
We Trip The Light
FANTASTIC

Forensic Science International

An international journal dedicated to the applications of medicine and science in the administration of justice

Forensic Science International is an international journal publishing original contributions in the many different scientific disciplines pertaining to the forensic sciences. Fields include forensic pathology and histochemistry, chemistry, biochemistry and toxicology (including drugs, alcohol, etc.), biology (including the identification of hairs and fibres), serology, odontology, psychiatry, anthropology, the physical sciences, firearms, and document examination, as well as investigations of value to public health in its broadest sense, and the important marginal area where science and medicine interact with the law.

Review Articles and Preliminary Communications (where brief accounts of important new work may be announced with less delay than is inevitable with major papers) may be accepted after correspondence with the appropriate Editor. Case Reports will be accepted only if they contain some important new information for the readers.

Submission of Articles: Manuscripts prepared in accordance with Instructions to Authors should be sent to the Editor-in-Chief or one of the Associate Editors according to their area of expertise as listed below. If there is any doubt, a preliminary letter, telefax or telephone enquiry should be made to the Editor-in-Chief or his Assistant.

ELSEVIER

Forensic Science International 164 (2006) 87–92

Forensic Science International

www.elsevier.com/locate/forsciint

Review

Time of death dependent criteria in vitreous humor—Accuracy of estimating the time since death

Burkhard Madea *, Alexander Rödig

Institute of Legal Medicine, University of Bonn, Stiftsplatz 12, D-53111 Bonn, Germany

Received 3 June 2005; received in revised form 16 November 2005; accepted 3 December 2005
Available online 24 January 2006

Abstract

Since more than 40 years reports on the rise of potassium concentration [K^+] in vitreous humor have been published with different statements concerning the accuracy of death time estimation. In the last years several statistical approaches for a more accurate estimation of the time since death have been reported. While in most investigations the PMI has been used as the independent and [K^+] as the dependent variable in linear regression analysis between PMI and [K^+], recently it has been suggested to use [K^+] as the independent variable for regression analysis. Changing the variables would lead to a higher accuracy of death time estimation. This has also been recommended for regression analysis between hypoxanthine concentration [Hx] and time since death.

This hypothesis has been checked on independent cases with potassium and hypoxanthine in vitreous humor. Linear regression with [K^+] or [Hx] as independent variable has revealed a slightly more accurate death time estimation compared to a linear regression with PMI as independent variable. Thus, e.g. the accuracy could have been improved from ±25.96 to ± 23.27 h by using [K^+] as independent variable.

Another statistical approach has re-evaluated six large studies on the rise of vitreous [K^+] using a local regression analysis (Loess procedure). Based on this re-evaluation an accuracy of death time estimation has been recommended (95% limits of confidence of ±1 h in the early PMI and ±10 h, 110 h postmortem) which has surpassed even optimistic results of earlier investigations. This recommended accuracy of death time estimation has been checked on a random sample of 492 cases. Only 153 cases have been within the predicted postmortem interval, 339 lay outside with a systematic overestimation of the time since death.

Keywords: Potassium; Vitreous humor; Death time; Regression analysis

Contents

1. Introduction

The postmortem rise of the potassium concentration [K^+] in vitreous humor (VH) has been known for 40 years and has been recommended for the estimation of the time since death [1,3–5,9–13,15,17,18,23,27,28,31–33]. However, a practical application has been hampered by different results concerning the accuracy of death time estimation [17,21]. Optimistic results of early investigations with an accuracy of death time estimation of ±9.5 h in a time period up to 104 h postmortem [33] could not have been confirmed by succeeding investigations [1,3,9,10,17,30].

* Corresponding author. Tel.: +49 228 73 83 15; fax: +49 228 73 83 68.
E-mail address: b.madea@uni-bonn.de (B. Madea).

0379-0738/$ – see front matter
doi:10.1016/j.forsciint.2005.12.002

The correlation and the strength of correlation between [K^+] and time since death depends on different factors such as cause of death, duration of agonal period, ambient temperature, etc. [4,5,17,21]. These factors influencing the accuracy of death time estimation can partly be taken into consideration by using internal standards (e.g. urea concentrations as indicator of an antemortem electrolyte dysregulation) [17,21].

Meanwhile new methods like capillary zone electrophoresis have been applied to vitreous humor analysis with encouraging results [2,7,34,35]. Furthermore, vitreous humor pre-treatment before analysis and analytical methods have been identified as important factors for the accuracy of [K^+] determination and therefore also death time estimation [6,8,20,24,28].

In the last years several statistical approaches for a more accurate estimation of the time since death have been recommended:

(1) In most investigations, the PMI has been used as indepedant and [K^+] as dependant variable in linear regression analysis between PMI and [K^+]. According to a recommendation of Munoz et al., however, [K^+] should be used as independent variable for regression analysis. According to the authors this approach leads to a higher accuracy of death time estimation. This can also be applied to the correlation between hypoxanthine concentration [HX] and time since death [25,26,29].
(2) A statistical re-evaluation of six greater studies on the rise of vitreous [K^+] [1,3,10,17,30,33] using a local regression analysis (Loess procedure) has revealed an accuracy of death time estimation (95% confidence limits of $\pm$1 h in the early postmortem period and $\pm$10 h, 110 h postmortem) which has surpassed even optimistic results of earlier investigations [14].

The approach of Lange et al. [14] was as follows: a re-analysis of six studies on vitreous [K^+] revealed that the relationship between [K^+] and pmi is not completely linear and the residual variability of [K^+] as a function of pmi is not constant. Thus, two main assumptions of the simple linear model, linearity and constant variance, were not supported by the data. The conclusion of the authors was that it is clearly problematic to report statistical summaries such as a slope of an estimated regression line and the reliability of that estimation based on a model with faulty assumptions. Even after rescaling the data in an attempt to achieve linearity in the [K^+]–pmi relationship and to stabilize residual variation, the relationship continued to be non-linear and its variability unstable. Therefore, as a new approach for modelling [K^+] and pmi that accomodates non-linearities and changing residual variability a local regression model, specifically a Loess smooth curve, was fitted seperately to the data from each of the six studies. The Loess smooth curve adapted locally to the changing and possibly non-linear relationship between [K^+] and pmi across their observed ranges. The data from all six studies were then combined to yield a single Loess curve with 95% confidence bands. The estimated Loess curve and confidence bands were used in an inverse prediction method to construct low, middle and high estimates at given values of [K^+] (in an appendix to their paper Lange et al. give some details on the Loess method and the inverse prediction method) [14].

Based on 766 cases from 6 studies on potassium in vitreous humor and time since death and the calculated ''single Loess curve'' 95% confidence limits for increasing [K^+] values were published [14]. However, these 95% confidence limits and the table on estimating the time since death from measured [K^+] derived from their statistical analysis (Table 1) are not comprehensible, taking into consideration the real values of the six studies [1,3,10,17,30,33]. According to Table 1 a potassium concentration of 7 mmol/l reveals a mean time since death of 7 h with a lower 95% confidence limit of 6 h, an upper 95% confidence limit of 8 h; a potassium concentration of 17 mmol/l reveals a mean time since death of 69 h, a lower 95% limit of 66 h and an upper limit of 72 h.

Aim of the present paper was to test the results of both studies

- higher accuracy of death time estimation by using analyte concentrations as independent variable and time since death as dependent variable [25,26];
- validity of the accuracy of death time estimation based on the re-evaluation by Lange et al. [14];

using own independent cases as well as cases reported in forensic literature.

Table 1
Estimated values of postmortem interval for various increasing values of potassium obtained from combining all 790 cases and the Loess procedure

Measured vitreous potassium concentration (mmol/l)	Estimated PMI (h)		
	Lower 95% value	Mean value	Upper 95% value
5.9	2	3	4
6.4	3	5	6
7.0	6	7	8
7.5	8	10	12
8.0	11	13	15
8.5	14	16	19
9.1	18	21	22
10.1	23	25	27
11.1	29	30	32
12.1	33	35	38
13.0	39	41	44
13.9	44	47	50
14.9	51	54	57
15.9	58	61	64
17.0	66	69	72
18.3	74	77	81
19.7	81	85	90
21.1	89	94	100
22.6	98	103	111
24.2	106	113	123

From Lange et al. [14].

Table 2
Regression parameters of the linear regression for estimating the time since death from vitreous potassium: correlation coefficient, standard deviation, 95% confidence limits

Data	Own cases ($n = 170$)		Cases from Munõz et al. 2001 [26] ($n = 176$)	
	$[K^+]$ dependent variable	PMI dependent variable	$[K^+]$ dependent variable	PMI dependent variable
Rise (PMI/K^+)	4.76	3.82	5.78	4.02
Intercept (PMI)	−29.05	−16.46	−32.31	−19.57
Mean value of residues (real minus calculated)	0.055	0.000	−0.02	0.000
Standard deviation (h)	13.25	11.87	4.37	3.65
95% confidence limits	±25.96	±23.27	±8.56	±7.15
Postmortem interval	up to 133 hpm		up to 29 hpm	
R^2	0.801		0.695	

Compared are accuracies of estimating the time since death on two random samples with $[K^+]$ as dependent or independent variable. Own random sample ($n = 170$) and cases by Munoz et al. [26] ($n = 176$).

2. Case material and statistical calculations

Vitreous humor has been routinely obtained by scleral puncture near the outer canthus using a 10 ml syringe and a no. 20 needle. Any specimen that has not been crystal clear has been rejected. Most of the samples have been frozen at −70 °C until determinations could have been performed. For analysis only the supernatant has been used after centrifugation for 10 min at 3000 rpm. The analysis of vitreous humor has been performed on the selective analyser Hitachi 705 (purchased by Boehringer/Mannheim) [17]. [Hx]-determination has been performed using a high performance liquid chromatography method [19]. Cause of (sudden) death was mainly due to coronary artery diseases, head injury, traffic accidents, falls from height, etc. Sudden death means that the duration of the agonal period was much below 6 h, mainly in the scope of some minutes.

Statistical calculations have been based on

- 170 own cases with vitreous potassium;
- 176 cases with vitreous potassium from Munoz et al. [26];
- 198 cases with vitreous hypoxanthine;

to check the hypothesis that a change of variables with analyte concentration as independent variable reveals a more accurate death time estimation. For the statistical calculation using [Hx] own cases ($n = 64$) and the cases of Munoz et al. [25] ($n = 134$) have been used together, since causes of death, sample acquisition, pre-treatment and analytical procedure have nearly been identical and full data had been published by Munoz et al. ''to facilitate comparative studies'' [26]. The two groups have also been analysed separately. For vitreous potassium the cases of Munoz et al. [26] and the own ones have been analysed separately, too (see results in Table 2).

Statistical significance has been checked using Pitman's T ($\alpha = 5\%$).

To test the validity of predicted times since death for various increasing $[K^+]$ values using the table of Lange et al. [14] a combined random sample of 523 cases has been used (347 consecutive own cases; 176 cases from Munoz et al. [25]). This has been necessary to have enough cases available for the 20 $[K^+]$ concentration groups.

3. Results and discussion

3.1. Accuracy of estimating the time since death by using $[K^+]$ and [Hx] as independent variable

A linear regression analysis with the $[K^+]$ as independent variable using 170 own consecutive cases (PMI up to 133 h) has proved to be more accurate than a linear regression with the PMI as independent variable.

Compared to the classic approach the accuracy has increased from ±25.96 to ±23.27 h.

The material of Munoz et al. [26] shows a rise in accuracy of ±1.4 h (from ±8.56 to ± 7.15 h); however, Munoz et al. only have studied a postmortem interval of less than 29 h (Table 2).

The rise in accuracy of death time estimation as described above has also been found when using the hypoxanthine concentration as independent variable to predict the PMI. In a random sample of 198 cases the accuracy has risen from 15.89 to 13.69 h (Table 3).

The rise in accuracy analysing the data of Munoz et al. ($n = 134$) separately has even been higher: it has increased from ±12.57 to ±9.09 h (notice: the observed interval has contained only cases with a PMI < 29 h). When only the own cases

Table 3
Regression parameters of the linear regression for estimating the time since death from vitreous hypoxanthine [Hx]: correlation coefficient, standard deviation, 95% confidence limits

Data	Own cases ($n = 64$) and cases from Munoz et al. ($n = 134$) [25] $\sum n = 198$	
Method	PMI as dependent variable	HX as dependent variable
Rise (PMI/Hx)	0.22	0.29
Intercept (PMI)	−2.24	−7.85
Mean value of residues (real minus calculated)	0.000	0.000
Standard deviation (h)	6.98	8.11
95% confidence limits	±13.69	±15.89
Postmortem interval	up to 96.8 hpm	
R^2	0.742	

Compared are accuracies of estimating the time since death on a random sample with [Hx] as dependent or independent variable. For statistical analysis own cases ($n = 64$) and cases by Munoz et al. [25] ($n = 134$) were used.

($n = 64$) have been used for statistical analysis the rise of the accuracy has been – due to the longer PMI studied – from ±23.41 to ±19.88 h.

Using the analyte as independent variable a significant rise in accuracy could have been observed for [K^+] and [Hx] (Pitman's T, $\alpha = 5\%$).

Already Lucy and Aytwoyd [16] have confirmed the approach of Munoz et al. [25,26]. The rise of accuracy by changing the variables can be declared as follows.

A regression line is computed by a mathematical procedure known as ''least squares fitting'' (Fig. 1). In this procedure a term that describes the sum of the squared distances of the data points from the regression line is minimized. It is mathematically expedient and commonly practiced to minimize only the vertical distances (the residuals) and not the perpendicular distances. By using this approach, however, two regression lines can be obtained, depending on which variable is put on the *y*-axis. This variable is called the ''dependent'' variable as its value is estimated from the ''independent'' variable on the *x*-axis. Linear regression models simply describe a statistical relationship, therefore the terms ''dependent'' and ''independent'' do not indicate a causal relationship.

The obtained result is a one-way estimation. The regression line $y = a + bx$ must not be simply converted to $x = 1/b(y - a)$ in order to predict in the other direction. This is a result from the vertical distances (parallel to the *y*-axis) being minimized. If a simple conversion is performed, the wrong distances (still parallel to the *y*-axis and not parallel to the *x*-axis as needed) are minimized. As a result the so obtained regression line does not fit optimally to the data. To change the direction of prediction a completely new regression is required.

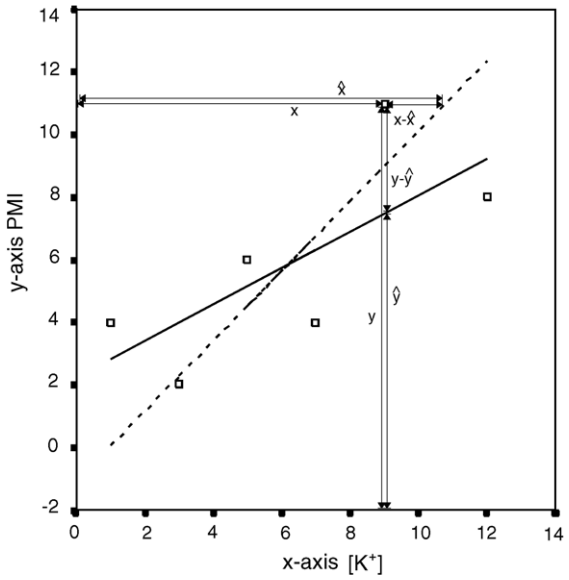

Fig. 1. Diagram of ''least squares fitting''. Two regression lines are shown where the PMI is used as both dependant and independent variable. Each square represents a data point but the values are chosen for illustration purposes only. If the PMI is used as dependant variable it is estimated from the potassium concentration. Then the sum of squares of the residuals ($y - \hat{y}$) parallel to the *y*-axis is minimized. This leads to the solid regression line. To predict the potassium concentration from the PMI the obtained regression line must not be simply converted but a new one has to be computed where the sum of squares of the new residuals ($x - \hat{x}$) parallel to the *x*-axis has to be minimized. This leads to the dashed line. It can be clearly seen that two different regression lines are obtained. The angle between the two lines depends on R^2. An R^2 of 1 leads to two identical lines, an R^2 of 0 to two lines perpendicular to each other.

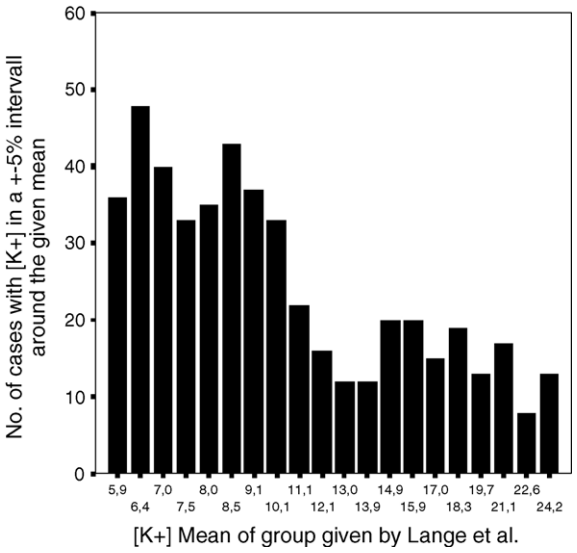

Fig. 2. Distribution of cases ($N = 492$) on the 20 potassium concentration groups according to Lange et al. using an interval of ±5% around the potassium concentrations.

Although a significant rise in accuracy can be obtained by using the analyte as independent variable this is negligible for practical purposes since the accuracy of death time estimation for vitreous [K^+] is only increased by 1.7 h from ±25.96 to ±23.27 h (see Table 2) in the time interval up to 133 hpm.

In the early pmi as studied by Munoz et al. (below 29 h) the rise of accuracy is also of limited importance since other methods of death time estimation work with a higher accuracy in this time period [22].

3.2. Re-evaluation of the data of Lange et al.

To re-evaluate the validity of the table of Lange et al. [14] from 523 cases (347 own cases and 176 cases reported by Munoz et al. [25,26]) with measured potassium concentration and known time since death 492 cases (94%) have been selected in which the potassium concentration has been within a 10% interval (±5%) around the increasing potassium values given by Lange et al. (Table 1). The distribution in 20 groups according to the 20 potassium values of Table 1 can be seen in Fig. 2. It has been necessary to combine both random samples (own cases and cases of Munoz) to have enough cases within the 20 increasing [K^+] concentration groups.

One hundred and fifty three of the selected 492 cases have revealed a postmortem interval within the predicted PMI for the given potassium concentration, 339 lay outside of the interval (Table 4).

There has been a mean difference of minus 6 h between estimated time since death according to Table 1 and actual time since death and a standard deviation of ±12 h.

Table 4
Overview of cases ($n = 492$) with [K^+] within 10% around the mean values according to Lange et al. (Table 1)

	Frequency, n	Percentage
Cases within the postmortem interval corresponding to the potassium concentration according to Table 1		
No	339	68.9
Yes	153	31.1
Total	492	100.0

PMI was calculated for the respective [K^+] according to Table 1. Three hundred and thirty nine PMI were outside the PMI according to Table 1, 153 inside.

Fig. 3 shows a widening gap between estimated and actual time since death with an increasing potassium concentration corresponding to an increasing time since death.

When from the original 523 cases only those cases with a [K^+] concentration within 1% (±0.5%) around the increasing [K^+] values in Table 1 ($n = 75$) have been selected the results have not been better: only 38.7% ($n = 29$) of the cases have been within the predicted PMI, 61% ($n = 46$) outside.

The deviation from the mean predicted time since death has been −5.1 h, the standard deviation ±12.6 h. The 95% limits of confidence have been ±24.7 h and have confirmed results of previous studies with a much wider range of scatter [1,3,9–13,17,31]. The results which have been derived from the metaanalysis of Lange et al. [14] have revealed a systematic over-estimation of the time since death and are not useful in practice.

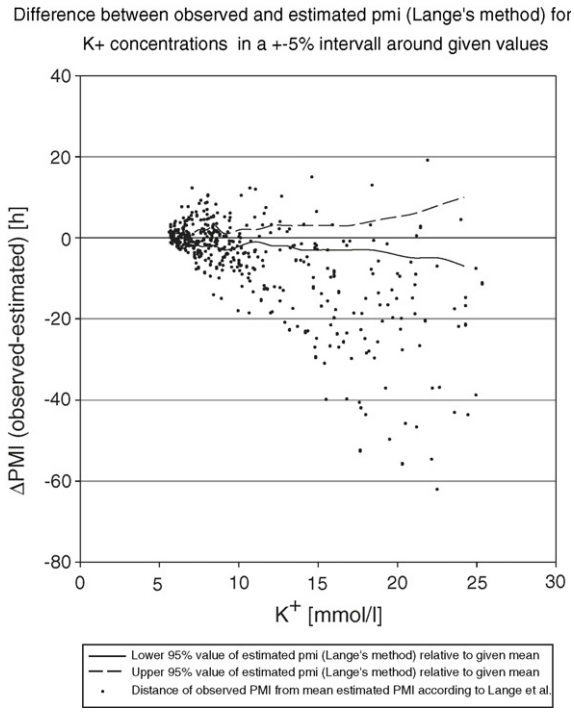

Fig. 3. Deviations between real and extrapolated time since death over the potassium concentration. Each point represents the difference between the observed pmi and estimated pmi according to Lange et al. Those cases with potassium concentrations in a ±5% interval around the given concentrations were included. The two lines represent the upper and lower value of the 95% confidence interval according to Lange et al. relative to the given mean.

4. Conclusion

For estimating the time since death using a linear regression with a postmortem interval and an analyte concentration the postmortem interval should be used as dependent variable.

This procedure recommended already by Munoz et al. [25,26] reveals a higher accuracy of death time estimation.

Although only a slight but statistically significant increase of the accuracy of death time estimation can be achieved, this is the correct method for statistical analysis.

The calculation of the time since death based on the table published by Lange et al. [14] reveals a systematic over-estimation of the time since death and the accuracy of death time estimation cannot be confirmed.

References

[1] L. Adelson, I. Sunshine, N.B. Rushforth, M. Manforth, Vitreous potassium concentration as an indicator of the postmortem interval, J. Forensic Sci. 8 (1963) 503–514.
[2] G. Bocaz-Beneventi, F. Tagliaro, F. Bortolotti, G. Manetto, J. Havel, Capillary zone electrophoresis and artificial neural networks for estimation of the post-mortem interval (PMI) using electrolyte measurements in human vitreous humor, Int. J. Legal Med. 116 (1) (2002) 5–11.
[3] J.I. Coe, Postmortem chemistries on human vitreous humor, Am. J. Clin. Pathol. 51 (1969) 741–750.
[4] J.I. Coe, Vitreous potassium as a measure of the postmortem interval: an historical review and critical evaluation, Forensic Sci. Int. 42 (1989) 201–213.
[5] J.I. Coe, Postmortem chemistry update—emphasis on forensic applications, Am. J. Forensic Med. Pathol. (1993) 91–117.
[6] J. Coe, F.S. Apple, Variations of vitreous humor chemical values as a result of instrumentation, J. Forensic Sci. 43 (1985) 604–607.
[7] K.E. Ferslew, A.N. Hagardorn, M.T. Harrison, W.F. McCormick, Capillary ion analysis of potassium concentrations in human vitreous humor, Electrophoresis 19 (1) (1998) 6–10.
[8] U. Garg, R. Althahabi, M. Brod, Th. Young, Ch. Blanchora, Hyaluronidase as a liquifying agent for chemical analysis of vitreous humor, Society of Forensic Toxicologists 2002, (2002.
[9] L. Hansson, U. Uotila, R. Lindfors, K. Laiho, Potassium content of the vitreous body as an aid in determining the time of death, J. Forensic Sci. 11 (1966) 390–394.
[10] W.M.H. Hughes, Levels of potassium in the vitreous humor after death, Med. Sci. Law (1965) 150–156.
[11] F.A. Jaffe, Chemical postmortem changes in the intraocular fluid, J. Forensic Sci. 7 (1962) 150–156.
[12] R.A. James, P.A. Hoadley, B.G. Sampson, Determination of postmortem interval by sampling vitreous humour, Am. J. Forensic Med. Pathol. 18 (2) (1997) 158–162.
[13] S. Komura, S. Oshiro, Potassium levels in the aqueous and vitreous humor after death, J. Exp. Med. 122 (1977) 65–68.
[14] N. Lange, S. Swearer, W.Q. Sturner, Human postmortem interval estimation from vitreous potassium: an analysis of original data from six different studies, Forensic Sci. Int. 66 (1994) 159–174.
[15] J.T. Lie, Changes in potassium concentration in the vitreous humor after death, Am. J. Med. Sci. (1967), 32/136–39/143.
[16] D. Lucy, B. Aytwoyd, Commentary on Munoz et al. (2001) J. Forensic Sci. 46, 20–213, J. Forensic Sci. 46 (2001) 1527.
[17] B. Madea, C. Henßge, W. Hönig, A. Gerbracht, References for determining the time of death by potassium in vitreous humor, Forensic Sci. Int. 40 (1989) 231–243.

[18] B. Madea, N. Hermann, C. Henßge, Accuracy of estimating the time since death by vitreous potassium—comparison of two different equations, Forensic Sci. Int. 46 (1990) 277–284.
[19] B. Madea, H. Käferstein, N. Hermann, G. Sticht, Hypoxanthine in vitreous humor and cerebrospinal fluid-marker of postmortem interval and prolonged (vital) hypoxia? Forensic Sci. Int. 65 (1994) 19–31.
[20] B. Madea, Is there recent progress in the estimation of the postmortem interval by means of thanatochemistry? Forensic Sci. Int. 151 (2005) 139–149.
[21] B. Madea, C. Henssge, Eye changes after death, in: C. Henssge, B. Knight, Krompecher Th, B. Madea, L. Nokes (Eds.), The Estimation of the Time Since Death in the Early Postmortem Period, second ed., Edward Arnold, London, 2002, pp. 103–133.
[22] B. Madea, C. Henssge, Time since death, in: J. Payne-James, A. Busuttil, W. Smock (Eds.), Forensic Medicine: Clinical and Pathological Aspects, Greenwich Medical Media Limited, London, 2003, pp. 91–114.
[23] B. Madea, C. Kreuser, S. Banaschak, Postmortem biochemical examination of synovial fluid—a preliminary study, Forensic Sci. Int. 118 (2001) 29–35.
[24] A.R. McNeil, A. Gardner, S. Stables, Simple method for improving the precision of electrolyte measurements in vitreous humor, Clin. Chem. 45 (1) (1999) 135–136.
[25] J.I. Munoz Barús, J.M. Suárez-Penaranda, X.L. Otero, M.S. Rodríguez-Calvo, E. Costas, X. Miguéns, L. Concheiro, Improved estimation of postmortem interval based on differential behaviour of vitreous potassium and hypoxantine in death by hanging, Forensic Sci. Int. 125 (2002) 67–74.
[26] J.I. Munoz, J.M. Suárez-Penaranda, X.L. Otero, M.S. Rodríguez-Calvo, E. Costas, X. Miguéns, L. Concheiro, A new prespective in the estimation of postmortem interval (PMI) based on vitreous $[K^+]^*$, J. Forensic Sci. 46 (2) (2001) 209–214.
[27] H.N. Naumann, Postmortem chemistry of the vitreous body in man, Arch. Opthalmol. 62 (1959) 356–363.
[28] D.J. Pounder, D.O. Carson, K. Johnston, Y. Orihara, Electrolyte concentration differences between left and right vitreous humor samples, J. Forensic Sci. 43 (3) (1998) 604–607.
[29] T.O. Rognum, S. Hauge, S. Uyasaeter, O.D. Saugstad, A new biochemical method for estimation of postmortem time, Forensic Sci. Int. 51 (1991) 139–146.
[30] K. Stegmaier, Untersuchungen über die postmortale Kaliumkonzentration in Glaskörperinhalt und Kammerwasser und ihre Beziehung zur Todeszeit. MD Thesis, Marburg University, 1971.
[31] R.L. Stevens, R.G. Richards, Vitreous humor chemistry: the use of potassium concentration for the prediction of the postmortem interval, J. Forensic Sci. 32 (1987) 503–509.
[32] W.Q. Sturner, G.E. Ganther, The postmortem interval, Am. J. Clin. Pathol. 42 (1964) 137–144.
[33] W.Q. Sturner, The vitreous humor, postmortem potassium changes, Lancet 1 (1963) 807–808.
[34] F. Tagliaro, G. Manetto, F. Cittadini, D. Marchetti, F. Bortolotti, M. Marigo, Capillary zone electrophoresis of potassium in human vitreous humour: validation of a new method, J. Chromatogr. B Biomed. Sci. Appl. 733 (1–2) (1999) 273–279.
[35] F. Tagliaro, F. Bortolotti, G. Manetto, F. Cittadini, V.L. Pascali, M. Marigo, Potassium concentration differences in the vitreous humour from the two eyes revisited by microanalysis with capillary electrophoresis, J. Chromatogr. A 924 (1–2) (2001) 493–498.

ELSEVIER

Forensic Science International 164 (2006) 93–97

Forensic Science International

www.elsevier.com/locate/forsciint

Persons found 'Not Criminally Responsible on Account of Mental Disorder': A comparison of British Columbia, Canada and Hunan, China

Xiaoping Wang [a,b,*], James D. Livingston [b,c], Johann Brink [b,d], Emlene Murphy [b]

[a] *Mental Health Institute of the 2nd Xiangya Hospital, Central South University, Changsha, Hunan 410011, China*
[b] *Forensic Psychiatric Services Commission, Port Coquitlam, BC, Canada*
[c] *School of Criminology, Simon Fraser University, Burnaby, BC, Canada*
[d] *Department of Psychiatry, University of British Columbia, Vancouver, BC, Canada*

Received 18 November 2004; received in revised form 8 November 2005; accepted 4 December 2005
Available online 19 January 2006

Abstract

Current research literature contains very few international, cross-cultural comparison studies of persons adjudicated 'Not Criminally Responsible on Account of Mental Disorder' (NCRMD). This study explores and compares the demographic differences between persons found NCRMD in British Columbia, Canada and Hunan, China. Eight variables such as sex, age, education level, marital status, conviction history, psychiatric history, and index offence are compared between the Canadian and Chinese cohorts. The Canadian and Chinese cohorts were similar in sex and psychiatric history. The divorce rate, educational level, and conviction histories were significantly higher, and the age was significantly older in the Canadian cohort. The Chinese cohort had higher levels of murder and attempted murder index offences. Differences between the two cohorts can be explained in terms of legislative and cultural differences.

Keywords: Mentally ill offender; Forensic psychiatry; China; Canada

1. Introduction

The Chinese forensic psychiatric system is rarely described in the English literature. Chinese historical records from the past two millennia contain occasional references related to persons who commit violent crimes and are pardoned by the courts on account of their mental disorders [1]. After the foundation of the Chinese Republic in 1911, a new criminal law was introduced to waive or reduce the punishment for persons suffering from mental disorders who commit crimes [1]. In 1949, the People's Republic of China was founded and a Soviet-style forensic psychiatric system was established [1]. In 1979, the Second Session of the Fifth National People's Congress adopted the Chinese *Criminal Code*—the first comprehensive set of criminal laws and criminal procedures for China.

One *Criminal Code* guides the criminal justice system in China and the legal system is based on a Civil Law model. According to Article 14 of the Chinese *Criminal Code*, individuals are criminally responsible for 'international crimes' resulting from a clear knowledge that one's own act will cause socially dangerous consequences, and of hope for or indifference to the occurrence of those consequences. Since 1997, when the Fifth Session of the Eighth National People's Congress Code amended the *Code*, the *Criminal Code* has contained provisions to absolve mentally ill persons who commit crime from bearing full criminal responsibility [2,3]. Article 18 of the Chinese *Criminal Code* articulates the following mental disorder provisions:

1. A mentally ill person who causes dangerous consequences at a time when he is unable to recognize or unable to control his own conduct is not to bear criminal responsibility after being established through accreditation of legal procedures; but his family or guardian shall be ordered to subject him to strict surveillance and arrange for his medical treatment. When necessary, he will be given compulsory medical treatment by the government.
2. A person whose mental illness is of an intermittent nature shall bear criminal responsibility if they commit a crime during a period of mental normality.

* Corresponding author. Tel.: +86 731 5292182; fax: +86 731 5360162.
E-mail address: xiaop6@hotmail.com (X. Wang).

0379-0738/$ – see front matter
doi:10.1016/j.forsciint.2005.12.001

3. A mentally ill person who commits a crime at a time when they have not yet completely lost their ability to recognize or control their own conduct shall bear criminal responsibility but they may be given a lesser or a mitigated punishment.
4. An intoxicated person who commits a crime shall bear criminal responsibility.

Of the four mental disorder subsections of Article 18, only the first involves the treatment and disposition of mentally ill offenders. Article 19 also enables a deaf-mute or a blind person who commits a crime to receive a lesser or mitigated punishment, or a complete exemption from punishment.

In Canada, the legal guidelines for the 'Not Criminally Responsible of Mental Disorder' defence are laid out in Section 16 of the *Criminal Code*:

1. No person is criminally responsible for an act committed or an omission made while suffering from a mental disorder that rendered the person incapable of appreciating the nature and quality of the act or omission or of knowing that it was wrong.
2. Every person is presumed not to suffer from a mental disorder so as to be exempt from criminal responsibility by virtue of subsection 1, until the contrary is proved on the balance of probabilities.
3. The burden of proof that an accused was suffering from a mental disorder so as to be exempt from criminal responsibility is on the party that raises the issue.

The guidelines for managing persons adjudicated NCR-MD is laid out section 672 of the *Code*, which is also known as the mental disorder provisions. Section 672 provides the policies and procedures for every juncture of the forensic mental healthcare system, including assessments, appeals, dispositions, and hearings. The mental disorder provisions of the Canadian *Code* were reformed in 1992 with the enactment of Bill C-30 and more recently, in 2005, with the enactment of Bill C-10 [4,5]. Similar to the Chinese *Code*, the Canadian *Code* holds individuals legally responsible for criminal acts that are committed during periods of mental normality, transient mental states caused by external factors, or self-induced states caused by drug or alcohol consumption [6,7]. Unlike the Chinese *Code*, the mental disorder provisions in Canada impose no legally bound obligations on family members or guardians.

A review of the current literature reveals very few international, cross-cultural comparison studies of NCR-accused persons. The purpose of the current study is to build on this literature by comparing and contrasting characteristics of persons adjudicated NCRMD in British Columbia, Canada and Hunan, China.

2. Methods

2.1. Sample

The Canadian cohort is from a previously published study of persons found NCRMD between February 4, 1992, and February 4, 1998, in British Columbia, Canada [8]. The Province of British Columbia is located on the West coast of Canada and has a population of 4,146,600 [9]. Approximately, 10% of residents of British Columbia are of Chinese descent [10]. Forensic psychiatric services in British Columbia are delivered through a centralized, highly specialized system consisting of a 190-bed forensic psychiatric hospital and six forensic psychiatric community clinics. The Canadian cohort contains 276 persons who were adjudicated NCR-MD from 1992 to 1998. Demographic and index offence information for the cohort was obtained through a comprehensive review of hospital charts. In British Columbia, less than 1% of adults charged with a criminal offence are referred for a forensic psychiatric assessment on issues pertaining to criminal responsibility. For example, in 2003 there were 63,000 adults who were charged with a criminal offence in British Columbia and approximately 300 were referred for an NCRMD assessment [11].

The Chinese cohort is composed of persons found NCRMD from June 1, 1998, and June 1, 2003, in Hunan, China. Hunan Province is located in the central south of China and has a population of 65,320,000 among them 48,080,000 live in rural area [12]. Hunan is divided into 14 cities and 90 counties and its socioeconomic development is on the middle level of China. After the Chinese *Criminal Code* amendments in 1997, the 15 forensic psychiatric assessment centers in Hunan Province were integrated into 2 assessment centers. Hunan Province also has a 90-bed forensic security hospital where seriously violent NCR-accused persons are detained for an indefinite period. Most NCR-accused persons in Hunan Province are detained and treated in a general psychiatric hospital for a period of 1–3 months. The less violent cases are discharged to the community directly by police. The Chinese cohort contains 354 cases that were selected from a database of persons referred for an evaluation at one of the forensic psychiatric assessment centers in Hunan Province. Approximately, more than half of forensic psychiatric evaluations in Hunan Province are conducted through the sampled forensic psychiatric assessment centre. Demographic and index offence information for the Chinese cohort was gathered through the database of the assessment center. Similar to British Columbia, a low percentage of adults charged with a criminal offence in Human are referred for a forensic psychiatric assessment on issues pertaining to criminal responsibility. For instance, in 2003 there were 58,962 adults who were charged with a criminal offence in Hunan and 337 were referred for an NCRMD assessment at the two psychiatric assessment centers of Hunan Province [13]. At this particular assessment centre, there were total 654 cases referred for assessment of criminal responsibility; of which, 45.9% were judged no-NCRMD and 13.7% were granted diminished responsibility.

2.2. Data analysis

Seven variables, including sex, age, education level, marital status, conviction history, psychiatric history, and index offence, were available for both Canadian and Chinese cohorts. The information was integrated into a database and statistical analyses were performed using the Statistical Package for Social Sciences (SPSS).

Table 1
Demographic and background data

Variables	Hunan cohort ($n = 354$)	BC cohort ($n = 276$)
Sex (1.11 (0.292))[a]		
Male	82.2%	85.5%
Female	17.8%	14.5%
Marital status (177.979 (0.000))[a]		
Never married (%)	40.7	62.3
Married (%)	53.4	7.0
Common law (%)	0	4.0
Divorced/separated (%)	5.1	25.6
Widowed (%)	0.8	0.4
Unknown (%)	0	0.7
Age at the time of NCRMD (in years) ($t = 3.721$, d.f. = 626, $P = 0.000$)	32.64 ± 9.17	35.59 ± 10.69
Age (years) (19.008 (0.000))[a]		
≤21	6.5%	10.4%
22–29	33.6%	26.0%
30–40	42.1%	36.4%
>40	17.8%	27.1%
Highest grade attained (in years) ($t = 15.917$, d.f. = 623, $P = 0.000$)	7.06 ± 2.70	10.22 ± 2.10
Conviction history before index offence yes (%) (271.170 (0.000))[a]	2.8	63.2
Psychiatric history before index offence yes (%) (0.525 (0.469))[a]	82.5	76.5

[a] χ^2 (P).

3. Results

Both cohorts were composed of approximately 80–85% males and 15–20% females. A Chi-square analysis revealed no significant differences in the proportion of males and females in the Chinese and Canadian cohorts. Approximately 80–85% of individuals in both the cohorts had a psychiatric history prior to the index offence. Again, a Chi-square analysis revealed no significant differences in the psychiatric histories of the Chinese and Canadian cohorts (see Table 1). Significant differences between the two cohorts were found in the marital status, age, educational level, and conviction history variables. The Chinese cohort was significantly more likely to be married and the Canadian cohort was significantly more likely to have never been married and/or divorced. The average age of the Canadian cohort was 35.6 years, which was significantly older than the Chinese cohort who had an average age of 32.6 years. A greater proportion of the Canadian cohort was above the age of 40 at the time of the NCRMD adjudication. On average, the highest grade level attained by the Canadian cohort was 10, whereas, on average, the highest grade level attained by the Chinese cohort was 7. A t-test revealed that the Canadian cohort had significantly more years of education than did the Chinese cohort.

The two cohorts also significantly differed in criminal histories and index offences. While only 3% of the Chinese cohort had a criminal conviction prior to the index offence, 63% of the Canadian cohort had a history of criminal convictions.

Table 2
Index offence for NCRMD assessment

Index offence	Hunan cohort (%)	BC cohort (%)
Murder/attempt	68.6	10.5
Sexual assault	2.3	7.3
Assault	22.0	45.5
Robbery	0.8	1.8
Weapons	0	6.5
Property	0	10.2
Nuisance	6.2	14.9
Theft	0	3.3

χ^2 (P) = 238.298 (0.000).

The most serious index offence for 68.6% of the Chinese cohort was murder or attempted murder, compared with only 10.5% of the Canadian cohort. Accordingly, a greater proportion of the Canadian cohort was charged with assault, property, and nuisance-related offences. Table 2 presents the index offence for the two subject groups.

4. Discussion

While it is limited in scope, the current comparison study has yielded interesting results. Given the relatively stable prevalence rates of mental illness internationally and across genders, it is unsurprising that the two cohorts share similarities. The Chinese and Canadian cohorts are similar in the proportion of males and females and have similar psychiatric histories. The results reveal that the conviction histories are significantly higher in the BC cohort, which could be explained by the different rates of offending behavior in the two countries. In 1997, the reported crime rates of the general population in BC and China were 13,757.7/100,000 and 135.9/100,000, respectively [14,15]. The crime rate in the Hunan province approached the average level of China. The crime rate in British Columbia is higher that the Canadian crime rate. The authors speculate that an alternative or additional explanation for this discrepancy in crime rates may relate to differences in societal and/or cultural attitudes towards crime committed by persons afflicted with mental disorder. Anecdotal evidence suggests that, in comparison with Canada, the public in Hunan province and the rest of China has a higher tolerance for non-violent, less serious offences such as nuisance or property related crimes committed by persons with mental illness. Such socially offensive behavior is less likely to be reported to the police and, therefore, less likely to result in criminal proceedings. Unfortunately, no scientific data is available to support this speculation.

In British Columbia, as in the rest of Canada, the government assumes the cost for the hospital and community care of all persons with severe mental illness. In China, however, the cost of such care is not totally born by government agencies. The cost of mental health care is beyond the financial capacity of many Chinese citizens, especially those living in rural areas of China. A recent survey from Fuyang, Anhui Province indicates that 35.2% of people with schizophrenia, 46.2% of people with mood disorder, and 61.5% of people with

mental retardation do not receive any psychiatric treatment [16]. It is, therefore, understandable that the early diagnosis and treatment of mental illness may be much better in British Columbia than that in Hunan, which can prevent mentally ill persons from committing crimes during their active stage of the disease. This may explain why NCR-accused persons in the Chinese cohort are significantly younger in comparison with persons in the Canadian cohort. Of particular interest is the higher proportion of Chinese NCR-accused persons who between the age of 22–29 years, which is the highest risk onset age period of schizophrenia. The divorce rate and educational level are significantly higher in the Canadian cohort as compared with the Chinese cohort, which are similar to that of the general population rates, respectively. The census showed that the unmarried and divorce rates in Hunan (1997) and BC (1996) are 19.64%, 798.5/100,000 and 30.5%, 7900/100,000, respectively among age 15 years and above group (12, Statistic Canada, 1996).

The present study indicates that the rates of serious offences such as murder/attempt murder are significantly higher, and the rates of the other less serious index offences are much lower in the Hunan cohort as compared with the BC cohort. The higher crime rates of general population in British Columbia and the underreported rate of crimes committed by persons with mental illness in Hunan are reasonable explanations for this finding. As well, the amendments to the Canadian *Criminal Code* in 1992 have made the NCRMD defense a more appealing option for defendants and legal counsel, which resulted in a substantial increase in the number of individuals entering the forensic psychiatric system for relatively less serious crimes [8].

Some limitations of the current study include methodological and sampling issues. Firstly, the data was collected in different periods for the two cohorts. Secondly, the Hunan cohort did not cover all NCRMD subjects of this province. Thirdly, the legal standards for the NCRMD defense differ between China and Canada. Lastly, the use of different and non-commensurate diagnostic systems precluded the comparison of some very important variables such as diagnosis.

Based on the author's experience of working in China and Canada, some main differences in forensic psychiatric service between Canada and China are described below:

1. In China, forensic psychiatric assessment establishments have to be designated by provincial government. Every assessment session requires the attendance of at least three psychiatrists, who have the equivalent qualifications of assistant professor of psychiatry. The psychiatric assessment reports need to be co-signed by all three attending psychiatrists. In Canada, the usual practice is to have one psychiatrist evaluate the subject independently on issues of criminal responsibility.
2. Canada does not have the defence of diminished responsibility and, therefore, the only defence available to persons suffering from a mental disorder during the commission of a criminal act is NCRMD. However, a lawyer may prefer to use a guilty-plea strategy, rather than an NCRMD verdict, if they feel that a conviction and sentence would be more advantageous for their client. In China, both the partial defence of diminished responsibility and the defence of NCRMD are available to mentally disordered accused persons. Sometimes, jails in Human refuse to receive persons who use the diminished responsibility defence because they lack the appropriate psychiatric treatment services.
3. In Canada, the criteria for the NCRMD defence focuses on the cognitive capacity of the accused person at the time of the offence and, occasionally, a person is found NCRMD without having been psychotic. In China, the criteria for NCRMD depend on cognitive and impulsive control functioning a the time of the offence, and the defence require that the person was psychotic at the time of the offence.
4. In China, only a small subset of NCR-accused persons, typically those who are seriously violent, are detained in the forensic psychiatric hospital for indefinite period by government. Most NCR-accused persons in China brought to a general psychiatric hospital by family members and are detained for treatment-purposes for approximately 1–3 months. Some of the less violent cases are discharged to community directly without any conditions. In Canada, the *Criminal Code* amendments established three disposition options – custody in a hospital, conditional discharge and absolutely discharge – that the Courts and provincial Review Boards must consider for NCR-accused persons. The Canadian *Code* clearly articulates the factors that the Courts and Review Boards must consider when determining the disposition for NCR-accused persons. In British Columbia, almost an equal number of NCR-accused persons are detained in custody or released to the community immediately following their NCRMD adjudication [8].

In summary, this paper provides a descriptive comparison of the legal standards for a finding of criminal non-responsibility in persons with mental disorder between the Hunan province in China and Canada. The results indicate significant differences in certain variables between the two cohorts that can be explained in terms of legislative, social, and cultural differences.

References

[1] X. Liu, Textbook of Forensic Psychiatry, second ed., People's Medical Publishing House, Beijing, China, 2004.
[2] G. Sun, Textbook of Criminal Law, Science Publishing House, Beijing, China, 2002.
[3] Z. Zheng, Forensic Psychiatric Foundation, Shanghai Science Technology Publishing House, Shanghai, China, 1997.
[4] Bill C-30, An Act to Amend the Criminal Code and to Amend the National Defence Act and the Young Offenders Act in Consequence Thereof (assented to 1991, c. 43, s. 4, proclaimed in force February 4, 1992).
[5] Bill C-10, An Act to Amend the Criminal Code (Mental Disorder) and to Make Consequential Amendments to Other Acts (assented to 2005, S.C. 2001, c.13 proclaimed in force January 1, 2006).
[6] R.v. Rabey, 37 C.C.C. (2d) 461, 79 D.L.R. (3d) 414 (Ont. C.A.), affd [1980] 2 S.C.R. 513, 54 C.C.C. (2d) 1, 15 C.R. (3d) 225, 1977.

[7] R.v. Stone, 2 S.C.R. 290, 134 C.C.C. (3d) 353, 24 C.R. (5th) 1, 1999.
[8] J.D. Livingston, D. Wilson, G. Tien, L. Bond, A follow-up study of persons found not criminally responsible on account of mental disorder in British Columbia, Can. J. Psychiatry 48 (6) (2003) 408–415.
[9] Statistics Canada, Population by Sex and Age Group, 2003 (Table 051-0001), Ottawa, Ontario, 2003.
[10] Statistics Canada, Visible Minority Population, Provinces and Territories, Ottawa, Ontario, 2001.
[11] Statistics Canada, Adults and Youth Charged, by Detailed Offences for Canada, Provinces and Territories, Annual (Table 252-0014), 2003.
[12] Hunan Statistic Bureau, Hunan Annual Statistic, Chinese Statistic Publishing House, 1998.
[13] Hunan Statistic Bureau, Hunan Annual Statistic, Chinese Statistic Publishing House, 2003.
[14] Statistics Canada, 1997 Crime Statistics, by Detailed Offences, Annual (Table 252-0013), Ottawa, Canada.
[15] L. Chen, Criminal tendency prediction of the 21st century in China, J. Hunan Public Security College 12 (4) (2000) 22–26.
[16] K. Zhang, S. Wang, X. Wei, et al., A survey and analysis of the recognized and therapeutic condition on mental disorders at urban and rural district in Fuyang, Chin. J. Mental Health 17 (3) (2003) 197–199.

ELSEVIER

Forensic Science International 164 (2006) 98–101

Forensic Science International

www.elsevier.com/locate/forsciint

Cluster analysis of a forensic population with antisocial personality disorder regarding PCL-R scores: Differentiation of two patterns of criminal profiles

Hilda Clotilde Penteado Morana [a,*], Fernando Portela Câmara [b], Julio Arboleda-Flórez [c]

[a] *Institute of Psychiatry, São Paulo University, Rua Marquês de Paranaguá, 36, ap. 62, Consolação, São Paulo, SP, CEP 01303-050, Brazil*
[b] *Epidemiology Sector, IMPPG, University of Brazil (UFRJ), Rua Pinheiro Machado 25/405, 22231-090 Rio de Janeiro, RJ, Brazil*
[c] *Department of Psychiatry, Queen's University, Kingston, Ont., Canada K7L 3N6*

Received 7 January 2005; received in revised form 10 November 2005; accepted 4 December 2005
Available online 24 January 2006

Abstract

Fifty six cases of a forensic population were submitted to a cluster analysis to observe the aglomerative behavior in relation to the total scores of the items comprising the PCL-R *Psychopathy Checklist Revised* [R.D. Hare, Manual for the Hare Psychopathy Checklist-Revised, Multi-Health System, Toronto, 1991]. The analysis indicated two independent types of antisocial personality disorders, not identified in the PCL-R in its standardized form, one of them being strongly associated with criminal conduct and the other with psychopathic personality. Such clusters were stable when the analysis was replicated with other hierarchical algorithms, and also, they were independently extracted via the *k*-means method without having previously fixed the value for *k*. One of the clusters concentrated the PCL-R highest scores, indicating that it is the prototypical psychopathic character determinant.

Keywords: Psychopathy; Antisocial personality disorder; Psychopathy checklist (PCL-R); Rorschach test; Cluster analysis; Forensic psychiatry

1. Introduction

In a former study a (Brazilian) Portuguese-language version of *Psychopathy Checklist Revised* (PCL-R) was validated from a forensic population sample of 56 male subjects classified as psychopaths and non-psychopaths [2]. Subjects were evaluated through psychiatric and neurological examinations, review of judicial records, Rorschach and PCL-R. Thirty three subjects were correlated to global personality disorder (GPD) and 23 to partial personality disorder (PPD), respectively, subtypes of antisocial personality disorder. The group identified as presenting GPD was statistically related to the category defined by Hare [2] as psychopaths and PPD as non-psychopaths. A control group of 30 subjects without criminological or psychiatric history was also evaluated with the same instruments.

Hare considers that in forensic environment identifying *psychopaths* is the main concern, since they present three times more chances of relapsing into criminal activity, and four times more likely to relapse into violent crimes. Therefore, *non-psychopath* subjects are identified via PCL-R only as those not reaching the cut-off score for psychopathy, presenting forensic relevance for category division purposes to the author.

Regarding the cut-off score for the Brazilian version of the PCL-R addressed in the former study [2], the value of 23 was set as cut-off score for the purpose of differentiating psychopaths and non-psychopaths. This cut-off score is defined as minimum necessary value to consider an individual as bearing the prototypical traits of psychopathy or global personality disorder. The score range of 12–22.9 was determined as the interval defining individuals bearing partial personality disorder or mild psychopaths, and normal individuals, i.e., presenting no sorts of personality deviation, are defined below the score of 12.

In comparison to the Rorschach test, the PCL-R in the Portuguese language presented a sensitivity level of 84.8% and specificity of 100%, as it was possible to exclude all true non-psychopaths, also presenting a strong agreement level (Kappa

* Corresponding author. Tel.: +55 11 3214 3084; fax: +55 11 3214 2765.
E-mail addresses: hildacpm@uol.com.br (H.C.P. Morana), fp3camara@yahoo.com.br (F.P. Câmara), ja9@post.queensu.ca (J. Arboleda-Flórez).

0379-0738/$ – see front matter
doi:10.1016/j.forsciint.2005.12.003

index = 0.87). Although the sample was not large ($n = 33$), the validity of the Rorschach test and the high sensitivity and agreement levels reinforce the cut-off score 23 as representative for the Brazilian forensic population.

For this paper, we have submitted that forensic population (56 cases) to a cluster analysis of the total scores of the items comprising the PCL-R, aiming to characterize possible subtypes of antisocial personality disorder which are familiar to the forensic practice.

Cluster analysis has been published previously by Cooke and Michie [3]. However, these authors work with factor analysis that requires a very large data. Besides this matter they are looking for a superordinate Hare's PCL-R psychopathic construct made up of correlated clusters or factors. The difference of what is presented on this study is that we are using cluster analysis as a descriptive/exploratory technique made up by similarities and not by factors or *eigenvalues*. This technique fill better our findings on personality structure, once we are interested in clinical observation, trying to identify antisocial personality disorders subtypes based on a forensic population using PCL-R as an exploratory tool.

2. Material and methods

2.1. Forensic population

PCL-R items "*interview and information schedule*", "PCL-R *quickscore form*" and "*the rating booklet*" have been translated into the Portuguese language (Brazil) with the author's agreement (Dr. Robert Hare) and its cut-off established for a forensic population selected from several penal facilities in the State of São Paulo, Brazil, except for one individual, who was selected from an outpatient facility [2]. This population was a random sample of 56 male individuals was taken from all those who had a diagnosis of antisocial personality disorder (ASPD) in the files. The diagnosis of antisocial personality disorder was confirmed according to ICD-10 criteria. Of these 56 individuals, 33 were diagnosed with global personality disorder (GPD) and the remaining 23 were diagnosed with subtype partial personality disorder (PPD) by the Rorschach test [1]. Average age was 27.9 years with a range of 35 (16–51). A sample of 30 individuals from the normal population with no criminal or psychiatric history and no diagnosis of ASPD was used as control, after be examined and tested by the Rorschach test. All subjects were informed about the nature and objectives of the study and assured about the confidentiality and privacy of the respective protocols. Written informed consent was obtained from all subjects. This study receives ethical approval by the Ethics Review Committee of Clinical Hospital from São Paulo University.

2.2. Rorschach test

The Rorschach tests were carried out according to the guidelines proposed by Silveira [4], and adapted to the Brazilian population by Coelho [5]. As this study required diagnostic accuracy of the personality conditions, the Exner criteria [6] for Rorschach was not utilized.

Table 1
Total score for PCL-R in GPD, PPD and control groups

F1	GPD	PPD	*N*	F2	GPD	PPD	*N*	F0	GPD	PPD	*N*
1	26	11	8	3	43	14	4	11	33	7	7
2	53	35	32	9	38	9	4	17	30	7	1
4	31	7	5	10	57	29	16	20	22	3	0
5	51	23	16	12	47	14	5				
6	65	45	2	13	57	25	11				
7	66	25	3	14	59	36	34				
8	63	27	4	15	42	13	6				
16	54	37	0	18	28	6	0				
				19	13	2	0				

2.3. Statistical analysis

Total PCL-R scores from GPD ($n = 33$), PPD ($n = 23$) and control groups were analyzed for hierarchical clustering patterns, *k*-means clustering test, descriptive and basic statistic tests using the Statistica 5.0.

3. Results

3.1. Characteristics of the investigated forensic population

Table 1 shows the total scores of each item comprising the PCL-R for groups GPD, PPD and NM (control) in the investigated population. We see that group GPD presents the highest scores, while group NM has the lowest ones and group PPD obtains intermediate scores. All three groups were significantly different from one another (Kruskal Wallis, $p < 0.001$). However, in relation to the distributions, groups GPD and PPD present strong correlation ($r = 0.88$) with each other, and weak correlation when related to group NM (0.39 and 0.49, respectively).

Table 2 summarizes the descriptive statistic of the population used in the former study [2]: NM or control ($n = 30$), PPD ($n = 23$) and GPD ($n = 33$), and Fig. 1 illustrates the respective box and whisker plots.

3.2. Cluster analysis of the forensic population based on the total scores of their PCL-R

Cluster analysis of the forensic population PCL-R total scores was performed in an unsupervised way using a hierarchic polythetic agglomerative method. We used the Ward's method for dendrogram (or tree diagram) classification method, using single or squared Euclidean distance measures.

Table 2
Descriptive statistic of the forensic group population studied in this paper

Groups	*n*	Mean	Minimum	Maximum	S.D.
GPD	20	43.90	13.00	66.00	15.63
PPD	20	18.75	2.00	45.00	12.96
NM	20	7.90	0.00	34.00	9.80

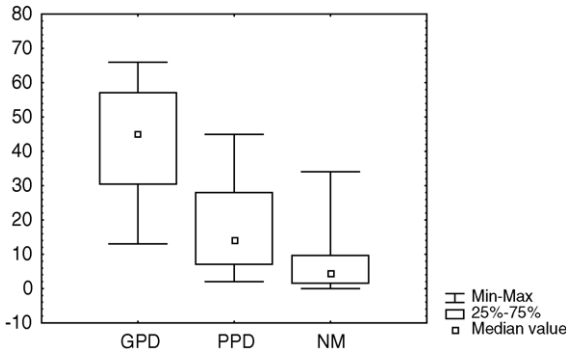

Fig. 1. Box and whisker plots of the forensic group population studied in this paper.

Two different clusters, which we named A and B, were obtained from the forensic population analysis, formed by groups GPD and PPD (Fig. 2). The same clusters were replicated by others methods, showing stability and the addition of the NM group does not modified the result.

The same clusters, A and B, were obtained again when the non-hierarchical *K*-means clustering method was used for testing the significance for two clusters ($k = 2$, $p < 0.0001$).

Cluster A is formed by items 2, 5, 6, 7, 8, 10, 13, 14, 16, most of them (2, 5, 6, 7, 8, 16) belong to Factor 1 of the PCL-R, which assesses dimensional traits of personality [1], and the other three (10, 13 and 14) belong to Factor 2, which assesses trends toward criminal behavior. Cluster B is formed by items 1, 3, 4, 9, 11, 12, 15, 17, 18, 19, 20, most of them (3, 9, 12, 15, 18 and 19) belong to Factor 2 and only two (1, 4) belong to Factor 1, the other three items do not relate to the PCL-R factors (11, 17 and 20).

Cluster A concentrates the highest scores of groups GPD and PPD (Table 2). Table 3 shows the total scores of each group in the clusters, indicating a highly significant difference (Chi-square, $p < 0.0001$) in favor of Cluster A.

Table 3
total scores of groups GPD and PPD in clusters A and B

Groups	Cluster A	Cluster B
GPD	525	353
PPD	282	93

4. Discussion

Morana et al. [2] identified two subtypes of ASPD by using the Rorschach test: GPD and PPD; next, she related them to psychopaths and non-psychopaths identified by PCL-R [1]. Populations GPD, PPD and NM [2] perform differently on PCL-R score. While groups GPD and NM, respectively, reach the highest and lowest scores, group PPD takes an intermediate position, closer to group NM, but with sufficient statistical difference to make up a distinct group (Mann–Whitney test, $p = 0.002$). On the other hand, groups GPD and PPD, despite different in their total scores (Mann–Whitney test, $p < 0.001$) are strongly correlated ($r = 0.88$). Groups GPD and PPD make up two different clusters (100% dissimilar) hence, these can be considered as quantitatively distinct within the ASPD category (to which they identify by correlation).

In relation to PCL-R scores, groups GPD and PPD, assessed either separately or as a group (forensic population) show the presence of two clusters, which we refer to as A and B (Fig. 2). These clusters were stable when the analysis was repeated with other algorithms, as well as independently extracted by the *k*-means method. Cluster A is made up by items 2, 5, 6, 7, 8, 10, 13, 14 and 16, most fitting in PCL-R Factor 1, which evaluates dimensional personality traits. Only three of the items in this cluster (10, 13 and 14) fit Factor 2 (which evaluates criminal behavior trends). This cluster classifies the profile of individuals defined as having a sharp sense of self-importance, manipulative, lacking feelings of remorse or guilt, insensitive, indifferent to others and not taking responsibility for their acts. Their criminal behavior characteristics are: subject to poor

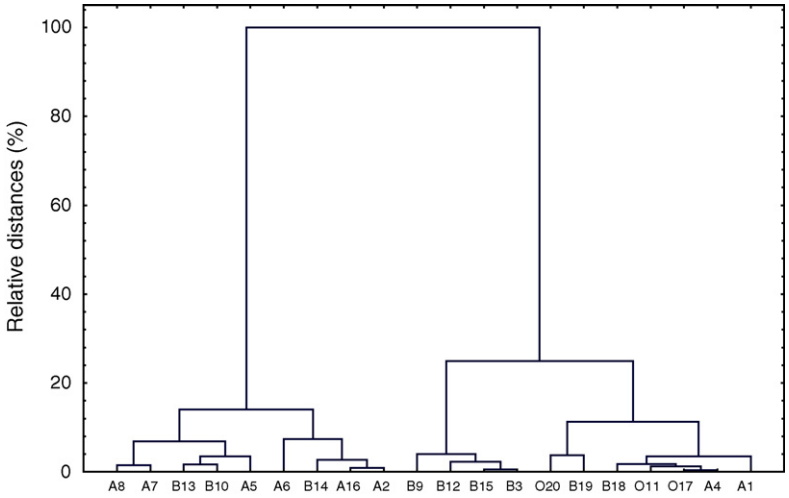

Fig. 2. Clusters A (left branch) and B (right branch) obtained by the Ward's algorithm from the forensic population studied in this paper. The numbers represents the PCL-R items.

behavioral controls, lack of realistic and long term goals and impulsivity. This type is close to the concept of prototypical psychopath as defined by Hare [1]. It is verified that these individuals' affective structure is globally impacted [2]. He is a mischievous type, who acts on impulse and on the spur of the moment, with no planning, and insensitivity and indifference to others are their most severe traits. A corroborating factor is that they present a sole trait not found in the control group, namely, failure to accept responsibility for their own actions. The most prevalent traces were a sharp sense of self-importance, feeling no guilt or accepting no responsibilities for their own actions and impulsiveness. The least prevalent traits were those related to criminal behavior traits and tending to glibness.

Hare [7] subdivides PCL-R Factor 1 into *Interpersonal* Facet and *Affective* Facet. However, of Cluster A presents the four factors from the *affective* facet, such as defined by Hare (insensitivity and affective indifference, and inability to accept responsibility for their own actions and lack of remorse or guilt). Not necessarily will this type perform criminal acts, however, should they do, such acts will be more severe, as personality impairment takes place in the overall integration of psychic processes (global personality disorder) leading to total indifference. Rehabilitation of this type seems unlikely. Traits connected to a strictly typical behavior of criminality are not associated with this type. As a matter of fact, Hare [7], in his latest studies, modifies his original conception of psychopathy as a condition, prevalently linked to criminality. That is, the idea that the author is more recently offering refers to the psychopath as a ''snake in suit'' [7]. He defines this type precisely as evidenced by Cluster A: an insensitive type yet not necessarily bearing a criminal profile, and for this reason, more easily found in corporations, institutions, universities or governmental offices, among other environments [8]. In our analysis, Facet 1 (affective), an essential characteristic of this group, is largely absorbed in Cluster A.

Cluster B is formed by items 1, 3, 4, 9, 11, 12, 15, 17, 18, 19, 20, most of which from Factor 2 (3, 9, 12, 15, 18 and 19), which evaluates anti-social tendencies, as well as the three items not fitting in any of the PCL-R factors (11, 17 and 20). This cluster classifies an unstable, typically criminal profile, characterized by deceitful, with intense need of stimulation, a parasitic life style, promiscuous sexual behavior, unstable marital relations and general irresponsibility toward all people and things. These individuals' criminal lives start early, presenting conduct disorders in childhood and juvenile delinquency. Criminal history is vast, versatile, where escapes and relapsing into crime is likely. This cluster is associated with the descriptions of commonly recurring criminals, frequently found in Brazilian prisons [2] and not meeting Hare's prototypical concept of psychopathy [1].

We believe that Cluster A describes the most prominent traits of the prototypical psychopath. In clinical practice, we have empirically identified subjects presenting prevalence of Cluster A traits as a spurious individual with the most injury factors of insensitivity and indifference. In this sense, traits relating to this personality profile remove psychopaths from a strictly forensic setting, thus Hare's [7] current identification of the type as a ''snake in suit''. Moreover, Hare is designing a new version of PCL-R that allows companies to detect corporate psychopaths before they can do serious damage in the workplace [8]. Babiak [9] and Sherman [10] have yet published some previous studies about this matter. This cluster identifies 9 of the 20 PCL-R items as most essential traits connected to criminal personality and personality structure, according to our analysis. It is possible that, on this assumption, a prototypical psychopath may form a specific cluster within the classification of ASPD, and on the other hand, be identifiable as a category by a reliable test bases, for instance, on the findings of this paper.

Cluster B, in turn, describes the most prominent traits of a typical felon. In clinical practice, it is empirically identified that a subject presenting prevalent trends of Cluster B presents himself as a ''slacker'' whose main objective is to obtain, with no working efforts, power assets and status.

References

[1] R.D. Hare, Manual for the Hare Psychopathy Checklist-Revised, Multi-Health System, Toronto, 1991.
[2] H.C.P. Morana, J. Arboleda-Flórez, F. Portela Câmara, Identifying the cutoff score for the PCL-R scale (psychopathy checklist-revised) in a Brazilian forensic population, Forensic Sci. Int. 147 (1) (2005) 1–8.
[3] D.J. Cooke, C. Michie, Refining the construct of psychopathy: towards a hierarchical model, Psychol. Assess. 13 (2001) 171–188.
[4] A. Silveira, Prova de Rorschach: Elaboração do Psicograma, Edbras, São Paulo, 1985.
[5] L. Coelho, Rorschach Clínico: Manual Básico, Terceira Margem, São Paulo, 2000.
[6] J.E. Exner Jr., A Rorschach Workbook for the Comprehensive System, fourth ed., Rorschach Workshops, Asheville, 1995.
[7] R.D. Hare. Psychopathy and Risk for Recidivism and Violence. Avaliable at http://www.rededor.com.br/cbnu/portugues/publications.php (Publicações, conference paper 2).
[8] R.D. Hare, F. Hugues, M.A. Hervé, Hare, P-SCAN Research Version (Hare P-SCAN) Business Scan 360 test. Multi-Health System, Toronto, Ontario, Canada, 1999.
[9] P. Babiak, Psychopathic manipulation at work, in: C.B. Gacono (Ed.), The Clinical and Forensic Assessment of Psychopathy. A Practitioner's Guide, Lawrence Erlbaum Associates, Publishers, 2000.
[10] C. Sherman, Industrial psychopaths' can thrive in business, Clin. Psychiatry News 28 (5) (2000) 38, © 2000 International Medical News Group. Available URL: http://www.lifepsych.com/linksworkarticle01psychopath.htm.

ELSEVIER

Forensic Science International 164 (2006) 102–109

Forensic Science International

www.elsevier.com/locate/forsciint

Potentiality of 3D laser profilometry to determine the sequence of homogenous crossing lines on questioned documents

Giuseppe Schirripa Spagnolo *

Dipartimento di Ingegneria Elettronica, Università degli Studi "Roma Tre", Via Della Vasca Navale 84, I-00146 Roma, Italy

Received 19 July 2005; received in revised form 30 November 2005; accepted 5 December 2005
Available online 20 January 2006

Abstract

The determination of the sequence of line crossings is still a current problem in the field of forensic documents examination. Optical examination, lifting technique, ESDA technique, and electron microscopy are the most widely used methods for the determination of the writing order of crossing texts. However, at present many examinations of intersecting lines result in an inconclusive opinion, particularly if the same type and colour of ink is involved. This paper presents the potentiality of the 3D laser profilometry, which has been to determine the chronological sequence of homogenous ''crossing lines''. The laser profilometry, illustrated in this paper, has been developed on a conoscopic holography based system. It is a non-contact three-dimensional measuring system that allows producing holograms, even with incoherent light, with fringe periods that can be measured precisely to determine the exact distance to the point measured. This technique is suitable to obtain a 3D micro-topography with high resolution also on surfaces with unevenness reflectivity (usual for the paper surface). The proposed technique is able to obtained 3D profile in non-invading way. Therefore, the original draft are not physically or chemically modified, allowing a multi-analysis in different times. The experiments performed with line crossings database show that the proposed method is able of ''positive identification'' of writing sequence in the majority of the tests. In absence of a positive identification, the result has been ''inconclusive'' (no false determination did occur in this work).

Keywords: Forensics; Questioned documents; 3D laser profilometry; Topography; Crossing line; Determination of writing sequence

1. Introduction

Even with the advent of electronic communication, electronic signatures and a whole array of electronic business transactions, the paper based document remains widely used and trusted for any business and legal documents. Besides, the problem of forgery remains an ever present problem and is still of great interest in forensic science. There are occasions when documents used in criminal activities or in the course of civil litigation are either altered or created specifically for the purpose of deception.

A difficult problem in questioned document examination is the determination of the order of crossed line.

The determination of the order of crossing lines is appropriate in cases of suspicions that the content of a document has been altered at a later date by adding a part to it, for instance in a will or signed legal agreement (blank signature). Therefore, the determination of sequence of crossing strokes [1–3] can provide important information when investigating fraud.

A variety of techniques can be employed to view an intersection. Optical examination, lifting technique, ESDA technique, and electron microscopy are the most widely used methods for the determination of the writing order of crossing texts. Unfortunately, many examinations of intersecting lines result in an inconclusive opinion, particularly when two inks are similar in colour and composed of the same type of ink. For these reasons, one of the most appealing challengers for questioned document examiners is the improvement of techniques, which can be used for determination of sequence of lines of homogenous intersection (crossing lines made by the same type of ink or media).

Handwriting on a common paper sheet allows to observe how, the pen-tip, besides releasing the ink, deforms the paper. In other words, the writing pressure leaves some impressions; several or less deep ones according to:

* Tel.: +39 06 55177046
E-mail address: schirrip@uniroma3.it.

0379-0738/$ – see front matter
doi:10.1016/j.forsciint.2005.12.004

- writing pressure (amount of pressure exerted on the point of a pen during the act of writing);
- underlying material (sheet of paper lying on a metal surface or on a paper block);
- writing material (fountain, pencil, ball point pen interact in different way with the paper);
- type of paper used (the production process determines the size and the morphology of the layers of fibers in the paper).

Therefore, a three-dimensional analysis of handwriting gives information on stroke sequence and on the pressure applied to the paper during writing, so as pen-up (stroke end vertex) and pen-down (stroke start vertex). The process of writing on a common paper sheet is similar to the writing on the sand (the paper sheet, for the writing, behaves as plastic material).

In Fig. 1 we see two eight drawn on the sand. The writing dynamics of two different 'eight' symbols is evident. The second stroke, when crosses the first stroke, modifies the produced groove in the sand according to the object used for the writing. In particular, it is possible to note the presence of some 'bumps' along the first stroke. These bumps are located at the sides of the second stroke that crosses the first one. The presence of these irregularities is localized in the strokes' crossing zone, along the first stroke line.

In this paper, we propose the use of the 3D laser profilometry, realized by means of the conoscopic holography, to transform seemingly flat handwritten letters into landscapes of hills and valleys that reveal the pressure and stroke sequence used to create each word documents. Conoscopic holography is a non-contact three-dimensional measuring technique that makes possible to produce holograms, even with incoherent light, with fringe periods that can be measured precisely to determine the exact distance to the point measured. It is suitable to obtain 3D micro-topography with high resolution also on surface with unevenness reflectivity (this situation is usual on the surface of the handwritten document). The technique is able to obtained 3D profile in non-invading way. Therefore, the system leaves the investigated surface unaltered so that the questioned document can be studied by means of other destructive or non-destructive technique in different time, also in case of forensic analysis with the necessity to preserve the original sample.

The determination of the 3D micro-topography, in the field of forensic document examination, can be obtained using the scanning electron microscope (SEM) [4,5] or atomic force microscopy [6]. SEM and AFM are promising 3D-techniques, but have a limited range in the vertical direction ($\sim$5 μm) and in the scanning area ($<$2 cm^2); while by means of laser profilometry a 3D micro-topography overcoming the limits imposed by the use of the techniques SEM and AFM is possible. In fact, with the laser profilometry technique non-destructive examination of ''wide'' zones of documents can be made.

The 3D laser profilometry has been introduced, as a useful tool for the examination of crossing lines, in Refs. [3,7]. The aim of this paper is to study the potentiality of this method and, despite of complicating inhomogeneous structure of the paper and the writing impression, determine the writing sequence when the inks are chemically and optically mixed at the crossings (homogenous crossing lines).

This paper is organized as follows: in Section 2, the conoscopic holography and used conoscopic range finder are briefly described. In Section 3, the proposed method is described and the experimental results are presented. The conclusions are presented in Section 4.

2. Conoscopic holography and conoscopic range finder

A conoscopic range finder (based on conoscopic holography) is well suited to provide an accurate 3D profile of handwritten documents. At present, cheap conoscopic systems, well adapted to work in the field, are available.

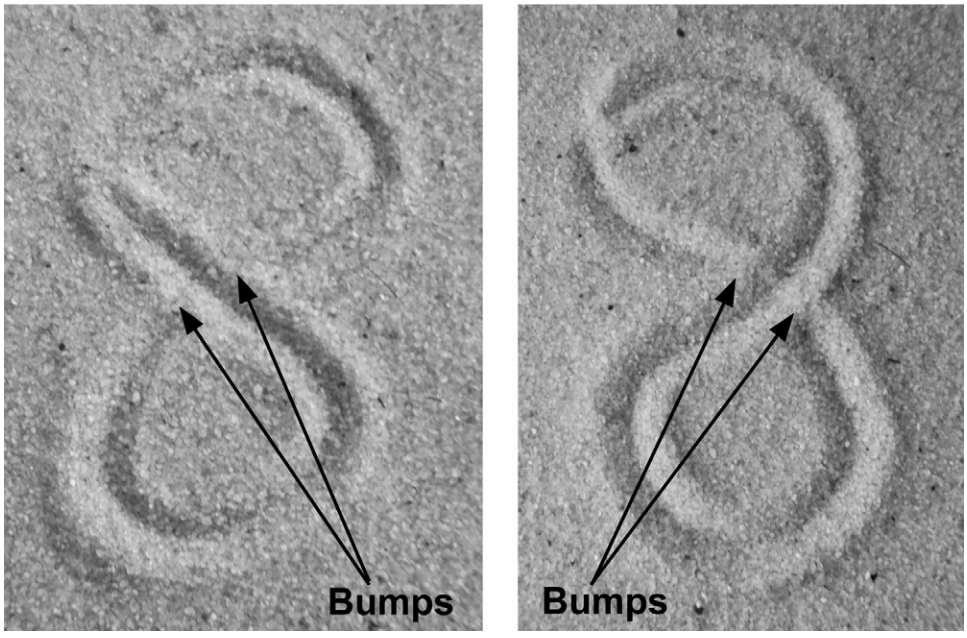

Fig. 1. Eight drawn, with different dynamics, on the sand.

Conoscopic holography has already been described in depth many times [7–9], here we present only what is necessary to understand the following discussion.

Based on crystal optics, conoscopic holography is a simple implementation of a particular type of polarized light interference process. In the basic interference set-up, a light beam is projected on a diffusive object. The reflected beam creates a light point source, which is dispersed in all directions. A complete solid angle of the diffuse light is analyzed with the conoscopic optical system. The measurement process corresponds to the retrieval of the distance of illuminated point from a fixed reference plane.

In order to obtain a better understanding of the system functionality the behavior of a single ray needs to be comprehended.

A single ray, emitted by light point source at a given angle is polarized using a polarizer.

This wave polarized at 45° to the principal axes of the crystal is incident on it (see Fig. 2). The wave is separated into two polarization components. In a uniaxial crystal the two polarized waves propagate at different velocities. The velocity of one ray is isotropic and it is designated as an ordinary ray, while the other one has an anisotropic velocity, i.e. it is designated as an extraordinary ray. Thus, two super-imposed rays emerge from the crystal with a phase difference and with orthogonal polarizations to each other. In order to obtain interference between these two rays, an analyzer (polarizer) is inserted at the point for which the rays emerge from the crystal.

For a complete solid angle, each emerging ray will have a different phase difference between the ordinary and extraordinary rays. At a given plane, the collections of all the rays will create an intensity figure—the conoscopic image. This image can be recorded by means of CCD array or matrix. The parameters of conoscopic image will depend on the angular distribution of the rays inside the crystal. The latter depends on the position of the point in space. Recording and analyzing the image, one is capable of retrieving the distance of the illuminated point from a fixed reference plane. An important point is that each detector of the CCD carries out an independent measure. Conoscopy is, in principle, a triangulation method of distance measurement duplicated many times. In particular, a standard triangulation system measures the angle of a single ray, while the conoscopic system measures the angle of each ray in a complete solid angle. Therefore, conoscopic procedure is much more precise, stable and robust, but requires more computations.

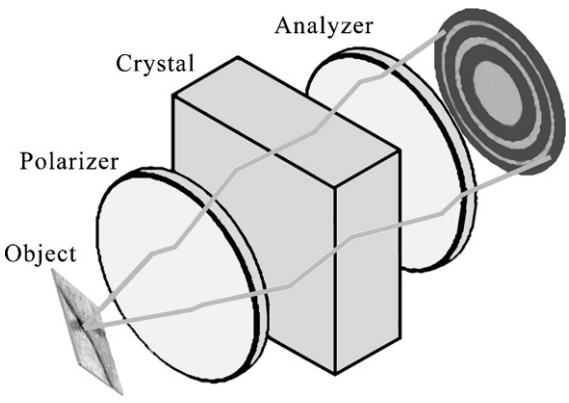

Fig. 2. Conoscopic principle.

Conoscopic range finder offer specific benefit:

- Simplicity in the set-up. This makes simple the procedure of measure.
- Much greater stability than classical interferometer because the geometrical paths of both split wavefronts are almost the same. The system is able to work outside laboratory (it is possible to work in field, in other words where the questioned document is kept).
- By switching the polarization axis of one polarizer (see Fig. 2), two complementary holograms of the same point can be obtained. Indeed, we will calculate the ratio between the difference and the sum of both interferograms ('contrast' calculation). Most of the intensity inhomogeneities (optical noise) can be in this way eliminated. So the conoscopic probe measurements are independent from intensity modulation induced by the object albedo and surface with unevenness reflectivity (which is usual on the surface of the handwritten document).
- Large range in vertical direction is possible.
- Collinearity and minimal aperture. The conoscopic techniques need a minimal angular aperture to recover the wavefront curvature and they can work in an on-axis configuration with respect to the projected laser beam. Therefore, measuring is also possible inside holes or cutting. This characteristic is very important when there is the interest to reconstruct the 3D micro-topography 3D micro-topography of crossing line with high resolution. In fact, only with a collinear measurement system it is possible to reconstruct all the characteristics present in the crossing zone.

All this characteristics make conoscopic holography well suited to reconstructing the 3D micro-topography of handwritten documents. As far as we know, for application on questioned document, no commercial micro-profiling equipment with potentiality of the conoscopic holography is available.

Our system (Optimet MiniConoscan 3000) has vertical resolution and the dynamical range of 0.2 and 2000 μm, respectively. The system used in this work is in the fix-probe configuration. The fix-probe configuration consists of keeping the conoscopic probe fixed and placing the questioned document to be analyzed on a translation-table. The maximum dislocation of the translation-table is 12 cm with a position accuracy of 1 μm/10 mm. The documents are resting on a support made of porous copper. By evacuating the air through the microscopic holes in this material, the position of the document remains unaltered throughout the measurement.

3. Three-dimensional analysis of handwritten documents

The conoscopic range finder determines the micro-topography of the examined surface. The resulting 3D profile shows the pen-tip strokes as an impression in the paper.

A typical handwritten document surface profile consists of roughness, pen-tip strokes (waviness) and form (in many cases the paper sheet may also contain significant form such as deformations) [10]. It is important to notice that:

- The paper roughness range is, usually, 2–8 μm. It depends on the type of paper used [11,12].
- The pen-tip strokes depth range is between 2 and 50 μm. This is the range of depth analyzed, with our conoscopic range finder, in our tests. The range of variability depends on writing pressure and used material.
- The deformations of paper sheets, present mainly when we use soft underlying support and when the paper is in no good condition (e.g. sheet humidified or rubbed), can be also 100 times greater than the pen-tip stroke impression.

Fig. 3a shows 3D view of raw data from the analysis of handwritten symbol "€".

This raw data contain information on pen-tip strokes, paper roughness and paper deformation. So, after the acquisition of the data, 3D image processing and filtering are necessary to obtain a surface model that can be used to identify the stroke that describes the handwriting [13].

The first step is to identify and eliminate the paper deformation by means of suitable 3D filter. The handwriting of a word or symbol cause the incision of the sheet, besides, it causes a global deformation on the sheet. Fig. 3b shows the global deformation drawn out by means of "3D form removal" techniques. The 3D view of the symbol "€", after the operation of "form removal", is shown in Fig. 3c. The filtered data is then passed through a new elaboration to separate the roughness and waviness components of the surface. Fig. 3d shows the roughness component present on the paper sheet. The pen-tip strokes (waviness) impression is shown in Fig. 3e. Finally, 3D view of the pen-tip strokes, with a mirror along the z-axis, is shown in Fig. 3f.

Observing the reconstructed 3D image, strokes appear like furrows, but for recognizing the crossing dynamics the observer needs to pay attention to some particular characteristics. A first activity to perform is to verify the presence of some 'bumps', irregularities in the grooves produced in the paper by the pen-tip used for the writing. These bumps are located at the sides of the second stroke that crosses the first one. The presence of these irregularities is localized in the strokes' crossing zone, along the first handwritten stroke line, and they have to stand out against the paper depression created by the double pen passage. The strokes' and bumps' visibility depend both on the kind of paper and used per.

However, when we are in presence of homogenous intersection with lines effected with similar writing pressure

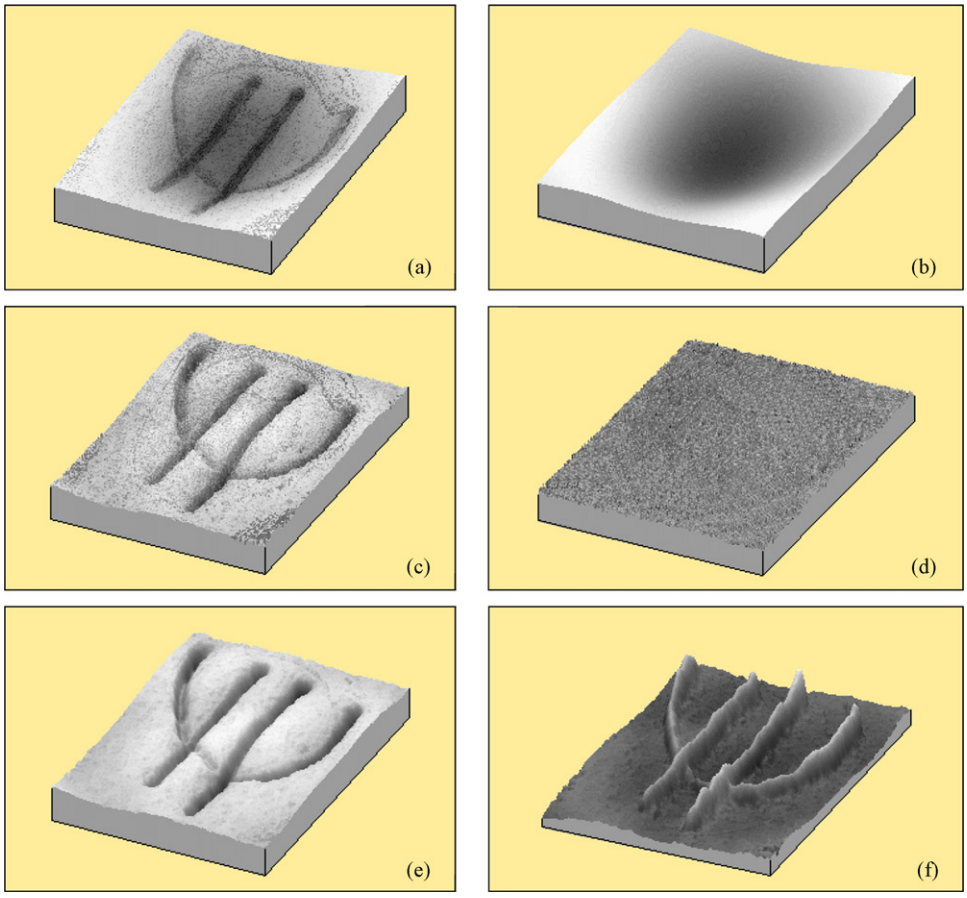

Fig. 3. 3D image processing for separation of roughness, waviness and form in a handwritten document. (a) 3D original data; (b) 3D form—deformation of sheet; (c) 3D profile of the euro symbol, after the operation "form removal"; (d) paper roughness; (e) pen-tip strokes–waviness; (f) 3D view of the pen-tip strokes with a mirror along the z-axis.

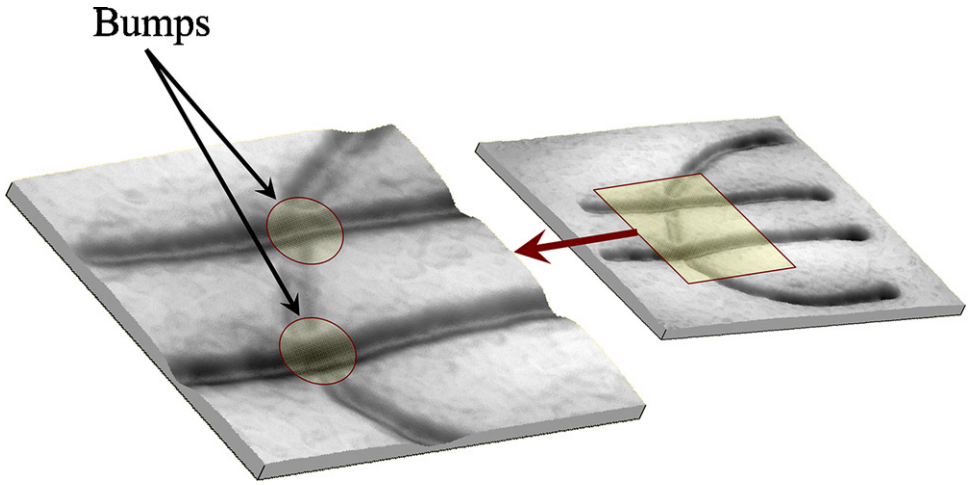

Fig. 4. 3D view of the strokes' profile. It is possible to note the regularity in the horizontal lines. The presence of bumps is evident.

and when indented impression of stroke is one or two times the roughness, the bumps are always present and evident.

Fig. 4 shows a typical example of analysis. This example was realized using a common black ballpoint pen on 80 g/m^2 white paper commonly used for printing and photocopying. It clearly shows that the horizontal lines, of symbol "€", were made after curvilinear stroke. Therefore, the shapes are continuous, whereas curvilinear stroke is interrupted. As can be noted, a characteristic of the second stroke is that it 'cuts' the first one. Using this assertion it is easier to reconstruct the crossing dynamic.

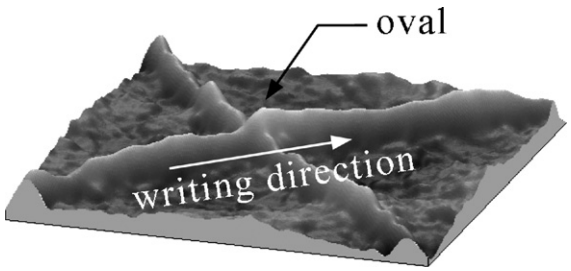

Fig. 5. 3D view, with a mirror along the z-axis, of crossing zone of two pen-tip strokes. In this image, it is possible to note the presence of an "oval".

Fig. 5 shows 3D view an other example of analysis. It shows 3D view of a crossing zone of two strokes, with a mirror along the z-axis. In Fig. 5, we note the presence of an "oval" structure, with its longitudinal axis in the direction of second line, where the two strokes are really crossed.

The oval structure is due to the additional impression left by the last written line leaves in the existing groove of the first pen stroke. Moreover, when the second line is less indented in comparison with the first, this "oval" is deformed along the writing direction of the second line. When the pen-tip arrives at the zone of crossing, where the first line is present, it downs within the groove already clear. Successively it goes up again smoothing the first groove (see Fig. 6). Therefore, from the

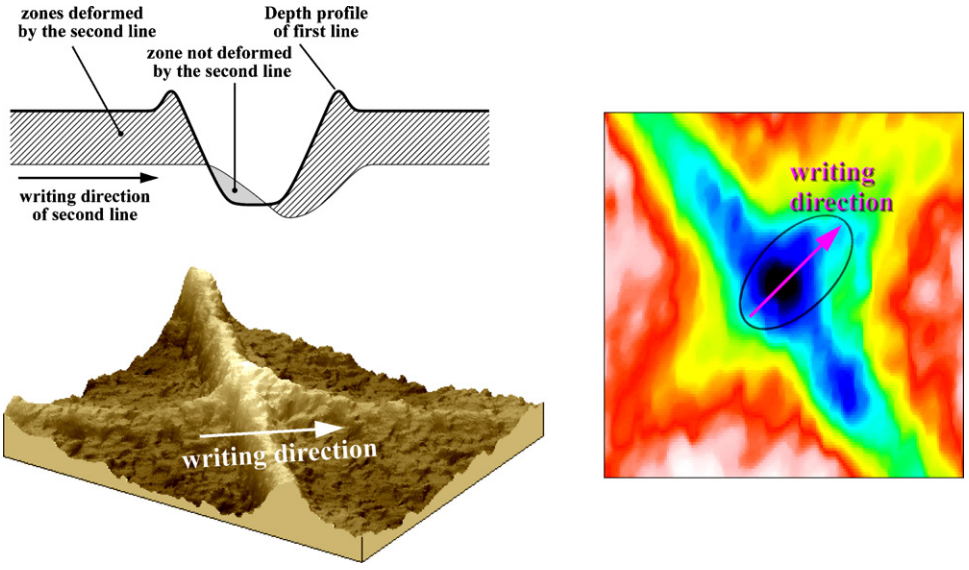

Fig. 6. Deformation of the "oval" in the direction of writing.

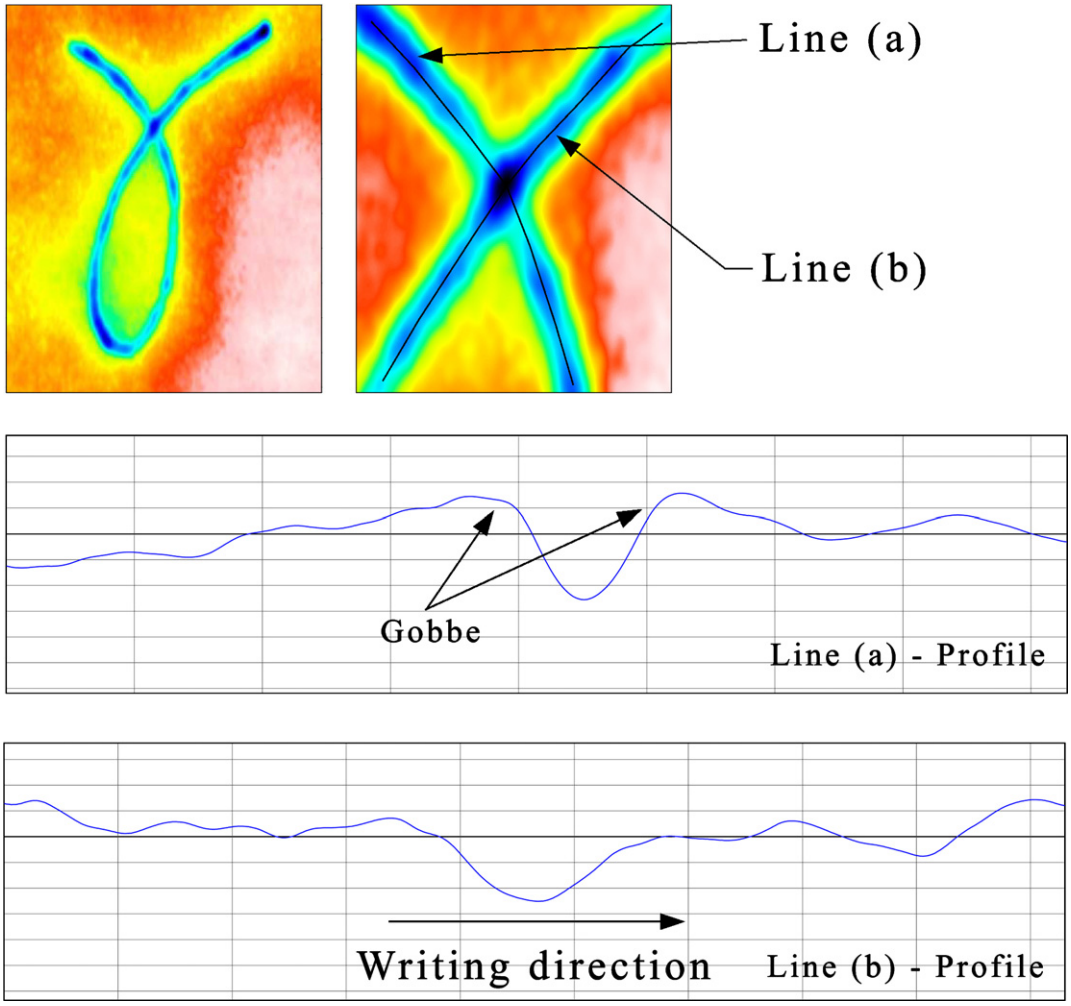

Fig. 7. Profilometry along the lines of writing.

analysis of the ‘‘oval’’ structure it is possible, at any time, to go back to the direction used for tracing the second stroke. The analysis of the direction of writing can be effected, with more effectiveness, by means of profilometry along the handwritten lines. Fig. 7 shows this type of analysis made on the geek ‘‘gamma’’.

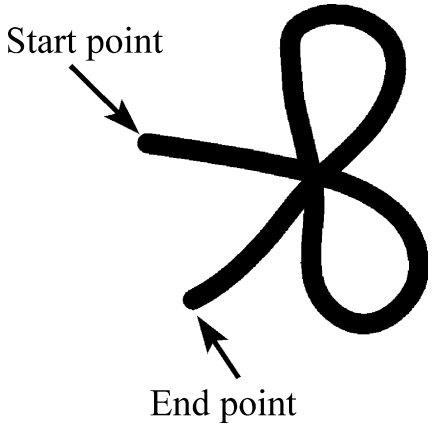

Fig. 8. Scrip with more two lines intersecting.

Analyzing Fig. 7 it is possible to note that along the firth line are present two ‘‘evident’’ bumps. The presence of these bumps, in the profile along the line (a), assures that this line is what we have traced for first. The presence of these bumps, in our example, assures that the line (a) is what has been traced for first. The profile along the line (b) shows an interesting characteristic. The pen-tip ‘‘falls’’ in the furrow (impression) done by the first line. This fallen deforms, even, the paper (increases the impression in the cross point). Subsequently, the peak of the pen, going up from the hole, smoothes the slant. The side of the profilometry that shows a softer profile indicates the writing direction.

Our method is also able to resolve complex stroke sequence. Fig. 8 shows a handwritten script with more than two lines intersecting. The 3D view, relating to this script is shown in Fig. 9. It is possible to see that, even in this case, the correct sequence of drawing order is recovered.

Our method allows to analyze cross lines marked with different pressure. In Fig. 10, we show an analysis done on the geek ‘‘gamma’’ handwritten with a non-constant pressure (the first part has high writing pressure, instead the second part has low pressure). The example shows crossing lines with the first written line more marked compared to the second. Analyzing

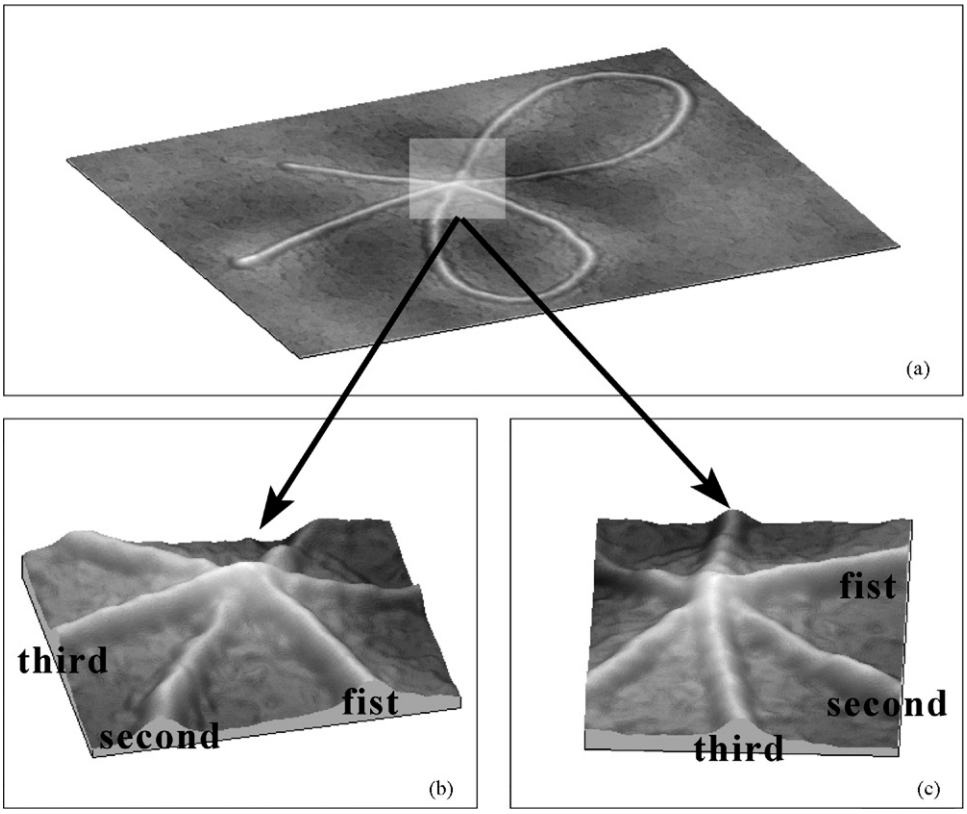

Fig. 9. 3D view of script with more two lines intersecting. (a) The micro-topography of the symbol. (b and c) The 3D reconstruction of the intersection from two different geometrical points of view.

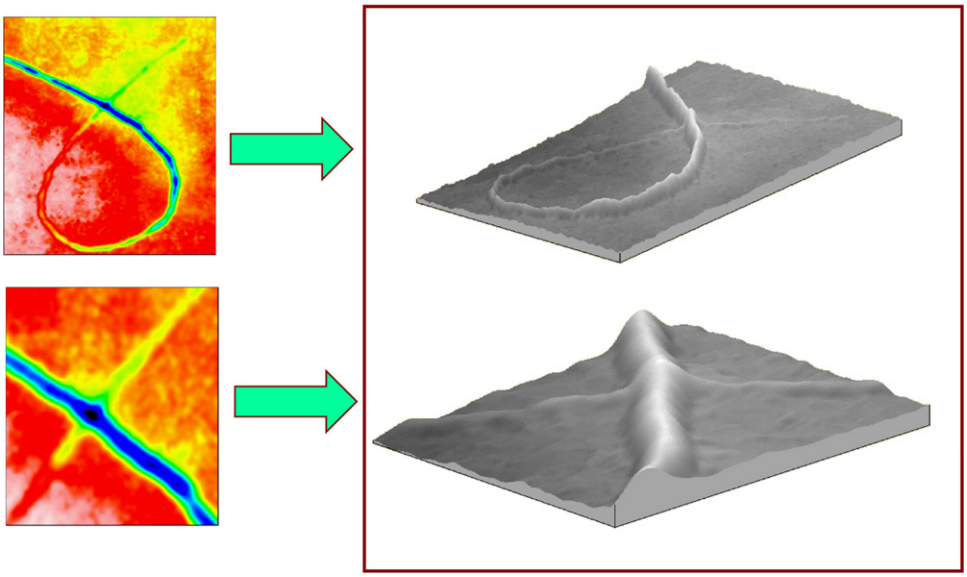

Fig. 10. "Crossing lines" problem of intersection when the lines have very different depth profile.

Fig. 10, the possibility to determine the writing sequence in unambiguous way is evident. Also in this case the second line changes the morphology of the first stroke. It is possible to note a second impression over the deformation caused by the first line.

To confirm the potentiality of the proposed technique, to detect the dynamics of the strokes' superposition, we have used 120 homogeneous intersections made by 120 different persons of different age. Every single intersection has been done using the same pen. We have used six different types of pen, two different types of paper (80 and 120 g/m^2 white paper commonly used for printing and photocopying) and two different underlying supports. On one hand, the strokes were

Table 1
Synthesis of results obtained for each kind of pen

Category of pen	Positive identification (correct classification) (%)	Inconclusive (%)	Number of experiments
BIC pen	98	2	45
Ballpoint pen with fine point	90	10	10
Fountain pen	45	55	15
Liquid ink pen	65	35	20
Felt pen	35	65	20
Felt pen with fine point	75	25	10

made on a ''soft'' underground consisting of pile of 0.3 cm of 80 g/m^2 paper; on one hand, the strokes were made on a ''hard'' underground consisting of metal plate. In particular, we have realized five samples for every single combination pen-paper-support. The five different intersections have been carried out using the symbols: €, +, ×, γ, and α. In this way we have simulate homogeneous intersection made in different direction. Subsequently, the sample data has been tested, with our method, in blind way, by two different persons independently. The two scientists have achieved similar results. These results are reported, in a synthetic way, in Table 1.

From the results reported in the table, is possible to notice that under no circumstance a false determinations has been effected. Besides, it is possible to notice that the cases of inconclusiveness relate to a depth profile.

Generally, by means of the tests effected it is possible to conclude that if the profile, left by the writing media, is at least two times the mean roughness of the paper, the determination is possible with success.

4. Conclusion

In this paper, we have presented the potentiality of the 3D micro-topography to study the sequence of homogenous crossing lines on questioned documents. The method is applicable where the questioned document is an original and contains a crossing between two media that will allow the determination of the sequence of introduction onto the paper. In this work, 3D micro-topography is obtained by means of conoscopic holography, which has same advantages over other 3D profile techniques. In particular, greater stability; large range of measure in vertical direction; ''wide'' zones of documents can be analyzed; measurements are independent from intensity modulation induced by the object unevenness reflectivity.

The method works well and it allows, in most of the cases, to recover correct stroke sequenced of a handwritten script. Besides, the method is able of analyzing the pressure variations used during the writing. The main potentiality over the ''traditional'' methods and is that it allows to determine, with success, the sequence intersection made by two mixed inks of similar colour (e.g. when the inks are chemically and optically mixed at the crossings).

The principal limit is the inability to analyze intersection if the profile, left by the writing media, is similar to the mean roughness of the paper. Other limit is the time consumed to acquire data. For this reason, it is essential to carry out studies for the improvement of the used hardware.

References

[1] G. Poulin, Establishing the sequence of strokes: the state of the art, Int. J. Forensic Doc. Examiners 2 (1996) 16–32.
[2] D. Ellen, The Scientific Examination of Documents, Methods and Techniques, second ed., Taylor & Francis, London, 1997.
[3] V. Berx, J. De Kinder, A 3D view on the 'crossing lines' problem in document investigation, Proc. SPIE 4709 (2002) 102–110.
[4] P.A. Waeschle, Examination of line crossing by scanning electron microscopy, J. Forensic Sci. 24 (1979) 569–578.
[5] S. Tollkamp, H.G. Fackler, Use of low voltage SEM in the detection of forgeries, Int. J. Forensic Doc. Examiners 2 (1996) 333–341.
[6] S. Kasas, A. Khanmy-Vital, G. Dietler, Examination of line crossings by atomic force microscopy, Forensic Sci. Int. 119 (2001) 290–298.
[7] G. Schirripa Spagnolo, C. Simonetti, L. Cozzella, Superposed strokes analysis by conoscopic holography as an aid for a handwriting expert, J. Opt. A: Pure Appl. Opt. 6 (2004) 869–874.
[8] G.Y. Sirat, Conoscopic holography. I. Basic principles and physical basis; II. Rigorous derivation, J. Opt. Soc. A 9 (1992) 70–90.
[9] Y. Malet, G.Y. Sirat, Conoscopic holography application: multipurpose rangefinders, J. Opt. 29 (1998) 183–187.
[10] ANSI B46.1, Surface Texture (Surface Roughness Waviness and Lay), The American Society of Mechanical Engineer, 2002.
[11] T.E. Conners, S. Banerjee, Surface Analysis of Paper, CRC Press, 1995.
[12] Tappi Press, Tappi Test Methods: 2002–2003, Tappi Press, Atlanta, GA, USA, 2002.
[13] J. Raja, B. Muralikrishnan, Fu. Shengyu, Recent advances in separation of roughness, waviness and form, Precis. Eng. J. Int. Soc. Precis. Eng. Nanotechnol. 26 (2002) 222–235.

ELSEVIER

Forensic Science International 164 (2006) 110–115

Forensic Science International

www.elsevier.com/locate/forsciint

Adolescent homicides in Finland: Offence and offender characteristics

Camilla Hagelstam [a,1], Helinä Häkkänen [a,b,1,*]

[a] Department of Psychology, Criminal and Forensic Psychology Research Group, University of Helsinki, Finland
[b] National Bureau of Investigation, Criminal Intelligence Division, Jokiniemenkuja 4, P.O. Box 285, FIN-01301 Vantaa, Finland

Received 15 June 2005; received in revised form 8 November 2005; accepted 6 December 2005
Available online 19 January 2006

Abstract

Approximately 9% of the homicides in Finland are committed by adolescents under 20 years of age. The purpose of this study was to investigate the offence and offender characteristics in homicidal adolescents. Forensic psychiatric evaluation statements of adolescent offenders accused of a homicide during 1990–2001 were reviewed retrospectively ($n = 57$). In 38% of the cases, there were multiple offenders. In 58% of the cases, the victim was an acquaintance, in 25% a stranger, in 12% a family member and in 5% of the cases an (ex)intimate partner. Sixty-nine percent of the offenders were intoxicated and 21% under the influence of drugs at the time of the killing. The most frequent motives were an argument (25%) and a robbery (25%). Sixty-four percent of the offenders had developmental problems and 42% had a crime history. Approximately half were diagnosed as having a conduct or a personality disorder, but 32% of the offenders were considered not to suffer from a mental illness or substance abuse. For 63%, the level of intellectual functioning was average or above average. There were signs of more than one form of violence in 54% of the cases and 28% of the cases contained excessive violence. The use of multiple and excessive violence was significantly related to the offender age, multiple offenders, offender–victim relationship and substance abuse, but not related to having developmental problems, crime history or mental illness.

Keywords: Homicide; Adolescence; Motive; Excessive violence

1. Introduction

In Finland, the rates of homicides per capita have for decades been about double the rate of the most of the other West European democracies and triple the rate of the other Nordic countries [1,2]. Annually, approximately 9% of all homicides are committed by adolescents under 20 years of age [3]. In 1999–2001, however, the number of homicidal adolescents per year nearly doubled compared to previous years [3]. This led to a sensational reporting of the Finnish commercial media.

The research literature on homicidal adolescents is substantial (e.g. [4–7]). For example, previous research has identified three distinct groups of adolescent murderers: clearly psychotic subjects, subjects engaged in severe interpersonal conflict and subjects committing homicides in the course of another crime [8]. In addition, it has been suggested that there are certain characteristics distinguishing homicidal adolescents from non-violent delinquents: criminally violent family members, gang participation, alcohol abuse and severe educational difficulties [9,10], as well as neuropsychiatric impairment, abuse history and extensive aggressive history [11,12]. Within the psychodynamic approach, it has been addressed, e.g. that violence among homicidal adolescents is egosyntonic and that the offenders have an extreme capacity to dehumanise others [13,14].

Several studies focusing on the sociocultural factors seem to agree that a marked psychopathology, in terms of severe physical abuse [11], sexual abuse [12], exposure to extreme violence [15] and parental mental illness [16] exist in the families of homicidal adolescents [7,17], although contradictory results have also been presented [18]. Studies focusing on the psychopathology have suggested that both conduct disorder and personality disorder, often overlapping with substance abuse, are common diagnoses among adolescent killers (e.g. [19,20]) with associated learning difficulties [9,21]. However, previous research results regarding the level of intellectual functioning are controversial; homicidal adolescents have been found to be both above-average and below-average (e.g. [22–24]). Also, previous research results regarding the incidence of psychosis are mixed (e.g. [10,11,16,19,24–26]).

According to previous research, adolescent homicide offenders have often engaged in other criminal activity prior

* Corresponding author. Tel.: +358 9838 8661.
E-mail address: helina.hakkanen@krp.poliisi.fi (H. Häkkänen).
[1] Both authors contributed equally.

0379-0738/$ – see front matter
doi:10.1016/j.forsciint.2005.12.006

to the homicide [9,10], and occasionally extreme violence during childhood has been reported [12]. Approximately, 45–70% of the offenders are intoxicated at the time of the killing [10,12] and substance abuse is common [20,28].

In summary, the research literature has recognized the clinical diversity of homicidal adolescents, but is often American origin and generally limited to case-reports or small groups of cases referred to psychiatric services. Previous research has rarely focused on non-clinical samples or on the nature of the offences. It would seem useful for investigative, legal and treatment purposes, if it was possible to identify offender related factors associated with the nature of adolescent homicidal violence. For example, a previous study suggests that the degree of violence used in adolescent homicides is excessive [28], but other offence characteristics have been very little examined. To understand these crimes better, an examination of the crime scene behaviors and offender characteristics on homicidal adolescents was undertaken. The present study is part of a series of studies on homicides in Finland [29–31].

2. Methods and material

Information concerning homicides was obtained from the Finnish National Authority of Medicolegal Affairs (NAMA) organising forensic psychiatric evaluations. In Finland, roughly 90% of homicide cases are solved by the police, and a large proportion of homicide offenders go through a forensic psychiatric evaluation as a part of the trial procedure [32]. According to the Finnish law, courts decide if a forensic psychiatric evaluation should be conducted. Both the prosecutor and the defence are allowed to request for the evaluation. After deciding on the evaluation, the court asks the NAMA to arrange it. Forensic psychiatric evaluations include data gathered from various sources (family members, relatives, medical and criminal records, school and military), psychiatric evaluation, standardised psychological tests, interviews by a social worker and a psychologist, evaluation of the offender's physical condition and observation of the offender by the hospital staff. The overall quality and reliability of Finnish forensic psychiatric evaluations is considered high by both courts and scientists [33].

The NAMAs' archives were searched for all homicide cases for the period from 1990 to 2001. Cases where the homicide was conducted while the offender was 18 years old or younger were identified and collected for data analysis. The minimum age of criminal liability in Finland is 15 years: therefore the sample consists of offenders between 15 and 18 years of age. The Finnish police computerized Criminal Index File was searched for additional information on the selected cases. The Criminal Index File includes both quantitative data (e.g. the age and sex of the victim and the offender) and an open-ended narrative appendix. All cases were retrospectively analysed for the offender–victim relation and several variables regarding the offence and offender characteristics. The list of variables was created based on the information derived from the forensic examination statements and earlier studies on similar issues [29–31,34]. The relation between victim and offender was divided into the following groups: family member, (ex)intimate, acquaintance, stranger and other. A case was referred to the 'acquainted' group, if the parties knew each other at least by name or by sight and the 'stranger' group if they did not know each other at all. The interrater reliability of the variables has been assessed in our previous study, where the similar data collection procedure was used [29,31]. The NAMA and the Ministry of Interior approved the study.

3. Results

There were altogether 57 adolescent offenders accused of homicide and subject to forensic psychiatric evaluation during the 11-year period. It was not possible to estimate the representative of the whole sample by comparing the number of offenders in the present sample to the number of overall adolescent homicide offenders (the Statistics Finland clusters offenders into the following age groups: $\leq$14 years, 15–17 years and 18–20 years). However, the number of 15–17-year-old offenders corresponded to 60% of all 15–17-year-old offenders suspected of a homicide within the time period [35].

There were altogether 50 homicide cases with 55 victims in the sample. There were multiple victims in four cases: three offenders killed two victims and one offender killed three victims. In 38% of the cases, there were multiple offenders: in 14 cases two offenders, in two cases three offenders and in three cases four offenders.

3.1. Age and gender

The mean age of victims (information known for 37 victims) was 36.11 years (range 10–79, S.D. = 19.46 years). Adult victims (66%) outnumbered child or adolescent victims (<18 years, 22%), and elderly victims (>65 years, 12%). Thirty-four percent of the victims (n = 13) were female. The mean age for offenders was 17.05 years (range 15–18, S.D. = 0.97). Of the offenders, 9% (n = 5) were 15 years old, 18% (n = 10) were 16 years old, 33% (n = 19) were 17 years old and 40% (n = 23) were 18 years old at the time of the killing. Three offenders were females. Offender and victim age did not correlate at a significant level.

3.2. Offender–victim relationship and circumstances

In 58% of the cases, the victim was an acquaintance, in 25% a stranger, in 12% a family member and in 5% of the cases an (ex)intimate partner. Half of the female victims were acquaintances, the rest distributed uniformly across other groups. According to the records, 69% of the offenders were intoxicated at the time of the offence, and 21% were under the influence of drugs (no consistent information concerning drug and alcohol levels in blood was available as the records usually do not include additional information on the level of intoxication). There were several motives for the killings: in 25% of the cases, the motive was specified as an argument, in 25% a robbery and in 12% a family conflict. In 39% of the

cases, the motive could not be specified (e.g. the offender claimed for memory loss, accident, mental disorder or denied his/her involvement in the killing). The motive was significantly related to the number of offenders. In cases with a robbery motive, there were more frequently multiple offenders (78% versus 29% in others, $\chi^2 = 7.371$, $p < 0.05$, Fisher's).

3.3. Crime scene and additional violence

In 88% of the cases, the victim(s) was/were found at the scene of the killing. In 54% of the cases, the body was found in an apartment, and in 40% outdoors. None of the bodies of the victims who were family members or (ex)intimate partners were found outdoors. In contrast, 36% of the acquaintance and 83% of the stranger victims' bodies were found outdoors. In 12% of the cases, the body had been moved and in 14% of the cases, it was (partly) covered or placed inside a bag when found. In 27% of the cases, something was stolen from the scene or the victim (in none of these cases the victim was an intimate partner or a family member).

In 54% of the cases, there were signs of more than one form of violence. Table 1 presents the distribution regarding the form of violence. The most frequent form of violence was stabbing, followed by stabbing and hitting and kicking.

Use of multiple forms of violence was most frequent when the victim was a stranger (71%), followed by an acquaintance (61%), family member (43%) and (ex)intimate partner (33%). In addition, it was more frequent when the case involved multiple offenders (68% versus 54%, $\chi^2 = 2.566$, $p < 0.11$), although the difference only approached a significant level. Further, the use of multiple form of violence was significantly related to offender age. In all, 87% of the 15–16-year-old offenders used multiple forms of violence compared to 50% of the 17–18-year-old offenders ($\chi^2 = 6.174$, $p < 0.01$, Fisher's). Victims' gender did not have a significant effect.

Sadistic features and desecration of the body were rare. None of the cases involved burning the victim, using a gag, or penetration with an object. In three cases, the victim's body was mutilated. Altogether four cases, which all involved acquaintance victims, were classified as having a sexual or sadistic feature. One of these cases involved urinating on the victim and necrophilia, one case urinating and binding the victim, one case vaginal penetration and necrophilia and one case vaginal penetration. In three of these cases, there were multiple offenders.

Table 1
Form of violence in 50 homicides by adolescents

	n	%
Stabbed	13	26
Stabbed and hit/kick	9	18
Shot	7	14
Blunt instrument and hit/kick	5	10
Blunt instrument, stabbed and hit/kick	5	10
Strangled and hit/kick	3	6
Blunt instrument	2	4
Stabbed and strangled	2	4
Blunt instrument, strangled and hit/kick	2	4
Strangled	1	2
Stabbed, hit/kick and suffocated	1	2
Total	50	100

3.4. Offender crime history

Previous crime history was defined as having an entry in the criminal record (which covered the preceding 10 years), or self-reporting a crime. However, it should be noted that the Finnish criminal record lacks information on crimes committed before the age of 15. In all, 42% of the offenders had a crime history. The most frequently occurring crimes were theft (25%), assault (16%) and drunken driving (14%). Having crime history was not related to offender age.

3.5. Offender childhood environment

A large proportion of the offenders had experiences problems in their childhood environment. Of them, 28% had been placed in an institution, 54% had parents with alcohol problems and 32% had witnessed or experienced physical violence at home. In 16% of the cases, the offender had personally experienced physical violence at home. In all, 64% of the offenders scored positive for at least one of these developmental variables. Further, 21% of the offenders were positive for paternal crime and 16% had a history of physical abuse (none had a history of sexual abuse). Thirty-four percent of the offenders perceived their relationship with their father and 21% with their mother, as poor. Altogether 54% of the offenders had been in contact with the mental health services. The first contact with the mental health services had been in average of 4.5 years before the killing (S.D. = 3.8 years).

3.6. Living conditions and psychiatric diagnosis

At the time of the killing, 39% of the offenders were unemployed, 23% were in vocational school, 16% in comprehensive school, 10% working and 5% were in high school. The average IQ was 96.4 (S.D. = 10.2, min = 72, max = 114). For 63% of the offenders, the level of intellectual functioning was average or above average. Only five offenders (9%) were known to have an ongoing mental health services contact at the time of the killing. Eleven offenders (19%) were known to have been self-destructive or suicidal (self mutilation, suicide attempts and serious threats). Altogether 39% of the offenders were diagnosed with alcohol dependency and 12% with drugs dependency. In all, 74% of the offenders consumed alcohol weekly and 37% took illicit drugs on a regular basis. The prevalence of conduct disorder was 40%. Fifty-seven percent of the 18-year-old offenders and 53% of the 17-year-old offenders were diagnosed as having a personality disorder (the DSM manual technically does not allow for the personality disorder diagnosis until age 18; however, some of the 17-year-old offenders were 18 years old at the time of the forensic psychiatric evaluation). In three cases the personality disorder was diagnosed as being mixed, in another two cases borderline,

in one case dependent, and in the rest of the cases antisocial. Four offenders (7%) were diagnosed as having schizophrenia. Five offenders were considered, due to their severe mental illness, not to be criminally responsible for the killing. Of the offenders, approximately one out of three (32%) was considered not to have a mental disorder or substance dependence.

3.7. Use of excessive violence

For further analysis, the cases were classified as having excessive violence present if the case contained sadistic or sexual features, mutilation or more than three forms of violence, or if it contained more than 19 stab wounds (this was the average number of stab wounds on the victims, with a S.D. of 20.1, min = 1, max = 120 wounds). By using these criteria, 28% of the cases were considered to include excessive violence. The use of excessive violence was related to the case involving multiple offenders (52% of the cases with multiple offenders involved excessive violence compared to 13% of the cases with a single offender, $p < 0.01$ Fisher's) and the victim offender relationship (being more frequent among acquaintances and strangers than family members or intimates, 35% versus 0%, respectively, $p < 0.05$, Fisher's). The offender age did not have a significant effect and the effect of the victim gender approached a significant level (excessive violence being more frequent among male than female victims, 35% versus 8%, respectively, $p < 0.08$ Fisher's). The use of excessive violence at the killing was not significantly related to early developmental problems, having a crime history or mental disorder (e.g. personality disorder). However, both alcohol dependency and drug dependency were significantly related with the use of excessive violence ($\chi^2 = 4.778$, $p < 0.05$; Fisher's $p < 0.01$, respectively). Of those using excessive violence, 64% were diagnosed with an alcohol dependency and 71% with a drug dependency.

4. Discussion

This study analysed the offender and offence characteristics among Finnish homicidal adolescents. The present results support partly the long-standing understanding that a large proportion of adolescent homicide offenders share a constellation of psychological, cognitive, educational and family system disturbance [9,17,27,28,36]. However, the present results suggest that this conception cannot be generalised to all homicidal adolescents. Several offenders in our sample had not been involved in criminal activities, had not parents with alcoholism or mental illness and had not witnessed or experienced family abuse. This difference with regard to previous studies is probably partly due to the differences in data gathering: the present sample was not collected within the clinical context. Also, previous studies have been criticised for the general lack of control groups, confounding factors, small samples and dependence on retrospective self-reports of prior abuse [36,37,38]. However, it should be noted that the absence of physical abuse history in the present study does not exclude possible mental abuse or cruelty. Some parents may have not, for example, given enough time to their children or they may have stressed materialistic aspects of life or simply neglected their children.

The victims and methods of killing observed in the present study were fairly similar to previous large-scale studies on adolescent homicides [9,27,37]. In congruent with previous studies, there was a low rate of major psychopathology [9,16,26,27], but the frequency of offenders being intoxicated or under the influence of drugs was slightly higher (e.g. [27]). Compared to the general pattern of homicides in Finland [3], in the present data the motive ''robbery'' was substantially more frequent suggesting that among adolescent homicide offenders acts of instrumental violence are more frequent. This mode of violence is planned, purposeful and unemotional, and it often serves an outer (financial or sexual) goal. The relatively low rate of prior arrests for violent crimes in our sample fits in previous research [26,27], and highlights further the fact that homicide can occur in adolescents who do not have anger control problems. The importance of this finding is that it suggests that the offender is opportunistic rather than impulsive and may not show any emotional warning signals. These results are in accordant with previous results on adolescent homicide [37], juvenile sexual homicide [39] and adolescent mass murderers [40]. The present results are also in accordant with previous results showing that approximately a quarter of the adolescent homicides are theft related, with the likelihood increasing if the victim is a stranger [37]. Furthermore, in many of these homicides there were multiple offenders [41].

Excessive violence was present in at least every third homicide. This is in accordance with previous results, and suggests an unambivalent need to maximize injuries [28]. Given the absence of psychosis, and the fact that excessive violence was related to multiple offenders suggests that it may reflect adolescent development—approval and validation seeking from peers. It may be hypothesised that in several of the pairings, one offender may have been the dominant personality, who reinforced the use of violence based on a pathologically sense of entitlement. Further, the use of excessive violence was associated with substance dependency but interestingly not with factors such as personality disorder or early developmental problems. This suggests that the use of excessive violence in adolescent homicides is something that steams from situational, rather than individual factors. Further, four cases (8%) involved sexual or sadistic elements (e.g. penetration, necrophilia, urinating, binding). Further, two of these homicides involved an elderly (>65-year-old) victim. It is of note, that in all of these four cases there were multiple offenders and none of these offender(s) were diagnosed as psychotic, or had an ongoing psychiatric contact. All of these offenders in these four cases had at least an average IQ and previous crime history or physical violence at childhood home was evident in only one offender. Two of these offenders had personality disorder.

Our study has some limitations, and it should be considered only preliminary and descriptive. Our sample size is smaller than ideal, and we did not utilize a comparison or control group.

Therefore, the characteristics identified in the present study cannot be used to predict adolescent murder. Further, limitations of the forensic psychiatric evaluation system have been discussed previously [30] and will be only shortly presented here. In sum, at present the district courts order independently a full-scale forensic psychiatric evaluation, e.g. there is no systematic procedure in the Finnish court of law in ordering the forensic psychiatric evaluation. Further, due to the lack of a detailed uniform register within the police, district courts, forensic pathologist or national homicide statistics, it is difficult to estimate how well the present sample represents all homicidal adolescents within the time frame. The present study suggested that 60% of the 15–17-year-old homicide offenders during 1991–2001 were evaluated and included in the data. However, the use of equal time frame may lead to an underestimated figure as the forensic evaluation lasts for 2–3 months and may be finished at a different year as the homicide. Further, the national homicide data maintained by Statistics Finland is based on police data regarding the number of suspects in homicides. Whether or not these suspects are in fact prosecuted (and therefore the forensic evaluation is considered) is another issue. This evaluation is further hindered by the fact that the national crime statistics reported the number of offenders prior to 1996 as gross value, where one offender is represented in terms of the number of victims [42]. One can assume, however, that due to the fact that homicides by adolescents are rare events, a forensic psychiatric evaluation is more like to be ordered to the offender in these cases. However, during 1991–2001 there were seven offenders who were less than 15 years old at the time of the homicide: these have not been included in the sample (due to a lack of legal proceeding).

Previous research on homicidal adolescents has rarely investigated the nature of the offences in association with the offender characteristics, with the exception of the victim and offender relationship. However, investigations of the background characteristics of adolescent homicidal offenders and their offence characteristics may be useful for police investigations in prioritizing suspects in unsolved homicide cases. In line with this approach, Dolan and Smith showed that the method of killing among homicidal adolescents was not associated with the physical, sexual or emotional abuse history, except for mutilation which was more frequent among the abused offenders [27]. However, practical utility of the results is hindered due to mutilation being a rare behaviour, occurring for example in only four cases in the present sample. For the purpose of criminal psychological profiling, some cautious comparisons of the present results and previous studies on Finnish homicides will be performed. Firstly, in the present data, the proportion of stranger victims was 25% which is higher than the 10% prevalence of stranger victims in the general homicide data [3]. Secondly, it has previously been reported that 11% of the Finnish homicides have multiple offenders [3,43]. In the present sample, the corresponding figure was 38%. Thirdly, robbery as a motive is more frequent among adolescents than in all homicides where robbery occurs in only approximately 5% of the cases [3,43]. It thus seems that young offenders plan robberies together which may escalate into excessive violence contrary to adults, who more frequently kill due to drinking quarrels. The low percentage of (ex)intimates is most likely due to the offenders' age. Further, the relatively low percentage of family member victims may be due to the infrequency of major psychopathology; a factor that has previously been associated among homicide offenders with an increased risk of killing family members [29,44–46].

Adolescent murder is a very low-frequency yet very high intensity event, therefore rendering generalisation is virtually impossible. Despite the methodological limitations, the present study is a systematic gathering of data on adolescent murder and it charts a path for further research. In sum, the characteristics of homicidal adolescents, although often highly problematic, sometimes do not stand out as significantly different from the characteristics of other youngsters. Therefore, it may prove beneficial to address what is it that drives youngsters to commit homicide rather than perpetrate non-lethal violence, leaving aside the effects of chance in determining whether violent act results in death or not. Specifically, the results invite further study on adolescent homicides committed in the course of other criminal activity and in groups.

Acknowledgements

Grateful acknowledgement is given to the National Authority of Medicolegal Affairs for their co-operation in this study. This study was supported by a grant from the Finnish Cultural Foundation to the first author. The second author would like to thank the Academy of Finland (personal Grants No. 75697 and No. 211176) for financial support on the series of Finnish homicide studies.

References

[1] G. LaFree, K.A. Drass, Homicide trends in Finland and 33 other nations since 1995: Is Finland still exceptional? in: T. Lappi-Seppälä (Ed.), Homicide in Finland: Trends and Patterns in Historical and Comparative Perspective, The National Research Institute of Legal Policy, Publication no. 181, Helsinki, 2001.
[2] C.G. Salfati, A European perspective on the study of homicide, Homicide Stud. 5 (2001) 286–291.
[3] M. Lehti, Henkirikokset 1998–2000. Tutkimus poliisin tietoon vuosina 1998–2000 tulleista henkirikoksista. Tilastokeskus ja Oikeuspoliittinen tutkimuslaitos 194, Helsinki (Homicides, Homicide Offenders and Victims in Finland in 1998–2002, Statistics Finland and The National Research Institute of Legal Policy, Publication no. 194, Helsinki), 2002.
[4] T.D. Crespi, S.A. Rigazio-DiGilio, Adolescent homicide and family pathology: implications for research and treatment with adolescents, Adolescence 31 (1996) 353–367.
[5] K.M. Heide, Youth homicide: a review of the literature and a blueprint for action, Int. J. Offender Ther. Comp. 47 (2003) 6–36.
[6] K.M. Heide, Young Killers: The Challenge of Juvenile Homicide, Thousand Oaks, Sage Publications, 1999.
[7] D.M. Shumaker, R.J. Prinz, Children who murder: a review, Clin. Child Family Psychol. Rev. 3 (2000) 97–115.
[8] E. Benedek, D. Cornell (Eds.), Juvenile Homicide, American Psychiatric Press, Washington, DC, 1989.
[9] K.G. Busch, R. Zagar, J.R. Hughes, J. Arbit, R.E. Bussell, Adolescents who kill, J. Clin. Psychol. 46 (1990) 472–485.
[10] R. Zagar, J. Arbit, R. Sylvies, K. Busch, J.R. Hughes, Homicidal adolescents: a replication, Psychol. Rep. 67 (1990) 1235–1242.

[11] D.O. Lewis, E. Moy, L.D. Jackson, R. Aaronson, N. Restifo, S. Serra, A. Simos, Biopsychosocial characteristics of children who later murder: a prospective study, Am. J. Psychiatry 142 (1985) 1161–1166.
[12] D.O. Lewis, R. Lovely, C. Yeager, G. Ferguson, M. Friedman, G. Sloane, H. Friedman, J.H. Pincus, Intrinsic and environmental characteristics of juvenile murderers, J. Am. Acad. Child Adolesc. Psychiatry 27 (1988) 582–587.
[13] D. Miller, J. Looney, The prediction of adolescent homicide: episodic dyscontrol and dehumanization, Am. J. Psychoanal. 34 (1974) 187–198.
[14] C.M. Greco, D.G. Cornell, Rorschach object relations of adolescents who committed homicide, J. Pers. Assess. 59 (1992) 574–583.
[15] C.R. Pfeiffer, Psychiatric hospital treatment of assaultive homicidal children, Am. J. Psychother. 34 (1980) 197–207.
[16] P. Hellsten, O. Katila, Murder and other homicide, by children under 15 in Finland, Psychiatric Q. Suppl. 39 (Suppl.) (1965) 54–74.
[17] P.J. Darby, W.D. Allan, J.H. Kashani, K.L. Hartke, J.C. Reid, Analysis of 112 juveniles who committed homicide: characteristics and a closer look at family abuse, J. Family Violence 13 (1998) 365–375.
[18] W. Tuteur, J. Glotzer, Further observations on murdering mothers, J. Forensic Sci. 11 (1966) 373–383.
[19] W.C. Myers, J.P. Kemph, DSM-III-R classification of murderous youth: help or hindrance? J. Clin. Psychiatry 51 (1990) 239–242.
[20] A. Labelle, J.M. Bradford, D. Bouget, B. Jones, M. Carmichael, Adolescent murderers, Can. J. Psychiatry 36 (1991) 583–587.
[21] J.R. Hays, K.S. Solway, D. Schreiner, Intellectual characteristics of juvenile murderers versus status offenders, Psychol. Rep. 43 (1978) 80–82.
[22] W.C. Myers, P.J. Mutch, Language disorders in disruptive behavior disordered homicidal youth, J. Forensic Sci. 37 (1992) 919–922.
[23] W.C. Myers, K. Scott, Psychotic and conduct disorder symptoms in juvenile murderers, Homicide Stud. 2 (1998) 160–175.
[24] I.B. Sendi, P.G. Blomgren, A comparative study of predictive criteria in the predisposition of homicidal adolescents, Am. J. Psychiatry 132 (1975) 423–428.
[25] D.O. Lewis, S.S. Shanok, M. Grant, E. Ritvo, Homicidally aggressive young children: neuropsychiatric and experiential correlates, Am. J. Psychiatry 140 (1983) 148–153.
[26] K.S. Walshe-Brennan, A socio-psychological investigation of young murderers, Br. J. Criminol. 17 (1977) 58–63.
[27] M. Dolan, C. Smith, Juvenile homicide offenders: 10 years' experience of an adolescent forensic psychiatry service, J. Forensic Psychiatry 12 (2001) 313–329.
[28] S. Bailey, Adolescent who murder, J. Adolesc. 19 (1996) 19–39.
[29] H. Häkkänen, T. Laajasalo, Homicide crime scene actions in a Finnish sample of mentally ill offenders, Homicide Stud. 10 (2006) 1.
[30] H. Häkkänen, Homicide by ligature strangulation in Finland: offence and offender characteristics, Forensic Sci. Int. 152 (2005) 61–64.
[31] T. Laajasalo, H. Häkkänen, Background characteristics of mentally ill homicide offenders—a comparison of five diagnostic groups, J. Forensic Psychiatry Psychol. 15 (2004) 451–474.
[32] J. Pajuoja, Väkivalta ja Mielentila. Oikeussosiologinen tutkimus syyntakeisuussäännöksistä ja mielentilatutkimuksista. Suomalainen Lakimiesyhdistys. Jyväskylä (Violence and Mental Health, Finnish Law Association, Jyväskylä), 1995.
[33] M. Eronen, E. Repo, H. Vartiainen, J. Tiihonen, Forensic psychiatric organization in Finland, Int. J. Law Psychiatry 23 (2000) 541–546.
[34] N. Långström, M. Grann, A. Tengström, N. Lindholm, A. Woodhouse, G. Kullgren, Extracting data in file based forensic psychiatric research: some methodological considerations, Nordic J. Psychiatry 53 (1999) 61–67.
[35] Statistics Finland. Yearbooks of Justice Statistics, Statistics Finland, Helsinki, 1991–2001.
[36] D.G. Cornell, E.P. Benedek, D.M. Benedek, Juvenile homicide: prior adjustment and a proposed typology, Am. J. Ortopsychiatry 57 (1987) 383–393.
[37] J.C. Rowley, C.P. Ewing, S. Singer, Juvenile homicide: the need for an interdisciplinary approach, Behav. Sci. Law 5 (1987) 3–10.
[38] P.J. Hardwick, M.A. Rowton-Lee, Adolescent homicide: towards assessment of risk, J. Adolesc. 19 (1996) 263–276.
[39] W.C. Myers, L. Monaco, Anger experience, styles of anger expression, sadistic personality disorder, and psychopathy in juvenile sexual homicide offenders, J. Forensic Sci. 45 (2000) 698–701.
[40] J.R. Meloy, A.G. Hempel, K. Mohandie, A. Shiva, T. Gray, Offender and offence characteristics of a non-random sample of adolescent mass murderers, J. Am. Acad. Child Adolesc. Psychiatry 40 (2001) 719–728.
[41] C.P. Ewing, When Children Kill: The Dynamics of Juvenile Homicide, Lexington Books, Toronto, 1990.
[42] M. Lehti, J. Kivivuori, Väkivaltarikokset (Violen Crimes), in: T. Lappi-Seppälä, J. Kivivuori (Eds.), Rikollisuustilanne 2002. Oikeuspoliittinen tutkimuslaitos 200, Helsinki (Crime trends in Finland, The National Research Institute of Legal Policy, Publication no. 200, Helsinki), 2003.
[43] J. Kivivuori, Suomalainen henkirikos: teonpiirteet ja tekojen olosuhteet vuosina 1988 ja 1996. Oikeuspoliittinen Tutkimuslaitos 159, Helsinki, 1999 (Patterns of Criminal Homicide in Finland, The National Research Institute of Legal Policy, Publication No. 159, Helsinki).
[44] H. Putkonen, J. Collander, M. Honkasalo, J. Lönnqvist, Personality disorders and psychoses form two distinct subgroups of homicide among female offenders, J. Forensic Psychiatry 12 (2001) 300–312.
[45] E. Steury, M. Choinski, Normal'' crimes and mental disorder: a two-group comparison of deadly and dangerous felonies, Int. J. Law Psychiatry 18 (1995) 183–207.
[46] H. Gillies, Homicide in the West of Scotland, Br. J. Psychiatry 128 (1976) 105–127.

ELSEVIER

Forensic Science International 164 (2006) 116–121

Forensic Science International

www.elsevier.com/locate/forsciint

Ethanol production by *Candida albicans* in postmortem human blood samples: Effects of blood glucose level and dilution

Daisuke Yajima [a,*], Hisako Motani [a], Katsuhiko Kamei [b], Yayoi Sato [a], Mutsumi Hayakawa [a], Hirotaro Iwase [a]

[a] *Department of Legal Medicine, Graduate School of Medicine, Chiba University, 1-8-1 Inohana, Chuo-ku, Chiba City, Chiba 260-8670, Japan*

[b] *Chiba University Research Center for Pathogenic Fungi and Microbial Toxicoses, 1-8-1 Inohana, Chuo-ku, Chiba City, Chiba 260-8670, Japan*

Received 25 April 2005; received in revised form 5 December 2005; accepted 6 December 2005
Available online 20 January 2006

Abstract

We present two cases in which the ethanol concentration in blood samples taken after death continued to increase in the absence of any remarkable increase in *n*-propanol concentration. Species of bacteria and yeasts, including *Candida albicans* were isolated from these samples. We then examined whether *C. albicans*, the most common yeast in the general environment, was able to produce ethanol in human blood stored at room temperature. Ethanol production increased as the glucose concentration increased, indicating that *C. albicans* produced ethanol from the glucose. Our results also suggested that *C. albicans* produced ethanol more easily in blood diluted by intravenous infusions that included glucose than in undiluted blood. These findings are useful for the evaluation of postmortem ethanol production in subjects whose blood has been diluted by infusions with glucose. Furthermore, there was no quantitative relationship between the amount of *n*-propanol detected and the amount of ethanol production: *n*-propanol appears to be an unreliable index of putrefaction and postmortem ethanol production by *C. albicans*. It is possible for the blood ethanol level to be high and *n*-propanol not to be detected, even if the subject has not been drinking alcohol. We reconfirmed the necessity of immediately adding sodium fluoride to samples for ethanol analysis to prevent postmortem ethanol production.

Keywords: Ethanol; Postmortem production; *n*-Propanol; *Candida albicans*; Putrefaction

1. Introduction

Ethanol analysis is the assay performed most frequently in forensic autopsies. Some samples are putrefied, contaminated, or destroyed, and ethanol can be produced in these samples. Some forensic pathologists look on *n*-propanol as an index of putrefaction. Nanikawa et al. [1] concluded that the amount of ethanol production post mortem is 20 times higher than that of *n*-propanol, whereas other forensic pathologists consider that there is currently no reliable standard of interpretation of postmortem ethanol production [2,3]. We encountered two cases in which the ethanol concentration of blood samples taken post mortem increased with time, with no remarkable increase in *n*-propanol concentration. This postmortem ethanol production is thought to be the work of such microorganisms as *Candida albicans*, but there have been only a few reports on the production of ethanol by *C. albicans* in postmortem blood [4–11].

Our aim was to identify whether *C. albicans* produces ethanol in blood samples and whether this microorganism could produce ethanol without producing *n*-propanol. Furthermore, we discuss the conditions under which *C. albicans* could easily produce ethanol and reconfirm that sodium fluoride prevents *C. albicans* from producing ethanol.

2. Case reports

2.1. Case A

A 24-year-old man died instantly when his car collided with a parked car. An autopsy was performed about 35 h after death. The results of ethanol analysis of his blood sample are shown in Fig. 1. The cause of death was brain stem death by destruction of the posterior cerebral artery. The first ethanol analysis gave a blood ethanol concentration of 0.59 mg/mL. The concentration

* Corresponding author. Tel.: +81 43 226 2078; fax: +81 43 226 2079.
E-mail address: yajima.d@graduate.chiba-u.jp (D. Yajima).

0379-0738/$ – see front matter
doi:10.1016/j.forsciint.2005.12.009

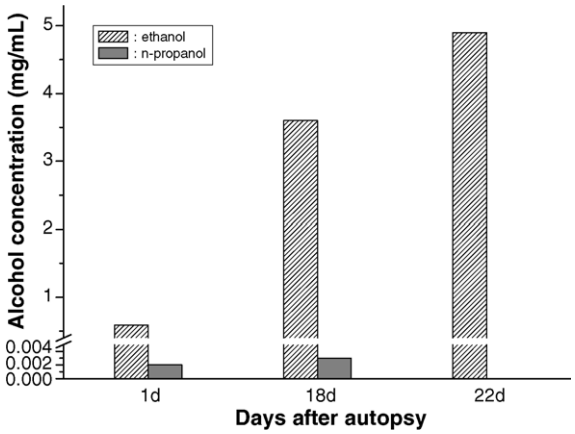

Fig. 1. Alcohol concentration in blood sample A over time.

then increased from day to day, even though the blood was stored in a refrigerator (at 2–10 °C). Twenty-two days after death the value was 4.9 mg/mL, and the *n*-propanol concentration was low (around 0.002–0.003 mg/mL).

2.2. Case B

A 48-year-old inebriated man was run over by a car while he was lying on the road. Shortly after hospitalization he died. An autopsy was performed about 10 h after death. The results of ethanol analysis of his blood sample are shown in Fig. 2. The cause of death was exsanguination due to destruction of the aorta. In a pattern similar to that of case A, the first analysis gave a blood ethanol concentration of 2.1 mg/mL. The level in the sample then rose, and 20 days after death it was 9.6 mg/mL. Although *n*-propanol was detected, the values were very small (around 0.004–0.03 mg/mL).

3. Experimental procedure

3.1. Materials and methods

3.1.1. Blood samples

We collected peripheral blood from four healthy volunteers. The blood was handled with aseptic technique. Heparin was added, and the samples were stored in a refrigerator at 4 °C (normal blood samples). In some experiments, the blood samples were stored after deactivation (deactivated blood samples) (see below).

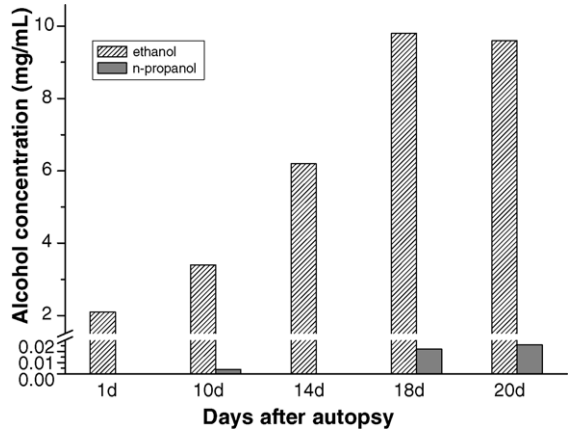

Fig. 2. Alcohol concentration in blood sample B over time.

3.1.2. Deactivation

Collected blood was incubated in a 56 °C water bath for 30 min to deactivate complement and white blood cells and to inhibit coagulation during the experiments.

3.1.3. Candida albicans

A clinically isolated strain of *C. albicans* (IFM46851) was cultured on potato dextrose agar (PDA) medium for more than 1 day. *C. albicans* (yeast) was added to each sample with a platinum loop. Aseptic technique was followed throughout the experiment.

3.1.4. Experiments

3.1.4.1. Experiment 1. Six-milliliter normal blood samples were stored in 30-mL glass vials at room temperature (24 °C) after the addition of yeast. Ethanol, *n*-propanol, and glucose analyses were performed 0, 2, 4, 8, and 12 (13) days after addition of yeast. Blood samples with glucose levels of about 7 mg/mL were prepared by adding a very small quantity of highly concentrated glucose solution to 6 mL of deactivated blood sample. The blood samples with added glucose were stored after the addition of yeast and analyzed as described above. Furthermore blood samples with glucose were also analyzed every 12 h until 48 h after the addition of yeast.

3.1.4.2. Experiment 2 (the influence of dilution by infusion on ethanol production). We mixed blood and the commercial intravenous infusion Solita-T No. 1 (Ajinomoto Pharma Co. Ltd., Tokyo, Japan), which includes glucose, in the following ratio. And then analyses were performed. The ratios of normal blood sample to infusion were 6–0 mL (undiluted blood), 4–2 mL, and 3–3 mL. The drip infusion contained 90 mM Na^+, 70 mM Cl^-, 20 mM L-lactate, and 26 mg/mL glucose.

3.1.4.3. Experiment 3 (the influence of blood elements on ethanol production). We mixed deactivated blood and water in the following ratios: 6 mL:0 mL (undiluted blood), 4 mL:2 mL, 3 mL:3 mL, and 2 mL:4 mL. Mixtures with glucose levels of 7 mg/mL were then prepared.

3.1.4.4. Experiment 4 (the influence of deactivation on ethanol production). Normal and deactivated blood samples with glucose levels of 7 mg/mL were prepared.

3.1.4.5. Experiment 5 (the influence of sodium fluoride on ethanol production). Sodium fluoride was added at 1–2% to blood samples with glucose levels of 7 mg/mL. After addition of the yeast, the samples were stored and analyzed every 12 h until 48 h after yeast addition.

3.1.5. Determination of blood glucose level

Samples were analyzed by an enzyme method (Gluc-DH method) [12].

3.1.6. Ethanol and n-propanol analysis

Ethanol concentrations were determined by headspace gas chromatography [13]. The analytical conditions were as follows: instruments, Shimadzu GC-9 (FID detector) (Kyoto, Japan); column, glass column 2.1 m × 3.2 mm (inner diameter) with Chromosorb W 60/80 AW-DMCS polyethylene glycol 1000 25%; temperature of column 100 °C, and of injection 140 °C; and internal standard, *t*-butanol.

4. Results

4.1. Limits of quantitation for alcohol measurements

The limit of quantitation was less than 0.001 mg/mL for both ethanol and *n*-propanol.

4.2. Identification of microorganisms in samples from the autopsy cases

The microorganisms identified in each sample are shown in Table 1. They were common environmental microorganisms, and all have been reported as capable of producing ethanol [4].

4.3. Ethanol and n-propanol production and glucose concentration over time

In experimental samples without added glucose, no ethanol or *n*-propanol was detected on any day (data not shown). In contrast, in samples with added glucose, ethanol was detected. Concentrations of ethanol, *n*-propanol, and glucose are shown in Figs. 3 and 4.

In the analyses performed at intervals over 13 days, ethanol concentrations in samples with added glucose peaked 2 days after the addition of yeast and then gradually decreased. Small concentrations of *n*-propanol were detected (Fig. 3).

On day 0, the glucose concentration of samples without additional glucose was around 0.8 mg/mL and that of samples with additional glucose was around 7 mg/mL. After 2 days, the glucose concentrations of both kinds of samples had decreased dramatically.

In the analyses performed every 12 h until 48 h, ethanol was detected 12 h after the addition of yeast and glucose; its concentration gradually increased and peaked after about 36–48 h (Fig. 4). Small amounts of *n*-propanol were detected. The glucose concentration gradually decreased, and almost all had been consumed by 48 h.

Table 1
Microorganisms identified in samples A and B

Sample A	① *Candida albicans* ② *Candida parapsilosis*
Sample B	① *Corynebacterium* sp. ② *Escherichia coli* ③ *Candida tropicalis*

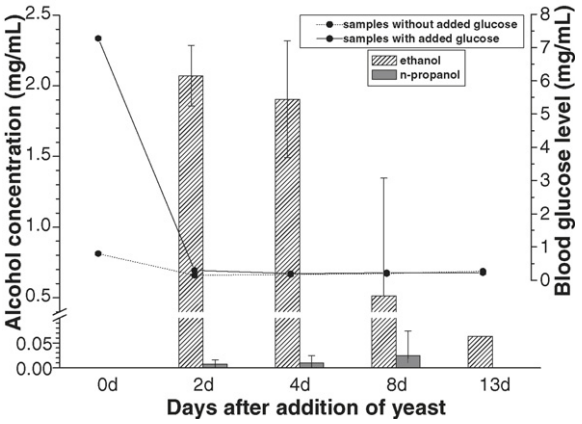

Fig. 3. Alcohol and glucose concentrations of experimental samples with and without added glucose ($n = 4$) (Experiment 1).

4.4. Ethanol and n-propanol production and glucose concentrations in experimental samples diluted by addition of intravenous infusions containing glucose

Concentrations of ethanol, *n*-propanol, and glucose in experimental samples diluted by the addition of intravenous infusions containing glucose are shown in Fig. 5. Ethanol was detected on day 2, and its level increased from then until day 4 or 8. The maximum levels were 2.2 mg/mL (blood to infusion ratio 4:2) and 3.3 mg/mL (blood to infusion ratio 3:3). Only low levels of *n*-propanol were detected. In undiluted experimental samples, no ethanol or *n*-propanol was detected (data not shown).

Although theoretical glucose concentrations would have been about 9.20 mg/mL (blood to infusion ratio 4:2) and about 13.4 mg/mL (blood to infusion ratio 3:3), the averages of measured glucose concentrations on day 0 were 9.93 and 13.88 mg/mL, respectively. Glucose concentrations decreased over time in all experimental samples. Almost all glucose had been consumed by 4 or 8 days.

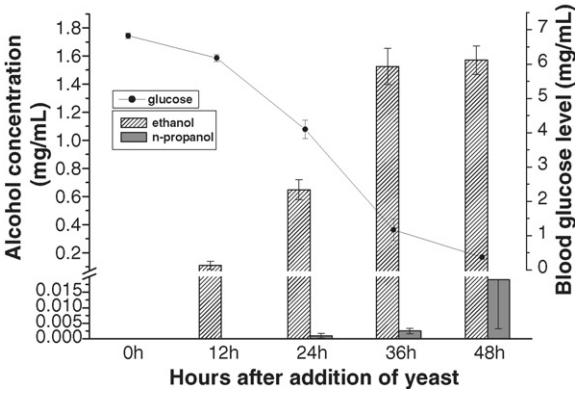

Fig. 4. Alcohol and glucose concentrations in experimental samples with added glucose ($n = 4$) (Experiment 1).

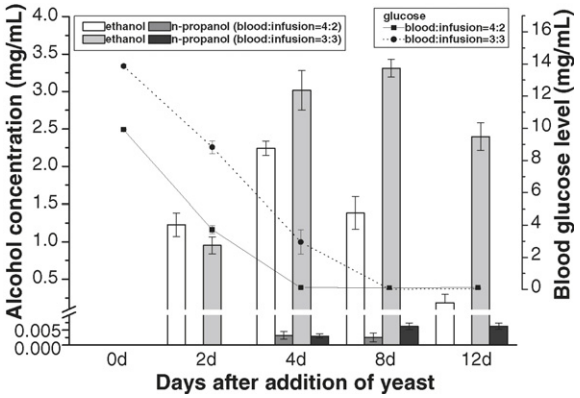

Fig. 5. Alcohol and glucose concentrations of samples diluted by infusions containing glucose ($n = 4$) (Experiment 2).

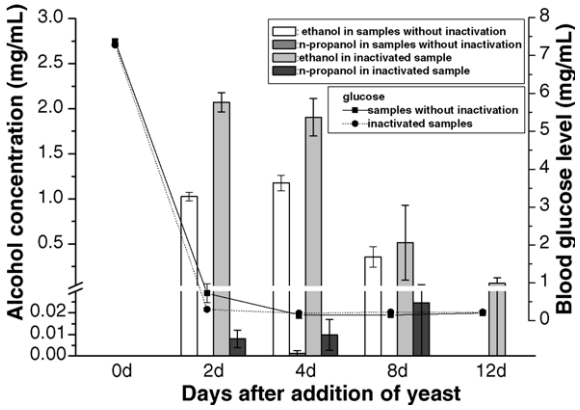

Fig. 7. Comparison of alcohol production in deactivated and control samples with added glucose ($n = 4$) (Experiment 4).

4.5. Influence of blood elements on ethanol production

We examined whether blood elements such as red blood cells and the many kinds of protein present influenced ethanol production. Ethanol and glucose concentrations of samples diluted and undiluted by water are shown in Fig. 6. The same tendency was seen in both undiluted and diluted samples.

4.6. Effects of blood deactivation on ethanol production

The concentrations of ethanol, *n*-propanol, and glucose in control and deactivated samples are shown in Fig. 7.

The glucose concentrations of samples with and without deactivation were nearly equal and decreased similarly. However, there was a difference in ethanol production between the two sample types. More ethanol was produced in deactivated samples than in control samples.

4.7. Effects of sodium fluoride

No ethanol or *n*-propanol was detected in samples with added sodium fluoride. Glucose concentrations did not decrease (data not shown).

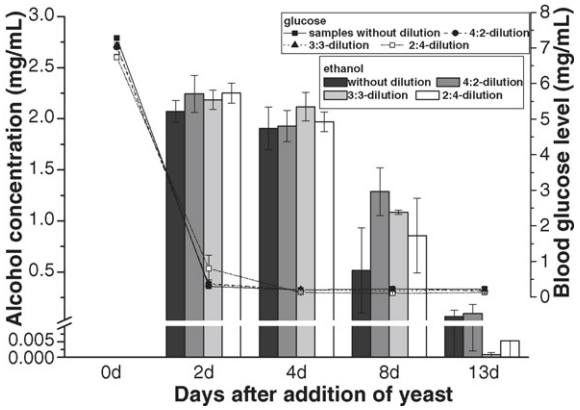

Fig. 6. Alcohol and glucose concentrations of experimental samples with and without dilution by water ($n = 4$) (Experiment 3).

5. Discussion

5.1. Microorganisms isolated

The microorganisms isolated from the forensic samples are species common in the general environment. We therefore thought that the samples might have been contaminated at the time of collection. In both cases, the blood had been taken from traffic accident victims with heavy body damage, so it was also possible that the blood had been contaminated before autopsy. In cases of heavy body damage, invasion of the blood by microorganisms can begin at an early stage. Samples from such cases would easily be susceptible to putrefaction.

C. albicans is one of the most common yeasts in the general environment. It produces ethanol under certain conditions [4,5,10,14]. In our experimental samples, we did not detect ethanol in any of the samples to which *C. albicans* had not been added. Therefore, it was clear that *C. albicans* was producing ethanol in the blood under our experimental conditions when glucose was added.

5.2. Relationship between glucose concentration and ethanol production

Microorganisms can produce ethanol from a variety of substrates [2,4]. Glucose is one of the best substrates [4]. In our experimental samples, as the ethanol concentration increased the glucose concentration decreased (Figs. 3 and 4). This fact suggests that glucose is a good substrate for ethanol production in the blood by *C. albicans*. The greater the initial concentration of glucose, the greater the quantity of ethanol production (Fig. 5).

According to Dawes, the maximum theoretical yield is two molecules of ethanol for each molecule of glucose fermented (51 mg ethanol/100 mg glucose) [4]. For example, as in Fig. 5, when the mixtures of blood and intravenous infusion with 9.93 and 13.88 mg/mL glucose were completely fermented, the theoretical ethanol concentrations would have been 5.1 and 7.1 mg/mL, respectively. Our experimental results were smaller

than the theoretical values. We assumed that glucose was consumed by glycolysis; furthermore, the ethanol concentration decreased after it peaked, suggesting that the ethanol itself was being metabolized. This result suggests that, under some conditions, microorganisms can completely consume ethanol when the initial concentration of ethanol is very low. Therefore, if ethanol were present in the blood of a living person, it might not be detected after death owing to its consumption by microorganisms.

Blood glucose levels in corpses vary. One report maintains that blood glucose levels can rise above 7 mg/mL in some corpses [15]. It is easily possible for ethanol to be produced in diabetics, in people who have received glucose infusions (as in our experiment), or in people who have high blood glucose levels at the time of death owing to some other hormonal condition.

The ethanol concentration rose from 0.59 to 4.9 mg/mL (+4.3 mg/mL) over 21 days in case A and from 3.4 to 9.6 mg/mL (+6.2 mg/mL) over 10 days in case B. According to the reference previously cited [4], in case A, a 4.3 mg/mL increase in ethanol concentration was derived from an 8.44 mg/mL increase in blood glucose level. In case B, a 6.2 mg/mL increase in ethanol concentration was equivalent to a 12.16 mg/mL increase in blood glucose level. These elevations of ethanol concentration could therefore theoretically be explained if the blood glucose level at the time of death were more than 8.44 mg/mL in case A and more than 12.16 mg/mL in case B. We can assume that infusion of fluids containing glucose can increase the blood glucose level by up to more than 10 mg/mL. The patient in case B was in fact hospitalized and received intravenous drip infusion.

We did not analyze blood glucose in our two autopsy cases, because there were no samples left for analysis. Nevertheless, from our results it seems likely that hyperglycemia was present at the time of death.

5.3. Factors affecting postmortem ethanol production

In Fig. 6, there were no differences in ethanol production among samples that differed in terms of only the concentrations of blood elements. That is, changes in the concentrations of such elements had no effect on ethanol production.

Sodium fluoride is an inhibitor of glycolytic enzymes. It has many inhibitory effects on coagulation, glucose consumption, and putrefaction of blood samples [16]. When we added sodium fluoride at 1–2% to experimental samples, no ethanol or *n*-propanol was produced. We can reconfirm that, in patients with diabetes, patients with suspected hyperglycemia resulting from infusion with glucose, and those with rapid putrefaction owing to severe tissue damage, sodium fluoride should be added to the samples immediately.

In Fig. 7, the results suggest that ethanol is produced more easily in deactivated experimental samples. In blood samples that are not deactivated, it is possible that the yeasts are killed because complement is active or neutrophils are alive.

5.4. Validity of n-propanol as an index of postmortem ethanol production

Ethanol production in corpses is due to the activity of microorganisms. Some forensic pathologists look on *n*-propanol as a good index of putrefaction and postmortem ethanol production by microorganisms. One opinion is that the postmortem ethanol concentration is about 20 times higher than the *n*-propanol production [1,17–19]. However, in our study, the amount of ethanol produced by *C. albicans* was much more than 20 times the *n*-propanol concentration. We found no quantitative relationship between the two substances. Furthermore, in some samples, no *n*-propanol was detected.

C. albicans is a common yeast present in the general environment and is found in the human digestive system. We assume that this yeast is active in putrefaction. Our study can be viewed as a model for a phenomenon similar to that occurring in common putrefaction, and our results suggest that *n*-propanol cannot be used as a reliable index of postmortem ethanol production by yeasts.

When we discuss postmortem ethanol production, we should consider together such factors as the situation surrounding death, the subject's history, information on sample collection, and the ethanol concentration in the vitreous humor: *n*-propanol is just one factor that we need to consider [20].

References

[1] R. Nanikawa, S. Kotoku, Medico-legal evaluation of the ethanol levels in cadaveric blood and urine, Yonago Acta Med. 15 (1971) 61–69.
[2] C.L. O'Neal, A. Poklis, Postmortem production of ethanol and factors that influence interpretation: a critical review, Am. J. Forensic Med. Pathol. 17 (1996) 8–20.
[3] K. Ziavrou, V.A. Boumba, T.G. Vougiouklakis, Insights into the origin of postmortem ethanol, Int. J. Toxicol. 24 (2005) 69–77.
[4] E. Janet, L.A. Corry, Review of possible sources of ethanol ante- and postmortem: its relationship to the biochemistry and microbiology of decomposition, J. Appl. Bacteriol. 44 (1978) 1–56.
[5] K.-E. Sjolin, Postmortem production of alcohol, Acta Med. Legal Soc. 9 (1956) 262–276.
[6] K. Nakabayashi, Studies on the alcohol concentration in cadaveric blood, cisternal fluid and urine, Jpn. J. Legal Med. 21 (1967) 174–203.
[7] W. Schwerd, Die Beurteilung von Alkohol befunden im Leihenblut, Dtsch. Z. ges. Gerichtl. Med. 43 (1954) 221–231.
[8] E. Weinig, L. Lautenbach, Die Beurteilung von Alkohol befunde in Leichenblutproben, Blutalkohol 1 (1962) 222–233.
[9] E. Ostenhaus, K. Johannsmeier, Postmortale Entstehung von Alkoholen durch faulnis, Dtsch. Z. ges. Gerichtl. Med. 57 (1966) 281–284.
[10] G. Landsberg, Über den Alkoholgehalt tierischer Organe, Z. Physiol. Chem. 41 (1904) 505–523.
[11] J. Chang, S.E. Kollman, The effect of temperature on the formation of ethanol by *Candida albicans* in blood, J. Forensic Sci. 34 (1989) 105–109.
[12] Von D. Banauch, W. Brümmer, W. Ebelting, et al., Eine glucose-dehydrogenase für die Glucose-Bestimmung in Körperflüssigkeiten, Z. Klin. Chem. Klin. Biochem. 13 (1975) 101–107.
[13] The Japanese Society of Legal Medicine, Alcohol analysis, in: Manual for Forensic Toxicology Analysis of the Japanese Society of Legal Medicine, Kijima Press, Fukuoka, Japan, 1999, pp. 20–21.
[14] H. Gormsen, Yeasts and the production of alcohol post mortem, J. Forensic Med. 1 (1954) 107–171.

[15] H. Iwase, M. Kobayashi, M. Nakajima, T. Takatori, The ratio of insulin to C-peptide can be used to make a forensic diagnosis of exogenous insulin overdosage, Forensic Sci. Int. 115 (2001) 123–127.
[16] R.J. Lewis, R.D. Johnson, M.K. Angir, N.T. Vu, Ethanol formation in unadulterated postmortem tissues, Forensic Sci Int. 146 (2004) 17–24.
[17] Y. Kosaka, Studies on the ethanol concentrations in bloods and other body fluids of cadavers, Jpn. J. Legal Med. 24 (1970) 32–47.
[18] R. Nanikawa, Gas chromatographic determination of the ethanol in biological materials and its application to the practice of legal medicine, Jpn. J. Legal Med. 26 (1972) 316–327.
[19] K. Ameno, Medicolegal studies on the ethanol concentrations in blood and urine of cadavers, Jpn. J. Legal Med. 35 (1981) 83–102.
[20] I.V. Lima, A.F. Midio, Origin of blood in decomposed bodies, Forensic Sci Int. 106 (1999) 157–162.

ELSEVIER

Forensic Science International 164 (2006) 122–125

Forensic Science International

www.elsevier.com/locate/forsciint

Comparison of pulmonary autopsy findings of the rats drowned at surface and 50 ft depth

Akın Savas Toklu [a,*], Nevzat Alkan [b], Aydın Gürel [c], Maide Cimsit [a], Damla Haktanır [c], Sefika Körpınar [a], Sevim Purisa [d]

[a] *Istanbul University, Istanbul Faculty of Medicine, Department of Underwater and Hyperbaric Medicine, 34093 Capa-Istanbul, Turkey*
[b] *Istanbul University, Istanbul Faculty of Medicine, Department of Forensic Medicine, 34093 Capa-Istanbul, Turkey*
[c] *Istanbul University, Faculty of Veterinary, Department of Pathology, 34320 Avcilar-Istanbul, Turkey*
[d] *Istanbul University, Cerrahpasa Faculty of Medicine, Department of Biostatistic, 34098 Cerrahpasa-Istanbul, Turkey*

Received 11 January 2005; received in revised form 9 November 2005; accepted 6 December 2005
Available online 19 January 2006

Abstract

Introduction: When a body is recovered from the water after a fatal SCUBA diving accident, it is useful to know if the diver was under pressure or not when he/she took his/her last breath, in order to determine the cause and manner of the death. If the victim was under pressure, the air remained in the lungs of the diver will be equal to the environmental pressure. If the body comes to the surface, the air in the lung will expand according to the Boyle's Gas Law and give mechanical damage to the surrounding tissues, due to decreases in environmental pressure. We designed an experimental study to see the difference in pulmonary autopsy findings of the rats that drowned under normobaric and hyperbaric conditions.

Method: Forty five male, 250–300 g, Sprague Downey adult rats were divided into three groups. Two groups of rats were drowned under normobaric conditions (Groups DS Group DSS) and the third group at 50 ft pressure (Group DD). The pulmonary autopsy findings of the groups were compared. In the light microscopy, the number of the microscopic fields (×10) containing at least one emphysematous area with longitudinal dimension greater than 300 μm were compared among the groups.

Results: The gross examination revealed a prominent swelling of the lungs in all rats in the Group DD, in comparison to that of the Groups DS and DSS. The number of the microscopic fields, which included at least one emphysematous area with longitudinal dimension greater than 300 μm out of 150 fields from each of the groups DS, DSS and DD, were 88, 101 and 115 respectively. The difference between the group DS and DD was found to be statistically significant.

Conclusion: We conclude that in investigating the fatal diving accidents, pulmonary autopsy findings give valuable information whether the death occurred at the surface or at the depth.

Keywords: Diving; Fatal; Accident; Pulmonary; Autopsy; Drowning; Barotrauma

1. Introduction

When a body is recovered from the water, there are several questions that should be answered. The two most critical questions are: (1) Was the victim alive or dead when he dived into the water? (2) Is the cause of death drowning? If the body recovered was equipped with diving gears, it is more than probable that the body belongs to a diver. If evidence is without doubt in favor of homicide or suicide, then the incident cannot be regarded as a fatal diving accident. But if it is a diving accident, a few more questions must be answered such as; Was the diver under pressure, which means if the diver was at depth, when he or she drowned?

Self-contained underwater breathing apparatus (SCUBA) diving is a fascinating recreational but dangerous activity. The risk of hypothermia and drowning are combined with those of hyperbarism and change in ambient pressure [1]. Although severe diving injuries and fatal accidents are rare, minor accidents frequently occur. It is estimated that three to nine deaths per 100,000 divers occur annually in the United States [2]. Drowning is the leading cause of death in fatal diving accidents [3]. When a body is recovered from the water after a

* Corresponding author. Tel.: +90 532 4125168; fax: +90 212 4142034.
E-mail address: akin@toklu.net (A.S. Toklu).

0379-0738/$ – see front matter
doi:10.1016/j.forsciint.2005.12.010

fatal SCUBA diving accident, one of the following conditions is more likely to have occurred;

(1) Diver drowned at the surface and the body remained at the surface until the recovery.
(2) Diver drowned at the surface, the body sank and came to the surface before the recovery, after remaining at the bottom for some time.
(3) Diver drowned at the surface and sunken body remained at the bottom until the recovery.
(4) Diver drowned at depth (under pressure) and the body remained at the bottom until the recovery.
(5) Diver drowned at depth (under pressure) and the body came to the surface before the recovery.

The investigation of a fatal diving accident by technical, medical and legal personnel is critical to provide useful information for determining the cause and manner of the death [4]. It is known that the lungs are not fully filled with water and some air remains in the lungs in drowning cases [5]. In the last two conditions above (4 and 5), the pressure of the air remained in the lungs of the victim will be equal to the environmental pressure. In both conditions, since the environmental pressure decreases while the body comes to the surface, the air will expand according to the Boyle's Gas Law and give mechanical damage to the surrounding tissues. Therefore, it can be presumed that, the pulmonary autopsy findings of the victims that drowned at normobaric or hyperbaric conditions differ from each other. It may be possible to find out if the diver was under pressure or not when he/she took his/her last breath by investigating the autopsy findings in the lungs.

We have conducted an experimental animal study on rats as a model for investigating diving fatalities under the conditions mentioned above. The study based on comparison of the autopsy findings in the lungs of the rats that drowned at the surface and drowned at 50 ft depth.

2. Material and method

2.1. Animals

In this study, 45 male, 250–300 g, Sprague Downey adult rats, which were cared by Istanbul University, Institute of Experimental Researches, under the surveillance of a veterinarian, were divided into three groups and named as Group Drowned at Surface (DS), Group Drowned at Surface and Sunken (DSS) and Group Drowned at Depth (DD). Each group consisted of 15 rats.

2.2. Drowning and pressurization procedures

The rats in Group DS and Group DSS were drowned at the surface (pressure: 1 ATA). The rats in a cage (13 cm × 30 cm × 35 cm) were immersed in a plastic container (17 cm × 28 cm × 43 cm) filled with fresh tap water at room temperature. The rats remained underwater for about 2–3 min until they were drowned. The rats in Group DSS were pressurized to 50 ft in 2 min, for 30 min, after being drowned at the surface. A recompression chamber with the volume of 0.4 m^3 was used to pressurize the rats on air. The rats in Group DD were drowned at 50 ft (pressure: 2.5 ATA) and decompressed after they remained under that pressure for 30 min.

2.3. Autopsy, sampling and pathology

The rats were removed from the water 1 h after drowning. The time interval between the death and the autopsy procedure was between 90 and 120 min. Thoracic cavities were opened to examine the lungs. The lungs were removed after recording macroscopic features. Then, incisions were applied throughout the lungs by a blade and the whole lungs were fixed in 10% saline-buffered formalin solution for 48 h. About 0.5-cm-thick sections, perpendicular to the bronchioles and blood vessels were excised from the proximal, medial and distal regions of each lobe. Then the tissue samples were embedded in paraffin wax and cut as about 5–6 μm-thick slices. The sections were stained with hematoxylene–eosine (HE).

2.4. Light microscopy

After examining the samples in general by a blinded pathologist, 10 different high-power fields (HPF, ×10) were selected randomly on the each of 45 specimens that were prepared from the upper, lower and the medial parts of the lungs of every rat in each group. Emphysematous areas in each microscopic field were examined using OLYMPOS Eyepiece Micrometer, 10/100, *XY* to determine areas longitudinal dimensions were greater than 300 μm. We compared the number of the fields containing at least one emphysematous area with longitudinal dimension greater than 300 μm in each group. For statistical analysis, Chi-square test was used.

3. Results

3.1. Necropsy findings

There were no significant gross pathologic changes observed at necropsy of the rats in Group DS. The lungs were slightly enlarged and seemed congested with petechial hemorrhages in Group DSS. There was also slight reddish foamy fluid emerging from the incisions applied to the visceral pleura, prior to the formalin-saline fixation. In Group DD, which were drowned under the pressure of 2.5 ATA (15-m-depth), macroscopic examination revealed a prominent swelling of the lungs in all of the rats, in comparison to that of the other two groups. The lungs were fairly enlarged and protruded through the opening of thoracic cavity. The congested lungs covered the whole mediastinum bilaterally, and petechial hemorrhages were seen on pale reddish pleural surface. The surfaces of the incisions were frail and the leakage of a dusty pink, frothy fluid was detectable.

3.2. Histological features

In Group DS, the respiratory capillaries were dilated and filled with erythrocytes. The expansion of the alveoli was not

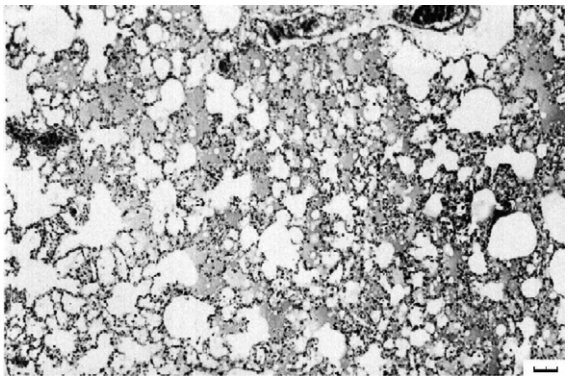

Photo 1. In Group DSS, proteic, amorphous, eosinophilic material was observed in the alveolar spaces. H&E, scale bar is 100 μm.

prominent. The epithelia of the dilated alveoli were flattened in some areas and the thinning of the interalveolar septae was detectable. In some areas rupture of two to three alveoli formed spaces of vesicular emphysema. In Group DSS, the blood vessels and the pulmonary capillaries were filled with erythrocytes and proteinous, amorphous, eosinophilic material was observed within the alveolar spaces (Photo 1). The thinning and rupture of the interalveolar walls in Group DSS was much more detectable than Group DS. The number of bullous emphysematous fields was more numerous. In Group DD, the blood vessels including pulmonary capillaries were found to be empty. The alveolar expansion was quite detectable with the presence of some froth within. In most of the microscopic fields examined, over-expansion of the alveoli resulted in flattening of the epithelia, thinning and even rupture of the interalveolar walls. Thus, communication among numerous alveoli yielded wide bullous emphysematous spaces (Photo 2). The number of the microscopic fields, which included at least one emphysematous area with longitudinal dimension greater than 300 μm out of 150 fields from each of the Groups DS, DSS and DD, were 88, 101 and 115, respectively. The difference between the Groups DS and DD was found to be statistically significant ($p = 0.001$) (Table 1).

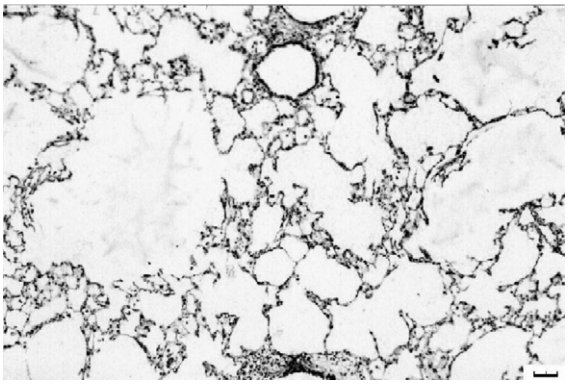

Photo 2. Wide bullous emphysematous areas in Group DD. H&E, scale bar is 100 μm.

Table 1
Number of microscopic fields, which includes at least one emphysematous area with or without longitudinal dimension greater than 300 μm out of 150 microscopic fields are shown in the table (columns "LD > 300 μm" and "LD < 300 μm")

Groups	LD > 300 μm	LD < 300 μm	p
DS	88	62	
DSS	101	49	0.120*
DD	115	35	0.001**

* $p > 0.05$ (Chi-square test is used for comparing with DS).
** $p < 0.05$ (Chi-square test is used for comparing with DS).

4. Discussion

In our study, the time interval between the death and the autopsy changed from 90 to 120 min. Therefore, the study may not be a good model for fatal diving accidents where the body is rescued after a substantial period of time underwater. Typical morphological signs of drowning (e.g. upper airway froth, emphysema aquosum, subpleural and intrapulmonary hemorrhages) may not be present when the body is in an advanced stage of putrefaction [6]. But the mechanical effect of the expanding air remained in the lung may be noticeable in the autopsy of the bodies, in case of drowning under pressure, even after a longer time.

Pulmonary barotrauma is a form of diving disease, which may be fatal and may cause similar findings as the findings in our study, such as pneumothorax, parenchymal hemorrhage, interstitial emphysema and rupture of alveolar walls. In such an accident it might be possible to find embolized gas in cardiovasculatory system. In this case, the detection of oxygen in embolized gas may differentiate deaths due to pulmonary barotrauma from those with post-mortem pulmonary damage [7]. In such cases radiological examination by modern digital cross-sectioning techniques, such as magnetic resonance imaging and multislice computed tomography are valuable measures to detect gas bubbles in blood vessels and various tissues [8]. In our model, pulmonary damage occurred after the death of the rats and it is unlikely that the gas bubbles enter into the blood vessels since the circulation ceased beforehand.

In a fatal diving accident, the death might not have occurred where the body was found. In investigating a fatal diving accident it is critical to know if the death occurred under pressure (at depth) or not (at surface). While a positive buoyant body may sink after the occurrence of death at the surface, a negative buoyant body may come to the surface after the death of the person at the bottom. Bühlmann has reported that heavy streaming and obstacles, exhaustion, hypothermia, misestimation and panic reactions, technical problems, a loss of consciousness due to pre-existing medical condition, suicide, hyperoxia and nitrogen narcosis may lead to drowning [9]. In some of these conditions, such as hyperoxia and nitrogen narcosis, the divers should be under pressure when they died. In such accidents pulmonary autopsy findings may give an idea if the last breath was taken under pressure or not. In this study, we

found that pulmonary autopsy findings in the rats drowned under pressure (Group DD) were significantly different than those drowned under normobaric conditions (Groups DS and DSS), due to mechanical damage of the expanding air in the lungs of Group DD during decompression. The number of wide bullous emphysematous spaces was higher in Group DD, which could be interpreted as an effect of high-pressure (2.5 ATA). There were also the same size emphysematous spaces in Groups DS and DSS although fewer than in Group DD. Therefore, in practical case-work, the detection of large emphysematous areas in the lung cannot be considered as a decisive finding and evaluation should also include necropsy findings. There were erythrocytes and proteinous, amorphous, eosinophilic material in the alveolar spaces of the rats in Group DSS. We believe that the negative pressure in some air containing alveoli as a result of increased environmental pressure after drowning caused this erythrocytes and material leakage into the alveolar space. General histological features in all of the groups such as the over-expansion of the alveoli, flattening of the epithelia, thinning and rupture of the interalveolar walls, emphysema aquosum were in accordance with the findings in the study done by Brinkmann et al. [10].

If pulmonary autopsy findings after a fatal diving accident imply that the drowning has occurred at the surface, then the possibilities such as decompression sickness, external traumatic events, pre-existing medical problems or hypothermia might be underlying reasons for drowning. However, if the findings suggest that the last breath was taken under pressure, then the factors such as equipment failure, nitrogen narcosis, oxygen toxicity, panic reaction or obstacles at the bottom, etc., might be the initiating factors for fatal diving accident.

5. Conclusion

We conclude that in investigating the fatal diving accidents, pulmonary autopsy findings will give valuable information clarifying if the death occurred at the surface or at depth.

Acknowledgment

We would like to thank you Turkish Underwater and Hyperbaric Medical Society for supporting the study.

References

[1] A.A. Bühlmann, Phsiologie und Pathophysiologie des Tauchens, Schweiz Z Sportmed 29 (1981) 5–11.
[2] W.P. Morgan, Anxiety and panic in recreational scuba divers, Sports Med. 20 (1995) 398–421.
[3] D.H. Elliott, P.B. Bennett, Underwater accidents, in: Peter Bennett, David H. Elliott (Eds.), The Physiology and Medicine of Diving, W.B. Saunders Company Ltd., 1993, pp. 238–252.
[4] I.M. Calder, A method for investigating specialised accidents with special reference to diving, Forensic Sci. Int. 27 (1985) 119–127.
[5] W.U. Spitz, Drowning, in: W.U. Spitz (Ed.), Spitz and Fisher's Medicolegal Investigation of Death, Charles C. Thomas, Springfield, 1993 pp. 498–516.
[6] B. Knight, Forensic Pathology, Edward Arnold, London, 1991 pp. 360–374.
[7] I. Pedal, Autopsie und Histologie nach Todesfallen beim Sporttauchen, in: M. Oehmichen, U. van Laak, K. Püschel, M. Birkholz (Eds.), Der Tauchunfall, Schmid-Römhild, Lübeck, 1994, pp. 129–140.
[8] T. Plattner, M.J. Thali, K. Yen, M. Sonnenschein, C. Stoupis, P. Vock, K. Zwygart-Brügger, T. Kilchör, R. Dirnhofer, Virtopsy-postmortem multislice computed tomography (MSCT) and magnetic resonance imaging (MRI) in a fatal scuba diving incident, J. Forensic Sci. 48 (6) (2003) 1347–1355.
[9] A.A. Bühlmann, Tauchmedizin, fifth rev. ed., Springer, Berlin, 2002 .
[10] B. Brinkmann, G. Fechner, K. Puschel, Lung histology in experimental drowning, Z Rechtsmed 89 (4) (1983) 267–277.

ELSEVIER

Forensic Science International 164 (2006) 126–130

Forensic Science International

www.elsevier.com/locate/forsciint

Stability of Δ^9-tetrahydrocannabinol (THC) in oral fluid using the Quantisal™ collection device

C. Moore *, M. Vincent, S. Rana, C. Coulter, A. Agrawal, J. Soares

Immunalysis Corporation, 829 Towne Center Drive, Pomona, CA 91767, United States

Received 30 August 2005; received in revised form 6 December 2005; accepted 6 December 2005
Available online 19 January 2006

Abstract

This article details the stability of Δ^9-tetrahydrocannabinol (THC) in oral fluid during collection, extraction and storage. Oral fluid is being increasingly used as the specimen of choice for the detection of drug use in various applications. Studies to determine the extraction efficiency of THC from the collection buffer and stability under various laboratory storage conditions were carried out. THC was extracted from the collection pad and buffer with an average efficiency over 80% and was stable in Quantisal™ oral fluid extraction buffer when stored at refrigerated temperatures. Fluorescent lighting caused THC losses of over 50%, however the presence of the pad reduced the loss. In the dark, the loss of THC at room temperature was approximately 20% over 14 days. When stored with the serum separators in place, THC losses were significant. After 3 days, THC concentration was reduced by almost 30%, and after 14 days, 60% of the drug was lost and the losses were not concentration dependent.

Keywords: Oral fluid; Tetrahydrocannabinol; Stability

1. Introduction

Oral fluid is becoming increasingly popular in many areas of drug testing as a diagnostic fluid, partly due to the ease and non-invasiveness of collection [1]. Applications for oral fluid analysis are being reported in roadside testing [2,3], epidemiological studies [4,5] and in clinical settings [6,7].

Δ^9-tetrahydrocannabinol (THC) is the predominant analyte detected in oral fluid following marijuana ingestion [8]. The concentrations detected are generally low in the hours after smoking. Huestis and Cone reported high concentrations (5800 ng/mL) immediately after intake, but within 12 h, the oral fluid THC concentration had declined below 1 ng/mL [9]. Kintz et al. [10] described a wide range of concentration from 1 to 103 ng per collection device (in this case, a Salivette). There is concern regarding the stability of the drug since THC adheres to polystyrene surfaces, and degrades during storage. While data regarding THC in oral fluid is limited, the drug in other matrices has been widely studied. As long ago as 1984, Johnson et al., reported significant loss of THC from whole blood when stored in silanized glass tubes at room temperature after 2 months, while the samples stored at 4 and −10 °C were relatively stable. After 6 months at room temperature the THC had degraded by as much as 90% [11]. Christophersen [12] reported that the concentration of THC in blood stored frozen, for 4 weeks at −20 °C, was relatively unchanged, but when stored in polystyrene containers, the loss was 60–100%. Two research groups looked at the loss of the THC metabolite, THC–COOH, in various types of glass or plastic containers, both concluding that at refrigerated temperatures, the losses of the metabolite were minimized [13,14].

Oral fluid using the Quantisal™ collection system is stored in buffer in a polypropylene tube. Since in some situations, the specimen may need to be re-analyzed some time after the original test, the storage of the specimen is a key issue. The present study reports on the stability of THC in collection buffer under various conditions.

2. Materials and methods

2.1. Materials

Quantisal™ collection devices were obtained from Immunalysis Corporation (Pomona, CA). Δ^9-Tetrahydrocannabinol

* Corresponding author. Tel.: +1 909 482 0840; fax: +1 909 482 0850.
E-mail address: cmoore@immunalysis.com (C. Moore).

0379-0738/$ – see front matter
doi:10.1016/j.forsciint.2005.12.011

(THC) and tri-deuterated Δ^9-tetrahydrocannabinol (d3-THC) were obtained from Cerrilliant (Round Rock, TX). Solid-phase extraction columns (Trace-N, Part #TN-315C) were obtained from SPEWare (San Pedro, CA). All solvents were of HPLC grade and chemicals were of ACS grade or better. The derivatizing agent, *N*,*O*-bis trimethylsilyl]trifluoroacetamide + 1% trimethylchlorosilane (BSTFA + 1% TMCS) was obtained from Pierce Chemical Co. (Rockford, IL).

2.2. Methods

Multiple Quantisal™ collection devices were selected from different lots. Each device contained 3 mL of buffer. The oral fluid collector incorporated a volume indicator, which turned blue when 1 mL of oral fluid (±10%) had been collected. Therefore, approximately 4 mL of specimen was available for analysis. The oral fluid concentration was diluted 1:3 due to the presence of the buffer. A synthetic oral fluid matrix, which matched the immunoassay responses of three human negative oral fluid samples was prepared, comprising 25 mM phosphate buffered saline (pH 7.0), 30 mM sodium bicarbonate, 0.1% albumin, amylase and 0.1% Proclin 300 as a preservative. Synthetic oral fluid was fortified with THC at various concentrations, then the pad was dipped into the oral fluid until 1 mL had been absorbed. The pad was then placed into the extraction buffer.

2.2.1. Extraction procedure

Quantisal™ buffer (2 mL, equivalent to 0.5 mL neat oral fluid) was removed from the collector. Deuterated d3-THC (40 μL of a 1 μg/mL solution) was added to each sample giving an internal standard concentration of 20 ng/mL, and 0.1 M sodium acetate buffer (pH 4.5, 1 mL) was added to the samples.

The solid-phase extraction columns were conditioned with methanol (0.5 mL) and 0.1 M acetic acid (100 μL). The samples were poured into the columns at a flow rate of 1 mL/min. The columns were washed with deionized water:acetic acid (80:20, 1 mL) followed by deionized water:methanol (40:60, 1 mL). The columns were dried for 5 min at 30 psi. The THC was eluted using hexane:glacial acetic acid (98:2, 0.8 mL), and the eluent evaporated to dryness. The samples were reconstituted in ethyl acetate (50 μL) and transferred into auto sampler vials. The derivatizing agent, BSTFA + 1% TMCS (20 μL) was added, and the vials were capped. The specimens were heated at 60 °C/15 min prior to analysis using gas chromatography–mass spectrometry (GC/MS). With each assay, a complete calibration curve was analyzed using concentrations of 0, 1, 2, 4 and 8 ng/mL THC.

2.2.2. Analytical procedure

An Agilent Technologies 6890 gas chromatograph coupled to a 5973 mass selective detector (MSD) operating in electron impact mode was used for analysis (GC/MS). The system was capable of fast gas chromatography and incorporated an inert source.

The gas chromatographic column was 5% phenyl–95% methyl silicone DB-5, 0.25 mm ID, 0.25 μm film thickness, 15 m length (J&W Scientific, Palo Alto, CA) and the injection temperature was 250 °C. The injection volume was 2 μL and the injection mode was splitless. The oven was programmed from 125 °C for 30 s; ramped at 40 °C/min to 250 °C, where it was held for 1.3 min; then ramped at 70 °C/min to 300 °C. The transfer line was held at 280 °C, the MS source was held at 230 °C and the quadrupole at 150 °C. The ions monitored were 374.2 and 389.3 for deuterated THC; 371.2, 386.2 and 303.1 for THC. The limit of quantitation of the assay was 1 ng/mL and the limit of detection was 0.5 ng/mL. The accuracy of the assay at 2 ng/mL was −0.03 ng/mL (98.3%) and the precision was 2.57% ($n = 5$).

2.2.3. Fortification of oral fluid

While it is true that very high concentrations of THC can be detected immediately after smoking, the concentrations of THC at 4 and 8 ng/mL were selected for our study since they approximate the levels found in samples from marijuana users hours after smoking. Losses from a collection device are much more of an issue at low levels than high, since any degradation may cause false negative results. Additionally, the United States Federal Drug Testing proposals for THC in oral fluid suggest a cut-off concentration of 2 ng/mL so our fortified samples were at twice and four times the cut-off.

2.2.4. Stability assessment

Separate experiments were carried out to assess the stability of THC under various conditions:

A. Stability of THC when collected with the Quantisal™ device.
B. Effect of collection pad under fluorescent light and in the dark.
C. Effect of serum separator tube.

2.2.4.1. Stability of THC when collected with the Quantisal™ device. Oral fluid (1 mL) containing THC at a concentration of 8 ng/mL, was collected by the pad, and the pads were placed in the extraction buffer. The devices were separated into two groups, one set was refrigerated (2–8 °C) and one set remained at room temperature. Immediately before analysis, the pads were separated using a serum separator provided with the kit. Three devices were analyzed at each time point over 14 days. The Day 1 time-point is the specimen having being stored overnight following spiking, to reflect delivery time to a laboratory.

2.2.4.2. Effect of collection pad under fluorescent light and in the dark. Three sets of devices were selected for each experimental group. Oral fluid (1 mL) containing THC at a concentration of 8 ng/mL was spiked onto individual collection pads, and the pads were placed in the collection buffer. The devices were separated into two groups and kept at room temperature (22–28 °C). One set of collection devices was kept in the dark, separated into sets retaining the pad, and sets with the pad removed. The other set of devices was stored under fluorescent light, separated into those with the pad remaining and those with the pad removed.

Table 1
Loss of THC when stored in oral fluid collection buffer with the pad

Days	Sample 1			Sample 2			Sample 3		
	8 ng/mL	Ext Eff	%Day 1	8 ng/mL	Ext Eff	%Day 1	8 ng/mL	Ext Eff	%Day 1
(a) Refrigerated conditions (2–8 °C)									
1	7.1	89.8	100	6.4	80.5	100	6.3	79.1	100
3	6.5		90.4	6.3		97.9	6.2		98.8
7	6.2		86.3	6.1		94.8	5.9		94.3
10	6.5		90.4	6.4		100	6.3		100
14	6.5		90.5	6.0		94.4	5.8		91.6
(b) Room temperature (22–28 °C)									
1	6.6	83.1	100	6.2	77.8	100	6.5	81.7	100
3	5.7		87.0	5.7		91.6	5.9		93.8
7	5.4		82.1	5.8		94.2	5.3		84.2
10	5.4		81.2	5.1		82.9	5.2		82.6
14	4.7		71.1	5.2		84.7	5.0		79.9

2.2.4.3. Effect of serum separator tube. Three sets of devices were selected for each experimental group. Oral fluid (1 mL) containing THC at two concentrations (4 and 8 ng/mL) was spiked onto individual collection pads, and the pads were placed in the extraction buffer.

Two concentrations were chosen to assess the losses, if any, due to concentration. The samples were stored in the buffer at room temperature overnight, then the pads were separated using serum separator tubes, which remained in the sample. The samples were stored and analyzed at various time points over 14 days.

3. Results

The extraction efficiency for all experiments was calculated by analyzing the samples the day after spiking since THC is known to adhere to surfaces and materials. In this way, the ''Day 1'' value is equivalent to the amount of drug available after collection, and is less than 100% of the spiking solution. The percentage released from the pad is the extraction efficiency of the buffer and is used as a reference point (100%) in order to calculate subsequent losses.

3.1. Stability of THC when collected with the Quantisal™ device

Replicates of three collection devices were analyzed over 14 days. The results are shown in Table 1 and Fig. 1. While the pads were fortified at 8 ng/mL, the recovery on Day 1 (less than 100%) is due to THC binding to the collection pad. The extraction efficiency of THC from the pad into the buffer (Lot #E 3597) was 82% (CV 5.2%), to which the other measurements are compared. When stored under refrigerated conditions, even after 14 days the loss of THC was less than 10% (Table 1a). At room temperature, the THC loss averages 20% after 14 days (Table 1b).

3.2. Effect of collection pad under fluorescent light and in the dark

Collection devices were analyzed over 14 days after storage in the dark and under fluorescent light (Fig. 2), with and without the collection pad being present. The extraction efficiency of THC from the buffer (Lot #E 3906) was 86.9% (CV 1.43%)

When stored under fluorescent lighting, the loss of THC was over 50%, however the presence of the pad reduced the

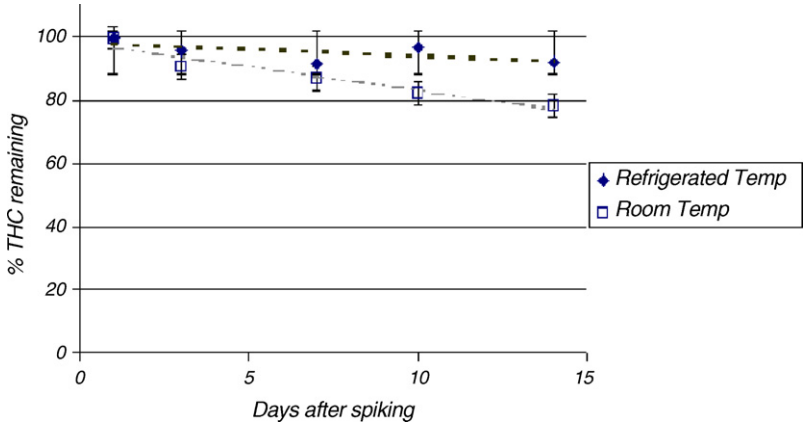

Fig. 1. Variability of THC loss from oral fluid buffer for 14 days at room temperature (22–28 °C) and at refrigerated temperature (2–8 °C); ($n = 3$).

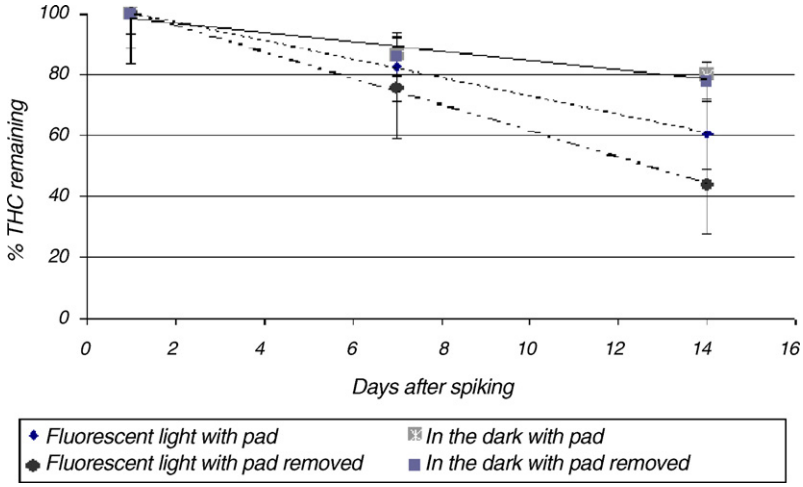

Fig. 2. Stability of THC in oral fluid buffer in the dark and under fluorescent light ($n = 3$).

Table 2
Loss of THC when stored in oral fluid collection buffer under fluorescent light and in the dark (mean values; $n = 3$)

With pad				Without pad			
Days	ng/mL	Ext Eff	%Day 1	Days	ng/mL	Ext Eff	%Day 1
(a) Fluorescent lighting							
1	6.8	85.5	100	1	6.9	86.3	100
7	5.6		82.6	7	5.2		75.6
14	4.1		60.5	14	3.0		43.7
(b) In the dark							
1	7.0	87.6	100	1	7.0	88.2	100
7	6.0		86.2	7	5.9		85.9
14	5.5		79.7	14	5.3		77.5

Table 3
Effect of the serum separator tube (mean values; $n = 3$)

Days	4 ng/mL spike	Ext Eff	%Day 1	8 ng/mL spike	Ext Eff	%Day 1
1	3.8	96	100	6.9	86.5	100
3	2.7		70.3	5		72.2
7	2.0		53.6	3.3		48.5
14	1.4		38.5	2.9		42.4

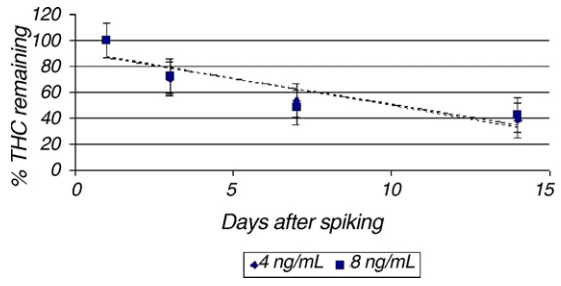

Fig. 3. Stability of THC in oral fluid buffer with the serum separator present ($n = 3$).

loss (Table 2a). When kept in the dark, the loss of THC at room temperature was approximately 20% over 14 days whether the pad was present or not (Table 2b).

3.3. Effect of serum separator tube

When an oral fluid specimen is collected, the pad is placed in buffer for transportation to the laboratory. At the testing facility, a serum separator is used to push down on the pad and release the maximum amount of fluid into the buffer for testing. The separator generally remains in the collection tube after use.

The pads were spiked at both 4 and 8 ng/mL of THC and were stored with the serum separators in the extraction buffer at room temperature, then analyzed at various time points for 14 days (Table 3, Fig. 3). The loss of THC from the specimens was remarkable. Even after 3 days, THC concentration was reduced by almost 30%, and after 14 days, 60% of the drug was lost. The losses were not concentration dependent since both levels were reduced by similar percentages at the same time points.

4. Discussion

Stability is an important consideration in the use of specimens for accurate determination of analyte concentrations. As described in Section 1, the stability of THC in blood and plasma has been reported under various conditions and in different containers. THC degrades at room temperature in plasma or blood, particularly when stored in plastic containers.

This is the first report of stability of THC in the Quantisal™ collection system under different conditions. Crouch [15] reported on the effects of the collection device on drug concentration and stability, but the Quantisal™ was not included in that study. Crouch noted that THC in the Intercept® device was relatively stable for 6 weeks when stored frozen, however, THC stability was marginal under refrigerated conditions and poor at room temperature.

In contrast, our results using the Quantisal™ collection device show that if fluorescent light and plastic surfaces are

avoided (e.g. serum separator is not allowed to remain in the sample) along with refrigeration of the specimen, or storage in the dark, THC extraction is in excess of 80% for the collection buffer and loss due to degradation is less than 20% over 2 weeks, making it a good candidate for oral fluid collection.

5. Summary

In summary, THC is extracted from the collection pad and buffer with an average efficiency over 80% and is stable in oral fluid collection buffer when stored at refrigerated temperatures. Oral fluid specimens must not be stored with the serum separators in place, since the THC adheres to the polystyrene tube and substantial losses are observed. Storage, or extended exposure under fluorescent light must be avoided.

References

[1] R.E. Choo, M.A. Huestis, Oral fluid as a diagnostic tool, Clin. Chem. Lab. Med. 42 (11) (2004) 1273–1287.
[2] S.W. Toennes, G.F. Kauert, S. Steinmeyer, M.R. Moeller, Driving under the influence of drugs – evaluation of analytical data of drugs in oral fluid, serum and urine, and correlation with impairment symptoms, Forensic Sci. Int. 152 (2–3) (2005) 149–155.
[3] N. Samyn, G. De Boeck, A.G. Verstraete, The use of oral fluid and sweat wipes for the detection of drugs of abuse in drivers, J. Forensic Sci. 47 (6) (2002) 1380–1387.
[4] M. Fendrich, T.P. Johnson, J.S. Wislar, A. Hubbell, V. Spiehler, The utility of drug testing in epidemiological research: results from a general population survey, Addiction 99 (2) (2004) 197–208.
[5] T. Johnson, M. Fendrich, Modeling sources of self-report bias in a survey of drug use epidemiology, Ann. Epidemiol. 15 (5) (2005) 381–389.
[6] H. Liu, M.R. Delgado, Therapeutic drug concentration monitoring using saliva samples. Focus on anticonvulsants, Clin. Pharmacokinet. 36 (6) (1999) 453–470.
[7] M. Berkovitch, T. Bistritzer, M. Aladjem, P. Burtin, T. Dagan, Z. Chen-Levi, R. Freedom, G. Koren, Clinical relevance of therapeutic drug monitoring of digoxin and gentamicin in the saliva of children, Ther. Drug Monit. 20 (3) (1998) 253–256.
[8] D.B. Menkes, R.C. Howard, G.F. Spears, E.R. Cairns, Salivary THC following cannabis smoking correlates with subjective intoxication and heart rate, Psychopharmacology (Berlin) 103 (2) (1991) 277–279.
[9] M.A. Huestis, E.J. Cone, Relationship of delta 9-tetrahydrocannabinol concentrations in oral fluid and plasma after controlled administration of smoked cannabis, J. Anal. Toxicol. 28 (6) (2004) 394–399.
[10] P. Kintz, V. Cirimele, B. Ludes, Detection of cannabis in oral fluid (saliva) and forehead wipes (sweat) from impaired drivers, J. Anal. Toxicol. 24 (7) (2000) 557–561.
[11] J.R. Johnson, T.A. Jennison, M.A. Peat, R.L. Foltz, Stability of delta 9-tetrahydrocannabinol (THC), 11-hydroxy-THC, and 11-nor-9-carboxy-THC in blood and plasma, J. Anal. Toxicol. 8 (5) (1984) 202–204.
[12] A.S. Christophersen, Tetrahydrocannabinol stability in whole blood: plastic versus glass containers, J. Anal. Toxicol. 10 (4) (1986) 129–131.
[13] K.D. Roth, N.A. Siegel, R.W. Johnson, L. Litauszki, L. Salvati, C.A. Harrington, L.K. Wray, Investigation of the effects of solution composition and container material type on the loss of 11-nor-delta 9-THC-9-carboxylic acid, J. Anal. Toxicol. 20 (5) (1996) 291–300.
[14] P.R. Stout, C.K. Horn, D.R. Lesser, Loss of THCCOOH from urine specimens stored in polypropylene and polyethylene containers at different temperatures, J. Anal. Toxicol. 24 (7) (2000) 567–571.
[15] D.J. Crouch, Oral fluid collection: the neglected variable in oral fluid testing, Forensic Sci. Int. 150 (2–3) (2005) 165–173.

ELSEVIER

Forensic Science International 164 (2006) 131–137

Forensic Science International

www.elsevier.com/locate/forsciint

Sensitivity of autopsy and radiological examination in detecting bone fractures in an animal model: Implications for the assessment of fatal child physical abuse

C. Cattaneo [a,*], E. Marinelli [a], A. Di Giancamillo [b], M. Di Giancamillo [c], O. Travetti [c], L. Vigano' [a], P. Poppa [a], D. Porta [a], A. Gentilomo [a], M. Grandi [a]

[a] *Istituto di Medicina Legale, Università degli Studi, Milano, Italy*

[b] *Dipartimento di Scienze e Tecnologie Veterinarie per la Sicurezza Alimentare, Università degli Studi di Milano, Italy*

[c] *Dipartimento di Scienze Cliniche Veterinarie e Radiologia Veterinaria Clinica e Sperimentale, Università degli Studi, Milano, Italy*

Received 25 March 2005; received in revised form 30 May 2005; accepted 10 December 2005

Available online 8 February 2006

Abstract

Skeletal injuries are often strong indicators of child abuse and their detection is therefore crucial. The aim of this study was to compare the sensitivity of three diagnostic approaches, namely autopsy, traditional (conventional) radiology, and computed tomography on ''battered'' piglets, in order to verify the sensitivity of each method, with respect to the true number of bone fractures assessed once the piglet was skeletonised (osteological control). Four newborn cadaver piglets who had died from natural causes were severely beaten post-mortem in every district of the body. Traditional radiography, computed tomography (CT) and autopsy were performed. The piglet was then macerated until skeletonised and the number of all fractures present recorded (osteological control).

On the cranium, traditional radiology revealed only 35% circa of actual fractures, autopsy detected only 31% ($P < 0.01$ for both comparisons versus osteological control), whereas CT imaging detected all fractures actually present. For ribs, radiology detected only 47% of all fractures present, and autopsy 65% circa ($P > 0.05$ for both comparisons versus osteological control), while CT scans detected 34% ($P < 0.01$). In suspected cases of fatal child abuse, we suggest that the bones of specific districts be directly analysed either at autopsy or by collecting specific diagnostic sites, such as parts of the rib cage, and subjecting them to maceration. The removed areas could be replaced with artificial material for cosmetic purposes. The authors stress the importance of combined radiological, CT scan, autopsy and osteological survey in the detection of perimortem bone fractures.

Keywords: Bone fractures; Autopsy; Radiology; Osteology; Child physical abuse

1. Introduction

Child abuse, whether it be sexual, physical, psychological or manifested as neglect, is certainly one of the most disconcerting types of crime of our society. In the United States, according to data concerning child abuse and neglect known to child protection agencies, in 2001, 903,000 children experienced or were at risk for child abuse and/or neglect. Fifty-nine percent of these victims suffered neglect, 19% were physically abused, 10% were sexually abused and 7% were emotionally or psychologically abused. Furthermore, 1300 children died from maltreatment: 35% of these deaths were from neglect and 26% from physical abuse [1]. Infants seem to be at greatest risk of homicide during the first week of life, with the highest risk being in the first days [2,3]. However, many researchers and practitioners believe that child fatalities due to abuse and neglect are underreported. This may be due to inaccurate reporting of the number of children who die each year as a result of abuse and neglect, lack of national standards for child autopsies or death investigations and the use in some states of medical examiners who do not have specific child abuse and neglect training.

It is therefore crucial to establish common and thorough guidelines for assessing possibly abused children, both in the

* Corresponding author at: Istituto di Medicina Legale, Università degli Studi, Via Mangiagalli 37, 20133 Milano, Italy. Tel.: +39 02 50315678/9; fax: +39 02 50315724.

E-mail address: cristina.cattaneo@unimi.it (C. Cattaneo).

0379-0738/$ – see front matter © 2006 Published by Elsevier Ireland Ltd.
doi:10.1016/j.forsciint.2005.12.016

hospital and at the autopsy table. It is consequently fundamental to be aware of the sensitivity of investigative tools used, such as clinical observation (for the living), autopsy (for the dead), and radiology.

Regardless of whether one is referring to the living or the dead, bone fractures are perhaps the most important and problematic issue as far as detectability is concerned. According to some authors, skeletal injuries occur in 36–50% of abused children [4,5]. Other authors [6] specify that 76% of cases occur in the first 3 years.

Whereas external and internal soft tissue traumatic injuries will eventually show up at a thorough clinical examination or at the autopsy table, the presence of bone fractures, whose distribution, number, and age are crucial, is not as easy to detect, particularly if very recent or if inflicted in the circumstances of a lethal event and therefore just barely ante-mortem. Furthermore, if the detection of bone fractures is difficult in the living, where signs of soft tissue inflammatory reactions and bone callus formation may be present, the problem becomes even more difficult when the child dies immediately after the abuse. In this case signs of child abuse may consist of very subtle soft tissue lesions and especially bone fractures—the latter being, at times, particularly difficult to detect when healing processes (and therefore callus formation) have not taken place. Furthermore, haemorrhaging of surrounding soft tissues may be slight and barely detectable upon autopsy, particularly in the paravertebral and posterior vertebral regions (e.g. costo-spinal junction, transverse processes, spinous processes), or, if present, can be hidden by decomposition processes which in the case of infants are particularly rapid. In other words, regardless of whether we are dealing with shaken baby syndrome or other forms of physical child maltreatment which involve blunt force injury, it may be difficult yet crucial to identify a bone fracture upon autopsy or radiological assessment.

In actual fact, it is not known precisely how sensitive such procedures are: physical markers of trauma may go undetected through clinical and radiological assessment because of the low sensitivity of some diagnostic protocols, particularly autoptic and radiological ones. Regardless of their site, frequency and distribution [7–9], it is evident that bone fractures are a frequent event and must be looked for.

Advantages and limitations of several methods of assessing the living have been studied. The limits of scintigraphy [10] and MRI technology [11] are well known in the living and are inapplicable in practice on dead bodies. Belfer et al. [12] on a population of 203 living children found that skeletal survey for occult fractures was crucial in suspected cases. Kleinman et al. 1988 [13] showed how much more sensitive bone scans can be with respect to detecting posterior rib fractures. However, very little literature exists on the actual sensitivity of autopsy and radiology for the detection of recent bone fractures. Such studies obviously need to be performed on dead bodies.

Kleinman et al. [14] performed a study on 78 ribs removed from seven infants who had died with posterior rib fractures, by in situ radiography and computed tomography. Results showed that frontal radiography was insensitive in identifying these fractures and revealed only periosteal reaction (healing processes). Furthermore, CT scans were better for detecting fractures at the costovertebral junction but were less sensitive for fractures of the rib head.

Williamson and Perrot [15] tried to correlate radiographic findings with those found at autopsy in 108 cases of dead infants, showing that routine autopsy would have missed fractures detected radiologically. Kleinman and Schlesinger [16] studied the detectability of artificially produced rib fractures on humans and rabbits but focused only on the biomechanics of posterior rib fractures. Thomsen et al. [17] in their study on 28 children showed that rib fractures and metaphyseal fractures may not be detected at gross examination and therefore X-rays should performed. Finally, Klotzbach et al. [18] applied a protocol, on three cases of fatal physical child abuse, which involved autopsy, radiography (including contact radiography of suspected lesions) and histology for detecting and aging bone fractures.

All the above-mentioned studies assess the advantages of different types of radiological techniques or of combined traditional radiological and histopathological techniques. No study has however verified the actual sensitivity of radiology, CT scan and autopsy on control cases. In order to do this it is in fact necessary to verify, after radiological assessment, all fractures which are actually present on bone by studying the cleaned skeleton.

The aim of this study was therefore to compare three diagnostic approaches, namely autoptic, radiological and tomographic, on simulated battered cases of piglets, in order to assess the sensitivity of each method with respect to the true number of bone fractures observable once the piglet was macerated and skeletonised.

2. Materials and methods

2.1. Animals

Four 3-kg newborn piglets, who had died under the weight of the mother or of natural causes, were acquired under the authorisation of the Azienda Sanitaria Locale (ASL) and severely beaten (post-mortem) in every district of the body. The thoracic region was severely compressed antero-posteriorly and latero-laterally and cranium and limbs were beaten with a hammer. This random approach was aimed at producing the maximum number of fractures. Dynamics were not taken into consideration since the goal of the study was not to verify the mode of production of fractures but simply to maximize their number and distribution in order to check the sensitivity of the applied tests.

A negative control piglet, with no lesions, was also included in the study.

2.2. Radiological assessment

2.2.1. Traditional radiography

Traditional radiography was performed first, followed by CT scanning. The piglet's body was divided into four different

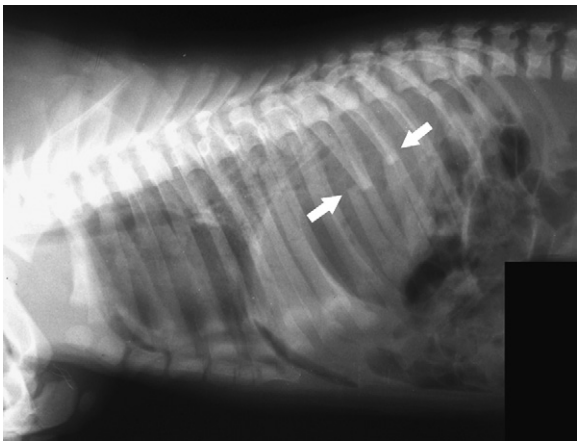

Fig. 1. Traditional radiography. Latero-lateral view of the thorax: note the superimposed multiple rib fractures (arrows).

body regions as follows: head, ribs, anterior limbs and posterior limbs. All piglets underwent two-view radiographic series of the head (latero-lateral and ventro-dorsal views) and limbs (medio-lateral and cranio-caudal views), perpendicular to eachother. Another series of four projections for the thorax, namely latero-lateral, ventro-dorsal, right 45° ventral-left dorsal oblique and left 45° ventral-right dorsal oblique, was performed (the first two and last two projections are, also, perpendicular to eachother). All radiographs were interpreted by at least two radiologists, and the numbers of fractures per region recorded. Fractures were diagnosed when radiotransparencies in the bones were identified (Figs. 1–3).

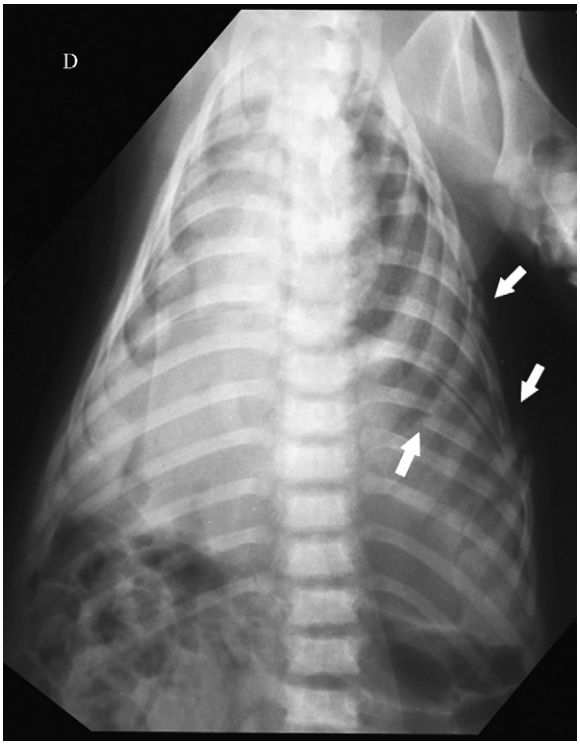

Fig. 2. Traditional radiography. Ventro-dorsal view of the thorax: it is possible to detect the exact localization of the left rib fractures at the level of 5th, 6th, 7th, 8th, 9th, 10th, 11th and 12th ribs (arrows).

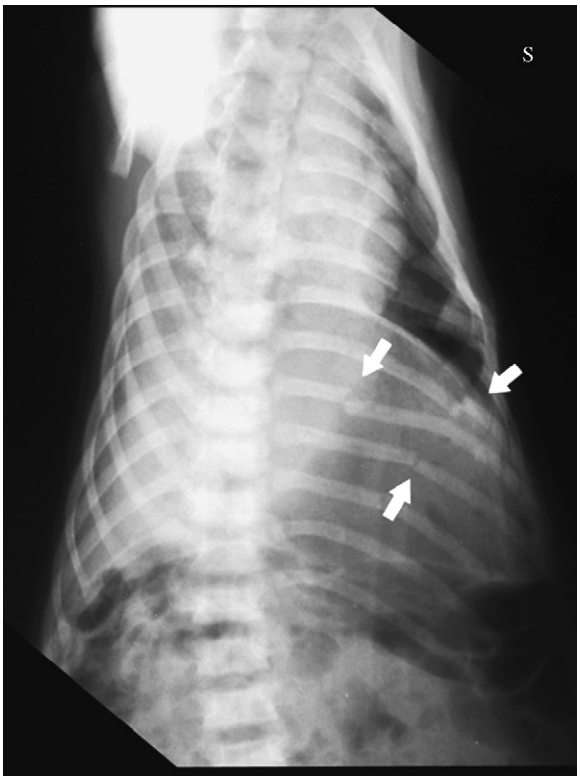

Fig. 3. Traditional radiography. Right 45° ventral-left dorsal oblique views of the thorax: it is possible to detect the exact localization of the left rib fractures at the level of 5th, 6th, 7th, 8th, 9th, 10th, 11th and 12th ribs (arrows).

2.2.2. Helical CT scan examination

All piglets subsequently underwent helical CT (PQ 2000S, Philips) of the whole body, and diagnosis of bone fractures was based on identifying low-density areas. Vertical and horizontal scout scans of the entire body were performed on each piglet. Piglets were imaged in the supine position and the forelegs extended flat on the table, except for the head which was in the prone position.

Typical scan parameters were: thick/index 3 mm, pitch 1:1, scan time 1.0 s, tube potential 120 kV and mA was 150 for the head and 175 for ribs and legs. Hard tissue algorithms were always employed.

The imaging study data were obtained from the imaging reports made before autopsy and osteological analysis. All CT scans were interpreted by at least two radiologists, and the numbers of fractures per region recorded (Fig. 4).

2.3. Autopsy

Autopsies were performed by two pathologists on all piglets applying the most thorough protocol suggested in these cases. First a linear incision was made from the chin to the pubic symphysis; then standard detachment of soft tissues from the thorax allowed exploration of the ribs and clavicle anteriorly. After sternotomy, standard evisceration was performed. Posteriorly, a Y-shaped incision was performed in order to reveal scapulae and spinal processes, from the nuchal crest to the sacrum. The cranial vault was exposed via a saggital

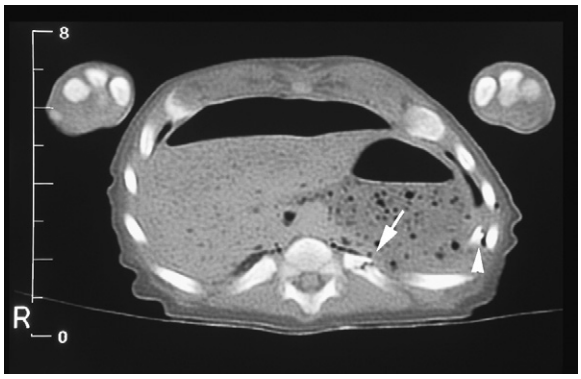

Fig. 4. Computed tomography. CT scan obtained at the level of the 10th vertebral body where a paravertebral fracture of the 10th left rib can be seen (arrow). On the same image one can recognize a second line of fracture and fragment of the 9th rib (arrowhead).

incision of the skin. Long bones were explored by a vertical incision of the front and hind limbs. All visible fractures were then recorded (Fig. 5).

2.4. Osteological assessment

After autopsy all the piglets were macerated until full skeletonisation was reached. The skeleton was then remounted anatomically and all visible fractures were recorded (bone, site, number) (Fig. 6).

Due to their high number, fractures were grouped as pertaining to the head; anterior limbs; posterior limbs; ribs.

2.5. Statistical analysis

Statistical analysis of the data was performed using SAS statistical software [19]. All numerical results were expressed as means ± pooled S.E. Differences between means were evaluated by two-way ANOVA, where skeletal regions and techniques were the main factors. Homogeneity of variances was checked. When variances were heterogeneous, logarithmic transformations of individual values were used before statistical analysis. Logarithmic estimates were converted to number

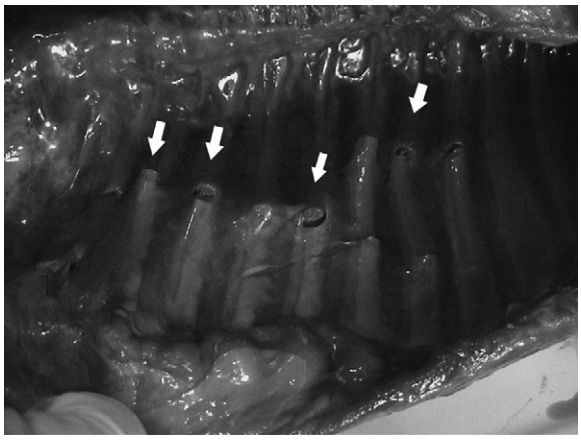

Fig. 5. Autopsy. Exploration of the thoracic cavity: note the numerous rib fractures, some of which are indicated by the arrows.

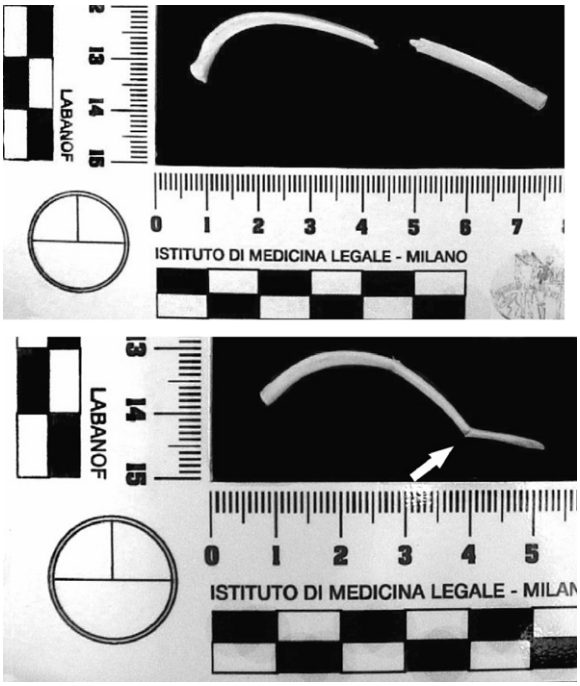

Fig. 6. Osteological control. Skeletonised ribs: example of complete (a) and incomplete (b) bone fractures.

of fractures. Differences were considered significant when $P < 0.05$.

3. Results

The total number of fractures actually present on the skeletons of the 4 piglets was 110 (26 on the cranium, 62 on the ribs, 11 on anterior limbs and 11 on posterior limbs).

Comparisons between traditional radiography, computed tomography, autopsy and osteological analysis in the detection of bone fractures are summarised in Fig. 7.

From Fig. 7 one can notice that on the cranium, traditional radiology showed about 35% of actual fractures, autopsy detected only 31%, whereas there is a flawed result for CT scans, where more fractures were recorded with respect to single linear fractures present at osteological control. For ribs (thorax), radiology detected only 47% of all fractures present, CT scans 34% and autopsy about 65%. No fractures were present on the vertebrae. All fractures were detected by all methods on posterior limbs, whereas for anterior limbs radiology and CT scans detected only 73% of fractures and autopsy only about 91%.

From a statistical point of view, keeping in mind however the low number of fractures for some districts, there were no significant differences in the number of fractures detected with the different diagnostic techniques both for posterior limbs and anterior limbs. Detectability of fractures induced in cadaver piglet heads with CT from a statistical point of view did not differ from the osteological control ($P > 0.05$), whereas traditional radiology and autopsy proved to be less efficient in a statistically significant manner ($P < 0.01$). Detection of rib fractures by autopsy did not differ from osteological analysis

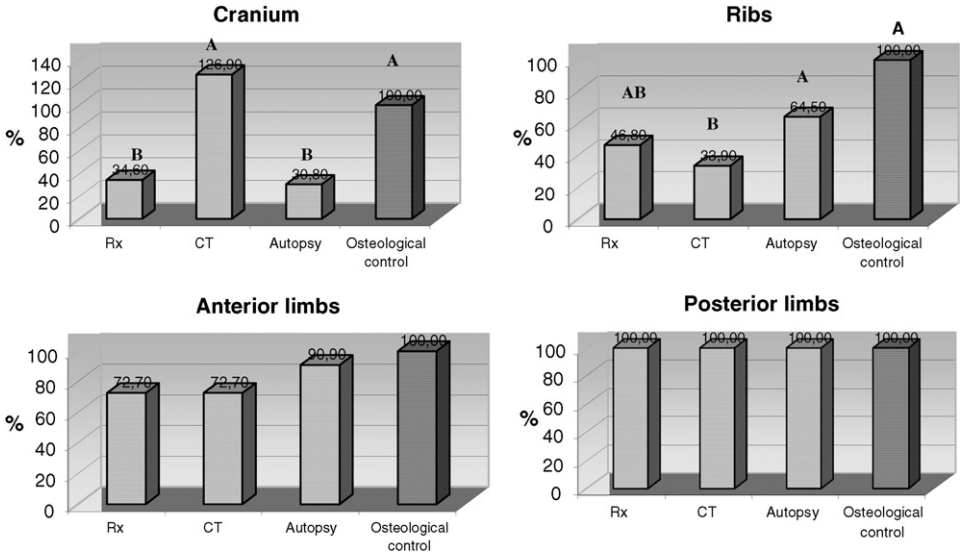

Fig. 7. Fractures detected in the various anatomical regions expressed as percentage of total fractures present in the osteological control. The histograms show the percentage of fractures detected by the methods Rx (traditional radiology), CT (computed tomography) and autopsy with respect to the sum total (100%) found upon osteological analysis. A, B differ significantly ($P < 0.01$).

($P > 0.05$), but detectability by CT scan was significantly lower ($P < 0.01$); furthermore, there were no statistically significant differences between traditional radiography, autopsy and the osteological control.

4. Discussion

In this study, the sensitivity of autopsy and radiological procedures in detecting bone fractures was assessed. A thorough autopsy, radiological and CT protocol was applied on beaten dead piglets. Results were then compared to the true number of fractures present, visible after skeletonisation of the piglets. Although this study, which was performed on dead animals, does not reflect the actual ante-mortem situation, and although there are significant anatomical differences between piglets and human infants, it does provide useful and interesting information on the sensitivity of the autopsy and of this particular kind of radiological assessment.

The most interesting results concern the cranium and the thorax (ribs in particular). No statistically significant differences were found among the techniques applied as concerns the number of fractures recorded both in anterior limbs and posterior limbs ($P > 0.05$), confirming that traditional radiology was valid in detecting bone fractures at these sites. Results concerning the cranium were quite complicated to interpret. Autopsy and traditional radiology detected only about one-third of all fractures present. As far as the autopsy is concerned, this is due to the fact that many fractures on the facial skeleton obviously go undetected. Traditional radiology, on the other hand, may present problems in interpreting superimposed bone structures which can cause one to underestimate the number of actual fracture lines present. CT scans, on the other hand, showed an excess of fractures: this error depends on the orientation of the CT slice with respect to the orientation of the fracture line. Furthermore on CT scans it is very difficult to distinguish between a single long fracture and shorter linear fractures which closely follow one another, and this may lead to an overestimation of the number of fractures. Detectability of fractures induced in cadaver piglet heads revealed to be good with CT scans (disregarding the risk of excess in scoring) when compared to osteological analysis, but statistically significant differences were seen with traditional radiology and autopsy. These results show a lack of sensitivity of traditional methods, which may be alarming. The infant skull consists of extremely thin bones that lack the rigidity and strength of adult ones. In addition, the bones of the infant skull are separated by loose cranial sutures. Consequently, the immature skull is fairly resistant to fracturing except in the setting of significant trauma [20]. The presence of fractures in infants is thus a strong indicator of relevant trauma. Results of this study seem to indicate that all infants and children with suspected cranial injury should undergo, especially prior to autopsy, cranial CT scan, as already suggested by the American Academy of Pediatrics [21]. In the case of cadavers, osteological analysis should also be recommended, although it may be impossible to apply for body conservation purposes.

Even more alarming are the results concerning rib fractures. The importance of rib fractures in the diagnosis of child abuse has been appreciated for a long time [22–26]. Rib fractures are lesions which are highly specific for infant abuse [27–29] and are reported as 5–27% of all fractures occurring in abused children [30,31]. They are therefore crucial. In our study, the detection of all rib fractures proved difficult. Traditional radiology detected only 47%: this may be due to anatomical superimposition in the orientations adopted (which however were those suggested by the literature), or to the small size of the bones, combined with the lower contrast present due to lack of air in the underlying lungs. CT scans detected only 34%, regardless of the use of helical CT scanning: this low sensitivity

could be due to the orientation of the scan direction, with respect to rib curvature, which does not allow for an in toto observation of every single rib. Autopsy detected only 65%: in this case it should be stressed that because fractures were produced post-mortem there were no vital soft tissue reactions to guide the pathologist in looking for an underlying fracture. Thus in the case of fractures induced ante-mortem the score could be higher. Nonetheless, one should keep in mind that haemorrhaging, at times, in soft tissue may not be evident, particularly in the posterior paravertebral regions and in decomposed bodies.

This study has therefore shed some light on the possible limits of autopsy, traditional radiology and CT scans in detecting all bone fractures truly present.

Autopsy and traditional radiographs have the advantage of being easily performed and interpreted. Furthermore, radiographs may easily detect calluses and therefore reveal old fractures—which is another crucial step in the diagnosis of child physical abuse. It is important to detect all recent perimortem fractures. For this purpose, CT may ameliorate the situation for some regions, but not for all. Careful osteological analysis of particularly ''at risk'' areas may be crucial, and in the case of the rib cage, may be performed by cautiously removing all soft tissue from bone in situ (a time consuming process) or by removing parts of the rib cage and preparing them for osteological analysis. In the latter case, one should then replace the removed area with artifacts for cosmetic purposes.

5. Conclusion

Skeletal injuries are often the strongest indicators of child abuse and their detection is therefore of fundamental importance [21]. It is well recognized that certain patterns of injury are sufficiently characteristic to permit a sturdy diagnosis of inflicted injury [32]. Most infants who die from inflicted injury have fractures at multiple sites, and documenting skeletal injuries in a thorough and systematic way is crucial for establishing the cause and manner of death.

This study confirms the possibly low sensitivity of autoptic and radiological analysis particularly in the detection of all fractures of the cranium and thoracic osseous elements. According to the authors, in cases of suspected fatal physical abuse, the bones of specific districts should be either directly analysed upon autopsy (by peeling off periosteal soft tissue, closely observing articulation sites—a time consuming process) or by collecting specific ''crucial'' sites, such as parts of the rib cage, and replacing them with artificial material for cosmetic purposes. The authors stress the importance of combined radiological, CT scan, autopsy and osteological survey in the study of cases of possible fatal physical child abuse.

Acknowledgments

The authors wish to thank Enrico Silingardi and Alessandro Travetti of the Sezione Cinofila del Corpo Volontari Protezione Civile di Milano for supplying the piglets for this study.

References

[1] National Centre for Injury Prevention and Control. www.cdc.gov/ncipc/default.htm.
[2] Committee on Child Abuse and Neglect, Distinguishing sudden infant death syndrome from child abuse fatalities, Pediatrics 94 (1994) 124–126.
[3] L. Paulozzi, M. Sells, Variation in homicide risk during infancy. United States and 1989–1998, Centers for Disease Control and Prevention, Morbidity Mortality Weekly Rep. 51 (09) (2002) 187–189.
[4] C.J. Hobbs, Skull fracture and the diagnosis of abuse, Arch. Dis. Child. 59 (1984) 246–252.
[5] J.A. Monteleone, Child Maltreatment: A Comprehensive Photographic Reference Identifying Potential Child Abuse, Medical Publishing, St. Louise, 1994.
[6] C.F. Johnson, Inflicted injury versus accidental injury, Pediatr. Clin. N. Am. 37 (1990) 791–814.
[7] J. King, D. Diefendorf, J. Apthorp, V.F. Negrete, M. Carlson, Analysis of 429 fractures in 189 battered children, J. Pediatr. Orthoped. 8 (1988) 585–589.
[8] R.T. Loder, C. Bookout, Fracture patterns in battered children, J. Orthoped. Trauma 5 (1991) 428–433.
[9] P.K. Kleinman, S.J. Marks, J. Richmond, D. Blackbourne, Inflicted skeletal injury: a post-mortem radiologic–histopathologic study, Am. J. Radiol. 165 (1995) 647–650.
[10] J.J. Conway, M. Collins, R.R. Tanz, M.A. Radkowski, E. Anandappa, R. Hernandez, E.L. Freeman, The role of bone scintigraphy in detecting child abuse, Sem. Nucl. Med. 23 (1993) 321–332.
[11] K.W. Feldman, E. Weinberger, J.M. Milstein, C.L. Fligner, Cervical spine MRI in abused infants, Child Abuse Neglect 21 (1997) 199–205.
[12] R.A. Belfer, B.L. Klein, L. Orr, Use of skeletal survey in the evaluation of child maltreatment, Am. J. Emerg. Med. 19 (2001) 122–124.
[13] P.K. Kleinman, S.C. Marks, V.I. Adams, B.D. Blackbourne, Factors affecting visualization of posterior rib fractures in abused infants, Am. J. Radiol. 150 (1988) 635–638.
[14] P.K. Kleinman, S.C. Marks, M.R. Spevak, J.M. Richmond, Fractures of the rib head in abused infants, Radiology 185 (1992) 119–123.
[15] S.L. Williamson, L.L. Perrot, The significance of postmortem radiographs in infants, J. For. Sci. 35 (1990) 365–368.
[16] P.K. Kleinman, A.E. Schlesinger, Mechanical factors associated with posterior rib fractures: laboratory and case studies, Pediatr. Radiol. 27 (1997) 87–91.
[17] T.K. Thomsen, B. Elle, J.L. Thomsen, Post-mortem radiological examination in infants: evidence of child abuse? Foren. Sci. Int. 90 (1997) 223–230.
[18] H. Klotzbach, G. Delling, E. Richter, J.P. Sperhake, K. Püschel, Post-mortem diagnosis and age estimation of infants' fractures, Int. Leg. Med. 117 (2003) 82–89.
[19] SAS Institute Inc., Version 8, SAS Institute, Cary, NC, 2000.
[20] J.A. Lancon, D.E. Haines, A.D. Parent, Anatomy of the shaken baby syndrome, New Anat. 253 (1998) 13–18.
[21] American Academy of Pediatrics, Diagnostic imaging of child abuse, Paediatrics 105 (2000) 1345–1348.
[22] F.W. Smith, D.L. Gilday, J.M. Ash, M.D. Green, Unsuspected costo-vertebral fractures demonstrated by bone scanning in the child abuse syndrome, Pediatr. Radiol. 10 (1980) 103–106.
[23] E.F. Lis, G.S. Frauenberger, Multiple fractures associated with subdural hematoma in infancy, Paediatrics 6 (1950) 890–892.
[24] P.V. Woolley Jr., W.A. Evans, Significance of skeletal lesions in infants resembling those of traumatic origin, JAMA 158 (1955) 539–543.
[25] A. Marie, Hematome sousdural du nourrisson associe a des fractures des membres, Semaine Hospitale 30 (1954) 1757.
[26] F. Silverman, Roentgen manifestations of unrecognized skeletal trauma in infants, Am. J. Roentgenol. 69 (1953) 413–426.
[27] J.M. Cameron, L. Rae, The radiological diagnosis, in: J.M. Cameron, L. Rae (Eds.), Atlas of the Battered Child Syndrome, Churchill Livingstone, London, England, 1975, pp. 20–50.
[28] P.S. Thomas, Rib fractures in infancy, Ann. Radiol. 20 (1977) 115–122.

[29] P.K. Kleinman, S.C. Marks, B.D. Blackbourne, The metaphyseal lesion in abused infants: a radiologic–histopathologic study, Am. J. Radiol. 146 (1986) 895–905.
[30] B. Akbarnia, J.S. Torg, J. Kirkpatrick, S. Sussman, Manifestations of the battered-child syndrome, J. Bone Joint Surg. Am. 56 (1974) 1159–1166.
[31] I.R. Barret, K. Kozlowski, The battered child syndrome, Australas. Radiol. 23 (1979) 72–82.
[32] P.K. Kleinman, Skeletal imaging strategies, in: E. Corra (Ed.), Diagnostic Imaging of Child Abuse, Mosby-Year Book Inc., Missouri, 1998 , pp. 237–241.

ELSEVIER

Forensic Science International 164 (2006) 138–147

Forensic Science International

www.elsevier.com/locate/forsciint

Synthesis by-products from the *Wacker* oxidation of safrole in methanol using ρ-benzoquinone and palladium chloride

M. Cox [a,*], G. Klass [b]

[a] *Forensic Science South Australia, 21 Divett Place, Adelaide, 5000 SA, Australia*

[b] *University of South Australia, City West Campus, 61-73 North Terrace, Adelaide 5000 and Mawson Lakes Campus, Mawson Lakes Boulevard, Mawson Lakes, SA 5095, Australia*

Received 25 May 2005; received in revised form 13 December 2005; accepted 15 December 2005
Available online 25 January 2006

Abstract

This paper reports the identification of a number of by-products, which are produced during the *Wacker* oxidation of safrole to 3,4-methylenedioxyphenyl-2-propanone (MDP2P) using ρ-benzoquinone and palladium chloride when methanol is utilised as the solvent. Also described is the retrieval of these compounds from illicit samples from a clandestine laboratory, which was uncovered in South Australia in September 2003.

Keywords: Safrole; MDP2P; 3,4-Methylenedioxymethamphetamine; By-products; *Wacker* oxidation

1. Introduction

Most of the 3,4-methylenedioxymethamphetamine (MDMA) available in Australia is produced in clandestine laboratories in The Netherlands and Belgium [1]. We have recently observed a resurgence of clandestine laboratories engaged in the manufacture of MDMA within South Australia, with four ecstasy laboratories having been uncovered in the years 2003 and 2004. *Wacker* oxidation of safrole to 3,4-methylenedioxyphenyl-2-propanone (MDP2P) using palladium chloride, ρ-benzoquinone and methanol was being utilised at one of the laboratories (Scheme 1).

Many unknown components were encountered in the gas chromatograms (GCs) of samples taken from the scene and we have since attempted to unambiguously identify some of these unknown compounds.

It was thought that some of these compounds may be route specific and as such, their identification may aid in the determination of the method by which an illicit drug might be manufactured. For example linking or discriminating information might be required to establish a connection between a drug seizure found in possession of a suspect with another batch of drugs or with the source laboratory. Manufacturing information also gives law enforcement agencies an indication as to which chemicals should be subject to sales control and monitoring. A number of papers have been devoted to the route specific markers associated with the various different synthetic routes to 3,4-methylenedioxyamphetamine and 3,4-methylenedioxymethamphetamine but at this stage it appears that the production of the precursor MDP2P via the *Wacker* oxidation of safrole has received little attention [2–11].

The goals of this work included the synthesis of the anticipated by-products and their comparison with the unidentified by-products from the *Wacker* oxidation of safrole and then followed by screens for the presence of these compounds in illicit preparations.

2. Experimental procedure

2.1. Chemicals and reagents

All solvents used in this work were of analytical grade and were purchased from Aldrich Chemical Company. All of the reagents used in this work were acquired from Aldrich Chemical Company.

* Corresponding author. Tel.: +61 8 8226 7700; fax: +61 8 8226 7777.
E-mail address: cox.matthew@saugov.sa.gov.au (M. Cox).

0379-0738/$ – see front matter © 2005 Elsevier Ireland Ltd. All rights reserved.
doi:10.1016/j.forsciint.2005.12.019

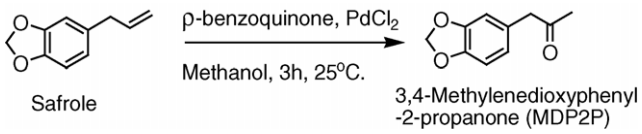

Scheme 1.

2.2. Instrumentation

Sample analysis was effected with gas chromatography–mass spectrometry (GC–MS), viz. a Hewlett Packard 6890 plus gas chromatograph equipped with a Hewlett Packard 5973 mass selective detector (MSD) and electronic pressure programming. Helium was used as a carrier gas; the column was a 15 m × 0.25 mm × 0.25 μm DB-1 capillary.

The mass spectrometer operated from 30 to 450 amu in electron impact (EI) mode with an ionization energy of 70 eV. A solvent delay of 1.50 min was applied. The injector temperature was 300 °C. The initial column temperature was 90 °C for 4 min and then ramped at 45 °C over 4.67 min.

2.3. Synthesis procedures

2.3.1. Wacker oxidation of safrole in methanol using ρ-benzoquinone

This conversion was done by roughly following the procedure of *Methyl Man* [12]: a solution containing safrole (17.8 g, 162.1 mmol) and methanol (10 mL) was added dropwise over a period of 60 min to a solution containing palladium chloride (0.2 g, 1.1 mmol), ρ-benzoquinone (15 g, 138.8 mmol), methanol (40 mL) and distilled water (5 mL). The reaction mixture was stirred for 3 h, by which time GC analysis indicated that all of the safrole had been consumed. After this time the insoluble solid material was filtered from the reaction mixture and 10% hydrochloric acid solution (170 mL) was added. The aqueous mixture was extracted with dichloromethane (3 × 30 mL) and the organic extracts were combined. The organic phase was then washed with saturated sodium bicarbonate solution (2 × 30 mL), saturated sodium chloride solution (3 × 30 mL) and 5% sodium hydroxide solution (3 × 30 mL). The organic phase was then dried ($MgSO_4$), filtered and evaporated to give a straw yellow oil. Analysis by GC indicated a product mixture represented by Fig. 1.

2.3.2. Wacker oxidation of safrole in ethanol using ρ-benzoquinone

The above procedure was duplicated but ethanol replaced methanol as the solvent.

3. Results and discussion

MDP2P was synthesised in our laboratory by following the procedure of *Methyl Man* [12]. After a 3 h reaction time and work-up, GC analysis indicated that all of the safrole starting material had been consumed (Fig. 1).

The oxidation of safrole to MDP2P is accompanied by the reduction of ρ-benzoquinone to hydroquinone and this compound is observed in the crude reaction mixture prior to alkaline work-up. Significantly, 4-methoxyphenol was also noted as a reduction product of ρ-benzoquinone, but was also lost to the aqueous phase during alkaline work-up. The presence of this compound has been implicated in the synthesis of *para*-methoxyphenyl-2-propanone [13].

Isosafrole (A) and the major product MDP2P (B) were recognisable products amongst a number of unknown minor products from the reaction (unknowns 1–5, Fig. 1). Unknown compounds 1–5 are the subjects of this communication.

3.1. Unknown 1

The retention time of unknown compound 1 was 4.90 min. The base peak (165 amu) and the molecular ion (194 amu) suggested that unknown 1 was consistent with a reduced safrole structure with a methoxy group positioned at the benzylic position (Fig. 2).

1-(3,4-Methylenedioxyphenyl)-1-methoxypropane (1) was synthesised for comparison with unknown 1 (Fig. 3).

1-(3,4-Methylenedioxyphenyl)-1-methoxypropane (1) was synthesised by reaction of ethyl magnesium bromide with

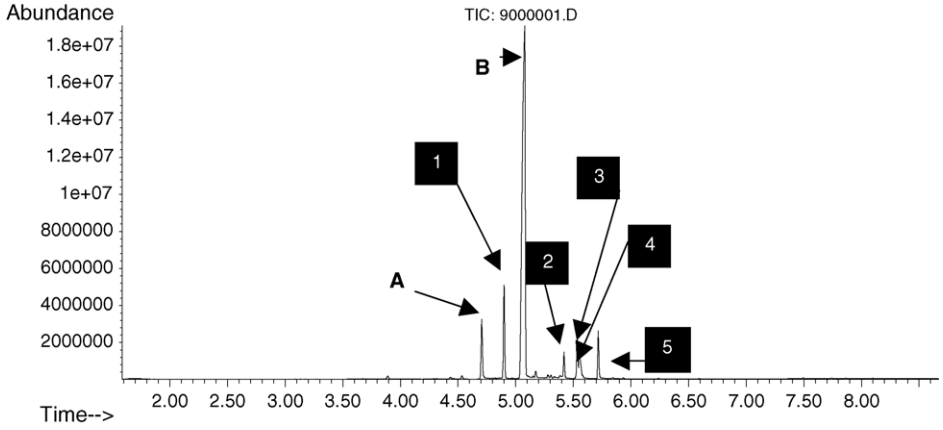

Fig. 1. GC of the *Wacker* oxidation of safrole after work-up and a 3 h reaction time. Peak identities; (A) isosafrole, 1: unknown 1, (B) MDP2P, 2: unknown 2, 3: unknown 3, 4: unknown 4, 5: unknown 5.

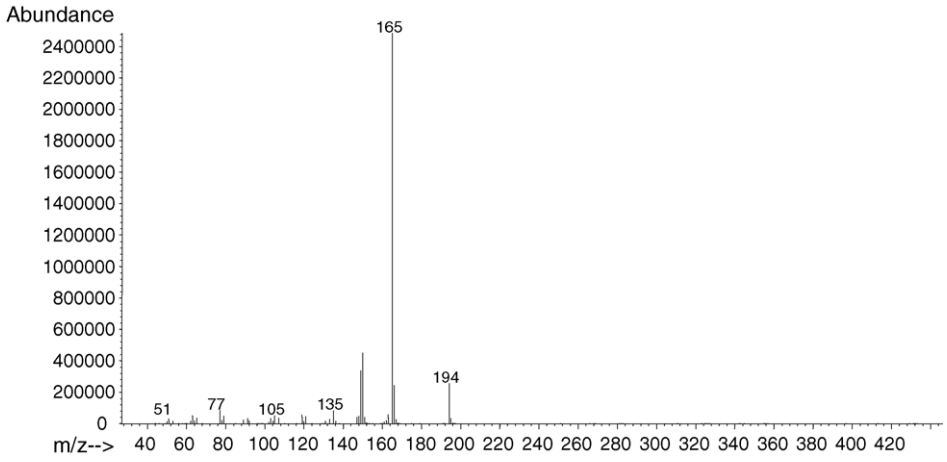

Fig. 2. Mass spectrum of unknown compound 1, at retention time = 4.90 min.

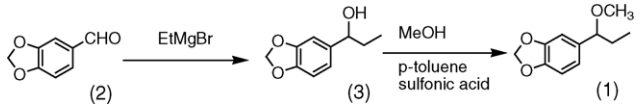

Scheme 2.

piperonal (2), which gave 1-(3,4-methylenedioxyphenyl)-1-hydroxypropane (3), which was then converted to the methoxy derivative by solvolysis of (3) in methanol with ρ-toluene-sulfonic acid (Scheme 2).

The mass spectrum of synthesised (1) was identical with the mass spectrum of unknown 1. The retention time was checked by co-injection of synthesised (1) with the product mixture from the *Wacker* oxidation of safrole and this resulted in the symmetrical enhancement of the peak eluting at 4.90 min. This co-injection procedure was applied to all of the unknown compounds mentioned in this report. We concluded that the identity of unknown 1 was 1-(3,4-methylenedioxyphenyl)-1-methoxypropane (1).

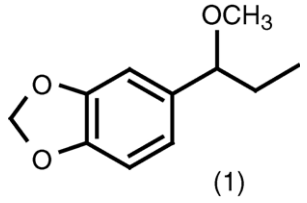

Fig. 3. Proposed structure of unknown compound 1.

3.2. Unknown 2

The retention time of unknown 2 was 5.42 min. The mass spectrum of this compound contained a base peak of 165 amu and a molecular ion of 208 amu, which suggested that this compound contained a methoxy substituent at the benzylic position as well as a carbonyl group (Fig. 4).

1-(3,4-Methylenedioxyphenyl)-1-methoxypropan-2-one (4) was synthesised for comparison with unknown 2 (Fig. 5).

Bromination of MDP2P (5) with bromine resulted in the predominant formation of the singly brominated species, 1-(3,4-methylenedioxyphenyl)-1-bromopropan-2-one (6) and 1-(3,4-methylenedioxyphenyl)-3-bromopropan-2-one (7). Initially it was thought that direct substitution of (6) with sodium

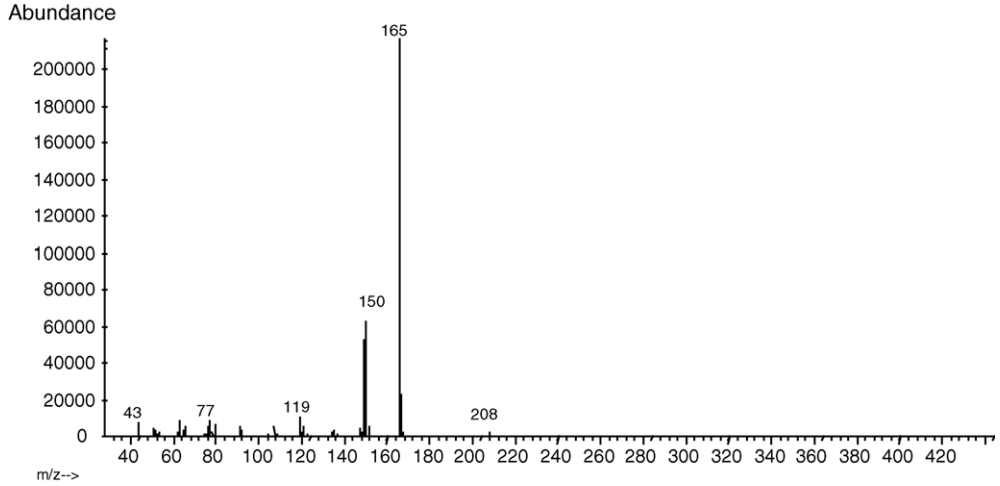

Fig. 4. Mass spectrum of unknown compound 2, at retention time = 5.42 min.

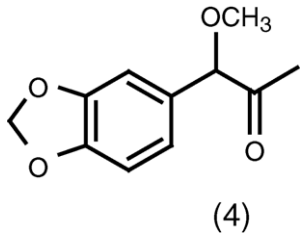

Fig. 5. Proposed structure of unknown compound 2.

methoxide might give (4). When a mixture of (6) and (7) was refluxed with sodium methoxide a compound was predominantly formed with identical mass spectral fragmentation and retention time to the third unknown compound which eluted at 5.54 min as well as trace amounts of (4). Solvolysis of (6) in methanol produced larger amounts of (4) and unreacted (7), but high yields of (4) (along with unreacted (7)) were obtained when (6) was treated with silver nitrate in methanol (Scheme 3).

The mass spectrum and retention time of synthesised (4) was identical with unknown 2. We concluded that the identity of unknown 2 was 1-(3,4-methylenedioxyphenyl)-1-methoxypropan-2-one (4). Compound (4) has recently been identified in MDP2P prepared by the per-acid oxidation of isosafrole [14].

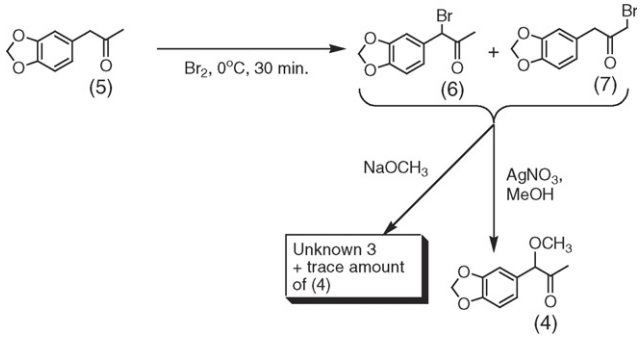

Scheme 3.

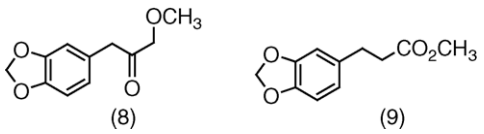

Fig. 7. Proposed structures of unknown compound 3.

Therefore, (4) cannot be considered as route specific for this oxidation process.

3.3. Unknown 3

The base peak of 135 amu of unknown 3, which eluted at 5.54 min suggests a vacant benzylic position but the molecular ion of 208 amu suggests the presence of a methoxy group and a carbonyl group in the molecule (Fig. 6).

Possible structures of the third unknown compound are shown in Fig. 7.

As mentioned above when a mixture of (6) and (7) was refluxed with sodium methoxide a compound was produced with identical mass spectral fragmentation and retention time as unknown compound 3. Direct substitution of (7) with methoxide may produce (8) (Scheme 4).

An alternative mechanism involving *Favorskii* re-arrangement of (6) or (7) with methoxide through the cyclopropanone

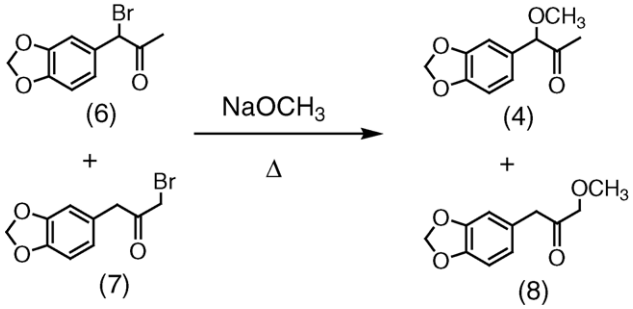

Scheme 4.

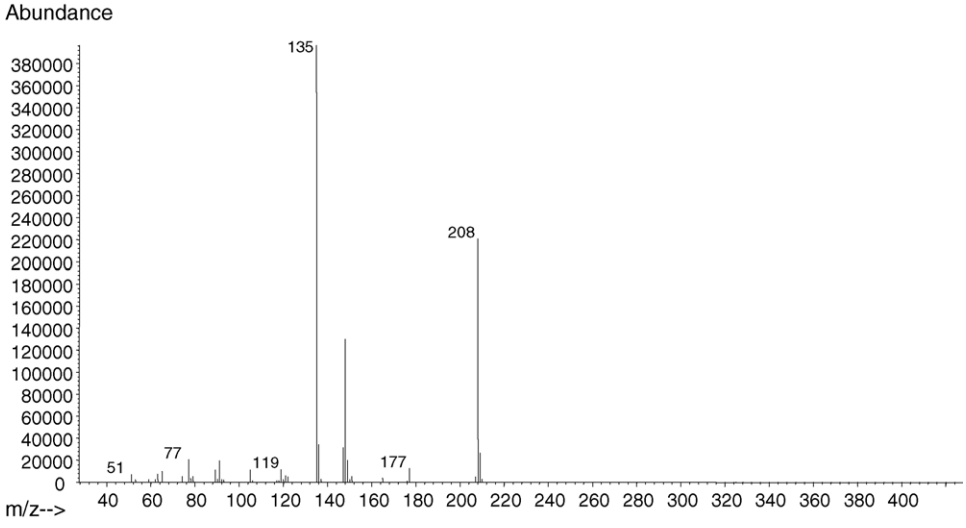

Fig. 6. Mass spectrum of unknown compound 3, at retention time = 5.54 min.

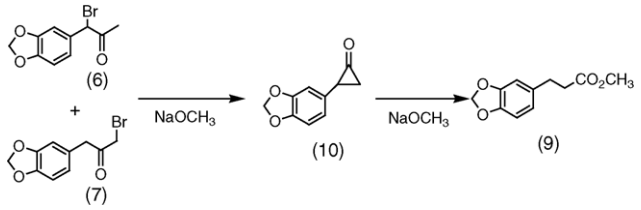

Scheme 5.

intermediate (10) to (9) could also have occurred [15] (Scheme 5). Since (8) or (9) could both theoretically be produced from (7) (when heated with sodium methoxide) then more work was required to unambiguously identify the structure of unknown compound 3.

Further identification of unknown compound 3 was required despite the production of a compound with identical features during the reaction of sodium methoxide with a mixture of compounds (6) and (7) (above). Methyl 3-(3,4-methylenedioxyphenyl)propanoate (9) was synthesised as per Scheme 6. The conjugated ester (13) was produced by *Knoevenagel* condensation of piperonal (11) with malonic acid, followed by esterification of the conjugated acid (12). Reduction of the conjugated ester (13) with sodium in methanol resulted in the formation of 3-(3,4-methylenedioxyphenyl)propanol (14) and the *Michael* type addition product 3-(3,4-methylenedioxyphenyl)-3-methoxypropanol (15). The alcohol (14) was then oxidised with acidified dichromate to the acid (16), which was then esterified to give (9).

The spectral features and elution time of synthesised (9) was identical with the third unknown compound. We concluded that the third unknown compound was methyl 3-(3,4-methylenedioxyphenyl)propanoate (9).

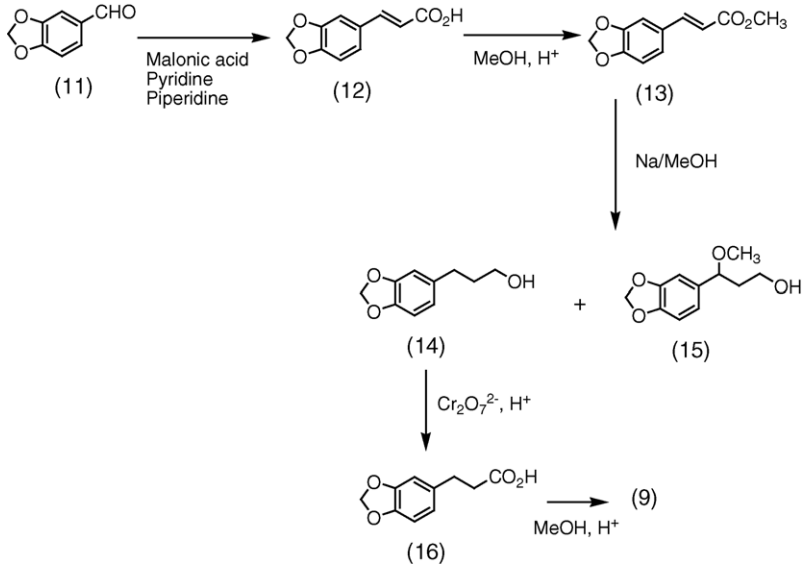

Scheme 6.

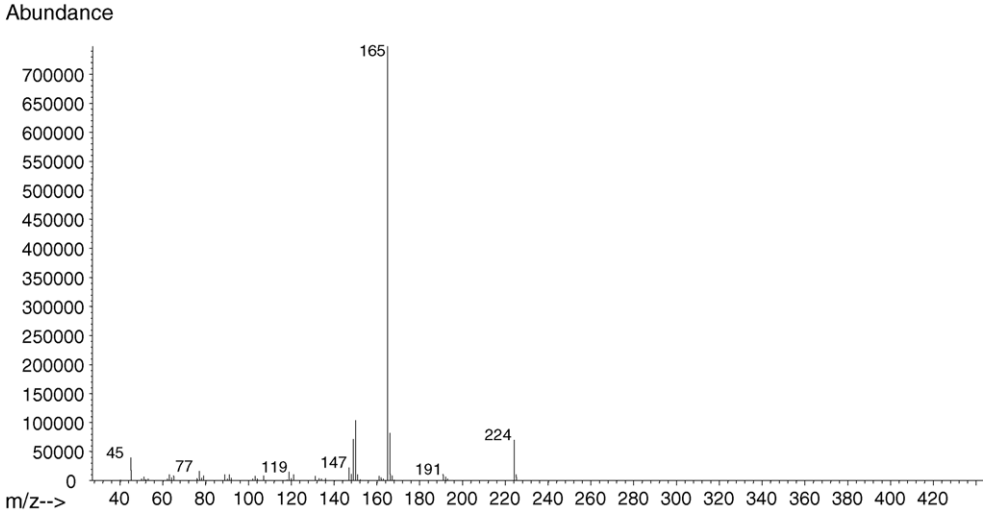

Fig. 8. Mass spectrum of unknown compound 4, at retention time = 5.56 min.

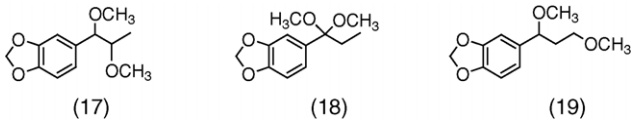

Fig. 9. Proposed structures of unknown compound 4.

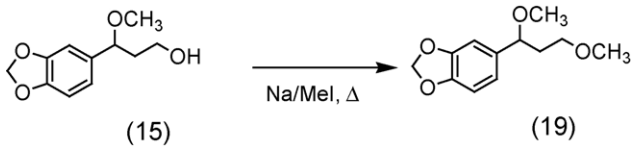

Scheme 7.

3.4. Unknown 4

Unknown compound 4 eluted at 5.56 min and contained fragment ions consistent with a methoxy group at the benzylic position, but in this case the parent ion suggested that another methoxy group was present (Fig. 8).

Possible structures of the fourth unknown compound are shown in Fig. 9.

Both diastereomers of (17) were synthesised and found to have very similar mass spectral fragmentation with unknown compound 4, but neither diastereomer of (17) matched the retention time. The dimethylacetal (18) of 3,4-methylenedioxyphenylpropan-1-one (MDP1P) was synthesised in trace amounts but neither the mass spectrum nor the elution time matched the fourth unknown compound. 1-(3,4-Methylenedioxyphenyl)-1,3-dimethoxypropane (19) was synthesised from (15) by methylation of the sodium salt with methyl iodide in anhydrous 1,2-dimethoxyethane (Scheme 7).

The mass spectrum and retention time of synthesised (19) were identical with those of the fourth unknown compound, which eluted at 5.56 min and we concluded that the fourth unknown compound was 1-(3,4-methylenedioxyphenyl)-1,3-dimethoxypropane (19).

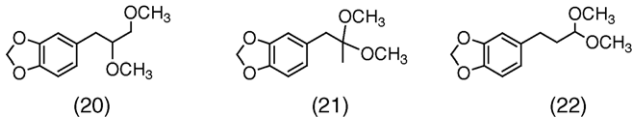

Fig. 11. Proposed structures of unknown compound 5.

3.5. Unknown 5

Unknown compound 5 eluted at 5.71 min and contained a base peak of 135 amu and a parent ion of 224 amu, which suggested that the structure of the final unknown compound contained an unsubstituted benzylic position but the molecular ion suggested that the unknown compound contained two methoxy groups (Fig. 10).

Possible structures of the fifth unknown compound are shown below in Fig. 11.

Dimethyl safrole glycol (20) was synthesised by permanganate oxidation of safrole to give safrole glycol followed by methylation with sodium hydride and methyl iodide, but neither retention time nor the mass spectrum of (20) matched unknown compound 5. The dimethyl acetal (21) of MDP2P was

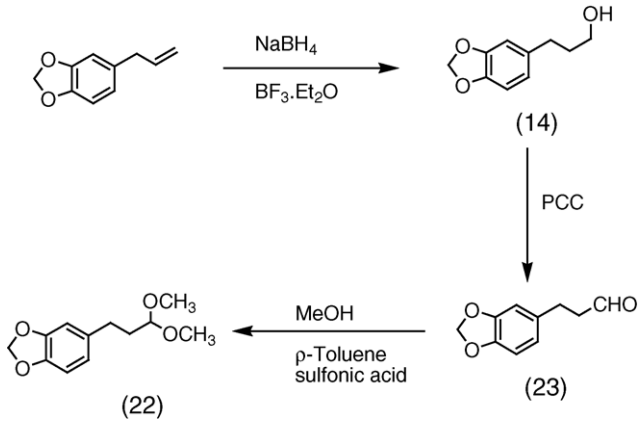

Scheme 8.

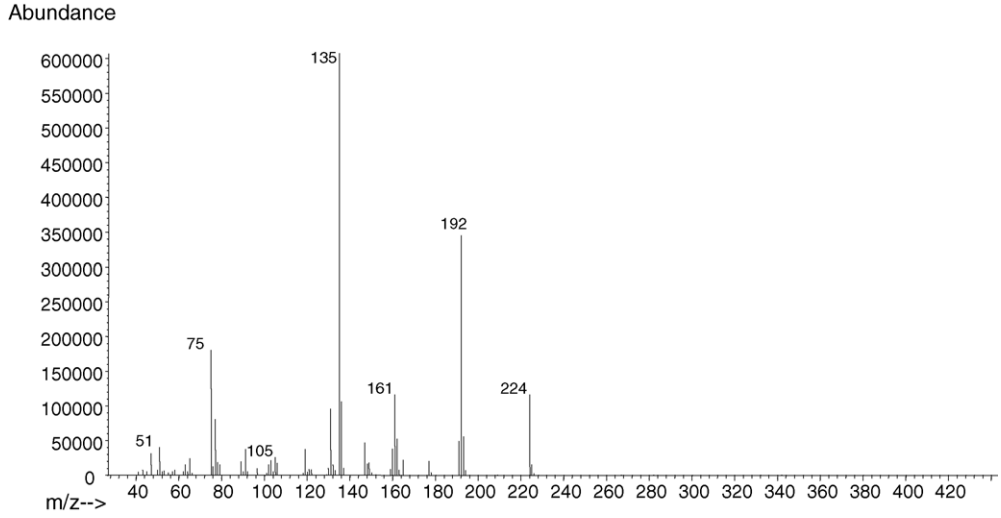

Fig. 10. Mass spectrum of unknown compound 5, at retention time = 5.71 min.

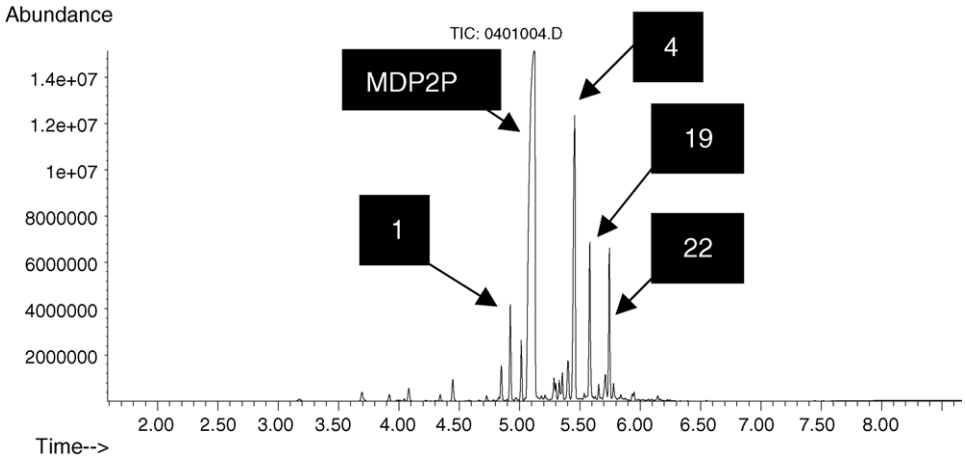

Fig. 12. GC plot of crude MDP2P located at the MDMA laboratory.

Fig. 13. Mitsubishi design tablets, which were being produced at the clandestine laboratory in Willunga (2003).

synthesised and neither the retention time nor the mass spectrum of (21) matched those of unknown compound 5.

Compound (22) was synthesised by initial hydroboration of safrole to give 3-(3,4-methylenedioxyphenyl)propanol (14) which was then selectively oxidised to 3-(3,4-methylenedioxyphenyl)propanal (23) with pyridinium chlorochromate followed by the formation of the dimethylacetal (22) in methanol with ρ-toluenesulfonic acid (Scheme 8).

The mass spectrum and retention time of synthesised (22) were identical with those of the fifth unknown compound, which eluted at 5.71 min and we concluded that the fifth unknown compound was 3-(3,4-methylenedioxyphenyl)-1,1-dimethoxypropane (22).

The next phase of this study involved the investigation of the retrieval of some of these by-product chemicals from samples taken from a clandestine laboratory, which was employing the *Wacker* oxidation of safrole to manufacture MDP2P. Police uncovered the laboratory in September 2003 at a rural property in Willunga, about a 1-h drive south of Adelaide, South Australia. A large array of chemicals and equipment was present at the scene. The vast majority of the chemicals had nothing to do with drug production, but some of the chemicals, including *sassafras oil*, pointed to MDMA manufacture. A sample of crude MDP2P from the laboratory was analysed for the presence of any of the neutral by-products mentioned previously; the chromatogram is presented in Fig. 12.

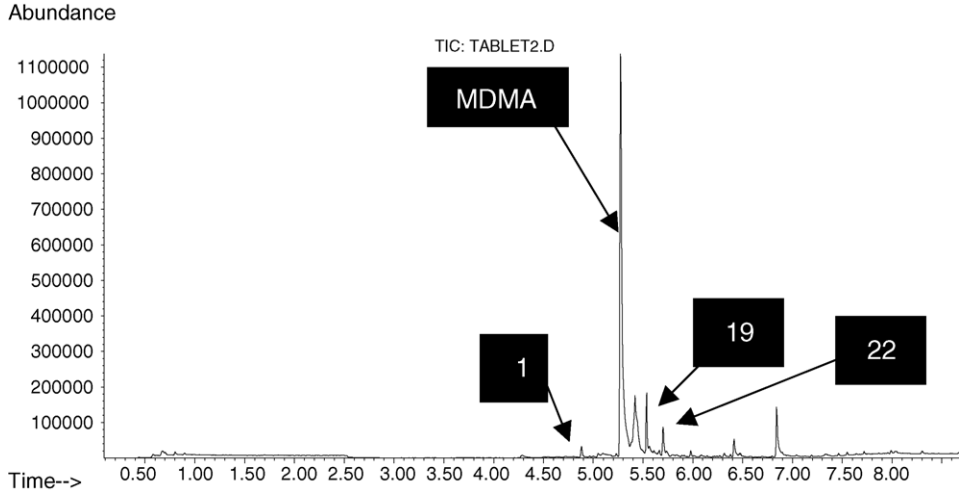

Fig. 14. GC SPME profile of a *Mitsubishi* tablet using a 100 μm polydimethylsiloxane fibre.

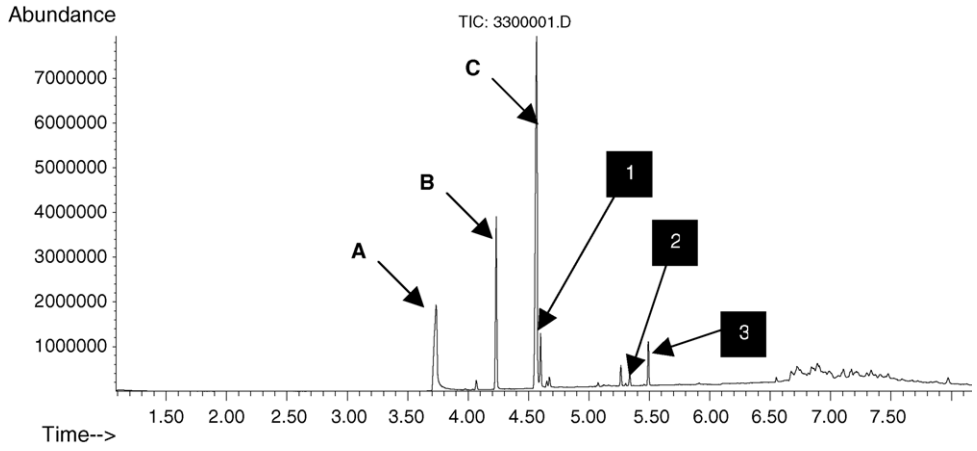

Fig. 15. GC plot of crude MDP2P manufactured by the *Wacker* oxidation of safrole in ethanol. Peak identities; (A) piperonal, (B) isosafrole, (C): MDP2P, 1: unknown 1, 2: unknown 2, 3: unknown 3.

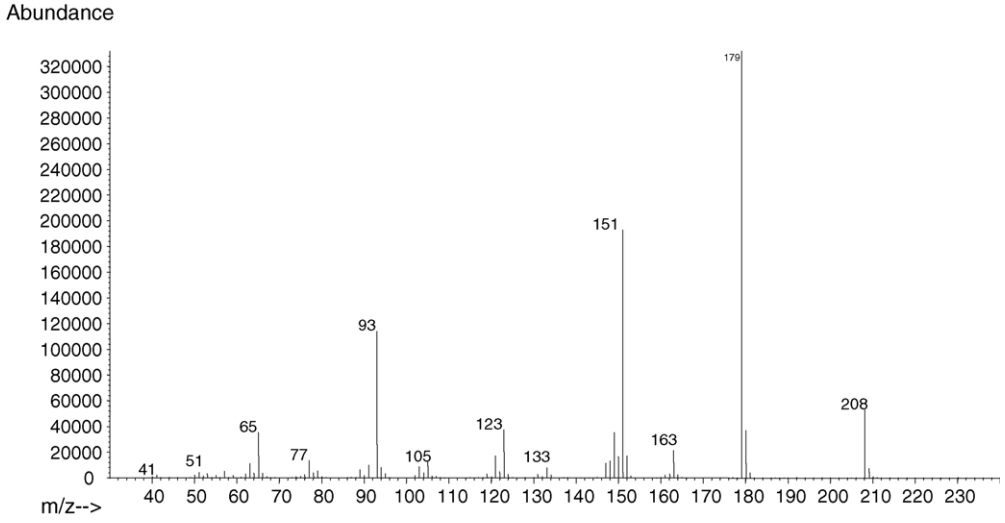

Fig. 16. Mass spectrum of unknown compound 1 from the *Wacker* oxidation of safrole in ethanol.

The chromatographic result shows the presence of 1-(3,4-methylenedioxyphenyl)-1-methoxypropane (1), 1-(3,4-methylenedioxyphenyl)-1-methoxypropan-2-one (4), 1-(3,4-methylenedioxyphenyl)-1,3-dimethoxypropane (19) and 3-(3,4-methylenedioxyphenyl)-1,1-dimethoxypropane (22). The presence of these compounds in this combination may be considered as markers for the *Wacker* oxidation of safrole to MDP2P.

In addition to crude MDP2P, MDMA powder and MDMA tablets were located. The MDMA had been synthesised using the alumina amalgam method where nitromethane was employed as the nitrogen source. The MDMA tablets were impressed with the *Mitsubishi* logo (Fig. 13).

The tablets were investigated for the presence of the compounds described here. It was expected that they could be present due to their neutral character, but this would be dependent on the purification processes, which had been used to prepare the MDMA tablets. The laboratory operator had used vacuum distillation for purification of safrole (from sassafras oil), MDP2P and MDMA free base. The ultimate test of the utility of these by-products as markers for the *Wacker* oxidation of safrole would be to retrieve these materials from the final MDMA tablets, which were being produced in this laboratory. Solid-phase microextraction (SPME) was investigated as a tool for non-destructive recovery of the drug manufacturing impurities and the chromatographic result of the sampled *Mitsubishi* design tablet is presented in Fig. 14.

The presence of (1), (19) and (22) in the final MDMA tablets indicates that trace amounts of these materials carry through to the final MDMA even after purification by vacuum distillation. The ultimate fate of ketone (4) during the reductive amination

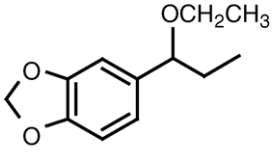

(24)

Fig. 17. Proposed structure of unknown compound 1 from the *Wacker* oxidation of safrole in ethanol.

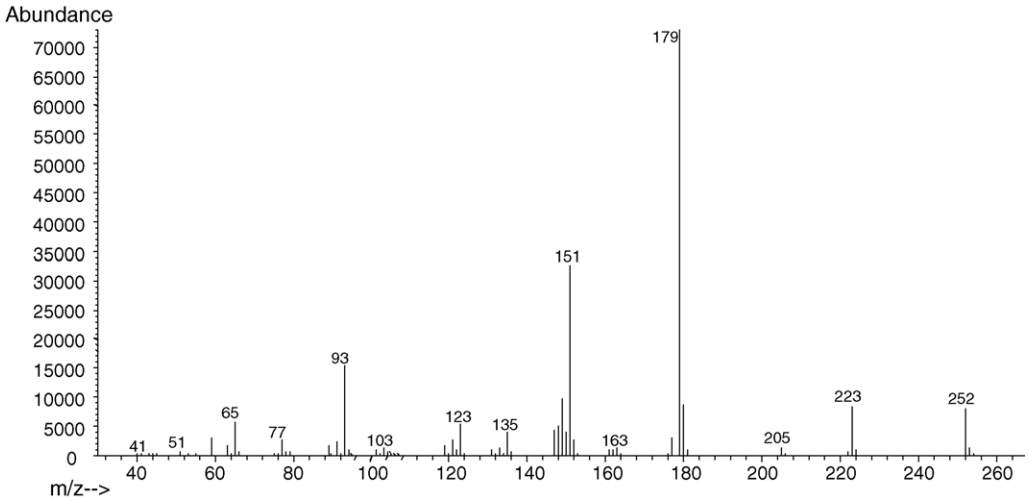

Fig. 18. Mass spectrum of unknown compound 2 from the *Wacker* oxidation of safrole in ethanol.

step is not known at this stage, but it is conceivable that this material may also be reductively aminated, but we were unable to detect *N*-methyl-2-methoxy-1-methyl-2-(3,4-methylenedioxyphenyl)-ethanamine in the final MDMA tablets. This material has been reported as a reductive amination product of (4) [14].

3.6. Ethanol mediated Wacker oxidation of safrole

We have also investigated the use of an alternative solvent in the *Wacker* oxidation. Ethanol is widely available as methylated spirits and although we have not detected the use of this solvent for the *Wacker* oxidation we thought that ethanol might be a convenient alternative for some underground chemists. Whereas *Wacker* oxidation of safrole in methanol is complete within 3 h we observed the reaction was sluggish in the case of ethanol and the reaction required 24 h for completion. The chromatographic result of the *Wacker* oxidation of safrole in ethanol is presented in Fig. 15.

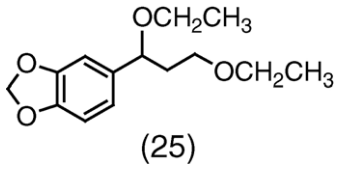

(25)

Fig. 19. Proposed structure of unknown compound 2 from the *Wacker* oxidation of safrole in ethanol.

The MDP2P produced during the *Wacker* oxidation of safrole in ethanol was accompanied by the formation of the known compounds isosafrole and piperonal. Piperonal was not detected in the methanol mediated *Wacker* oxidation but this may be due to a shorter reaction time than when using ethanol. The extra reaction time may allow oxidative cleavage of the produced isosafrole. By-product formation appeared in general to be less, but we have tentatively assigned the structures of some of the trace by-product components as having ethoxy substitution rather than the corresponding methoxy substitution.

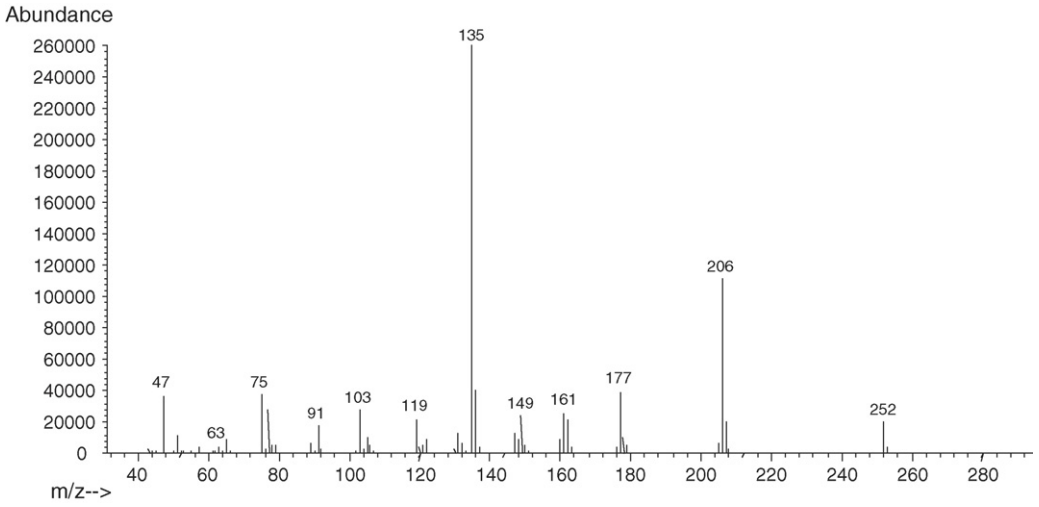

Fig. 20. Mass spectrum of unknown compound 3 from the *Wacker* oxidation of safrole in ethanol.

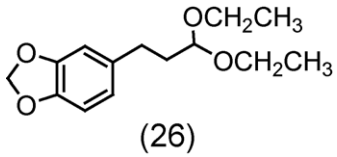

(26)

Fig. 21. Proposed structure of unknown compound 3 from the *Wacker* oxidation of safrole in ethanol.

3.6.1. Unknown 1

Unknown compound 1 from Fig. 15 has a base peak of 179 amu and a molecular ion of 208 amu and is consistent with an ethoxy group positioned at the benzylic position (Fig. 16).

This mass spectrum may represent the structure of 1-(3,4-methylenedioxyphenyl)-1-ethoxypropane (24) (Fig. 17).

3.6.2. Unknown 2

Unknown compound 2 from Fig. 15 has a base peak of 179 amu and a molecular ion of 252 amu and is consistent with two ethoxy groups in the molecule with one of them positioned at the benzylic position (Fig. 18).

This mass spectrum may represent the structure of 1-(3,4-methylenedioxyphenyl)-1,3-diethoxypropane (25) (Fig. 19).

3.6.3. Unknown 3

Unknown compound 3 from Fig. 15 has a base peak of 135 amu and a molecular ion of 252 amu and is consistent with two ethoxy groups in the molecule with none of them positioned at the benzylic position (Fig. 20).

This mass spectrum may represent the structure of 3-(3,4-methylenedioxyphenyl)-1,1-diethoxypropane (26) (Fig. 21).

4. Conclusions

It has been found that 1-(3,4-methylenedioxyphenyl)-1-methoxypropane (1), 1-(3,4-methylenedioxyphenyl)-1-methoxypropan-2-one (4), methyl 3-(3,4-methylenedioxyphenyl)-propanoate (9), 1-(3,4-methylenedioxyphenyl)-1,3-dimethoxypropane (19) and 3-(3,4-methylenedioxyphenyl)-1,1-dimethoxypropane (22) are produced during the *Wacker* oxidation of safrole to MDP2P using ρ-benzoquinone and palladium chloride with methanol as the solvent. Furthermore we have demonstrated the retrieval of (1), (4), (19) and (22) from clandestinely produced MDP2P and (1), (19) and (22) from final MDMA tablets (having been synthesised by this route). Ethanol is a viable alternative to methanol for the *Wacker* oxidation of safrole but similar by-products with ethoxy substitution are likely produced instead of the methoxy substituted by-products. It should be noted, however, that the presence of these impurities depends a great deal upon the exact technique by which purification of the intermediary and final products is performed i.e., solvent extraction and/or vacuum distillation etc.

References

[1] Australian Illicit Drug Report 2001–2002. Commonwealth of Australia, 2003.
[2] A.M.A. Verweij, Clandestine manufacture of 3,4-methylenedioxymethylamphetamine (MDMA) by low pressure reductive amination. A mass spectrometric study of some reaction mixtures, Forensic Sci. Int. 45 (1990) 91–96.
[3] C.R. Clark, J. DeRuiter, F.T. Noggle, GC–MS identification of amine-solvent condensation products formed during analysis of drugs of abuse, J. Chromatogr. Sci. 30 (1992) 399–404.
[4] A.M.A. Verweij, Impurities in illicit drug preparations: 3,4-(methylenedioxy)amphetamine and: 3,4-(methylenedioxymethyl)amphetamine, Forensic Sci. Rev. 4 (1992) 137–146.
[5] M. Bohn, G. Bohn, G. Blaschke, Synthesis markers in illegally manufactured 3,4-methylenedioxyamphetamine and 3,4-methylenedioxymethamphetamine, Int. J. Legal Med. 106 (1993) 19–23.
[6] A.M.A. Verweij, A.G.A. Sprong, a note about some impurities in commercially available piperonylmethylketone, Microgram XXVI (1993) 209–213.
[7] R.J. Renton, J.S. Cowie, M.C.H. Oon, A study of the precursors, intermediates and reaction by-products in the synthesis of 3,4-methylenedioxymethamphetamine and its application to forensic drug analysis, Forensic Sci. Int. 60 (1993) 189–202.
[8] C.R. Clark, J. DeRuiter, S. Andurkar, F.T. Noggle, Analysis of 3,4-methylenedioxyphenyl-2-propanone and 3,4-methylenedioxyamphetamine prepared from isosafrole, J. Chromatogr. Sci. 32 (1994) 393–402.
[9] P. Gimeno, F. Besacier, H. Chaudron-Thozet, J. Girard, A. Lamotte, A contribution to the chemical profiling of 3,4-methylenedioxymethamphetamine (MDMA) tablets, Forensic Sci. Int. 127 (2002) 1–44.
[10] C.R. Clark, J. DeRuiter, F.T. Noggle, Gas chromatographic and mass spectrometric analysis of samples from a clandestine laboratory involved in the synthesis of ecstacy from sassafras oil, J. Chromatogr. Sci. 29 (1991) 168–173.
[11] T. Lukaszewski, Spectroscopic and chromatographic identification of precursors, intermediates, and impurities of 3,4-methylenedioxyamphetamine synthesis, J. Assoc. Off. Anal. Chem. 61 (1978) 951–967.
[12] Methyl Man, benzoquinone Wacker oxidation of safrole in methanol, http://www.rhodium.ws/chemistry/wacker.benzo-meoh.html.
[13] D. Waumans, N. Bruneel, B. Hermans, J. Tytgat, A rapid and simple GC/MS screening method for 4-methoxyphenol in illicitly prepared 4-methoxyamphetamine (PMA), Microgram J. 1 (3–4) (2003) 184–189.
[14] M. Swist, J. Wilamowski, D. Zuba, J. Kochana, A. Parczewski, Determination of synthesis route of 1-(3,4-methylenedioxyphenyl)-2-propanone (MDP-2-P) based on impurity profiles of MDMA, Forensic Sci. Int. 149 (2005) 181–192.
[15] J. March, Advanced Organic Chemistry, 4th ed., John Wiley and Sons, New York, 1992.

ELSEVIER

Forensic Science International 164 (2006) 148–154

Forensic Science International

www.elsevier.com/locate/forsciint

A quantitative differentiation method for plastic bags by infrared spectroscopy, thickness measurement and differential scanning calorimetry for tracing the source of illegal drugs

Valerio Causin [a,*], Carla Marega [a], Pietro Carresi [b], Sergio Schiavone [b], Antonio Marigo [a]

[a] *Dipartimento di Scienze Chimiche dell'Università, via Marzolo 1, 35131 Padova, Italy*
[b] *Sezione di Chimica, Esplosivi ed Infiammabili, Reparto Carabinieri Investigazioni Scientifiche, Viale Tor di Quinto, 151-00191 Roma, Italy*

Received 5 July 2005; received in revised form 5 December 2005; accepted 15 December 2005
Available online 23 January 2006

Abstract

Fifty shopping bags, commonly encountered in the packaging of drug doses, were characterized by thickness measurements, infrared spectroscopy and differential scanning calorimetry. By these very straightforward and inexpensive techniques, without sample preparation, nearly all the considered samples could be discriminated. Ninety-seven percent of the possible pairs of white, apparently similar dull polymer films were differentiated. The rather large degree of variability existing in grocery bags, even though they are mass produced, was shown, confirming that these items can be useful in tracing the source of illicit drug doses.

Keywords: Forensic science; Plastic materials; Drug packaging; Polymers; Polyethylene; Infrared spectroscopy; Differential scanning calorimetry

1. Introduction

The characterization of plastic packaging material may be a problem of relevant importance in forensic science. Plastic bags are used to conceal body parts of a victim or other crime related materials [1] and to pack illicit drugs [2–4] and may be of interest in arson related investigations [5,6]. In particular, a thorough examination of the packaging used to contain drugs can help in tracing their source. In order to be useful, though, the characterization of such materials should be complete enough to discriminate apparently similar plastic films, differing by manufacturer or manufacturing batch. An assessment of which characteristics are less common, and thus more significant, is important to determine the evidential value of the forensic results presented to the Court. The more of these features the items are found to have in common, the greater are the chances that they came from the same single source.

Polymers are quite versatile materials under this point of view, because slight variations in the production process may bring about a variety of differences in chemical and physical properties that may be exploited for forensic science purposes [6–12].

A number of methods have been proposed for the analysis of plastic packaging films, among which UV–vis [2] and infrared (IR) spectroscopy [2], differential scanning calorimetry (DSC) [5], pyrolysis–gas chromatography [13], gas chromatography–mass spectrometry [14] and elemental analysis [15,16], but their effectiveness in discriminating specimens of the same polymer basis (i.e. mass produced articles) has rarely been accounted for.

The purpose of this paper is to show that a combination of widely available and inexpensive techniques such as IR spectroscopy, DSC and thickness measurement can discriminate apparently similar grocery bags. These bags are quite often used by Italian drug smugglers for packaging of individual doses. A number of times our labs were requested by the Court to correlate cut plastic bags seized in the smuggler's premises with the portions of plastic film that wrapped the illicit substances that had been sold to the drug-addicts of the zone.

* Corresponding author. Tel.: +39 049 8275153; fax: +39 049 8275161.
E-mail address: valerio.causin@unipd.it (V. Causin).

0379-0738/$ – see front matter
doi:10.1016/j.forsciint.2005.12.024

Fifty shopping bags of different shops were analyzed, produced by different manufacturers. Inter- and intra sample variations were investigated, along with the diversity among samples of the same lot or from different batches of the same producers.

2. Experimental

2.1. Samples

All the major supermarket chains in the Venice, Italy, region were visited to obtain samples of shopping bags. A number of plastic bags were also acquired in medium and small-size shops. A total of 50 samples were collected from 31 different stores, 16 of which were colored. The manufacturer and batch code, when present on the plastic film, were noted and recorded.

2.2. General examination and thickness measurements

The films were visually observed by the naked eye and under a DM4000M (Leica) microscope under cross polarized light in the transmission and reflection mode. The thickness was measured by a Digico 1 (Tesa) micrometer, with a $\pm 2\,\mu m$ precision. A single layer of plastic was measured for each sample. Five replicates were acquired and the average was calculated. The standard deviations computed on the basis of replicate data were always smaller than the precision of the instrument, so an error of $\pm 2\,\mu m$ was associated to the averages.

2.3. Infrared spectroscopy

IR absorption spectra were acquired on a Nexus FTIR spectrometer (Thermo Nicolet) in attenuated total reflection (ATR) mode with a smart endurance accessory (Thermo Nicolet) equipped with a diamond ATR crystal. A MIR Globar source was used and the detector was of the DTGS type. The spectral region spanned from 4000 to 650 cm^{-1}, with a resolution of 4 cm^{-1}. Two hundred and fifty-six scans were collected in the acquisition of the IR spectrum of each sample. Nicolet Omnic software was used for the treatment of spectra. The ATR correction routine of the Nicolet Omnic software was applied to ATR data.

2.4. Differential scanning calorimetry

All the measurements were carried out with a model 2920 calorimeter (TA Instruments) operating under N_2 atmosphere. Tiny portions of the samples, weighing about 5 mg, were closed in aluminum pans. A heating rate of 10 °C/min up to 200 °C was set in order to observe the polymer melting peak. After erasure of thermal history by a 5 min isotherm at 200 °C, the sample was cooled down to room temperature at 10 °C/min and heated again to 200 °C at the same rate. Indium of high purity was used for calibrating the DSC temperature and enthalpy scales. The choice of the baseline in enthalpy evaluations has been standardized for all samples. In order to quantify the repeatability of the measurements, five replicates were recorded for selected samples (Aa1, B, D, F and M) and their standard deviations were computed. A 3% error on the enthalpy associated to melting endotherms and a 2% error on the enthalpy of crystallization was obtained. All the remaining samples were analyzed twice, a third confirmation replicate was performed if the two previous measurements differed by more than 3% in case of melting peaks or 2% in case of crystallization exotherms.

3. Results and discussion

A visual examination of the samples collected was the first step of the characterization procedure adopted in this work. Of the 50 samples collected, 16 were colored in shades that were readily distinguishable by the naked eye. The appearance of the film (shiny or dull) was noted, along with features like cuts, folds, perforations or seals. Only one textured bag (sample O) was encountered in the survey of the shops visited during the sampling campaign, making this feature a quite significant one when evaluating comparisons. The existence of machine marks and defects in the printing of some bags was observed and recorded, and could be of interest in casework in which comparisons were requested between whole bags used for the packaging of drugs [2]. Moreover, the name of the manufacturer and the lot number was often printed on the bag, a detail that could be of great help in cases like those mentioned before. The work reported in this paper was aimed at a different type of comparison, in which it must be determined if different film portions were cut from the same bag. This is the analysis most widely requested by Italian Courts, because they are often interested in linking a dealer, who prepared and packed single doses from a quantity of drugs, to the drug-addicts to whom the doses were sold. Pieces of plastic film are also known to be used for the drug packages ingested by ''body stuffers'' [3,4], so their characterization can be exploited in reconstructing the dynamics also of international traffic of illegal substances. To the knowledge of the authors, no systematic study was reported on the European market about this specific type of forensic analytical problem.

After a simple visual examination step, 34 white and dull samples appeared indistinguishable and thus requested a more thorough instrumental characterization. Table 1 shows the characterization data collected for these samples. Each specimen was identified by a capital letter that designates the shop that supplied it. A lower case letter was added to the code of the sample if different manufacturers produced bags for the same shop. Samples Aa1 and Aa2 were supplied to the same shop by the same manufacturer but differed in size. The data shown in Table 1 are the average of the various replicates performed on each sample. When more than one specimen was available, as in the case of products coming from different lots (vide infra Table 2), the datum shown is the average of all the measurements that were carried out.

By IR spectrometry it was found that all the considered bags were made of polyethylene (PE). Although the polymer matrix was the same for every sample, an examination of IR spectra showed that additives were sometimes present, so that three

Table 1
Characterization data for the 34 white, dull plastic films

Sample	IR grouping	Thickness (μm)	T_m^I (°C)	ΔH_m^I (J/g)	T_c (°C)	ΔH_c (J/g)	T_m^{II} (°C)	ΔH_m^{II} (J/g)
Aa1	2	15	128.6	156 ± 5	117.1	150 ± 5	130.5	167 ± 5
Aa2	2	12	128.2	148 ± 12	117.2	142 ± 12	130.2	158 ± 14
Ab	3	13	129.1	182 ± 3	117.7	177 ± 4	130.9	196 ± 3
Ac	3	9	127.7	172 ± 5	116.2	161 ± 4	129.4	186 ± 5
B	2	11	126.4	115 ± 5	117.0	104 ± 3	128.8	119 ± 4
C	1	18	127.7	169 ± 5	115.9	152 ± 4	129.2	171 ± 5
D	1	11	128.9	191 ± 6	117.8	183 ± 4	131.0	204 ± 6
E	1	24	122.0	110 ± 3	111.2	127 ± 3	122.6	118 ± 3
F	1	16	126.8	153 ± 5	115.7	140 ± 3	128.5	162 ± 5
G	3	19	127.9	168 ± 5	116.8	156 ± 4	130.1	176 ± 5
H	3	40	109.4	117 ± 3	98.5	99 ± 2	110.3	123 ± 4
I	3	15	127.2	170 ± 5	116.0	162 ± 4	128.9	187 ± 6
J	1	45	123.5, 131.1	136 ± 4	114.3, 118.7	127 ± 3	126.9	144 ± 4
K	1	12	129.2	152 ± 5	115.6	143 ± 3	130.2	163 ± 5
L	3	35	123.0	109 ± 3	111.8	124 ± 3	123.3	114 ± 3
M	3	19	127.3	165 ± 5	115.8	147 ± 4	128.9	171 ± 5
N	1	14	129.1	173 ± 5	118.2	166 ± 4	131.3	184 ± 5
O	1	21	131.6	182 ± 5	118.5	182 ± 4	133.4	191 ± 5
P	1	18	128.3	151 ± 4	116.8	145 ± 3	130.3	163 ± 5
Q	1	14	127.5	140 ± 4	116.5	130 ± 3	129.3	150 ± 4
R	1	18	129.6	160 ± 5	117.4	158 ± 4	131.8	170 ± 5
S	1	14	128.6	154 ± 4	116.1	147 ± 3	130.2	165 ± 5
T	2	22	127.7	140 ± 4	115.8	131 ± 3	129.5	150 ± 4
U	1	19	124.7	108 ± 3	114.0	96 ± 2	125.7	114 ± 3
V	3	38	110.6	84 ± 2	99.7	74 ± 2	110.4	89 ± 2
W	1	4	129.4	166 ± 5	117.1	160 ± 4	131.0	178 ± 5
X	2	18	127.6	113 ± 3	116.6	105 ± 2	129.7	119 ± 3
Y	1	6	128.7	154 ± 4	116.6	147 ± 3	130.4	166 ± 5
Z	1	6	128.3	145 ± 4	116.3	140 ± 3	130.3	157 ± 5
Γ	1	10	127.6	160 ± 5	115.7	141 ± 3	129.1	165 ± 5
Δ	1	20	119.4	104 ± 3	108.1	90 ± 2	120.4	94 ± 2
Θ	1	23	128.4	163 ± 5	116.6	153 ± 4	129.8	173 ± 5
Λ	1	7	129.3	168 ± 5	116.8	164 ± 4	131.2	182 ± 5
Φ	2	4	127.6	132 ± 4	117.0	130 ± 3	129.6	143 ± 4

The error on thicknesses is ±2 μm, that on temperatures ±0.5 °C. T_m^I and ΔH_m^I denote the temperature and enthalpy of melting measured in the first heating ramp, T_c and ΔH_c are the temperature and enthalpy of crystallization, T_m^{II} and ΔH_m^{II} are the melting temperature and enthalpy measured in the second heating ramp. In sample J, a double peak of fusion was encountered and so two T_m^I and T_c values are shown.

main groups could be identified. In Fig. 1, the IR spectra of the bags pertaining to these three categories are displayed. As can be seen, group 1 films are composed of plain PE. The absence of detectable additives and the constancy of the relative intensity ratio between the signals did not allow for any further differentiation by IR within group 1. Calcium carbonate was used as a filler in group 2 bags and some characteristic peaks appeared at 1430 and at 876 cm^{-1}. Qualitative identification of the additive characterizing this group was done by subtracting the spectrum of pure PE from that of these polymers. As shown in Fig. 2, the subtraction result coincides with that of reference calcium carbonate. Samples within group 2 could be further differentiated on the basis of the relative intensities of the polyethylene peaks at 1461 and 1471 cm^{-1} and that of calcium carbonate at 1430 cm^{-1}. While in samples Aa1, Aa2, T and Φ the signals due to PE were preponderant with respect to that of the filler, in the case of bags B and X, the relative intensities were inverted because a larger quantity of carbonate was added by the manufacturer (Fig. 3).

The polymers of group 3 were different from those of the other two categories because a number of weak signals appeared along with those of neat PE. The more visible, although broad, peaks were at around 3350 cm^{-1} and at about 1600–1650 cm^{-1} (Fig. 1). Additional bands were visible at 1740, 1120 and 1045 cm^{-1} (Fig. 4). The scarce intensity of these signals did not allow for an effective subtraction procedure that could lead to a positive identification of the compound that originated them. A similar profile was also observed by Roux et al. [2], who ascribed it to vinyl acetate occasionally added as a comonomer to ethylene to obtain ethylene/vinyl acetate polymers (EVA). A second hypothesis was that group 3 bags were mixed with a pro-oxidant such as a metal salt (i.e. Fe(II)-stearate) that may catalyze thermal and photo-oxidation in degradable PE [14]. This would explain the presence of the peak at 1740 cm^{-1}, due to partial oxidation of the film. Although the appearance of these signals was consistent in replicate analyses (and thus was suitable for qualitative characterization), their weak intensity did not allow a quantitative assessment of the relative content of additive and PE.

The discriminating power (DP) of the techniques employed was calculated as the ratio between the number of differentiated

Table 2
Characterization data for samples pertaining to the same and different lots

Sample	Production lot	Thickness (μm)	T_m^I (°C)	ΔH_m^I (J/g)	T_c (°C)	ΔH_c (J/g)	T_m^{II} (°C)	ΔH_m^{II} (J/g)
Aa1	38015	15	128.6	160	117.1	154	130.7	170
		17	128.4	162	117.2	157	130.3	175
		14	128.9	158	117.1	151	130.6	169
		12	128.8	154	117.0	151	130.7	167
		12	128.6	159	117.3	153	130.5	171
		14	129.2	151	117.0	144	131.0	160
		14	128.0	152	117.2	148	130.0	162
		17	128.0	149	111.2	144	130.1	160
Aa2	38294	11	127.9	139	117.1	134	130.0	148
	38323	13	128.4	156	117.3	151	130.4	168
Ab	04/04	9	129.2	184	118.3	182	131.2	199
	41/04	13	129.7	185	117.2	179	131.4	200
	41/04	15	128.6	182	117.6	176	130.5	194
	45/04	13	128.8	179	117.8	173	130.6	192
B	1AUG2004	13	126.7	123	116.9	106	129.2	122
		11	126.4	107	117.0	98	128.7	112
		12	125.7	114	116.7	104	128.1	119
		9	126.4	116	117.1	107	128.7	122
		10	126.7	113	117.2	103	129.1	118

The error on thicknesses is ±2 μm, that on temperatures is ±0.5 °C. The relative error on enthalpies is ±2%. T_m^I and ΔH_m^I denote the temperature and enthalpy of melting measured in the first heating ramp, T_c and ΔH_c are the temperature and enthalpy of crystallization, T_m^{II} and ΔH_m^{II} are the melting temperature and enthalpy measured in the second heating ramp.

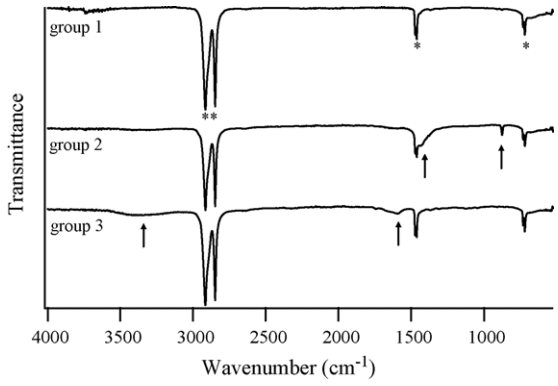

Fig. 1. IR spectra of the three groups of polymers encountered in the study. The arrows indicate the diagnostic bands for each category. The IR bands of PE are indicated by (*) in the topmost spectrum.

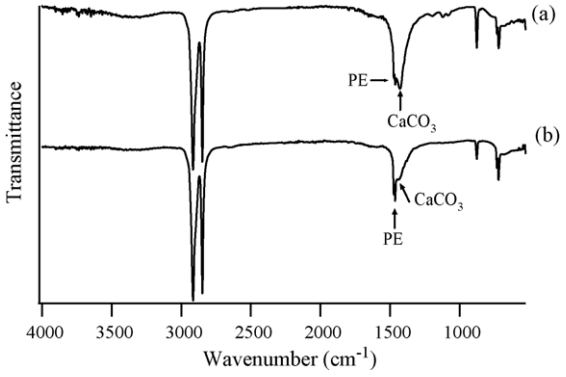

Fig. 3. IR spectrum of samples (a) B and (b) Aa1. Arrows show the characteristic peaks of PE and calcium carbonate useful for differentiation within group 2, according to the different relative intensity between polyethylene peaks at 1461 and 1471 cm^{-1} and that of calcium carbonate at 1430 cm^{-1}.

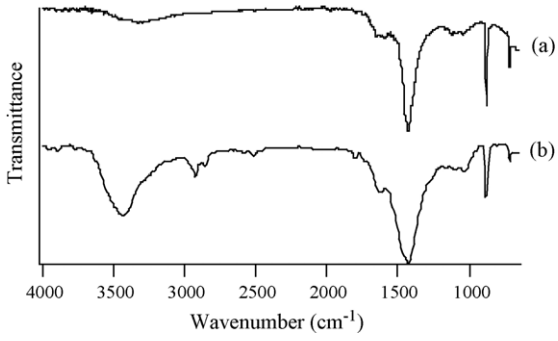

Fig. 2. (a) Subtraction result of pure PE from the IR spectrum of a group 2 sample. (b) IR spectrum of calcium carbonate.

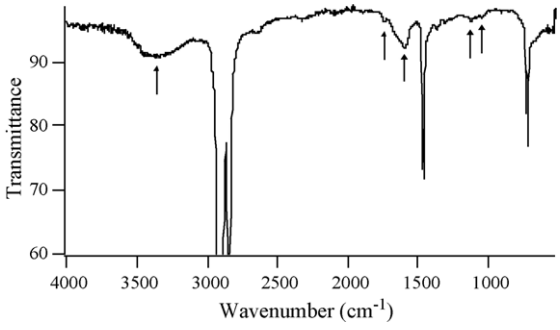

Fig. 4. Particular of the weaker, diagnostic peaks (arrows) of the IR spectrum of a group 3 sample.

pairs over the number of possible pairs [17]. The DP of IR spectroscopy was 0.60. This DP is remarkably lower than that reported by Roux et al. [2], who studied samples coming from Australia and Asia, though. A much lower variability in polymer composition was found to be present in the Italian market.

The characterization was further refined by thickness measurements, whose results are shown in Table 1. A larger DP (0.69) was obtained on the basis of this method, a quite remarkable achievement for a very easy and inexpensive technique. For some of the samples shown in Table 1, it was possible to obtain specimens pertaining to the same and different lots. The results of their characterization are shown in Table 2. As may be seen, some variability in thickness exists among plastic films produced by the same manufacturer in different times and on the basis of this feature lots 04/04 and 41/04 of sample Ab could be deemed as different. Bags of the same lot also showed dishomogeneity, with some of the items of sample Aa1 (lot 38015) distinguishable on the basis of thickness alone. The amount of intra and inter-lot samples is too small to be able to rigorously conclude, under a statistical point of view, that differentiation between or within production lots is possible with this procedure. However, these results are encouraging because they showed that some degree of dishomogeneity indeed exists.

In order to refine a discrimination procedure suitable for this type of plastic packaging films, DSC was applied. A triple ramp was programmed. The first heating was aimed at determining the melting behavior of the sample as a function of the raw material used and of its thermal history. The signals obtained by the subsequent cooling and heating ramps, since they followed the erasure of the thermal history, were dependent only on the microstructure of the polymer employed for the manufacturing of the plastic film. Two different thermal behaviors were found for the 34 white and dull samples. A single signal was predominantly observed for the first and second melting and for the crystallization processes (Fig. 5). This is consistent with the employment of high density PE (HDPE), while if a shoulder appeared in the thermogram, that was an indication that HDPE had been blended with low density PE (LDPE) [18] (Fig. 6). Only five of the considered samples, E, J, L, U and Δ, displayed a double peak, so it can be

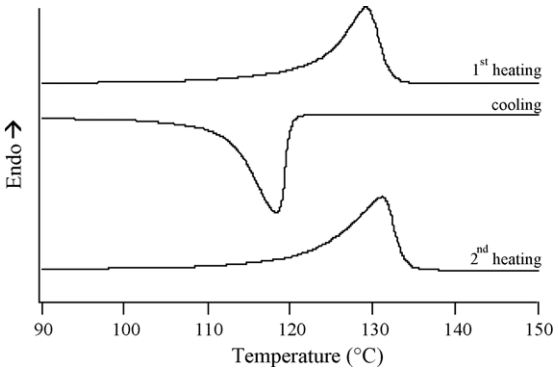

Fig. 5. First melting endotherm (top), crystallization exotherm (middle) and second melting endotherm (bottom) of sample Ab.

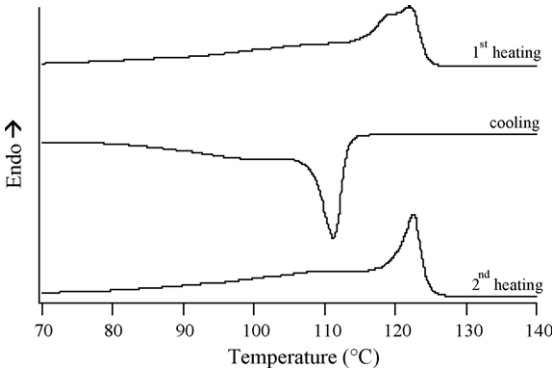

Fig. 6. First melting endotherm (top), crystallization exotherm (middle) and second melting endotherm (bottom) of sample E.

concluded that grocery bags made of HDPE–LDPE are rather rare items (hence more interesting under a forensic point of view). Sample J produced a very peculiar DSC pattern, with a very well separated double peak (Fig. 7). Moreover, in the thermogram of sample H an additional crystallization exotherm, not present in the other considered films, appeared at about 60 °C, giving a supplementary discrimination feature for this item (Fig. 8).

The signals were integrated to measure the enthalpy associated with the melting and crystallization processes. In

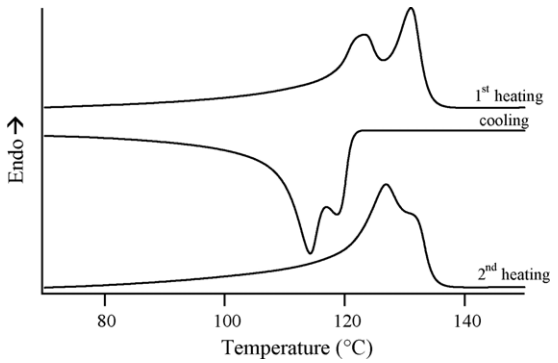

Fig. 7. First melting endotherm (top), crystallization exotherm (middle) and second melting endotherm (bottom) of sample J.

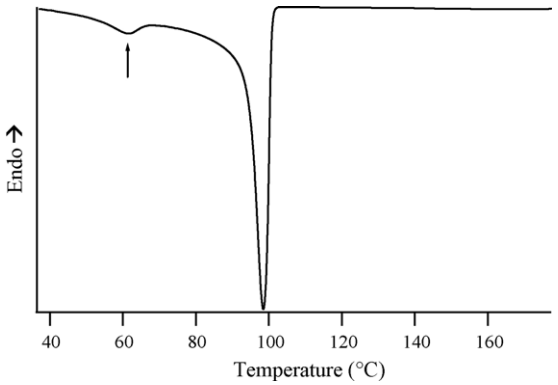

Fig. 8. Crystallization exotherm of sample H. The arrow shows the additional signal at about 60 °C.

particular, the melting enthalpy is proportional to the crystallinity of the material and is a quantity deeply dependent on the processing that was applied to the material during the manufacturing. Tables 1 and 2 show the peak temperatures and the enthalpies associated with the thermal processes detected. The errors associated to these data were evaluated by running replicates on the same samples and calculating the standard deviations: the uncertainty on temperatures was $\pm 0.5\ ^{\circ}C$, the relative error on enthalpies was $\pm 3\%$ for endothermal peaks and 2% for exothermal crystallization signals. In some samples, i.e. E, H, J, L, U, V and Δ the differences in thermal behavior were evident based on their melting or crystallization temperatures. An even greater variability was observed if enthalpies were taken into account. The DP of the first melting enthalpy was 0.77, on the basis of crystallization enthalpy 81% of the possible pairs of samples were discriminated and if the second melting enthalpy was considered the DP was lowered to 0.76. The large dependence of thermal data on slight variations in the manufacturing process is evident if the data in Table 2 are examined. Comparing the enthalpies of samples either of the same and of different lots of the same manufacturer, a significant diversity was observed. This confirmed that DSC is a very efficient method in polymer analysis for distinguishing otherwise similar samples, its only drawback being the relatively large sample size (5 mg) sometimes unrealistic for some samples of forensic interest (e.g. fibers) but affordable in many others, like polymeric packages.

Finally, using all available techniques, IR, thickness measurements and DSC, a comparison was made between all the possible pairs of white, dull samples (colored ones were readily distinguishable by the naked eye) and the DP was therefore computed. IR grouping and thickness proved very useful to rapidly rule out coarsely incompatible samples, while DSC was more effective in the refining of the comparison. The DP associated to the application of this complete sequence of analyses on the 34 white and dull samples was 97%.

4. Conclusion

By an examination procedure consisting of visual examination, thickness measurement, IR spectroscopy and DSC nearly all the grocery bags examined in this work could be discriminated. This can be of help, for example, when the Court is interested in linking the drug packaging to the smugglers who wrapped up the illicit substances. Care was taken to use very straightforward techniques and to avoid sample preparation, in order to meet the double aim of producing easily interpretable results without altering the items. Excluding those samples that were readily distinguishable by visual examination, the use of the three instrumental techniques allowed to discriminate 97% of the possible pairs of white, apparently similar dull polymer films. The aim of this study was that of showing that a rather large degree of variability exists in mass produced articles such as grocery bags. This possibility of discrimination lies in the influence that slightly different parameters in the production processes have on the structure of the polymer obtained. Even though this study was limited to the Italian market, it showed that different materials are used in Europe with respect, for instance, to Australia or Asia [2]. A comparison based on simple and inexpensive techniques can therefore help the Court in tracing the source of illicit drug doses with significant results. Polymeric materials are too often neglected in investigations because of their alleged scarce ‘‘uniqueness’’. Not only judges and lawyers, but also other forensic scientists, often think that, being industrial products, it is not possible to link the polymeric evidence found, for example, on the crime scene to a well-circumstantiated single source. This study showed instead that plastic films used for grocery bags have enough physical and chemical characteristics to allow for the retrieve of a big amount of information.

References

[1] V. Berx, J. De Kinder, 3D measurements on extrusion marks in plastic bags, J. Forensic Sci. 47 (2002) 976–985.
[2] C. Roux, S. Bull, J. Goulding, C. Lennard, Tracing the source of illicit drugs through plastic packaging—a database, J. Forensic Sci. 45 (2000) 94–114.
[3] K. Püschel, S. Stein, S. Stobbe, A. Heinemann, Analysis of 683 drug packages seized from ‘‘body stuffers’’, Forensic Sci. Int. 140 (2004) 109–111.
[4] S.A. Koehler, S. Ladham, L. Rozin, A. Shakir, B. Omalu, J. Dominick, C.H. Wecht, The risk of body packing: a case of a fatal cocaine overdose, Forensic Sci. Int. 151 (2005) 81–84.
[5] T. Tsukame, M. Kutsuzawa, H. Sekine, H. Saitoh, Y. Shibasaki, Identification of polyethylene by differential scanning calorimetry—application to forensic science, J. Therm. Anal. Calorimetry 57 (1999) 847–851.
[6] E.C. Ihms, D.W. Brinkman, Thermogravimetric analysis as a polymer identification technique in forensic applications, J. Forensic Sci. 49 (2004) 505–510.
[7] G.S.H. Lee, K.M. Brinch, K. Kannangara, M. Dawson, M.A. Wilson, A methodology based on NMR spectroscopy for the forensic analysis of condoms, J. Forensic Sci. 46 (2001) 808–821.
[8] M.C. Grieve, K.G. Wiggins, Fibers under fire: suggestions for improving their use to provide forensic evidence, J. Forensic Sci. 46 (2001) 835–843.
[9] V. Causin, C. Marega, G. Guzzini, A. Marigo, Forensic analysis of poly(ethylene terephthalate) fibers by infrared spectroscopy, Appl. Spectrosc. 58 (2004) 1272–1276.
[10] Z. Shen, J.J. Thomas, G. Siuzdak, R.D. Blackledge, A case study on forensic polymer analysis by DIOS-M: the suspect who gave us the SLIP, J. Forensic Sci. 49 (2004) 1028–1035.
[11] V. Causin, C. Marega, S. Schiavone, A. Marigo, Employing GRIM in fiber analysis: a simple method for evaluating the crystallinity of acrylics, Forensic Sci. Int. 149 (2005) 193–200.
[12] V. Causin, C. Marega, S. Schiavone, A. Marigo, A quantitative differentiation method for acrylic fibers by infrared spectroscopy, Forensic Sci. Int. 151 (2005) 125–131.
[13] F.C.-Y. Wang, The microstructure exploration of thermoplastic copolymers by pyrolysis–gas chromatrography, J. Anal. Appl. Pyrolysis 71 (2004) 83–106.
[14] L. Burman, A.-C. Albertsson, Chromatographic fingerprinting—a tool for classification and for predicting the degradation state of degradable polyethylene, Polym. Degrad. Stabil. 89 (2005) 50–63.
[15] U. Simmross, R. Fischer, F. Düwel, U. Müller, Quantitative determination of cadmium in polyethylene using total reflection X-ray fluorescence

(TXRF) spectroscopy, Fresenius J. Anal. Chem. 358 (1997) 541–545.
[16] K.E. Nissen, J.T. Keegan, J.P. Byrne, Characterization of plastic films from trace element analysis using inductively coupled plasma-mass spectrometry, Can. J. Anal. Sci. Spectrom. 43 (1998) 122–128.
[17] K.W. Smalldon, A.C. Moffat, The calculation of discrimination power for a series of correlated attributes, J. Forensic Sci. Soc. 13 (1973) 291–295.
[18] T. Tsukame, Y. Ehara, Y. Shimizu, M. Kutsuzawa, H. Saitoh, Y. Shibasaki, Characterization of microstructure of polyethylenes by differential scanning calorimetry, Thermochim. Acta 299 (1997) 27–32.

ELSEVIER

Forensic Science International 164 (2006) 155–158

Forensic Science International

www.elsevier.com/locate/forsciint

The value of examination aids in victim identification: a retrospective study of an airplane crash in Nepal in 2002

Roman Bux [a,*], Detlef Heidemann [b], Markus Enders [a], Hansjürgen Bratzke [a]

[a] *Centre of Forensic Medicine, J.W. Goethe-University, Frankfurt/Main, Germany*
[b] *Dental School, J.W. Goethe-University, Frankfurt/Main, Germany*

Received 4 February 2005; received in revised form 9 December 2005; accepted 20 December 2005
Available online 24 January 2006

Abstract

After the crash of an airplane in Nepal in the year 2002, the dental status of the 14 European victims was examined at autopsy as well as after additional removal of the soft tissue and compared with antemortem findings which were available in 11 cases. Re-examination of all jaws showed that nine composite fillings and seven root fillings as well as one parapulpal pin could not be detected during autopsy. Because tooth-coloured restorations may be overseen even by an experienced expert, the findings underline the necessity of performing a full resection of both jaws and removal of the soft tissue. Furthermore, X-ray analysis of the jaws and the use of phosphoric acid or ultra violet radiation for recognizing tooth-coloured restorations are recommended.

Keywords: Dental identification; Mass disaster; Tooth-coloured dental fillings; Forensic odontology; Radiography

1. Introduction

On August 22, 2002, a twin-engine DHC-6 Twin Otter with 15 passengers and three crew-members flying from Jomsom to Pokhara, Nepal, crashed into a mountain near Pokhara. All 18 passengers and crew were killed. After an autopsy in Kathmandu, a second autopsy of the 14 European victims was performed at the Centre of Legal Medicine, Frankfurt/Main, Germany, to enable identification of the corpses which was complicated by the extensive fragmentation of the bodies.

2. Material and methods

The autopsies which were performed by two forensic pathologists, in the presence of members from the Identification Commission of the Bundeskriminalamt (IDKO). Each team consisted of two forensic pathologists, a dentist, an autopsy assistant, a secretary and a photographer. When applicable personal documents, jewellery, remains of the clothing and anthropological data (sex, age, body size, scars, etc.) were recorded to supplement the dental findings.

For postmortem dental examination maxilla and mandible were excised, cleaned and examined by the dentist at daylight and artificial light, using magnifying glasses. The findings were recorded in postmortem Interpol DVI forms. In 11 cases, antemortem dental records were available, transcribed into antemortem Interpol DVI forms and compared with the postmortem findings. No antemortem radiographs were available as they were not asked for by the IDKO a.m.-team.

After completing identification procedures, the soft tissue was removed, the jaws were X-rayed and re-examined by the same dentist 6 months later. The ante and postmortem data were compared with findings of the re-examination.

3. Results

At autopsy the corpses were found severely damaged, partly fragmented showing signs of heavy blunt external forces. The injuries were consistent with an airplane crash. The 14 victims (13 German and one British citizen) were between 35 and 64 years old, seven males and seven females.

* Corresponding author at: Centre of Legal Medicine, J.W. Goethe-University, Kennedyallee 104, D-60596 Frankfurt am Main, Germany.
Tel.: +49 69 6301 5277 fax: +49 69 6301 83461.
E-mail address: bux@em.uni-frankfurt.de (R. Bux).

0379-0738/$ – see front matter © 2006 Elsevier Ireland Ltd. All rights reserved.
doi:10.1016/j.forsciint.2005.12.025

The antemortem (a.m.) dental findings, the postmortem (p.m.) data obtained at autopsy and after removal of the soft tissue are presented in Table 1. Of 11 victims (78.6%) an antemortem dental status was available covering a time range between 6 months and 13 years. Only in one case, the p.m. findings at autopsy were identical with the a.m. data. In the other cases, discrepancies up to 10 fillings were observed. In three cases, the a.m. status was found to be incorrect; the retention of two wisdom teeth and two torsions (tooth 13 and 41) had not been noted, one filling (tooth 13) could not be confirmed.

Table 1
The dental status of the victims a.m., at autopsy and after removal of the soft tissue; differences to the previous finding bold typed

Number	Sex	Age	a.m. findings	p.m. findings (autopsy)	p.m. findings (re-ex.)
1	Female	58 a	n/a	Maxilla missing; composite fillings: 33, 34, 35, 44; gold crowns: 36, 37, 38; ceramic crown: 45; silver crown: 48; ceramic bridge: 45–48	**Root filling: 36**
2	Female	35 a	Fillings (not specified): 11, 13, 14, 15, 16, 17, 26, 27, 36, 46	**No filling: 13; fractured tooth 35, filling missing**; mandible fractured	No differences to previous findings
3	Female	44 a	amalgam fillings: 16, 26, 46	**Cement fillings: 15, 16, 26; amalgam filling: 36; retention: 38, 48**; p.m. missing: 12, 13, 43; p.m. fracture: 11	**Composite filling: 26**
4	Male	44 a	Amalgam fillings: 16, 17, 24, 36; composite fillings: 26, 45; metal crown: 46; gold inlay: 47	**Composite fillings: 16, 28**	**Composite filling: 45: parapulpal pin: 26**
5	Female	35 a	Amalgam fillings: 14, 15, 17, 24, 25, 26, 35, 36, 46; composite filling: 45; missing teeth: 18, 28, 38, 48	**Amalgam filling: 16; composite filling: 11**; p.m. missing: 21, 31, 32, 33; p.m. fracture: 12, 22	No differences to previous findings
6	Female	45 a	Composite filling: 47; gold inlays: 15, 16, 17, 26, 27, 36, 46; missing teeth: 18, 28, 38, 48	**Composite fillings: 11, 14, 24, 35, 37, 44, 45; amalgam filling: 12**	**Composite filling: 41**
7	Male	43 a	n/a	Amalgam fillings: 35, 47; composite fillings: 11, 12, 13, 21. 23, 34, 44; gold inlays: 15, 16, 17, 25, 26, 46; metal crowns: 14, 24, 45; gold crowns: 27, 36, 37; torsion: 33, 43; missing teeth: 18, 28, 38, 48; p.m. missing: 31, 32	**Root filling: 26**
8	Female	39 a	Composite fillings: 15, 17; ceramic crowns: 14, 25, 26, 34, 35, 37; ceramic bridge: 24–26; missing tooth: 46	**Composite fillings: 11, 16, 21, 23, 33; missing tooth: 28; amalgam fillings: 18, 27, 36, 47, 48; torsion: 13, 41**; p.m. missing: 32	**Composite filling: 22; root filling: 25**
9	Male	51 a	Amalgam fillings: 17, 18, 21, 22, 28, 35, 48; ceramic crowns: 13, 16, 24, 27, 44, 45, 47; ceramic bridges: 13–16, 24–27, 45–47; crown: 36; missing teeth: 37, 38	**Composite filling: 22; Ceramic crowns: 17, 18; ceramic bridge: 13–17; gold crown: 48**; missing segments: 24–28, 42–38	**Composite filling: 21; root fillings: 13, 45**
10	Female	43 a	Amalgam fillings: 15, 16, 17, 27, 34, 45, 46; composite filling: 24, 25; ceramic crown: 12, 13, 22, 23, 26; gold crown: 35, 37, 47; ceramic bridge: 13–23; gold bridge: 35–37; missing teeth: 18, 28, 38	**Amalgam filling: 14; missing tooth: 48**; filling 34 lost	**Root fillings: 24, 47**
11	Male	64 a	n/a	Missing segments: 16–18, 23–28; segment 42–32 fragmented, not clearly interpretable; missing teeth: 11, 12, 15, 21, 22, 37, 38; amalgam fillings: 13, 14, 34, 35, 36, 44, 45, 48; metal crown: 46; gold crown: 47; p.m. missing: 43	**Composite fillings: 13, 14, 31, 32**
12	Male	43 a	Amalgam filling: 28; metal crown: 46; missing teeth: 26, 38, 47	**Amalgam fillings: 16, 17, 18**; p.m. fracture: 14	No differences to previous findings
13	Male	45 a	Amalgam fillings: 15, 16, 17, 26, 27, 36, 37, 46, 47; composite fillings: 12, 21, 22; missing teeth: 14, 18, 25, 28 (diminutive), 34, 38, 44, 48; fixed dental brace maxilla, mandible	p.m. missing: 11	No differences to previous findings
14	Male	48 a	Composite fillings: 11, 12, 17, 18, 21, 22, 23; ceramic crowns: 16, 26, 33, 34, 45; metal crown: 37, 47; ceramic bridge: 34–35; metal bridges: 36–37, 45–47	**Amalgam fillings: 24, 25, 27, 38, 44, 48**; missing segment: 12–18; segment 42–32 heavily fragmented, not interpretable	No differences to previous findings

Since the names of the 14 passengers were known (closed disaster), their identification could be performed on the basis of dental findings, in four cases in combination with anthropological data and personal belongings.

Re-examination of the jaws after removal of the soft tissue by the same investigator 6 months later revealed that in six victims nine composite fillings and one parapulpal pin had not been detected at autopsy. Radiographs further revealed seven root fillings in five victims which were neither mentioned in the a.m. notes nor diagnosed during autopsy.

4. Discussion

Proper identification of disaster victims is an important medico-legal objective. Apart from visual identification, which is often complicated by the severe destruction of the corpses, personal belongings, physical characteristics and other anthropological findings, finger prints, dental examination and genetic data may be used [1]. In cases of dismembered human bodies a multidisciplinary approach has been found to be most promising [2–4]. With well documented postmortem findings and sufficient antemortem data, exist dental identification has great practical value in routine forensic casework [5–10]. A review of mass disasters indicates that the success rate of dental identification varies within a wide range. Of 28 victims of a bus accident in Spain 16 (57%) could be identified with the help of their dental status [11]. Of 94 recovered victims of the M/S Estonia which sunk in 1994, 57 (60%) could be identified by comparing their a.m. and p.m. dental data [12]. The dental identification of war victims in Croatia had success rates of 16–25% [13,14] and was hindered by the lack of sufficient a.m. records [15]. Dental identification may be difficult in high-impact and high-temperature accidents with extensive dental fracturing [16] or if teeth or parts of the jaws were lost in the course of recovery, transportation of the body [3,17].

Postmortem X-rays are considered to be important tools in dental identification, especially if a p.m. orthopantomography (OPG) could be compared to an a.m. OPG [18,19]. Therefore, efforts have been made to improve the techniques of postmortem dental radiology [20,21] and even the technique to obtain post mortal OPGs [19,22]. The results of a British study where 198 dental radiographs taken from 22 skulls indicated that root morphology and alignment were found facilitating matching [23], are in accordance with the suggestion to compare a.m. and p.m. OPGs for identification purposes whenever possible [12,24]. In cases of fragmented jaws intra-oral radiographs should be obtained. Because up to 40% of dental filling materials is not detectable by radiography [25], an additional careful visual dental examination is required. Recently, a new technique was introduced to improve the visual detection of tooth-coloured dental restorations by etching with 37% phosphoric acid [26], which may help to avoid overlooking of dental fillings. The reliability of the findings may be illustrated by the NMR (numerical-morphological-radiographic) Certainty Index [27], which documents the number of points of concordance between the a.m. and p.m. data.

According to dental examination of 17,880 teeth from mass graves in Croatia prosthetic appliances were most useful for identification (30%), followed by teeth extractions (25%) and teeth restorations in 20% [28]. But also dental anomalies like diastemas, displaced and rotated teeth can be important [29], stressing the need of carefully maintained dental records.

Since at least 12 concordant findings are requested to enable positive dental identification [30] dental patterns were thoroughly investigated in epidemiological studies indicating a huge diversity. A certain number of points of concordance between the a.m. and p.m. dental status should not be overstressed, even when a.m. radiographs are not available [31,32]. The suggestion that rare dental findings should be used for identification even if they are the single concordance [33] is in contrast to a report of the incorrect identification of a military pilot with a very similar dental record to his co-pilot. In this case, only the correct evaluation of the shape of the amalgam restorations allowed positive identification. In both victims, all third molars had been removed and there were identical amalgam restorations in all molars except in one [34].

In this study, the initial examination of every jaw associated with the autopsy was performed by an odontologist with considerable experience in dental identification. The p.m. findings of all victims were recorded in p.m.-forms and then compared with the a.m. findings. Dental identification was made in ten cases which showed between 6 and 21 points of concordance, but only in three cases the criteria of Keiser–Nielsen [30] were met. Nevertheless the findings allowed preliminary identification due to the special constellation of a small number of victims in a closed disaster. To eliminate the remaining uncertainty, a second examination of the jaws after removal of the soft tissue was performed and led to the disclosure of nine composite fillings and one parapulpal pin. This additional points of concordance with the a.m. records improved significantly the certainty of the identification. The fact that only one of the 11 a.m. records available was completely concordant with the p.m. findings underlines the importance of accurate a.m. records. Dentists should be aware that their clinical documentation might be an important aid in identification and should thus be kept accurate and topical. In our cases the absence of a.m. radiographs, which had not been asked for by the a.m.-team, did not hamper the identification process. But in open disasters or a higher number of victims a.m. radiographs should definitely be made available.

5. Conclusion

The study demonstrates that high quality tooth-coloured dental restorations may be overlooked even by an experienced dentist. A good light-source and magnification devices should be standard for the examination of teeth and jaws. Therefore the removal of the jaws is recommended in all cases where the identification through the dental status is intended, especially in an open disaster and in children with no or only a few teeth restorations. Removing the jaws by the neck dissection will leave the face entirely unaffected and avoids disfigurement. Additionally, intra-oral radiography of the jaws, (if possible an

orthopantomography (OPG)) or radiography of the resected jaws should be performed. Phosphoric acid and ultra violet light [35] should be used to facilitate the visual identification of tooth-coloured restorations.

References

[1] B. Brinkmann, Harmonization of medico-legal autopsy rules. Committee of Ministers. Council of Europe., Int. J. Legal Med. 113 (1999) 1–14.

[2] Y. Bilge, P. Kedici, Y. Alakoc, K. Ulkuer, Y. Ilkyaz, The identification of a dismembered human body: a multidisciplinary approach., Forensic Sci. Int. 137 (2003) 141–146.

[3] K. Rötzscher, S. Benthaus, B. Höhmann, Schutz oder Management? Katastrophenschutz in der Bundesrepublik Deutschland, Rechtsmedizin 8 (1998) 201–206.

[4] C. Hsu, N.E. Huang, L.C. Tsai, L.G. Kao, C.H. Chao, A. Linacre, JC-I. Lee, Identification of victims of the 1998 Taoyuan Airbus crash accident using DNA analysis, Int. J. Legal Med. (1999) 43–46.

[5] D. Heidemann, Identifizierungsarbeiten in Ramstein, Zahnärztl. Mitt. 78 (1988) 2116–2123.

[6] S. Sakoda, B. Zhu, K. Ishida, S. Oritani, M. Fujita, H. Maeda, Dental identification in routine forensic casework: clinical and postmortem investigations, Leg. Med. (Tokyo) 2 (2000) 7–14.

[7] D. Sweet, Why a dentist for identification? Dent. Clin. North America 45 (2001) 237–251.

[8] E. Ndiokwelu, J. Miquel, N. Coudert, Identification of victims of catastrophes: introduction to the role of forensic odontology, Odontostomatol. Trop. 26 (2003) 33–36.

[9] I. Pretty, L. Addy, Associated postmortem dental findings as an aid to personal identification, Sci. Justice 42 (2002) 65–74.

[10] M. Richardson, By their teeth shall ye know them, Br. Dent. J. 191 (2001) 459–464.

[11] A. Valenzuela, I.H.S. Martin-de, T. Marques, N. Exposito, J. Bohoyo, The application of dental methods of identification to human burn victims in a mass disaster, Int. J. Legal Med. 113 (2000) 236–239.

[12] H. Soomer, H. Ranta, A. Penttilä, Identification of victims from the M/S Estonia, Int. J. Legal Med. 114 (2001) 259–262.

[13] H. Brkic, D. Strinovic, M. Slaus, J. Skavic, D. Zecevic, M. Milicevic, Dental identification of war victims from Petrinja in Croatia, Int. J. Legal Med. 110 (1997) 47–51.

[14] H. Brkic, D. Strinovic, M. Kubat, V. Petrovecki, Odontological identification of human remains from mass graves in Croatia, Int. J. Legal Med. 114 (2000) 19–22.

[15] J. Dumancic, Z. Kaic, V. Njemirovskij, H. Brkic, D. Zecevic, Dental identification after two mass disasters in Croatia, Croat. Med. J. 42 (2001) 657–662.

[16] A. Titsas, J. Kieser, Odontological identification in two high-impact, high-temperature accidents, J. Forensic Odontostomatol. 17 (1999) 44–46.

[17] R. Oliveira, R. Melani, J. Antunes, E. Freitas, L. Galvao, Postmortem tooth loss in human identification processes, J. Forensic. Odontostomatol. 18 (2000) 32–36.

[18] A. Haertig, A. Bonnin, L. Lehoux, R. Auffret, Role du panoramique dentaire lors des procédures d'identification, J. Radiol. 72 (1991) 489–490.

[19] A. Du Chesne, S. Benthaus, K. Teige, B. Brinkmann, Post-mortem orthopantomography–an aid in screening for identification purposes, Int. J. Legal Med. 113 (2000) 63–69.

[20] S. Benthaus, Systematic aspects of roentgen identification–practical methods and new aids, Arch. Kriminol. 200 (1997) 95–106.

[21] S. Benthaus, K. Rötzscher, H. Engel, Der Einsatz mobiler Röntgentechniken bei der odonto-stomatologischen Identifizierung von Katastrophenopfern, Rechtsmedizin 9 (1999) 155–158.

[22] K. Rötzscher, T. Solheim, Befunderhebung postmortem, in: K. Rötzscher (Ed.), Forensische Zahnmedizin, Springer, Berlin, Heidelberg, 2000, pp. 181–203.

[23] S. Sholl, G. Moody, Evaluation of dental radiographic identification: an experimental study, Forensic Sci. Int. 115 (2001) 165–169.

[24] S. Lee, J. Choi, C. Yoon, C. Kim, K. Shin, The diversity of dental patterns in the orthopantomography and its significance in human identification, J. Forensic Sci. 49 (2004) 784–786.

[25] A. Du Chesne, S. Benthaus, B. Brinkmann, Forensic identification value of roentgen images in determining tooth-colored dental filling materials, Arch. Kriminol. 203 (1999) 86–90.

[26] S. Benthaus, C.A. Du, B. Brinkmann, A new technique for the postmortem detection of tooth-coloured dental restorations, Int. J. Legal Med. 111 (1998) 157–159.

[27] S. Benthaus, K. Rötzscher, B. Brinkmann, B. Knell, H. Waes van, J. Bonnetain, J. Hutt, Qualitätsrichtlinien bei der zahnärztlichen Identifikation unbekannter Leichen. Definition eines international verbindlichen Standards, Newslett. AKFOS 6 (1999) 56–65.

[28] H. Brkic, J. Keros, Z. Kaic, J. Cadez, Hereditary and environmental dental findings in identification of human remains, Coll. Antropol. 24 (Suppl. 1) (2000) 79–83.

[29] V. Delattre, P. Stimson, Self-assessment of the forensic value of dental records, J. Forensic Sci. 44 (1999) 906–909.

[30] S. Keiser-Nielsen, Dental identification: certainty V probability, Forensic Sci. 9 (1977) 87–97.

[31] B. Adams, The diversity of adult dental patterns in the United States and the implications for personal identification, J. Forensic Sci. 48 (2003) 497–503.

[32] B. Adams, Establishing personal identification based on specific patterns of missing, filled, and unrestored teeth, J. Forensic Sci. 48 (2003) 487–496.

[33] C. de Villiers, V. Phillips, Person identification by means of a single unique dental feature, J. Forensic Odontostomatol. 16 (1998) 17–19.

[34] R. Cecchi, L. Cipolloni, M. Nobile, Incorrect identification of a military pilot with international implications, Int. J. Legal Med. 110 (1997) 167–169.

[35] D. Clark, R. Ruddick, Postmortem detection of tooth coloured dental restorations by ultra violet radiation, Acta Med. Legal Soc. (Liege) 35 (1985) 278–284.

ELSEVIER

Forensic Science International 164 (2006) 159–163

Forensic Science International

www.elsevier.com/locate/forsciint

Quantitative LC–MS determination of strychnine in urine after ingestion of a *Strychnos nux-vomica* preparation and its consequences in doping control

P. Van Eenoo *, K. Deventer, K. Roels, F.T. Delbeke

Doping Control Laboratory (DoCoLab), Ghent University-UGent, Department of Clinical Biology, Microbiology and Immunology, Technologiepark 30B, B-9052 Zwijnaarde, Belgium

Received 4 October 2005; received in revised form 1 December 2005; accepted 23 December 2005
Available online 31 January 2006

Abstract

A simple, fast and sensitive method for the quantitative determination of strychnine residues in urine has been developed and validated. The method consists of a liquid–liquid extraction step with ethyl acetate at pH 9.2, followed by LC–MS/MS in positive atmospheric pressure chemical ionization (APCI)-mode. The method is linear in the range of 1–100 ng/mL and allows for the determination of strychnine at sub-toxicological concentrations. The accuracy of the method ranged from 1.3% to 4.4%. The method was used to determine the excretion profile of strychnine after the ingestion of an over-the-counter herbal preparation of *Strychnos nux-vomica*. Each volunteer ingested a dose equivalent to 380 μg of strychnine. This dose is lower than the prescription dose but results in the detection of strychnine for over 24-h post administration. Maximum detected urinary concentrations ranged from 22.6 to 176 ng/mL. The results of this study show that the use of this type of preparation by athletes can lead to a positive doping case.

Keywords: Strychnine; Urine; Doping; Liquid chromatography; Mass spectrometry

1. Introduction

The alkaloid strychnine was first isolated from *Strychnos ignatii* beans in 1818. The commercial source of strychnine is however the dried seed *Strychnos nux-vomica* [1]. Although strychnine is highly toxic [2], several homeopathic *Strychnos nux-vomica* preparations are available as an over-the-counter product in Belgium.

Strychnine has been one of the earliest substances used to enhance performance in sports. Already in the nineteenth century cyclists reportedly used cocktails of caffeine, cocaine, alcohol, ether and strychnine in endurance events [3] and perhaps the first reported drug-related death in sports (Arthur Linton in 1896) was due to strychnine [4]. Today, strychnine still appears on the list of prohibited substance in sports [5] and is one of the few substances for which an individual minimum required performance limit (MRPL) has been specified [6]. This MRPL for strychnine is set at 200 ng/mL [6].

Several methods for the detection of strychnine in bio-fluids via gas chromatography [7–9] and liquid chromatography [10] have been published. These methods were developed mainly for toxicology and the limits of detection are near or above the MRPL required by WADA. Recently, methods using liquid chromatography–tandem mass spectrometry (LC–MS/MS) for the quantitative detection of strychnine in seeds [11] and insects [12] and the qualitative detection in urine [13] have been published. The limits of detection of these methods are lower than those previously developed for toxicological purposes. Taking into account the popularity and growth of the supplement/homeopathy market, it seems necessary to test if the implementation of this new technique would allow for the detection of strychnine after the use of over-the-counter preparations. In addition, it needs to be tested if the use of a herbal preparation could result in inadvertent doping positive cases.

2. Materials and methods

2.1. Materials

Strychnine and nalorphine were purchased from Sigma (St. Louis, USA). Analytical grade potassium carbonate, sodium

* Corresponding author. Tel.: +32 9 3313290; fax: +32 9 3313299.
E-mail address: Peter.VanEenoo@UGent.be (P. Van Eenoo).

0379-0738/$ – see front matter
doi:10.1016/j.forsciint.2005.12.029

hydrogen carbonate and acetic acid were purchased from Merck (Darmstadt, Germany), acetonitrile was from Biosolve, HPLC grade methanol from Acros (Geel, Belgium), ethyl acetate from Panreac (Barcelona, Spain) and HPLC grade water from Fisher (Loughborough, UK). The herbal preparation Nux-vomica MT was bought as an over-the-counter product in a local pharmacy and was from Homeoden-Heel (Belgium).

2.2. Excretion study

The study was performed with four healthy male volunteers. The study protocol was reviewed and approved by the ethical committee of the institution (Ghent University Hospital). Each volunteer signed a statement of informed consent. Each volunteer ingested ten drops (equivalent to 380 μg of strychnine) of the over-the-counter Nux-vomica preparation. Urine samples were collected before (0 h) and quantitatively 2, 4, 6, 9 and 12 h after intake during the administration period. Additional samples were taken 24, 36 and 48 h after administration.

All urine samples were either analyzed directly or stored at −20 °C awaiting analysis. Urinary pH, volume and density were measured and all samples were analyzed in duplicate. When necessary, urine samples were diluted with water in order to obtain concentrations in the range of the calibration curve.

2.3. Sample preparation

The method was adapted from a previously published screening method for diuretics and beta-blockers [13]. The internal standard solution (50 μL nalorphine, 20 μg/mL) was added to 2.0 mL of urine and the urine was made alkaline with 200 mg $NaHCO_3/K_2CO_3$ (2:1).

Liquid–liquid extraction was performed by rolling for 10 min with 5 mL ethyl acetate. After centrifugation (2500 rpm) the organic layer was transferred into a new tube and evaporated until dry under oxygen free nitrogen (OFN) at 40 °C. The residue was dissolved in 200 μL mobile phase.

In each batch of samples, a blank urine sample, a system blank (aqua bidest) and a quality control sample (spiked at 10 ng/mL) were analyzed concurrently.

2.4. Apparatus

2.4.1. Chromatography

Separation of the compounds was performed on a cyanopropyl column (100 mm × 4.6 mm, 3 μm; Chrompack, Antwerp, Belgium) using a P4000 pump and a model AS3000 autosampler (TSP, San Jose, USA). The mobile phase consisted of acetonitrile and 1% acetic acid in water. Gradient elution at a flow rate of 1.0 mL/min was as follows (Fig. 1): 90% acetic acid (1%) decreased linear to 64% in 6.5 min followed by an increase to the initial acetic acid (1%) concentration, which is maintained for 5 min before the next injection (equilibration time). The total run time of the method was 12 min. The injection volume was 50 μL.

2.4.2. Mass spectrometry

Ionization of the analytes was carried out on a LCQ-Deca instrument (Thermo, San Jose, USA) using atmospheric pressure chemical ionization (APCI) in the positive ionization mode. The capillary temperature and evaporator temperature were maintained at 200 and 300 °C, respectively. The drying gas was maintained at 80 units while the auxiliary gas was set to 10 units. The capillary voltage was maintained at 10 V. The needle discharge current was set arbitrarily to 5 μA.

For MS/MS experiments $m/z = 335$ and $m/z = 312$ were chosen as precursor ions in the APCI+-mode for strychnine and nalorphine, respectively. The relative collision energies for both compounds were set at 38% and 36%, respectively. The collision energies were determined in such a way that the precursor ion would still be present in the product spectrum with a relative intensity of maximum 20%. The isolation width for the precursor ion was set at 3. The activation q-value and ionization time were set to 0.250 and 30 ms, respectively.

2.5. Validation

A five-point calibration curve was generated by spiking blank urine with strychnine in triplicate at 1, 5, 10, 50 and 100 ng/mL. The averages of these measurements were used to construct the calibration curve. The area ratio of the product ions of strychnine ($m/z = 264$) and the internal standard ($m/z = 270$) were plotted versus the concentration.

The precision and accuracy of the method were tested at three levels (1, 10 and 100 ng/mL). Precision was assessed as the percentage relative standard deviation (%R.S.D.) of both repeatability (within-day) and reproducibility (between-day and different analysts) for a selected compound and level. Maximum allowed tolerances for reproducibility and repeatability can be calculated from the Horowitz-equation $R.S.D._{max} = 2^{(1-0.5 \log C)}$ (C = concentration (μg/mL) × 10^{-6}). The maximum allowed tolerances for repeatability and reproducibility are $2/3 R.S.D._{max}$ and $R.S.D._{max}$, respectively [14].

Accuracy was defined as the difference between the calculated amount and the specified amount for the selected compound and expressed as a percentage [15].

Selectivity was tested by analysing reference mixtures containing several structurally related doping agents which are routinely screened for including alkaloids and stimulants. The

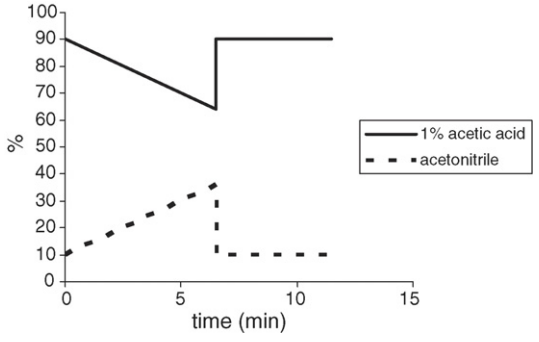

Fig. 1. Mobile phase composition, flow: 1 mL/min.

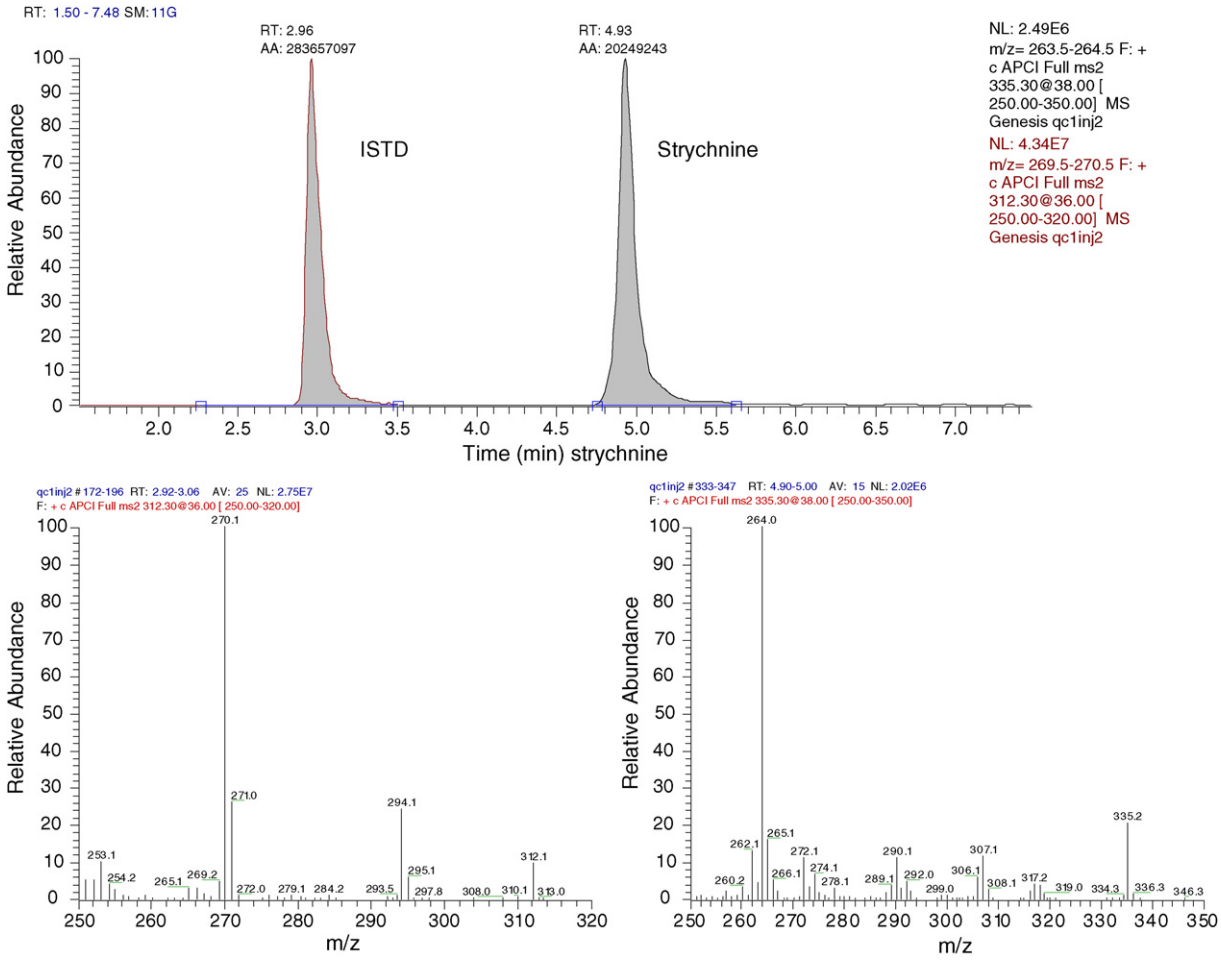

Fig. 2. Ion chromatograms (*m/z* 270 and *m/z* 264) and product spectra of nalorphine (ISTD) and strychnine in a quality control urine spiked at 10 ng/mL.

Table 1
Accuracy (between-day), repeatability, reproducibility and tolerance limits of the LC–MS method at three concentrations (1, 10 and 100 ng/mL)

Concentration (ng/mL)	Accuracy (%), $n = 18$	Repeatability (%), $n = 6$	Reproducibility (%), $n = 18$	R.S.D.$_{max}$ (%)	2/3 R.S.D.$_{max}$ (%)
1	+1.3	2.5	11.5	45	30
10	+3.4	6.1	7.5	32	21
100	+4.4	3.9	6.4	23	15

Including the lowest point of the calibration curve for strychnine.

concentration of the substances in these mixtures was 1 μg/mL. The limit of quantification (LOQ) of the method was defined as the lowest concentration where acceptable reproducibility and accuracy could be guaranteed. The limit of detection (LOD) was defined arbitrarily as 1/2LOQ. The product spectrum of strychnine in six samples spiked at the LOD was compared to a strychnine reference sample and conformity with the WADA guidelines [16] was checked (*m/z* 335, 307, 290 and 264 were used for comparative purposes).

Extraction recovery of strychnine was investigated. For this purpose blank urine samples ($n = 6$) were spiked at three levels (1, 50, 100 ng/ml) and extracted together with blank (not spiked) urine samples ($n = 6$). The extracts of the blank urine samples were then spiked at the same levels simulating a 100% recovery. Finally, both sets of samples were evaporated and analyzed with the described LC–MS method. The obtained peak areas of the two sets of samples were compared (Fig. 1).

Table 2
Recovery of strychnine[a]

Concentration (ng/mL)	Recovery (%), $n = 6$
1	79.3 ± 6.4
10	83.6 ± 1.8
100	83.0 ± 1.9

[a] Values are presented as mean ± standard deviation ($n = 6$).

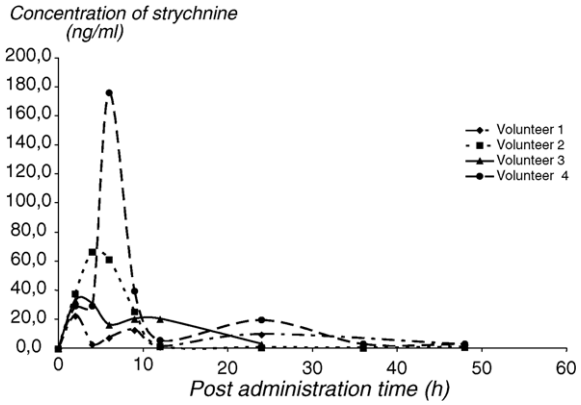

Fig. 3. Urinary excretion profile of strychnine in the urine samples from four volunteers (380 μg of strychnine administered as a *Strychnos nux vomica* extract).

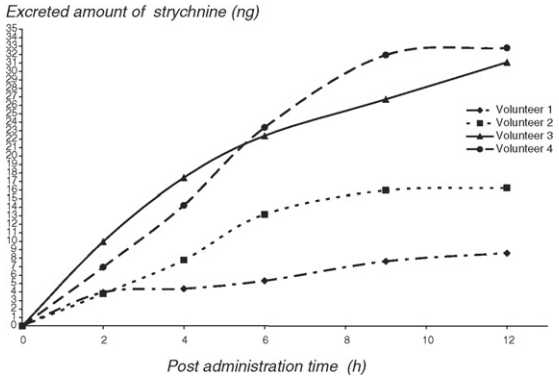

Fig. 4. Excreted amount of strychnine in urine within the first 12-h post administration of 380 μg for the four volunteers.

3. Results

The ion chromatograms and product spectra for strychnine and nalorphine in a quality control sample spiked at 10 ng/mL are shown in Fig. 2.

The study was performed over a 2-month period and three calibration curves were generated. The correlation coefficients (r^2) of the calibration curves always exceeded 0.99. Data on accuracy, repeatability and reproducibility of the method is given in Table 1. The LOQ was 1 ng/mL and the LOD was 0.5 ng/mL. The product spectra obtained in the samples spiked at the LOD were in agreement with the minimum requirements of WADA for the unequivocal identification of a prohibited substance.

The extraction recovery of strychnine is presented in Table 2.

The excretion profiles (urinary concentration) of the 4 volunteers are shown in Fig. 3 and the cumulative excretion profiles are given in Fig. 4.

4. Discussion

The vast majority of reversed phase (in particular C18) HPLC separations take place on silica based stationary phases. However, silica suffers from poor peak shape for basic compounds. In particular for strychnine the problem of tailing peaks is commonly known for silica based reversed phases [13]. Instead of a C18-column, a cyano-based column was applied. Since separation of polar compounds on this type of column is based on polar–polar interactions, tailing was less prevalent (Fig. 2) and did not influence quantification. The fragmentation pattern in APCI in this study (Fig. 2) was comparable as the one previously published for the detection of strychnine in seeds using an ESI-interface [11].

Based upon the correlation coefficient, it can be concluded that the method showed good linearity in the range of 1–100 ng/mL. This concentration range is lower than the limits of quantitative detection of other methods previously described. However, as shown in Table 1, the method allows for an accurate, reproducible measurement of these low, sub-toxicological concentrations in urine, compliant to generally accepted criteria [14,15].

Therefore, this method is capable of detecting and quantifying strychnine in urine at levels expected in doping analysis.

Indeed, low maximum urinary strychnine concentrations (23–176 ng/mL) in the volunteers, would remain undetected via the methods routinely applied in toxicology [7,9]. Although the MRPL from WADA (200 ng/mL) is not reached, strychnine would be detected in doping control laboratories [13]. Indeed, the WADA technical document specifically states that an MRPL is not a reporting limit but a performance limit that should easily be achieved on a day-to-day basis. Hence, the limits of detection of doping control laboratories should be below the mandatory MRPL-levels.

As shown in Fig. 3 strychnine remained detectable for 24–48-h post administration. The cumulative excretion profiles (Fig. 4) indicate that 2.2–8.6% of all ingested strychnine was excreted unchanged in urine during the first 12-h post administration. As shown in Fig. 4, the difference in maximum attained urinary concentration for volunteer 4 compared to the others (Fig. 3) is caused by a difference in the volume of urine excreted. Taking into account the profiles in Fig. 3 and the detection of small concentration of strychnine in urine until 48-h post administration, it seems that the amounts excreted unchanged in this study are in agreement with previously published results [17].

5. Conclusions

A quantitative LC–MS method for the quantitative determination of strychnine in urine after the ingestion of sub-toxicological concentrations of an over-the-counter *Strychnos nux-vomica* preparation has been developed. The method allowed for the detection of strychnine up to 48 h post the oral administration of 380 μg of the active substance. The use of over-the-counter preparations containing *Strychnos nux-vomica* extracts could lead to adverse analytical findings in doping analysis.

Acknowledgements

P.V.E. and K.D. wish to thank the Flemish Ministry of Health for financial support and the Belgian National Lottery for the purchase of the LCQ-DECA® instrument.

The technical assistance of F. Van Eeckhaute is also gratefully acknowledged.

References

[1] J.A. Perper, Fatal strychnine—a case-report and review of the literature, J. Forensic Sci. 30 (1985) 1248–1255.
[2] Y. Gaillard, G. Pepin, Poisoning by plant material: review of human cases and analytical determination of main toxins by high-performance liquid chromatography–(tandem) mass spectrometry, J. Chromatogr. B 733 (1999) 181–229.
[3] T. Donohoe, N. Johnson, Foul Play? Drug Abuse in Sports, Blackwell, Oxford, 1986.
[4] M. Verroken, Drug use and abuse in sport, Best Pract. Res. Clin. Endocrinol. 14 (2000) 1–23.
[5] World Anti-Doping Agency (WADA), 2005 prohibited list, http://www.wada-ama.org/.
[6] World Anti-Doping Agency (WADA), Minimum required performance limits for detection of prohibited substances, TD2004MRPL, version number 1.0, http://www.wada-ama.org/.
[7] E.P. Marques, F. Gil, P. Proença, P. Monanto, M.F. Oliveira, A. Castanheira, D.N. Vieira, Analytical method for the determination of strychnine in tissues by gas chromatography/mass spectrometry: two case reports, Forensic Sci. Int. 110 (2000) 145–152.
[8] M. Barrosso, E. Gallardo, C. Margalho, S. Avila, E.P. Marques, D.N. Vieira, M. Lopez-Rivadulla, Application of solid phase microextraction to the determination of strychnine in blood, J. Chromatogr. B 816 (2005) 29–34.
[9] T.G. Rosano, J.D. Hubbard, J.M. Meola, T.A. Swift, Fatal strychnine poisoning: application of gas chromatography and tandem mass spectrometry, J. Anal. Toxicol. 24 (2000) 642–647.
[10] C. Duverneuil, G. Lorin de la Grandmaison, P. de Manzancourt, J.C. Alvarez, Liquid chromatography/photodiode array detection for determination of strychnine in blood: a fatal case report, Forensic Sci. Int. 141 (2004) 17–21.
[11] Y.H. Choi, Y.M. Sohn, C.Y. Kim, K.Y. Oh, J. Kim, Analysis of strychnine from detoxified Strychno nux-vomica seeds using liquid chromatography–electrospray mass spectrometry, J. Ethnopharmacol. 93 (2004) 109–112.
[12] R.S. Stahl, W.M. Arjo, K.K. Wagner, C. Furcolow, D.L. Nolte, J.J. Johnston, Development of a high performance liquid chromatography/mass spectroscopy method for the determination of strychnine concentrations in insects used to assess potential risks to insectivores, J. Chromatogr. B 811 (2004) 257–262.
[13] K. Deventer, P. Van Eenoo, F.T. Delbeke, Simultaneous determination of beta-blocking agents and diuretics in doping analysis by liquid chromatography mass spectrometry with scan-to-scan polarity switching, Rapid Commun. Mass Spectrom. 19 (2005) 90–98.
[14] W. Verwaal, M. van Bavel, A. Boot, J. Bravenboer, F. de Goei, C. Maas, A. Van der Putten, De Ware(n) Chemicus 26 (1996) 106.
[15] F. Bressolle, M. Bromet-Petit, M. Audran, Validation of liquid chromatographic and gas chromatographic methods—applications to pharmacokinetics, J. Chromatograph. B 686 (1996) 3–10.
[16] World Anti-Doping Agency (WADA), Identification criteria for qualitative assays, incorporating chromatography and mass spectrometry, TD2003IDCR, version number 1.2, http://www.wada-ama.org/.
[17] A.C. Moffat, J.V. Jackson, M.S. Moss, B. Widdop (Eds.), Clarke's Isolation and Identification of Drugs in Pharmaceuticals, Body Fluids, and Post-mortem Material, second ed., The Pharmacautical Press, London, 1986, pp. 976–977.

ELSEVIER

Forensic Science International 164 (2006) 164–167

Forensic Science International

www.elsevier.com/locate/forsciint

Death scene evaluation in a case of fatal accidental carbon monoxide toxicity

Antioco Franco Sedda *, Gabriele Rossi

FIS ION – TRIGA Reactor, ENEA Casaccia, s.p. Anguillarese 301, 00060 Rome, Italy

Received 12 December 2005; received in revised form 22 December 2005; accepted 23 December 2005
Available online 24 January 2006

Abstract

Exposure of humans to high concentrations of carbon monoxide can result in death, due to the formation of carboxyhaemoglobin (COHb), which impairs the oxygen carrying capacity of the haemoglobin. Carbon monoxide is responsible of a great number of accidental domestic poisonings and deaths throughout the world, particularly in homes that have faulty or poorly vented combustion appliances. A case is reported, in which a 21-year-old woman was found dead, due to carbon monoxide poisoning from a gas water heater, despite the puzzling evidence that the heater has been used for more than 10 years without any problem. An evaluation of the exposure to CO was performed, by measuiring the rate of production of CO from the heater, and using the Coburn–Forster–Kane equation to describe the kinetics of the poisoning process. The death was attributed to an accidental poisoning from carbon monoxide due to a sum of unfortunate circumstances.

Keywords: Carbon monoxide; Carboxyhaemoglobin; Unvented heater; Coburn–Forster–Kane equation

1. Introduction

Carbon monoxide is a colourless, odourless gas, poisonous to humans [1]. Although low concentrations (50–120 ppb) are considered a normal constituent of the natural environment, about 60% of the carbon monoxide found in the non-urban troposphere is attributed to human activities as a product of the incomplete combustion of carbon-containing fuels, and ambient concentrations of carbon monoxide near urban and industrial areas substantially exceed global background levels.

Vehicle emissions in industrial countries account for about 50–60% of total emissions; the other categories of carbon monoxide emissions are other fuel combustion sources, such as steam boilers, industrial processes and solid waste disposal.

Exposure to additional carbon monoxide can be detrimental to human health, and exposure to higher concentrations can result in death. The health effects of carbon monoxide are largely the result of the formation of carboxyhaemoglobin (COHb), but, in addition to its reaction with haemoglobin, carbon monoxide combines with myoglobin, cytochromes and metalloenzymes such as cytochrome *c* oxidase and cytochrome P-450.

The formation of COHb is a reversible process, but due to the affinity of carbon monoxide to haemoglobin, the elimination half-time varies, depending on the initial levels of COHb and the ventilation rate of the individuals. This might lead to accumulation of COHb, and even relatively low concentrations of carbon monoxide might produce substantial blood levels of COHb [2].

The COHb levels below 10% are usually not associated with symptoms. At COHb saturations of 10–30%, neurological symptoms of carbon monoxide poisoning can occur, such as headache, dizziness, weakness, nausea, confusion, disorientation and visual disturbances [3].

Dyspnoea, increases in pulse and respiratory rates, and syncope are observed with continuous exposure, producing COHb levels from 30 to 50%. At COHb levels higher than 50%, coma, convulsions and cardiopulmonary arrest may occur.

2. Case report and Investigation

A 21-year-old white woman was found dead, crouched in a shower cabin of a small building, situated beside the country

* Corresponding author. Tel.: +39 06 30483806; fax: +39 06 30484874.
E-mail address: antioco.sedda@casaccia.enea.it (A.F. Sedda).

0379-0738/$ – see front matter
doi:10.1016/j.forsciint.2005.12.028

house where the victim lived with the family; the jet of warm water was still running on the naked body.

The building, composed of a single large room, was used as laundry and as lavatory facility, had a window and an access door, both made with a frame of aluminum equipped with rubber seals, and a total volume of about 26 cubic meters; the window and door were closed when the body was discovered.

A schematic drawing of the room is shown in Fig. 1. It can be seen that the orientation of the major axis of the building was 60°N.

The pale cherry pink colour of the victim immediately suggested a carbon monoxide poisoning; a spectrophotometric measurement of the blood was performed at the local Legal Medicine Institute, and furnished a value of 60% of COHb.

Apart from the CO intoxication, the medical status of the victim was quite good, and no sign of underlying disease has been found on the victim from the autopsy examination; the absence of important disease, past and present, was also obtained from the family doctor.

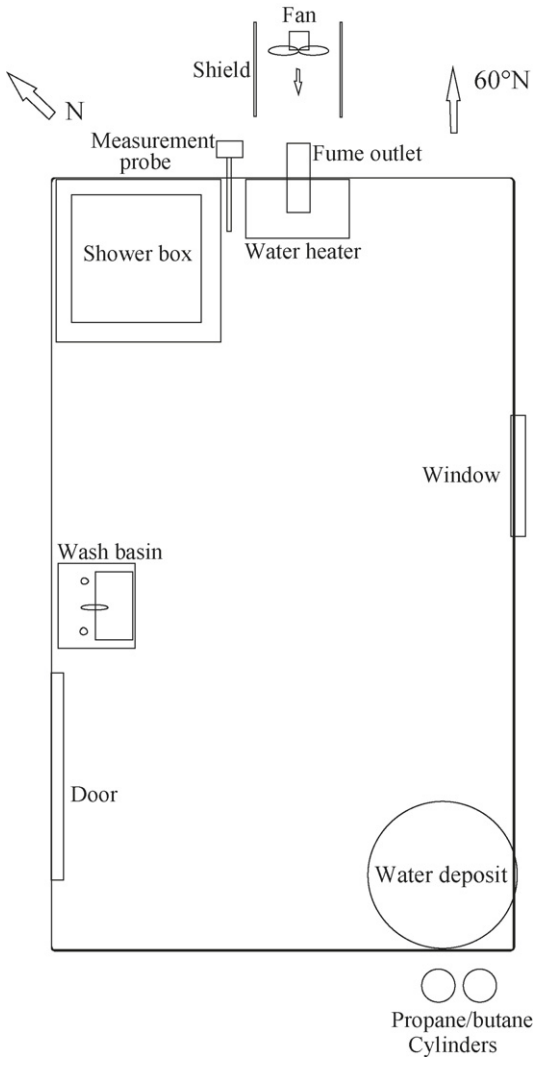

Fig. 1. Schematic drawing of the room in which the accident occurred, and of the experimental setup for the measurements.

A complete toxicological screen was also performed, and no trace of illicit drugs or alcohol was found in the blood.

The psychiatric status of the victim, according to the relatives, friends and family doctor witnesses, was quite normal, without depression or psycological problems that could indicate a possible suicide.

The relatives told to the investigators that the woman entered into the room about 45–50 min before the discovery of the body, to take a shower.

They also indicated that, being a cold and cloudy day, the woman had ignited the heater about 10–15 min before taking the shower, to warm the room.

The hot water was produced by an unvented heater, with power of 250 Kcal/min, installed inside the room, beside the shower cabin (Fig. 1).The heater used has a combustible propane/butane mixture coming from a cylinder standing outside the building.

The air-exhaust pipe of the heater had a total length of about 1 m and a diameter of 10 cm; the fumes from the heater were conveyed in a vertical pipe, connected by an elbow to an horizontal pipe, which crossed the wall of the building.

The exit of the horizontal exhaust pipe ended under the edge of the roof, it was only covered with a wide mesh metallic net, probably to prevent the entry of birds and other little animals, and was aligned along the major axis of the building.

According to numerous witnesses, all the members of the family used the shower frequently after the work in the fields, especially during the summer, in order to avoid to making the bathroom of the house dirty; no health problem has never been reported following the use of the shower, for more than 10 years of use, by the members of the family before the accident, apart from an occasional ‘‘bad smell’’.

The elevated value of COHb in the blood indicated an exposure to high concentrations of CO, which seemed not compatible with a safe use of the room for long periods.

The prosecuting attorney decided to test the heater, and clarify the cause of the death with the help of an expert.

3. Methods

A hole of 1 cm of diameter was made across the wall, and a remote sampling probe for the analysis of CO was introduced up to the shower cabin. The probe was connected to a detector WHOLER A91-IR, equipped of O_2, CO_2, NO and CO electrochemical sensors [4,5], and, after the ignition of the heater, a constant stream of warm water was produced in the shower.

A second measurement technique, which uses visual colorimetric detector tubes (MSA-AUER – Sigma–Aldrich), was also used as a confirmation technique. The measurement is based on the reaction: $5CO + I_2O_5 \rightarrow I_2 + 5CO_2$; the iodine-coloured layer in the tube corresponds in length to the carbon monoxide concentration in the sample [6].

On the day of the accident, a light wind was blowing in the site, as resulted from the weather parameters registrations of a near military airport. At the same time of the accident, a relatively constant wind of 2 knots was blowing, with direction 57°N–60°N.

In order to test if the presence of the wind had prevented the exit of the fumes, the measurements have been performed both in normal condition, and simulating a constant 2 knots wind.

During the measurements, the door and the window were closed.

A large, variable speed, fan has been fixed in front of the exit of the horizontal air-exhaust pipe, with the rotation axis at an angle of 60°N (the same of the wind); a large mesh grid has been interposed in order to render the flow laminar, and the speed of the fan has been varied to obtain near the pipe a constant wind speed, measured by a digital anemometer, of 2 knots (±0.2).

All the measurements were conducted in triplicate; the data from the electrochemical detector and from the colorimetric detector always differed not more than 7%.

4. Results

The obtained values of CO concentration versus time are reported in Fig. 2, both in the presence and in the absence of wind.

The curve in the absence of wind shows that, after a plateau of 15–20 min from ignition, the CO concentration rapidly raised, reaching after 35 min the value of 1000 ppm, which although highly dangerous, is seldom lethal in the case of a short-time exposure.

The same curve in presence of a wind of 2 knots blowing in the same direction of the horizontal air-exhaust pipe changed dramatically. After 20 min from ignition a concentration of 2000 ppm is reached, a value which, for an exposure of 5–10 min, can cause incapacitation, lethargy, drowsiness, dizziness and confusion.

After only 35 min from ignition, in the presence of wind, the CO concentration raised to 6300 ppm, a value generally considered fatal even for a short time exposure.

An evaluation of the time of exposure to CO which has been necessary to reach the value of 60% for COHb was attempted in our case, by using the Coburn–Forster–Kane equation [7]. A standard set of physiological values were introduced in the formula (ventilation volume and frequency, initial CO concentration in blood for non smokers), evaluated by using the known physiological data of the victim (age, weight, height, initial Hb %).

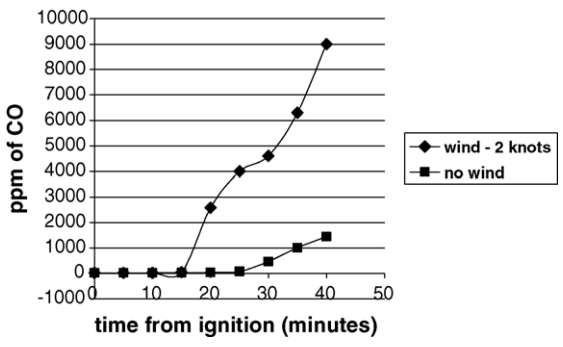

Fig. 2. Measured values of CO concentration vs. time in the presence, and in the absence of wind.

Coburn–Forster–Kane equation

$$A\,[\mathrm{HbCO}]_t - (\mathrm{BV_{CO}} + \mathrm{PI_{CO}})\}/\{A\,[\mathrm{HbCO}]_0 - (\mathrm{BV_{CO}} + \mathrm{PI_{CO}})\} = e^{-tAV}b^B$$

where, $A = P_{c,O_2}/M[Hb_{O_2}]$, $B = 1/DL_{CO} + PL/VA$, P_{c,O_2} is the average partial pressure of O_2 in lung capillaries (mm Hg), At sea level $PI_{O_2}(159) - 49 = 110$; $PI_{O_2} = 148.304 - 0.0208$; PI_{CO}, M the the ratio of the affinity of blood for CO to that for O_2, approximately 218. $[HbO_2]$ is in ml of O_2 per ml blood, or = 0.22 − $[HbCO]_t$. $[HbCO]_t$ in ml of CO per ml blood at time t, or = $[COHb\%]_t$ 0.0022 {term to be solved for}. DL_{CO} the diffusivity of the lung for CO (ml/min/mm Hg), or = $35V_{O_2}$, $e^{0.33}$, $V_{O_2} = RMV/22.274 - 0.0309$. RMV the respiratory minute volume (L/min.); PL the barometric pressure minus the vapor pressure of water (i.e. 49) at body temperature (mm Hg); V_{CO} the rate of endogenous CO production (ml/min.); approximately 0.007 ml/min.; PI_{CO} the partial pressure of CO in inhaled air (mm Hg); V_A is alveolar ventilation rate (ml/min), or = 0.933 V_E − 132 f; $_{VE}$ the ventilation volume (ml/min.); f the ventilation frequency; $[HbCO]_0$ is in ml of CO/ml blood at the beginning of the exposure (approximately 0.8% COHb, or 0.0176 ml CO/ml blood for a non-smoker); e the base of natural logarithms (2.7182); t the exposure duration (min);and V_b is the blood volume (ml); assume 74 ml/kg body weight.

By starting with an initial CO concentration of 50 ppm, a calculation of $[HbCO]_t$ by the complete Coburn–Forster–Kane equation was performed.

The obtained $[HbCO]_t$ value was re-introduced in the equation as new starting value of $[HbCO]_0$, and a new complete calculation was performed, by using the CO concentration of the curve of Fig. 2 (ppm CO versus time of ignition, obtained with a simulated wind of 2 knots) corresponding to the first minute of exposure.

The calculation was repeated, with steps of 1 min, and was stopped when the calculated $[HbCO]_t$ reached the value experimentally found in the blood of the victim.

The result revealed that a presence in the room of 33 (±7) minutes fom ignition of the heater (including the 10 min warm up of the room) was required to reach the value of 60% for COHb, the uncertainty in the determination of the exposure time (±7 min) being mainly due to the experimental variability of the measured CO concentration versus time, and to the unknown ventilation volume and respiratory frequency of the victim.

5. Discussion

Carbon monoxide is readily absorbed from the lungs into the bloodstream.

When in equilibrium with ambient air, the COHb content of the blood will depend mainly on the concentrations of inspired carbon monoxide and oxygen.

However, if equilibrium has not been achieved, the COHb concentration will also depend on the duration of exposure, pulmonary ventilation and the COHb concentration originally present before inhalation of the contaminated air [7–9].

Although approximate prediction of COHb concentration can be made by assuming a linear relationship of CO concentration to uptake [3,11–13], the Coburn–Forster–Kane equation is the most complete approach available to modeling carbon monoxide uptake. Disadvantages of its use are the large number of variables that it contains and the fact that the value of many of the variables must be obtained from other equations [10,14,15].

A study of 22 deaths produced from unvented gas heaters showed in the blood of the victims a mean COHb of 49.5%, with minimum value of about 30% and a maximum of 75% for COHb [16].

Another study examined the distribution of COHb among survivors (mean = 28.1%, $n = 159$) and fatalities (mean 62.3%, $n = 101$); the 50% survival probability was associated approximately with 50% of COHb [17].

In conclusion, the value of COHb found in the blood of the victim, the CO concentration reached in the room, and the exposure time evaluated by us were fully coherent with the witness of the relatives of the victim.

During the accident different unfortunate circumstances were contemporaneously present in the room, which caused the death of the victim:

The room was not provided with the vent aperture that must be present for unvented heaters; in the present case a permanent aperture of more than 100 cm^2 was mandatory, according to the national regulations for this kind of heaters.

During the day of the accident the weather was cold, and differently from usual (as indicated by the relatives of the victim), the window of the room has been completely closed. The measurements of CO concentration performed with the window only partially opened was sufficient to drop the maximum value of CO concentration, after 40 min from ignition, to 180 ppm (data not shown), clearly demonstrating the utmost importance of a minimum of air circulation for a safe use of unvented heaters.

In installations such as coal-, gas- or oil-fired heating of power generating plants, or external combustion boilers, the formation of carbon monoxide is lowest at a ratio near the stoichiometric air/fuel ratio (from 11:1 vol. for methane to 30:1 vol. for propane/butane mixture). At lower than stoichiometric ratios, high carbon monoxide concentrations reflects the relatively low oxygen concentration, while higher than stoichiometric ratios, resulting in decreased flame temperatures and shorter residence time, also increases carbon monoxide emissions.

Emissions were observed to vary in time during a heater run and increase when room or chamber oxygen levels decreased [18–21].

The wind, that was present at the date and time of the accident, directed in the same direction of the air-exhaust horizontal pipe, not only hindered the elimination of CO from the room, but contributed to raise the room CO_2 concentration. This fact decreased the O_2 concentration, and increased the CO production rate, in a ''catastrophical'' circle which rapidly raised the respirable CO concentration of the room to lethal values, leading to confusion, drowsiness, lethargy, and finally to the death of the victim.

After the report of the above mentioned measurement, the court attributed the death to accidental poisoning from carbon monoxide, due to a sum of unfortunate circumstances, caused from the widespread underestimation [22] of an insidious life threatening hazard.

References

[1] T. Meredith, A. Vale, Carbon monoxide poisoning, Br. Med. J. 296 (1988) 77–79.

[2] H. Hauck, M. Neuberger, Carbon monoxide uptake and the resulting carboxyhemoglobin in man, Eur. J. Appl. Physiol. Occup. Physiol. 53 (2) (1984) 186–190.

[3] D.A. Purser, in: P.J. DiNenno, et al. (Eds.), Toxicity assessment of combustion products, 2nd ed., Handbook of the Society of Fire Protection Engineering, 1995.

[4] H.W. Bay, K.F. Blurton, H.C. Lieb, H.G. Oswin, Electrochemical measurement of carbon monoxide, Am. Lab. 4 (1972) 57–58, 60–61.

[5] H.W. Bay, K.F. Blurton, J.M. Sedlak, A.M. Valentine, Electrochemical technique for the measurement of carbon monoxide, Anal. Chem. 46 (1974) 1837–1839.

[6] A.G. Drägerwerk, Dräger Tube Handbook, 9th ed., Drägerwerk, Lübeck, 1994.

[7] R.F. Coburn, R.E. Forster, P.B. Kane, Considerations of the physiological variables that determine the blood carboxyhemoglobin concentration in man, J. Clin. Invest. 44 (1965) 1899–1910.

[8] C.G. Douglas, J.S. Haldane, JB.S. Haldane, The laws of combination of haemoglobin with carbon monoxide and oxygen, J. Physiol. 44 (1912) 275–304.

[9] P. Halebian, C. Sicilia, R. Hariri, R. Inamdar, G.T. Shires, A safe and reproducible model of carbon monoxide poisoning, Ann. NY. Acad. Sci. 435 (1984) 425–428.

[10] M.L. McCartney, Sensitivity analysis applied to Coburn–Forster–Kane models of carboxyhemoglobin formation, Am. Ind. Hyg. Assoc. J. 51 (1990) 169–177.

[11] V.A. Benignus, M.J. Hazucha, M.V. Smith, P.A. Bromberg, Prediction of carboxyhemoglobin formation due to transient exposure to carbon monoxide, J. Appl. Physiol. 76 (4) (1994) 1739–1745.

[12] W.H. Forbes, F. Sergent, F.J.W. Roughton, The rate of carbon monoxide uptake by normal men, Am. J. Physiol. 143 (1945) 594–608.

[13] J.E. Peterson, R.D. Stewart, Predicting the carboxyhemoglobin levels resulting from carbon monoxide exposures, J. Appl. Physiol. 39 (1975) 633–638.

[14] J.S. Britten, RA.M. Myers, Effects of hyperbaric treatment on carbon monoxide elimination in humans, Undersea Biomed. Res. 12 (1985) 431–438.

[15] P.B. James, Hyperbaric and normobaric oxygen in acute carbon monoxide poisoning, Lancet 2 (8666) (1989) 780–799.

[16] Tyrrell EA, Kale DA., U.S. Consumer Product Safety Commission, memorandum, 1 Feb 1979.

[17] J. Pach, Analysis of predictive factors in acute carbon monoxide poisonings, Folia Med. Cracoviensia 20 (1978) 159–168.

[18] K.R. Cooper, R.R. Alberti, Effect of kerosene heater emissions on indoor air quality and pulmonary function, Am. Rev. Respir. Dis. 129 (1984) 629–631.

[19] J. Faure, P. Arsac, P. Chalandre, Prospective study in carbon monoxide intoxication by gas water heaters, Hum. Toxicol. 2 (1983) 422–425.

[20] M.P. Humphreys, C.V. Knight, J.C. Pinnix, Residential wood combustion impacts on indoor carbon monoxide and suspended particulates, in: Proceedings of the 1986 EPA/APCA Symposium on Measurement of Toxic Air Pollutants, Raleigh, NC, (EPA-600/9-86-013), April 1986, (1986), pp. 736–747.

[21] B. Brunekreef, H.A. Smit, K. Biersteker, Boleij JSM, E. Lebret, Indoor carbon monoxide pollution in The Netherlands, Environ. Int. 8 (1982) 193–196.

[22] L.T. Jorgen, K. Troels, Intoxication at home due to carbon monoxide production from gas water heaters, Forensic Sci. Int. 36 (1–2) (1988) 69–72.

ELSEVIER

Forensic Science International 164 (2006) 168–171

Forensic Science International

www.elsevier.com/locate/forsciint

Application of pericardial fluid to the analysis of morphine (heroin) and cocaine in forensic toxicology

María Teresa Contreras [a], Antonio F. Hernández [b,*], Marisa González [c], Susana González [c], Rosa Ventura [c,d], Antonio Pla [b], Juan Luis Valverde [a], Jordi Segura [c,d], Rafael de la Torre [c,d]

[a] *National Institute of Toxicology, Department of Barcelona, Spain*
[b] *Department of Legal Medicine and Toxicology, University of Granada School of Medicine, Avda. Madrid, 11, 18071 Granada, Spain*
[c] *Pharmacology Research Unit, Institut Municipal d'Investigació Mèdica (IMIM), Barcelona, Spain*
[d] *Universitat Pompeu Fabra, Barcelona, Spain*

Received 28 July 2005; received in revised form 27 December 2005; accepted 31 December 2005
Available online 26 January 2006

Abstract

In this study opiates (morphine and codeine) and cocaine and its related metabolites (benzoylecgonine and cocaethylene) were analyzed in pericardial fluid by GC/MS. This is the first study reporting levels of drugs of abuse in this body fluid. The analytical method used has been previously validated and then applied to 54 drug-related deaths in the Barcelona area (Spain). Median levels were as follows: morphine 589 ng/ml, range 19–8857 ($n = 49$); codeine 26 ng/ml, range 15–343 ($n = 35$); cocaine 78 ng/ml, range 10–220 ($n = 14$), benzoylecgonine 742 ng/ml, range 20–3386 ($n = 15$), and cocaethylene 36 ng/ml, range 9–100 ($n = 13$). In addition, a comparative study of the concentration of opiates and cocaine in pericardial fluid by both semi-quantitative EMIT d.a.u.® and GC/MS (used as reference) was performed. Fairly good correlations for opiates ($r = 0.905$) and cocaine ($r = 0.859$) were found; however, the consistently low results of EMIT in the analysis of cocaine comparing to GC/MS could be caused by matrix effect. In spite of that, it raises the possibility of using the immunoassay as a preliminary technique in forensic toxicology.

Keywords: Pericardial fluid; Drugs of abuse; Opiates; Cocaine; GC/MS; Immunoassay

1. Introduction

The interpretation of toxicological data in cases of drug-related deaths and drug overdoses is not a simple matter. A number of known conditions can make it difficult, such as an adequate database to compare the analytical results, post-mortem degradation (spontaneous or enzymatic), post-mortem redistribution of drugs, and the simultaneous consumption of two or more drugs. Forensic toxicologists have been using different viscera as samples for toxicological analysis, although preferences were further turned to biological fluids, because they are easier to handle and pose less analytical drawbacks than solid organs.

As most drugs are distributed to their site of action by blood, drug concentration measurements in this body fluid provide the best information as to the potential effect on behaviour, clinical symptoms, or vital functions [1]. However, blood samples are not always available due to the cause of death or the post-mortem processes that interfere with the amount and/or the quality of the sample. It has been reported that in some fatal cases of poisoning, in addition to blood and urine, cerebrospinal fluid, vitreous humour, bile, meconium, and other body fluids are useful for toxicological analysis [2–5]. In this respect, pericardial fluid may be an alternative sample to blood for toxicological examinations in drug-related deaths. This body fluid is an ultrafiltrate of plasma with an extremely similar amount of proteins and is located within a tight compartment so that it is almost free of contamination by pathogens [6]. The usual volume of 5–20 ml is enough for analytical purposes.

The objective of the present study was to investigate the occurrence in pericardial fluid of opiates (morphine and codeine) and cocaine and its metabolites (benzoylecgonine and cocaethylene). Cocaethylene is not a true metabolite of cocaine but it appears when cocaine is coadministered with ethyl

* Corresponding author. Tel.: +34 958 249927; fax: +34 958 206107.
E-mail address: ajerez@ugr.es (A.F. Hernández).

0379-0738/$ – see front matter
doi:10.1016/j.forsciint.2005.12.030

alcohol by means of a transesterification reaction. The analytical method used has been previously validated [7] and applied to 54 drug-related deaths. The second aim of this study was to ascertain the application of a semi-quantitative EMIT® d.a.u.™ assay to pericardial fluid, which might be of interest in forensic toxicology as a preliminary result. This procedure was compared to GC/MS used as reference.

2. Material and methods

2.1. Collection of samples

Pericardial fluid samples (4–6 ml) from 54 drug-related deaths in the Barcelona area were collected in polypropylene tubes by using plastic syringe. Permission from the President of the Catalonian Supreme Court of Justice (ref T.S./G.P. 68196) was obtained in advance. Samples were stored at −20 °C until analysis.

2.2. Preparation of pericardial fluid for opiate analysis

The procedure has been reported elsewhere [7]. Briefly, 50 μl of a mixture of internal standards solution (200 ng of morphine-D3 and codeine-D3 in methanol) was added to 1 ml of pericardial fluid. The pH of the sample was adjusted to approximately 5.2 by adding 1 ml of 1.1 M sodium acetate buffer (pH 5.2). The mixture was vortexed, and then 50 μl of β-glucuronidase (HP2 from Helix Pomatia, Sigma Chemicals, St. Louis, MO) was added and incubated at 37 °C for 12 h in a water bath. Then 350 μl of 1.0 M potassium hydroxide was added to adjust the pH to 9.0, the mixture was centrifuged at 2500 rpm for 5 min, poured into Bond-Elut Certify™ columns (Varian, Harbon City, USA), and gently sucked through.

Columns were previously conditioned with 2 ml of methanol and 2 ml of deionized (Milli Q) water and prevented from running dry. After applying the samples, columns were successively washed with 2 ml of deionized water, 1 ml of 0.1 M acetate buffer pH 4.0 and 2 ml of methanol. Finally, analytes were eluted with 2 ml of a freshly prepared mixture of chloroform:isopropanol (80:20, v/v) containing 2% ammonia. The eluates were collected and evaporated to dryness under a gentle nitrogen stream at 40 °C in a water bath. Residues were kept in a vacuum oven for 30 min at 50 °C and then derivatised with 100 μl of *N*-methyl-*N*-trimethylsilyl-trifluoroacetamide (MSTFA). The mixture was vortexed for 10 s and then heated at 60 °C for 5 min in a heating block. After being cooled at oom temperature, 20 μl of *N*-methyl-bis-trifluoroacetamide (MBTFA) were added and vortexed for 10 s. The mixture was heated again at 60 °C for 10 min in the heating block, cooled at room temperature and 1 μl aliquots of the derivatised extract were injected into the GC/MS system (split ratio 10:1). This consisted of a Hewlett-Packard 5890A Series II gas chromatograph equipped with an HP-Ultra 1 capillary column (cross-linked methylsilicone, 0.2 mm × 25 m) and coupled to an HP 5971A mass-selective detector. The injector port and detector temperatures were operated at 280 °C. The oven temperature was increased from 100 to 290 °C, at 20 °C/min, with a final hold time of 5 min. The mass spectrometer was operated in electron impact mode and three diagnostic ions for each compound were monitored (SIM): *m/z* 429, 414 and 401 for morphine-bis-*O*-TMS; *m/z* 371, 313, and 178 for codeine-bis-*O*-TMS. Three characteristic ions for each deuterated analogue were monitored at *m/z* + 3, respectively.

2.3. Preparation of pericardial fluid for cocaine analysis

The procedure has been reported elsewhere [7]. Briefly, 50 μl of a mixture of internal standards solution (200 ng of benzoylecgonine-D3 and cocaine-D3, and 100 ng of cocaethylene-d_8 in methanol) was added to 1 ml of pericardial fluid. The pH of the sample was adjusted to 7.0 by adding 1 ml of 0.1 M pH 7.0 sodium phosphate buffer. The mixture was vortexed, centrifuged at 2500 rpm for 5 min, poured into Bond-Elut Certify™ columns, and gently sucked through.

Columns were previously conditioned with 2 ml of methanol and 2 ml of 0.1 M sodium phosphate buffer pH 7.0 and prevented from running dry. After applying the samples, columns were successively washed with 3 ml of deionized water, 3 ml of 0.1 M HCl, and 9 ml of methanol. Finally, analytes were eluted with 2 ml of a freshly prepared mixture of chloroform:isopropanol (80:20, v/v) containing 2% ammonia. The eluates were collected and evaporated to dryness under a gentle nitrogen stream at 40 °C in a water bath. Residues were kept in a vacuum oven for 30 min at 50 °C and then derivatised with 70 μl of pentafluoropropionic anhydride (PFPA) and 30 μl of hexafluoroisopropanol (HFIP). The mixture was vortexed for 10 s and then heated at 70 °C for 10 min in a heating block, then cooled at room temperature, and evaporated to dryness under a gentle nitrogen stream at 40 °C. The residue was reconstituted with 50 μl of ethyl acetate and 1 μl aliquots of the derivatized extract were injected into the same GC–MS system mentioned above. In this case, an HP-ultra 2 capillary column (5% phenylmethylsilicone gum, 0.2 mm × 12.5 m) was used. The oven temperature was increased from 100 to 280 °C (20 °C/min), with a final hold time of 4 min. Three diagnostic ions for each compound were monitored (SIM): *m/z* 439, 334, and 318 for benzoylecgonine-HFIP; *m/z* 303, 272, and 182 for cocaine, and *m/z* 317, 272, and 196 for cocaethylene. Two characteristic ions for each deuterated analogue were monitored (*m/z* 442 and 321 for benzoylecgonine-D3-HFIP, *m/z* 306 and 185 for cocaine-D3; and *m/z* 325 and 204 for cocaethylene-d_8).

2.4. Analysis of pericardial fluid for opiates and cocaine by immunoassay

A semi-quantitative determination of opiates and cocaine was carried out in pericardial fluid by using EMIT® d.a.u.™ assays (Dade Behring) in a Vitalab Viva analyzer. The calibration curve for the assay was built with four points from the calibrator solutions supplied by the manufacturer. The points selected were as follows: 0 (blank, water); 150 ng/ml (calibrator A – 300 ng/ml – diluted with water at 1:1, v/v); 300 ng/ml (calibrator A); and 1333 ng/ml (morphine) or 1000 ng/ml (benzoylecgonine) obtained by diluting the calibrator B (morphine 4000 ng/ml;

benzoylecgonine 2000 ng/ml) with water at 1:2 and 1:1 (v/v), respectively.

3. Results and discussion

This is the first paper reporting levels of some drugs of abuse in pericardial fluid and may begin the database for further comparison purposes. To our best knowledge, only one study has previously addressed the measurement of drugs in pericardial fluid [8], although it focussed on acidic and neutral drugs and several pesticides, but not on drugs of abuse.

In this study, 54 cases of drug-related death were included. Combinations of at least two or more drugs were found in 92.6% of cases, one of them being morphine. This figure is slightly higher than the 82% reported by Darke et al. [9] and the 85% reported by Gerostamoulos et al. [10]. Morphine appeared together with cocaine in 35% of the cases, with ethanol in 28%, and with benzodiazepines in 65%. According to the ''Plan Nacional sobre las Drogas'' [11], 88% of the 489 drug-related deaths reported throughout Spain in 1999 were opiate-related deaths, and 63.3% cocaine-related deaths. In our study we found 94.4% and 37.0%, respectively. The ''Plan Nacional sobre las Drogas'' reports that males comprised 86.7% of drug-related deaths cases, and that the mean age was 32.8 years. These figures are very similar to the 90.7% and 29.9 years found in our study.

The concentrations of opiates (morphine and codeine) and cocaine (and metabolites) in pericardial fluid are shown in Table 1. If mean levels of these drugs are compared to those found in blood (data retrieved from forensic casework files and not shown) it is observed that morphine and cocaine concentrations in pericardial fluid are roughly two-fold those found in blood. However, the mean value for benzoylecgonine in pericardial fluid is about 50% higher than that found in blood. In contrast, the mean concentration of codeine is almost identical in both body fluids. It appears that both cocaine and benzoylecgonine are likely to be accumulated in pericardial fluid where they remain longer than in blood.

Table 2 shows the comparative analysis of the concentration of opiates and cocaine in pericardial fluid measured by both semi-quantitative EMIT d.a.u.™ and GC/MS (used as reference). This study was undertaken to ascertain the potential usefulness of the immunoassay for the rapid estimation of drugs of abuse levels in pericardial fluid as a preliminary analysis. As compared to GC/MS, the EMIT assay found slightly lower concentrations of opiates in pericardial fluid, although the differences failed to be statistically significant ($p = 0.107$). A strong correlation was found between both procedures ($r = 0.905$, $p < 0.001$, $n = 42$) and the regression equation obtained was the following:

$$[\text{Opiates (morphine plus codeine)}]\ \text{by GC/MS} = 0.733 \times [\text{opiates by EMIT}] + 456.61$$

More divergent results were found in the case of cocaine, as the mean concentration detected by EMIT was about 2.5 times lower than that found by GC/MS. Nevertheless, a fairly good correlation was obtained between both procedures ($r = 0.859$, $p < 0.001$, $n = 12$). The regression equation obtained was:

$$[\text{Cocaine and metabolites}]\ \text{by GC/MS} = 1.54 \times [\text{cocaine by EMIT}] + 480.04$$

At first glance, the EMIT assay should have obtained higher concentrations of both types of drugs of abuse, as the antibody may cross-react with other minor metabolites (in addition to the main compound) that were not determined by GC/MS. Besides, EMIT usually gives rise to more misleading (false positive) results due to matrix-effect and other types of interferences that do not occur with GC/MS. The consistently low results of EMIT in the analysis of cocaine comparing to GC/MS could be caused by matrix effect. The matrix interference of pericardial fluid on EMIT was checked by spiking blank pericardial fluid with known amounts of morphine and cocaine (0, 150, 500, and 1000 ng/ml). The following results were obtained, respectively, for each drug: linearity 0.995 and 0.893; variability 0.6% and 0.7%; recovery 108% and 116%. Since EMIT assay is designed for use only with human urine, other substances may interfere with the test and give false results. When pericardial fluid instead of urine was used for cocaine assay, the different in nature of these body fluids could result in the suppression of the EMIT results. One of the possible interference could be caused by the presence of higher concentration of sodium chloride in the pericardial fluid than urine as this compound is known to mask the cocaine assay using EMIT. This assumption is

Table 1
Levels of opiates and cocaine (and metabolites) in pericardial fluid (ng/ml)

	Mean ± S.D.	Range	Median	*N*
Morphine	1022 ± 1351	19–8857	589	49
Codeine	45 ± 57	15–343	26	35
Cocaine	89 ± 72	10–220	78	14
Benzoylecgonine	994 ± 931	20–3386	742	15
Cocaethylene	42 ± 31	9–100	36	13

Table 2
Comparative analysis of opiates and cocaine in pericardial fluid (ng/ml) analyzed by semi-quantitative EMIT d.a.u.™ and GC/MS

Drug	Parameter	EMIT	GC/MS[a]	Ratio
Opiates	Mean ± S.D.	888 ± 1734	1106 ± 1406	1.12 ± 1.26
	Median	556	677	0.70
	N	46	46	42
	Range	11–11770	19–8968	0.10–6.29
Cocaine	Mean ± S.D.	189 ± 473	1114 ± 975	0.35 ± 0.31
	Median	46	798	0.34
	N	23	15	12
	Range	0–1462	30–3535	0.00–0.80

In the case of opiates, the paired *t*-test failed to show significant differences between the semi-quantitative EMIT and GC/MS (963.2 ± 1797.4 vs. 1162.5 ± 1456.2, respectively, $p = 0.107$; $n = 42$). By contrast, in the case of cocaine statistically significant differences were found as semi-quantitative EMIT obtained lower levels than GC/MS (532.6 ± 558.9 vs. 1300.8 ± 1001.2, respectively, $p = 0.001$; $n = 12$).

[a] Includes morphine and codeine (opiates), and cocaine, benzoylecgonine and cocaethylene (cocaine).

supported by the electrolyte levels of blank pericardial fluid (163 mEq/l of sodium and 113 of chloride), in contrast to blank urine (37 mEq/l and 50, respectively).

The lower specificity of the antibody against benzoylecgonine for cocaine (Behring, instructions for users) might also explain the discrepancies; however when benzoylecgonine levels in pericardial fluid measured by GC/MS are compared with the semi-quantitative EMIT for cocaine (whose antibody is raised against benzoylecgonine), the differences still remain. No satisfactory explanation for the discrepancies can be drawn at this time. Anyway, EMIT seems to be of usefulness only as a preliminary assay and, although a rather good estimation of GC/MS values could be inferred from the regression equations calculated (mostly in the case of opiates), a GC/MS confirmation is mandatory as it is a current rule in forensic toxicology. Further investigations addressing this issue should be done to gain insight on the EMIT–GC/MS correlations and for potential applications.

In conclusion, this is the first paper reporting levels of drugs of abuse (morphine and cocaine) in pericardial fluid. The number of samples studied ($n = 49$ and 14, respectively) provides reference values, such as mean, median levels and range, that might be used for comparison purposes. However, further studies are warranted to support the role of pericardial fluid in forensic toxicology.

Acknowledgements

Authors are grateful to Dade Behring for supplying the EMIT d.a.u.™ reagents and to Isabel J. Macdonald for her assistance in language reviewing.

References

[1] C.N. Chiang, R.L. Hawks, Implications of drug levels in body fluids: basic concepts, NIDA Res. Monogr. 73 (1986) 62–83.
[2] E.M. Koves, Use of high-performance liquid chromatography-diode array detection in forensic toxicology, J. Chromatogr. A 692 (1995) 103–119.
[3] K.L. Crump, I.M. McIntyre, O.H. Drummer, Simultaneous determination of morphine and codeine in blood and bile using dual ultraviolet and fluorescence high-performance liquid chromatography, J. Anal. Toxicol. 18 (1994) 208–212.
[4] B.K. Logan, R. Luthi, The significance of morphine concentrations in the cerebrospinal fluid in morphine caused deaths, J. Forensic Sci. 39 (1994) 699–706.
[5] A.M. Bermejo, I. Ramos, P. Fernández, M. López-Rivadulla, A. Cruz, M. Chiarotti, N. Fucci, R. Marsilli, Morphine determination by gas chromatography/mass spectroscopy in human vitreous humor and comparison with radioimmunoassay, J. Anal. Toxicol. 16 (1992) 372–374.
[6] A.T. Gibson, M.B. Segal, A study of the composition of pericardial fluid, with special reference to the probable mechanism of fluid formation, J. Physiol. (Lond.) 277 (1978) 367–377.
[7] M.T. Contreras, Aplicación del líquido pericárdico al análisis de drogas de abuso en Toxicología forense, Doctoral thesis, Servicio de Publicaciones, Universidad de Granada, 2002.
[8] F. Moriya, Y. Hashimoto, Pericardial fluid as an alternative specimen to blood for postmortem toxicological analyses, Leg. Med. (Tokyo) 1 (1999) 86–94.
[9] S. Darke, I. Topp, H. Kaye, W. Hall, Heroin use in New South Wales Australia 1996–2000: 5 year monitoring of trends in price, purity, availability and use from the Illicit Drug Reporting System (IDRS), Addiction 97 (2002) 179–186.
[10] J. Gerostamoulos, V. Staikos, O.H. Drummer, Heroin-related deaths in Victoria: a review of cases for 1997 and 1998, Drug Alcohol Depend. 61 (2001) 123–127.
[11] Observatorio Español sobre Drogas, Informe no. 4, Plan Nacional sobre drogas, Ministerio del Interior, Madrid, 2001.

ELSEVIER

Forensic Science International 164 (2006) 172–178

Forensic Science International

www.elsevier.com/locate/forsciint

Analysis of hallucinogenic constituents in *Amanita* mushrooms circulated in Japan

Kenji Tsujikawa [a,*], Hiroyuki Mohri [b], Kenji Kuwayama [a], Hajime Miyaguchi [a], Yuko Iwata [a], Akinaga Gohda [b], Sunao Fukushima [b], Hiroyuki Inoue [a], Tohru Kishi [a]

[a] *National Research Institute of Police Science, First Chemistry Section, 6-3-1, Kashiwanoha, Kashiwa, Chiba 277-0882, Japan*
[b] *Forensic Science Laboratory, Fukuoka Prefectural Police HQ, 7-7, Higashikouen, Hakata-ku, Fukuoka 812-8576, Japan*

Received 5 January 2006; accepted 6 January 2006
Available online 7 February 2006

Abstract

The constituents of seven mushrooms sold as *Amanita muscaria* or *Amanita pantherina* (five *A. muscaria* and two *A. pantherina*) and four ''extracts purported to contain *A. muscaria*'' products that are currently circulated in Japan were determined. All mushroom samples were identified as *A. muscaria* or *A. pantherina* by macroscopic and microscopic observation. The dissociative constituents, ibotenic acid (IBO) and muscimol (MUS), were extracted with 70% methanol twice and determined by gas chromatography/mass spectrometry. The IBO (as the hydrate)/MUS contents were in the range of <10–2845 ppm/46–1052 ppm in the cap of *A. muscaria* and 188–269 ppm/1554–1880 ppm in the cap of *A. pantherina*. In the caps, these compounds had a tendency to be more concentrated in the flesh than in the cuticle. On the other hand, the IBO/MUS contents in the stem were far lower than in the caps. In the ''extracts purported to contain *A. muscaria*'' products, IBO/MUS were detected below the lower limit of calibration curve (<10 ppm/<25 ppm) or not detected. However, these samples contained other psychoactive compounds, such as psychoactive tryptamines (5-methoxy-*N,N*-diisopropyltryptamine and 5-methoxy-*N,N*-dimethyltryptamine), reversible monoamine oxidase inhibitors (harmine and harmaline) and tropane alkaloids (atropine and scopolamine), which were not quantified. This is the first report of the chemical analysis of *Amanita* mushrooms that are circulated in the drug market.

Keywords: *Amanita muscaria*; *Amanita pantherina*; Ibotenic acid; Muscimol; GC/MS

1. Introduction

Amanita muscaria, known by the name ''fly agaric,'' is a psychotropic mushroom that is traditionally used for religious or recreational purposes in Siberia, North-East Asia and India [1,2]. This mushroom has been recently reported as being used as an intoxicant in several countries [3,4]. In Japan, not only *A. muscaria* but also *Amanita pantherina*, a dissociative mushroom similar to *A. muscaria*, are circulated via the Internet or in ''smoke shops.'' In addition, ''extracts purported to contain *A. muscaria*'' products are also in circulation. In 2003, the Japan Poison Information Center received four cases of intoxication caused by ''extracts purported to contain *A. muscaria*'' products [5].

A. muscaria and *A. pantherina* contain two dissociative constituents, ibotenic acid (IBO) and muscimol (MUS) (Fig. 1). IBO is a powerful agonist of the *N*-methyl-D-aspartic acid (NMDA) receptor [6]. Nielsen et al. reported that IBO was converted by decarboxylation to MUS in mouse brain homogenates [7]. MUS, which acts as a potent $GABA_A$ agonist [8], has more potent neuropharmacological activity [9–11].

There are several reports on the contents of IBO/MUS in *A. muscaria* and *A. pantherina* in natural products. Determination of IBO/MUS in mushrooms was performed using paper chromatography [12], high performance liquid chromatography [13–15], single-column chromatography [16] and gas chromatography/mass spectrometry (GC/MS) [17]. However, an analysis of samples that are circulated in the drug market has not yet been reported. In this study, we report on the chemical analysis of *Amanita* mushrooms and ''extracts purported to contain *A. muscaria*'' products that are circulated in Japan.

* Corresponding author. Tel.: +81 4 7135 8001; fax: +81 4 7133 9173.
E-mail address: tujikawa@nrips.go.jp (K. Tsujikawa).

0379-0738/$ – see front matter
doi:10.1016/j.forsciint.2006.01.004

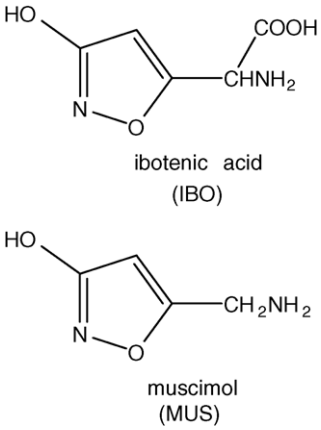

Fig. 1. Chemical structures of ibotenic acid (IBO) and muscimol (MUS).

2. Experimental

2.1. Samples and chemicals

Eleven samples were used in this study; seven were dried mushrooms sold as *A. muscaria* or *A. pantherina* (five *A. muscaria* (see Fig. 2A) and two *A. pantherina* (see Fig. 2B)), and four were "extracts purported to contain *A. muscaria*" products (see Fig. 2C and D). These samples were obtained from "smoke shops" or via the Internet in Japan.

IBO hydrate was obtained from Biosearch Technologies (Novato, CA, USA). MUS was obtained from Sigma (St. Louis, MO, USA). *N*,*O*-Bis(trimethylsilyl)trifluoroacetamide (BSTFA) with 10% trimethylchlorosilane (TMCS) was obtained from Pierce Chemical Co. (Rockford, IL, USA). All other chemicals used in the experiments were of analytical grade.

2.2. Optical microscopic examination

A microscopic examination was performed using the method reported by Walting [18]. A 2.5% potassium hydroxide solution was used as a swelling agent and to return the dried tissues to their previous state. Small pieces of the gills were cut from the fruit-body and mounted on a glass slide, while directly in the 2.5% potassium hydroxide solution. After covering with a glass cover-slip, it was tapped with a rubber-tipped pencil to separate the tissues from each other. Observation was carried out using a biological microscope. The sizes of the spores were measured with Image J (Wayne Rasband, National Institute of Health, USA) and an average of 12 spores was measured for each sample.

Melzer's staining reaction was used for detecting amyloid, pseudoamyloid, or nonamyloid of the spores. Staining was performed using the method described in Ref. [19]. Small pieces of the gills were cut from the fruit-body and mounted on a glass slide, while directly in the 2.8% ammonia solution. After washing by water, the samples were swelled in the Melzer's reagent (composition as follows: 0.5 g of iodine, 1.5 g of potassium iodide, 22 g of chloral hydrate and 20 g of water) and were observed under a biological microscope.

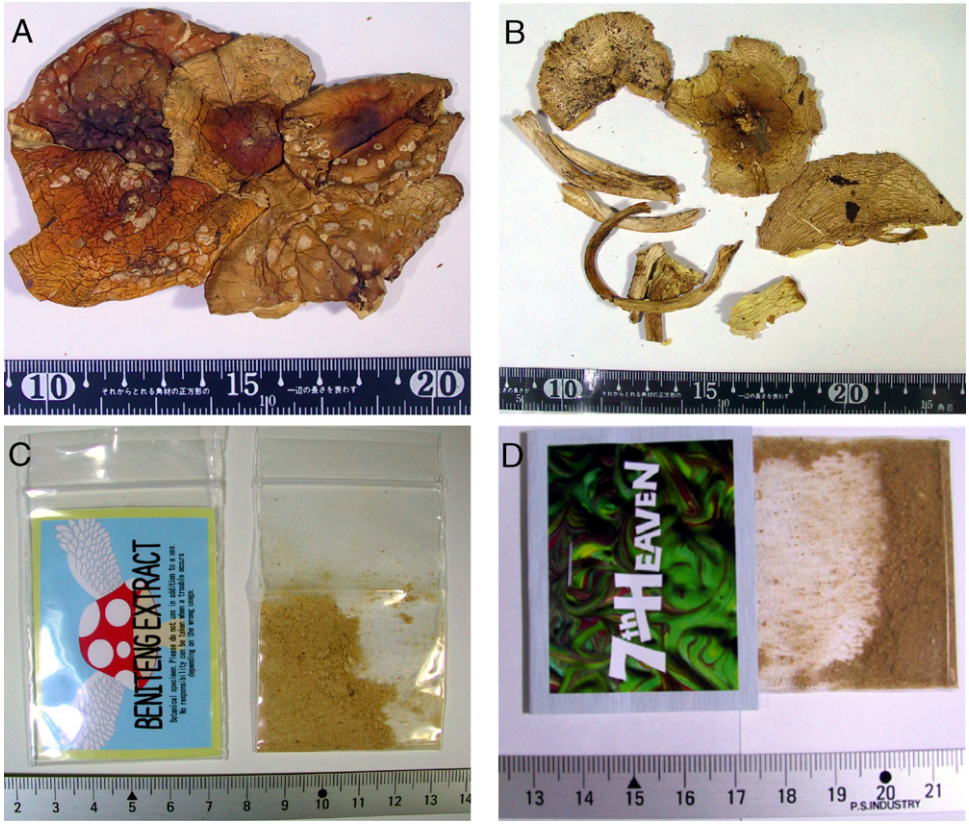

Fig. 2. Representative photographs of the samples: (A) *A. muscaria*; (B) *A. pantherina*; (C and D) "extracts purported to contain *A. muscaria*" products.

2.3. Chemical analysis

2.3.1. Extraction procedure of IBO and MUS

For the extraction of IBO and MUS, a previously reported method [13] was used with minor modifications as follows. The dried mushrooms were cut into the sections of caps and stems, and the cuticle and flesh in a part of the caps were also separated. Each section was ground to a fine powder in a mortar. Fifty milligrams of the powdered mushrooms or ''extracts purported to contain *A. muscaria*'' products were extracted twice with 2 mL of 70% aqueous methanol by shaking for 1 min followed by ultrasonication for 5 min. After centrifugation at 3000 rpm for 3 min, 200 μL of the supernatant was transferred to a separate vial and the solution evaporated to dried under a stream of nitrogen. The residues were derived by reaction with a mixture of 50 μL of BSTFA containing 10% TMCS and 50 μL of ethyl acetate containing 20 μg/mL *n*-pentadecane as an internal standard (IS) at 80 °C for 30 min. A 1 μL aliquot was used for gas chromatography/mass spectrometry.

2.3.2. Calibration curve

Calibration curves for IBO/MUS were constructed by plotting the blank-subtracted peak area ratio of the target compound to IS versus the concentration of IBO/MUS. Blank-subtraction was performed by subtracting the peak area ratio of the blank from that of the samples. An entire cap of sample no. 4 (*A. muscaria*) was used as blank, because it contained lower concentrations of IBO/MUS than the other *Amanita* mushrooms determined in this study. IBO/MUS were added to the blank extract in the following blank-subtracted final concentrations: IBO hydrate (10, 25, 50, 150, 400 ppm) and MUS (25, 50, 150, 400, 1000, 2000 ppm). The regression parameters for the slope, intercept and correlation coefficient were calculated by weighted ($1/x$) linear regression using the Correlation2-2 freeware (http://homepage3.nifty.com/m_nw/j-frame.htm).

The determination of IBO/MUS in the blank sample (no. 4) was performed by the standard addition method. Calibration curves were constructed by adding standards to the blank extract and plotting the blank-subtracted peak area ratio of the target compound to IS versus the concentration of IBO/MUS. The final concentrations of adding standards are as follows: IBO hydrate (0, 10, 25, 50 ppm) and MUS (0, 25, 50, 150 ppm). The regression parameters were calculated by the above mentioned software.

Tests to determine the precision and accuracy of the method were performed using the blank mushroom extract that had been spiked with IBO hydrate and MUS. The concentrations spiked were as follows: 20, 80, 300 ppm for IBO hydrate and 40, 300, 1500 ppm for MUS, respectively. The accuracy of the assay was evaluated by percent deviation (%DEV) from the nominal concentration using the formula: $\%DEV = 100 \times$ (mean back calculated concentration − nominal concentration)/nominal concentration. Intra- and inter-assay precision is expressed as the coefficient of variation (CV, %) of the experimental values at each concentration.

2.3.3. Extraction procedure for drug screening analysis

For other active ingredients (e.g. abused drugs, natural pharmacologically-active compounds, etc.) in ''extracts purported to contain *A. muscaria*'' products, general drug screening was performed by a modified Stas-Otto's isolation method, as summarized in Fig. 3. After the extraction procedure, a 1 μL aliquot was used for GC/MS.

2.3.4. Apparatus and chromatographic conditions

GC/MS analysis was performed with a GCMS-QP5050A (Shimadzu, Kyoto, Japan) equipped with a DB-5 ms capillary column (30 m length, 0.25 mm i.d. and 0.25 μm film thickness, J&W). The temperature of the injector and the interface was set at 250 °C. The oven temperature was held at 100 °C (for IBO/MUS) or 50 °C (for general drug screening) for 1 min, then increased to 300 °C at 15 °C/min and held for 5 min. Helium was used as the carrier gas (head pressure at 72.3 kPa at 100 °C or 67.5 kPa at 50 °C, total flow 53.0 mL/min). The mass spectrometer was operated under the electron ionization (EI) mode at an ionization energy of 70 eV. For qualification, the analysis was performed in the scan mode (mass range: *m/z* 40–450 for IBO/MUS, and *m/z* 40–600 for general drug screening). For quantification, the MS was programmed for selected ion monitoring (SIM) detection of *m/z* 257 (IBO), *m/z* 243 (MUS) and *m/z* 57 (IS).

3. Results and discussion

3.1. Morphological examinations

For identification of the species of the mushrooms sold as *A. muscaria* or *pantherina*, we performed macroscopic and microscopic examination. The morphologic features of mushroom samples are summarized in Table 1. Some important morphological features such as stems and gill attachment could not be obtained from the samples, because there were no stems in most of the packages of the mushroom samples. Therefore, identification of species in this study was mainly performed by macroscopic features of caps and microscopic features of spores. Morphologic features of the samples were almost fully in accordance with the description of *A. muscaria* and *A. pantherina* in Refs. [20,21]. The color of caps of the mushrooms sold as *A. muscaria* tended to be yellowish in comparison with the references, but we presumed that this was caused by fading during drying. Judging comprehensively, all mushroom samples could be identified as *A. muscaria* and *A. pantherina* as described on the package of the samples.

3.2. Chemical examinations

Fig. 4 shows total ion chromatogram (TIC) and mass chromatograms resulting from an *A. muscaria* (sample no. 1) in the scan mode. The peaks for IBO-*tri*-TMS, MUS-*di*-TMS and IS had retention times of 9.1, 7.0 and 7.3 min, respectively. The peaks of IBO-*tri*-TMS and MUS-*di*-TMS were not detected in the extract of edible mushrooms like *Lentinus edodes* (''shiitake''), *Flammulina velutipes* (''enokitake'') and *Pleurotus ostreatus*

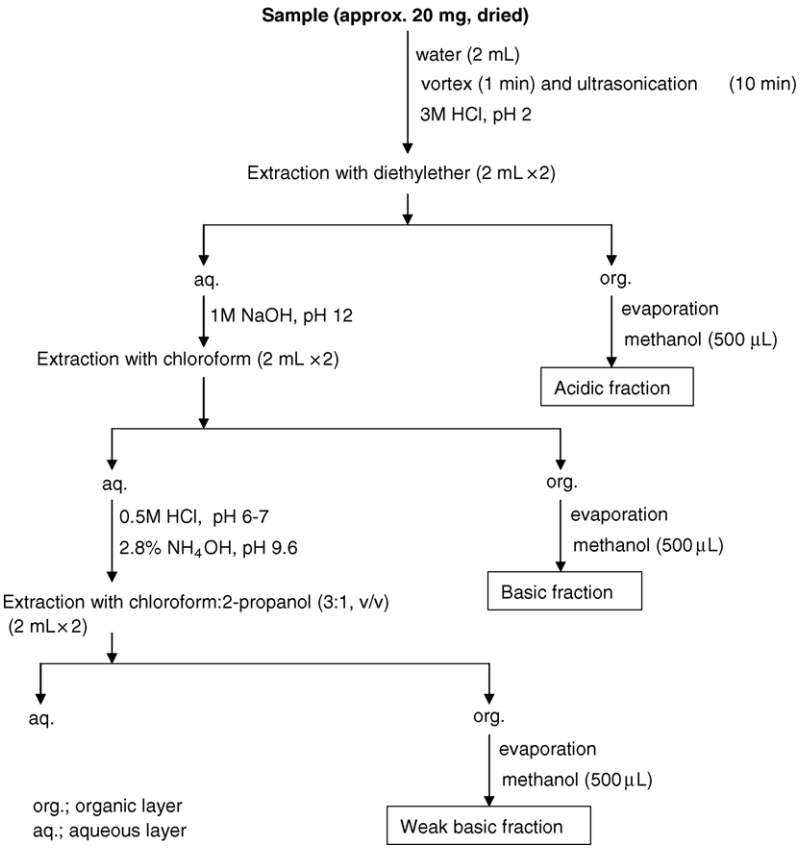

Fig. 3. Extraction procedures for other active constituents in "extracts purported to contain *A. muscaria*" products.

("hiratake"). Each derivative was stable for at least 10 h at room temperature. The mass spectra of IBO-*tri*-TMS and MUS-*di*-TMS are shown in Fig. 5. The fragmentations of these mass spectra were previously reported by Repke et al. [17].

Table 1
Morphologic characteristics of *A. muscaria* and *A. pantherina* used in this study

Species	Description
A. muscaria	Macroscopic feature *Cap*: 4–10 cm broad, plane shape, pale brown to orange color, strewn with whitish-brown warts *Gill*: whitish-brown color *Subcuticle*: white color
	Microscopic feature *Spores*: 9.5–9.9 μm × 6.6–7.0 μm, colorless, elliptical-ovate, smooth surface and nonamyloid *Basidia*: colorless, 4-sterigmate
A. pantherina	Macroscopic feature *Cap*: 3.5–6.5 cm broad, plane shape, gray-brown color, strewn with whitish-brown warts *Gill*: whitish-brown color *Subcuticle*: white color
	Microscopic feature *Spores*: 10.5–11.4 μm × 7.2–7.4 μm, colorless, elliptical-ovate, smooth surface and nonamyloid *Basidia*: colorless, 4-sterigmate

Repke et al. performed trimethylsilylation at 140 °C for 30 min with BSTFA, and they reported that shorter reaction times or lower reaction temperature resulted in the presence of variable amounts of a partially derivatized product, presumably IBO-*di*-TMS [17]. In the present study, by adding 10% TMCS to the BSTFA, IBO could be completely converted to IBO-*tri*-TMS at 80 °C for 30 min.

In the early stage of the experiment, IBO/MUS in the mushroom samples were extracted four times with 70% aqueous methanol to investigate the efficiency of the extraction. As shown in Fig. 6, almost all of IBO/MUS were recovered from the mushrooms in two extractions. Hereafter, two extractions were used for the quantitative analysis of IBO/MUS.

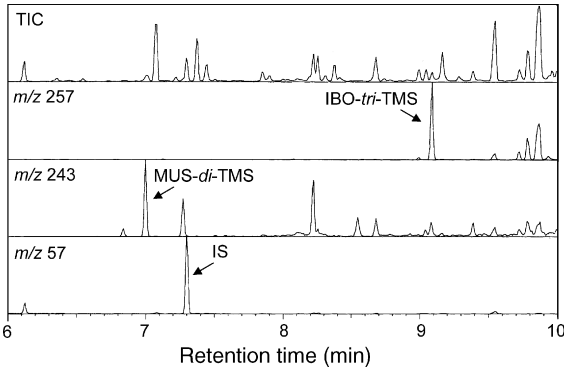

Fig. 4. TIC and mass chromatograms resulting from an *A. muscaria* (sample no. 1) in the scan mode.

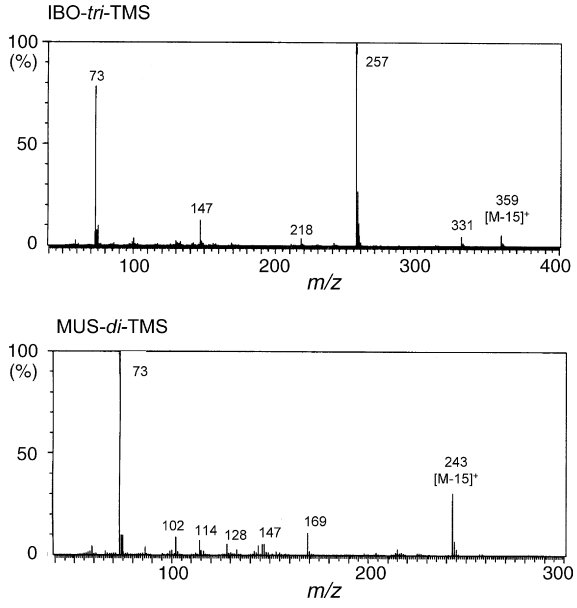

Fig. 5. EI mass spectra of IBO-*tri*-TMS and MUS-*di*-TMS.

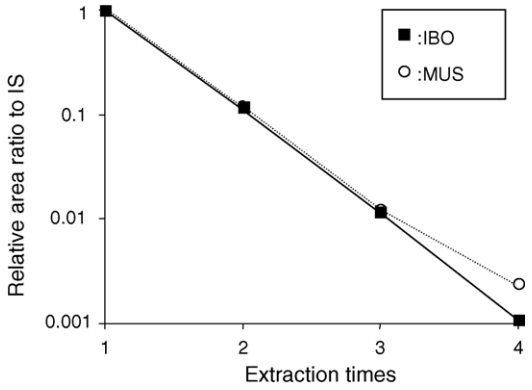

Fig. 6. Recovery of IBO and MUS in *A. muscaria* after repeated extraction. The *Y*-axis is relative area ratio to the first extract and the *X*-axis denotes extraction times. Each data point represents the mean of triplicate determinations.

Initially, we attempted to construct calibration curves by adding IBO/MUS standards to extracts of edible mushrooms such as *L. edodes*, *F. velutipes* and *P. ostreatus*. However, this approach was not feasible for IBO because of matrix differences. Therefore, we selected *A. muscaria* sample no. 4 as a blank mushroom, because it contained lower levels of IBO/MUS than the other *Amanita* mushroom samples. The calibration curves were linear over the concentration range of 10–400 ppm for IBO (as hydrate) and 25–2000 ppm for MUS with correlation coefficients that were routinely greater than 0.99. Samples that were found to contain IBO or MUS in excess of the upper limits of linearity were reanalyzed after dilution with the blank extract. Table 2 shows accuracy and intra- and inter-assay precision data. The intra-assay accuracy was between −6.3 and 4.5% deviation from nominal values. The CV for the intra- and inter-assay was between 3.5 and 12.8% at three concentrations of the two analytes.

Table 2
Summary of analytical accuracy and precision

	Nominal concentration (ppm)					
	IBO			MUS		
	20	80	300	40	300	1500
Accuracy ($n = 5$)						
Mean observed concentration (ppm)	20.9	82.6	303.4	37.5	291.9	1488.2
%DEV	4.5	3.2	1.1	−6.3	−2.7	−0.8
Precision ($n = 5$)						
Intra-assay (CV, %)	9.8	4.4	12.3	10.1	3.7	6.9
Inter-assay (CV, %)	7.9	6.6	12.8	11.3	3.5	7.0

In applying this quantification procedure, it is necessary to be careful for the following reasons:

(i) Application of this method is limited in the case of obtaining an *Amanita* mushroom which contained much lower levels of IBO/MUS than others.
(ii) Correction of the blank may confound calculation of the IBO/MUS concentrations in the samples.
(iii) The lower limits of calibration curves were dependent on the IBO/MUS levels in the blanks. There is the possibility of evaluation as ‘‘below the lower limits of calibration curves’’ despite detecting IBO/MUS peaks clearly, in case of using the highly-concentrative mushroom as a blank.

Table 3 summarizes the IBO/MUS contents in the dried mushroom samples. The total contents of IBO/MUS in the caps were <10–2845 ppm/46–1052 ppm in *A. muscaria* and 188–269 ppm/1554–1880 ppm in *A. pantherina*. Some reports have appeared in regard to IBO/MUS contents in naturally growing *A. muscaria* and *A. pantherina*. Benedict et al. reported that the IBO content was in the range of 0.17–0.18% in dried *A. muscaria* [12]. Tsunoda et al. reported that the IBO/MUS contents in the dried Japanese *A. muscaria* caps were in the range of 192–1260 ppm/13–58 ppm [14]. The IBO contents in our samples were in general agreement with the previously reported data, however, our MUS data were higher than the

Table 3
IBO and MUS contents of *Amanita* mushrooms

Sample no.	IBO (ppm)		MUS (ppm)	
	Cap	Stem	Cap	Stem
A. muscaria				
1	612	ND	286	ND
2	97	–	472	–
3	342	–	254	–
4	<10	–	46	–
5	2845	–	1052	–
A. pantherina				
1	188	<10	1880	64
2	269	–	1554	–

(ND) not detected; (–) no sample.

Table 4
IBO and MUS contents in the cuticle and flesh of caps of *Amanita* mushrooms

Sample no.	IBO			MUS		
	Concentration (ppm)		*B*/*A* ratio	Concentration (ppm)		*B*/*A* ratio
	Cuticle (*A*)	Flesh (*B*)		Cuticle (*A*)	Flesh (*B*)	
A. muscaria						
1	84	527	6.3	239	425	1.8
2	54	1366	25.2	35	558	15.9
3	58	322	5.6	54	202	3.7
4	<10	<10	–	<25	125	>5.0
5	187	732	3.9	297	774	2.6
A. pantherina						
1	508	985	1.9	1304	3544	2.7
2	491	377	0.8	929	1242	1.3

(–) *B*/*A* ratio could not be calculated.

previous reports. Drying *A. muscaria* in the sun or with a heater caused an increase in MUS in the mushroom by decarboxylation of IBO, but a lot of IBO was lost [15]. MUS is not biogenic and can be regarded as IBO artifact. We speculate that *A. muscaria* sold in the drug market were dried in the sun or with a heater to increase the MUS content. Concerning the IBO concentration in *A. pantherina,* our results were lower than the findings reported by Benedict et al. (4600 ppm in an American *A. pantherina*) [12].

On the other hand, there were no stems in the packages of most of the mushroom samples, and the IBO/MUS levels in stems were far lower than that in caps. This tendency is in agreement with findings reported by Tsunoda et al. [14] who found lower concentrations of IBO/MUS in the stem than in the cap of *A. muscaria*.

The thresholds for observation of central nervous system disturbances in humans were 30–600 mg of IBO or about 6 mg of MUS [9]. In another reports, effects were measurable about 1 h after ingestion of 50–90 mg of IBO or 7.5–10 mg of MUS in human volunteers. These effects continued for 3–4 h, with some residual effects lasting as much as 10–24 h in some subjects [10,11]. The symptoms caused by ingestion of purified IBO/MUS in volunteers were as follows: hallucination, delirium, muscular spasm and sleep [9,22]. Some parts of the symptoms caused by IBO were presumed to be attributed to MUS derived from IBO by its decarboxylation.

Judging from the MUS concentration in the *Amanita* mushrooms used in this study, it is estimated that the ingestion of approximately 7–30 g of *A. muscaria* caps (except for sample no. 4) or approximately 4–5 g of *A. pantherina* caps would be sufficient to cause central nervous effects. The former amount is consistent with the ''recommended dosage'' (1–30 g of dried *A. muscaria* caps) claimed on the Erowid Internet site (http://www.erowid.org/plants/amanitas/amanitas.shtml). Minimum units circulated in Japan (10 g for *A. muscaria* and 4 g for *A. pantherina*) are also approximately equal to the estimated amounts.

Moreover, we separately determined the IBO/MUS contents in the cuticle and in the flesh of the caps of mushrooms (Table 4). Our findings indicated that the flesh contained a higher concentration than the cuticle in most samples. This result was in agreement with findings reported by Gore and Jordan [16] and Erowid's claim that the material just under the cuticle of *A. muscaria* was the most ''active'' portion.

In Japan, ''extracts purported to contain *A. muscaria*'' products rather than dried mushrooms are mainly circulated. However, judging from their amounts (approximately 0.3–0.5 g) in one package (Table 5), their IBO/MUS contents were too low (below the lower limit of calibration curves or not detected) to evoke dissociative effect. On the other hand, other psychoactive chemicals such as hallucinogenic tryptamine derivatives (5-methoxy-*N,N*-diisopropyltryptamine (5-MeO-DIPT) and 5-methoxy-*N,N*-dimethyltryptamine (5-MeO-DMT), reversible monoamine oxidase (MAO) inhibitors (harmine and harmaline) and tropane alkaloids (atropine and scopolamine)) were detected in these products by the modified Stas-Otto's method (Table 5). However, these chemicals were not quantified. These compounds were presumed to be artificially added, because these are not contained in the *Amanita* mushrooms. 5-MeO-DIPT has been controlled by the Narcotics and Psychotropics Control Law in Japan since 2005. The other chemicals contained in these products are not controlled as of yet.

Table 5
IBO/MUS contents and other chemicals contained in the ''extracts purported to contain *A. muscaria*''

Sample no.	Concentration (ppm)		Other contents
	IBO	MUS	
1	ND	<25	5-MeO-DIPT
2	<10	<25	5-MeO-DIPT
3	<10	<25	5-MeO-DIPT, harmaline, harmine, atropine
4	ND	<25	5-MeO-DMT, 5-MeO-DIPT, harmaline, harmine, atropine, scopolamine, caffeine

(ND) not detected; 5-MeO-DIPT, 5-methoxy-*N,N*-diisopropyltryptamine; 5-MeO-DMT, 5-methoxy-*N,N*-dimethyltryptamine.

5-MeO-DMT, which is an orally-inert tryptamine derivative [23], will be orally psychoactive by coadministration with MAO inhibitors such as harmine and harmaline [24]. This is very dangerous for public health because a severe intoxication case caused by the combination of 5-MeO-DMT and harmine was reported [25]. Moreover, MAO inhibitors may potentiate pharmacological effects of tropane alkaloids [26,27]. We therefore conclude that psychotic symptoms caused by the ingestion of these products can be attributed to multiple effects of added psychoactive chemicals.

4. Conclusion

This is the first report on chemical analysis about *Amanita* mushrooms and ‘‘extracts purported to contain *A. muscaria*’’ products circulated in the drug market. This study indicated that *Amanita* mushrooms contained high enough levels of IBO/MUS to cause central nervous effects, and that ‘‘extracts purported to contain *A. muscaria*’’ products contained other psychoactive chemicals (e.g. hallucinogenic tryptamines) in place of IBO/MUS. These results will be very useful for comprehension of drugs circulated in the Japanese illicit drug markets.

References

[1] M. Saar, Ethnomyocological data from Siberia and North-East Asia on the effect of *Amanita muscaria*, J. Ethnopharmacol. 31 (1991) 157–173.
[2] S. Hajicek-Dobberstein, Soma siddhas and alchemical enlightenment: psychedelic mushrooms in Buddhist tradition, J. Ethnopharmacol. 48 (1995) 99–118.
[3] J.H. Halpern, Hallucinogens and dissociative agents naturally growing in the United States, Pharmacol. Ther. 102 (2004) 131–138.
[4] J. Riba, M. Valle, G. Urbano, M. Yritia, A. Morte, M.J. Barbanoj, Human pharmacology of ayahuasca: subjective and cardiovascular effects, monoamine metabolite excretion, and pharmacokinetics, J. Pharmacol. Exp. Ther. 306 (2003) 73–83.
[5] Y. Kuroki, The latest tendency of uncontrolled substances inquires to JPIC, Jpn. J. Toxicol. 17 (2004) 241–243 (in Japanese).
[6] T.A. Verdoorn, R. Dingledine, Excitatory amino acid receptors expressed in *Xenopus* oocytes: agonist pharmacology, Mol. Pharmacol. 34 (1988) 298–307.
[7] E.O. Nielsen, A. Schousboe, S.H. Hansen, P. Krogsgaard-Larsen, Excitatory amino acid: studies on the biochemical and chemical stability of ibotenic acid and related compounds, J. Neurochem. 45 (1985) 725–731.
[8] E.J. Nestler, S.E. Hyman, R.C. Malenka, Molecular Pharmacology: A Foundation for Clinical Neuroscience, McGraw-Hill, New York, 2001, p. 10.
[9] F.G. Waser, The pharmacology of *Amanita muscaria*, in: D.H. Efron, B. Holmstedt, N.S. Kline (Eds.), Ethnopharmacological Search for Psychoactive Drugs, U.S. Public Health Service Publication, Washington, DC, 1979, pp. 419–439.
[10] C.H. Eugster, Isolation structure and synthesis of central active compounds from *Amanita muscaria* (L. ex Fr.) Hooker, in: D.H. Efron, B. Holmstedt, N.S. Kline (Eds.), Ethnopharmacological Search for Psychoactive Drugs, U.S. Public Health Service Publication, Washington, DC, 1979, pp. 416–419.
[11] W.S. Chilton, The course of an intentional poisoning, McIlvanea 2 (1975) 17–18.
[12] R.G. Benedict, V.E. Tyler Jr., L.R. Brady, Chemotaxonomic significance of isoxazole derivatives in *Amanita* species, Lloydia 29 (1966) 333–341.
[13] K. Tsunoda, N. Inoue, Y. Aoyagi, T. Sugahara, Simultaneous analysis of ibotenic acid and muscimol in toxic mushroom, *Amanita muscaria*, and analytical survey on edible mushrooms, J. Food Hyg. Soc. Jpn. 34 (1993) 12–17.
[14] K. Tsunoda, N. Inoue, Y. Aoyagi, T. Sugahara, Changes in concentration of ibotenic acid and muscimol in the fruit body of *Amanita muscaria* during the reproduction stage (food hygienic studies of toxigenic basidiomycotina II), J. Food Hyg. Soc. Jpn. 34 (1993) 18–24 (in Japanese).
[15] K. Tsunoda, N. Inoue, Y. Aoyagi, T. Sugahara, Change in ibotenic acid and muscimol contents in *Amanita muscaria* during drying, storing or cocking, J. Food Hyg. Soc. Jpn. 34 (1993) 153–160 (in Japanese).
[16] M.G. Gore, P.M. Jordan, Microbore single-column analysis of pharmacologically active alkaloids from the fly agaric mushroom *Amanita muscaria*, J. Chromatogr. 243 (1982) 323–328.
[17] D.B. Repke, D.T. Leslie, N.G. Kish, GLC–mass spectral analysis of fungal metabolites, J. Pharm. Sci. 67 (1978) 485–487.
[18] R. Watling, Hallucinogenic mushrooms, J. Forensic Sci. Soc. 23 (1983) 53–66.
[19] R. Imazeki, T. Hongo, Books of Fungi in Japan Illustrated in Color, second ed., Hoikusya, Tokyo, Japan, 1977, p. 5 (in Japanese).
[20] R. Imazeki, T. Hongo, Books of Fungi in Japan Illustrated in Color, second ed., Hoikusya, Tokyo, Japan, 1977, p. 44 (in Japanese).
[21] D.T. Jenkins, R.H. Petersen, A neotype specimen for *Amanita muscaria*, Mycologia 68 (1976) 463–469.
[22] W. Theobald, O. Büch, H.A. Kinz, P. Krupp, E.G. Stenger, H. Heimann, Pharmacological and experimental investigations of two components of the fly agaric, Arzneim. Forsch. 18 (1968) 311–315.
[23] B.L. Roth, Hallucinogens, Pharmacol. Ther. 101 (2004) 131–181.
[24] J. Ott, Phamepena-psychonautics: human intranasal, sublingual and oral pharmacology of 5-methoxy-*N*,*N*-dimethyltryptamine, J. Psychoactive Drugs 33 (2001) 403–407.
[25] D.E. Brush, S.B. Bird, E.W. Boyer, Monoamine oxidase inhibitor poisoning result from Internet misinformation on illicit substances, J. Toxicol. Clin. Toxicol. 42 (2004) 191–195.
[26] Drug Package Insert of Atropine Sulfate Injection, Tanabe Seiyaku Co., Ltd.
[27] Drug Package Insert of PAN-SCO Injection, Opium Alkaloids and Scopolamine Injection, Takeda Pharmaceutical Co., Ltd.

ELSEVIER

Forensic Science International 164 (2006) 179–182

Forensic Science International

www.elsevier.com/locate/forsciint

The use of mitochondrial cytochrome oxidase I gene (COI) to differentiate two UK blowfly species – *Calliphora vicina* and *Calliphora vomitoria*

Carole Ames [a], Bryan Turner [b], Barbara Daniel [a,*]

[a] *King's College London, Department of Forensic Science and Drug Monitoring, 150 Stamford Street, London SE1 9NH, UK*
[b] *Department of Life Science, King's College London, SE1 9NN England, UK*

Received 27 October 2004; received in revised form 10 January 2006; accepted 11 January 2006
Available online 28 February 2006

Abstract

Traditionally identification of forensically important insects has been carried out based upon morphological differences between species. However insect evidence found at a crime scene may on occasion be difficult to distinguish by morphological techniques and under these circumstances another method of accurate identification is required.

This work utilises a cytochrome oxidase I partial mitochondrial gene region (COI) to distinguish the two of the main UK blowfly species – *Calliphora vicina* (Robineau Desvoidy) and *Calliphora vomitoria* (Linnaeus) (Diptera:Calliphoridae).

Seventeen interspecific differences in COI sequence were located. Use of the restriction enzyme *Sfc*I on this gene region provides a simple method for distinguishing between *C. vicina* and *C. vomitoria*.

Keywords: Forensic entomology; Cytochrome oxidase I (COI); *Calliphora vicina*; *Calliphora vomitoria*; Mitochondrial gene

1. Introduction

Insect evidence is used in forensic science, amongst other things, to aid in estimating time of death of a corpse (post-mortem interval, PMI). This estimation is based upon the time taken for insects developing on a corpse to reach the stage present when the body is found. Insect species have different developmental lifecycle timings and therefore, to utilise the correct developmental information, species need to be accurately identified. This can be done based upon morphological differences [1]. However under the far from ideal circumstances of a crime scene the larval forms and eggs of many forensically important dipteran species are difficult to distinguish as their morphological differences may be obscured or badly preserved. [2]. Definitive identification may be achieved by rearing larvae to adults but this can be time consuming and require the larvae to be collected live and kept in conditions suitable for continued development.

The use of DNA techniques can not only provide a suitable alternative but may also give information on population substructures [3]. This identification can be carried out on any lifecycle stage without further rearing and on dead, preserved or live samples. DNA techniques are also relatively insensitive to the methods of preservation or age of samples [4].

Recent use of molecular markers for forensic species has focussed on the use of mitochondrial DNA [2]. Mitochondria are present in high numbers within cells and hence mitochondrial DNA is present in a much higher copy number than nuclear DNA [5]. It is therefore the preferred target when dealing with incomplete or aged tissue samples [5–7]. Previous work on mitochondrial DNA has used regions of the cytochrome oxidase gene (COI) to differentiate Calliphoridae. Wallman and Donnellan [8] have demonstrated that COI can be used for identification of the most forensically important species of blowflies from south-eastern Australia.

Another recent study using a region of the COI gene (278 bp) [9] identified 45 regions that distinguished species from three genera – *Lucilla, Calliphora* and *Chrysomya.* These researchers used two species of C*alliphora* (*Calliphora augur* (Fabricius) and *Calliphora dubae* (Acquart)) and located three areas in the COI gene that showed variation between these two species.

* Corresponding author. Tel.: +44 20 7848 3841; fax: +44 20 7848 3843.
E-mail address: barbara.daniel@kcl.ac.uk (B. Daniel).

0379-0738/$ – see front matter
doi:10.1016/j.forsciint.2006.01.005

In the UK the first arrivals at a corpse are often the blowflies, *Calliphora vicina* (Robineau-Desvoidy) and/or *Calliphora vomitoria* (Linnaeus). The aim of this study was to use the COI gene to differentiate these two species of Calliphoridae.

2. Materials and methods

2.1. Samples

Wild adult specimens were obtained from various locations across England and Wales. Flies were immediately killed and placed in 99% ethanol and frozen until extraction. Laboratory populations of both species were used as a source for all other samples used in this work. These have been maintained in cages for several generations within the laboratory.

Sequence analysis was carried out on 100 adult flies from each species. In addition for each species three replicates of each developmental stage (eggs, each larval stage and pupae). Also included were triplicate DNA extractions from single adult legs and wings and from empty pupal cases.

2.2. DNA extraction

DNA was extracted using the QIAamp DNA Mini Kit (QIAGEN, UK) according the manufacturer's Tissue protocol. DNA was eluted in 100 μl ddH_2O. DNA was then quantified using PicoGreen (Molecular Probes, OR, USA) according to manufacturer's protocol.

2.3. Polymerase chain reaction (PCR)

A region of the COI gene was amplified using primers described in Simon et al. [10]. C1-N-2191 (5′-CCCGGTAAAATTAAAATATAAACTTC-3′) and C1-J-1718 (5′-GGAGGATTTGGAAATTGATTAGTTCC-3′).

PCR reactions were carried out using a total reaction volume of 50 μl. Fifty picomolar of each primer were added to a final concentration of 1 μM. Approximately 1 ng of extracted DNA was added to each reaction. Sterile water was added to a volume of 25 μl. Samples were then heated for 1 min at 94 °C before 25 μl of Readymix™ Red Taq™ PCR Reaction Mix (Sigma, UK) was added. This reaction mix contains 1.5U Taq DNA polymerase, 1.5 mM $MgCl_2$, 0.2 mM dNTPs and buffer (10 mM Tris–HCl, 50 mM KCl) in the 50 μl final volume.

Samples were then loaded onto the GeneAmp® PCR System 9700 Thermal Cycler (PE Applied Biosystems, USA). The following cycles were run 94 °C for 2 min; 30 cycles of [94 °C for 30 s; 60 °C for 30 s; 72 °C for 60 s]; 72 °C for 15 min; 4 °C to finish.

2.4. Sequencing

Sequencing of the purified PCR products was carried out on an Applied Biosystems (Foster City, CA, USA) 310 Genetic Analyser according to manufacturer's protocols. Both forward and reverse samples were sequenced.

2.5. Comparison of sequences

Sequences were analysed using BioEdit Sequence Alignment Editor Software. Initially, forward and reverse sequences from the same sample were compared and any discrepancies resolved. Samples were then compared using CLUSTAL X [11] to find any interspecific differences.

2.6. Restriction enzyme digests

From the consensus sequences, theoretical restriction sites within the sequences were established. The restriction enzyme *Sfc*I (New England Biolabs) was chosen to digest the samples. Each reaction mix consisted of 0.5 μl *Sfc*I (1U), 2 μl 10× NEB Buffer 4 (50 mM potassium acetate; 20 mM Tris–acetate; 10 mM magnesium acetate; 1 mM DTT), 0.2 μl 100× BSA, approximately 1 μg DNA with ddH_2O to make the total volume 20 μl. Reactions were incubated for 1 h at 37 °C.

Samples (5 μl) were subjected to electrophoresis on a 2% agarose gel and visualised with ethidium bromide.

3. Results

This DNA extraction technique (QIAGEN spin column) yielded adequate DNA for cytochrome oxidase amplification in all samples tested. DNA concentrations ranged from 0.2 ng/μl from a single wing to 30 ng/μl for a complete adult fly. For comparable developmental stages or structures there was little variation in DNA yield between the two species. The PCR amplification of the cytochrome oxidase region produced a fragment of 523 bp for all samples. Approximately 400 bp were sequenced and these were compared by pairwise alignment (CLUSTAL X). Consensus sequences for *C. vicina* and *C. vomitoria* mitochondrial COI partial gene regions can be located in GenBank (accession numbers AY536642 and AY536643).

There are 17 differences between the species sequences for COI and these are highlighted in Fig. 1. The base numbering is relative to the consensus sequence established and is not an indication of location within the mitochondrial genome.

The differences consist of 17 base substitutions. From these results a level of 4% variation between species can be calculated for this part of the gene. All substitutions produced synonymous changes in the amino acid sequence for this part of the COI gene.

There were single intraspecific differences observed in 17 samples. One sample had two intraspecific nucleotide differences. All these were located at positions distinct from the 17 interspecific variations in sequence.

Samples were then digested with the restriction enzyme *Sfc*I. Digestion of this *C. vicina* COI region with this enzyme produces three fragments (63, 239 and 273 bp) and digestion of the *C. vomitoria* COI region produces fragments (250 and 273 bp). Fig. 2 illustrates the banding pattern of the two blowfly

```
                    10         20         30         40         50         60         70         80
                    ....|....| ....|....| ....|....| ....|....| ....|....| ....|....| ....|....| ....|....|
C. vicina           ccttccctcg gataaacaat ataagtttct gacttttacc tcctgcatta actttactat tagtaagtag tatagtagaa
C. vomitoria        .a........ a.....t... .......... .......... .......... .......... .......... ..........

                    90         100        110        120        130        140        150        160
                    ....|....| ....|....| ....|....| ....|....| ....|....| ....|....| ....|....| ....|....|
C. vicina           aacggagctg gaacaggatg aactgtttac ccacctttat cttctaatat cgctcatgga ggagcttctg ttgatttagc
C. vomitoria        .......... ....t..... .........t .......... .......... t..a...... .......... ..........

                    170        180        190        200        210        220        230        240
                    ....|....| ....|....| ....|....| ....|....| ....|....| ....|....| ....|....| ....|....|
C. vicina           tatttttctc ttacacttag caggaatttc ttcaatttta ggagctgtaa attttattac tacagttatt aatatacgat
C. vomitoria        .......... .....t.... .......... .......... .......... .......... .......... ..........

                    250        260        270        280        290        300        310        320
                    ....|....| ....|....| ....|....| ....|....| ....|....| ....|....| ....|....| ....|....|
C. vicina           caacaggaat tacattcgac cgaataccat tatttgtttg atctgtagta attacagctt tattactttt attatcttta
C. vomitoria        .......t.. ...c...... .......... .......... ...a...... ........c. .......... ..........

                    330        340        350        360        370        380        390        400
                    ....|....| ....|....| ....|....| ....|....| ....|....| ....|....| ....|....| ....|....|
C. vicina           ccagtattag caggtgctat tactatatta ttaacagatc gaaatcttaa tacatcattc tttgacccag caggaggagg
C. vomitoria        .......... ....a..... .......... .......... .......... ...t...... .......... ..........

                    410
                    ....|....| ....
C. vicina           agacccaatc ttgt
C. vomitoria        ...t.....t ..a.
```

Fig. 1. Sequence differences between *C. vicina* and *C. vomitoria* partial cytochrome oxidase I gene region. Base positions are relative to the sequence established in this work and not the insect mitochondrial genome. Symbol '.' in the *C. vomitoria* sequence represents an identical base to the *C. vicina* sequence.

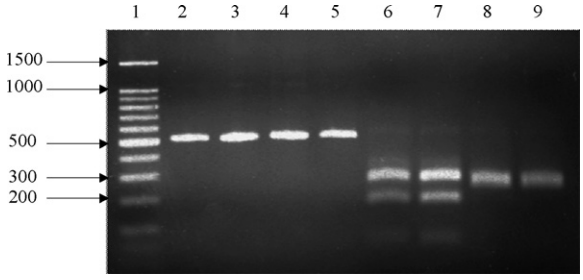

Fig. 2. Restriction enzyme *Sfc*I digest. Lane 1 contains a 100 bp ladder. Numbers represent number of DNA basepairs. Lanes 2 and 6 – undigested and digested *Calliphora vicina* replicate one COI partial gene region. Lanes 3 and 7 – undigested and digested *Calliphora vicina* replicate two COI partial gene region. Lanes 4 and 8 – undigested and digested *Calliphora vomitoria* replicate one COI partial gene region. Lanes 5 and 9 – undigested and digested *Calliphora vomitoria* replicate two COI partial gene region.

species when run on an agarose gel and stained with ethidium bromide. The *C. vomitoria* digestion fragments run as an unresolved doublet on this 2% agarose gel system. However, the two species can be easily distinguished as the *C. vicina* digestion fragments (239 and 273 bp) appear as two distinct bands.

4. Discussion

Use of QIAGEN spin columns provides a DNA extraction method capable of extracting amplifiable mitochondrial DNA from all the lifecycle stages including single eggs, adult legs and wings and empty pupal cases.

After sequencing this 414 bp mitochondrial COI gene region there appears to be 17 species-specific differences present. As expected, the sequence did not vary between adults and immature forms. These data would therefore allow an entomologist to distinguish between specimens of *C. vicina* and *C. vomitoria*, in cases where morphological differentiation was difficult. This agrees with Sperling et al. [12], who demonstrated that mtDNA COI sequences (along with COII and $tRNA^{leu}$) could be used to identify the immature larvae of other forensically interesting Diptera (*Lucilla illustris*, *Phormia regina* and *Phaenicia sericata*).

This study showed interspecific variation of 4% between *C. vicina* and *C. vomitoria*. This is similar to the work of Wells and Sperling [13] that found greater than 3% variation between Chrysomyinae fly species. When the region sequenced in this study is compared with other forensically important UK dipteran species already deposited in GenBank there is 2.3% variation between the *Calliphora* samples in this study and the important *Lucilia* species. This partial COI sequence also provides unique nucleotides to differentiate between *Lucilia* species (ranging from one unique site in *Lucilia sericata* and *Lucilia caesar* to seven in *Lucilia ampullacea*).

The DNA sequence from 212 individuals matched the consensus sequence (GenBank accession numbers AY536642 and AY536643). Seventeen individuals displayed different single base variations in this partial gene region. There was one individual sample with 2 bp differences to the consensus sequence (0.48% variation).

These intra specific results are similar to those found by other researchers. Wells and Sperling [13] reported intraspecific level of variation within the COI and COII sequence for chrysomyinae flies of below 1%. Likewise, Otranto et al. [14], who used COI to distinguish between *Hypoderma* larvae, reported a rate of intraspecific variation ranging from 0.14% to 1.59%.

None of the samples used in this study demonstrated intraspecific variation at any of the 17 interspecific base

substitution positions and therefore not at the *Sfc*I restriction enzyme sites. This is important as variation at these sites might lead to false species identification.

5. Conclusions

This work has therefore indicated that the use of the COI region followed by a *Sfc*I restriction enzyme digest provides a simple and relatively fast method of accurately distinguishing between two of the main UK *Calliphora* blowfly species. This region of the COI gene also provides potential variation between other forensically important blowfly species.

Acknowledgements

Helene Le Blanc from The University of Derby for providing some samples. Steven Tann-Ailward for help with sample collection.

References

[1] K.G.V. Smith, A Manual of Forensic Entomology, The British Museum (Natural History), London and Cornell University Press, London, 1986, p. 205.
[2] D. Otranto, J. Stevens, Molecular approaches to the study of myiasis causing larvae, Int. J. Parasitol. 32 (11) (2002) 1345–1360.
[3] D.M. Hillis, C. Moritz, Molecular Systematics, Sinauer Associates. Massachusetts, USA, 1990, p. 587.
[4] S. Pääbo, J.A. Gifford, A.C. Wilson, Mitochondrial DNA sequences from a 7000-year-old brain, Nucleic Acids Res. 16 (1988) 9775–9787.
[5] J.M. Butler, Forensic DNA Typing, Academic Press, London, 2001, p. 322.
[6] Y. Malgorn, R. Coquoz, DNA typing for identification of some species of Calliphoridae. An interest in forensic entomology, For. Sci. Int. 102 (1999) 111–119.
[7] S. Vincent, J.M. Vian, M.P. Carlotti, Partial sequencing of the cytochrome oxydase b subunit gene I: a tool for the identification of European species of blow flies for postmortem interval estimation, J. For. Sci. 45 (4) (2000) 820–823.
[8] J.F. Wallman, S.C. Donnellan, The utility of mitochondrial DNA sequences for the identification of forensically important blowflies (Diptera: Calliphoridae) in southeastern Australia, For. Sci. Int. 120 (1–2) (2001) 60–67.
[9] M.L. Harvey, I.R. Dadour, S. Gaudieri, Mitochondrial DNA cytcochrome oxidase I gene: potential for distinction between immature stages of some forensically important fly species (Diptera) in western Australia, For. Sci. Int. 131 (2003) 134–139.
[10] C. Simon, F. Frati, A. Beckenbach, B. Crespi, H. Liu, P. Flook, Evolution, weighting, and phylogenetic utility of mitochondrial gene-sequences and a compilation of conserved polymerase chain-reaction primers, Ann. Ent. Soc. Am. 87 (6) (1994) 651–701.
[11] J.D. Thompson, D.G. Higgins, T.J. Gibson, CLUSTAL W: improving the sensitivity of progressive multiple sequence alignment through sequence weighting, position specific gap penalties and weight matrix choice, Nucleic Acids Res. 22 (1994) 4673–4680.
[12] F.A.H. Sperling, G.S. Anderson, D.A. Hickey, A DNA-based approach to the identification of insect species used for postmortem interval estimation, J. For. Sci. 39 (2) (1994) 418–427.
[13] J.D. Wells, F.A.H. Sperling, DNA-based identification of forensically important Chrysomyinae (Diptera: Calliphoridae), For. Sci. Int. 120 (1–2) (2001) 110–115.
[14] D. Otranto, D. Traversa, B. Guida, E. Tarsitano, P. Fiorente, J.R. Stevens, Molecular characterization of the mitochondrial cytochrome oxidase I gene of Oestridae species causing obligate myiasis, Med. Vet. Ent. 17 (3) (2003) 307–315.

ELSEVIER

Forensic Science International 164 (2006) 183–192

Forensic Science International

www.elsevier.com/locate/forsciint

Carrion fly (Diptera: Calliphoridae) larval colonization of sunlit and shaded pig carcasses in West Virginia, USA

James E. Joy [a,*], Nicole L. Liette [b], Heather L. Harrah [b]

[a] Department of Biological Sciences, Marshall University, One John Marshall Way, Huntington, WV 25755, USA
[b] Department of Integrated Sciences and Technology, Marshall University, One John Marshall Way, Huntington, WV 25755, USA

Received 4 February 2005; received in revised form 25 August 2005; accepted 11 January 2006
Available online 23 February 2006

Abstract

Two pig (*Sus scrofta* L.) carcasses were placed in sunlit and shaded plots in September 2003, and again in May 2004. Mean ambient temperatures between sunlit and shaded plots were not significantly different in either September or May, but mean ambient temperatures at sunlit and shaded plots in 2004 were significantly higher than corresponding means for sunlit and shaded plots in 2003. Mean maggot mass temperatures were significantly higher than ambient plot temperatures for all four experimental plots (i.e., sunlit and shaded carcasses in both 2003 and 2004). In addition, maggot mass temperatures on sunlit carcasses were positively, and significantly, correlated with ambient temperatures, whereas there was no significant correlation between maggot mass and ambient temperatures at shaded plots. Carcass decomposition proceeded more rapidly in 2004 in the presence of higher ambient temperatures, and sunlit carcasses decomposed faster than shaded ones in both 2003 and 2004 experiments. *Phaenecia coeruleiviridis* (Macquart) and *Phormia regina* (Meigen) third instars dominated collections on all four carcasses, but there was little temporal overlap between these species with third instars of the former dominating collections in the early portion (≈40%) of each experimental period (with the exception of the shaded carcass in 2004 where both species were co-dominant), and the latter assuming dominance in the latter portion (≈60%). Lower accumulated degree hour values were calculated for instar development on 2004 carcasses subjected to higher ambient temperatures.

Keywords: Forensic entomology; Postmortem interval; *Phaenecia coeruleiviridis*; *Phormia regina*

1. Introduction

Medicocriminal entomology utilizes information derived from either the temperature-dependent development of insects (primarily flies) or the succession of arthropods on human corpses or animal carcasses to form an estimate of the time elapsed since death, or postmortem interval (PMI) [1]. Extensive coverage of the medicocriminal entomology literature is available [2].

Laboratory studies under controlled temperature and/or light conditions [3–9] have provided valuable information on the development of carrion and flesh flies, but it is recognized that field studies are necessary to gain a better insight on fly development under variable climatic conditions. Indeed, the need for increased efforts in the field was recently emphasized [10]. Encouragingly, the desired field work in medicocriminal entomology is continuing, as evidenced by recent investigations [11–13].

A recent study of carrion fly development in West Virginia [11] was preceeded by investigations in nearby states of Tennessee [14,15], South Carolina [16,17], Virginia [18], Illinois [19,20], Maryland [21], Missouri [22], and from Washington, DC [23,24]. The purpose of the present investigation is to expand our understanding of carrion fly development by utilizing pig carcasses in sunlit and shaded field conditions at different times of the year (September and May). We have also sampled at regular intervals, giving equal emphasis to daytime and nighttime collections, to gain a more complete picture of larval development in fluctuating ambient temperatures.

2. Materials and methods

2.1. Study site and sample plots

Two experimental plots were established at the Huntington, West Virginia Sanitary Landfill in Cabell County (N38°25′ and

* Corresponding author. Tel.: +1 304 696 3639; fax: +1 304 696 7136.
E-mail address: joy@marshall.edu (J.E. Joy).

0379-0738/$ – see front matter © 2006 Elsevier Ireland Ltd. All rights reserved.
doi:10.1016/j.forsciint.2006.01.008

W82°23′, elevation 230 m). One plot was situated in the open (i.e., exposed to continuous sunlight during the day) on a hard packed gravel substrate with a sparse amount of emergent grasses; *Ambrosia artemisiifolia* L. (common ragweed), *Festuca elatior* L. (meadow fescue) and *Melilotus* sp. (sweet clover). The second plot was situated 40 m from the first in a shaded area with a canopy of *Cercis canadensis* L. (red bud), *Acer negundo* L. (box elder), *Aesculus octandra* Marsh (yellow buckeye) and *Ailanthus altissima* (Mill.) (tree-of-heaven), and a ground cover of *Lonicera japonica* Thumb. (Japanese honeysuckle), *Eupatorium rugosum* Houtt. (white snakeroot), *Parthenocissus quinquefolia* (L.) (Virginia creeper), and *Geum vernum* (Raf) (spring avens).

2.2. Experimental design and sampling methodology

Two experimental periods were selected for the study; 5–14 September 2003 and 18–25 May 2004. On 11 July 2003 two pigs that had died of natural causes were double bagged in 50-gal plastic garbage bags immediately after death and frozen. Carcasses were thawed at room temperature (≈22 °C) for 72 h, then weighed, prior to the beginning of the September experimental period. Carcasses were then transported to the experimental plots where they were removed from their respective bags. One carcass (23 kg) was placed in the sunlit plot with the second carcass (24 kg) similarly located in the shaded plot at 07:00 h (hour zero) on 5 September 2003. Carcasses were covered with a wooden frame (measuring 90 cm long × 50 cm wide × 40 cm high) supporting 2.5 cm hexnetting to prevent disturbance by scavengers.

Carcasses at both plots were examined every 6 h over a 240 h experimental period for the presence of eggs and/or larvae of carrion flies. A sample of 50–75 larvae was collected at the first appearance of instars and at subsequent 12 h intervals with jeweler's forceps or metal micro-spoon from different areas (i.e., oral/nasal cavities, thoracic/abdominal cavities, anal region) of each carcass. Larvae in these samples were killed in the field immediately after collection by placing them in boiling water heated in a small (1 l) sauce pan over a butane camp stove. After killing, larvae were placed in appropriately labeled (hour from 0 h, sunlit or shaded carcass) bottles containing 70% ethanol. Larvae were then returned to the lab where the fixing solution was decanted and replenished with fresh 70% ethanol.

Ambient temperatures were recorded at 0 h, and at 6 h intervals at both sunlit and shaded plots throughout the course of the 240 h experimental period (Figs. 1 and 2). Maggot mass temperature readings were first recorded at 36 h and continued at 6 h intervals as long as maggot masses were present (Figs. 1 and 2). All temperature readings were taken with a digital thermometer to the nearest 0.1 °C. There was no precipitation during the course of the 2003 experimental period.

The same general experimental procedure was followed for the May 2004 experiment, with two pigs that died of natural causes being frozen on 13 May 2004. The May 2004 experiment differed in four respects: (1) the sunlit and shaded pigs weighed 24 and 26 kg, respectively; (2) the experimental

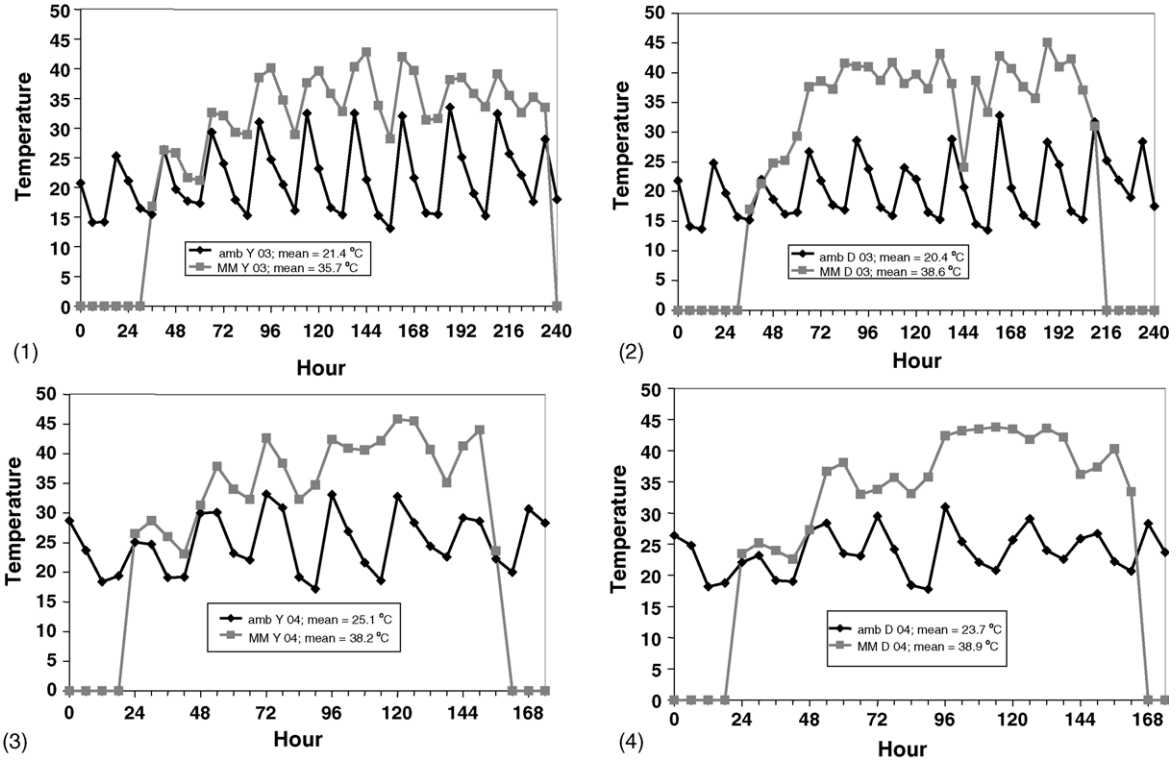

Figs. 1–4. Ambient (◆) vs. maggot mass (■) temperatures (°C) recorded at experimental carcasses in 2003 and 2004. Amb Y03 and Amb D03 represent ambient temperatures at sunlit and shaded carcasses in 2003, respectively. Amb Y04 and Amb D04 are ambient temperatures at sunlit and shaded carcasses in 2004. MM denotes maggot mass temperatures for those respective experimental periods. An X-bar indicates mean temperatures for all ambient or maggot mass points in an experimental period.

Table 1
Extrapolation method used to estimate ADH in the absence of a data logging system

Hour	September 2003						May 2004					
	Sunlit plot			Shaded plot			Sunlit plot			Shaded plot		
	Amb. (°C)	Hourly rate	Est. ADH	Amb. (°C)	Hourly rate	Est. ADH	Amb. (°C)	Hourly rate	Est. ADH	Amb. (°C)	Hourly rate	Est. ADH
0	**20.7**	–	0	**21.8**	–	0	**28.7**	–	0	**26.4**	–	0
1	19.6	−1.10	19.6	20.5	−1.28	20.5	27.9	−0.83	27.9	26.1	−0.27	26.1
2	18.5	−1.10	38.1	19.2	−1.28	39.8	27.0	−0.83	54.9	25.9	−0.27	52.0
3	17.4	−1.10	55.5	18.0	−1.28	57.7	26.2	−0.83	81.1	25.6	−0.27	77.6
4	16.3	−1.10	71.8	16.7	−1.28	74.4	25.4	−0.83	106.5	25.3	−0.27	102.9
5	15.2	−1.10	87.0	15.4	−1.28	89.8	24.6	−0.83	131.1	25.1	−0.27	128.0
6	**14.1**	−1.10	101.1	**14.1**	−1.28	103.9	**23.7**	−0.83	154.8	**24.8**	−0.27	152.8
7	14.1	+0.017	115.2	14.0	−0.067	117.9	22.8	−0.88	177.6	23.7	−1.10	176.5
8	14.1	+0.017	129.3	14.0	−0.067	131.9	21.9	−0.88	199.5	22.6	−1.10	199.1
9	14.2	+0.017	143.5	13.9	−0.067	145.8	21.1	−0.88	220.6	21.5	−1.10	220.6
10	14.2	+0.017	157.7	13.8	−0.067	159.6	20.2	−0.88	240.8	20.4	−1.10	241.0
11	14.2	+0.017	171.9	13.8	−0.067	173.4	19.3	−0.88	260.1	19.3	−1.10	260.3
12	**14.2**	+0.017	186.1	**13.7**	−0.067	187.1	**18.4**	−0.88	278.5	**18.2**	−1.10	278.5
13	16.1	+1.85	202.2	15.6	+1.85	202.7	18.6	+0.17	297.0	18.3	+0.10	296.8
14	17.9	+1.85	220.1	17.4	+1.85	220.1	18.7	+0.17	315.8	18.4	+0.10	315.2
15	19.8	+1.85	239.9	19.3	+1.85	239.3	18.9	+0.17	334.7	18.5	+0.10	333.7
16	21.6	+1.85	261.5	21.1	+1.85	260.4	19.1	+0.17	353.8	18.6	+0.10	352.3
17	23.4	+1.85	284.9	23.0	+1.85	283.4	19.3	+0.17	373.0	18.7	+0.10	371.0
18	**25.3**	+1.85	310.2	**24.8**	+1.85	308.2	**19.4**	+0.17	392.4	**18.8**	+0.10	389.8
174	–	–	3647	–	–	3436	–	–	4339	–	–	4120
240	–	–	5155	–	–	4891	–	–	–	–	–	–

Actual ambient temperature readings recorded at 6 h intervals (e.g., at 6, 7–12, 13–18 h, etc. throughout entire experimental periods for both years) are shown in boldface type. Extrapolated hourly temperatures appear in normal font. The difference between the ending temperature of a 6 h period (in boldface) and the ending 6 h period immediately following (again in boldface) is divided by 6 to determine the hourly rate of decrease or increase (− or +) within that 6 h period. This estimate assumes a constant hourly rate which, of course, did not likely occur, but since no notable temperature variations were experienced in any given 6 h period, the calculations of such hourly rate estimates are believed to be quite close to actual hourly temperature conditions. Total ADH values for 174 and 240 h (for 2004 and 2003 experimental periods, respectively) are given, as well.

period, beginning at 01:00 h (hour zero) on 18 May, was shorter (174 h) because higher ambient temperatures contributed to faster carcass decomposition; (3) larval instar collections were made every 6 h rather than at 12 h intervals; (4) there were three precipitation events with ppt measured by a rain gauge to the nearest 1.0 mm (shown in appropriate figures).

2.3. Calculation of ADH (accumulated degree hours)

Ambient temperatures were recorded at both sunlit and shaded plots for hour zero and at 6 h intervals thereafter in both 2003 and 2004. The estimated hourly rate of temperature decrease (or increase) was extrapolated by measuring the difference in ambient temperatures at the end of each 6 h collection interval (Table 1).

2.4. Data recording and statistical treatment

First and second instars were recorded by observation without regard to species diagnosis. Third instars were identified by characters of posterior spiracles, tubercules, and body spination with the aid of a Zeiss stereomicroscope at 40–60 magnifications. Only third instars were measured because they could be identified as either *Phaenecia coeruleiviridis* or *Phormia regina.* Whenever possible 20 of the largest third instars of each species, from each sampling period (at 12 h intervals in 2003 and 6 h intervals in 2004), were measured to the nearest 0.1 mm using a stereomicroscope equipped with a calibrated ocular micrometer. If <20 individuals of either species were present in a sample, all were used to calculate mean length. Length measurements of individual third instars were recorded on an Excel spreadsheet and adjustments were made to the program to reflect the appropriate 95% confidence limits for a given sample size (i.e., $n = 20$, or $n < 20$). Statistical tests and levels of significance are given in the narrative or figures, as appropriate.

Evaluation of maggot mass temperatures as a function of ambient temperatures at each of the four carcasses was done by testing the null hypothesis that the slope of the regression equation was equal to zero (i.e., H_o:$b = 0$) [25]. Values for the test statistic t and levels of probability are given in the narrative where appropriate.

3. Results

3.1. Ambient plot temperatures

Mean ambient temperatures for sunlit (21.4 °C) versus shaded (20.4 °C) plots in September 2003 (Figs. 1 and 2), were not significantly different ($t_{0.05,80} = 0.843$); nor was there a significant difference ($t_{0.05,58} = 1.165$) between ambient means for sunlit (25.1 °C) versus shaded (23.7 °C) plots in May 2004 (Figs. 3 and 4).

Mean ambient temperatures for experimental plots in 2003 (Figs. 1 and 2) were, however, significantly lower than corresponding means for 2004 (Figs. 3 and 4): 21.4 °C versus 25.1 °C ($t_{0.05,69} = 2.660$) for 2003 and 2004 sunlit plots, respectively; 20.4 °C versus 23.7 °C ($t_{0.05,69} = 3.014$) for 2003 and 2004 shaded plots.

3.2. Maggot mass temperatures

Maggot mass temperatures were recorded from the initial appearance of first instars, but temperatures of maggot masses did not depart noticeably from ambient temperatures until early third instars were first observed on the carcasses (Figs. 1–4). With the appearance of third instars (beginning at 84 h on sunlit and shaded carcasses in 2003, and at 48 and 54 h on sunlit and shaded carcasses, respectively, in 2004) recorded mean maggot mass temperatures were significantly higher than mean ambient temperatures at all carcasses: 35.7 °C versus 21.4 °C ($t_{0.05,65} = 10.59$), 2003 sunlit carcass (Fig. 1); 38.6 °C versus 20.4 °C ($t_{0.05,61} = 13.68$), 2003 shaded carcass (Fig. 2); 38.2 °C versus 25.1 °C ($t_{0.05,47} = 8.40$), 2004 sunlit carcass (Fig. 3); 38.9 °C versus 23.7 °C ($t_{0.05,47} = 13.22$), 2004 shaded carcass (Fig. 4).

Mean maggot mass temperatures in 2004 on sunlit and shaded carcasses (at 38.2 and 38.9 °C, respectively) were not significantly different ($t_{0.05,35} = 0.419$), but the mean maggot mass temperature of 38.6 °C on the shaded carcass in 2003 was significantly higher than its 2003 sunlit counterpart mean of 35.7 °C ($t_{0.05,45} = 2.27$).

While ambient temperatures at both sunlit and shaded plots in 2004 were significantly higher than ambient temperatures for corresponding plots in 2003, mean maggot mass temperatures in sunlit and shaded carcasses in 2004 were essentially the same as their 2003 counterparts. For example, the mean maggot mass temperature of 38.2 °C on the 2004 sunlit carcass was not significantly higher than the 35.7 °C recorded for maggot masses on the 2003 sunlit carcass ($t_{0.05,43} = 1.71$). Similarly, the mean maggot mass temperature of 38.9 °C on the 2004 shaded carcass was not significantly different from the 38.6 °C mean for maggots from the shaded 2003 carcass ($t_{0.05,38} = 0.214$).

Maggot mass temperatures (at sampling hours when third instars were present) recorded on sunlit carcasses paralleled ambient temperatures at sunlit plots in both September 2003 and May 2004 (Figs. 1 and 3). This relationship (i.e., maggot mass temperature as a function of ambient temperature) was positive and significant for both September 2003 (Fig. 5; $b \neq 0$, $t_{0.05,24} = 4.729$, $P < 0.001$) and May 2004 (Fig. 6; $b \neq 0$, $t_{0.05,17} = 2.258$, $P = 0.037$). Conversely, while maggot mass temperatures on shaded carcasses exhibited a positive relationship with shaded plot ambient temperatures, that correlation was not significant for either September 2003 (Fig. 7; $b = 0$, $t_{0.05,20} = 0.435$, $P = 0.669$) or May 2004 (Fig. 8; $b = 0$, $t_{0.05,16} = 0.952$, $P = 0.355$).

3.3. Carcass decomposition

Two features of carcass decomposition were readily observed. First, carcass decomposition occurred more rapidly

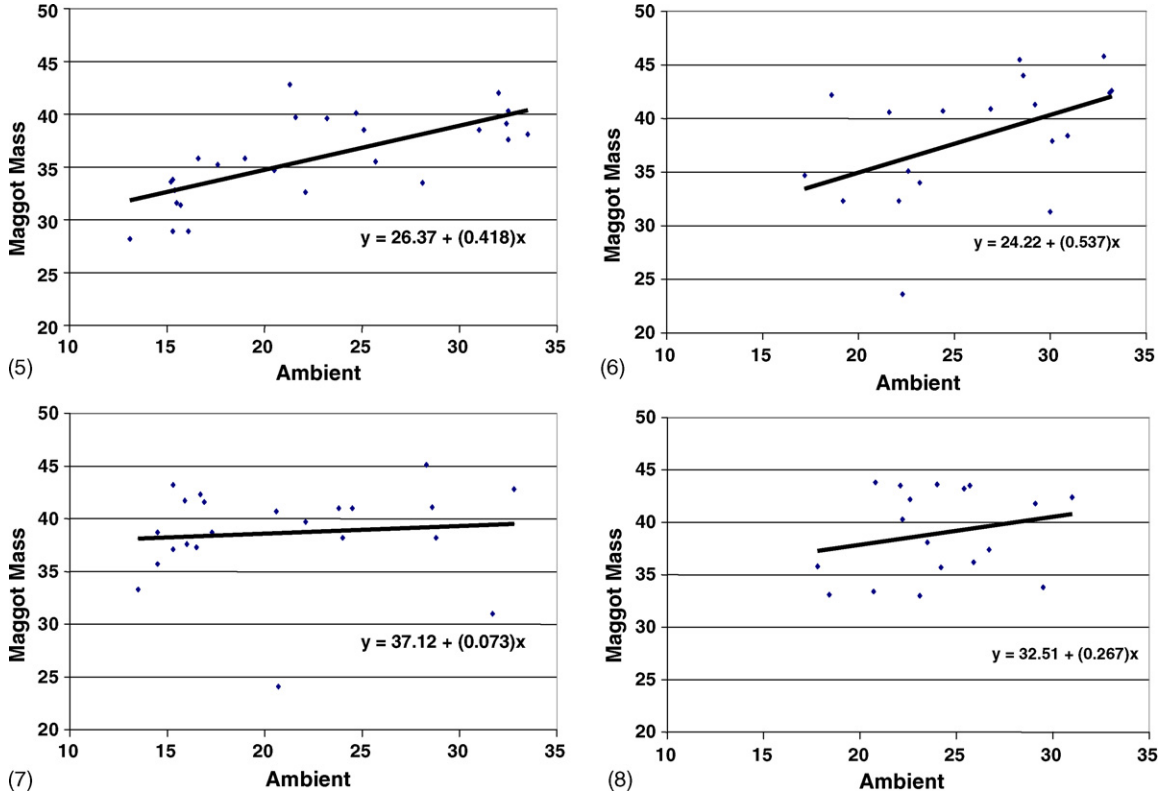

Figs. 5–8. Linear regressions for maggot mass temperature (°C, *y*-axis) as a function of ambient temperature (°C, *x*-axis): Y03, sunlit 2003; Y04, sunlit 2004; D03, shaded 2003; D04, shaded 2004.

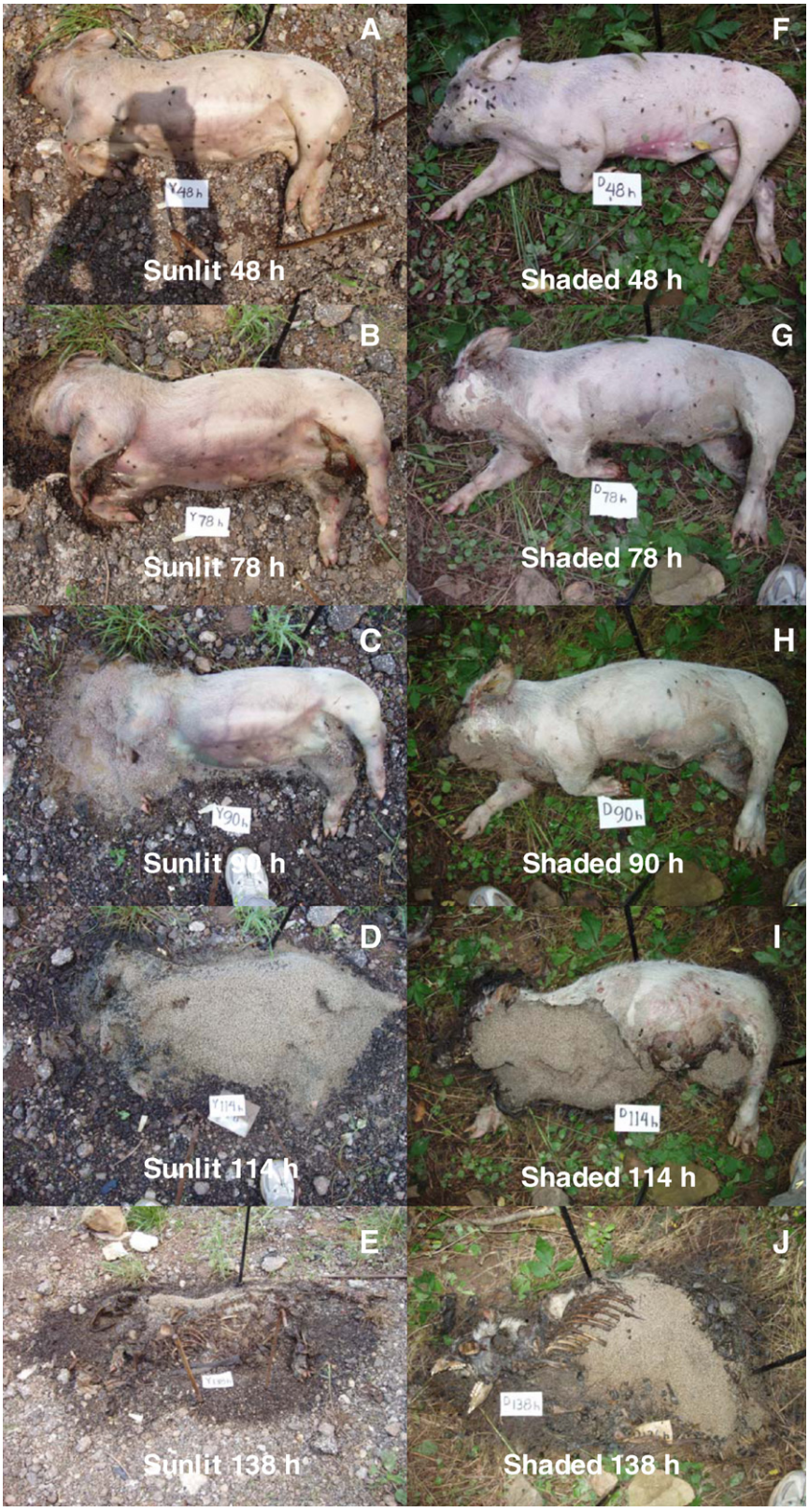

Fig. 9. Decomposition stages for the sunlit pig carcass (A–E) are matched with comparable stages for the shaded pig carcass (F–J) at selected observation periods in 2004.

in the significantly higher ambient temperatures of 2004 (Fig. 9A–J) than in 2003 (Fig. 10A–D). For example, sunlit carcasses at 48 h in 2004 (Fig. 9A) and 84 h in 2003 (Fig. 10A) are at comparable levels of decomposition—coincident with the first appearance of third instars at each carcass. More dramatically, however, in 2004 both sunlit and shaded carcasses were in a greater state of decomposition after 114 h (Fig. 9D and I) than were 2003 sunlit and shaded

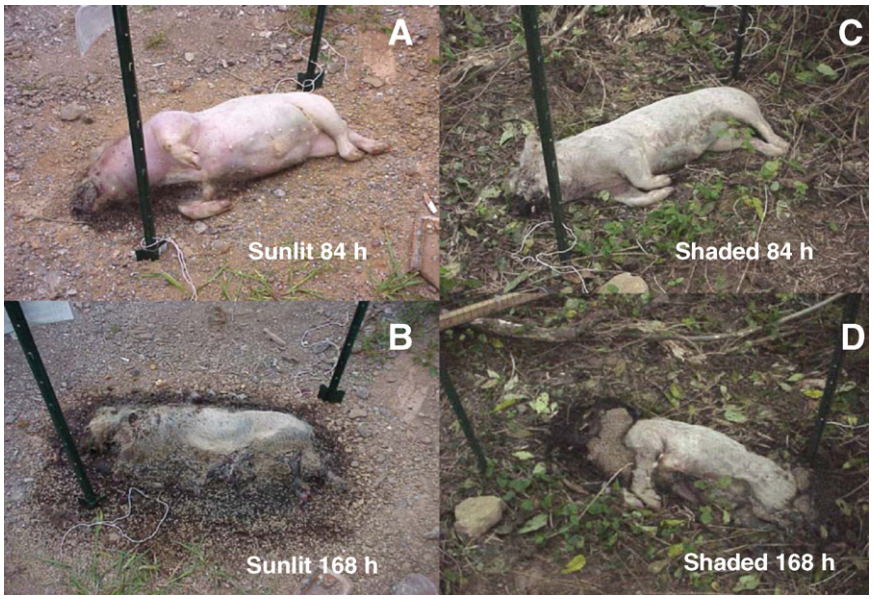

Fig. 10. Decomposition stages for the sunlit pig carcass (A and B) are matched with comparable stages for the shaded pig carcass (C and D) at selected observation periods in 2003.

carcasses at 168 h (Fig. 10B and D). Second, sunlit carcasses decomposed more rapidly than shaded ones in each experimental period. At 48 h, in 2004 when a better photographic series was available, sunlit and shaded carcasses were at comparable levels of decomposition (Fig. 9A and F), but by 78 h bloating was more advanced in the sunlit carcass (Fig. 9B) versus the shaded one (Fig. 9G) and decomposition associated with maggot colonization in the head region of the sunlit carcass is more evident, as well. In comparisons at 90 h, and thereafter, decomposition of the sunlit carcass (Fig. 9C–E) was noticeably advanced over its shaded counterpart (Fig. 9H–J) even though mean ambient temperatures at the sunlit and shaded plots in 2004 were not significantly different.

3.4. Larval activity

Maggot development was slower in 2003 on carcasses exposed to lower ambient temperatures (Table 2), resulting in a greater number of accumulated degree hours (ADH) calculated for instar development in 2003 than in 2004 (Table 3).

There was no attempt to speciate first and second instars, but third instars of carrion flies, identified as *P. coeruleiviridis* and *Phormia regina,* first appeared at 84 h on both sunlit and shaded carcasses in 2003 (Tables 2 and 3; Figs. 11 and 12). In 2004, *Phormia regina* third instars first appeared at 48 and 60 h on sunlit and shaded carcasses, respectively, followed somewhat later by *P. coeruleiviridis* on those carcasses (Tables 2 and 3; Figs. 13 and 14).

Table 2
First appearance of first (1st), second (2nd) and third (3rd) instars by mean ambient temperature (°C) in 2003 and 2004 experimental periods

Hour	September 2003									May 2004								
	Sunlit carcass					Shaded carcass				Sunlit carcass					Shaded carcass			
	N	°C	1st	2nd	3rd	°C	1st	2nd	3rd	*N*	°C	1st	2nd	3rd	°C	1st	2nd	3rd
24	5	19.1				18.8				5	23.1	X			22.1	X		
30	6	18.7				18.3				6	23.3		X		22.3			
36	7	18.2	X			17.9	X			7	22.7				21.8		X	
42	8	19.2				18.4				8	22.3				21.5			
48	9	19.3		X		18.4		X		9	23.0			X[a]	22.1			
54	10	19.1				18.2				10	23.8			X[b]	22.7			
60	11	19.0				18.0				11	23.8				22.8			X[a]
66	12	19.8				18.8				12	23.6				22.8			
72	13	20.1				19.0				13	24.4				23.3			X[b]
78	14	20.0				18.9												
84	15	19.7			X[a,b]	18.8			X[a,b]									

N, number of observations used to determine mean values.
[a] *P. coeruleiviridis.*
[b] *Phormia regina.*

Table 3
First appearance of first (1st), second (2nd) and third (3rd) instars by ADH for 2003 and 2004 experimental periods

Hour	September 2003							May 2004							
	Sunlit carcass				Shaded carcass				Sunlit carcass				Shaded carcass			
	1st	2nd	3rd	ADH	1st	2nd	3rd	ADH	1st	2nd	3rd	ADH	1st	2nd	3rd	ADH
24				447	X			439	X			529	X			514
30				558				543		X		678				651
36	X			653				636				807		X		776
42				784				750				922				890
48		X		919		X		871			X[a]	1075				1033
54				1030				974			X[b]	1255				1200
60				1135				1073				1411			X[a]	1354
66				1281				1208				1547				1493
72				1438				1351				1718			X[b]	1654
78				1561				1467								
84			X[a,b]	1659			X[a,b]	1571								

[a] *P. coeruleiviridis*.
[b] *Phormia regina*.

P. coeruleiviridis third instars were dominant early on sunlit carcasses (84–132, and 54–90 h for 2003 and 2004, respectively). This dominance was characterized by two features: (1) a greater number of *P. coeruleiviridis* individuals in those hourly samples; (2) mean third instar lengths were greater (often significantly so) for *P. coeruleiviridis* than *Phormia regina* (Figs. 11 and 13). After 132 h (in 2003) and 90 h (in 2004), however, *Phormia regina* third instars assumed dominance on the sunlit carcasses and remained so throughout the experimental periods (Figs. 11 and 13).

Conversely, on shaded carcasses, *P. coeruleiviridis* dominance was less evident in the early collection periods (84–120, and 60–102 h for 2003 and 2004, respectively), but from 132 to 216 h (in 2003) and 108 to 162 h (in 2004) *Phormia regina* third instars dominated both in terms of numbers in hourly samples, and in their mean lengths (Figs. 12 and 14).

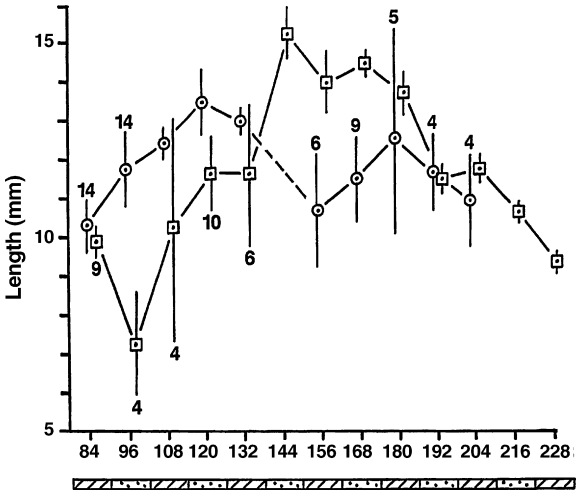

Fig. 11. Third instar lengths on the 2003 sunlit carcass by hour of collection. Open circles, mean *P. coeruleiviridis* lengths; open squares, mean *Phormia regina* lengths. Vertical lines, 95% confidence limits. Numbers above and below vertical lines represent number of *P. coeruleiviridis* and *Phormia regina* third instars, respectively, in collection samples used to calculate means and 95% confidence limits. Where there are no numbers above or below c.l. lines, the third instar sample size was 20. Dashed line indicates that no *P. coeruleiviridis* third instars were in the 144 h sampling period. Numbers on the *y*-axis are instar lengths; numbers along the *x*-axis refer to hours of collection samples. Timeline bar below collection hours indicates 7 PM sample (stippled) and 7 AM sample (cross-hatched). There was no precipitation between 84 and 228 h.

4. Discussion

P. coeruleiviridis and *Phormia regina* larvae dominated carcasses in the present study; not surprising given that these two species were the most common calliphorids recently reported from Southwest Virginia [13]. Still, in the present study those two species did not overlap temporally on carcasses to a great extent. In general, *P. coeruleiviridis* third instars were the initial colonizers of carcasses, but over time their representation in collections declined, and *Phormia regina* assumed the dominant role. This corresponds to previous investigations [22,25] where adult *P. coeruleiviridis* were first drawn to fresh carcasses, but then steadily declining in

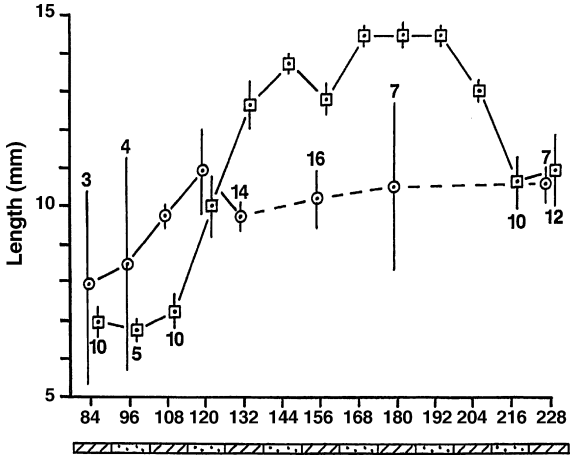

Fig. 12. Third instar lengths on the 2003 shaded carcass by hour of collection. Designations for means, confidence limits, numbers of instars in samples by species, collection hours and time line bar are the same as in Fig. 11. Dashed lines indicate hours when no *P. coeruleiviridis* third instars were present in collections.

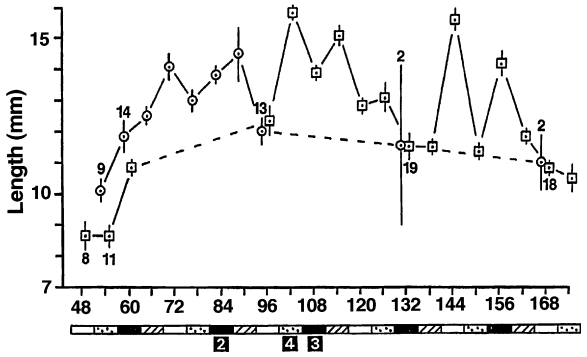

Fig. 13. Third instar lengths on the 2004 sunlit carcass by hour of collection. Designations for means, confidence limits, numbers of instars in samples by species, and collection hours are the same as in Fig. 11. Dashed line from 60 to 96 h indicates hours when no *Phormia regina* third instars were in collection samples. Other dashed lines indicate sample hours when there were no *P. coeruleiviridis*. Time line bar below collection hours indicates collections at 1 PM (open portion of bar); 7 PM (stippled portion); 1 AM (black portion); 7 AM (cross-hatched portion). Numbers below time line bar indicate periods of precipitation as: 2, 4 and 3 mm of rainfall, respectively.

numbers, being replaced by *Phormia regina* as carcass decomposition progressed. Thus, a ''wave'' of *P. coeruleiviridis* passed through the sunlit and shaded carcasses from 84 to 132, and 84 to 120 h, respectively, in 2003 yielding dominance to *Phormia regina* after 132 and 120 h on those carcasses. Similarly, in 2004, *P. coeruleiviridis* third instars dominated the sunlit carcass from 54 to 90 h yielding dominance to *Phormia regina* from 96 h through the remainder of the experimental period at 174 h. Only on the 2004 shaded carcass was this early pattern suppressed, as third instars of both species were co-dominant from 60 to 102 h before *Phormia regina* assumed its typical pattern of dominance throughout the latter portion of the experimental period. Other investigators [26] graphed a pattern reminiscent to that of the present study with third instars of the tribe Luciliini appearing before those of the Phormiini on both exposed and shaded pig carcasses in Washington State.

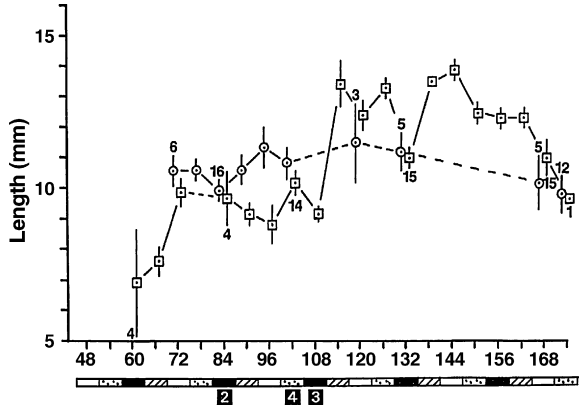

Fig. 14. Third instar lengths on the 2004 shaded carcass by hour of collection. Designations for means, confidence limits, numbers of instars in samples by species, and collection hours are the same as in Fig. 11. There were no *Phormia regina* third instars in the 78 h sample. Dashed lines beyond 102 h indicate sample hours where there were no *P. coeruleiviridis*. Time line bar below collection hours same as in Fig. 13.

Additionally, by the fourth day *Phormia regina* was the dominant (or only) species reared from all sites [12]; an observation similar to our 2004 experimental period where *Phormia regina* assumed the dominant role at 96 and 108 h on sunlit and shaded carcasses, respectively. Other workers, however, have stated that no difference in temporal occurrence was observed for arthropod taxa on pig carcasses in Hawaii [27].

Phormia regina has been characterized as a cool weather species [25,28,29], and this conformed to another finding [13] that *Phormia regina* was the dominant spring calliphorid species. Still, some surprise was expressed in finding that *Phormia regina* was co-dominant with *P. coeruleiviridis* in late-June to July when the mean temperature was as high as 24.5 °C (at an elevation of 608 m) [13]. Other workers [17,30] have verified that *Phormia regina* is common in June and July. Our observations support those of previous investigations since *Phormia regina* was clearly dominant in the latter portions of experimental periods when mean ambient temperatures varied from 20.4 to 25.1 °C at four different experimental plots.

Mean maggot mass temperatures (when third instars were present) were significantly higher than mean ambient temperatures at all four experimental plots; a finding that, with the possible exception of maggots colonizing small carcasses in the winter [31], is a universally reported phenomenon [11,13,16,17,32–34]. Maggot masses may not always exhibit stable temperatures [26] and, indeed, may be a function of ambient temperatures [35]. Our findings revealed that maggot mass temperatures on both 2003 and 2004 sunlit carcasses (Figs. 5 and 6) were positively (and significantly, i.e., $b \neq 0$) correlated with sunlit plot ambient temperatures, whereas there was no significant relationship (i.e., $b = 0$) between maggot mass and ambient temperature at shaded carcasses (Figs. 7 and 8).

Since accelerated development of larval carrion flies has been reported at higher temperatures in both laboratory [4,7,9] and field [11,14,21,26] experiments, the observation that larval development proceeded at a greater rate on both sunlit and shaded carcasses in 2004 when mean ambient temperatures were significantly higher than in 2003 (Table 1) was expected.

Accumulated degree hour (ADH) values calculated for the 2004 sunlit and shaded carcasses were lower for each instar than comparable ADH values for corresponding instars on the 2003 carcasses (Table 3). The difference was striking for *Phormia regina* third instars which were initially collected at 1075 ADH on the 2004 sunlit carcass (subjected to a higher mean ambient temperature), whereas third instars of this species did not appear until 1659 ADH on the sunlit 2003 carcass (Table 3). Lower accumulated degree days, or hours, associated with higher ambient temperatures is not a newly reported phenomenon since an accumulated degree day (ADD) value of 353.9 for *Phormia regina* (egg to adult) at 23.0 °C versus an ADD of 480.5 at 16.1 °C has been calculated [9]. Similarly, larval development (in terms of ADH) of *Protophormia terraenovae* was essentially the same at temperatures of 23–35 °C, but at 12.5 °C the ADH was ≈3.5 greater [36].

Thus, the relationship between ambient temperature and instar development may be linear over favorable temperature ranges, but becomes nonlinear in instances when temperature falls below a certain threshold level.

Present study variation in ADH values appears to be associated with the amplitude of ambient temperature fluctuations in 2003 vis-à-vis 2004. For example, from 0 to 84 h (the period required for the initial appearance of third instars in the 2003 sunlit carcass sample) there were three temperature readings >25 °C, but nine readings <20 °C; with four of those ≤15.5 °C (Fig. 1). In contrast, from 0 to 48 h (the period required for the initial appearance of *Phormia regina* third instars in the 2004 sunlit carcass sample) there were also three ambient temperature readings >25 °C, but only four readings <20 °C, the lowest being 18.4 °C (Fig. 3).

Growth/developmental rates depend upon biochemical reactions, and temperature limits may be imposed on growth through rate-limiting enzymatic reactions [37,38], and/or temperature sensitive endocrine mechanisms which result in modified concentrations of molting and juvenile hormones [38]. Thus, in 2003, minimum ambient temperatures appear to have approached the developmental minimum threshold which resulted in the continued accumulation of degree hours, but with apparent inactivation of control enzymes there was little corresponding larval growth/development. In modeling insect growth, a development curve for *Phormia regina* third instars demonstrated that rate of development was remarkably constant between 20 and 30 °C., whereas from 20 to 15 °C (and especially below 17 °C) the rate of third instar development slowed dramatically [10]. This appears to fit with our data suggesting that third instars, of both species, continued their development on 2004 carcasses (when minimum ambient temperatures seldom fell below 19 °C), whereas those instars exhibited a lower rate of development on 2003 carcasses subjected to minimum ambient temperature periods of <17 °C.

The effect of light on carrion fly larval development is seldom mentioned in the forensic literature, even though many phenomena known among insects (including, "... emergence and other ecdyses ...") appear sensitive to photoperiodic response [39]. Our data revealed that *P. coeruleiviridis* third instars were larger on sunlit than shaded carcasses in both 2003 (Figs. 11 and 12) and 2004 (Figs. 13 and 14). Since mean ambient temperatures between sunlit and shaded plots for 2003 (21.4 °C versus 20.4 °C) and 2004 (25.1 °C versus 23.7 °C) were not significantly different, sunlight may have influenced *P. coeruleiviridis* larval development. This is not an entirely unexpected outcome because maggots in open pasture are reported to be more advanced developmentally than those in wooded areas [14], with other workers observing that; "... increased temperature and/or direct sun on a corpse ..." catalyzed maggot growth [26]. In addition, significantly greater development of *Phormia regina* third instars on sunlit versus shaded raccoon carcasses has been documented; leading investigators [11] to conclude that, "... sunlight affected, in some synergistic manner, the development of *Phormia regina* larvae."

5. Conclusions

In this study we document increased rates of carcass decomposition in higher versus lower ambient temperatures, and for sunlit versus shaded carcasses. And, as universally recognized, maggot mass temperatures are significantly higher than ambient temperatures for carcasses in both sunlit and shaded settings. New findings include the lack of temporal overlap between *P. coeruleiviridis* and *Phormia regina* third instars colonizing carcasses, suggesting an evolutionary adaptation that reduces competition between these species for food and space resources. In addition, maggot mass temperatures, under certain circumstances (e.g., on sunlit carcasses), may be a function of ambient temperatures. We also corroborate the seldom reported phenomenon that ADH (or ADD) values decrease with corresponding increases in ambient temperatures, indicating that low ambient temperature thresholds reduce larval development rates appreciably. There appear to be two areas that need additional investigative attention to increase the accuracy of PMI estimates: (1) a more precise determination of low temperature development thresholds for various carrion fly species; (2) the effects of light (as intensity and photoperiod) on larval development.

Acknowledgments

We thank Carol Niekamp for procurement of pigs for use in our experiments, and Larry Lunsford, Head of the Huntington, WV Department of Sanitation, for his assistance in establishing and securing the experimental site. Our appreciation is also extended to Dan Evans for identifying plant species at our experimental site, James Amrine and Terri Stasney for their help in identifying adult and larval stages of *P. coeruleiviridis* and *Phormia regina*, and Daniel Blair for his assistance with computer graphics.

References

[1] R.D. Hall, Introduction: perceptions and status of forensic entomology, in: J.H. Byrd, J.L. Castner (Eds.), Forensic Entomology: The Utility of Arthropods in Legal Investigations, CRC, Boca Raton, FL, 2001, pp. 1–15.

[2] J.H. Byrd, J.L. Castner, Forensic Entomology: The Utility of Arthropods in Legal Investigations, CRC, Boca Raton, FL, 2001.

[3] L.M. Peairs, The relation of temperature to insect development, J. Econ. Entomol. 1 (1914) 174–181.

[4] A.S. Kamal, Comparative study of thirteen species of sarcosaprophagous Calliphoridae and Sarcophagidae (Diptera) I, Bionomics. Ann. Entomol. Soc. Am. 51 (1958) 261–270.

[5] I. Hanski, An interpolation model of assimilation by larvae of the blow fly, *Lucilia illustris* (Calliphoridae) in changing temperatures, Oikos 28 (1977) 187–195.

[6] R. Dallwitz, The influence of constant and fluctuating temperatures on development rate and survival of pupae of the Australian sheep blowfly *Lucilia cuprina*, Entomol. Expl. Appl. 36 (1984) 89–95.

[7] B. Greenberg, Flies as forensic indicators, J. Med. Entomol. 28 (1991) 565–577.

[8] J.H. Byrd, J.F. Butler, Effects of temperature on *Cochliomyia macellaria* (Diptera: Calliphoridae) development, J. Med. Entomol. 33 (1996) 901–905.

[9] G.S. Anderson, Minimum and maximum development rates of some forensically important Calliphoridae (Diptera), J. Forensic Sci. 45 (2000) 824–832.
[10] J.H. Byrd, J.C. Allen, Computer modeling of insect growth and its application to forensic entomology, in: J.H. Byrd, J.L. Castner (Eds.), Forensic Entomology: The Utility of Arthropods in Legal Investigations, CRC, Boca Raton, FL, 2001, pp. 303–329.
[11] J.E. Joy, M.L. Herrell, P.C. Rogers, Larval fly activity on sunlit versus shaded raccoon carrion in southwestern West Virginia with special reference to the black blowfly (Diptera: Calliphoridae), J. Med. Entomol. 39 (2002) 392–397.
[12] E.J. Watson, C.E. Carlton, Spring succession of necrophilous insects on wildlife carcasses in Louisiana, J. Med. Entomol. 40 (2003) 338–347.
[13] K.L. Tabor, C.C. Brewster, R.D. Fell, Analysis of the successional patterns of insects on carrion in Southwest Virginia, J. Med. Entomol. 41 (2004) 785–795.
[14] H.B. Reed Jr., A study of dog carcass communities in Tennessee, with special reference to the insects, Am. Midl. Nat. 59 (1958) 213–245.
[15] W.C. Rodriguez, W.M. Bass, Insect activity and its relationship to decay rates of human cadavers in east Tennessee, J. Forensic Sci. 28 (1983) 423–432.
[16] J.A. Payne, A summer carrion study of the baby pig *Sus scrofa* Linneaus, Ecology 46 (1965) 592–602.
[17] J.K. Tomberlin, P.H. Adler, Seasonal colonization and decomposition of rat carrion in water and on land in an open field in South Carolina, J. Med. Entomol. 35 (1998) 704–709.
[18] R.D. Hall, L.H. Townsend Jr., The blow flies of Virginia (Diptera: Calliphoridae). The insects of Virginia: no. 11, Res. Div. Bull. 123, Virginia Polytechnic Institute and State University, Blacksburg, VA, 1977.
[19] D.L. Baumgartner, Spring season survey of the urban blowflies (Diptera: Calliphoridae) of Chicago, Illinois, Gt. Lakes Entomol. 21 (1988) 119–121.
[20] D. Liu, B. Greenberg, Immature stages of some flies of forensic importance, Ann. Entomol. Soc. Am. 82 (1989) 80–93.
[21] F. Introna Jr., T.W. Suman, J.E. Smialek, Sarcosaprophagous fly activity in Maryland, J. Forensic Sci. 36 (1991) 238–243.
[22] R.D. Hall, K.E. Doisey, Length of time after death: effect on attraction and oviposition or larviposition of midsummer blow flies (Diptera: Calliphoridae) and flesh flies (Diptera: Sarcophagidae) of medicolegal importance in Missouri, Ann. Entomol. Soc. Am. 86 (1993) 589–593.
[23] W.D. Lord, E.P. Catts, D.A. Scarboro, D.B. Hadfield, The green blow fly, *Lucilia illustris* (Meigen), as an indicator of human postmortem interval: a case of homicide from Fort Lewis, Washington, Bull. Soc. Vector Ecol. 11 (1986) 271–275.
[24] W.D. Lord, R.W. Johnson, F. Johnson, The blue bottle fly, *Calliphora vicina* (=*Erythrocephala*) as an indicator of human postmortem interval: a case of homicide from suburban Washington, D.C., Bull. Soc. Vector Ecol. 11 (1986) 276–280.
[25] R.R. Sokal, F.J. Rohlf, Biometry: The Principles and Practice of Statistics in Biological Research, 3rd ed., W.H. Freeman and Company, New York, 1995.
[26] B.S. Shean, L. Messinger, M. Papworth, Observations of differential decomposition on sun exposed v. shaded pig carrion in coastal Washington State, J. Forensic Sci. 38 (1993) 938–949.
[27] K.A. Hewadikaram, M.L. Goff, Effect of carcass size on rate of decomposition and arthropod succession patterns, Am. J. Forensic Med. Pathol. 12 (1991) 235–240.
[28] D.G. Hall, The Blowflies of North America, The Thomas Say Foundation, Entomological Society of America, Lanham, MD, 1948.
[29] J.H. Byrd, J.L. Castner, Insects of forensic importance, in: J.H. Byrd, J.L. Castner (Eds.), Forensic Entomology: The Utility of Arthropods in Legal Investigations, CRC, Boca Raton, FL, 2001, pp. 43–79.
[30] M.D. Johnson, Seasonal and microseral variations in the insect populations on carrion, Am. Midl. Nat. 93 (1975) 79–90.
[31] C.C. Deonier, Carcass temperatures and their relation to winter blowfly populations and activity in the southwest, J. Econ. Entomol. 33 (1940) 166–170.
[32] J.R. Goodbrod, M.L. Goff, Effects of larval population density on rates of development and interactions between two species of *Chrysoma* (Diptera: Calliphoridae) in laboratory culture, J. Med. Entomol. 27 (1990) 338–343.
[33] E.N. Richards, M.L. Goff, Arthropod succession on exposed carrion in three contrasting tropical habitats on Hawaii Island, Hawaii, J. Med. Entomol. 34 (1997) 328–339.
[34] G.D. De Jong, J.W. Chadwick, Decomposition and arthropod succession on exposed rabbit carrion during summer at high altitudes in Colorado, USA, J. Med. Entomol. 36 (1999) 833–845.
[35] L.G. Higley, N.H. Haskell, Insect development and forensic entomology, in: J.H. Byrd, J.L. Castner (Eds.), Forensic Entomology: The Utility of Arthropods in Legal Investigations, CRC, Boca Raton, FL, 2001, pp. 287–302.
[36] B. Greenberg, T.I. Tantawi, Different developmental strategies in two boreal blow flies (Diptera: Calliphoridae), J. Med. Entomol. 30 (1993) 481–484.
[37] P.J.H. Sharpe, D.W. DeMichele, Reaction kinetics of poikilotherm development, J. Theor. Biol. 64 (1977) 649–670.
[38] H.T. Ratte, Temperature and insect development, in: K.H. Hoffman (Ed.), Environmental Physiology and Biochemistry of Insects, Springer, Berlin, 1984, pp. 33–66.
[39] S.D. Beck, Insect thermoperiodism, Ann. Rev. Entomol. 28 (1983) 91–108.

ELSEVIER

Forensic Science International 164 (2006) 193–200

Forensic Science International

www.elsevier.com/locate/forsciint

Species identification using sequences of the trnL intron and the trnL-trnF IGS of chloroplast genome among popular plants in Taiwan

Li-Chin Tsai [a,c], Yung-Chien Yu [b], Hsing-Mei Hsieh [c], Jenn-Che Wang [a], Adrian Linacre [d], James Chun-I Lee [e,*]

[a] *Department of Life Science, National Taiwan Normal University, 88 Ting-Chow Road, Sec. 4, Taipei 116, Taiwan, ROC*
[b] *Chang-Hua County Police Bureau, National Police Administration, 778, Sec. 2, Jhongjheng Road, Changhua, Changhua 500, Taiwan, ROC*
[c] *Department of Forensic Science, Central Police University, 56 Shu-Jen Road, Kwei-San, Taoyuan 33334, Taiwan, ROC*
[d] *Centre for Forensic Science, Department of Pure & Applied Chemistry, University of Strathclyde, Glasgow G1 1XW, United Kingdom*
[e] *Department of Forensic Medicine, College of Medicine, National Taiwan University, No.1 Jen Ai Road, Section 1, Taipei 100, Taiwan, ROC*

Received 8 December 2005; received in revised form 13 January 2006; accepted 13 January 2006
Available online 20 February 2006

Abstract

Forensic botanical comparison can be hampered by the lack of appropriate DNA databases. While DNA sequence databases for many mitochondrial loci have been established for the identification of animal species, less is known regarding the genomes of plants. We report on the use of the trnL intron and the trnL-trnF intergenic spacer (IGS) in the chloroplast genome and establish a DNA sequence database for plant species identification. The DNA sequences at these two loci from commonly encountered plants, including monocots and dicots, were aligned to establish a DNA database of local plants. The database comprises 373 individual sequences representing 80 families, 206 genera and 269 species. These plant species can be grouped to species level using both sequence and length polymorphisms at these loci. To validate the database for future forensic purposes, we sequenced 20 blind samples and searched the local database and the databases of GenBank and EMBL. Fifteen of these 20 samples used in blind trial testing matched their respective species from our local DNA database but only 6 matched species registered in the GenBank and EMBL databases. The sequences of two species used in the blind trial did not match any sequence registered in any of these databases. Cluster analysis was performed to demonstrate the family and genus distribution of samples. Neighbor-joining trees of the two DNA regions from 70 samples of the local database and 10 of the species used in the blind trials were constructed and clustered to both family and genus. The bootstrap values of the trnL intron were higher than most of those of the trnL-trnF IGS. The sequence database described in this study can be used to identify plant species using DNA sequences of the trnL intron and trnL-trnF IGS of chloroplast genome and illustrates its value in plant species identification.

Keywords: trnL intron; trnL-trnF IGS; Species identification; Plant DNA database; Cluster analysis

1. Introduction

Botanical evidence at crime scenes can be fragmentary, preventing accurate species identification of a plant based upon traditional morphological characteristics. This may therefore compromise the value of botanical evidence and lead to this type of evidence being ignored by many investigators. DNA technology has long been used in animal wildlife studies and in animal studies for forensic purposes with two main outcomes; species identification and identification of the individual organism. DNA profiling offers the same prospect with botanical samples. For many botanical species there is a limited knowledge of the genome and therefore whole genome screening methods such as DNA fingerprinting [1–4], RAPD [5–8] and AFLP [9,10] have been used. While these methods are adequate as a means of rapid screening, the problem of reproducibility, especially from degraded specimens, prevents their use in routine forensic investigations. More recently, the direct sequencing of specific loci has been the method of choice for plant species identification [11–19].

Previous phylogenetic relationships and botanical taxonomic studies among higher taxonomic level have used coding regions of polymorphic gene loci [20–24]. Since non-coding regions have faster rates of evolution, these loci have been used

* Corresponding author. Fax: +886 2 23218438.
E-mail address: jimlee@ntumc.org (J.-I. Lee).

0379-0738/$ – see front matter © 2006 Elsevier Ireland Ltd. All rights reserved.
doi:10.1016/j.forsciint.2006.01.007

as markers for phylogenetic, evolutionary and taxonomic study at lower taxonomic levels [11–19]. Among the non-coding regions, the intron of the trnL (UAA) and intergenic spacer (IGS) of the trnL-trnF (GAA) in the chloroplast genome are suitable for phylogenetic study from intra-species to inter-family level [13–19,25–30]. This feature provides an opportunity for species identification using these markers in forensic cases. The length of these regions is another advantage for forensic application as they are usually shorter than 700 bp for most of species examined to date and therefore they can be directly amplified and sequenced.

There are more than 4000 species of vascular plants in Taiwan which include more than 1000 species of native plants [31]. Although some of the sequences of the two loci of many common plants in Taiwan can be searched from DNA databases, such as the EMBL or GenBank DNA databases, most of the species are still unregistered. For forensic purposes, our laboratory has screened the sequences of the intron of the trnL and the trnL-trnF IGS in the chloroplast genome of plants found in Taiwan. DNA sequences of the two loci could be amplified and directly sequences from collected plants since there are multiple copies of chloroplasts and the primers used are based upon conserved DNA sequences.

2. Materials and methods

2.1. Sample collection

Leaf samples were collected from 373 individuals of 80 families, 206 genera and 269 species which usually grow in Taiwan and their species was confirmed by morphological identification. Within the study there were 32 species (8 families and 27 genera) of monocots and 237 species (72 families and 179 genera) of dicots. For 59 of the 269 tested species between 2 and 6 individual samples were analyzed to determine any intra-species variation. Another 20 samples were randomly collected from the northern Taiwan for blind testing.

2.2. DNA extraction

Approximately 10 mg of leaf samples was pulverized under liquid nitrogen in a mortar. The powder was transferred to a 1.5 ml microcentrifuge tube and DNA was extracted by the commercial kit (Plant Genomic DNA Miniprep System, Viogene, Taipei, Taiwan). The isolated DNA was quantified with 0.7% agarose gel electrophoresis and ultra-violet detection by spectrophotometer, and stored at −20 °C until used.

2.3. PCR amplification

The universal primers [18,19] for algae and land plants targeting exon regions were used to amplify the intron of the trnL and the trnL-trnF IGS. Both PCR amplifications were performed in separate tubes but under the same conditions. They were in a 50 μl volume containing 0.3 μM each of primers, reaction buffer (10 mM Tris–HCl, pH 8.3, 2.5 mM $MgCl_2$, 50 mM KCl, 0.1%, w/v, gelatin), 200 μM dNTP, 2.5 units of VioTaq DNA polymerase (Viogene) and 10 ng of genomic DNA. The amplifications were conducted in a 2400 Perkin-Elmer thermal cycler (Applied Biosystems) under the following conditions: denaturation at 94 °C for 1 min, annealing at 55 °C for 1 min and extension at 72 °C for 2 min for 35 cycles, and followed by a 7 min extension at 72 °C.

2.4. DNA sequencing

PCR products were checked on a 2% agarose gel electrophoresis and purified with the PCR-M™ Clean Up System (Viogene), and sequenced using both the forward and reverse primers in a PCR amplification and using the ABI PRISM™ BigDye™ Terminator Cycle Sequencing Ready Reaction Kit. The cycle sequencing products were analyzed with POP-7™ performance optimized polymer (Applied Biosystems) and detected by ABI 3730 DNA Analyzer.

2.5. Local DNA database establishment

The sequences of all the collected samples of the chloroplast trnL intron and trnL-trnF IGS were imported by the BioEdit software [32] for comparison purposes.

2.6. Blind testing

The sequences of 20 blind samples were compared with those of the local DNA database by the BLAST program of the BioEdit software, and the database of GenBank and EMBL by the FASTA program of the GCG computer package (Wisconsin Package, Version 10.2, Genetic Computer Group (GCG), Madison, WI, USA). Cluster analysis was performed in order to investigate the best fit of the blind samples in the local database. Sequences were aligned using the PileUp program of GCG computer package. The gap creation penalty and gap extension penalty were 5 and 1 for the two loci. The genetic distances were generated with Kimura's two-parameters, the cluster trees were constructed with neighbor-joining (using bootstrap tests with 1000 replications) and maximum-likelihood by the Phylip package. The programs of GCG and Phylip package are available from http://bioinfo.nhri.org.tw (National Health Research Institute, Taiwan).

3. Results and discussion

3.1. PCR amplification and sequencing

Species were chosen from those that cover a wide range of geographical regions from plain to middle elevation. The species included both monocots and dicots encompassing herbs to woody plants. In this study, 373 individuals (80 families, 206 genera and 269 species) were collected. Universal primers can be used to successfully amplify for all the plants tested and produced a distinct PCR product that could be visualized by agarose gel electrophoresis. All these PCR products were successfully sequenced using both primer sets.

Table 1
The size distributions of PCR products in different classifications

Classification	trnL intron (bp)	trnL-trnF IGS (bp)	Taxon composition	Percentage
All samples	354–942	206–756	80 families, 206 genera, 269 species	100
Monocots	467–942	343–501	8 families, 27 genera, 32 species	13
Dicots	354–703	206–756	72 families, 179 genera, 237 species	87

3.2. Sequence analysis of the DNA database in this study

All sequences of the trnL intron and the trnL-trnF IGS in this study were aligned with the programs of the GCG computer package. The size of PCR products was found to be highly diverse among these samples with the trnL intron found to be larger than that of the trnL-trnF IGS for almost all of the collected species. The size of the PCR products are widely distributed ranging from 354 bp to 942 bp for the trnL intron and from 206 bp to 756 bp for the trnL-trnF IGS among the samples collected. The PCR products of the trnL intron are between 500 bp and 700 bp in size approximately 94% of species tested and for the trnL-trnF IGS approximately 90% of the species exhibited between 300 bp and 500 bp in size. The size distribution of PCR products at the two loci among different classifications is shown in Table 1. The size variation

Table 2
The smallest and largest PCR products of the trnL intron and trnL-trnF IGS within the same family

Family	Species	trnL intron (bp)	trnL-trnF IGS (bp)	Family	Species	trnL intron (bp)	trnL-trnF IGS (bp)
Acanthaceae (4, 4)[a]	*Justicia procumbens*	555	285	Primulaceae (3, 7)	*Anagalis arvensis*	556	318
	Staurogyne concinnula		400		*Androsace umbellate*	587	428
	Hypoestes purpurea	589		Rubiaceae (8, 10)	*Paederia foetida*	355	
Asteraceae (23, 29)	*Galinsoga parviflora*	444			*Spermacoce latifolia*		470
	Conyza sumatrensis		452		*Ophiorrhiza pumila*		426
	Gnaphalium purpureum	527	387		*Geophila herbacea*	595	
Brassicaceae (4, 5)	*Cardamine impatiens*	574	630	Rutaceae (4, 4)	*Toddalia asiatica*	582	
	Cardamine flexuosa		472		*Zanthoxylum nitidum*		429
	Coronopus didymus	595			*Melicope semecarpifolia*	623	471
Caprifoliaceae (3, 3)	*Viburnum luzonicum*	577	459	Saxifragaceae (3, 3)	*Mitella formosana*	525	429
	Sambucus chinensis	604	437		*Hydrangea chinensis*	595	446
Caryophyllaceae (4, 6)	*Drymaria diandra*	618	300	Scrophulariaceae (6, 8)	*Mazus faurei*	568	418
	Silene fortunei Vis.		504		*Lindernia crustacea*	575	445
	Cerastium glomeratum	682		Solanaceae (2, 4)	*Solanum capsicoides*	572	
Campanulaceae (3, 3)	*Lobelia chinensis*	577	465		*Solanum capsicastrum*		482
	Peracarpa carnosa	593			*Tubocapsicum anomalum*	573	756
	Wahlenbergia marginata		396	Urticaceae (5, 10)	*Nanocnide japonica*	490	
Euphorbiaceae (6, 9)	*Aleurites Montana*	538	380		*Pilea peploides*		657
	Chamaesyce prostrata	703	520		*Boehmeria densiflora*		385
Fabaceae (8, 15)	*Kummerowia striata*	596			*Gonostegia hirta*	589	
	Bauhinia championii		506	Valerianaceae (2, 2)	*Valeriana flaccidissima*	571	420
	Trifolium repens	623	206		*Patrinia formosana*	588	441
Lamiaceae (7, 7)	*Clinopodium gracile*		364	Verbenaceae (4, 5)	*Duranta repens*	562	
	Salvia nipponica var. *formosana*	550			*Callicarpa formosana*		428
	Mosla dianthera	566	389		*Lantana camara*	570	408
Malvaceae (3, 3)	*Hibiscus taiwanensis*	624	478	Commelinaceae (3, 4)	*Amischotolype hispida*	869	405
	Urena lobata	675	472		*Rhopalephora scaberrima*	942	396
Moraceae (4, 10)	*Morus australis*	570	460	Cyperaceae (2, 4)	*Scleria terrestris*	467	456
	Humulus scandens		353		*Cyperus alternifolius* subsp. *flabelliformis*		407
	Broussonetia papyrifera	592			*Cyperus serotinus*	720	
Myrsinaceae (2, 4)	*Maesa perlaria* var. *formosana*	576	461	Liliaceae (3, 3)	*Tricyrtis formosana*	594	
	Ardisia brevicaulis	581	350		*Dianella ensifolia*		501
Oleaceae (3, 3)	*Chionanthus retusus*	549	421		*Ophiopogon intermedius*	603	436
	Osmanthus fragrans	550	437	Poaceae (15, 17)	*Alopecurus aequalis* var. *amurensis*	566	
Rosaceae (4, 6)	*Rubus alnifoliolatus*	570			*Centotheca lappacea*		463
	Duchesnea chrysantha	604	475		*Setaria palmifolia*		343
	Malus docmeri		485		*Eleusine indica*	630	

[a] Numbers of genus and species in this family respectively.

of PCR products in the trnL intron of the monocots is larger than that of dicots, however the variation of dicots is greater than monocots for the trnL-trnF IGS.

We randomly selected 27 families, each of which included more than two genera and these are shown in Table 2. The size of the PCR products of the two loci is illustrated and extreme lengths within the same family are indicated. These families showed high intra-family variation of the size of PCR products. For the trnL intron, the intra-family variation of PCR products is from only 1 bp (Slonaceae) to 253 bp (Cyperaceae) and from 6 bp (Malvaceae) to 300 bp (Fabaceae) for the trnL-trnF IGS. The intra-genus variation at the trnL intron is lower than 20 bp but for some genera at the trnL-trnF IGS the intra-genus variation can be nearly 180 bp in size (such as *Pilea* sp.). There were 59 species studied where greater than one sample was analysed to determine any intra-species variation. Little variation of intra-species was noted as for each species, with the exception of only a few, the samples produced similar sizes of PCR products. At the trnL intron of the 59 species, 44 exhibited no intra-species variation, 13 exhibited only 1 bp difference, one species exhibited a 2 bp difference and a further one species exhibited an 8 bp difference. At the trnL-trnF IGS locus for the same 59 species, 48 species showed no intra-species variation, 8 species showed a 1 bp difference, one species exhibited a 2 bp difference, one species exhibited a 4 bp difference and one species exhibited a significant 23 bp difference.

Comparison of the DNA sequences for the 269 species showed that they are unique with the exception of 5 pairs of species at the trnL-trnF IGS and with three of these five species pairs showing same sequences at the trnL intron. The three species pairs which produced the same sequences of trnL intron and trnL-trnF IGS loci are: *Ageratum conyzoides* and *Ageratum houstonianum*, *Ixeris chinensis* and *Ixeris debilis*, *Digitaria ciliaris* and *Digitaria setigera*. Two pairs of species produced the same sequences of trnL-trnF IGS loci but differ at the trnL intron: *Machilus thunbergii* and *Machilus zuihoensis*, *Ficus irisana* and *Ficus septica*. Among 59 species where more than one sample was analysed, intra-species variation of DNA sequences was observed in 20 of these species at the trnL intron and in 16 species at the trnL-trnF IGS. For comparison purpose, all sequences were compiled as a local DNA database using the BioEdit software.

3.3. Blind testing

In order to evaluate the probability that the trnL intron and the trnL-trnF IGS loci can be used to identify any sample to

Table 3
Search results of blind trial samples from the database in this study and in GenBank and EMBL

Blind samples	Search from the DNA database of this study			Fasta search from the database of GenBank and EMBL		
	Best similar sp. of trnL intron and trnL-F IGS	Similarity (%)		Best similar sp. of trnL intron and trnL-F IGS	Similarity (%)	
		trnL intron	trnL-F IGS		trnL intron	trnL-F IGS
Alstonia scholaris[a]	*Marsdenia formosana*	89.4	92.6	*Alstonia scholaris*	99.8	100.0
Ficus microcarpa	*Ficus microcarpa*	100.0	99.4	*Ficus benjamina*	100.0	99.7
Cassia surattensis[a]	*Chamaecrista mimosoides*	93.8	94.4	*Caesalpinia bonduc* (*Batesia floribunda*)[b]	96.6	92.3
Lantana camara	*Lantana camara*	99.8	100.0	*Lantana camara*	99.8	99.7
Duranta repens	*Duranta repens*	100.0	100.0	*Stachytarpheta dichotoma*	98.3	97.4
Pyracantha fortuneana[a]	*Malus docmeri*	99.5	98.1	*Pyracantha fortuneana*	100.0	100.0
Taraxacum officinale	*Taraxacum officinale*	100.0	100.0	*Taraxacum officinale*	100.0	100.0
Chionanthus retusus	*Chionanthus retusus*	100.0	100.0	*Chionanthus retusus*	100.0	100.0
Mallotus japonicus[a]	*Mallotus paniculatus*	99.7	97.0	*Humiria balsamifera* (*Acridocarpus austrocaledonicus*)[b]	87.2	70.4
Cinnamomum camphora[a]	*Machilus zuihoensis*	99.5	99.4	*Cinnamomum camphora*	100.0	100.0
Farfugium japonicum var. *formosanum*	*Farfugium japonicum* var. *formosanum*	100.0	100.0	*Farfugium japonicum*	99.7	97.9
Desmodium gracillimum[c]	*Desmodium gracillimum*	100.0	100.0	*Desmodium elegans* (*Glycine clandestina*)[b]	96.6	85.4
Salvia nipponica var. *formosana*[c]	*Salvia nipponica* var. *formosana*	100.0	100.0	*Salvia glutinosa*	99.5	100.0
Hibiscus taiwanensis[c]	*Hibiscus taiwanensis*	100.0	100.0	*Hibiscus macrophyllus* (*Hibiscus rosa-sinensis*)[b]	93.6	99.2
Pachycentria formosana[c]	*Pachycentria formosana*	100.0	100.0	*Adelobotrys boissieriana*	79.9	96.6
Damnacanthus angustifoliusc[c]	*Damnacanthus angustifolius*	100.0	100.0	*Morinda citrifolia* (*Dunnia sinensis*)[b]	94.2	94.6
Gonostegia matsuda[c]	*Gonostegia matsuda*	100.0	100.0	*Boehmeria calophleba*	94.1	93.7
Patrinia formosana[c]	*Patrinia formosana*	100.0	100.0	*Patrinia heterophylla*	99.5	99.7
Callicarpa pilosissima[c]	*Callicarpa pilossima*	100.0	100.0	*Callicarpa japonica* (*Callicarpa dichotoma*)[b]	99.8	99.7
Tricyrtis formosana[c]	*Tricyrtis formosana*	100.0	100.0	*Tricyrtis latifolia*	96.8	96.7

[a] Sequences of the species have not been collected in this study.
[b] Searching results of the best similar species of the sequences of trnL-trnF IGS.
[c] Species native to Taiwan.

species level, 20 samples were used to perform a blind trial. The sequences were compared with our local DNA database and the databases of GenBank and EMBL. The search results are shown in Table 3. Fifteen samples, nine of which are native to Taiwan, matched to a registered sequence on the local database with a homology of 99.4% or greater. However only six samples matched with a species registered with GenBank or EMBL, where the similarity for these species was 99.7%. It should be noted that none of these six species are native to Taiwan. The other five blind trial samples have not been added to this local DNA database, but three of them have already been registered in the GenBank and EMBL databases. The search results match their previous identification based upon the plant morphology with the results showing similarities of sequence greater than 99.8%. There were two species (*Cassia surattensis* and *Mallotus japonicus*) used in the blind trial testing that did

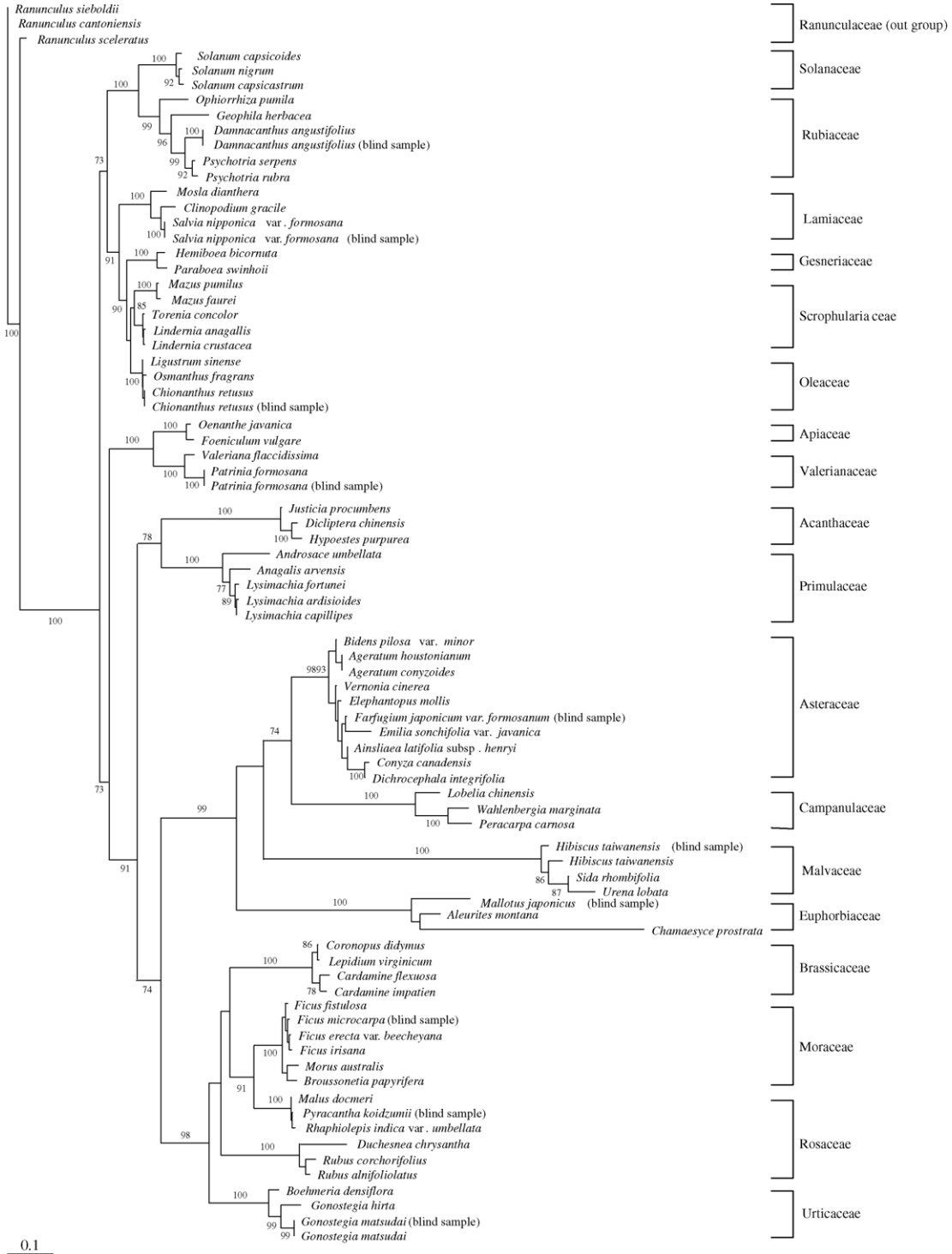

Fig. 1. Neighbor-joining tree of the trnL intron sequences from plant species used in this study. The bootstrap values at the nodes of the trees were obtained from 1000 replicates and shown in percentage.

not match any sequence registered previously in any of the databases. The results show that if the sequences of samples used in blind trial testing, or unknown samples, have already registered in the DNA database, near 100% homology should be obtained. This illustrates the need to expand the DNA database of plant for species identification.

3.4. Cluster analysis

To determine the genetic distance among different taxonomic levels of the two loci, we selected 70 species (19 families) from this database and 10 from the blind samples to perform cluster analysis. Three out-group species were selected

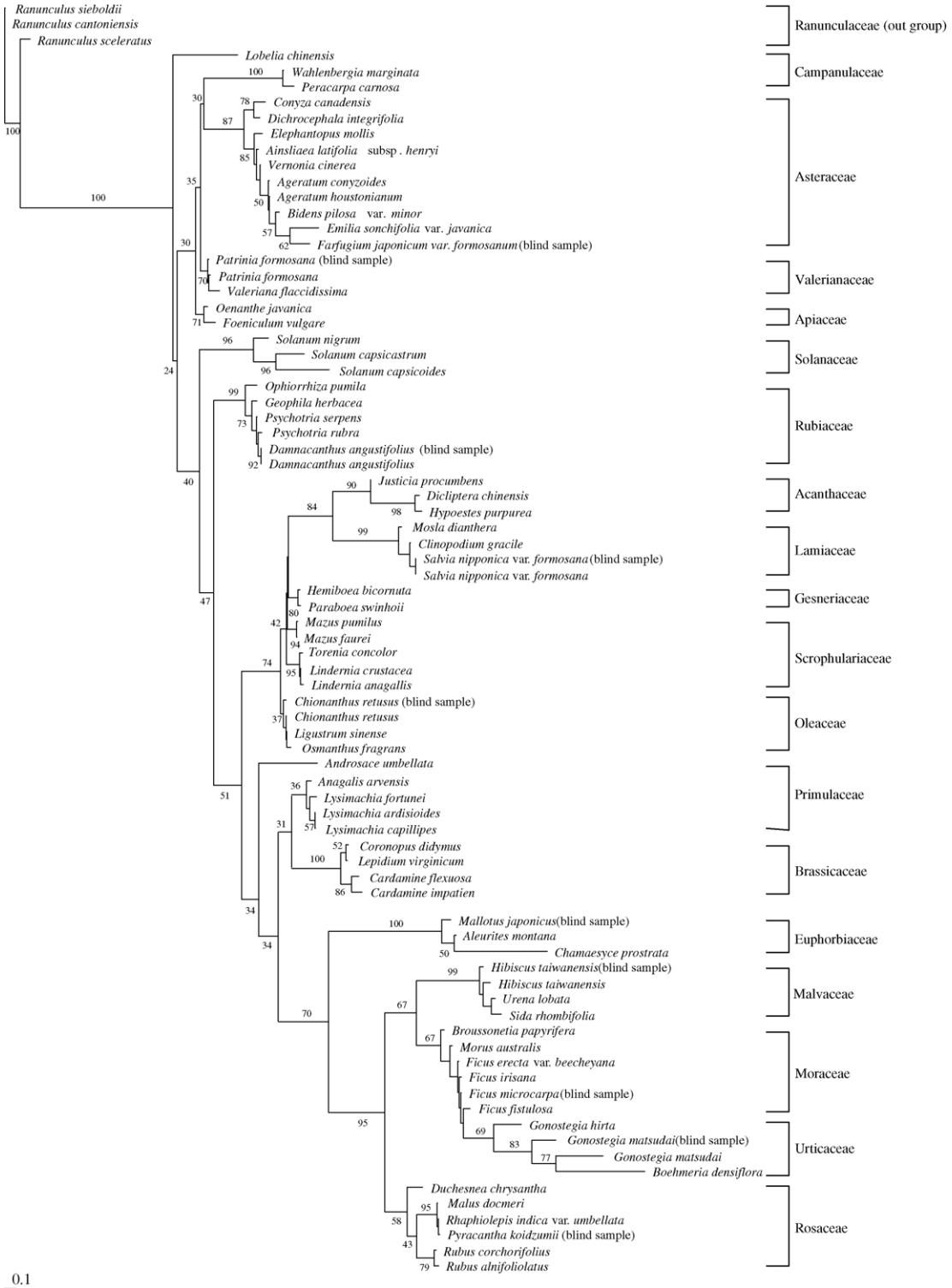

Fig. 2. Neighbor-joining tree of the trnL-trnF IGS sequences from plant species used in this study. The bootstrap values at the nodes of the trees were obtained from 1000 replicates and shown in percentage.

from the Ranunculaceae family and were chosen based on phylogenetic relationships of the angiosperm phylogeny group (APG) classification [33–36]. The size of PCR products at the trnL intron of selected samples (including blind trial samples) was between 355 bp and 549 bp and at the trnL-trnF IGS was between 203 bp and 548 bp. These selected samples are widely distributed in the Class of dicots and the lengths of these two loci show high diversity. It is difficult to determine the numbers of mutational steps due to insertions and deletions between different samples, therefore we have tried various conditions of gap creation penalty and gap extension penalty to establish the most likely alignments. Alignment of the selected samples at the trnL intron and the trnL-trnF IGS yielded the consensus sequences of 574 bp and 625 bp, respectively, with a gap creation penalty of 5 and gap extension penalty of 1. The cluster trees of the two DNA regions from the 80 samples were constructed by the methods of neighbor-joining and maximum-likelihood. The neighbor-joining trees at the two loci are shown in Figs. 1 and 2, and the cluster results are consistent with those of the maximum-likelihood (data not shown). Although the diversity of length at the two loci will be expected to affect the cluster result, the constructed trees show reasonable clusters in both family and genus among the selected samples and for those samples used in the blind trial testing. At the trnL intron all of the selected species are grouped into their respective families and genera and the bootstrap values for this locus are more than 800. The only exception was Rosaceae that was split into 2 groups. On the other hand, although most of the samples are grouped into their respective families and genera in the cluster tree of trnL-trnF IGS, most of the bootstrap values are lower than those of trnL intron. This is particularly the case for the families of Asteraceae, Valerianaceae, Apiaceae, Gesneriaceae, Oleaceae, Moraceae and Urtiaceae. The families of Campanulaceae, Scrophulariaceae and Primulaceae are split into 2 groups. These results indicate that the tree of the trnL intron is more reliable than the trnL-trnF IGS tree. These data are in line with the results of Taberlet et al. [18] and Fangan et al. [19] where these previous reports suggested that the sequences of the trnL intron in the plant kingdom are more conservative than those of the trnL-trnF IGS and could be more valuable for evolutionary studies at higher taxonomic levels.

4. Conclusion

Sequences of the trnL intron and the trnL-trnF IGS of chloroplast genome of 373 individuals from 80 families, 206 genera and 269 species of local popular plants were established. Pair-wise comparisons of the sequences indicated that there is no matching sequence among different families and genera. Samples can be identified to species level using these two loci. This was with the exception of three species pairs that produced the same sequence at the trnL intron and five species pairs at the trnL-trnF IGS. Using the new database blind trial tests produced more reliable results when compared to the databases of GenBank and EMBL, particularly for species native to Taiwan. The cluster analysis grouped the selected species and the species used in blind trials into their respective family and genus, with most of the bootstrap values of the trnL intron being higher than those of the trnL-trnF IGS. The species or genus of an unknown plant can be predicted using our plant DNA sequence database. This database therefore represents a valuable resource for forensic plant identification.

Acknowledgements

This study was supported in part by NSC 89-2420-H-015-005-QC, NSC 89-2420-H-003-005-QC, NSC 90-2420-H-015-001-QC, NSC 90-2420-H-003-001-QC, NSC 91-2420-H-015-001-QC, NSC 91-2420-H-003-001-QC from National Science Council and Department of Medical Research in NTUH, Taiwan, ROC.

References

[1] G. Caetano-Anolles, MAAP: a versatile and universal tool for genome analysis, Plant Mol. Biol. 25 (1994) 1011–1026.
[2] J.T. Epplen, H. Ammer, C. Epplen, C. Kammerbauer, R. Mitreiter, L. Roewer, W. Schwaiger, V. Steimle, H. Zischler, E. Albert, Oligonucleotide fingerprinting using simple repeat motifs: a convenient, ubiquitously applicable method to detect hypervariability for multiple purposes, EXS 58 (1991) 50–69.
[3] R.R. Prabhu, P.M. Gresshoff, Inheritance of polymorphic markers generated by DNA amplification fingerprinting and their use as genetic markers in soybean, Plant Mol. Biol. 26 (1994) 105–116.
[4] J.G.K. Williams, A.R. Kubelik, K.J. Livak, J.A. Rafalski, S.V. Tingey, DNA polymorphisms amplified by arbitrary primers are useful as genetic markers, Nucleic Acids Res. 18 (1990) 6531–6535.
[5] R. Gillan, M.D. Cole, A. Linacre, J.W. Thorpe, N.D. Watson, Comparison of *Cannabis sativa* by random amplification of polymorphic DNA (RAPD) and HPLC of cannabinoids: a preliminary study, Sci. Justice 35 (1995) 169–177.
[6] T. Demeke, R.P. Adams, R. Chibbar, Potential taxanomic use of random amplified polymorphic DNA (RAPD): a case study in *Brassica*, Theor. Appl. Genet. 84 (1992) 990–994.
[7] B. Koller, A. Lehmann, J.M. McDermott, C. Gessler, Identification of apple cultivars using RAPD markers, Theor. Appl. Genet. 85 (1993) 901–904.
[8] R.E. Veilleux, L.Y. Shen, M.M. Paz, Analysis of genetic composition of anther-derived potato by randomly amplified polymorphic DNA and simple sequence repeats, Genome 38 (1995) 1153–1162.
[9] P. Vos, R. Hogers, M. Bleeker, M. Reijans, T. Lee, M. Hornes, A. Frijters, J. Pot, J. Peleman, M. Kuiper, M. Zabeau, AFLP: a New Technique for DNA Fingerprinting, Nucleic Acids Res. 23 (1995) 4407–4414.
[10] H. Witsenboer, J. Vogel, R.W. Michelmore, Identification, genetic localization, and allelic diversity of selectively amplified microsatellite polymorphic loci in lettuce and wild relatives (*Lactuca* spp.), Genome 40 (1997) 923–936.
[11] B.G. Baldwin, S. Markos, Phylogenetic utility of the external transcribed spacer(ETS) of 18S-26S rDNA: congruence of ETS and ITS Trees of *Calycadenia* (Compositae), Mol. Phylogenet. Evol. 10 (1998) 449–463.
[12] G. Siniscalco Gigliano, Preliminary data on the usefulness of internal transcribed spacer I (ITS1) sequence in *Cannabis sativa* L. identification, J. Forensic Sci. 44 (1999) 475–477.
[13] M. Kojoma, K. Kurihara, K. Yamada, S. Sekita, M. Satake, O. Iida, Genetic identification of cinnamon (*Cinnamomum* spp.) based on the trnL-trnF chloroplast DNA, Planta Med. 68 (2002) 94–96.
[14] T. Yi, A.J. Miller, J. Wen, Phylogenetic and biogeographic diversification of Rhus (Anacardiaceae) in the Northern Hemisphere, Mol Phylogenet. Evol. 33 (2004) 861–879.
[15] S.D. Holt, L. Horova, P. Bures, Indel patterns of the plastid DNA trnL-trnF region within the genus Poa (Poaceae), J. Plant Res. 117 (2004) 393–407.

[16] T. Okaura, K. Harada, Phylogeographical structure revealed by chloroplast DNA variation in Japanese Beech (*Fagus crenata* Blume), Heridity 88 (2002) 332–339.
[17] A. Linacre, J. Thorpe, Detection of identification of cannabis by DNA, Forensic Sci. Int. 91 (1998) 71–76.
[18] P. Taberlet, L. Gielly, G. Pautou, J. Bouvet, Universal primers for amplification of three non-coding regions of chloroplast DNA, Plant Mol. Biol. 17 (1991) 1105–1109.
[19] B.M. Fangan, B. Stedje, O.E. Stabbetorp, E.S. Jnsen, K.S. Jakobsen, A general approach for PCR-amplification and sequencing of chloroplast DNA from crude vascular plant and algal tissue, Biotechniques 16 (1994) 484–494.
[20] M.T. Clegg, Chloroplast gene sequences and the study of plant evolution, Proc. Natl. Acad. Sci. U.S.A. 90 (1993) 363–367.
[21] H. Setoguchi, T.A. Osawa, J.C. Pintaud, T. Jaffre, J.M. Veillon, Phylogenetic relationships within Araucariaceae based on *rbcL* gene sequences, Am. J. Bot. 85 (1998) 1507–1516.
[22] R.J. Duff, D.L. Nickrent, Phylogenetic relationships of land plants using mitochondrial small-subunit rDNA sequences, Am. J. Bot. 86 (1999) 372–386.
[23] R. Hiesel, A.V. Haeseler, A. Brennicke, Plant mitochondrial nucleic acid sequences as a tool for phylogenetic analysis, Proc. Natl. Acad. Sci. U.S.A. 91 (1994) 634–638.
[24] D.L. Nickrent, R.J. Duff, D.A.M. Konings, Structural analyses of plstid-derived 16S rRNAs in holoparasitic angiosperms, Plant Mol. Biol. 34 (1997) 731–743.
[25] N. Fujii, K. Ueda, Y. Watano, T. Shimizu, Further analysis of intraspecific sequence variation of chloroplast DNA in *Primula cuneifolia* Ledeb. (Primulaceae): implications for biogeography of the Japanese alpine flora, J. Plant Res. 112 (1999) 87–95.
[26] R.G. Terry, R.S. Nowak, R.J. Tausch, Genetic variation in chloroplast and nuclear ribosomal DNA in Utah Juniper (*Juniperus osteosperma*, Cupressaceae): evidence for interspecific gene flow, Am. J. Bot. 87 (2000) 250–258.
[27] Y.W. Yang, P.Y. Tai, Y. Chen, W.H. Li, A study of the phylogeny of *Brassica rapa*, *B. nigra*, *Raphanus sativus*, and their related genera using noncoding regions of chloroplast DNA, Mol. Phylogenet. Evol. 23 (2002) 268–275.
[28] T. Fukuda, J. Yokoyama, H. Ohashi, Phylogeny and biogeography of the genus *Lycium* (Solanaceae): inferences from chloroplast DNA sequences, Mol. Phylogenet. Evol. 19 (2001) 246–258.
[29] E. Wallander, V.A. Albert, Phylogeny and classification of Oleaceae based on rps16 and trnL-F sequence data, Am. J. Bot. 87 (2000) 1827–1841.
[30] F.T. Bakker, A. Culham, R. Gomez-Martinez, J. Carvalho, J. Compton, R. Dawtrey, M. Gibby, Patterns of nucleotide substitution in angiosperm cpDNA trnL (UAA)- trnF (GAA) regions, Mol. Biol. Evol. 17 (2000) 1146–1155.
[31] Editorial Committee of the Flora of Taiwan, Flora of Taiwan, vols. 1–6, second ed., Department of Botany, National Taiwan University, Taipei, 1993–2003.
[32] T.A. Hall, BioEdit: a user-friendly biological sequence alignment editor and analysis. Program for Windows 95/98/NT, Nucl. Acids Symp. Ser. 41 (1999) 95–98.
[33] D.E. Soltis, P.S. Soltis, The role of phylogenetics in comparative genetics, Plant Physiol. 13 (2003) 1790–1800.
[34] K.W. Hilu, T. Borsch, K. Muller, D.E. Soltis, P.S. Soltis, V. Savolainen, M.W. Chase, M.P. Powell, L.A. Alice, R. Evans, H. Sauquet, C. Neinhuis, T.A.B. Slotta, J.G. Rohwer, C.S. Campbell, L.W. Chatrou, Angiosperm phylogeny based on *matK* sequence information, Am. J. Bot. 90 (2003) 1758–1776.
[35] The Angiosperm Phylogeny Group, An update of the Angiosperm Phylogeny Group classification for the orders and families of flowering plants: APG II, Bot. J. Linn. Soc. 141 (2003) 399–436.
[36] D.E. Soltis, P.S. Soltis, M.W. Chase, M.E. Mort, D.C. Albach, M. Zanis, V. Savolainen, W.H. Hahn, S.B. Hoot, M.F. Fay, M. Axtell, S.M. Swensen, L.M. Prince, W.J. Kress, K.C. Nixon, J.A. Farris, Angiosperm phylogeny inferred from 18S rDNA, rbcL, and atpB sequences, Bot. J. Linn. Soc. 133 (2000) 381–461.

ELSEVIER

Forensic Science International 164 (2006) 201–210

Forensic Science International

www.elsevier.com/locate/forsciint

Australian Federal Police seizures of illicit crystalline methamphetamine ('ice') 1998–2002: Impurity analysis

Ying Qi [a,b], Ian D. Evans [b], Adam McCluskey [a,*]

[a] *Chemistry Building, The University of Newcastle, University Drive, Callaghan, NSW 2308, Australia*
[b] *Australian Federal Police, 110 Goulburn Street, Sydney, NSW 2000, Australia*

Received 15 August 2005; received in revised form 21 January 2006; accepted 21 January 2006
Available online 20 March 2006

Abstract

Nineteen crystalline methamphetamine ('ice') seizures captured by the Australian Federal Police (AFP) at the Australian border between 1998 and 2002 were analysed. Using a modified gas chromatograph–mass spectrometry (GC–MS) impurity profiling approach of these samples we have identified >30 compounds associated with methamphetamine and/or its synthetic route. Major impurities detected include 1,2-dimethyl-3-phenylaziridine **8**, dimethylamphetamine **14**, *N*-formylmethamphetamine **24**, *N*-acetylmethamphetamine **25**, 1,3-dimethyl-2-phenylnaphthalene **32**, 1-benzyl-3-methylnaphthalene **33** and methamphetamine dimer **34**. These data are suggestive of ephedrine/pseudoephedrine as the main precursor of the 'ice' samples seized during 1998–2002. Additionally the two naphthalenes **32** and **33** further identified that 15 items in 9 seizures were produced via the more specific ephedrine/hydriodic acid/red phosphorus method.

One sample comprised 75% dimethylamphetamine and 9.7% methamphetamine, representing the first Australian seizure of imported dimethylamphetamine reported.

Keywords: Illicit drugs; Methamphetamine; 'Ice'; Impurity profiling; Gas chromatography–mass spectrometry

1. Introduction

The supply and abuse of illicit amphetamine-type stimulants (ATS) worldwide has increased considerably over the last few years, with methamphetamine accounting for almost 75% of seized ATS [1]. Impurities in illicit methamphetamine have been investigated and/or profiled by researchers around the world; detailed impurity information has been reported on the drugs seized in countries such as Norway [2], Japan [3], Thailand [4], the Philippines [5] and China [6], where methamphetamine abuse is one of the most serious drug issues.

A global survey indicated that Australia has the highest level of ecstasy abuse and ranks second after Thailand for methamphetamine abuse in 2001 [1]. Since 1997–1998, the detection of high purity crystalline methamphetamine ('ice') at the Australian border has dramatically increased from less than 1 kg in that year to over 233 kg in 2003–2004 [7].

Impurity profiling of the drug seizures, which characterises impurities associated with drug synthetic routes or handling and may provide information to help to identify relationship between drug seizures, drug sources and trafficking routes, therefore, has become an increasingly important aspect of criminal investigation. However, in the open literature there has been little information available on impurity characterisation or profiling of methamphetamine drug seizures in Australia, especially at the border level. Perkal et al. [8] profiled domestically manufactured methamphetamine seized in Vic., Australia, but did not mention any identities of the impurities.

As part of the Australian Illicit Drug Intelligence Program (AIDIP), this study of profiling crystalline methamphetamine ('ice') seized at the Australian border using gas chromatograph–mass spectrometry (GC–MS) – one of the most common profiling methods – aims to obtain impurity characteristics of the imported high purity methamphetamine drugs and to identify synthetic routes and the trend over recent years.

AFP Forensic Services provide physical guidance information of each seizure of illicit drugs at border level and the NMI provides chemical profiling information. Both the chemical and

* Corresponding author. Tel.: +61 249 216486; fax: +61 249 215472.
E-mail address: Adam.McCluskey@newcastle.edu.au (A. McCluskey).

0379-0738/$ – see front matter © 2006 Elsevier Ireland Ltd. All rights reserved.
doi:10.1016/j.forsciint.2006.01.010

physical profiles are combined onto a common database platform. The main objective of the program is to provide forensic intelligence product to the AFP intelligence group (and the partner agencies) via the Joint Drug Intelligence Team (JDIT).

2. Methods and materials

2.1. Sample preparation

Inoue et al.'s method [9] was utilised in this work. Thus, crystalline methamphetamine samples were ground and homogenised. A 50 mg portion of each sample was dissolved in 1 mL phosphate buffer solution (pH 10.5) (four parts of 0.1 M NaH_2PO_4 and 0.1 M Na_2HPO_4 mixture, pH 7, and one part of 10% sodium carbonate). Ethyl acetate spiked with four *n*-alkanes (C_{10}, C_{15}, C_{20} and C_{28}) as internal standards at 0.02 mg/L each was then added. The sample was thoroughly mixed by shaking on a vortex mixer for 5 min, followed by 5 min centrifuging at 3000 rpm. The upper organic layer was transferred to a 2 mL GC auto sampler vial for GC–MS analysis.

2.2. Reagents and chemicals

Buffer chemicals, sodium dihydrogen phosphate dihydrate ($NaH_2PO_4{\cdot}2H_2O$), disodium hydrogen phosphate dodecahydrate ($Na_2HPO_4{\cdot}12H_2O$) and sodium carbonate (Na_2CO_3), were analytical grade, sourced from BDH Ltd. (Australia). HPLC grade ethyl acetate solvent was sourced from Burdick & Jackson. Certified by-product samples for comparison purposes, *N*-acetylamphetamine, *N*-ethylamphetamine **13**, *N*,*N*-dimethylamphetamine **14**, *N*-formylamphetamine **22**, *N*-formylmethamphetamine **24** and 3,4-methylenedioxymethamphetamine (MDMA) were kindly supplied by the National Measurement Institute (NMI), Australia. Internal standards, *n*-alkanes (C_{10}, C_{15}, C_{20} and C_{28}), were kindly provided by Dr. H. Inoue, National Research Institute of Police Science, Japan.

2.3. GC–MS instrument and conditions

Analyses of the ethyl acetate extracts were carried out on an Agilent 6890N GC coupled with Agilent 5973 mass selective detector (MSD). Using an Agilent 7683 automatic liquid sampler, 1 μL sample was injected under splitless mode onto a DB-5, 30 m × 0.33 mm (i.d.) column with 1 μm film thickness. Helium flow was 2.0 mL/min; the inlet temperature was 250 °C. The following oven temperature program was used to run all the samples: initial temperature 50 °C held for 1 min; 10 °C/min to 300 °C; then the final temperature held for 10 min.

Analysis of each chromatogram was simplified using the Agilent Chemstation® data analysis, each peak was identified, where possible, using a combination of retention time; mass and abundance of the base peak (target ion); and one to three selected major ions.

3. Results

Nineteen seizures of crystalline methamphetamine from the Australian Federal Police (AFP) captured between 1998 and 2002 were analysed (note that the AFP are not involved in seizures within Australia). Typically the samples were off-white to white translucent crystals, or coarse powders. The seized methamphetamine was typically 77–84% pure. Within the 19 seizures there were a total of 73 discrete items, all of which were analysed as part of this work. The terms 'item' and 'sample' are used interchangeably in this work.

Table 1 lists the main impurities found, and their characteristic MS ions found as a result of GC–MS analysis. The identification numbers associated with the compounds correspond with the annotated peaks in Fig. 1.

Some compounds listed are not shown in the chromatograms in Fig. 1 since they are either not present or present only in trace quantities. The origins of some impurities given in Table 1 are not exclusive. As can be seen from Table 1, methamphetamine was found in high purity in all seizures excepting item 64 of Seizure XIX, which contains 75% dimethylamphetamine.

For most of the AFP 'ice' samples, the impurities listed in Table 1 account for >90% of the total impurity peak areas. Only in a small number of samples impurities that are not related to methamphetamine were detected. These include MDMA, cocaine, ketamine and dextromethorphan (DXM) and impurities often associated with these drugs such as 3,4-methylenedioxy-*N*-methylbenzylamine (MDB), *N*,*N*-dimethyl-3,4-methelenedioxyamphetamine and 1-[3,4-methylenedioxyphenyl]-2-propanol from MDMA and lidocaine, tropacocaine and ecgonidine methyl ester from cocaine. Common adulterants or contaminants including caffeine, aminopyrine and triprolidine were also present but only in a few samples at very low levels. It is probable that these impurities came from cross contamination during drug manufacturing or handling processes. The only exceptional case is item 20 of Seizure IX (Table 2; 67.5% methamphetamine), which contains large amount of dimethyl sulfone, **1**, which overloaded the GC column (Fig. 1(b)). Dimethyl sulfone is a common cutting agent in illicit methamphetamine [10]. We believe this is the first case of Australian 'ice' containing dimethyl sulfone reported.

In clandestine laboratory environments ATS's are synthesised mainly, but not exclusively, via reductive approaches: reductive amination, the Leuckart reaction and the ephedrine route [11,12]. In an attempt to identify the sources and manufacturing routes of the 'ice' seizures, 11 compounds (*cis*-/*trans*-1,2-dimethyl-3-phenylaziridine, **8a** and **8b**; benzyl methyl ketone (P2P), **9**; amphetamine, **10**; 1-phenyl-2-propanol, **11**; *N*,*N*-dimethylamphetamine, **14**; ephedrine/pseudoephedrine, **19**; *N*-formylmethamphetamine, **24**; *N*-acetylmethamphetamine, **25**; 1,3-dimethyl-2-phenylnaphthalene, **32**; 1-benzyl-3-methylamphetamine, **33**, and methamphetamine dimer, **34**) were selected mainly based on the information in the literature about their significance related to methamphetamine synthetic routes; their presence in the 'ice' samples analysed is summarised in Table 2.

Table 1
Impurities detected in Australian imported 'ice' samples

Compound no.	Name	Major ion	Origin	Compound no.	Name	Major ion	Origin
1	Dimethyl sulfone	79, 94	Adulterant for methamphetamine	**19**	Ephedrine/pseudoephedrine	58, 77, 105	Starting material (ephedrine route)
2	Benzaldehyde	106, 105, 77	By-product or methamphetamine pyrolysis product	**20a** and **20b**	3,4-Dimethyl-5-phenyloxazolidine (two isomers)	71, 56, 91	Ephedrine artefact [39]
3	Benzyl chloride	91, 126	Methamphetamine pyrolysis product	**21**	*N*-Methylephedrine	72, 105	By-product (ephedrine route)
4	2-Propenyl benzene	117, 118, 91	Methamphetamine decomposition or pyrolysis product [6,38]	**22**	*N*-Formylamphetamine	118, 72, 91	Intermediate in amphetamine (Leuckart route [2])
5	*N*,*N*-Dimethylbenzylamine	58, 135, 91	By-product	**23**	Bibenzyl	91, 182	Methamphetamine pyrolysis product
6	*N*-Methylbenzylamine	120, 121, 91	By-product	**24**	*N*-Formylmethamphetamine	86, 58, 118	Intermediate product (Leuckart route)
7	Benzyl alcohol	108, 79	Methamphetamine decomposition product	**25**	*N*-Acetylmethamphetamine	58, 100	By-product [40]
8a and **8b**	*cis*- and *trans*-1, 2-dimethyl-3-phenylaziridine	146, 105, 132	By-product (ephedrine route) [13]	**26a** and **26b**	Unidentified-4 (two isomers)	118, 147, 191	Unknown
9	Benzyl methyl ketone (1-phenyl-2-propanone, P2P)	43, 91, 134	Starting material (Leuckart and reductive amination routes); by-product (ephedrine route)	**27a** and **27b**	*cis*- and *trans*-3,4-dimethyl-5-phenyl-2-oxazolidone	57, 42, 191	By-product [4]
10	Amphetamine	44, 91, 120	Amphetamine contaminant or by-product	**28**	*N*-Formylephedrine	87, 86, 58	By-product (ephedrine route)
11	1-Phenyl-2-propanol	92, 91, 45	Intermediate (reductive amination route [28])	**29**	*N*-Acetylephedrine	58, 100	By-product
12	*N*-(1-Methyl-2-phenylethylidene) methenamine	56, 91, 147	Intermediate (reductive alkylation [25])	**30**	Benzylmethamphetamine	148, 91	By-product [25]
13	*N*-Ethylamphetamine	72, 44, 91	By-product	**31**	3,4-Dimethyl-2,5-diphenyl-oxazolidine	146, 147, 105	By-product
14	*N*,*N*-Dimethylamphetamine	72, 91	By-product	**32**	1,3-Dimethyl-2-phenylnaphthalene	232, 217, 108	By-product (ephedrine/hydriodic acid/red phosphorus route [13])
15	Unidentified-1	158, 56, 144	Unknown [15]	**33**	1-Benzyl-3-methylnaphthalene	232, 217, 108	By-product (ephedrine/hydriodic acid/red phosphorus route [13])
16a and **16b**	1-Phenylpropan-2-one oxime (*Z*- and *E*-isomers)	*Z*-91, 149, 116 *E*-91, 131, 116	By-product	**34**	Methamphetamine dimer (*N*1,*N*2 -dimethyl-*N*1-(1-methyl-2-phenylethyl) -1-phenyl-1,2-propanediamine)	238, 91, 120	By-product [4,15,24]
17	Unidentified-2	170, 68, 144	Unknown [15]	**35**	Unidentified-5	58, 208, 239	Unknown [4]
18	Unidentified-3	85, 148, 70	Unknown	**36**	Unidentified-6	105, 162, 77	Unknown

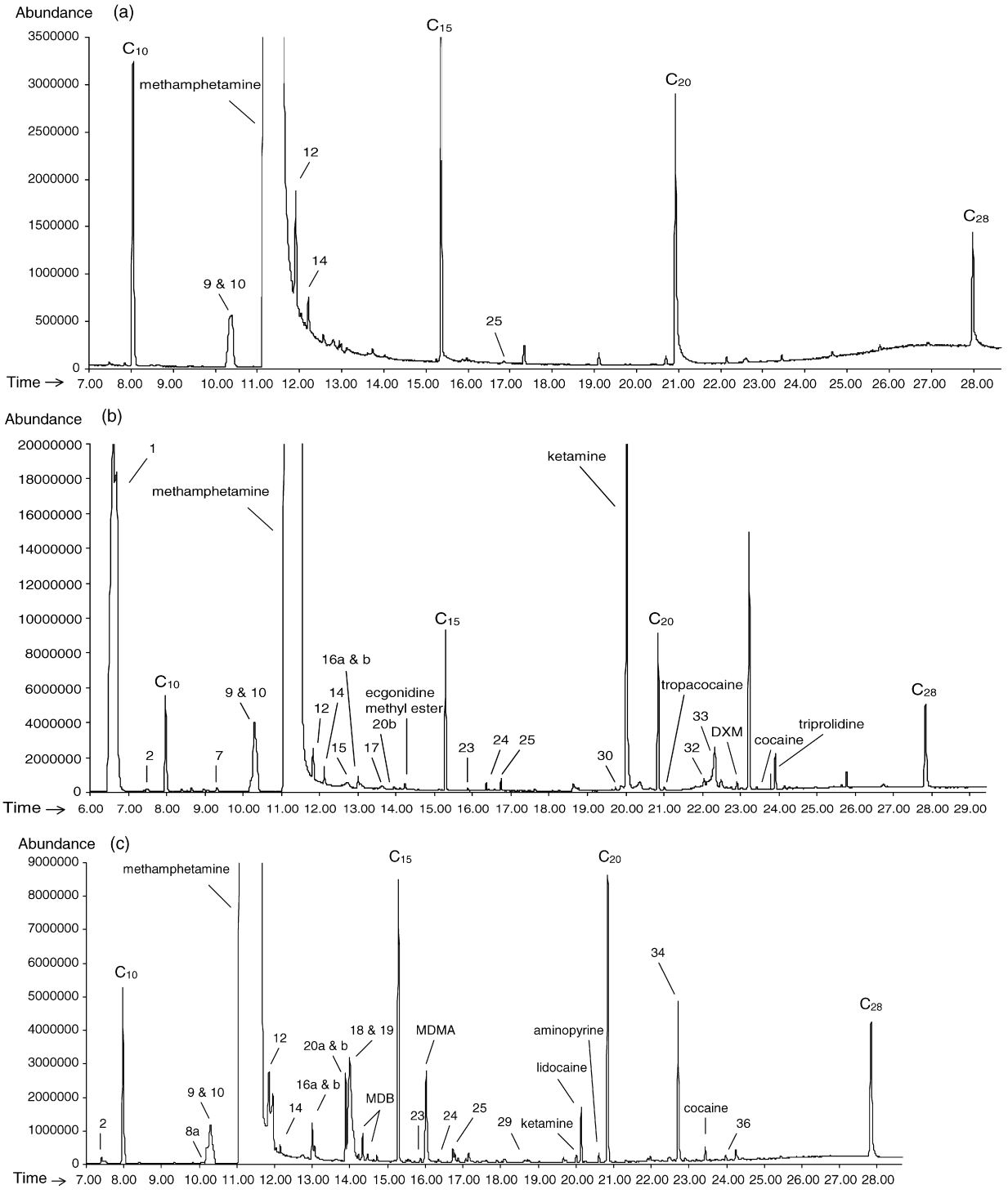

Fig. 1. Typical total ion chromatograms of crystalline methamphetamine samples: (a) Sample 4, methamphetamine 80.6%; (b) Sample 20, methamphetamine 67.5%; (c) Sample 50, methamphetamine 80.3%.

The results show that generally impurity profiles of methamphetamine samples in the same seizure show more similarities than that in different seizures, with some exceptions. Nevertheless, for samples from different seizures, the presence of impurities may also show similar characteristics. In terms of the impurity profiles of the 'ice' samples over the years no significant trend can be observed in the synthetic route used.

4. Discussion

The validity and use of GC and GC–MS methodologies for the analysis of methamphetamine drugs has been well covered in the literature with considerable method development and optimisation reported, viz. Inoue et al. [3], Tanaka et al. [13], Lambrechts et al. [14] and Dayrit and Dumlao [5] have all examined GC methodologies; Puthaviriyakorn et al. [4],

Table 2
Major impurities in Australian 'ice' samples

Year	Seizure no.	Sample no.	Methamphetamine purity (%)	**8**[a]	**9**[b] and **10**[c]	**11**[d]	**14**[e]	**19**[f]	**24**[g]	**25**[h]	**32**[i]	**33**[j]	**34**[k]
1998	I	1–3	82.2	√	√		√			√			√
	II	4–7	80.6–81.0		√	√	√			√			
	III	8	80.6	√	√		√		√	√			
	IV	9	82.4	√	√		√		√	√			
	V	10	79.8	√	√		√	√	√	√			√
	VI	11–13	80.2	√	√		√		√	√	√	√	
	VII	14–15	72.2	√	√		√	√[l]	√	√			
	VIII	16–19	78.8	√	√		√		√	√	√	√	
1999	IX	20	67.5		√		√		√	√	√	√	
	X	21	78.2	√	√	√	√	√	√	√	√	√	
	XI	22	79.4	√	√		√		√	√	√	√	
		23	81.0	√	√	√	√	√	√	√			√
		24	81.2	√	√	√	√		√	√	√	√	
	XII	25–27	80.9–81.0	√	√		√	√	√	√			
2000	XIII	28	78.0	√	√		√		√	√	√	√	√
	XIV	29	82.4	√	√	√	√		√	√	√	√	
		30	82.3	√	√		√		√	√			
		31–36	80.8–83.9	√	√	√	√		√	√			
	XV	37–38	81.7–83.5	√	√	√	√		√	√			
		39–43	81.1–82.9	√	√	√	√	√	√	√			
		44–45	81.1–81.4	√	√	√	√	√[l]	√	√			
2001	XVI	46	81.2	√	√	√	√		√	√			
		47–49	80.1–81.2	√	√	√	√			√			
	XVII	50	80.3	√	√		√	√	√	√	√	√	√
		51–54	79.9–81.1	√	√		√	√	√	√			√
	XVIII	55	77.7	√	√		√	√	√	√			√
		56–63	77.4–81.0	√	√	√	√	√	√	√			
2002	XIX	64	9.7		√		√[l]		√	√			
		65	81.5		√		√		√	√	√	√	
		66	80.3	√	√		√	√[l]	√	√			√
		67–73	79.2–80.7	√	√		√		√	√			√

[a] *cis*- and *trans*-1,2-dimethyl-3-phenylaziridine.
[b] Benzyl methyl ketone (P2P).
[c] Amphetamine.
[d] 1-Phenyl-2-propanol.
[e] *N*,*N*-Dimethylamphetamine.
[f] Ephedrine/pseudoephedrine (see text).
[g] *N*-Formylmethamphetamine.
[h] *N*-Acetylmethylamphetamine.
[i] 1,3-Dimethyl-2-phenylnaphthalene.
[j] 1-Benzyl-3-methylnaphthalene.
[k] Methamphetamine dimmer.
[l] Overloaded.

Koester et al. [15], Cantrell et al. [16] and Allen and Kiser [17] examined the use of MS approaches. Additionally, considerable sample preparation optimisation has been conducted by Tanaka et al. (choosing phosphate buffer pH 10.5 [18] and ethyl acetate extraction solvent [13] for the first time). Investigations into the most appropriate GC columns by Inoue et al. [9] (medium bore column) have led us to utilise a modified Inoue protocol [9]. In our hands we found that an increase in inlet temperature from 250 °C to 280 °C allowed for a significant increase in peak intensity of some early eluting peaks (notably methamphetamine thermal decomposition products, compounds **2**–**4**, **7** and **23** [19,20]) while not affecting the intensities of the remaining peaks (peaks **5** and **6** in Fig. 2). This is most probably a result in the increase in thermal decomposition of methamphetamine at the higher temperatures. Therefore, we chose 250 °C instead of 280 °C used by Inoue et al. [9] as the GC inlet temperature. Lower inlet temperatures were not chosen in order to accommodate low volatile compounds.

In all instances that we examined samples were completely dissolved in the phosphate buffer and the analytes were easily extracted using ethyl acetate as the extracting solvent.

4.1. Impurity identification

For impurities with certified standards available, identification was based on the match of both the retention time and mass spectrum of an unknown peak with that of the standard. Additional characterisation support was gained via library

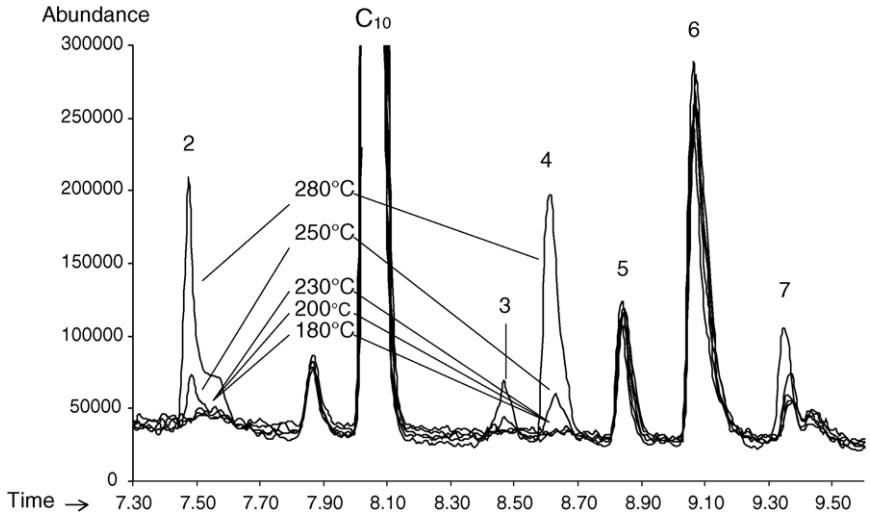

Fig. 2. Effect of GC inlet temperature on peak intensity of some volatile compounds.

spectrum matching. This approach allowed *N*-ethylamphetamine **13**, *N*,*N*-dimethylamphetamine **14**, *N*-formylamphetamine **22**, MDMA and *N*-formylmethamphetamine **24** to be identified in the seized samples. It is also confirmed that none of the samples contain *N*-acetylamphetamine.

Other impurities were identified via comparison with known literature reports. Thus, the mass spectrum and retention time associated with **12** are consistent with data reported by Zhang et al. [6] and Skinner [21] and assigned to *N*-(1-methyl-2-phenylethylidiene)methenamine. Compound **20** correlates well with 3,4-dimethyl-5-phenyloxazolidine, synthesised by Lewis et al. [22] using pseudoephedrine and formaldehyde. The oxazolidine, **20**, appeared in most of the AFP samples as two diastereomeric compounds, which co-eluted with ephedrine as also observed by Lewis et al. [22] and the UNDCP [23]. Using extracted ion chromatograms the two peaks of the oxazolidine isomers (m/z = 71, 56 and 91) could be explicitly distinguished from the ephedrine peak (m/z = 58, 77 and 105).

We observe **27** as a peak pair, with identical spectra, located between the peaks of *N*-acetylmethamphetamine **25** and *N*-formylephedrine **28**. The spectra match very well with that of a single peak appearing at a similar position in chromatograms of methamphetamine tablets (Ya Ba) and crystal identified by Puthaviriyakorn et al. [4] as *trans*-3,4-dimethyl-5-phenyl-2-oxazolidone via synthesis of an authentic sample. The researchers also reported the synthesis of both *cis*- and *trans*-3,4-dimethyl-5-phenyl-2-oxazolidone from ephedrine and pseudoephedrine, respectively, noting that both isomers have identical spectra.

Compounds **32** and **33** are assigned as 1,3-dimethyl-2-phenylnaphthalene and 1-benzyl-3-methylnaphthalene, respectively, with their spectra identical to those reported by Cantrell et al. [16] and Skinner [24]. Additionally, the two peaks with very similar spectra always appear simultaneously with a smaller peak of compound **32** in front of a much larger peak of compound **33** and thus easy to be identified even at very low levels.

Both the spectra of methamphetamine dimer [4,23] and *N*-methyl-*N*-(α-methylphenethyl)amino-1-phenyl-2-propanone [23,25] give similar spectra to **34** with abundant ions at m/z 238, 120 and 91. However, the spectrum of **34** shows more similarities to that of the dimer, lacking the distinct 190, 133 and 105 ions found in the propanone. Thus, **34** is assigned as the methamphetamine dimer.

Despite using the methods mentioned above, a number of impurities could not be identified, the most commonly occurring and significant, **15**, **17**, **18**, **26**, **35** and **36**, are listed in Table 1. Puthaviriyakorn et al. [4] found an impurity in Ya Ba tablets with identical spectrum as compound **35**, no identity was provided and this compound remains unidentified. Analysis of retention times and MS fragmentation patterns strongly suggest that **15** and **17** (m/z = 158, 144, 56 and 170, 144, 56, respectively) are identical to two unidentified impurities observed by Koester et al. [15] in methamphetamine samples. In this study the two impurities are present simultaneously in most cases. Ion 144 is a common mass fragment of indoles. Their wide peak shapes in chromatograms observed in this work may imply polar characteristics in the structure.

Exhaustive literature searching and spectral analysis failed to identify compounds associated with peaks **18**, **26** and **36** (Fig. 3). No evidence of similar spectra was found associated with impurities in methamphetamine or any other common illicit drugs. Interestingly compound **26** always appears as a double peak suggesting the presence of non-resolved stereoisomers.

4.2. Route identification

The 11 compounds chosen to be listed in Table 2 are expected to provide important information to help with the identification of synthetic routes of the AFP 'ice' samples.

Phenyl-2-propanone (P2P), **9**, and ephedrine/pseudoephedrine, **19**, are two most common starting materials for synthesising methamphetamine. While the presence of ephedrine/pseudoephedrine may indicate a synthetic route via ephedrine, P2P is a non-specific marker for both reductive amination and the Leuckart reaction since it is also a by-product

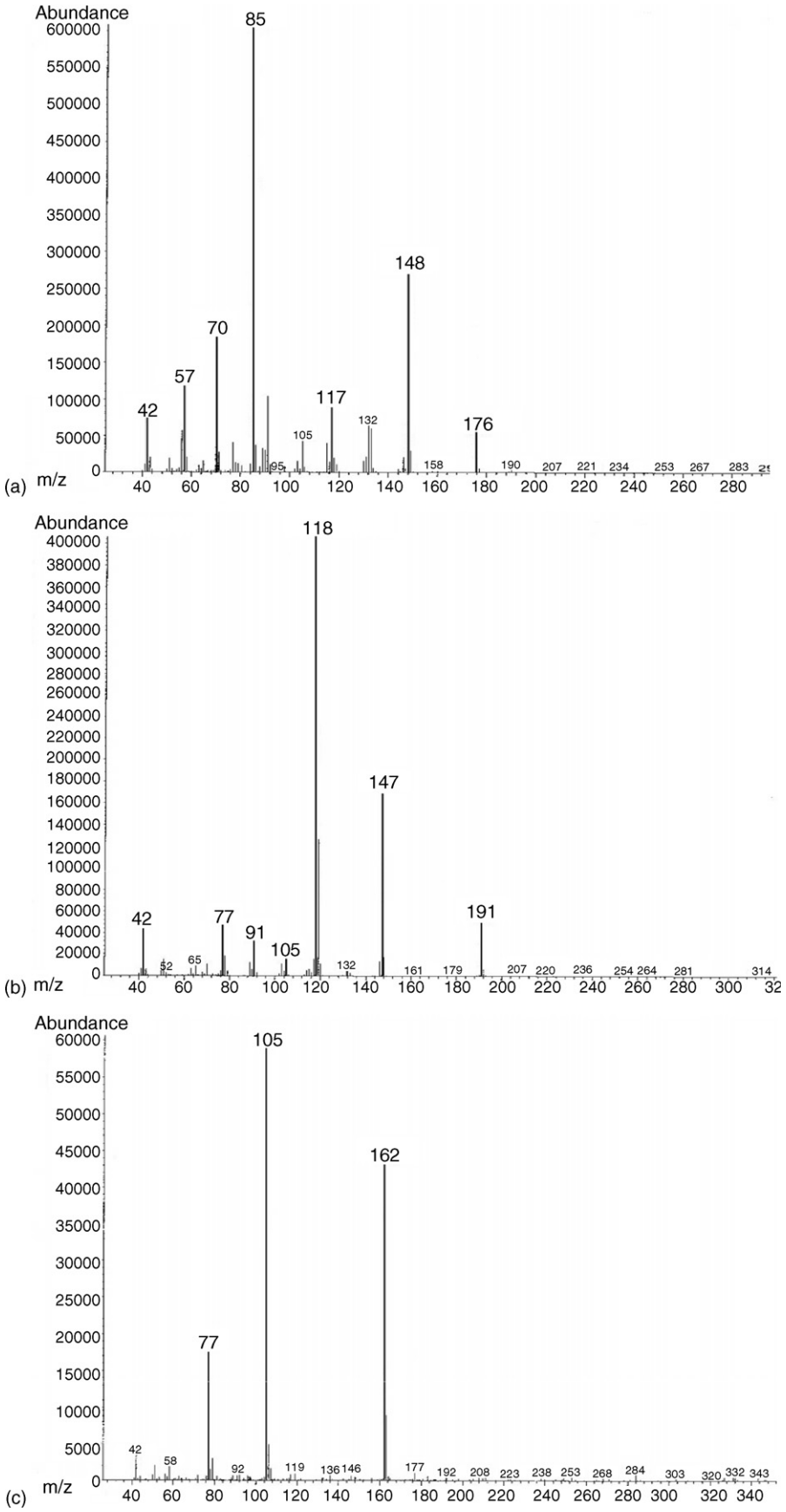

Fig. 3. Mass spectra of unknown impurities: (a) compound **18**; (b) compounds **26a** and **26b**; (c) compound **36**.

of the ephedrine route [16]. Evidentially P2P **9** has been found in methamphetamine synthesised from ephedrine [24,25]. In this study all samples contained P2P **9**, which is identified using extracted ion chromatograms although its peak is irresolvable from the much larger peak of amphetamine **10**. Ephedrine/pseudoephedrine **19** appeared in 30 samples of 9 seizures, which presumably indicates an ephedrine origin of these samples. The peak **19** in five of the samples was considerably (10–1000-fold) larger than other impurities noted, overloading the column. This is in keeping with the UNDCP methamphetamine profiling guide [23].

Route specific impurities or markers are the compounds that are only present in drugs synthesised via a certain route. *cis*- and *trans*-1,2-dimethyl-3-phenylaziridines **8** can be considered marker compounds as their formation during methamphetamine synthesis is specifically related to ephedrine/pseudoephedrine. It is proposed that during the synthetic reaction the intermediate haloephedrine (iodoephedrine or chloroephedrine) undergoes a ring closure to produce both the *cis* and *trans* aziridines [16,17,24]. However, the aziridines may not always be present in methamphetamine even though ephedrine is the precursor, as shown in the work by Windahl et al. [25]. As proposed by Cantrell et al. [16], under the acidic condition of the ephedrine/hydriodic acid/red phosphorus reaction, the aziridines may go through a ring opening process producing P2P intermediates; two P2P molecules then undergo self-condensation followed by dehydration to form 1-benzyl-3-methylnaphthalene **32** and 1,3-dimethyl-2-phenylnaphthalene **33** [13]. Since the P2P intermediate does not occur under non-acidic conditions, as found in the ephedrine route via chloroephedrine [17], the two naphthalenes are considered specific of the ephedrine/hydriodic acid/red phosphorus route.

Table 2 shows the presence of aziridines **8a** and/or **8b**, at trace levels in some instances, in 66 of the 73 AFP samples, an indication of ephedrine/pseudoephedrine synthetic origin. Additional support for this route in the majority of the samples analysed is in the detection of 1-benzyl-3-methylnaphthalene **32** and 1,3-dimethyl-2-phenylnaphthalene **33** in 15 of the samples, including 2 in which **8** was not detected (Table 2, Samples 20 and 65). Thus, it is highly probable that the 15 samples containing **32** and **33** were produced via the ephedrine/hydriodic acid/red phosphorous route.

Methamphetamine dimer **34** is another impurity that has been reported present in ephedrine synthesised methamphetamine. Tanaka et al. [18] assumed a production route of the dimer via condensation of 1,2-dimethyl-3-phenylaziridine and methamphetamine and successfully synthesised the dimer from the two compounds. In the present work, the presence of the dimer **34** in 20 samples in which the aziridines were also present confirms an ephedrine route of the drugs.

Methamphetamine synthesised from ephedra using hydriodic acid and red phosphorous typically contains two marker compounds: D-amphetamine (D-**10**) and D-*N*,*N*-dimethylamphetamine (D-**14**) [26]. Notwithstanding this, both **10** and **14** have been found in illicit methamphetamine from various synthetic routes including reductive amination [27], the Leuckart reaction [28] and the ephedrine/hydriodic acid/red phosphorus route [24], ephedrine/lithium–ammonia reduction [29]. According to Kram and Kruegel [28], **10** and **14** in Leuckart synthesised methamphetamine may come from the contamination of methylamine or methylformamide starting material by ammonia or dimethylformamide, respectively. It is also proposed that the two compounds in methamphetamine produced via the ephedrine or ephedra route are reduction products of norephedrine and methylephedrine, respectively, in the starting materials [26,29]. In this study both **10** and **14** were found in all the samples. We were unable to resolve any stereoisomers that may have been present; consequently, these two compounds are not indicative of any specific synthetic routes.

The inclusion of *N*-formylmethamphetamine **24** and *N*-acetylmethamphetamine **25** in Table 2 is based on that, firstly, compound **24** was considered by Kram and Kruegel [28] as the only impurity characteristic of the Leuckart route and, secondly, in the present study the two compounds were found always present simultaneously in the samples with the latter appeared as a larger peak. Results showed that **24** was present in most of the samples of ephedrine origin, which is indicated by the presence of the aziridines **8** and/or the naphthalenes **32** and **33**. Both compounds **24** and **25** were found by Puthaviriyakorn et al. [4] in Ya Ba tablets, which are well known to be produced from ephedrine. Therefore, **24** should not, in isolation, be considered a specific marker of Leuckart origin. Further investigation about the origin of this compound in ephedrine-derived methamphetamine is necessary. In addition, considering compounds **24** and **25** are often present simultaneously in the samples, it is unclear whether the formyl group in compound **24** undergoes methylation to form *N*-acetylmethamphetamine **25** during the process.

In a comprehensive methamphetamine impurity listing produced by Verweij [30], 1-phenyl-2-propanol **11** is the only compound from the reductive amination route that is not present in methamphetamine from other routes. In the present work, **11** was found in 35 samples, among which 31 are presumably from the ephedrine route due to the presence of the aziridines **8** and/or the naphthalenes **32** and **33**. It is possible that the occurrence of the propanol is due to the reduction of 1-phenylpropan-2-one oxime **16** [31], which was detected in most of the samples. In addition, considering that P2P is a common precursor for the propanol **11** under reductive conditions [32,33], it is not impossible that under suitable conditions compound **11** can be found in methamphetamine drugs where P2P is present.

To summarise, from the impurities detected and shown in Table 2 we have been unable to identify the synthetic origins of five samples: four samples from Seizure II and Sample 64 from Seizure XIX. All other samples contain evidence consistent with production via ephedrine. This is consistent with expectations for illicit methamphetamine trafficked to Australia mainly from the Southeast Asia region [34] where ephedrine is a major source of illicit methamphetamine production [35].

It is noteworthy that Sample 64 (Table 2, Seizure XIX) contains only 9.7% methamphetamine, but 75% dimethylamphetamine. Similar cases in which crystalline substances

suspected to be methamphetamine were found to be dimethylamphetamine have been reported in recent years in Japan [36,37] and Malaysia [38]. It is possible that these drugs were manufactured intentionally as suggested by Chan et al. [38], since dimethylamphetamine is not a controlled substance in some countries. This is the first case reported of dimethylamphetamine imported to Australia.

5. Conclusions

GC–MS characterisation of recent 'ice' seizures at the Australian border enabled a comprehensive evaluation of drug impurities. The method proved to be simple and efficient capable of dealing with samples with high-level methamphetamine and low level impurities. Information about the impurities in methamphetamine allowed identification of the drug synthetic routes. However, in some cases for the high purity methamphetamine, this information alone is insufficient to indicate any specific clandestine manufacturing routes. We are actively pursuing the identities of the unknown impurities via synthetic approaches and will report the outcomes of our efforts in due course.

One seized sample comprised 75% dimethylamphetamine, and 9.7% methamphetamine. This is the first recorded case of dimethylamphetamine importation into Australia.

Acknowledgements

This project was funded through the Australian Illicit Drug Intelligence Program (AIDIP) which is managed by the Australian Federal Police. We also thank Dr. Michael Collins (NMI) for useful discussions and Mr. Bruce Nelson (AFP) for his assistance in drug sample access.

References

[1] UNODC, Ecstasy and Amphetamines: Global Survey 2003, United Nations Office on Drugs and Crime, New York, 2003, United Nations Publication Sales No. E.03.XI.15.
[2] M. Lambrechts, K.E. Rasmussen, Leuckart-specific impurities in amphetamine and methamphetamine seized in Norway, Bull. Narcotics 36 (1984) 47–57.
[3] T. Inoue, K. Tanaka, T. Ohmori, Y. Togawa, S. Seta, Impurity profiling analysis of methamphetamine seized in Japan, Forensic Sci. Int. 69 (1994) 97–102.
[4] V. Puthaviriyakorn, N. Siriviriyasomboon, J. Phorachata, W. Pan-ox, T. Sasaki, K. Tanaka, Identification of impurities and statistical classification of methamphetamine tablets (Ya–Ba) seized in Thailand, Forensic Sci. Int. 126 (2002) 105–113.
[5] F.M. Dayrit, M.C. Dumlao, Impurity profiling of methamphetamine hydrochloride drugs seized in the Philippines, Forensic Sci. Int. 144 (2004) 29–36.
[6] Y. Zhang, H. Chen, X. Yu, Analysis of methamphetamine and its impurities by gas chromatography/mass spectrometry, Fenxi Huaxue 26 (1998) 1464–1467 (in Chinese).
[7] R. Rushby, 'Ice' cool detections by Australian Customs, UNODC Eastern Horizons 17 (2004) 6.
[8] M. Perkal, Y.L. Ng, J.R. Pearson, Impurity profiling of methylamphetamine in Australia and the development of a national drugs database, Forensic Sci. Int. 69 (1994) 77–87.
[9] H. Inoue, T. Kanamori, T. Iwata Yuko, Y. Ohmae, K. Tsujikawa, S. Saitoh, T. Kishi, Methamphetamine impurity profiling using a 0.32 mm i.d. nonpolar capillary column, Forensic Sci. Int. 135 (2003) 42–47.
[10] D.-T.T. Vu, SPME/GC–MS characterization of volatiles associated with methamphetamine: toward the development of a pseudomethamphetamine training material, J. Forensic Sci. 46 (2001) 1014–1024.
[11] A. Allen, T.S. Cantrell, Synthetic reductions in clandestine amphetamine and methamphetamine laboratories: a review, Forensic Sci. Int. 42 (1989) 183–199.
[12] W.H. Soine, Clandestine drug synthesis, Med. Res. Rev. 6 (1986) 41–74.
[13] K. Tanaka, T. Ohmori, T. Inoue, S. Seta, Impurity profiling analysis of illicit methamphetamine by capillary gas chromatography, J. Forensic Sci. 39 (1994) 500–511.
[14] M. Lambrechts, T. Klemetsrud, K.E. Rasmussen, H.J. Storesund, Analysis of Leuckart-specific impurities in amphetamine and methamphetamine, J. Chromatogr. 284 (1984) 499–502.
[15] C.J. Koester, B.D. Andresen, P.M. Grant, Optimum methamphetamine profiling with sample preparation by solid-phase microextraction, J. Forensic Sci. 47 (2002) 1002–1007.
[16] T.S. Cantrell, B. John, L. Johnson, A.C. Allen, A study of impurities found in methamphetamine synthesized from ephedrine, Forensic Sci. Int. 39 (1988) 39–53.
[17] A.C. Allen, W.O. Kiser, Methamphetamine from ephedrine: I. Chloroephedrines and aziridines, J. Forensic Sci. 32 (1987) 953–962.
[18] K. Tanaka, T. Ohmori, T. Inoue, Analysis of impurities in illicit methamphetamine, Forensic Sci. Int. 56 (1992) 157–165.
[19] M.-R. Lee, J. Jeng, W.-S. Hsiang, B.-H. Hwang, Determination of pyrolysis products of smoked methamphetamine mixed with tobacco by tandem mass spectrometry, J. Anal. Toxicol. 23 (1999) 41–45.
[20] M. Sato, K. Ito, H. Nagase, A smoking case in which dimethylamphetamine as a pyrolysis product of methamphetamine (MA) was detected in the urine of MA abuser, J. Health Sci. 50 (2004) 389–395.
[21] H.F. Skinner, Methamphetamine synthesis via reductive alkylation hydrogenolysis of phenyl-2-propanone with *N*-benzylmethylamine, Forensic Sci. Int. 60 (1993) 155–162.
[22] R.J. Lewis, E.F. Huffine, A.K. Chaturvedi, D.V. Canfield, J. Mattson, Formation of an interfering substance, 3,4-dimethyl-5-phenyl-1,3-oxazolidine, during a pseudoephedrine urinalysis, J. Forensic Sci. 45 (2000) 898–901.
[23] UNDCP, A Practical Guide to Methamphetamine Characterization/Impurity Profiling: Method Procedures, Mass Spectral Data of Selected Impurities, and Literature References: Scientific Section, Division for Operations and Analysis, United Nations International Drug Control Programme, 2000, Scientific and Technical Notes, SCITEC/17.
[24] H.F. Skinner, Methamphetamine synthesis via hydriodic acid/red phosphorus reduction of ephedrine, Forensic Sci. Int. 48 (1990) 123–134.
[25] K.L. Windahl, M.J. McTigue, J.R. Pearson, S.J. Pratt, J.E. Rowe, E.M. Sear, Investigation of the impurities found in methamphetamine synthesized from pseudoephedrine by reduction with hydriodic acid and red phosphorus, Forensic Sci. Int. 76 (1995) 97–114.
[26] K.M. Andrews, Ephedra's role as a precursor in the clandestine manufacture of methamphetamine, J. Forensic Sci. 40 (1995) 551–560.
[27] A.M. Van der Ark, A.B.E. Theeuwen, A.M.A. Verweij, Contamination in illegal amphetamine. 6. Identification of 2-phenylpropanol, amphetamine and *N*,*N*′-dimethylamphetamine in methamphetamine, Arch. Kriminol. 162 (1978) 171–175.
[28] T.C. Kram, A.V. Kruegel, The identification of impurities in illicit methamphetamine exhibits by gas chromatography/mass spectrometry and nuclear magnetic resonance spectroscopy, J. Forensic Sci. 22 (1977) 40–52.
[29] R.A. Ely, D.C. McGrath, Lithium–ammonia reduction of ephedrine to methamphetamine: an unusual clandestine synthesis, J. Forensic Sci. 35 (1990) 720–723.
[30] A.M.A. Verweij, Impurities in illicit drug preparations: amphetamine and methamphetamine, Forensic Sci. Rev. 1 (1989) 1–11.
[31] H.B. Hucker, B.M. Michniewicz, R.E. Rhodes, Phenylacetone oxime. Intermediate in the oxidative deamination of amphetamine, Biochem. Pharm. 20 (1971) 2123–2128.

[32] F. Kazemi, A.R. Kiasat, Reduction of carbonyl compounds to the corresponding alcohols with isopropanol on dehydrated alumina under microwave irradiation, Synth. Commun. 32 (2002) 2255–2260.
[33] A. Janusz, K.P. Kirkbride, T.L. Scott, R. Naidu, M.V. Perkins, M. Megharaj, Microbial degradation of illicit drugs, their precursors, and manufacturing by-products: implications for clandestine drug laboratory investigation and environmental assessment, Forensic Sci. Int. 134 (2003) 62–71.
[34] R. McKetin, The methamphetamine market in Australia, Centrelines 11 (2003) 2–4.
[35] K. Kulsudjarit, Drug problem in southeast and southwest Asia, Ann. N. Y. Acad. Sci. 1025 (2004) 446–457.
[36] M. Katagi, M. Tatsuno, A. Miki, M. Nishikawa, H. Tsuchihashi, Discrimination of dimethylamphetamine and methamphetamine use: simultaneous determination of dimethylamphetamine-N-oxide and other metabolites in urine by high-performance liquid chromatography–electrospray ionization mass spectrometry, J. Anal. Toxicol. 24 (2000) 354–358.
[37] M. Katagi, H. Tsuchihashi, Update on clandestine amphetamines and their analogues recently seen in Japan, J. Health Sci. 48 (2002) 14–21.
[38] K.B. Chan, Y.K. Chong, M. Nazarudin, The identification of D-*N*,*N*-dimethylamphetamine (DMA) in an exhibit in Malaysia, Microgram 1 (2003) 163–168.
[39] S.M.R. Wille, W.E.E. Lambert, Phenmetrazine or ephedrine? Fooled by library search, J. Chromatogr., A 1045 (2004) 259–262.
[40] C. Conn, M. Dawson, A.T. Baker, J. Keegan, B. Fryirs, Identification of *N*-acetylmethamphetamine in a sample of illicitly synthesized methamphetamine, J. Forensic Sci. 41 (1996) 645–647.

ELSEVIER

Forensic Science International 164 (2006) 211–220

Forensic Science International

www.elsevier.com/locate/forsciint

Quantitative characterization of morphological polymorphism of handwritten characters loops

R. Marquis [a,*], F. Taroni [a], S. Bozza [b], M. Schmittbuhl [c]

[a] *Institut de Police Scientifique, School of Criminal Sciences, BCH, University of Lausanne, CH-1015 Lausanne-Dorigny, Switzerland*

[b] *Team Research EA 3428, Dental Faculty, F-67085 Strasbourg, France*

[c] *Department of Statistics, University Ca' Foscari of Venice, San Giobbe, Cannaregio 873, I-30121 Venezia, Italy*

Received 23 May 2005; accepted 1 February 2006
Available online 9 March 2006

Abstract

A methodology based on Fourier descriptors that was previously validated has been applied to 13 writers in order to quantify the polymorphism degree of the shape of the loops of the handwritten characters *a*, *d*, *o* and *q*. In a first step, the discriminating power of the parameters extracted from these letters was investigated. The loop of the letter *d* appeared to be the most discriminant with a correct classification rate of 82.4%, whereas the least discriminant one was the loop of the letter *o* (69.7%). The second aim of the study was to extract grouping characteristics which make it possible to discriminate between writer sets, whatever the letter. Trends in the writing of loops could effectively be shown: the 13 writers of the study were separated into five main groups according to the shape and surface of their loops. The most discriminating features between the writer groups were the importance of the loops elongation and the surface of the loops. Finally, the differences between writers belonging to distinct groups could be characterized more precisely, and differences between writers belonging to the same group were revealed; the individual writings were distinguished by the variability of the parameters of shape and surface of their loops and the morphological distances between its different letters. The correct classification rates reached in this study suggest that carrying out an expertise of fragmentary samples of handwriting comprising only some loops is completely possible.

Keywords: Handwriting; Polymorphism; Shape analysis; Fourier descriptors

1. Introduction

Handwriting examination consists in describing handwriting features, such as elements of style or elements of execution, and studying their range of variation in order to individualize a particular writer through comparison. Characterization of these writing habits as well as the evaluation of the extent of their variability is essentially subjective. Few studies on Roman handwriting were concerned with this lack of objectivity and suggested solutions to provide an objective and quantitative description of writing habits from a forensic point of view. The feature vectors obtained from handwriting documents in previous studies were related to global (based on the handwriting image) [1–4], local (based on zones of interest of the handwriting image, such as lines, words or allographs) [5–12] or both [13,14] aspects of handwriting, but they did not reflect precise visual aspects of handwriting. These studies were merely focused on the development of techniques providing the most accurate identification rates possible, rather than the precise description of handwriting features as they are observed by examiners during the comparison process of handwriting samples.

In a first paper [15], a methodology based on Fourier descriptors was developed, validated and used to precisely characterize and objectively express the within-variability and the between-variability of the parameters of the shape of the loops of handwritten characters *o* in a population of three writers. This procedure was completely new, since the variability of the shape of loops had hitherto been described only in a subjective or partial way [8].

In this further part of the study, the developed methodology has been applied on a larger population of writers to quantify the morphological polymorphism of the loops of the

* Corresponding author. Tel.: +41 21 692 46 00; fax: +41 21 692 46 05.
E-mail address: raymond.marquis@unil.ch (R. Marquis).

0379-0738/$ – see front matter © 2006 Elsevier Ireland Ltd. All rights reserved.
doi:10.1016/j.forsciint.2006.02.008

handwritten characters *a*, *d*, *o* and *q*. Three main steps were accomplished to describe this polymorphism:

- the discriminating power of the parameters of shape and surface of the loops of the letters *a*, *d*, *o* and *q* was investigated and compared;
- then, the similarity of the loops shape between the writers was evaluated, in order to extract grouping characteristics which make it possible to discriminate between writer sets, whatever the letter;
- finally, the distinctive characteristics of each writing could be described according to the morphological distances between its different letters and the variability of their loops shape and surface parameters.

2. Materials and methods

2.1. Sampling

Approximately 100 individuals of the *Institut de Police Scientifique*, University of Lausanne, filled out five documents, where each document had to be written on a different day. On each one of these documents, they had to write 10 times a series of alphabet letters, in their usual way. Paper (standard blank paper of format A4) and pen (ball point pen Bic® Cristal™ with blue color ink) were provided to each participant. Among the collected samples, only the 13 writers showing closed loops for their characters *a*, *d*, *o* and *q* were retained. The total number of observations was 2325 (591 *a* loops, 547 *d* loops, 596 *o* loops and 591 *q* loops).

2.2. Image analysis procedure/size normalization/Fourier analysis

The extraction of the skeletons of the handwritten loops, as well as the size normalization of these skeletons and the Fourier analysis of their shape, were carried out according to the methodology described in detail in reference [15]. In addition, before normalizing the size of the loops, the surface enclosed in the loops was automatically calculated for each character by means of the Visilog 6.0® software.

2.3. Statistical analysis

S-plus® 2000 (Mathsoft Inc.) and SPSS® 12.0 (SPSS Inc.) were used to analyse the numerical data obtained.

Table 1
Surface and Fourier analysis of the handwritten loops *a* of the writers W1–W13: summary statistics[a] of the surface and the first four pairs of Fourier amplitudes (A_1–A_4) and phases (θ_1–θ_4)[b]

Writer	Statistics	Surface	A_1	A_2	A_3	A_4	θ_1	θ_2	θ_3	θ_4
W1	*X*	0.065	0.06	1.18	0.25	0.25	337.86	64.51	93.38	70.41
	S.D.	0.012	0.01	0.33	0.12	0.12	29.40	11.82	20.02	14.91
W2	*X*	0.072	0.07	0.43	0.23	0.11	337.38	57.51	93.87	72.63
	S.D.	0.012	0.01	0.23	0.12	0.06	25.03	24.14	22.64	17.81
W3	*X*	0.049	0.06	0.57	0.33	0.21	280.07	34.87	73.96	49.12
	S.D.	0.010	0.03	0.30	0.17	0.08	92.56	35.65	19.23	19.04
W4	*X*	0.058	0.11	1.16	0.31	0.27	350.13	66.85	124.56	73.30
	S.D.	0.018	0.04	0.50	0.14	0.18	45.75	24.07	11.18	20.32
W5	*X*	0.037	0.06	2.02	0.18	0.56	308.59	43.18	128.77	44.68
	S.D.	0.006	0.02	0.27	0.08	0.15	78.71	5.86	13.96	5.66
W6	*X*	0.031	0.13	1.92	0.23	0.46	365.94	51.53	115.93	53.33
	S.D.	0.008	0.05	0.41	0.10	0.18	30.28	7.90	14.03	10.84
W7	*X*	0.025	0.13	1.99	0.21	0.51	341.72	51.90	117.78	53.28
	S.D.	0.007	0.05	0.28	0.08	0.13	18.37	6.56	12.51	8.33
W8	*X*	0.028	0.10	1.93	0.21	0.56	358.56	56.45	123.93	57.91
	S.D.	0.005	0.05	0.23	0.10	0.13	37.15	5.92	15.50	5.83
W9	*X*	0.049	0.05	0.55	0.29	0.17	291.06	67.73	76.47	55.49
	S.D.	0.007	0.02	0.23	0.11	0.07	72.84	20.55	13.95	11.26
W10	*X*	0.147	0.08	1.08	0.21	0.20	339.80	83.50	100.65	80.11
	S.D.	0.054	0.03	0.32	0.08	0.09	35.88	8.23	13.83	8.12
W11	*X*	0.078	0.08	0.98	0.19	0.13	351.69	29.29	77.63	38.88
	S.D.	0.021	0.02	0.23	0.08	0.08	33.93	11.30	11.85	21.79
W12	*X*	0.025	0.19	1.70	0.38	0.50	340.52	70.08	97.05	66.98
	S.D.	0.005	0.05	0.26	0.19	0.10	22.81	6.53	9.83	4.75
W13	*X*	0.016	0.14	1.40	0.22	0.28	339.94	72.00	124.35	75.87
	S.D.	0.004	0.04	0.30	0.09	0.11	18.18	8.37	17.78	8.85

[a] *X*, mean; S.D, standard deviation.
[b] Surface is given in cm^2 and phases are given in degrees.

For each writer and for each letter, the mean and the standard deviation were calculated for the surface and for each pair of Fourier descriptors. All the analyses described below were performed on the surface and the pairs of Fourier descriptors of the contours.

To compare the discriminating power of the four letters *a*, *d*, *o* and *q*, four quadratic discriminant analyses were performed on the 13 writers. The estimation of the discriminating power was given by the rates of correct classification within the observations retained for validation, which represented 20% of the overall data.

Then, a quadratic discriminant analysis was applied on the 13 writers considering the four letters simultaneously. In order to estimate the between-writers variability, Mahalanobis distances between each pair of writers – a writer being characterized by his set of *a*, *d*, *o* and *q* loops – were calculated. Then, the Hotelling's *T* squared test was used to test differences in means between each possible pair of writers.

Finally, a quadratic discriminant analysis was separately applied on each writer considering the four letters simultaneously. Mahalanobis distances were calculated between each pair of letter sets for each writer. Euclidean distances were calculated between pairs of observations within each letter set for each writer; the within-writer variability was estimated through the mean and the standard deviation of these distances.

3. Results

The statistics of the Fourier descriptors (amplitudes and phases) of the handwritten characters *a*, *d*, *o* and *q* contours of each writer are summarised in Tables 1–4. Only the first four pairs of Fourier descriptors were retained, since the global shape of each character contour was practically reconstructed on the basis of these four Fourier harmonics, and because from the fifth harmonic, for the majority of the writers, the phase values were randomly distributed and were not specific of the writing shape of the characters loops.

3.1. Discriminating power of the shape of handwritten characters loops

An attempt to discriminate between the 13 writers of the study was conducted in applying a discriminant analysis on the data of each one of the letters *a*, *d*, *o* and *q*. The corresponding correct classification rates calculated with the observations retained for validation were 74.8%, 82.4%, 69.7% and 81.4%,

Table 2
Surface and Fourier analysis of the handwritten loops *d* of the writers W1–W13: summary statistics[a] of the surface and the first four pairs of Fourier amplitudes (A_1–A_4) and phases (θ_1–θ_4)[b]

Writer	Statistics	Surface	A_1	A_2	A_3	A_4	θ_1	θ_2	θ_3	θ_4
W1	*X*	0.055	0.12	1.03	0.24	0.22	339.35	62.33	97.81	67.92
	S.D.	0.012	0.05	0.40	0.10	0.13	27.36	11.71	18.51	17.03
W2	*X*	0.064	0.06	0.33	0.34	0.12	370.05	122.05	106.00	80.33
	S.D.	0.013	0.02	0.20	0.14	0.06	50.13	48.26	10.07	13.78
W3	*X*	0.038	0.10	0.77	0.16	0.17	308.66	18.13	59.52	31.41
	S.D.	0.010	0.03	0.30	0.11	0.09	27.57	18.96	41.22	28.93
W4	*X*	0.052	0.11	1.47	0.35	0.25	365.69	66.06	133.31	71.90
	S.D.	0.013	0.05	0.39	0.13	0.14	39.65	10.65	8.42	17.35
W5	*X*	0.040	0.06	1.90	0.31	0.46	345.52	45.89	131.34	45.66
	S.D.	0.007	0.03	0.24	0.08	0.14	64.77	4.62	5.95	4.89
W6	*X*	0.026	0.09	1.84	0.26	0.39	339.99	42.61	123.04	42.10
	S.D.	0.007	0.05	0.42	0.09	0.20	56.62	5.78	10.36	10.04
W7	*X*	0.017	0.13	2.27	0.29	0.62	314.75	49.85	129.76	49.27
	S.D.	0.005	0.07	0.34	0.09	0.19	22.17	4.17	13.25	5.29
W8	*X*	0.021	0.10	2.12	0.33	0.48	360.47	55.13	135.51	55.53
	S.D.	0.004	0.06	0.29	0.09	0.16	55.43	3.94	7.24	6.01
W9	*X*	0.059	0.07	0.49	0.15	0.11	301.35	49.42	62.72	48.04
	S.D.	0.007	0.02	0.18	0.08	0.06	30.51	18.78	29.53	22.70
W10	*X*	0.117	0.05	0.63	0.25	0.12	374.46	64.46	90.84	62.99
	S.D.	0.034	0.03	0.28	0.11	0.07	62.56	19.01	14.06	17.74
W11	*X*	0.071	0.08	1.76	0.20	0.45	400.00	−3.78	77.40	84.22
	S.D.	0.021	0.04	0.35	0.08	0.16	64.50	15.60	20.42	15.74
W12	*X*	0.025	0.12	1.21	0.36	0.18	343.00	63.50	130.98	77.55
	S.D.	0.004	0.05	0.32	0.12	0.09	39.43	6.67	13.25	15.34
W13	*X*	0.013	0.11	1.62	0.31	0.27	303.66	64.97	142.36	71.93
	S.D.	0.004	0.06	0.39	0.13	0.15	49.63	5.55	12.59	14.32

[a] *X*, mean; S.D, standard deviation.
[b] Surface is given in cm^2 and phases are given in degrees.

Table 3
Surface and Fourier analysis of the handwritten loops *o* of the writers W1–W13: summary statistics[a] of the surface and the first four pairs of Fourier amplitudes (A_1–A_4) and phases (θ_1–θ_4)[b]

Writer	Statistics	Surface	A_1	A_2	A_3	A_4	θ_1	θ_2	θ_3	θ_4
W1	*X*	0.059	0.13	1.36	0.25	0.31	329.36	57.98	87.07	64.25
	S.D.	0.017	0.05	0.34	0.13	0.12	26.64	8.96	17.46	9.65
W2	*X*	0.083	0.06	0.53	0.29	0.11	368.12	12.97	85.69	83.70
	S.D.	0.013	0.02	0.22	0.13	0.06	48.22	22.40	14.85	21.12
W3	*X*	0.045	0.07	0.62	0.38	0.18	309.04	126.88	80.23	58.38
	S.D.	0.010	0.03	0.29	0.16	0.07	83.68	39.44	14.86	29.21
W4	*X*	0.071	0.11	1.03	0.19	0.23	329.21	76.78	96.19	75.57
	S.D.	0.018	0.06	0.44	0.12	0.12	23.77	19.20	29.33	15.22
W5	*X*	0.043	0.07	1.18	0.13	0.29	296.85	54.72	122.88	53.12
	S.D.	0.007	0.02	0.26	0.07	0.08	33.61	6.22	41.32	6.31
W6	*X*	0.028	0.12	1.03	0.17	0.16	333.05	50.64	114.23	71.04
	S.D.	0.010	0.05	0.39	0.10	0.09	21.28	18.20	35.43	19.26
W7	*X*	0.030	0.14	1.70	0.23	0.35	350.32	51.81	100.50	52.68
	S.D.	0.004	0.04	0.36	0.10	0.16	23.67	10.04	8.48	15.04
W8	*X*	0.026	0.12	1.48	0.18	0.30	338.09	62.15	120.92	64.72
	S.D.	0.006	0.05	0.37	0.09	0.14	28.06	8.92	22.43	10.90
W9	*X*	0.065	0.04	0.36	0.21	0.10	313.96	119.00	78.21	61.30
	S.D.	0.009	0.02	0.18	0.11	0.05	61.34	39.73	20.25	17.52
W10	*X*	0.114	0.08	0.85	0.19	0.14	334.31	71.75	92.48	70.46
	S.D.	0.039	0.03	0.30	0.09	0.08	23.91	16.10	26.32	15.91
W11	*X*	0.074	0.08	1.00	0.30	0.24	398.71	−2.05	97.03	86.39
	S.D.	0.021	0.03	0.37	0.12	0.13	49.90	13.06	14.31	7.84
W12	*X*	0.027	0.12	0.75	0.24	0.13	328.60	53.73	126.58	66.61
	S.D.	0.006	0.04	0.26	0.11	0.09	19.51	33.48	30.44	14.60
W13	*X*	0.022	0.09	0.99	0.17	0.15	307.82	83.47	109.11	83.23
	S.D.	0.005	0.03	0.31	0.09	0.09	23.03	11.55	40.52	16.72

[a] *X*, mean; S.D, standard deviation.
[b] Surface is given in cm^2 and phases are given in degrees.

respectively. Furthermore, the multivariate means of the loops parameters based on each one of the four letters were different in a highly significant way according to the Hotelling's *T* squared test ($p < 0.01$) between each possible pair of writers.

3.2. Morphological characterization of groups of loops writings

The main groups of writers formed when applying a discriminant analysis on the features pertaining to one letter or another one were practically the same. Consequently, a discriminant analysis was performed on the four letters considered simultaneously in order to minimise the differences between the writers which were specific to one letter, thus allowing for the extraction of shape characteristics shared by different writers whatever the letter.

In this case, the first discriminant function accounted for 58.6% of the total variance, the second one 17.9%. The first two functions together explained 76.5% of the total variance of the data set. Within the observations retained for validation, 66.8% were correctly classified, i.e. allocated to the adequate writer. Once again, according to the Hotelling's *T* squared test (at $p < 0.01$), the differences in the multivariate means of the loop parameters between the writers were highly significant.

The graphic representation of the first two axes of the discriminant analysis (see Fig. 1) and the comparison of the Mahalanobis distances between the writers (see Table 5) suggested the constitution of five main groups among the 13 writers of the study: one group of one writer (W10), three groups of two writers (W1-W4, W2-W11 and W3-W9) and one group of six writers (W5-W6-W7-W8-W12-W13). The writing groups sharing shape characteristics are illustrated by the reconstructions of any *d* loops in Fig. 2, on the basis of the first four pairs of Fourier descriptors.

The first two discriminant functions were principally correlated with the same variables, which were the surface, the amplitude of the second harmonic (A_2) and the phase of the third harmonic (θ_3) (see Table 6).

The group formed by the writers W5, W6, W7, W8, W12 and W13 was distinguished from the other groups by the fact that these writers presented, in average, a very high value of the second amplitude of the loops of all the letters analysed. That was especially marked for the letter *a*: 2.02, 1.92, 1.99, 1.93, 1.70 and 1.40, respectively (see A_2 in Table 1). These high

values of the second amplitude indicated that the loops of these writers presented an important elongation. In addition, the loops of these writers presented very small surfaces, especially for the letter *q*: 0.031, 0.025, 0.020, 0.020, 0.022 and 0.015 cm^2, respectively (see surface in Table 4). Finally, these six writers were also characterized by high values of the third phase, more than 100° in average (see θ_3 in Tables 1–4), this means that the triangular contribution of their loops was slightly backward oriented.

The writers group W3–W9 was characterized by very low values of the second amplitude of the letters *a*, *d*, *o* and *q*. This amplitude was particularly reduced for the letter *q*: 0.50 and 0.47, respectively (see A_2 in Table 4). Thus, the loops of these writers presented a weak elongation. In addition, in average, the loops of these writers presented the lowest values of the third phase; one leaf of the triangular contribution of their loops was oriented at 68° in average (see θ_3 in Tables 1–4).

The writers W2–W11 were discriminated from the other writers groups by the high values of the surface of their loops. This characteristic led to associate these writers even if the values for the second amplitude were quite different between them; elongation was rather marked in the loops of the writer W11, contrary to those of writer W2 (see A_2 in Tables 1–4).

The group W1–W4 was characterized by moderate values of all the loops parameters which played an important role in the discrimination between-writers groups, namely the surface, the second amplitude and the third phase (see surface, A_2 and θ_3 in Tables 1–4).

The writer W10 constituted a group by himself, being characterized by the highest values of the surface of all his loops, in a very marked way for the letter *a*: 0.147 cm^2 (see surface in Table 1). Furthermore, the elongation of the loops of the writer W10 was not very marked, as indicated by the rather low value of the second amplitude of the loops of this writer: *a*: 1.08; *d*: 0.63; *o*: 0.85; *q*: 0.94 (see A_2 in Tables 1–4).

3.3. Morphological characterization of individual loops writings

Precise characterization of individual writings was then investigated, on the basis of the relationship between the shape and surface parameters of the loops of the different letters in each writing, as well as the extent of their variability. Four

Table 4
Surface and Fourier analysis of the handwritten loops *q* of the writers W1–W13: summary statistics[a] of the surface and the first four pairs of Fourier amplitudes (A_1–A_4) and phases (θ_1–θ_4)[b]

Writer	Statistics	Surface	A_1	A_2	A_3	A_4	θ_1	θ_2	θ_3	θ_4
W1	*X*	0.044	0.10	1.14	0.22	0.24	331.39	54.16	85.81	61.00
	S.D.	0.009	0.04	0.44	0.09	0.13	30.23	12.60	17.64	10.60
W2	*X*	0.054	0.06	0.88	0.24	0.14	396.57	31.60	96.23	83.77
	S.D.	0.012	0.02	0.33	0.12	0.08	41.46	48.85	17.20	20.97
W3	*X*	0.037	0.05	0.50	0.26	0.12	303.56	26.33	59.75	41.61
	S.D.	0.010	0.03	0.29	0.13	0.08	77.30	33.68	19.75	24.73
W4	*X*	0.038	0.10	1.52	0.27	0.33	355.53	54.68	105.03	78.92
	S.D.	0.011	0.04	0.49	0.13	0.20	38.17	15.05	17.33	24.26
W5	*X*	0.031	0.06	1.38	0.13	0.37	340.73	38.69	122.97	40.74
	S.D.	0.006	0.02	0.27	0.08	0.13	40.74	5.79	29.46	3.46
W6	*X*	0.025	0.10	1.82	0.25	0.35	402.74	32.39	105.88	33.55
	S.D.	0.005	0.04	0.44	0.10	0.18	32.22	9.46	9.68	15.73
W7	*X*	0.020	0.10	1.94	0.20	0.59	358.71	41.22	92.18	40.79
	S.D.	0.004	0.03	0.39	0.07	0.24	23.49	7.55	15.19	6.63
W8	*X*	0.020	0.13	2.01	0.30	0.47	389.13	41.45	118.80	43.73
	S.D.	0.004	0.05	0.34	0.12	0.19	30.92	5.18	10.03	6.63
W9	*X*	0.057	0.03	0.47	0.23	0.15	294.90	70.43	55.21	38.96
	S.D.	0.007	0.03	0.25	0.10	0.07	113.49	21.76	18.07	13.86
W10	*X*	0.102	0.06	0.94	0.21	0.16	311.47	74.91	87.34	71.90
	S.D.	0.028	0.03	0.36	0.11	0.08	59.66	13.12	22.47	13.84
W11	*X*	0.064	0.08	1.32	0.14	0.26	330.07	12.60	57.01	102.01
	S.D.	0.016	0.03	0.31	0.07	0.10	38.02	12.11	25.30	13.16
W12	*X*	0.022	0.19	1.73	0.46	0.52	345.57	63.72	91.38	61.22
	S.D.	0.003	0.04	0.28	0.16	0.16	27.25	7.25	6.36	5.33
W13	*X*	0.015	0.13	1.20	0.21	0.25	337.25	61.95	120.57	71.83
	S.D.	0.004	0.04	0.34	0.12	0.11	28.67	9.11	21.91	11.07

[a] *X*, mean; S.D, standard deviation.
[b] Surface is given in cm^2 and phases are given in degrees.

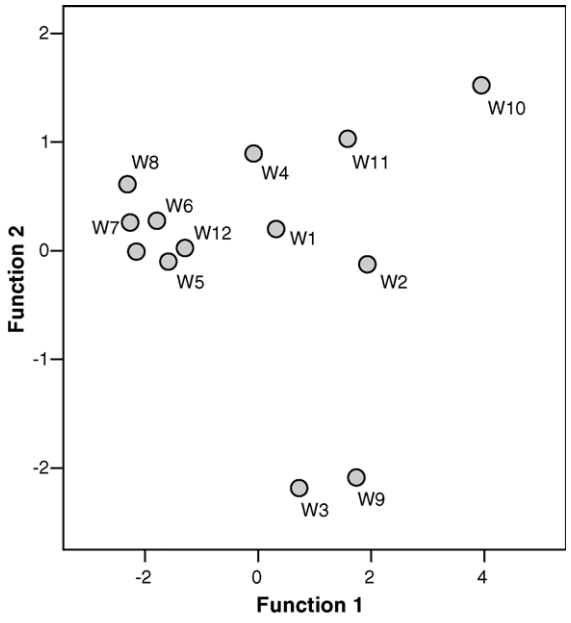

Fig. 1. Results of the discriminant analysis performed on the first four pairs of Fourier descriptors (A_1–A_4, θ_1–θ_4) and the surface of the contours of the loops *a*, *d*, *o* and *q* of the writers W1–W13: representation of the centroid of the loops of each writer on the first two discriminant functions.

writers were chosen within the 13, belonging to the same or different writers groups: W1, W5, W11 and W12. These writers were selected because they presented morphological characteristics appearing clearly different between them through the visualisation of their corresponding discriminant analysis (see Fig. 3). For each one of these writers and for each letter, Euclidean distances calculated between each possible pair of observations are illustrated in Fig. 4, while the Mahalanobis distances between the letters of each writer separately are given in Table 7 for these writers. Table 8 informs about the variables responsible for the discrimination between the letters in each writer.

In writer W1, the within-variability of the parameters of surface and shape within the set of observations for a letter was rather weak for all four sets of letters (see Fig. 4). However, the four letters clouds of points represented on the discriminant graph overlapped (see Fig. 3), since the distances between these sets were very low. The loops of the different letters were morphologically very similar, in the most marked way for the letters *a* and *d*, as indicated by the particularly small distance separating them (see Table 7). Nevertheless, the loops of the letter *q* could be slightly distinguished from the other letters by their smaller surface and their lower second phase (see surface and θ_2 in Tables 1–4); this means that elongation of *q* loops was closer to the horizontal axis compared to that of the other letters. Furthermore, W1 is the only writer in which the letter *o* is the most elongated letter, whereas this letter is the least elongated in the majority of the writers (see A_2 in Tables 1–4).

In writer W5, the variability of the loop parameters was the most extended for the letter *a* (see Fig. 4). The loops of letters *a* and *d* showed almost the same morphology, as demonstrated by the superimposition of their corresponding clouds of points on the discriminant graph, and the small distance separating them. On the contrary, the letters *o* and *q* were well discriminated and could be distinguished from the letters *a* and *d* (see Fig. 3 and Table 7). Letters *a* and *d* were characterized by a more pronounced elongation, as well as a more marked quadrangularity (see A_2 and A_4 in Tables 1–4). The triangularity of the letter *d* was two times more marked than that of the other letters (see θ_3 in Tables 1–4). Moreover, the letters *o* and *q* were mainly separated by their difference in orientation of their elongation (see θ_2 in Tables 3 and 4) and their quadrangular contribution (see θ_4 in Tables 3 and 4).

In writer W11, the greatest extent of variability of the loop parameters was observed in the letter *d* (see Fig. 4). The groups of the letters *d* and *q* were very close and practically superimposed. The distance between the group of the letter *a* and each one of the other letters was extremely high (see Fig. 3 and Table 7). The letters *d* and *q* presented both a distinctive orientation of the elongation which was almost horizontal (see θ_2 in Tables 2 and 4). The loops of the letter *a* were separated from the other letters by the low values of their second and fourth phases (see θ_2 and θ_4 in Tables 1–4) as well as the low value of their fourth amplitude (see A_4 in Tables 1–4). The letter *o* is distinguished from the other letters by its higher

Table 5
Discriminant analysis of the surface and the first four pairs of Fourier descriptors of the handwritten loops *a*, *d*, *o* and *q* of the writers W1–W13: Mahalanobis distances between each pair of writers

	W1	W2	W3	W4	W5	W6	W7	W8	W9	W10	W11	W12	W13
W1	0	6.32	7.96	1.67	8.86	5.75	8.48	8.90	8.72	16.45	7.57	5.06	8.53
W2		0	9.24	6.53	17.31	17.17	23.05	21.59	6.84	11.73	6.55	15.21	19.13
W3			0	12.64	13.82	14.17	17.26	19.46	2.41	26.63	14.84	13.23	18.14
W4				0	7.26	4.99	8.23	6.55	12.92	17.40	9.03	4.43	6.41
W5					0	3.52	4.06	3.64	16.95	32.03	17.68	8.57	8.31
W6						0	1.56	0.96	19.13	35.59	16.21	3.24	3.71
W7							0	0.92	23.01	41.35	20.03	4.62	6.48
W8								0	24.51	40.61	20.46	4.06	4.41
W9									0	18.32	15.88	18.32	21.91
W10										0	14.65	36.61	42.30
W11											0	18.55	23.27
W12												0	2.98
W13													0

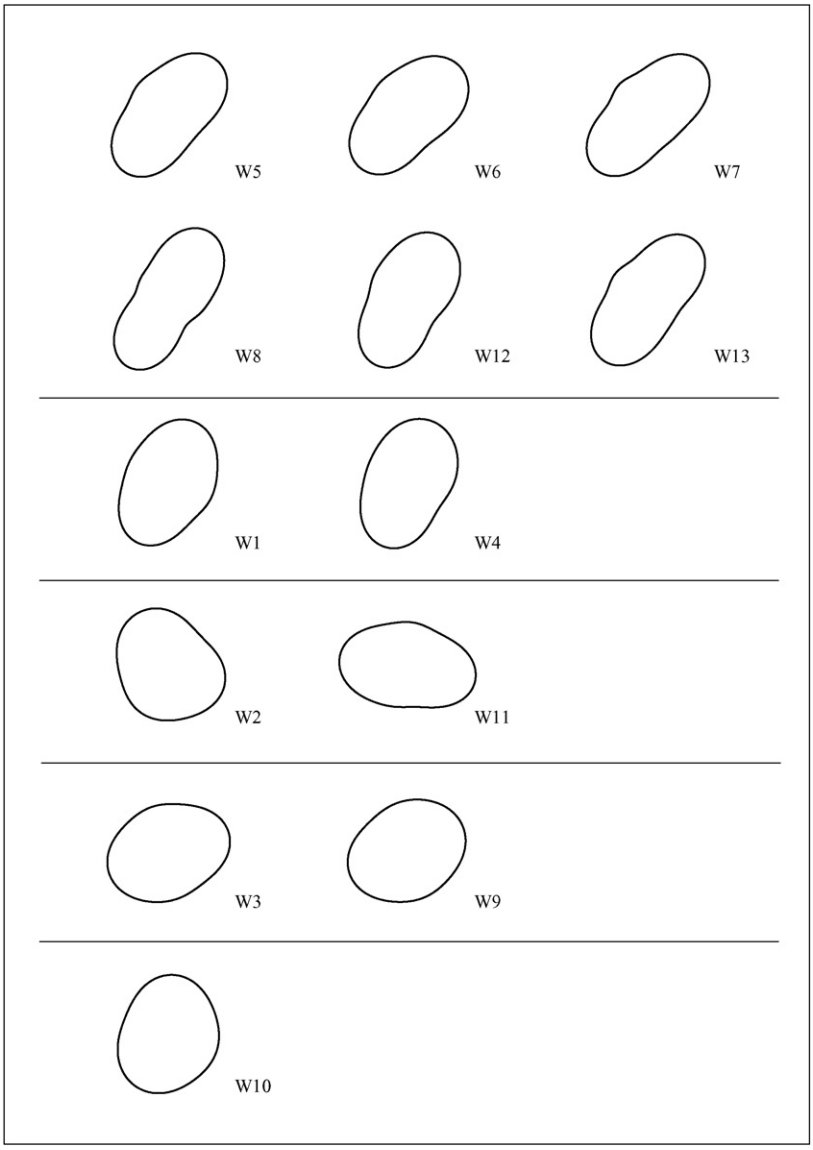

Fig. 2. Examples of reconstructions of *d* loops on the basis of the first four pairs of Fourier descriptors, one character being shown for each writer (W1–W13), to illustrate the five main groups of shape tendencies in loops writings (size is not illustrated here since it was normalized for the Fourier analysis).

Table 6
Discriminant analysis of the surface and the first four pairs of Fourier descriptors of the handwritten loops *a*, *d*, *o* and *q* of the writers W1–W13: correlation coefficient of the surface (*S*) and the Fourier amplitudes (A_1–A_4) and phases (θ_1–θ_4) with the first (r_1) and the second (r_2) discriminant functions

	r_1	r_2
S	0.796	0.466
A_1	−0.268	0.231
A_2	−0.438	0.548
A_3	−0.029	−0.022
A_4	−0.311	0.251
θ_1	−0.001	0.313
θ_2	0.024	−0.122
θ_3	−0.320	0.413
θ_4	0.111	0.372

third phase and its pronounced triangularity (see θ_3 and A_3 in Tables 1–4). The writer W11 is the only one in which the letter *o* is the most triangular.

In writer W12, the within-variability of the loops parameters of each letter was weak, especially for *a* and *q* (see Fig. 4). In this writer, observations of these letters presented a similar morphology, as demonstrated by the very low distance between these two letters groups. The letters *d* and *o* were distinctively separated from the other letter groups (see Fig. 3 and Table 7). The loops of the letter *o* were discriminated by their weaker elongation (see A_2 in Tables 1–4) and their less pronounced quadrangularity (see A_4 in Tables 1–4). Additionally, the loops of the letter *d* were characterized by a slightly less pronounced triangularity, as demonstrated by the lower value of their third amplitude compared to that of the letters *a*, *o* and *q* (see A_3 in Tables 1–4). In comparison with the other writers, W12 is all the same the writer whose loops are the most triangular on average.

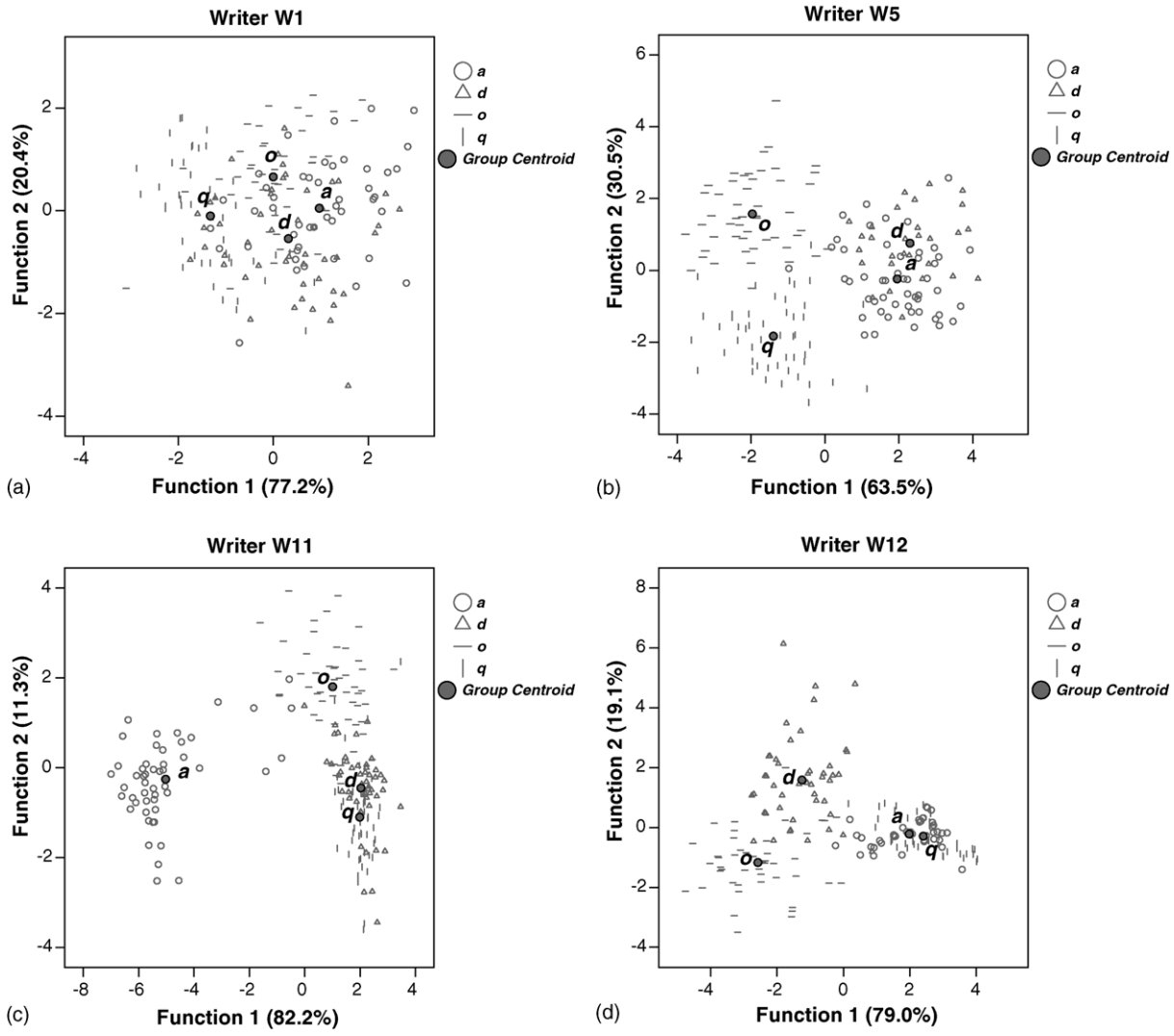

Fig. 3. Results of the discriminant analyses performed on the first four pairs of Fourier descriptors (A_1–A_4, θ_1–θ_4) and the surface of the contours of the loops *a*, *d*, *o* and *q* of the writer W1 (a), W5 (b), W11 (c) and W12 (d). Percentages given in parenthesis are the rates of variance explained by the corresponding functions.

4. Discussion

The methodology developed in a previous study to characterize objectively the global shape of the loops of handwritten characters was successfully validated. This procedure has now been applied to the loops of letters of other writers who were selected according to their habit to close their loops, and not on the basis of visual and subjective differences in the shape of their loops. The loops of the letters *a*, *d*, *o* and *q* were retained, as they all are circular bowls [16] and the first construction element of the corresponding letter.

This approach is new since it describes the shape of handwritten loops by decomposing it into specific contributions being visually understandable, and since variability of these parameters – within and between the writers, as well as within and between letters of a given writer – were detailed and quantified, allowing for an objective characterization of handwriting features, as well as their variability. The shape of loops of the handwritten characters *a*, *d*, *o* and *q* was described by using the Fourier descriptors. The decision criteria for determining the number of pairs of Fourier descriptors to be retained were based on the will to characterize the global shape of the loops without introducing random information assimilable to noise.

The discriminating power of the loops within the 13 writers of the study was different according to the letter. The loop of the letter *o* appeared to be the least discriminant one, as demonstrated by its lowest correct classification rate (69.7%). On the contrary, the loop of the letter *d* showed more individual characteristics of shape and size, as demonstrated by its better efficiency in the discrimination between the writers (correct classification rate of 82.4%). The order of these results is in agreement with the order of identification performances obtained by using micro-features of these letters (gradient, structural and concavity features extracted on the characters images) [17]. From these differences in discriminating power according to the letter, we deduce that all the individuals of the study did not form the loops of various letters in the same way; in a writer, shape parameters of various letters loops could be different.

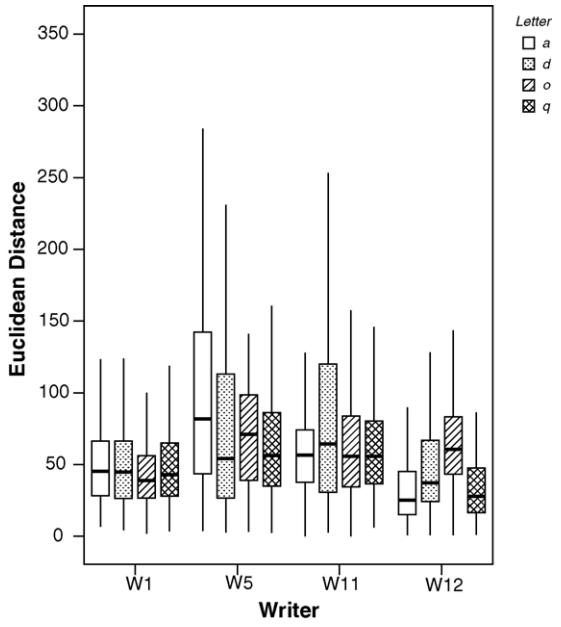

Fig. 4. Boxplots of Euclidean distances between all possible pairs of observations for each letter and each one of the writers W1, W5, W11 and W12. For a purpose of clarity, outliers were omitted from the figure.

Table 7
Variability of the surface and the first four pairs of Fourier descriptors of the loops *a*, *d*, *o* and *q* between each letter group of writers W1, W5, W11 and W12: Mahalanobis distances between each pair of letters groups (*n* = number of observations)

	n		*a*	*d*	*o*	*q*
W1	47	*a*	0	0.89	1.41	5.29
	49	*d*		0	1.55	2.96
	44	*o*			0	2.39
	46	*q*				0
W5	50	*a*	0	4.11	18.97	14.66
	30	*d*		0	20.25	21.02
	50	*o*			0	12.03
	49	*q*				0
W11	50	*a*	0	51.21	40.73	50.98
	50	*d*		0	8.52	5.56
	50	*o*			0	9.89
	50	*q*				0
W12	41	*a*	0	13.91	21.88	1.09
	47	*d*		0	9.35	17.04
	46	*o*			0	25.74
	40	*q*				0

Categories of loop writings presenting similar parameters of shape and surface of the loops *a*, *d*, *o* and *q* were established on the basis of discriminant analysis and between-writers distances. Then, even if all the writers did not form all the loops in the same way whatever the letter, main tendencies in size and shape could be highlighted and allowed for the characterization of groups of writers. The degree of dissimilitude between the groups of writers, as well as the degree of similitude between writers belonging to the same group, were quantified by the Mahalanobis distances calculated between the writers (see Table 5). The between-writers variability of the parameters of shape and surface of the loops of the letters *a*, *d*, *o* and *q* could thus be estimated in an objective way. The most discriminative features could be extracted from the discriminant analysis. In particular, the surface and the amplitude of the second harmonic were the variables contributing most to the separation or lack thereof between the writers. In other words, among the most discriminative characteristics were the size of the loops and the importance of their elongation.

The characteristics of the loops writing of each writer could be highlighted. The differences between writers belonging to distinct groups could be detailed, but it was also possible to reveal individual differences between writers belonging to the same group (see Fig. 3). For each writing, the variability of the size and shape parameters of the loops within each letter could be evaluated and compared (see Fig. 4). This variability, which is a quantitative representation of the natural variation (or consistency) of some aspects of handwriting, was different according to the writer and the letter. These results are in agreement with the hypothesis of the individuality of variations ranges of handwriting features [16]. Another major writing characteristic was the degree of morphological proximity between the loops of the different letters (see Table 7); the letters showing the strongest similitude were not always the same ones between the writers,

Table 8
Discriminant analyses of the surface and the first four pairs of Fourier descriptors of the handwritten loops *a*, *d*, *o* and *q* of the writers W1, W5, W11 and W12: correlation coefficient of the surface (*S*) and the Fourier amplitudes (A_1–A_4) and phases (θ_1–θ_4) with the first (r_1) and the second (r_2) discriminant functions

Variables	Writer W1		Writer W5		Writer W11		Writer W12	
	r_1	r_2	r_1	r_2	r_1	r_2	r_1	r_2
S	0.680	0.409	0.713	−0.148	−0.066	0.129	−0.129	−0.040
A_1	0.342	0.231	−0.068	0.177	0.028	0.028	0.353	−0.157
A_2	0.004	0.722	0.713	−0.148	0.209	−0.450	0.666	0.284
A_3	0.132	0.100	0.341	0.147	0.000	0.582	0.226	0.185
A_4	0.009	0.612	0.415	−0.171	0.236	−0.149	0.723	−0.195
θ_1	0.118	−0.293	0.042	−0.170	0.062	0.382	0.080	0.144
θ_2	0.405	−0.207	−0.173	0.774	−0.293	−0.376	0.122	0.137
θ_3	0.225	−0.441	0.065	0.013	−0.032	0.615	−0.435	0.298
θ_4	0.309	−0.162	−0.147	0.646	0.500	−0.056	−0.128	0.409

and the between-letters distances were different according to the writer. These differences in values and variability of the parameters of the loops between different letters, which were specific for a writer, suggest that it is of interest to compare the loops of the same letter when examining handwritten documents, and that each letter can provide additional information for writer identification. Indeed, the shape of a letter does not allow for the prediction of the shape of another letter, at least not for every writer.

A polymorphism of size and shape of loops of letters *a*, *d*, *o* and *q* could be shown in a quantitative and objective way. These parameters were useful to characterize peculiarities of any handwriting and to show general trends in the shape of handwritten loops; the most discriminative contributions could be highlighted, explaining the differentiation between-writers groups or between letters of a writer. Moreover, the high correct classification rates obtained showed that the retained parameters are also useful to associate loops with their corresponding writer. Then, in average, the variability of the shape and surface parameters were higher between the writers than within the writers.

Amplitudes and phases of the Fourier harmonics, directly related to precise contributions to the shape of loops, as well as size, were very relevant to the understanding of the differences between the writers groups or between the letters of each writer. Furthermore, from a practical point of view related to handwriting examination, one can conclude from the differences in discriminating power between the letters that it would be advisable to grant less weight to a correspondence of the shape of letters *o* than to that of letters *d* when comparing handwritten documents for writer identification.

In addition, characterization of local features, measured on the allographic level, is very relevant in order to examine documents containing little handwritten material. On the contrary, methods based on global features, such as texture analysis [1], require a sufficient amount of handwritten material that allows for a reliable description of the style of the questioned handwriting [18]. The correct classification rates reached in this study suggest that carrying out an expertise of fragmentary samples of handwriting comprising only some loops is completely possible.

Acknowledgement

This work was supported by a research grant (11–66787.01) from the Swiss National Science Foundation.

References

[1] H. Said, T. Tan, K. Baker, Personal identification based on handwriting, Pattern Recognit. 33 (2000) 149–160.

[2] M. Bulacu, L. Schomaker, Writer style from oriented edge fragments, Proceedings of the Tenth International Conference on Computer Analysis of Images and Patterns (CAIP 2003), Groningen, The Netherlands, 2003, pp. 460–469.

[3] A. Seropian, M. Grimaldi, N. Vincent, Writer identification based on the fractal construction of a reference base, in: Proceedings of the Seventh International Conference on Document Analysis and Recognition (ICDAR 2003), Edinburgh, Scotland, 2003, pp. 1163–1167.

[4] M. Wirotius, A. Seropian, N. Vincent, Writer identification from gray level distribution, in: Proceedings of the Seventh International Conference on Document Analysis and Recognition (ICDAR 2003), Edinburgh, Scotland, 2003, pp. 1168–1172.

[5] E.N. Zois, V. Anastassopoulos, Fusion of correlated decisions for writer verification, Pattern Recognit. (2001) 47–61.

[6] A. Bensefia, A. Nosary, T. Paquet, L. Heutte, Writer identification by writer's invariants, in: Proceedings of the Eighth International Workshop on Frontiers in Handwriting Recognition (IWFHR 2002), Niagara-on-the-Lake, Canada, 2002, pp. 274–279.

[7] C. Hertel, H. Bunke, A set of novel features for writer identification, Lecture Notes Comput. Sci. 2688 (2003) 679–687.

[8] G. Leedham, S. Chachra, Writer identification using innovative binarised features of handwritten numerals, in: Proceedings of the Seventh International Conference on Document Analysis and Recognition (ICDAR 2003), Edinburgh, Scotland, 2003, pp. 413–417.

[9] B. Zhang, S.N. Srihari, Analysis of handwriting individuality using word features, in: Proceedings of the Seventh International Conference on Document Analysis and Recognition (ICDAR 2003), Edinburgh, Scotland, 2003, pp. 1142–1146.

[10] L. Schomaker, M. Bulacu, Automatic writer identification using connected-component contours and edge-based features of uppercase western script, IEEE Trans. Pattern Anal. Mach. Intell. 26 (2004) 787–798.

[11] M. Tapiador, J.A. Sigüenza, Writer identification method based on forensic knowledge, in: Proceedings of the International Conference on Biometric Authentication (ICBA 2004), Hong Kong, China, 2004, pp. 555–561.

[12] C.-K. Li, N.-L. Poon, W.-K. Fung, C.-T. Yang, Individuality of handwritten numerals in local population, J. Forensic Sci. 50 (2005) 185–191.

[13] U.-V. Marti, R. Messerli, H. Bunke, Writer identification using text line based features, in: Proceedings of the Sixth International Conference on Document Analysis and Recognition (ICDAR 2001), Seattle, Washington, 2001, pp. 101–105.

[14] S.N. Srihari, S.-H. Cha, H. Arora, S. Lee, Individuality of handwriting, J. Forensic Sci. 47 (2002) 857–872.

[15] R. Marquis, M. Schmittbuhl, W.D. Mazzella, F. Taroni, Quantification of the shape of handwritten characters: a step to objective disrimination between writers based on the study of the capital character O, Forensic Sci. Int. 150 (2005) 23–32.

[16] R. Huber, A. Headrick, Handwriting Identification Facts and Fundamentals, CRC Press, Boca Raton, 1999, pp. 100 and 133–134.

[17] B. Zhang, S.N. Srihari, S. Lee, Individuality of handwritten characters, in: Proceedings of the Seventh International Conference on Document Analysis and Recognition (ICDAR 2003), Edinburgh, Scotland, 2003, pp. 1086–1090.

[18] A. Bensefia, T. Paquet, L. Heutte, Information retrieval based writer identification, in: Proceedings of the Seventh International Conference on Document Analysis and Recognition (ICDAR 2003), Edinburgh, Scotland, 2003, pp. 946–950.

ELSEVIER

Forensic Science International 164 (2006) 221–229

Forensic Science International

www.elsevier.com/locate/forsciint

A 'cold synthesis' of heroin and implications in heroin signature analysis Utility of trifluoroacetic/acetic anhydride in the acetylation of morphine

Luke R. Odell [a], Jana Skopec [b,1], Adam McCluskey [a,*]

[a] *Chemistry Building, School of Environmental and Life Sciences, The University of Newcastle, University Drive, Callaghan, NSW 2308, Australia*
[b] *AGAL, 1 Suakin Street, Pymble, NSW 2073, Australia*

Received 5 October 2005; received in revised form 25 January 2006; accepted 2 February 2006
Available online 23 March 2006

Abstract

Treatment of morphine, at room temperature, with a mixture of trifluoroacetic anhydride (TFAA) and acetic acid (20–30 min) affords good yields of heroin. GC–MS and HPLC examination shows that heroin produced by this route to be extremely clean, but the product contains slightly less heroin than observed via the more traditional acetic anhydride (AA) route (76.1% versus 83.55%); and greater quantities of 3-MAM and 6-MAM (6.9% versus 0.75% and 7.13% versus 0.63%). The concentration ratios of the major alkaloid impurities were found to be both production method (TFAA and AA) as well as morphine extraction methodology dependant. Data contained herein describe the impact of this new production method on current intelligence efforts, largely by-passing existing heroin signature programs and the UNDCP's efforts to restrict access to key synthetic precursors. Given the methodology dependency we find that examination of the major alkaloid ratios is unsuitable for the development of a new heroin signature program.

Further examination of the TFAA methodology allowed the identification of TFAA specific marker compounds, namely *bis*-trifluoroacetylmorphine (**30**), 3-trifluoroacetyl-6-acetylmorphine (**31**), 3-acetyl-6-trifluoroacetylmorphine (**32**) and trifluoroacetylcodeine (**33**). However, the hydrolytic lability of trifluroacetyl esters requires careful treatment of suspect samples, thus we propose a modification to existing HSP's in instances were the 6-MAM/WM ratio falls within the average minimum and maximum values of 6.17 and 17.32.

Keywords: Heroin; Signaure program; Acetylation of morphine; Cold synthesis

1. Introduction

Globally the heroin seized rises by about 5% per annum [1]. Within Australia these figures are even more disturbing as a result of record numbers of seizures, with the mid 1990s average of 250 kg per year increasing to between 450 and 730 kg per year since 2000 [2,3]. Indeed, despite education efforts within Australia a recent Australian National Drug Household survey indicates that domestic demand is on the increase and that the number of Australian heroin users has more than doubled since 1988 [4]. The semi-synthetic nature of heroin, being derived from morphine (Fig. 1) has facilitated the development and implementation of a series of heroin signature programs (HSP). In a HSP seized samples are analysed by a number of different analytical procedures with the aim of providing crucial drug trafficking and distribution intelligence. HSP typically analyses and evaluates the major synthetic impurities and adulterants. These approaches have been extensively examined and reported previously [1,5–37]. Worldwide, the impurity profiling of illicit drugs is being increasingly utilised as an intelligence-gathering tool, to support and complement the work of law enforcement agencies allowing an objective, comparative analysis of the level of commonality between samples [9–13,32,33]. The chemical information provided from an impurity profile can be used to provide tactical intelligence, which involves establishing links between different samples [14,15] and strategic intelligence, which refers to the identification of the source of a sample [28–30], the tracing of distribution routes and identifying new production processes [31].

To date HSP analysis rapidly allows South-West Asian (SWA) heroin to be identified by significant quantities of both

* Corresponding author. Tel.: +61 249216486; fax: +61 249215472.
E-mail address: Adam.McCluskey@newcastle.edu.au (A. McCluskey).
[1] Present address: AgriFor Scientific Pty Ltd, 46 Cook Road, Killara, NSW, Australia.

0379-0738/$ – see front matter © 2006 Elsevier Ireland Ltd. All rights reserved.
doi:10.1016/j.forsciint.2006.02.009

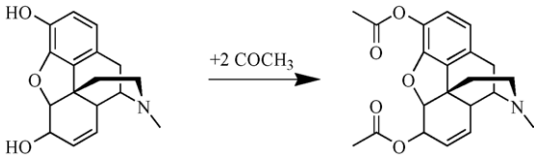

Fig. 1. Acetylation of morphine to yield diacetylmorphine (DAM, heroin).

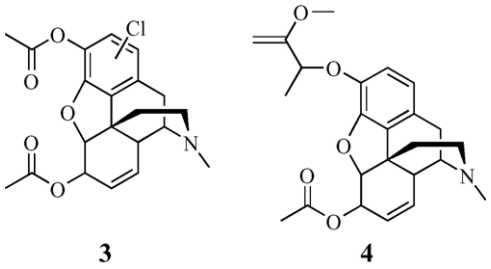

Fig. 2. Route specific markers detected in the illicit production of heroin.

papaverine (PAP) and noscapine (NOS); South-East Asian (SEA) heroin by an absence of these alkaloids; Mexican heroin by its unique appearance; and South American heroin by its high purity and low acetyl codeine (AC) content. Further, quantitative major component data have been used successfully by a number of authors to determine the source of heroin [9,10,12,17,19].

Whilst a HSP typically concentrates on determination of geographic origin, it is also possible to elicit information relating to the routes of synthesis used in the actual manufacture of seized DAM. Standard HSP analysis is based on acetic anhydride (AA) as the principle acetylating agent. However, AA is not the sole acetylating agent available in the clandestine manufacture of heroin. There are currently two other acetylating agents described in the literature: acetyl chloride, which affords 1-chloroheroin (**3**) as a route specific marker; and ethylene diacetate, which affords 3-[1-(1-carboxymethoxyethyl)]-6-acetylmorphine (**4**) as a route specific marker (Fig. 2) [5,38,39].

Over the past 30 years considerable work has been done developing parameters (Fig. 3, marker compounds **5**–**10**) for the profiling of heroin. During this period only three acetylating agents have been reported AA, acetyl chloride and ethylene diacetate, with the former being employed almost exclusively. The recent discovery of traces of trifluoroacetic acid in a seized sample promoted an investigation into the use of this and related reagents in the synthesis of heroin [40].

2. General techniques and instrumentation

All solvents used herein were of HPLC grade.

3. HPLC major impurity determination

The analyses were performed on a Perkin-Elmer ISS 200 Series HPLC equipped with an LC-235C diode array detector measuring at 240 and 225 nm. The chromatographic separation was achieved on an Alltec C_{18} column using a six-step methanol and phosphate buffer gradient (see Section 3.1) at a flow rate of 0.76 mL/min. The buffer (pH 2) comprised 1N sodium hydroxide (32 mL), phosphoric acid (11 mL) and hexylamine (3.5 mL) in millipore water (1000 mL).

3.1. Pump parameters

Step	Time (min)	Methanol (%)	Buffer (%)
1	10	5	95
2	20	30	70
3	6	30	70
4	10	80	20
5	4	80	20
6	10	5	95

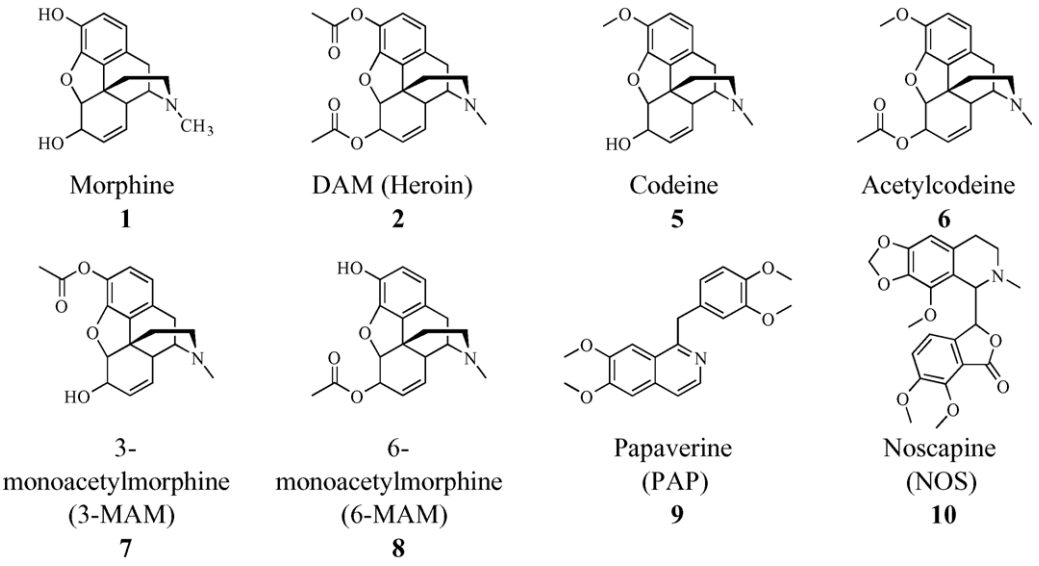

Fig. 3. Chemical structures of the major alkaloids found in, and as a result of, the illicit synthesis of heroin.

Table 1
Comparison of chemical yields and major component analyses for the synthesis of heroin via the TFAA or the AA route

Method	Target compounds								
	M	C	3-MAM	6-MAM	AC	DAM	NOS	PAP	Yield (%)
TFAA[a]	1.02 ± 1.13	0.09 ± 0.02	6.9 ± 1.63	7.13 ± 1.56	0.83 ± 0.11	76.1 ± 3.23	<0.01	<0.01	58 ± 5
AA[b]	0.16 ± 0.29	<0.01	0.75 ± 0.31	0.63 ± 0.28	1.12 ± 0.15	83.55 ± 5.93	<0.1	<0.1	64 ± 12

[a] Non-controlled precursor; reaction time 20–30 min; typically 3 equivalents TFAA; room temperature.
[b] Listed on the International Narcotics Control Board's 'RED LIST': see http://www.incb.org/incb/en/red_list.html; reaction time ≥ 2 h; typically 10 equivalents AA; requires heating 80–90 °C.

Each sample under investigation was weighed (10 mg) into a 10 mL volumetric flask. Propiophenone (1 μL) was added as an internal standard and the mixture diluted to 10 mL with the addition of the injection solvent (5% methanol, 95% buffer).

3.2. GC–MS analysis

The analyses were performed on a Hewlett-Packard 6890 gas chromatograph equipped with a 5973 quadrupole mass-selective detector and an Agilent 7683 series autoinjector. The chromatographic separation was achieved on a HP-5MS (5% phenyl methyl siloxane) capillary column (length 30 m, i.d. 0.25 mm, film thickness 0.25 μm) with helium carrier gas at a flow of 1.2 mL/min (pressure 88.9 kPa). The injection temperature was maintained at 260 °C, with 2 μL splitless injection. The column was heated at 100 °C for 1 min then increased at a rate 6 °C/min to 240 °C then 2 °C/min to 280 °C followed by 6 °C/min to 320 °C.

3.3. Acidic and neutral trace impurity analysis

All reaction vials, vial inserts, pipettes and centrifuge tubes were silanised, to replace active hydrogen groups, prior to use.

Each sample under investigation was weighed (50 mg) into a glass centrifuge tube. Sulphuric acid (1N, 4 mL) and extraction mixture (60:40 ether–dichloromethane; 4 mL) were added to the sample. The solution was vortexed (15 min) and then centrifuged (15 min, 1000 rpm). An aliquot (3 mL) of the organic phase was pipetted into a reaction vial. The solution was dried under a stream of nitrogen at 70 °C. The sample was then treated with a derivatisation solution (250 μL). The derivatising solution comprised BTFSA (1 mL), TMS (1%) and dichloromethane (1 mL). Next benzopinacolone (50 μL) was added as the internal standard, at a concentration of benzopinacolone/dichloromethane of 2.5 mg/mL. The reaction vial was capped and heated at 70 °C for 30 min. The solution was allowed to cool and transferred to a GC vial for analysis.

GC–MS trace component analysis was used to determine the relative amounts of the target compounds in each sample.

3.4. Major component analysis

To 1 mg of each sample was added dichloromethane (250 μL) followed by 50 μL of internal standard (prepared as described above).

4. Results and discussion

There is literature precedent for the use of trifluoroacetic anhydride as an ester promoter, with two methods commonly described, differing only in the order of reagent addition [41,42]. Dissolution of morphine in TFAA followed by the addition of acetic acid gives rise to very low yields of DAM, but significant quantities trifluoroacetyl esters; conversely dissolution of acetic acid in TFAA forming the mixed anhydride followed by addition of morphine proved to be an extremely clean, efficient and elegant route for the production of high quality DAM.

The TFAA methodology provides for a four to six-fold decrease in reaction time in the absence of both heat and a large reagent excess (Table 1). Interestingly, neither acetic acid nor TFAA are restricted precursors, and can thus be readily obtained from chemical suppliers [43]. From a drug

Table 2
Alkaloid ratios for the AA and TFAA reactions using the Tas, SWA and SEA procedures

Method[a]	Ratio[b]			
	C/WM	NOS/WM	PAP/WM	6-MAM/WM
Tas				
AA[c]	1.48 ± 0.22	<0.04	0.01 ± 0.02	0.80 ± 0.36
TFAA[d]	1.14 ± 0.10	<0.01	0.01 ± 0.02	9.86 ± 1.86
SWA				
AA[e]	10.69 ± 0.46	33.1 ± 1.25	4.61 ± 0.13	1.11 ± 0.39
TFAA[f]	10.92 ± 1.58	24.45 ± 8.63	4.7 ± 1.04	12.35 ± 4.27
SEA				
AA[e]	8.94 ± 0.3	0.21 ± 0.18	0.21 ± 0.23	0.28 ± 0.03
TFAA Base[e]	9.07 ± 0.09	0.25 ± 0.22	0.06 ± 0.2	9.54 ± 2.7
TFAA HCl[g]	9.78 ± 0.07	2.12 ± 0.34	0.26 ± 0.1	9.03 ± 1.31
Average				
AA[h]	5.56 ± 4.35	6.68 ± 13.93	0.99 ± 1.91	0.71 ± 0.42
TFAA[i]	6.5 ± 4.59	6.58 ± 11.34	1.24 ± 2.11	10.27 ± 2.79

[a] Tas: Tasmanian procedure; SWA: South-West Asian procedure; SEA: South-East Asian procedure.
[b] C = total codeine (C + AC); WM = (%DAM × 285.34/369.42) + (%MAM × 285.34/327.38)(%MAM).
[c] $n = 5$.
[d] $n = 8$.
[e] $n = 3$.
[f] $n = 5$.
[g] $n = 4$.
[h] $n = 11$.
[i] $n = 20$.

enforcement perspective the discovery of such a simple, rapid and facile method for DAM synthesis is significant. Not only does it offer the clandestine laboratories good yields with far greater throughput, but also the potential to circumvents the current UNDCP methods of tracking heroin production [43]. From Table 1, it is clear that the TFAA reaction gives rise to anomalous data outwith that anticipated in current HSP's. As can be seen from Table 1 the product produced via the TFAA route contains slightly less DAM (76.1%) than that observed via the more traditional AA route (83.55%); and greater quantities of 3-MAM (6.9% versus 0.75%) and 6-MAM (7.13% versus 0.63%). Furthermore all TFAA samples contained traces of morphine and codeine, whereas morphine was only detected in only two and codeine in none of the AA samples (data not shown). It is noteworthy to mention that trifluoroacetyl esters are notoriously unstable, readily hydrolysed under conditions required for analysis (see Section 6), meaning that their detection in clandestine laboratory samples is difficult [41,42], this is the most probable explanation for the increased concentrations of 3-MAM, 6-MAM, morphine and codeine detected.

Current HSP methodologies have evolved to deal with DAM synthesised via morphine acetylation by AA at elevated temperature, we thus felt it crucial that this new methodology be examined and key constituents analysed in an attempt to gather data as to how TFAA might impinge on existing HSP protocols. Accordingly we examined the amounts major illicit heroin components formed using the two methods (TFAA and AA) (Fig. 3 and Table 2) were compared by producing a number of replicate samples from three different morphine sources: Tasmanian poppy and typical South-West and South-East Asian morphine.

Table 2 highlights significant differences in the alkaloid ratios observed as a function of both the reaction method (TFAA or AA) and clandestine procedure employed. Variation in the noscapine, papaverine and codeine ratios between Tas, SWA and SEA series, can be explained by differences in the morphine extraction processes. The SWA procedure involves only a crude morphine extraction and consequently had the

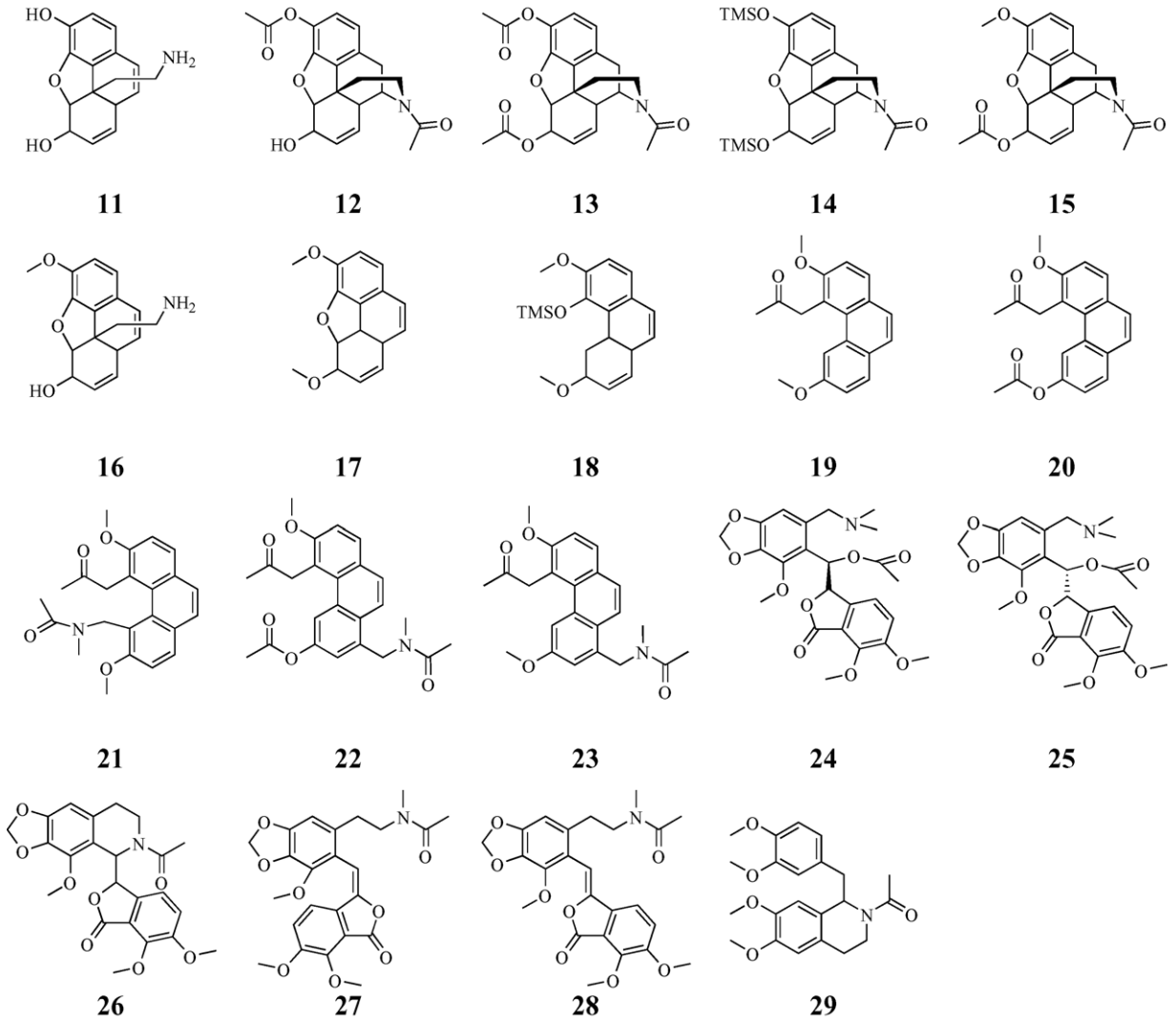

Fig. 4. Trace level impurities targeted by the Australian National Heroin Signature Program.

highest NOS/WM (33.1 and 24.45 versus SEA 0.21, 0.25, 2.12 and TAS <0.01) and PAP/WM (4.61 and 4.7 versus SEA 0.21, 0.06, 0.26 and TAS 0.01) ratios. In contrast, the SEA employs steps to remove the majority of noscapine and papaverine, which resulted in the smaller NOS/WM (0.21, 0.25, 2.12 versus 33.1 and 24.45) and PAP/WM (0.21, 0.06, 0.26 versus 4.61 and 4.7) ratios observed in this series. The morphine used in Tas series had been refined using an unknown chemical process, which removed the majority of non-morphine alkaloids.

Our data clearly illustrate that the amounts of these non-morphine alkaloids are related to the morphine extraction process and not the acetylating procedure. Consequently these ratios cannot be used as TFAA specific profiling parameters. In contrast, the 6-MAM/WM ratio is significantly higher for all TFAA produced samples (e.g. 9.86 versus 0.8 for Tas series) and remains constant irrespective of the morphine sample or clandestine procedure employed (TFAA reaction 9.86, 12.35 and 9.54, 9.03 for the Tas, SWA, SEA Base and HCl procedures, respectively). This indicates that the 6-MAM/WM ratio is both acetylating reagent and production process independent making it an ideal profiling parameter for the identification of the use of TFAA in the illicit synthesis of heroin.

Given that the major alkaloids are not suitable for determination of TFAA versus AA synthesis route we next turned our attention to analysis of the trace impurities (Fig. 4 and Table 3). Data presented in Table 3 clearly illustrate significant differences in the quantities of morphine related by-products; **11–13** and **15** are produced when AA is employed as the acetylating agent, e.g. **13**: 38.74, 51.13 and 100 for the Tas, SWA and SEA Base methods, respectively, as compared with the TFAA method, e.g. **13**: 7.19, 9.92 and 50.33 for the Tas, SWA and SEA methods, respectively. These compounds are formed by the *N*-acetylation followed by demethylation of morphine and codeine N-oxide, which are transient intermediates formed during the acetylation process [22]. Not surprisingly our data confirm the TFAA routes as milder, resulting in lower initial concentrations of these intermediate species and hence lower amounts of **11–13** and **15**.

Further examination of Table 3 reveals a contrast between the relative proportions of thebaine related products formed during the two reactions. All three series show that the AA procedure resulted in the formation of substantially greater amounts of impurities (e.g. **19**: AA method: 6.16, 97.79 and 0.84; TFAA method 0.47, 4.75 and 0.02 for the Tas, SWA and SEA methods, respectively), with the exceptions of **17** in the SEA series (AA: 0.2; TFAA: 0.4) and impurities **20–23** which were formed in essentially equal amounts. Control experiments, treating thebaine according to the TFAA protocol showed that the observed differences (AA versus TFAA methods) are a result of thebaine being not reacting under the TFAA conditions. The application of heat to thebaine in the presence of TFAA results in the rapid decomposition of

Table 3
Analysis of major alkaloids and impurities as a result of the AA and TFAA methods of DAM synthesis

Target compounds	Average response and procedure used[a]					
	Tasmanian		SWA		SEA	
	AA[b]	TFAA[c]	AA[d]	TFAA[d]	AA[d]	TFAA[d]
Morphine related compounds						
11	0.39 ± 0.04	0.07 ± 0.04	17.48 ± 1.97	2.47 ± 0.05	0.58 ± 0.14	0.37 ± 0.12
12	14.91 ± 0.98	4.46 ± 1.5	20.58 ± 2.01	10.95 ± 2.54	35.96 ± 6.46	20.25 ± 6.33
13	38.74 ± 1.22	7.19 ± 3.25	51.13 ± 0.85	9.92 ± 2.0	100 ± 5.30	50.33 ± 18.1
14	<0.05	<0.05	2.8 ± 0.54	0.83 ± 0.67	0.04 ± 0.02	0.09 ± 0.04
15	2.56 ± 0.37	0.3 ± 0.16	12.85 ± 1.16	1.82 ± 0.11	18.17 ± 4.70	6.52 ± 2.13
16	<0.05	<0.05	4.19 ± 0.02	0.13 ± 0.1	0.16 ± 0.05	0.17 ± 0.07
Thebaine related compounds						
17	2.13 ± 0.13	0.16 ± 0.06	61.36 ± 4.14	1.76 ± 0.69	0.2 ± 0.06	0.4 ± 0.05
18	5.32 ± 0.01	2.1 ± 1.28	100 ± 18.32	20.75 ± 2.45	2.41 ± 0.08	1.45 ± 0.33
19	6.16 ± 0.55	0.47 ± 0.34	97.79 ± 10.56	4.75 ± 0.35	0.84 ± 0.09	0.02 ± 0.01
20	0.22 ± 0.03	0.09 ± 0.03	4.87 ± 0.13	0.34 ± 0.26	0.24 ± 0.07	0.2 ± 0.09
21	0.12 ± 0.02	<0.05	9.11 ± 1.69	0.92 ± 0.31	0.03 ± 0.08	0.02 ± 0.02
22	<0.05	<0.05	3.11 ± 1.25	0.73 ± 0.52	0.01 ± 0.01	<0.05
23	<0.05	<0.05	6.22 ± 0.85	<0.05	<0.05	<0.05
Noscapine and *N*-norlaudanosine related compounds						
24	<0.05	<0.05	0.26 ± 0.05	<0.05	<0.05	<0.05
25	<0.05	<0.05	0.18 ± 0.01	<0.05	<0.05	<0.05
26	<0.05	<0.05	57.21 ± 1.33	3.52 ± 0.02	1.5 ± 0.23	<0.05
27	<0.05	<0.05	1.57 ± 0.01	0.14 ± 0.03	<0.01	<0.05
28	<0.05	<0.05	2.28 ± 0.10	0.06 ± 0.05	<0.01	<0.05
29	0.22 ± 0.15	<0.05	8.73 ± 3.8	5.93 ± 0.38	100 ± 9.9	7.74 ± 0.25

[a] Response was calculated against an internal standard (i.e. compound response/internal standard × 100), data are then normalised against largest response.
[b] $n = 3$.
[c] $n = 6$.
[d] $n = 2$.

thebaine. Thus, although thebaine decomposes when heated in TFAA, formation of **17**–**23** (the major AA decomposition products) is not the preferred pathway for this reaction [21].

Significantly greater amounts of noscapine and *N*-norlaudanosine related compounds were produced when the AA method was employed (e.g. **26**: AA: 57.21 and 1.5; TFAA: 3.52 and <0.05 for SWA and SEA, respectively) (Table 3). The formation of **24** and **25** proceeds through the addition of acetic acid across the double bond in **27** and **28** [22]. The absence of these compounds in samples produced using TFAA can be explained by the absence of acetic acid and the smaller quantities of **27** and **28** present in the mixed anhydride system. The formation of **26** proceeds through the precursor, noscapine N-oxide [22]. The increased abundance of this compound in the AA samples is believed to be a result of smaller quantities of noscapine N-oxide being formed during the TFAA synthesis. Subsequent cleavage of the C1–N bond affords **27** and **28**.

The formation of **29** involves the acetylation of the secondary amine group in *N*-norlaudanosine [22], which is a function of nucleophile strength, with increased prevalence for attack at the trifluoroacetyl carbonyl, of the mixed anhydride formed in situ, increasing with the reactivity of the nucleophile [41]. Hence the TFAA procedure favours trifluoroacetylation, decreasing the amount of **29** observed.

Our data clearly establish that the amounts of these trace impurities were significantly different between the two reactions. However, when comparisons are made between the Tas, SWA and SEA series these differences were shown to be highly dependent upon the morphine extraction procedure (e.g. **19**: 6.16 versus 0.47, 97.79 versus 4.75 and 0.84 versus 0.02 for Tas, SWA and SEA, respectively). Consequently based on this data set, the trace organic component of a seized sample cannot be used as a TFAA specific profiling parameter.

With the currently identified trace organic impurities unable to distinguish between the two reactions, an attempt was made to identify TFAA reaction specific marker compounds. During this investigation morphine, thebaine, oripavine, codeine, noscapine and papaverine were treated with AA and TFAA, analysed by GC–MS and their respective products compared (Fig. 5).

The reaction of noscapine, papaverine, thebaine and oripavine with TFAA failed to produce any detectable products, which could be used as TFAA markers. However, when morphine and codeine were treated with TFAA and AA significant differences in the reaction products were observed. Fig. 6 shows the appearance of peaks in the TFAA samples at 23.5 min (**30** m/z = 477), 25 min (**31** m/z = 423) and 26 min (**32** m/z = 423) in morphine and 24 min (**33** m/z = 395) in codeine, respectively. The molecular weights of these compounds suggest the addition of two CF_3CO groups (m/z = 194), one CF_3CO group and one CH_3CO group (m/z = 140) to morphine (m/z = 285) and one CF_3CO (m/z = 97) to codeine (m/z = 299), respectively, assuming the M-1 is detected in the GC–MS. We had anticipated that re-examination of our earlier preparations of heroin via the TFAA route that evidence for the formation of **30**–**33** would be forthcoming. This was not the case. However,

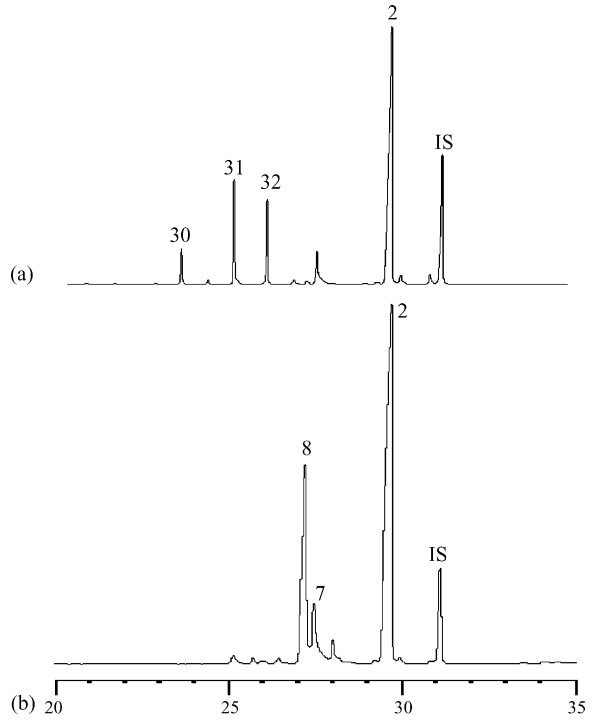

Fig. 5. (a) GC–MS analysis of a crude morphine sample after treatment with TFAA. R_t = 23.5 min = *bis*-trifluoroacetylmorphine (**30**); R_t = 26 min = *mono*-trifluoroacetylmorphine; R_t = 27.7 min = 3-MAM (**7**); R_t = 29 min = DAM (**2**); and R_t = 31 min = IS (benzopinacolone); (b) the same sample after typical pre-treatment for GC–MS analysis; R_t 27.2 min = 6-MAM (**8**); 27.7 min = 3-MAM (**7**); R_t = 29 min = DAM (**2**); and R_t = 31 min = IS (benzopinacolone).

the current HSP methodology involves a 1N H_2SO_4 extraction and derivitisation step prior to analysis, given the extremely labile nature of trifluoroacetyl esters it was deemed probable that the current methodology precluded the detection of these TFAA specific markers. Consequently we re-examined the TFAA heroin synthesis in the absence of the extraction and derivatisation steps, in these instances both **32** and **33** were detected in all SEA and SWA samples produced using TFAA (Fig. 6).

Structural assignment of **30** and **31** was based on MS fragmentation pattern analysis. MS analysis shows **30** to have $[M]^+$ of 423 which suggests the addition of one acetyl and one trifluoroacetyl ester to morphine. This is supported by a significant $[M\text{-}CH_2CO]^+$ (m/z = 381), $[M\text{-}CF_3COOH]^+$ (m/z = 310) and $[M\text{-}CH_2CO + CF_3COOH]$ (m/z = 268) ions. Additionally, the $[M\text{-}CH_2CHO]^+$ (m/z = 381) ion, which is characteristic of an aromatic acetate allowed the assignment of the acetate group to the 3-position [44]. The spectrum of 30 also showed significant peaks at m/z 215 and 174, which are characteristic of morphine skeleton fragmentation [45,46]. Similarly, **31** was determined to have $[M]^+$ of 395, which is consistent with the addition of a trifluoroacetyl group to codeine. This was confirmed by the $[M\text{-}CF_3COOH]^+$ (m/z = 282) base ion. The spectrum of **31** also showed characteristic codeine skeleton fragmentation peaks at m/z 229 and 188 supporting the assignment of **31** as trifluoroacetylcodeine [45,46].

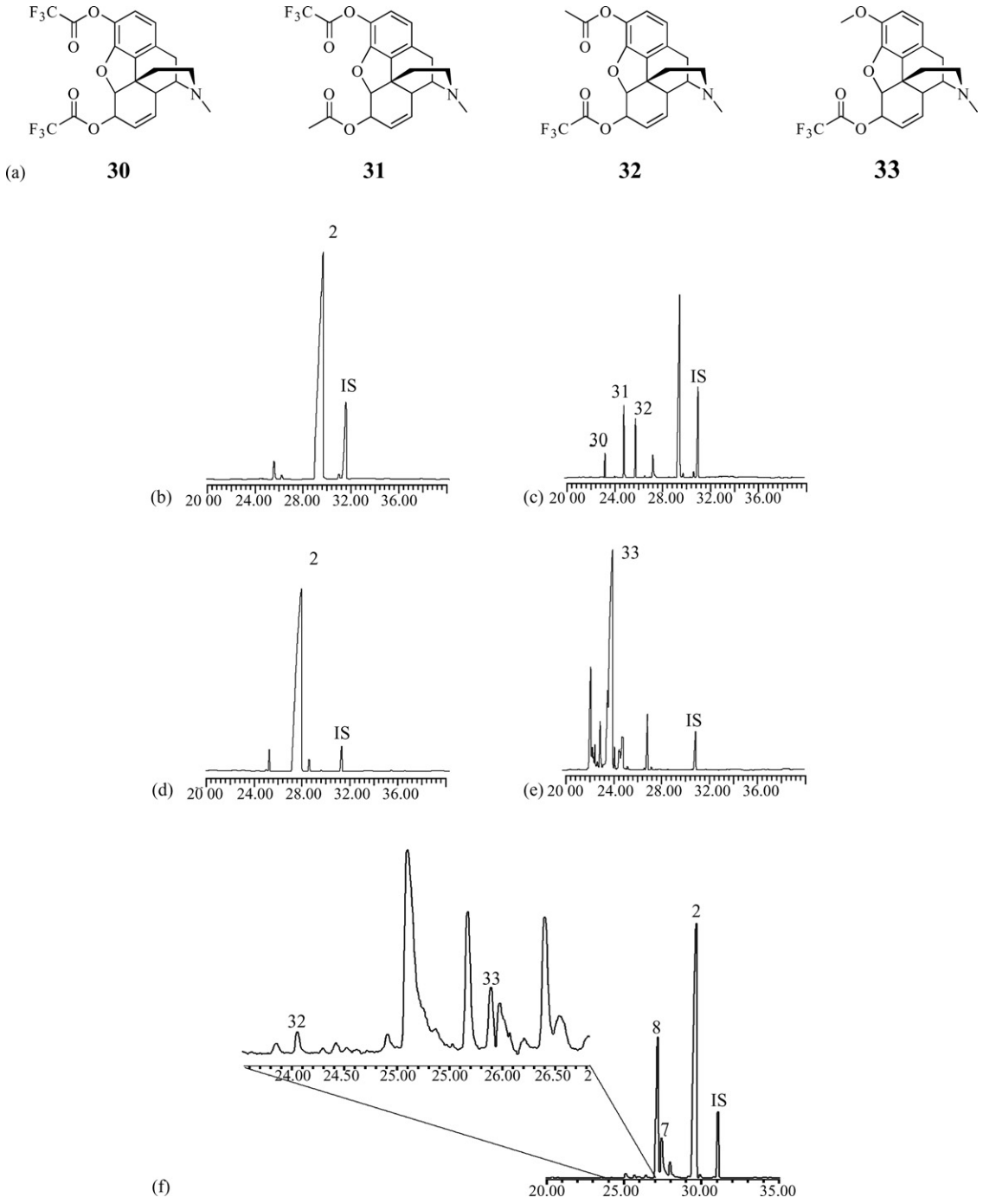

Fig. 6. (a) Chemical structures of TFAA specific markers identified in this work; (b) GC/MS trace of the crude reaction mixture arising from the reaction of morphine and AA; (c) GC/MS trace of the crude reaction mixture arising from the reaction of morphine and TFAA; (d) GC/MS trace of the crude reaction of codeine and AA; (e) GC/MS trace of the crude mixture arising from the reaction of codeine and TFAA. (f) GC–MS trace typical of DAM synthesis using TFAA; expanded section shows the presence of 3-acetyl-6-trifluoroacetylmorphine (**32**) and trifluoroacetylcodeine (**33**).

5. Conclusions

The use of TFAA provides a simple, quick and currently undetectable synthesis of heroin. To enable detection of this method a number of profiling parameters have been developed. In Australia, the routine profiling of heroin using major alkaloid analysis involves conversion of raw alkaloid concentration data into C/WM, NOS/WM, PAP/WM and 6-MAM/WM ratios and its origin assigned in accord with the UNDCP data [38]. Herein we suggest that if the 6-MAM/WM ratio of a seized sample falls within the average minimum and maximum values (6.17–17.32) then a presumption would be raised that the sample was made using the TFAA route. Any samples, which raise this presumption, would then be subjected to an additional test to confirm the origin of the product. A DAM sample with a large 6-MAM/WM ratio may

also be explained by incomplete acylation or poor sample storage [25,47,48]. Additionally the presence of **32** or **33** may be due to the presence of an alternate trifluorinated reagent (e.g. CF_3COCl).

6. Experimental

All solvents were HPLC grade or bulk solvents re-distilled from glass before use. Morphine used in the Tasmanian series was received from Tasmanian Alkaloids. In all other instances morphine utilised in synthesis was extracted (in a region specific manner) from samples seized by the Australian Federal Police using the methods described below. Thebaine, oripavine, morphine, codeine and papaverine reference standards were obtained from the National Analytical Reference Laboratory (NARL), Pymble, Australia.

6.1. Synthetic methods

6.1.1. Morphine extraction

Opium (40 g) was dissolved in boiling water (30 mL), to which was added $Ca(OH)_2$ (10 g) and the heating removed. The mixture was allowed to cool and stand overnight. The solution was filtered, the residue dissolved in boiling water (10 mL) and re-filtered. The combined filtrates were re-heated until the solution steamed, at this point the pH of the solution was adjusted to 8–9 with NH_4^+Cl and left to stand overnight. The solution was filtered to leave behind morphine base (2.61 g, 6.7%).

6.1.2. Morphine HCl

Morphine base (2.5 g) was dissolved in warm HCl (1 M, 25 mL) and 1 g of charcoal added. The solution was warmed for 10 min and then filtered. The filtrate was left to stand overnight and filtered to leave behind morphine hydrochloride (1.14 g, 41%).

6.2. Heroin synthesis

Trifluoroacetic anhydride synthesis.

6.2.1. Method 1

Glacial acetic acid (84 μL, 1.75 mmol) was added slowly to trifluoroacetic anhydride (311 μL, 2.1 mmol) in an ice bath and stirred for 10 min. Morphine (200 mg, 0.7 mmol) was added slowly and the mixture stirred for 20 min. The solution was then allowed to warm to room temperature and diluted with cold water (1 mL). The solution was put back in an ice bath and made basic (pH 8–10) with cold 10% sodium carbonate. The resulting aqueous solution was extracted with chloroform (3 × 10 ml), dried over $MgSO_4$ and evaporated to leave heroin base (157.6 mg, 78%).

6.2.2. Method 2

Trifluoroacetic anhydride (311 μL, 2.1 mmol) was added slowly to morphine (200 mg, 0.7 mmol) in an ice bath and stirred for 10 min. Glacial acetic acid (84 μL, 1.75 mmol) was added slowly and the mixture stirred for 20 min. The solution was then allowed to come to room temperature and evaporated under a stream of nitrogen. The residue dissolved in CH_2Cl_2 and analysed by GC–MS (see Section 2).

6.3. Acetic anhydride synthesis

Acetic anhydride (600 μL, 5.8 mmol) was added slowly to morphine (200 mg, 0.7 mmol). The resulting solution was heated and stirred at 85 °C for 2.25 h and allowed to cool to room temperature. The solution was diluted with cold water (1 mL). The solution was cooled on ice and made basic (pH 8–10) with cold 10% sodium carbonate. The resulting aqueous solution was extracted with chloroform (3 × 10 mL), dried over $MgSO_4$ and evaporated to leave diacetylmorphine base.

6.4. South-East Asian procedure

Diacetylmorphine base (from morphine hydrochloride) (60 mg, 0.16 mmol) was dissolved in acetone (6 mL), and concentrated HCl (18 mL) was added and the solution evaporated under a stream of nitrogen to leave behind diacetylmorphine hydrochloride (57 mg, 86%).

Acknowledgements

L.O. is grateful for financial support from the Australian Forensic Drug Laboratory (AGAL, Pymble, NSW, Australia). We are also grateful for the donation from the National Analytical Reference Laboratory of the alkaloid reference samples used in this work. We also thank the Australian Federal Police for allowing access to seized heroin samples, without which this work would not have been possible.

References

[1] United Nations Drug Control Program, World Illicit Drugs Report 2000–01, New York, 2001.
[2] Australian Bureau of Criminal Intelligence, Australian Illicit Drug Report 1998–99, 2000.
[3] Australian Bureau of Criminal Intelligence, Australian Illicit Drug Report 2000–01, 2002.
[4] Australian Institute of Criminology, 2001. Trends in the Prevalence of Drugs, Australia 1988–1998, National Drug Strategy Household Survey, Unit Record Files, 1988–1998, http://www.aic.gov.au/research/drugs/stats/prevalence/trendsdrugs88-98.html (3-25-2002).
[5] D.A. Cooper, in: M. Klein, F. Sapienza, H. McClain, I. Khan (Eds.), Clandestinely Produced Drugs and Precursors, United States Department of Justice Drug Enforcement Administration, Washington, DC, 1989.
[6] W.R. Heumann, Bull. Narc. 9 (1957) 34.
[7] M. Chiarotti, N. Fucci, C. Furnari, Comparative analysis of illicit heroin samples, Forensic Sci. Int. 50 (1991) 47–56.
[8] H. Neumann, Comments on the routine profiling of illicit heroin samples, Forensic Sci. Int. 44 (1990) 85–87.
[9] H. Neumann, Comparison of heroin by capillary gas chromatography in Germany, Forensic Sci. Int. 69 (1994) 7–16.
[10] P.J. O'Neil, P.B. Baker, T.A. Gough, Illicitly imported heroin products: some physical and chemical features indicative of their origin. Part II, J. Forensic Sci. 30 (1985) 681–691.
[11] B.A. Perillo, R.F.X. Klein, E.S. Franzosa, Recent advances by the US DEA in drug signature and analysis, Forensic Sci. Int. 69 (1994) 1–6.

[12] P.J. O'Neil, J.E. Pitts, Illicitly imported heroin products (1984–1989): some physical and chemical features indicative of their origin, J. Pharm. Pharmacol. 44 (1992) 1.
[13] H. Huizer, Analytical studies on illicit heroin II. Comparison of samples, J. Forensic Sci. 28 (1983) 40–48.
[14] A. Allen, D. Cooper, J. Moore, $\Delta^{16,17}$-Dehydroheroinium chloride: synthesis and characterization of a novel impurity detected in illicit heroin, J. Org. Chem. 48 (1983) 3951.
[15] K. Narayanaswami, H.C. Golani, R.D. Dua, Assay of major and minor constituents of opium samples and studies of their origin, Forensic Sci. Int. 14 (1979) 181.
[16] P.A. Hays, C.P. Goddard, M. Japp, I.J. Humphreys, The characterization of illicit heroin by the analysis of impurities using high-performance liquid chromatography, J. Forensic Sci. 24 (1984) 561.
[17] K. Narayanaswami, Parameters for determining the origin of illicit heroin samples, Bull. Narc. 37 (1985) 49.
[18] C. Barnfield, D.L. Byrom, A.V. Kemmenoe, S. Burns, The routine profiling of forensic heroin samples, Forensic Sci. Int. 39 (1988) 107–117.
[19] A. Johnson, L.A. King, Heroin profiling: predicting the country of origin of seized heroin, Forensic Sci. Int. 98 (1998) 47.
[20] R.B. Myors, S.V. Skopec, P.T. Crisp, R.J. Wells, Investigation of heroin profiling using trace organic impurities, Analyst 126 (2001) 679–689.
[21] A. Allen, D. Cooper, J. Moore, C. Teer, Thebaine rearrangements: nonclassical ring migrations, J. Org. Chem. 49 (1984) 3462.
[22] A. Allen, D. Cooper, J. Moore, M. Gloger, H. Neumann, Illicit heroin manufacturing by products: capillary gas chromatographic determination and structural elucidation of narcotine- and norlaudanosine-related compounds, Anal. Chem. 56 (1984) 2940.
[23] F. Bescier, H. Chaudron-Thozet, Chemical profiling of illicit heroin samples, Forensic Sci. Rev. 11 (1999) 105.
[24] A. Johnson, L.A. King, Heroin profiling: predicting the country of origin of seized heroin, Forensic Sci. Int. 95 (1998) 47.
[25] J.A. Sibley, Formation of O-6-acetylmorphine in the 'Homebake' preparation of heroin, Forensic Sci. Int. 44 (1996) 110.
[26] R.B. Myors, P.T. Crisp, S.Z. Skopec, R.J. Wells, Investigation of heroin profiling using trace organic impurities, Analyst 126 (2001) 679.
[27] M. Desage, R. Guilluy, J.L. Brazier, H. Chaudron, J. Girard, H. Cherpin, J. Jumeau, Gas chromatography with mass spectrometry or isotope-ratio mass spectrometry in studying the geographical origin of heroin, Anal. Chim. Acta 247 (1991) 249.
[28] F. Becacier, H. Chaudron-Thozet, M. Rousseau-Tsangaris, J. Girard, A. Lamotte, Comparative chemical analysis of drug samples: general approach and application to heroin, Forensic Sci. Int. 85 (1997) 113.
[29] S. Klemenc, In common batch searching of illicit heroin samples—evaluation of data by chemometrics methods, Forensic Sci. Int. 115 (2001) 43.
[30] K. Janhunen, M.D. Cole, Development of a predictive model for batch membership of street samples of heroin, Forensic Sci. Int. 102 (1999) 1.
[31] L. Stromberg, L. Lundberg, H. Neumann, B. Bobon, H. Huizer, N.W. van der Stelt, Heroin impurity profiling. A harmonisation study for retrospective comparisons, Forensic Sci. Int. 114 (2000) 67.
[32] M. Chiarotti, N. Fucci, Comparative analysis of heroin and cocaine seizures, J. Chrom. B 733 (1999) 127–136.
[33] P.J. O'Neill, P.B. Baker, T.A. Gough, Illicitly imported heroin products: some physical and chemical features indicative of their origin, J. Forensic Sci. 29 (1984) 899–902.
[34] B. Remberg, A. Nikiforov, G. Buchbauer, Fifty years of opium characterisation methods, Bull. Narc. XLVI (1994) 79–108.
[35] N.K. Nair, V. Navaratnam, V. Rajananda, An effective thin-layer chromatographic system for separating eight opiates and five adulterants, J. Chrom. A 366 (1986) 363.
[36] I.S. Lurie, Application of micellar electrokinetic capillary chromatography to the analysis of illicit drugs, J. Chrom. A 780 (1997) 265.
[37] P.A. Hays, I.S. Lurie, Quantitative analysis of adulterants in illicit heroin samples via revered phase HPLC, J. Liq. Chrom. 14 (1991) 3513.
[38] United Nations Drug Control Program, Recommended Methods for Testing Opium, Morphine and Heroin, United Nations, New York, 1998.
[39] DEA Special Testing and Research Laboratory, Ethylene diacetate—a substitute for acetic anhydride in heroin production, Microgram 20 (1987) 195.
[40] J. Skopec, S.Z. Skopec, unpublished results.
[41] J.M. Tedder, The use of trifluoroacetic anhydride and related compounds in organic synthesis, Chem. Rev. 55 (1955) 787.
[42] E.J. Bourne, M. Stacey, J.C. Tatlow, J.M. Tedder, Studies on trifluoroacetic acid Part I. Trifluoroacetic anhydride as a promotor of ester formation between hydroxy-compounds and carboxylic acids, J. Chem. Soc. (1949) 2976.
[43] United Nations Office on Drugs and Crime, http://www.unodc.org/unodc/en/undcp.html.
[44] F.W. McClafferty, F. Turecek, Interpretation of Mass Spectra, fourth ed., University Science Books, Mill Valley, 1993.
[45] G.A. Cordell, Introduction to Alkaloids, first ed., John Wiley and Sons, Brisbane Australia, 1981.
[46] D. Wheeler, T.H. Kinstle, K.L. Rinehart, Mass spectral studies of alkaloids related to morphine, J. Am. Chem. Soc. 89 (1967) 4494.
[47] H. Huizer, Analytical studies on illicit heroin I. The occurrence of O3-monoacetylmorphine, J. Forensic Sci. 28 (1983) 32.
[48] A.R.L. Wijesekera, D. Abeysinghe, K.C. Pathirana, Studies on the degradation of heroin, Forensic Sci. Int. 67 (1994) 147.

ELSEVIER

Forensic Science International 164 (2006) 230–234

Forensic Science International

www.elsevier.com/locate/forsciint

Morphological comparison between *Chrysomya rufifacies* (Macquart) and *Chrysomya villeneuvi* Patton (Diptera: Calliphoridae) puparia, forensically important blow flies

Kabkaew L. Sukontason [a,*], Paitoon Narongchai [b], Chaturong Kanchai [b], Karnda Vichairat [b], Somsak Piangjai [a], Worachote Boonsriwong [a], Nophawan Bunchu [a], Duanghatai Sripakdee [a], Tarinee Chaiwong [a], Budsabong Kuntalue [c], Sirisuda Siriwattanarungsee [a], Kom Sukontason [a]

[a] *Department of Parasitology, Faculty of Medicine, Chiang Mai University, Chiang Mai 50200, Thailand*
[b] *Department of Forensic Medicine, Faculty of Medicine, Chiang Mai University, Chiang Mai 50200, Thailand*
[c] *Electron Microscopy Research and Service Center (EMRSC), Faculty of Science, Chiang Mai University, Chiang Mai 50200, Thailand*

Received 28 April 2005; accepted 4 February 2006
Available online 9 March 2006

Abstract

In Thailand, the hairy maggots of the blow flies, *Chrysomya rufifacies* (Macquart) and *Chrysomya villeneuvi* Patton, are of forensic importance. Both flies are closely related species, not only in the morphological appearance of their larvae and puparia, but also on the aggressive feeding habit of the former. In our continuing studies of forensically important flies, identification of immature ones needs particular attention. In this study, we reported the morphological comparison between the puparia of these two blow fly species using scanning electron microscopy (SEM). Observation revealed that the cuticular sculpture of tubercles along the dorsal and lateral segments had markedly different features: with *C. rufifacies* having many sharp spines assembling only at the tip, while of *C. villeneuvi* bore stout spines throughout the tubercle. A larger number of globules at the bubble membrane on the dorsolateral border of the fifth segment was found in *C. villeneuvi* (average 225) than in *C. rufifacies* (average 35), and more papillae was observed on the anterior spiracle in *C. villeneuvi* (13–15) than in *C. rufifacies* (9–12). However, the morphology of distinct net-like patches of the integument and structure of the posterior spiracle of both species were almost identical. Morphological comparison in this study permitted identification of the puparia of both fly species, particularly in areas where they co-exist.

Keywords: *Chrysomya rufifacies*; *Chrysomya villeneuvi*; Puparia; Identification; Forensic entomology

1. Introduction

Fly specimens found in corpses and/or death scenes can be used as entomological evidence in forensic investigations of death, i.e. estimation of the postmortem interval, determination of toxic substances, antemortem trauma and verify relocation [1–4]. Not only are the eggs and larvae of flies important as evidence, but puparia is also found to provide valuable information long after the remains of the body have decomposed. Such examples of fly puparia used in investigations of a case scenario by either viable puparia or the empty puparial cases have been recorded [5]. Detection of toxic substances (e.g. drugs, pesticides, environmental pollutants) in fly puparia have also been reported [6–9]. However, prior to their use in forensic investigation, correct species identification of fly specimens collected from a corpse is mandatory, since the developmental rate of each species may be different by either temperature or toxic substance.

Chrysomya rufifacies (Macquart) and *Chrysomya villeneuvi* Patton are blow flies of forensic importance in many countries of the world including Thailand [1,4,5,10–13]. Both species share several similarities, for example the anatomical features of their larvae as ''hairy maggot'', geographical distribution, and aggressive feeding habit of the second and third instars [13,14]. Morphology of their larvae have been compared [14,15], however no comparison between their puparia has been found in the literature. We report, herein, the comparison of the morphological features between puparia of *C. rufifacies* and *C.*

* Corresponding author. Tel.: +66 53 945342; fax: +66 53 217144.
E-mail address: klikitvo@mail.med.cmu.ac.th (K.L. Sukontason).

0379-0738/$ – see front matter
doi:10.1016/j.forsciint.2006.02.012

villeneuvi, highlighting their important characteristics to identify them by SEM. This information will be beneficial for identification before puparia of these species are found in a corpse and/or at a death scene and used for further forensic analysis.

2. Materials and methods

Puparia of *C. rufifacies* were obtained from a laboratory colony maintained at the Department of Parasitology, Faculty of Medicine, Chiang Mai University. As for *C. villeneuvi*, puparia derived from the metamorphosis of numerous larvae collected from two unknown male human remains, which had been transferred to the Department of Forensic Medicine, Chiang Mai University, Thailand, for forensic investigation on 4 February 2004. These remains of unknown age were discovered in forested area in Lampang Province, northern Thailand (north latitude 18° and east latitude 99°).

For SEM observation, puparia of each species, which had been kept in 70% alcohol, were washed by shaking ≈20 min in a shaking bath. They were prepared for the SEM by mopping up water on the surface with filter paper and then gently placing onto double-stick tape on stubs and coating with gold for 30 s in a sputter-coating apparatus (SPI-MODULE^{TM} Coater Sputter,

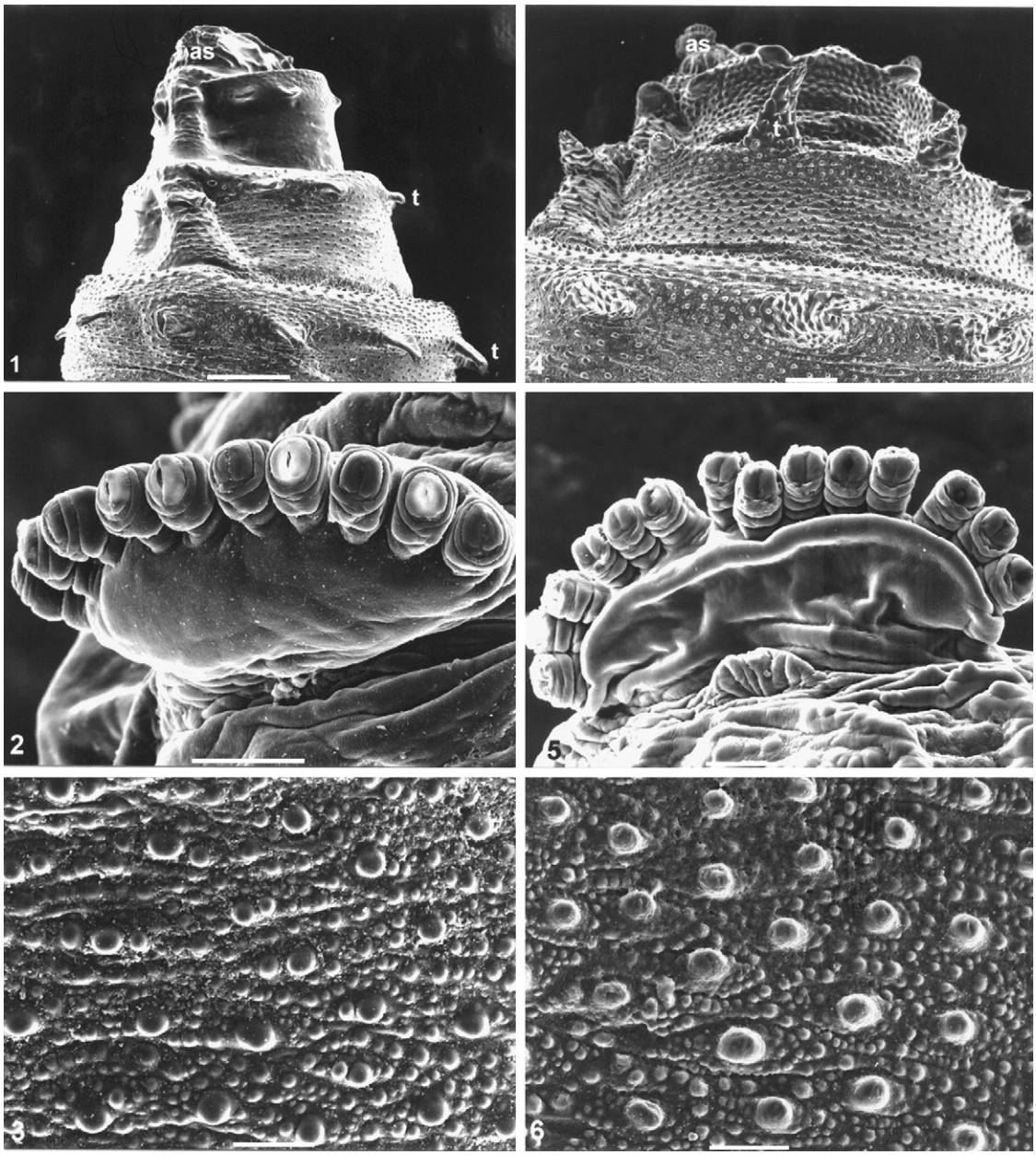

Figs. 1–6. Scanning electron micrographs of puparia of *C. rufifacies* and *C. villeneuvi*. (1) Anterior end of *C. rufifacies* showing anterior spiracle (as) and tubercles (t); bar = 500 μm. (2) Anterior spiracle of *C. rufifacies* having a single row of 10 papillae; bar = 50 μm. (3) Integument of *C. rufifacies* covered with distinct net-like patches; bar = 50 μm. (4) Anterior end of *C. villeneuvi* showing anterior spiracle (as) and tubercles (t); bar = 200 μm. (5) Anterior spiracle of *C. villeneuvi* having a single row of 14 papillae; bar = 50 μm. (6) Integument of *C. villeneuvi* covered with distinct net-like patches; bar = 50 μm.

USA). This enabled viewing under a JEOL JSM-5910LV scanning electron microscope (SEM; Tokyo, Japan) using a high vacuum mode.

3. Results

Puparia of *C. rufifacies* and *C. villeneuvi* were hairy in appearance; pointed anteriorly and blunt posteriorly. The former species measured 8.5 ± 0.4 mm in length ($n = 12$) and not statistically different from the latter, measured 8.3 ± 0.3 mm in length ($n = 12$) ($p > 0.05$; Mann–Whitney U test). At the anterior end, a pair of anterior spiracles was laterally prominent at the second segment (prothorax). Strong tubercles were strikingly noticeable, beginning at the fourth segment (Figs. 1 and 4). A single row of 10 papillae could be observed at the anterior spiracle of *C. rufifacies* (Fig. 2), in contrast to a single row of 14 papillae in *C. villeneuvi* (Fig. 5). The integument of the puparia of both species resembled each other, covered with distinct net-like patches (Figs. 3 and 6). Focusing on the tubercles along dorsal and lateral segments of the puparia, elongated tubercles were obviously different; those of *C. rufifacies* having slender spines assembling only at the tips (Fig. 7), and in contrast, those of *C. villeneuvi* bearing stout spines throughout the surface (Fig. 9). At the dorso-lateral margins of the fifth segment of the puparia, a group of globular structures called bubble membrane was detected. The number of globules was markedly distinct, with *C. rufifacies* having ≈35 globules (Fig. 8); while *C. villeneuvi* had ≈225 globules ($n = 2$) (Fig. 10). At the caudal segment, six pairs of elongated tubercles were similarly located marginally (Figs. 11 and 14). However, when focusing on the surface of these tubercles, a similar appearance to that seen in the third instar was observed. Tubercles of *C. rufifacies* possessed slender spines assembling only at the tips (Fig. 12); while short, stout spines existed throughout the surface in *C. villeneuvi* (Fig. 15). A pair of posterior spiracles was located centrally at the caudal segments (Figs. 11 and 14); nevertheless, no distinction was detected in the morphology characteristic of the posterior spiracles (e.g. shape and arrangement of posterior spiracular slits, position of button, arrays of posterior spiracular hairs) between *C. rufifacies* (Fig. 13) and *C. villeneuvi* (Fig. 16).

4. Discussion

Differentiation between puparia of *C. rufifacies* and *C. villeneuvi* is not simple, according to their hairy appearance and similar size. As morphological features previously described, puparia of both blow fly species shared some features that could not be differentiated, even when using SEM. These characteristics were the integument architecture of the net-like patches (see Figs. 3 and 6) and the morphology of the posterior spiracles (see Figs. 13 and 16). Geographically, *C. rufifacies* and *C.*

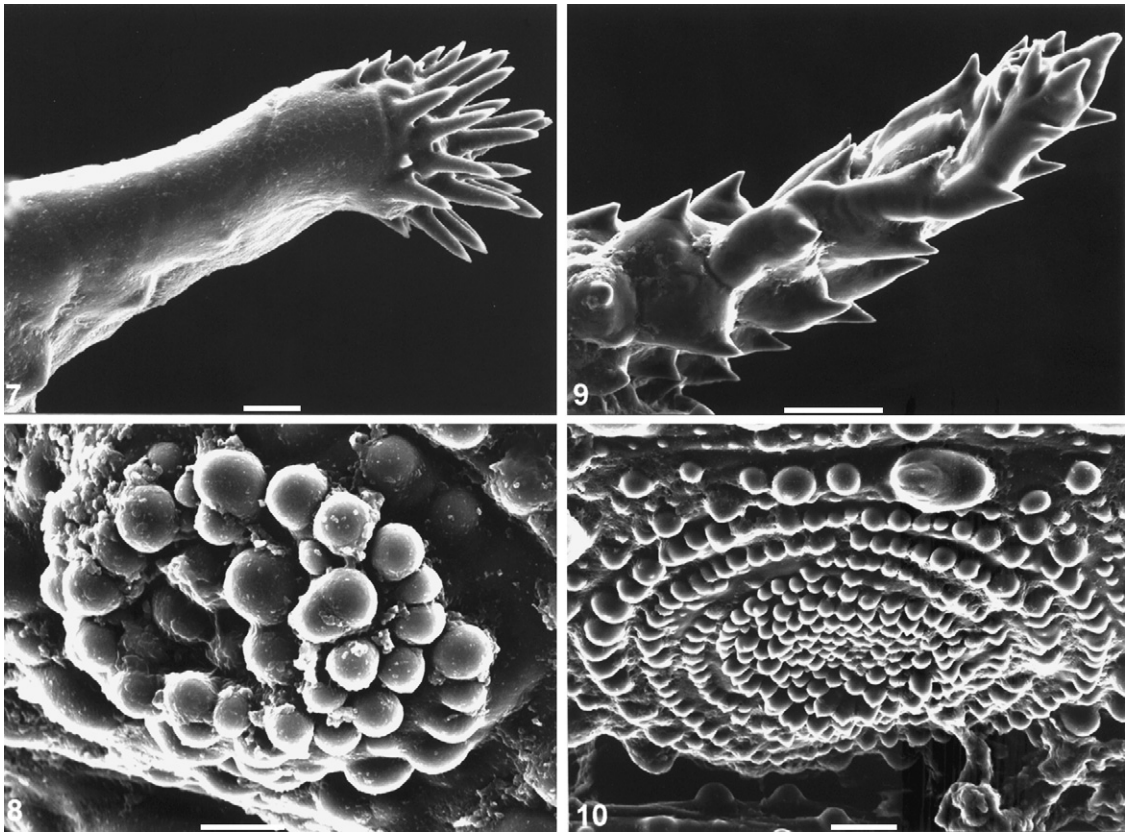

Figs. 7–10. Scanning electron micrographs of puparia of *C. rufifacies* and *C. villeneuvi*. (7) Elongate tubercle of *C. rufifacies* showing slender spines assembled only at the tip; bar = 20 μm. (8) Group of ≈35 globules of bubble membrane at the dorso-lateral margins of the fifth segment of *C. rufifacies*; bar = 10 μm. (9) Elongate tubercle of *C. villeneuvi* bearing stout spines throughout the surface; bar = 50 μm. (10) Group of ≈225 globules of bubble membrane of *C. villeneuvi*; bar = 20 μm.

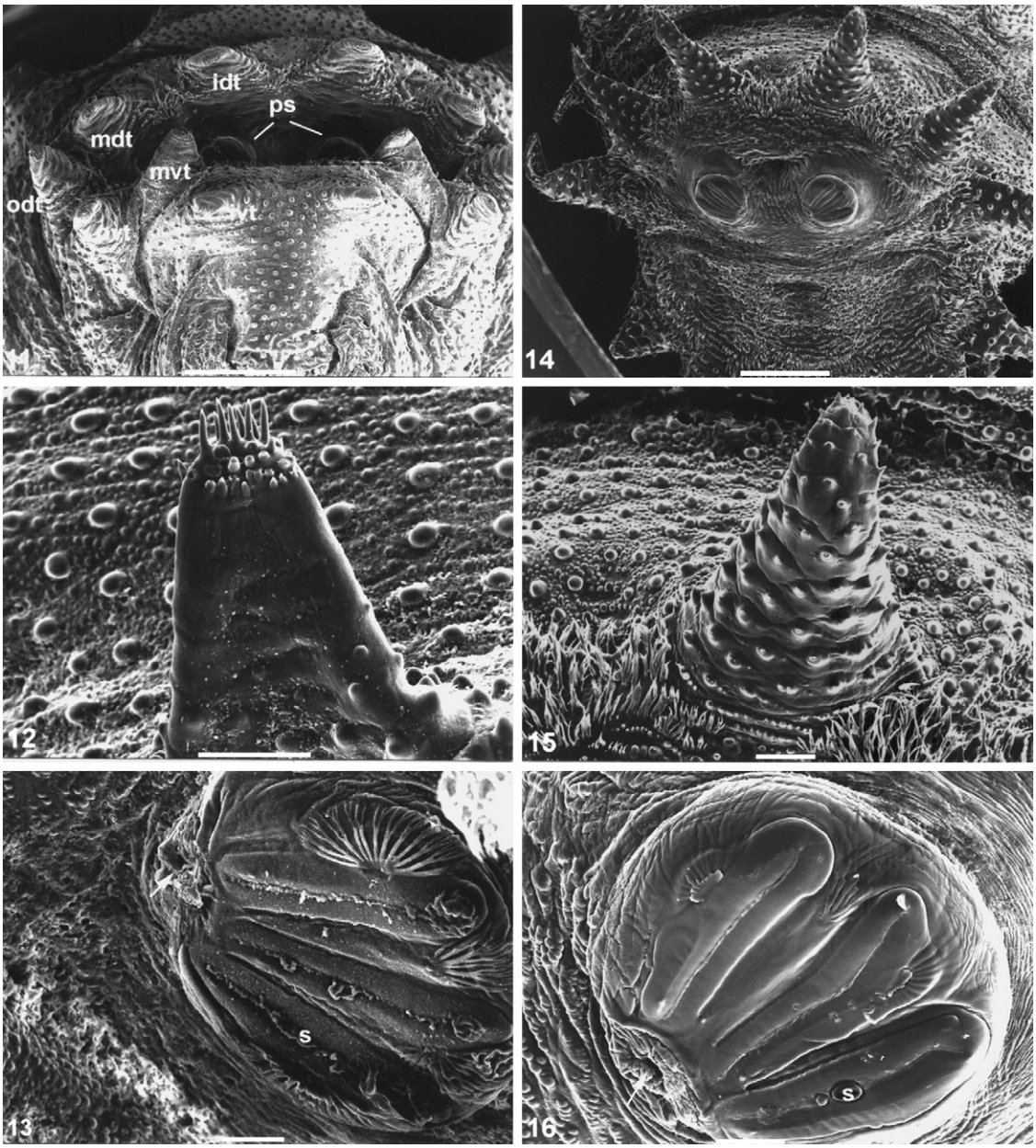

Figs. 11–16. Scanning electron micrographs of puparia of *C. rufifacies* and *C. villeneuvi*. (11) Caudal segment of *C. rufifacies* showing a pair of posterior spiracles (ps) and six pairs of tubercles along the margin. Idt, inner dorsal tubercle; mdt, median dorsal tubercle; odt, outer dorsal tubercle; ovt, outer ventral tubercle; mvt, median ventral tubercle; ivt, inner ventral tubercle, bar = 500 μm. (12) Inner dorsal tubercle of *C. rufifacies* having slender spines assembled only at the tip, bar = 100 μm. (13) Posterior spiracle of *C. rufifacies* indicating three slits(s). Arrow indicated button, bar = 50 μm. (14) Caudal segment of *C. villeneuvi* showing a pair of posterior spiracles and six pairs of tubercles along the margin, bar = 500 μm. (15) Inner dorsal tubercle of *C. villeneuvi*, bearing short, stout spines throughout the surface, bar = 100 μm. (16) Posterior spiracle of *C. villeneuvi* indicating three slits(s). Arrow indicated button, bar = 50 μm.

villeneuvi overlap in territories. *C. rufifacies* expand in distribution throughout tropical and subtropical areas, and North America [20], whereas *C. villeneuvi* are found in many Asian countries [China (Yunnan, Hainan Is.), Vietnam, Laos, Thailand, Malaysia, Indonesia (Sumatra), Nepal, India, and Sri Lanka] [21].

The results of this study clearly showed that puparia of *C. rufifacies* and *C. villeneuvi* could be morphologically differentiated. The most distinctive characteristic observed using SEM was the ornament of elongated tubercles of the puparia (see Figs. 7, 9, 12, and 15). The presence of slender spines assembling only at the tips of *C. rufifacies* tubercles (Figs. 7 and 12) corresponded with those seen in the third instar observed using SEM [13,16] or light microscopy [14]. Likewise, the short, stout spines existing throughout the surface in *C. villeneuvi* puparia (Figs. 9 and 15) agreed with those in third instar using light microscopy [14]. Another characteristic difference between the puparia of both species was the number of globules at the bubble membrane on the dorso-lateral border of the fifth segment, and this could only be observed by SEM. A larger number of globules was found in *C. villeneuvi* (Fig. 10) than in *C. rufifacies* (Fig. 8). Difference in the number of globules was one of the

characteristics used for differentiating puparia of forensically important fly species [17]. The final characteristic was the number of papillae on the anterior spiracle of the puparia. This character might be seen using light microscopy. Nine to 12 papillae were found in *C. rufifacies*, which agreed with the third instar previously reported [13,15,18,19], while 13–15 papillae were found in *C. villeneuvi*, which also agreed with the third instar previously reported [14,15].

The results presented herein enable identification of the puparia of both species, which have a hairy appearance.

Acknowledgements

We thank the Faculty of Medicine and Chiang Mai University, for publication cost.

References

[1] K.G.V. Smith, A Manual of Forensic Entomology, British Museum (Natural History), London, United Kingdom, 1986.
[2] R.D. Hall, Medicocriminal entomology, in: E.P. Catts, N.H. Haskell (Eds.), Entomology and Death, A Procedural Guide, Joyce's Print Shop, Clemson, SC, 1990, pp. 1–8.
[3] E.P. Catts, Problems in estimating the postmortem interval in death investigations, J. Agric. Entomol. 9 (1992) 245–255.
[4] B. Greenberg, J.C. Kunich, Entomology and the Law: Flies as Forensic Indicators, Cambridge University Press, United Kingdom, 2002.
[5] W.D. Lord, Case histories of the use of insects in investigations, in: E.P. Catts, N.H. Haskell (Eds.), Entomology and Death, A Procedural Guide, Joyce's Print Shop, Clemson, SC, 1990, pp. 9–37.
[6] M.L. Miller, W.D. Lord, M.L. Goff, B. Donnelly, E.T. McDonough, J.C. Alexis, Isolation of amitryptiline and nortryptiline from fly puparia (Phoridae) and beetle exuviae (Dermestidae) associated with mummified remains, J Forensic Sci. 39 (1994) 1305–1313.
[7] M.L. Goff, M.L. Miller, J.D. Paulson, W.D. Lord, E. Richards, A.I. Omori, Effects of 3,4-methylenedioxymethamphetamine in decomposing tissues on the development of *Parasarcophaga ruficornis* (Diptera: Sarcophagidae) and detection of the drug in postmortem blood, liver tissue, larvae, and puparia, J. Forensic Sci. 42 (1997) 276–280.
[8] R. Gagliano-Candela, L. Aventaggiato, The detection of toxic substances in entomological specimens, Int. J. Legal Med. 114 (2001) 197–203.
[9] M. Wood, M. Laloup, K. Pien, N. Samyn, M. Morris, R.A.A. Maes, E.A. de Bruijn, V. Maes, G. De Boeck, Development of a rapid and sensitive method for the quantitation of benzodiazepines in *Calliphora vicina* larvae and puparia by LC-MS-MS, J. Anal. Toxicol. 27 (2003) 505–512.
[10] M. Barreto, M.E. Burbano, P. Barreto, Flies (Calliphoridae, Muscidae) and beetles (Silphidae) from human cadavers in Cali, Colombia, Mem. Inst. Oswaldo Cruz 97 (2002) 137–138.
[11] K.L. Sukontason, K. Sukontason, P. Narongchai, S. Lertthamnongtham, S. Piangjai, J.K. Olson, *Chrysomya rufifacies* (Macquart) as a forensically-important fly species in Thailand: A case report, J. Vector Ecol. 26 (2001) 162–164.
[12] K. Sukontason, K.L. Sukontason, T. Chaiwong, N. Boonchu, S. Piangjai, H. Kurahashi, Hairy maggot of *Chrysomya villeneuvi* Patton (Diptera: Calliphoridae), a fly species of forensic importance, J. Med. Entomol. 40 (2003) 983–984.
[13] K.L. Sukontason, K. Sukontason, S. Lertthamnongtham, B. Kuntalue, N. Thijuk, R.C. Vogtsberger, J.K. Olson, Surface ultrastructure of *Chrysomya rufifacies* (Macquart) larvae (Diptera: Calliphoridae), J. Med. Entomol. 40 (2003) 259–267.
[14] K. Sukontason, K.L. Sukontason, S. Piangjai, P. Narongchai, W. Samai, N. Boonchu, D. Sripakdee, R. Ngern-klun, S. Siriwattanarungsee, Morphology of second and third instars of *Chrysomya villeneuvi* Patton (Diptera: Calliphoridae), a fly species of forensic importance, Forensic Sci. Int. 154 (2005) 195–199.
[15] B. Omar, Key to third instar larvae of flies of forensic importance in Malaysia, in: B. Greenberg, J.C. Kunich (Eds.), Entomology and the Law: Flies as Forensic Indicators, Cambridge University Press, Cambridge, 2002, pp. 120–127.
[16] J.D. Wells, J.H. Byrd, T.I. Tantawi, Key to third-instar Chrysomyinae (Diptera: Calliphoridae) from carrion in the Continental United States, J. Med. Entomol. 36 (1999) 638–641.
[17] D. Liu, B. Greenberg, Immature stage of some flies of forensic importance, Ann. Entomol. Soc. Am. 82 (1989) 80–93.
[18] H. Ishijima, Revision of the third stage larvae of synanthropic flies of Japan (Diptera: Anthomyiidae, Muscidae, Calliphoridae and Sarcophagidae), Jpn. J. Sanit. Zool. 18 (1967) 47–100.
[19] R.L. Kitching, The immature stages of the Old-World screw-worm fly, *Chrysomya bezziana* Villeneuve, with comparative notes on other Australasian species of *Chrysomya* (Diptera, Calliphoridae), Bull. Entomol. Res. 66 (1976) 195–203.
[20] D.L. Baumgartner, Review of *Chrysomya rufifacies* (Diptera: Calliphoridae), J. Med. Entomol. 30 (1993) 338–352.
[21] H. Kurahashi, L. Chowanadisai, Blow flies (Insecta: Diptera: Calliphoridae) from Indochina, Species Divers 6 (2001) 185–242.

ELSEVIER

Forensic Science International 164 (2006) 235–239

Forensic Science International

www.elsevier.com/locate/forsciint

The redistribution of selected psychiatric drugs in post-mortem cases

Kabrena E. Rodda, Olaf H. Drummer *

Victorian Institute of Forensic Medicine, Department of Forensic Medicine, Monash University, 57-83 Kavanagh Street, Southbank, Vic. 3006, Australia

Received 5 July 2005; received in revised form 12 January 2006; accepted 4 February 2006
Available online 22 March 2006

Abstract

The post-mortem redistribution of a number of psychiatric drugs was investigated. A portion of liver, the gastric contents and blood collected from heart and femoral sites was obtained from 13 cases and analyzed by liquid chromatography–mass spectrometry. Drugs detected included five selective serotonin reuptake inhibitors; venlafaxine, a serotonin/noradrenaline reuptake inhibitor; and risperidone, an atypical antipsychotic. Heart blood concentrations were significantly higher (3.4-fold on average) than those measured in femoral blood when results from all drugs were included together. The range for parent drug concentrations in these two blood specimens was 0.5–6.2. There was no significant correlation of the post-mortem interval, the liver concentration and content of drugs in the gastric contents to the heart:femoral blood concentration ratio. These data serve to demonstrate that variable increases in blood concentration occur post-mortem and limit the interpretative value of such toxicological data.

Keywords: Post-mortem redistribution; Psychiatric drugs; LC–MS

1. Introduction

Post-mortem redistribution, in which drug concentrations in blood specimens from various areas of the body change during the post-mortem interval, has been observed for many drugs. This is believed to occur largely through diffusion from a high to a low concentration and is believed to be time dependent. The extent to which a drug undergoes post-mortem redistribution is also dependent on protein binding and lipophilicity. Drugs with high volumes of distribution, i.e. greater than 3 L/kg, are thus more prone to post-mortem redistribution [1–3]. Diffusion of drug from the gastrointestinal tract into neighboring tissues has also been shown to contribute to redistribution [2,4,5]. An understanding of post-mortem tissue distribution is therefore important to determine the role of these drugs in the death process.

Tissue distribution of several serotonin reuptake inhibitors (SSRI) and atypical antidepressants has been studied [6–13]. In many cases, only one blood sample was taken, so it was impossible to determine if redistribution had actually occurred. In cases where both central and peripheral blood specimens were taken, no significant difference was seen for sertraline [8,11]. However, slight differences in paroxetine and fluoxetine concentrations were observed in central versus peripheral blood in one case of a subject who died in hospital [13], but neither drug was present on admission. It was suggested that the drugs were administered in hospital and the differences in concentration between the two specimens were most likely a result of incomplete absorption. In the two studies in which post-mortem peripheral and central blood venlafaxine and metabolite concentrations were compared, central blood concentrations were approximately 1.5–2 times those found in peripheral blood [8,9,12].

These studies do not allow a definitive conclusion to be made regarding redistribution of antidepressant drugs in general, or even many of the individual drugs already discussed. However, the uneven tissue distribution patterns often observed for these drugs, combined with their relatively high volumes of distribution (up to 28 L/kg), significant protein binding (0.27–0.99) and relatively high lipophilicity (log P = 2.9–5.4) suggest that post-mortem redistribution is very likely. We have assessed the degree of redistribution of selected psychiatric drugs by analyzing blood specimens collected from heart and femoral sites. Since the possibility exists for drugs in the stomach contents to diffuse into the liver or centrally collected blood, this heart:femoral blood concentration ratios were compared to drug concentrations measured in liver and stomach contents.

* Corresponding author. Tel.: +61 3 9684 4334; fax: +61 3 9682 7353.
E-mail address: olaf@vifm.org (O.H. Drummer).

0379-0738/$ – see front matter
doi:10.1016/j.forsciint.2006.02.013

2. Materials and methods

2.1. Specimen collection

Cases were selected based on circumstances where one or more of the target drugs were likely to have been used by deceased. Matched post-mortem femoral and heart post-mortem blood specimens were collected in 10 mL plastic tubes containing preservative (1% sodium fluoride and potassium oxalate) and were stored at −20 °C until assay. Specimens were classified according to their consistency (i.e. thin or watery looking or viscous) and color.

2.2. Specimen preparation

All cases were subject to a full toxicological examination for the presence of range of common drugs. When drugs were detected these were confirmed by standard GC–MS techniques. For quantification purposes parent drugs and where relevant metabolite concentrations were measured. The extraction technique used was performed based on a procedure described by McIntyre et al. [14] and modified for use with LC–MS as described previously using trazodone as internal standard [15,16].

2.3. LC–MS conditions

LC–MS analysis was performed on a 1100 Series HPLC (Agilent Technologies, Forest Hill, Vic., Australia) configured with a G1946A mass selective detector (MSD). It was operated in positive mode APES as described previously [15]. For quantification purposes, mass spectral detection was conducted in the SIM mode.

2.4. Post-mortem intervals (PMI)

The time of death, time of admission to the Institute and time of autopsy were recorded for each case included in this study. The post-mortem interval was the estimated time between death and autopsy. In cases where the time of death was unknown, the time of death was taken as the half-way point between when the subject had last been seen alive and when he or she was found dead.

2.5. Statistical analyses

Statistical evaluation of the data was performed using SigmaStat 2.03 (SPSS Inc.) and software on an IBM personal computer. Kruskal–Wallis one-way ANOVA at the 95% confidence interval were used to determine whether differences between heart and femoral blood concentrations were statistically significant. Pearson correlations were used to determine statistical significance of correlations between heart:femoral blood concentration ratios and each of the following pharmacokinetic parameters: volume of distribution (V_d), protein binding (F_b) and lipophilicity (log P). Values for log P were calculated using PALLAS Expert System V3.0 software [17].

2.6. Ethics review process

Ethics approval for the use of these specimens for the purposes of research was obtained through the Institute's Ethical Review Committee and informed consent was obtained from the senior next of kin.

3. Results

3.1. Effect of PMI and redistribution

A total of 13 cases were investigated. The PMI was 64 ± 17 h (range 42–90). In seven cases the exact time of death was known. There was no significant relationship between the PMI and the heart:femoral blood concentration ratio (Table 1).

3.2. Comparison of site of sampling and redistribution

The concentrations of drugs and their metabolites were compared in all 13 matched autopsy femoral and heart blood specimens (Table 1). Overall, differences in blood concentrations between the two sampling sites was statistically significant (non-parametric ANOVA, $p < 0.05$). The average heart:femoral blood concentration ratio was 3.4, although there was substantial variability within and between drugs. Heart:-femoral blood concentration ratios ranged from 0.50 to 6.2, although they averaged between 2–3:1. With the exception of norfluoxetine in case 2, the mean metabolite concentration ratios were similar to those of their parent drugs. In cases 4, 5 and 12, the heart blood specimen was noticeably lighter in color and therefore thinner than its corresponding femoral blood specimen. Cases 4, 5 and 12 accounted for the highest heart:femoral blood concentration ratios.

3.3. Redistribution from the gastrointestinal tract

Stomach contents were collected and assayed for drug residues in seven cases. Absolute amounts in the positive cases ranged from 0.05 to 2.0 mg. These values were all below the amount of drug contained in one standard tablet. With the exception of cases 2 and 4, the heart blood concentrations were not much higher than those in femoral including those cases for which drug residues were detected in the gastric contents.

3.4. Redistribution from the liver

Liver specimens were collected and analyzed for drug concentrations in 10 cases. Liver drug concentrations ranged from about 0.02 to 13 mg/kg. There was no significant difference in heart blood concentration ratio as a function of liver concentration when liver concentrations were dichotomized to less than and greater than or equal to 1 mg/kg (Table 1).

Table 1
Drug concentrations of selected psychiatric drugs in post-mortem heart and femoral blood and liver specimens in 13 cases and their corresponding heart:femoral ratio

Drug	Case no.	PMI (h)	Heart concentration (mg/L)	Femoral concentration (mg/L)	Heart:femoral ratio	Liver concentration (mg/kg)
Fluoxetine	2	43	0.93	0.15	6.2	3.9
Norfluoxetine	2	43	1.33	0.16	33	2.4
Fluvoxamine	3	46	0.59	0.75	0.79	12
Sertraline	6	53	0.36	0.24	4.8	n.t.
	8	76	0.05	0.05	1.0	3.3
N-Desmethyl sertraline	6	53	0.93	0.42	2.2	n.t.
	8	76	0.26	0.34	0.76	13
Citalopram	7	57	1.8	1.6	1.1	n.t.
Paroxetine	12	83	3.2	0.73	4.4	3.1
	13	90	0.49	0.44	1.1	n.t.
Venlafaxine	5	52	0.28	0.19	5.5	n.d.
	9	77	0.72	0.80	0.90	2.5
	10	79	0.05	0.05	1.0	0.08
	11	80	1.1	1.1	1.0	0.85
O-Desmethyl-venlafaxine	5	52	0.61	0.76	0.80	1.3
	9	77	1.0	1.1	0.91	3.1
	10	79	0.78	0.30	2.6	2.2
	11	80	1.4	0.92	1.5	1.6
Risperidone	1	42	0.01	0.02	0.50	0.05
	4	50	1.8	0.36	5.0	1.0
	8	76	0.33	0.22	1.5	0.22
9-OH-risperidone	1	42	0.01	0.008	1.3	0.05
	4	50	0.18	0.09	2.0	0.10
	8	76	0.50	0.25	2.0	<0.02

N.d.: not detected, n.t.: no liver tissue avaialble, PMI: post-mortem interval.

3.5. Effect of physiochemical properties and extend of redistribution

No significant correlation was observed between concentration ratios and any of the known physiochemical parameters specified in Table 2. There was also no significant difference in the result if drugs were categorized according to drug type (SSRI, SNARI and antipsychotic) or results for all drugs were tested together in one group. If results from previously published studies were also included, correlations still did not reach significance [8–13,18–21].

Table 2
Volumes of distribution (V_d), %protein bound (F_b) and lipophilicity (log P) values for drugs under investigation[a]

Compound	V_d (L/kg)	F_b	log P
Citalopram	15	0.80	3.7
Fluoxetine	26	0.94	4.7
Fluvoxamine	25	0.77	3.1
Paroxetine	16	0.95	3.6
Risperidone	1.2	~0.90	3.3
Sertraline	25	0.99	5.4
Venlafaxine	8	0.27	2.9

[a]log P values calculated using Pallas 3.0 software from CompuDrug [17].

4. Discussion

Individual heart:femoral concentration ratios greater than two were observed with fluoxetine, paroxetine, sertraline, venlafaxine and risperidone, however these were quite variable even for those drugs for which there was more than one case example. For example, the two sertraline cases had ratios of 4.8 and 1.0 and for the four venlafaxine cases the ratios ranged from 1.0 to 5.5. Previous studies on citalopram and venlafaxine have found higher heart:femoral concentration ratios, more in line with that measured in case 5 [9,12,20]. However, the citalopram, venlafaxine and *O*-desmethylvenlafaxine concentrations measured in other studies were not particularly different to those measured in the presented cases for either parent drug or metabolite.

The findings in this study are consistent with both the higher volumes of distribution and protein binding for citalopram and venlafaxine compared to the other drugs. The heart:femoral concentration ratio of *O*-desmethylvenlafaxine was slightly higher than that of venlafaxine (1.5:1 compared to 1.1:1). The difference in ratios between the presented results and those of other studies may be attributable to differences in parent drug:metabolite ratios. Jaffe found venlafaxine exhibited significant post-mortem redistribution, evidenced by an average autopsy:admission blood concentration ratio of

Table 3
Concentrations of psychiatric drugs in central and peripheral blood[a]

Reference	Blood concentrations		Ratio (central:peripheral)
	Central (mg/L)	Peripheral (mg/L)	
Citalopram			
[20]	1.16	0.88	1.32
Fluoxetine			
[8][b]	0.78–0.80 (0.42–0.70)	0.65 (0.53)	1.2 (0.79–1.3)
[19]	0.80 (0.65)	0.23 (0.25)	3.5 (2.6)
[18]	22 (6.8)	4.8 (4.5)	4.6 (1.5)
Fluvoxamine			
[21]	1.5	0.48	3.1
Paroxetine			
[8][b]	0.10–0.18	0.12	0.83–1.5
[13]	3.7	2.9	1.28
Sertraline			
[8][b]	0.38–0.48	0.25	1.5–1.9
[10]	0.23–0.46 (0.08–0.99)	0.23–0.82 (0.17–1.8)	0.56–1.36 (0.55–1.77)
[11]	0.49 (1.40)	0.63 (1.54)	1.29 (1.10)
Venlafaxine			
[8][b]	1.0–1.5	0.5	2.0–3.0
[9]	84 (15)	46 (7.1)	1.83 (2.11)
[12]	17–65 (7.1)	30–85 (5.6)	1.31–1.76 (0.79)

No data were available for risperidone.
[a] Metabolite concentrations listed in parentheses.
[b] Autopsy:admission blood ratios instead of heart:femoral ratios.

2.5:1 [8] (see Table 3). This finding is not surprising in light of the comparatively high volume of distribution of this drug. In contrast, fluvoxamine showed ratios somewhat lower to that reported elsewhere [21]. This also occurred for sertraline [10,11] (see Table 3). The heart:femoral concentration ratios of the metabolites norfluoxetine and 9-OH-risperidone generally reflected those of their parent drugs.

Studies have shown arterial–venous differences in drug concentrations during the drug absorption and distribution phase [3]. Therefore, if a person dies while a drug is still being distributed throughout the body, toxicological results may vary more and will less likely to be predicted than when absorption was complete. This may explain the lower heart:femoral ratios observed in my data for case 3. Since fluvoxamine acid metabolite concentrations were not measured in this case, it is not possible to make conclusions regarding the extent of ante-mortem drug absorption or distribution.

A study of post-mortem redistribution of paroxetine in the rat showed that increases in drug concentrations in post-mortem blood were accompanied by decreased drug concentrations in the lung over the post-mortem interval [22]. Similar conclusions were obtained using citalopram in the rat [23]. This was also observed in dog studies in which decreases in lung and liver concentrations of fluoxetine were accompanied by increases in heart blood concentrations over time [24].

It has also been suggested that in some cases of drug overdose, a certain amount of unabsorbed drug remains in the stomach and gastrointestinal tract (GIT), which can diffuse into abdominal blood vessels post-mortem. This would result in an increase in drug concentrations during the post-mortem interval [25]. Similarly, diffusion from the GIT has been shown to increase drug concentration in the liver in animal [25], and human cadaveric models [5]. In the cases presented here there was no apparent correlation observed between heart to femoral blood concentration ratio with either liver concentration or gastric contents of drugs.

No significant correlation was observed between concentration ratios and any of the known physiochemical parameters specified in Table 2. There was no significant difference in the result if drugs were categorized according to drug type (SSRI, SNARI and antipsychotic) or results for all drugs were tested together in one group.

The lack of any apparent correlation of any of the physiochemical parameters and the extent of heart to femoral blood concentration ratio does suggest that differences in the heart and femoral blood concentration reflects a number of processes that are either still unknown or, more likely, that these are factors are sufficiently variable as to not be predictable.

A significant weakness in our study was the absence of a specimen earlier than that taken at post-mortem. Earlier sampling was not possible due to legal and ethical restraints. It is conceivable that redistribution of whatever mechanism(s) occurs within the first several hours and that by 1–3 days even the femoral blood has become sufficiently elevated as to not be particularly useful [23]. It is also worth noting that even drugs in femoral blood will also be affected by redistribution (and other) processes. The collection of femoral blood reduces the extent of the changes but does not negate the changes.

This variability in heart and femoral blood concentrations suggests that blood concentration variations between heart and femoral blood are too variable to be predictive and allow some degree of certainty over possible estimates of peri-mortem blood concentrations. Nevertheless, these data reassert the need to ensure the site of blood collection is specified.

While more data are needed to understand the complex changes in drug concentration occurring after death these data serve to demonstrate again that post-mortem redistribution is a variable phenomenon and plays a major limiting factor in any interpretation of post-mortem drug concentration in blood.

Acknowledgements

This work was supported in part by the United States Air Force. KER conducted this research as part fulfillment of a dissertation towards a doctor of philosophy at Monash University. The authors thank Agilent Technologies Australia Pty Ltd. for providing loan of the LC–MS. The authors wish to thank the families of the deceased and the staff of the Victorian Institute of Forensic Medicine for providing access to tissue specimens.

References

[1] F.E. Barnhart, K.M. Bonnell, K.M. Rossum, Post-mortem drug redistribution, Forensic Sci. Rev. 13 (2001) 101–129.

[2] R.W. Prouty, W.H. Anderson, The forensic science implications of site and temporal influences on post-mortem blood–drug concentrations, J. Forensic Sci. 35 (2) (1990) 243–270.
[3] D.J. Pounder, The nightmare of post-mortem drug changes, Leg. Med. (1993) 163–191.
[4] F.J. Baud, A. Buisine, C. Bismuth, M. Galliot, E. Vicaut, R. Bourdon, et al., Arterio-venous plasma concentration differences in amitriptyline overdose, J. Toxicol. Clin. Toxicol. 23 (4–6) (1985) 391–406.
[5] D.J. Pounder, E. Adams, C. Fuke, A.M. Langford, Site to site variability of post-mortem drug concentrations in liver and lung, J. Forensic Sci. 41 (6) (1996) 927–932.
[6] J. Bidanset, C. Solerno, E.A. Dettling, A Case Report Involving Fluvoxamine in a Multi-drug Associated Death, Society of Forensic Toxicologists, San Juan, Puerto Rico, 1999.
[7] R.D. Budd, D.T. Anderson, Post-mortem Tissue Distribution of Venlafaxine: Six Case Studies, Society of Forensic Toxicologists, Denver, CO, 1996.
[8] P.D. Jaffe, H.P. Batziris, P. van der Hoeven, D. DeSilva, I.M. McIntyre, A study involving venlafaxine overdoses: comparison of fatal and therapeutic concentrations in post-mortem specimens, J. Forensic Sci. 44 (1) (1999) 193–196.
[9] B. Levine, A.J. Jenkins, M. Queen, R. Jufer, J.E. Smialek, Distribution of venlafaxine in three post-mortem cases, J. Anal. Toxicol. 20 (6) (1996) 502–505.
[10] B. Levine, A.J. Jenkins, J.E. Smialek, Distribution of sertraline in post-mortem cases, J. Anal. Toxicol. 18 (5) (1994) 272–274.
[11] B.K. Logan, P.N. Friel, G.A. Case, Analysis of sertraline (Zoloft) and its major metabolite in post-mortem specimens by gas and liquid chromatography, J. Anal. Toxicol. 18 (3) (1994) 139–142.
[12] A.T. Parsons, R.M. Anthony, J.E. Meeker, Two fatal cases of venlafaxine poisoning, J. Anal. Toxicol. 20 (4) (1996) 266–268.
[13] T. Vermeulen, Distribution of paroxetine in three post-mortem cases, J. Anal. Toxicol. 22 (6) (1998) 541–544.
[14] I.M. McIntyre, M.L. Syrjanen, K. Crump, S. Horomidis, A.W. Peace, O.H. Drummer, Simultaneous HPLC gradient analysis of 15 benzodiazepines and selected metabolites in post-mortem blood, J. Anal. Toxicol. 17 (4) (1993) 202–207.
[15] K.E. Goeringer, M. McIntyre, O.H. Drummer, LC–MS analysis of serotonergic drugs, J. Anal. Toxicol. 27 (1) (2003) 30–35.
[16] K.E. Rodda, B. Dean, I.M. McIntyre, O.H. Drummer, Brain Distribution of Selected Antipsychotics in Schizophrenia, Forensic Science International 157 (2–3) (2006) 121–130.
[17] C. Pallas, Expert System for Today's Chemists, CompDrug International Inc., San Francisco, 1999.
[18] J.R. Roettger, The importance of blood collection site for the determination of basic drugs: a case with fluoxetine and diphenhydramine overdose, J. Anal. Toxicol. 14 (3) (1990) 191–192.
[19] T.P. Rohrig, R.W. Prouty, Fluoxetine overdose: a case report, J. Anal. Toxicol. 13 (5) (1989) 305–307.
[20] K. Fu, R.J. Konrad, R.W. Hardy, R.M. Brissie, C.A. Robinson, An unusual multiple drug intoxication case involving citalopram, J. Anal. Toxicol. 24 (7) (2000) 648–650.
[21] G.W. Kunsman, R. Rodriguez, P. Rodriguez, Fluvoxamine distribution in post-mortem cases, Am. J. Forensic Med. Pathol. 20 (1) (1999) 78–83.
[22] T.C. Kupiec, L.V. Allen, G.P. Basmadjian, et al., Post-mortem Redistribution of Paroxetine using the Rat as a Model, American Academy of Forensic Sciences, San Francisco, CA, 1998.
[23] F.C. Kugelberg, M. Kingback, B. Carlsson, H. Druid, Early-phase post-mortem redistribution of the enantiomers of citalopram and its demethylated metabolites in rats, J. Anal. Toxicol. 29 (4) (2005) 223–228.
[24] R.C. Pohland, N.R. Bernhard, Post-mortem serum and tissue redistribution of fluoxetine and norfluoxetine in dogs following oral administration of fluoxetine hydrochloride (Prozac), J. Forensic Sci. 42 (5) (1997) 812–816.
[25] T. Hilberg, S. Rogde, J. Mørland, Post-mortem drug redistribution—human cases related to results in experimental animals, J. Forensic Sci. 44 (1) (1999) 3–9.

ELSEVIER

Forensic Science International 164 (2006) 240–248

Forensic Science International

www.elsevier.com/locate/forsciint

Automated PCR setup for forensic casework samples using the Normalization Wizard and PCR Setup robotic methods

S.A. Greenspoon [a,*], K.L.V. Sykes [a], J.D. Ban [a], A. Pollard [b], M. Baisden [a], M. Farr [c], N. Graham [d], B.L. Collins [a], M.M. Green [e], C.C. Christenson [f]

[a] *Virginia Department of Forensic Science, 700N. 5th St., Richmond, VA 23219, United States*
[b] *Virginia Department of Forensic Science, 830 Southampton Avenue, Suite 400, Norfolk, VA 23510-1028, United States*
[c] *Virginia Department of Forensic Science, 9797 Braddock Road #200, Fairfax, VA 22032-1744, United States*
[d] *Virginia Department of Forensic Science, 6600 Northside High School Road, Roanoke, VA 24019-2837, United States*
[e] *Montgomery County Department of Police Crime Laboratory, 2350 Research Blvd., Rockville, MD 20850, United States*
[f] *2490 E. Kentucky Avenue, Salt Lake City, UT 84117, United States*

Received 31 October 2005; received in revised form 25 January 2006; accepted 5 February 2006
Available online 20 March 2006

Abstract

Human genome, pharmaceutical and research laboratories have long enjoyed the application of robotics to performing repetitive laboratory tasks. However, the utilization of robotics in forensic laboratories for processing casework samples is relatively new and poses particular challenges. Since the quantity and quality (a mixture versus a single source sample, the level of degradation, the presence of PCR inhibitors) of the DNA contained within a casework sample is unknown, particular attention must be paid to procedural susceptibility to contamination, as well as DNA yield, especially as it pertains to samples with little biological material.

The Virginia Department of Forensic Science (VDFS) has successfully automated forensic casework DNA extraction utilizing the DNA IQ™ System in conjunction with the Biomek® 2000 Automation Workstation. Human DNA quantitation is also performed in a near complete automated fashion utilizing the AluQuant® Human DNA Quantitation System and the Biomek® 2000 Automation Workstation. Recently, the PCR setup for casework samples has been automated, employing the Biomek® 2000 Automation Workstation and Normalization Wizard, Genetic Identity version, which utilizes the quantitation data, imported into the software, to create a customized automated method for DNA dilution, unique to that plate of DNA samples. The PCR Setup software method, used in conjunction with the Normalization Wizard method and written for the Biomek® 2000, functions to mix the diluted DNA samples, transfer the PCR master mix, and transfer the diluted DNA samples to PCR amplification tubes. Once the process is complete, the DNA extracts, still on the deck of the robot in PCR amplification strip tubes, are transferred to pre-labeled 1.5 mL tubes for long-term storage using an automated method. The automation of these steps in the process of forensic DNA casework analysis has been accomplished by performing extensive optimization, validation and testing of the software methods.

Keywords: Forensic science; Automation; Biomek® 2000; Normalization Wizard; PCR; Short tandem repeats

1. Introduction

Forensic laboratories in the United States are facing escalating backlogs of DNA cases [1]. Advances in DNA typing technology have not only expanded the types of probative evidence available at crime scenes, but have compelled a substantial increase in the number of items submitted for DNA testing by virtue of the fact that detectives, prosecutors and defense attorneys want to leave "no stone unturned", and with advances in technology this can be accomplished. The tremendous demand for DNA analysis without a corresponding growth in forensic laboratory capacity has resulted in a large backlog of DNA casework samples nationally. One of several recommendations by the National Institute of Justice (NIJ) to help reduce the backlog, is to promote automation to expedite labor and time intensive procedures [2].

Automation of forensic casework DNA extraction is relatively new and its implementation posed particular challenges [3–7]. Since both the quantity and quality of the DNA contained within a casework sample is unknown, particular attention must be paid to procedural susceptibility to contamination, as well as DNA

* Corresponding author. Tel.: +1 804 786 0456; fax: +1 804 786 0456.
E-mail address: Susan.Greenspoon@dfs.virginia.gov (S.A. Greenspoon).

0379-0738/$ – see front matter
doi:10.1016/j.forsciint.2006.02.027

yield, especially as it pertains to samples with little biological material since these samples can be especially challenging [8,9]. Automation of forensic DNA quantitation is more widely practiced in forensic labs than the DNA extraction and PCR setup; this may be in part since automation of DNA quantitation has a great impact on casework throughput with little risk to the samples, such as the introduction of contaminants. Thus, validation and implementation are simplified [10–13]. Automation of the PCR setup for casework samples carries with it many of the same risks as for automated DNA purification. Special care must be taken to assess whether the system is susceptible to contamination and when making modifications to increase performance in other ways, such as the speed of the process, questions must be addressed as to whether the modifications introduce contamination or unanticipated problems.

The Virginia Department of Forensic Science (VDFS) initially began testing a beta version of the Biomek® 2000 Normalization Wizard (Beckman Coulter, Fullerton, CA) in combination with a PCR Setup method, written by Promega Corporation and modified by the VDFS, for DNA from bloodstains, buccal swabs and simulated casework samples. The experimental strategy was to separate the processes into steps that could be monitored for performance. The two major issues we wished to address were the accuracy of the Normalization Wizard when making the DNA dilutions and the performance of the PCR Setup method for fidelity of the PCR master mix and DNA dilution transfer, as well as susceptibility to contamination for the entire process and overall quality of the STR profile.

2. Materials and methods

2.1. Sample preparation and extraction

DNA samples were prepared from a collection, over a period of 8 years from volunteers at VDFS, of blood stains and buccal swabs. Blood stains were prepared from liquid blood placed onto blood stain cards (Whatman Inc., Florham Park, NJ) and buccal samples collected on sterile cotton swabs. A 5 mm square cutting or a 6 mm diameter punch of bloodstain and a 1/4 to 1/2 portion of buccal swab was used for the described experiments. Additionally, mock sexual assault samples were prepared from vaginal swabs and semen donated by VDFS employees. Previously collected and dried vaginal swabs were dipped into semen dilutions to prepare the mock post-coital swabs. Samples were extracted using the Biomek® 2000 Automation Workstation in conjunction with the DNA IQ™ System (Biomek/DNA IQ) as described [3,4].

2.2. DNA quantitation

DNA samples were quantitated using the AluQuant® Human DNA Quantitation System, a liquid, pyrophosphorylation enzymatic process [14,15], which was adapted to the Biomek® 2000 Automation Workstation for automated reaction setup. The minus probe reactions were removed since the AluQuant® reactions have been observed to contain little to no background signal (personal observation), thereby conserving sample and reagents. Luciferase/luciferin reagent was injected into the AluQuant® reactions to generate relative light units (RLU), light emitted in correlation with the amount of human DNA present. The Luminoskan luminometer (Thermo Electron, West Palm Beach, FL) in conjunction with the Ascent software program was used for Luciferase injection and data capture. Initially data were analyzed and DNA concentrations estimated using the AluQuant® Calculator 2.0. Samples that were greater than 4 ng/μL (the most concentrated standard used to generate the standard curve) would appear as >4 when the curve was extrapolated using Marquadt's Compromise algorithm. When this occurred, the operator had to manually estimate the concentration value. This was performed by dividing the sample RLU value by the 4 ng/μL standard RLU value and multiplying the attained value by 4. All DNA concentration data was then manually entered into an Excel spreadsheet in a format that the Normalization Wizard could recognize for import.

Experiments performed later employed the AluQuant® Calculator v3.0 which utilized a quadratic formula for standard curve extrapolation and also contained a Biomek® tab that allowed for the quantitation data to be transferred into a format for direct import into the Normalization Wizard (Fig. 1). No manual estimates of DNA concentrations were necessary.

2.3. Amplification parameters

Short tandem repeat (STR) typing was performed using the PowerPlex® 16 BIO multiplex (Promega Corp.) which includes the FGA, TPOX, D8S1179, vWA, Amelogenin, Penta E, D18S51, D21S11, TH01, D3S1358, Penta D, CSF1PO, D16S539, D7S820, D13S317, and D5S818 loci. The reagent volumes were halved for the amplification reaction, such that the final volume was 12.5 μL, rather than the 25 μL volume recommended by the manufacturer [16]. The target DNA concentration was set at 0.75 ng and the amplification parameters were modified as follows for amplification in a GeneAmp® PCR System 9600 Thermal Cycler (Applied Biosystems, Foster City, CA):

- 95 °C for 11 min, 96 °C for 1 min, then: 94 °C for 30 s, ramp to 60 °C (hold for 30 s), ramp 50 s to 70 °C (hold for 45 s), for 10 cycles;
- 90 °C for 30 s, ramp 60 s to 60 °C (hold for 30 s), ramp 50 s to 70 °C (hold for 45 s), for 21 cycles;
- 60 °C for 30 min and 4 °C soak.

2.4. STR typing and analysis

Before samples were loaded onto an acrylamide typing gel, 5 μL of each PCR product was electrophoresed in a 1% Nusieve (Cambrex, Rockport, ME) agarose gel containing Ethidium Bromide (product gel) to determine the success of the amplification and to assess the amount of amplified product to use for typing. The STR products were separated on a 6% PAGE Plus™ acrylamide gel (Amresco, Solon, OH) for

(A)

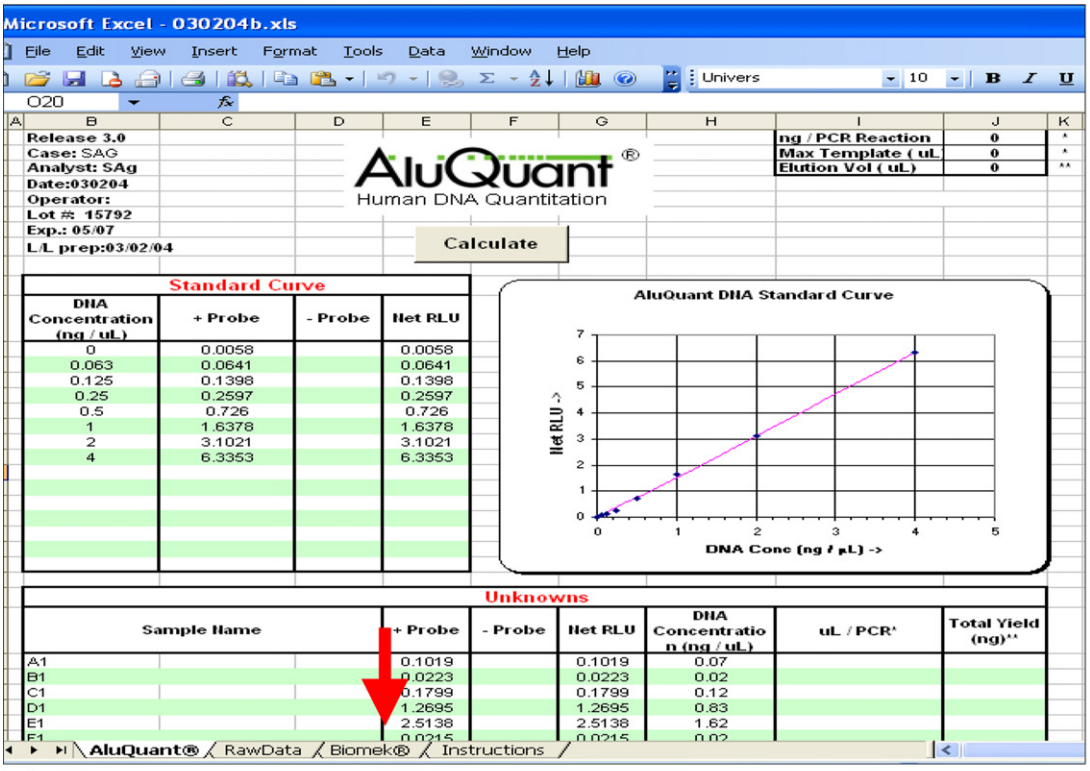

(B)

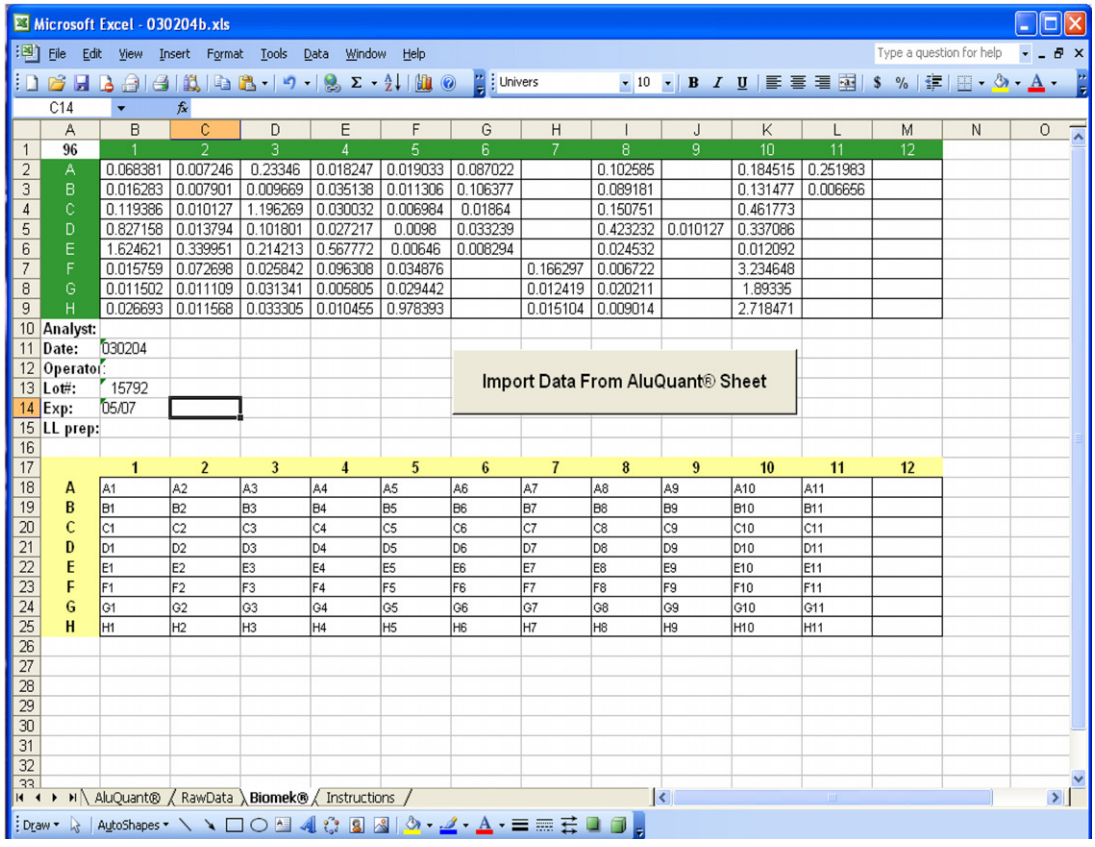

Fig. 1. (A) AluQuant® v3.0 spreadsheet containing DNA quantitation data and transfer to Biomek® import sheet. (B) Biomek® sheet with data in the proper format for import into the Normalization Wizard.

approximately 2 h at 60 W. Product gels were not utilized for all experiments. Those experiments where only blanks were evaluated did not necessitate visualization on a product gel, since the blank samples would likely display no PCR product, but were instead taken directly to the acrylamide gel (STR typing gel). Negative controls, reagent blanks and water blanks required the maximum sample volume (2 μL) mixed into the gel loading cocktail (final volume 6 μL); 3 μL of the gel loading cocktail were loaded into each well for electrophoresis. The Hitachi FMBIO® II and FMBIO® III Plus Fluorescent Imaging Analysis Systems (MiraiBio, Alameda, CA) were used to scan the images of the STR typing gels, the FMBIO Analysis and STaRCall software programs were used to analyze the gel images.

2.5. DNA Wizard and PCR Transfer

The Normalization Wizard software program, as configured by Beckman, was used in a stepwise fashion to generate customized DNA dilution methods. First, the Excel file or Biomek® sheet containing the AluQuant® quantitation data was imported into the Normalization Wizard. Next, the parameters for the method, such as the final DNA concentration and volume of sample used, were entered in the Configure Options step. Since 5 μL of diluted DNA, with a target concentration of 0.15 ng/μL, was used for the amplification reaction, it was determined that 8–10 μL should be used for the volume of DNA removed from each sample to provide a sufficient volume for those samples that would not be diluted. Pipetting and dispense heights and rates for the DNA extracts and the diluent were optimized by trial and error and the optimal values obtained were entered in the next step, the Configure Transfer step (Fig. 2). The View Plates step (Fig. 3), displayed the final DNA concentration, volume of sample used, and the volume of diluent added to the samples. Samples lower than the target concentration were highlighted to alert the user. Similarly, samples where the final concentration would exceed the target concentration, due to diluent volume limitations, were also highlighted. Moreover, at the View Plates step, individual samples can be excluded from the process (cherry picked) by the user.

Once all desired settings were entered and any wells to be excluded were marked, the final, Generate Method step, was employed. The user clicked the Generate Method button and the software program generated a customized dilution method for that plate of DNA extracts for the Biomek® 2000 Automation Workstation in a matter of seconds.

A summary of the normalization method was routinely obtained after the customized method had been created. The Normalization Wizard method provided a Summary Plate Map in the form of an Excel file at the completion of the process which summarized the settings for each well, such as original DNA sample concentration, amount of sample removed, amount of diluent and the final concentration achieved.

Once the Normalization Wizard method was finished, the PCR Setup method, which mixes the diluted DNA samples, adds the PCR master mix and transfers the DNA samples to the amplification tubes, was initiated. Our laboratory modified the version provided to us by Promega Corporation to reduce susceptibility to contamination so that the DNA dilutions were

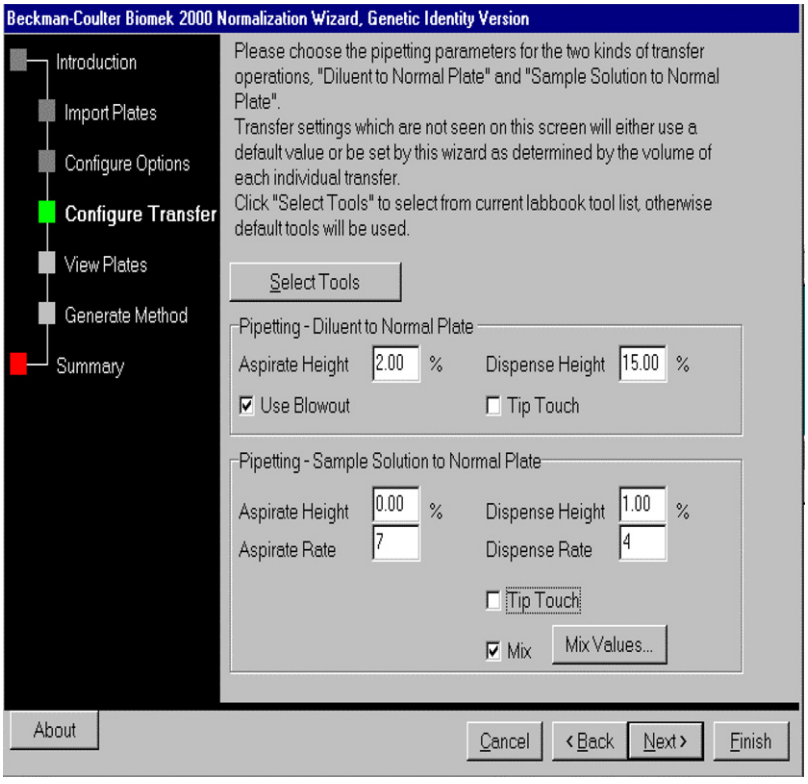

Fig. 2. Configure Transfer step of the Normalization Wizard software program.

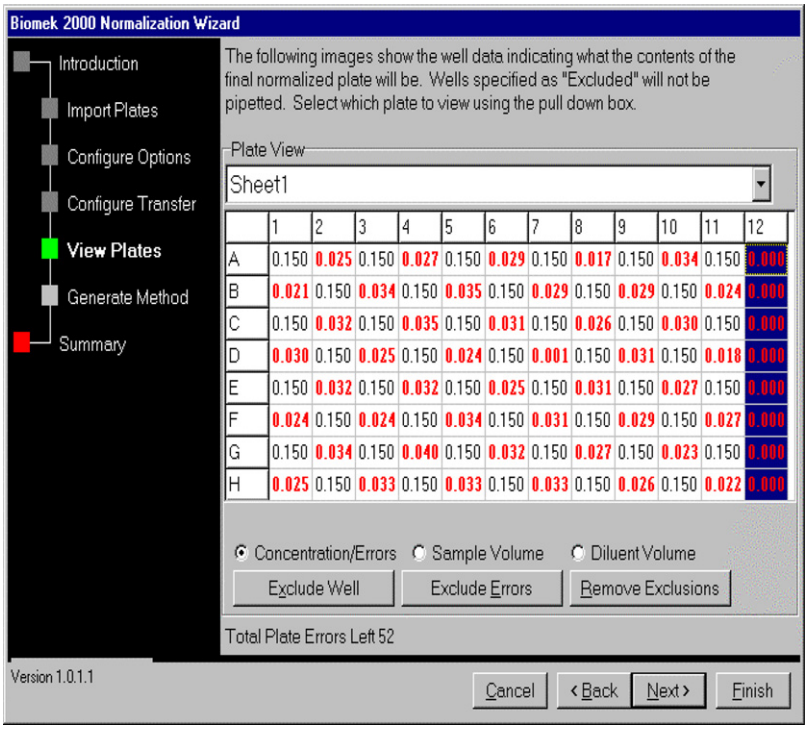

Fig. 3. View Plate function of the Normalization Wizard. Blue squares indicate wells that have been excluded, therefore no diluent or DNA extract will be pipetted into those wells. The concentration/errors button is checked therefore the screen display shows the wells in black type to indicate that the target DNA concentration will be reached for those samples. The wells with red type indicate an inability to generate the target DNA concentration either because the DNA is too dilute or too concentrated.

mixed, after which the PCR master mix, amplification tubes and positive and negative control tubes were uncapped and placed onto the deck, the PCR master mix was then aliquoted to the tubes followed by the diluted DNA samples.

Initially, 8-strip PCR tubes were used, however, individual PCR tubes replaced these since they could be opened one at a time and the tubes could be individually labeled.

2.5.1. Test of dilution accuracy by the Normalization Wizard

Using the same DNA and AluQuant® concentration data, dilutions were generated using a customized method created by the Normalization Wizard and manually. One PCR master mix was created for both the manually and robotically created DNA dilutions. For the STR typing gels, the same volume of each PCR product was used in the loading cocktail for the manually and robotically diluted samples and the corresponding samples were loaded adjacent to one another.

2.5.2. Contamination study

Four Normalization Wizard methods were generated corresponding to four different plates of DNA samples, for a total of 250 samples, arranged in a checkerboard pattern of alternating sample with a blank well, containing either water or TE^{-4}. The Normalization Wizard and the PCR Setup methods were carried out on the Biomek® 2000 Workstation and all PCR reactions amplified. All of the PCR reactions were visualized on product gels and all of the blanks were typed on STR typing gels. One set of samples, consisting of 17 DNA samples, 17 blanks and a positive (9947A) and negative control was taken through STR typing.

As part of the statewide implementation process, the Department's three regional laboratories also performed checkerboard tests for contamination following the same procedure as described above on an additional 768 samples. Thus the total number of samples assayed using the checkerboard test was 1018.

3. Results

3.1. Normalization Wizard dilution accuracy

The experimental design employed was to separate the Normalization Wizard and PCR Setup method processes so that individual steps could be carefully monitored for the aspects of the procedure that were of primary concern, i.e., is the automated DNA dilution accurate? Is the quality of the STR profiles produced comparable to a manual PCR setup? Does the automated DNA dilution and the addition of the PCR cocktail increase the susceptibility to contamination? After first investing time optimizing the system, such as plate choices and aspiration and dispense heights and rates, the initial experiment was to assess if the DNA dilutions performed by the Normalization Wizard were comparable to those performed manually. A total of 72 samples were tested in three independent Normalization Wizard runs. The same samples were also diluted manually using the same quantitation data. A single PCR master mix was created for both manually and

robotically created DNA dilutions. Once amplified, the manually diluted and robotically diluted samples were loaded adjacent to one another on the typing gels, using the same volumes, for easy performance comparison (Fig. 4). Among those 72 samples were a total of seven blanks all of which were devoid of any extraneous PCR product.

3.2. Contamination studies

Initially, four different checkerboard tests for contamination were performed. A well containing a DNA sample was alternated with a reagent blank or water blank well in an alternating, checkerboard pattern across the plate. This allows for sensitive detection of the horizontal and vertical transfer of material from one well to another. In those four initial checkerboard tests, a total of 250 samples were tested, half of which were blanks. Out of 125 blanks, two displayed extremely weak, single drop-in alleles, however, the source of the drop-in alleles could not be ascribed. The remaining 123 blanks showed no evidence of drop-in alleles and the 17 DNA profiles assessed by STR typing displayed the correct profiles and the locus balance and profile quality was identical to that produced manually (Fig. 5).

Furthermore, statewide six different Biomek® 2000 Automation Workstation operators, as part of their training and validation of the Normalization Wizard and PCR Setup methods for use in each of the Department's four laboratories (Central, Northern, Western and Eastern) performed additional checkerboard contamination tests. A total of 768 samples were taken through the automated PCR Setup process, half of which were blanks. All 384 blanks were taken through the entire STR typing process and a single, extremely weak drop-in allele was observed in six out of 384 blanks (data not shown). Again, the source of the drop-in alleles could not be ascertained. Additionally, a total of 204 DNA samples were taken through the entire STR typing process and displayed no alleles beyond the known profiles. Thus, a total of 1018 samples were tested in checkerboard contamination assays by seven different operators on five different robots and a total of eight, extremely faint single drop-in alleles were observed. None of the 221 samples containing DNA displayed any drop-in alleles. No sources for the drop-in alleles could be identified.

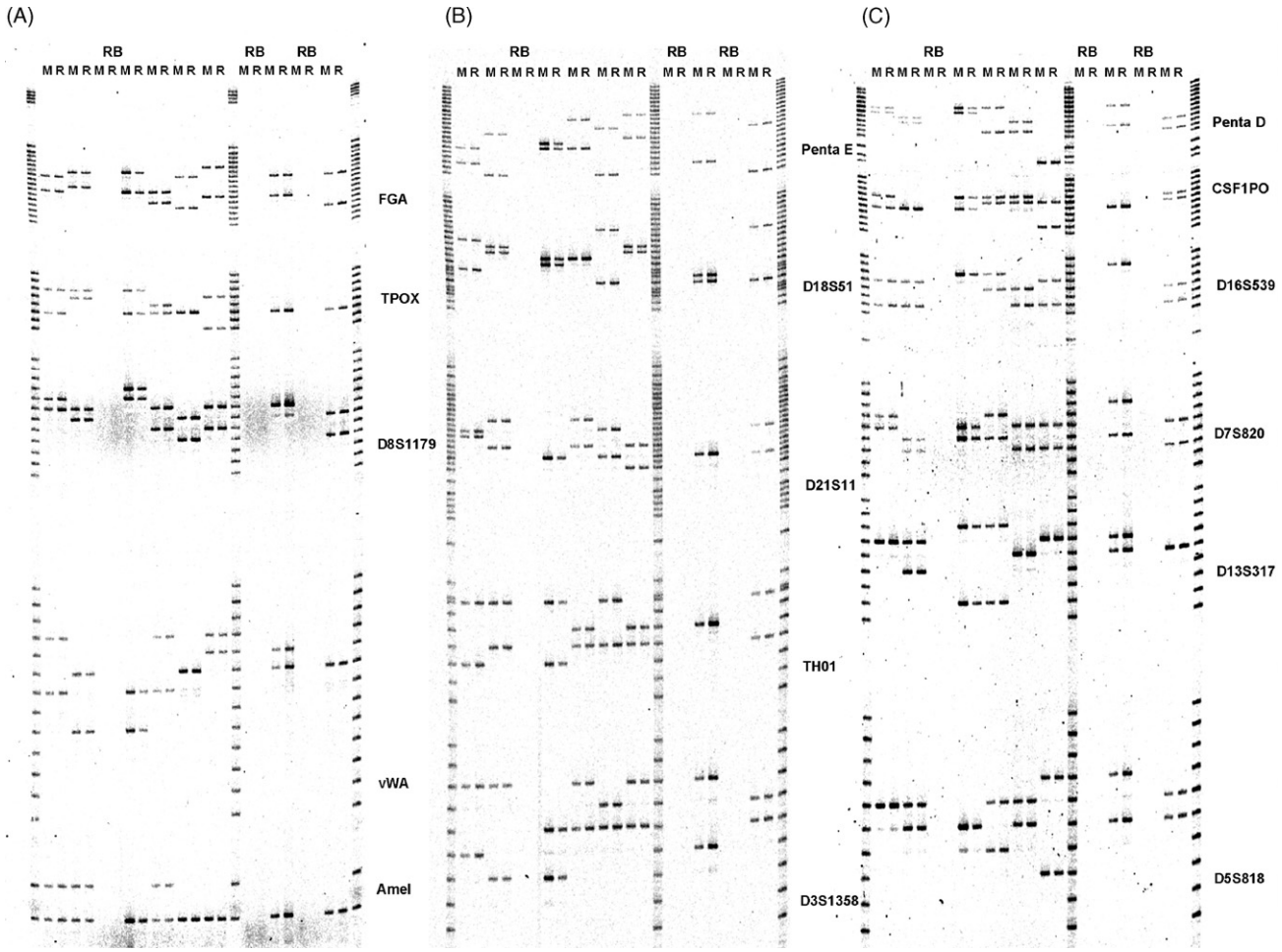

Fig. 4. STR typing gel displaying the test of the Normalization Wizard accuracy. (A) Gel image of the 598 nm filter scan (Rhodamine Red™-X) of a PowerPlex® 16 BIO System STR tying gel. (B) Gel image of the 505 nm filter scan (Fluorescein dye). (C) Gel image of the 577 nm filter scan (JOE dye). The 665 nm filter scan (Texas Red®-X dye) of the in-lane size standard (ILS600) is not shown. STR loci are indicated to the right of each allelic ladder. Key: Amel, Amelogenin locus; M, manual; R, robot; RB, reagent blanks. MiraiBio FMBIO II utilized for imaging.

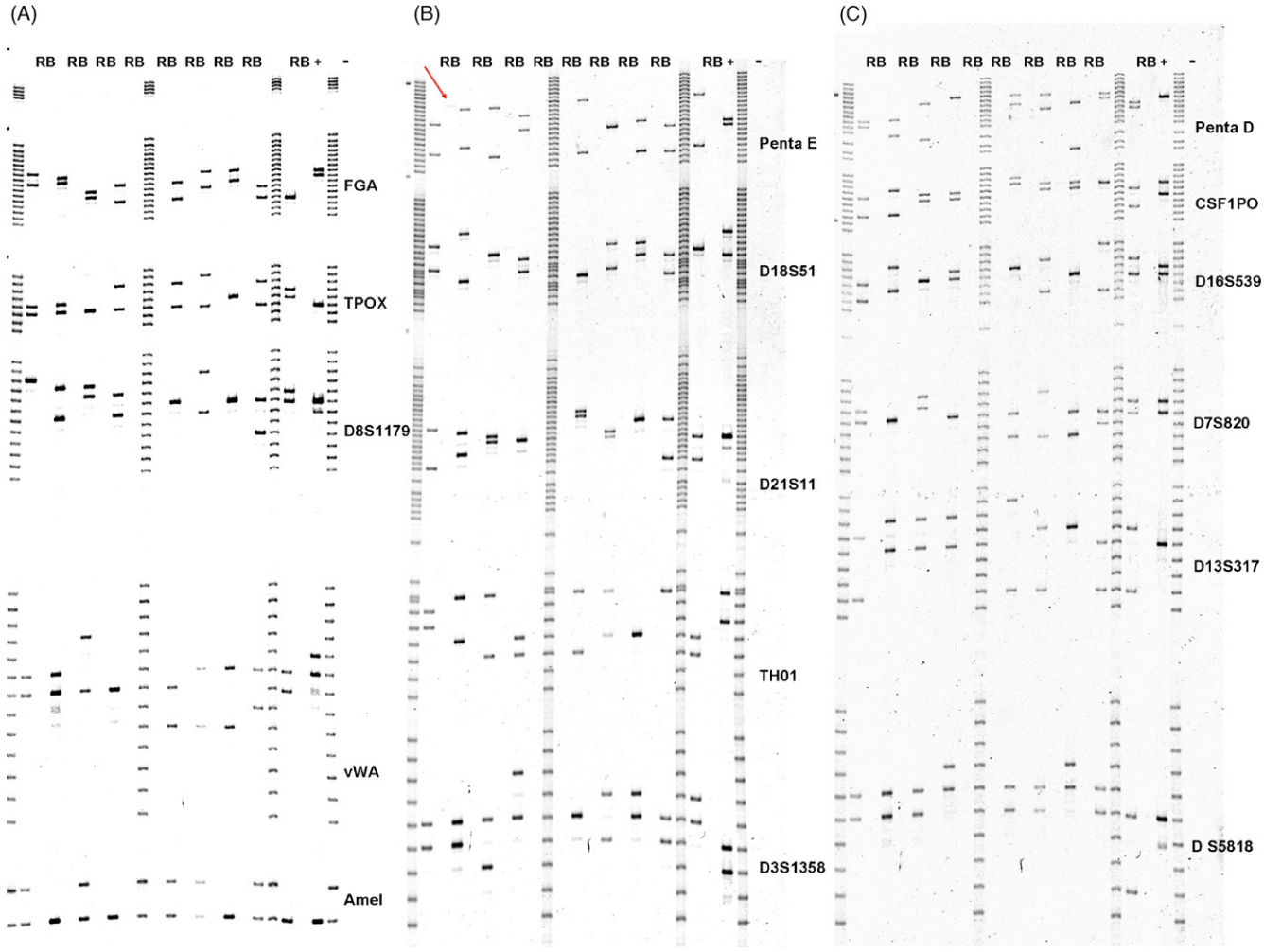

Fig. 5. STR typing gel displaying results of a checkerboard test. (A) Gel image of the 598 nm filter scan (Rhodamine Red™-X) of a PowerPlex® 16 BIO System STR typing gel. (B) Gel image of the 520 nm filter scan (Fluorescein dye). (C) Gel image of the 577 nm filter scan (JOE dye). The 650 nm filter scan (Texas Red®-X dye) of the in-lane size standard (ILS600) is not shown. STR loci are indicated to the right of each allelic ladder. Key: Amel, Amelogenin locus; RB, reagent blank. MiraiBio FMBIO III Plus™ utilized for imaging. Arrow points to a single faint drop-in allele at the Penta E locus.

Additionally, 120 samples, consisting of blood, buccal and mock sexual assault samples were taken through the Normalization Wizard and PCR Setup processes by the six Biomek® 2000 Automation Workstation operators as a competency test. The profiles from the samples were accurate and the reagent blanks showed no evidence of drop-in alleles (data not shown).

3.3. PCR Setup method modifications

The initial PCR Setup method contained these steps in the following order: PCR master mix was pipetted to the PCR tubes, the DNA dilutions were mixed and with the same pipette tips, transferred to the PCR tubes. First we observed that using the same tool to both mix the DNA dilutions and transfer the aliquots to the PCR tubes created inconsistencies in the amount of DNA solution transferred. Moreover, we considered the possibility that mixing the dilutions while the amplification tubes were open on the robot deck as well as the PCR master mix tube, might increase the incidence of drop-in alleles. Thus, the method was modified such that the DNA dilutions were first mixed without any open tubes on the deck. Next, the robot paused with a prompt to place the uncapped PCR master mix on the deck and to open the amplification tubes. Once the PCR master mix was dispensed, the diluted DNA sample aliquots were transferred. The PCR master mix was originally dispensed using a single pipette tip, but we modified this step so that it used the repeat pipette function and changed tips once a column.

4. Discussion

4.1. Normalization Wizard dilution accuracy

The dilution accuracy for two out of the three tests was assessed by STR typing on an acrylamide typing gel which allowed a direct performance comparison between the manually and robotically diluted samples (Fig. 4). One of the tests was assessed only through the product gel step. While

the STR typing results provided definitive results that the respective dilutions were virtually identical, the product gel still provided a gross analysis that corroborated the STR typing gel results, namely the PCR product obtained for the robotic dilutions appeared comparable to manual dilutions (data not shown). Moreover, the reagent blanks assessed through the STR typing gel (six reagent blanks) displayed no evidence of drop-in alleles. Thus, the dilutions performed by the Normalization Wizard were determined to be accurate.

4.2. Contamination studies

A total of 1018 samples were taken through the checkerboard contamination test statewide using five independent Biomek® 2000 Automation Workstations by seven different scientists. A total of eight, very weak, single drop-in alleles were observed out of the 509 blanks typed for the PowerPlex® 16 BIO loci and STR typing gels. The sources of the drop-in alleles could not be ascertained. The checkerboard contamination test can be difficult to perform flawlessly since there are many steps in the process in which a low level contaminant may be introduced that has nothing to do with the process that is being assessed: in this case the processes are the Normalization Wizard and the PCR Setup methods. For example, loading the cell lysates into wells for extraction that are surrounded by blank wells, particularly for very concentrated samples, requires pipetting skills and attentiveness. Additionally, manipulation of the samples in the strip PCR tubes using strip caps also requires great attentiveness and frequent glove changing to avoid any transfer of material from a concentrated sample to one of the surrounding reagent blanks. The extremely faint drop-in alleles were deemed not to be a threat to the integrity of the DNA typing process since these were observed in a small number of reagent blanks only when performing the checkerboard tests. Moreover, the 221 samples containing DNA taken through the entire STR typing process, even at low concentrations, showed no extraneous alleles.

4.3. PCR Setup method modifications

The modifications tested and implemented for the PCR Setup method by the VDFS were designed not only to reduce the possibility of sample-to-sample aerosol carry-over during the mixing step for the diluted DNA samples, but also to accelerate the entire process. Utilizing one set of larger volume pipette tips for the mixing step and another set of smaller volume tips for the DNA transfer step provided more accurate pipetting of the diluted DNA samples (K. Sykes, personal observations). Moreover, mixing the DNA samples, while keeping the amplification tubes and the PCR master mix tube closed and off the robot deck, further enhanced efforts to eliminate the threat of contamination by aerosols. The dispensing of the PCR master mix was quickened by using a repeat pipettor function and changing tips once a column, thereby reducing the time for the entire process (Normalization Wizard and PCR Setup) to approximately 40 min for 88 samples.

5. Conclusion

Advances in automation such as these presented in this paper, provide enhanced throughput capacity to forensic casework without a subsequent loss of quality. Enhancement of throughput is essential for forensic laboratories to decelerate case backlogs and to reduce the amount of time it takes to ''turn around'' a case [17]. The use of the Normalization Wizard teamed up with the PCR Setup method significantly reduces the amount of time it takes to setup the PCR amplification of samples. It takes approximately two to three hours to manually setup 88 samples for PCR amplification, while the Normalization Wizard and the PCR Setup methods combined take only about 40 min. However, it is of utmost importance that quality and confidence in the final product, the STR profiles obtained, is not jeopardized or undermined. There is a worldwide recognition of the need for advancements in forensic casework sample analysis and successful implementation of automated systems plays a critical role in that endeavor. But that advancement must be readily transferable among members of a laboratory as well as the instrumentation employed. This laboratory system wide study assessed the performance of the Normalization Wizard teamed up with the PCR Setup method and determined that it provides for a mostly hands off methodology for high throughput, customized sample amplification necessary for casework analysis. Backlog reduction is not the only advantage to advancing automation in forensic DNA analysis. By furthering throughput capacity while paying particular attention to the quality of the automated product, the forensic laboratories ability to assist in the successful investigation and closure of the large number of unsolved violent crimes can be utilized more fully [18].

Acknowledgments

The authors gratefully acknowledge all of the helpful advice provided by Allan Tereba and Paraj Madrekar (Promega Corporation).

References

[1] The President's initiative to advance justice through DNA technology, in Department of Justice Fact Sheet, U.S. Department of Justice, 2003.
[2] Report to Attorney General on Delays in Forensic DNA Analysis, National Institute of Justice, 2003.
[3] S.A. Greenspoon, J.D. Ban, Robotic extraction of mock sexual assault samples using the BioMek® 2000 and the DNA IQ™ System, Profiles DNA 5 (1) (2002) 3–5.
[4] S.A. Greenspoon, J.D. Ban, K. Sykes, E.J. Ballard, S.S. Edler, M. Baisden, et al., Application of the BioMek® 2000 Laboratory Automation Workstation and the DNA IQ™ System to the extraction of forensic casework samples, J. Forensic Sci. 49 (1) (2004) 29–39.
[5] M. Steinlechner, W. Parson, Automation and high through-put for a DNA database laboratory: development of a laboratory information management system, Croatian Med. J. 42 (3) (2001) 252–255.

[6] C.A. Crouse, S. Yeung, S. Greenspoon, A. McGuckian, J. Sikorsky, J. Ban, R. Mathies, Improving efficiency of a small forensic DNA laboratory: validation of robotic assays and evaluation of microcapillary array device, Croatian Med. J. 46 (4) (2005) 563–577.
[7] S.A. Montpetit, I.T. Fitch, P.T. O'Donnell, A simple automated instrument for DNA extraction in forensic casework, J. Forensic Sci. 50 (3) (2005) 555–563.
[8] T.M. Clayton, J.P. Whitaker, R. Sparkes, P. Gill, Analysis and interpretation of mixed forensic stains using DNA STR profiling, Forensic Sci. Int. 91 (1998) 55–70.
[9] P. Gill, Application of low copy number DNA profiling, Croatian Med. J. 42 (3) (2001) 229–232.
[10] M.C. Kline, D.L. Duewer, J.W. Redman, J.M. Butler, Results from the NIST 2004 quantitation study, J. Forensic Sci. 50 (3) (2005) 570–578.
[11] G. Tringali, A. Barbaro, E. Insirello, P. Cormaci, A.M. Roccazzello, Rapid and efficacious real-time quantitative PCR assay for quantitation of human DNA in forensic samples, Forensic Sci. Int. 146 (Suppl.) (2004) S177–S181.
[12] J.A. Nicklas, E. Buel, Development of an Alu-based, real-time PCR method for quantitation of human DNA in forensic samples, J. Forensic Sci. 48 (5) (2003) 936–944.
[13] AluQuant Human DNA Quantitation System Technical Bulletin #291, Promega Corporation.
[14] M.N. Mandrekar, A.M. Erickson, K. Kopp, B.E. Krenke, P.V. Mandrekar, R. Nelson, et al., Development of a human DNA quantitation system, Croatian Med. J. 42 (3) (2001) 336–339.
[15] S. Hayn, M.M. Wallace, M. Prinz, R.C. Shaler, Evaluation of an automated liquid hybridization method for DNA quantitation, J. Forensic Sci. 49 (1) (2004) 87–91.
[16] PowerPlex® 16 BIO System Technical Manual #D016, Promega Corporation.
[17] Attorney General's Report on the DNA Evidence Backlog, National Institute of Justice Plublications, April 2004.
[18] The Future of Forensic DNA Testing: Predictions of the Research and Development Working Group, National Institute of Justice Publications, November 2000.

ELSEVIER

Forensic Science International 164 (2006) 249–253

Forensic Science International

www.elsevier.com/locate/forsciint

Announcement of Population Data

Haplotypes for 13 Y-chromosomal STR loci in South Tunisian population (Sfax region)

Imen Ayadi [a], Leila Ammar-Keskes [b], Ahmed Rebai [a,*]

[a] *Bioinformatics Unit, Centre of Biotechnology of Sfax, PB"K" 3038 Sfax, Tunisia*
[b] *Laboratoire de Génétique Moléculaire Humaine, Faculté de Médecine, 3028 Sfax, Tunisia*

Received 9 June 2005; received in revised form 3 October 2005; accepted 3 October 2005
Available online 15 November 2005

Abstract

Nine Y-STR loci from the "minimal haplotype" (DYS19, DYS385a/b, DYS389I, DYS389II, DYS390, DYS391, DYS392, DYS393) included in Y-STR Haplotype Reference Databases (YHRD) with 4 additional Y-STRs (DYS436, DYS437, DYS438, DYS439) were analyzed by PCR using duplex and Y-PLEX^{TM}12 kit, followed by automatic genotyping in a sample of 105 Tunisian males originating from Sfax region (south Tunisia). Allelic frequencies and gene diversities for each Y-STR locus were determined. The high haplotype diversity (0.9932) and discrimination capacity (0.7714) show the usefulness of these loci for human identification in forensic studies and paternity tests in Tunisia. The most common haplotype was shared by 4.7% (5 individuals) of the sample was only found in samples from the Tunisian population reported in YHRD. One private allele for DYS392 (allele 17) was discovered and duplications were observed for five loci (DYS19, DYS389I, DYS393, DYS437 and DYS439).

Keywords: Y chromosome; STR; Y-Plex^{TM}12; Tunisian population; Haplotype; Forensic

Population: One hundred and five unrelated healthy males from the Sfax region located in south coastal part of Tunisia (see Fig. 1).

Extraction: Genomic DNA was extracted from blood using a phenol–chloroform protocol.

PCR: Amplification of the Y-STR loci was performed in two non-overlapping, multiplex PCR systems:

- **Duplex-amplification** (comprising loci DYS436 and DYS437): The primer sequences for DYS437 and DYS436 were described by Ayub et al. [1]. Polymerase chain reaction mixture contained 100–150 ng of template DNA in a total reaction volume of 50 μl including 5 μl GeneAmp 10× PCR Buffer I (Applied Biosystems), 2.5 mM $MgCl_2$, 0.5 μM of each primer, 200 μM dNTPs (Amersham) and 1.25 U AmpliTaq Gold DNA polymerase (Perkin-Elmer, Applied Biosystems). The PCR reactions were performed using a GeneAmp PCR system 9600 thermocycler (Perkin-Elmer). The PCR thermocycling parameters were as follows: pre-denaturation step at 95 °C for 10 min; 30 cycles at 94 °C denaturation for 30 s, annealing at 56 °C for 60 s and extension at 72 °C for 30 s and final extension at 72 °C for 10 min.
- **12Plex-amplification** was performed by the commercial kit Y-Plex^{TM}12 (Reliagene, New Orleans, LA) that amplifies 11 Y-STR loci (comprising DYS19, DYS385, DYS389I, DYS389II, DYS390, DYS391, DYS392, DYS393, DYS438 and DYS439) and a segment of the amelogenin gene, according to manufacturer's instructions but in a total reaction volume of 25 μl.

* Corresponding author. Tel.: +216 97 299 045; fax: +216 74 440 818.
E-mail address: ahmed.rebai@cbs.rnrt.tn (A. Rebai).

0379-0738/$ – see front matter
doi:10.1016/j.forsciint.2005.10.006

Fig. 1. Map of Tunisia showing the location of Sfax region.

Typing: The PCR products of loci DYS436 and DYS437 were analysed in 6% denaturing polyacrylamide sequencing gel and visualised by autoradiography.

The PCR products of the Y-Plex™12 kit were detected with the ABI PRISM® 3100-Avant Genetic Analyser (Applied Biosystems, Foster City, CA) using the Genemapper version 3.5 software (Applied Biosystems). The allele designations were determined by comparison of the PCR products with those of allelic ladders provided with the kit. Nomenclature of loci and alleles is according to the International Society of Forensic Genetics (ISFG) guidelines reported in Gill et al. [2].

Quality control: Allelic ladders, female DNA (negative control), male DNA (positive internal control) and the amelogenin (internal control), provided by Reliagene (Reliagene Tech.), were used in each reaction with the Y-plex™12 kit. For manual genotyping, female DNA 1347 (CEPH) amplified by a set of autosomal STR markers was used as control.

Results: The results are summarized in Tables 1 and 2.

Analysis of data: Allele frequencies were calculated by direct counting. Allele diversity was calculated as [3]

$$D = \frac{n}{n-1}\left(1 - \sum_{i=1}^{n} p_i^2\right),$$

where n is the sample size and p_i is the frequency of the ith allele. Haplotype diversity (HD) was calculated with the same equation using haplotype frequencies. For the Y-chromosome, haplotype diversity value is identical to the power of discrimination (PD) [4], and to the power of exclusion (CE) [5]. Standard errors for HD estimates were calculated according to the following equation [3]:

$$\text{S.E.} = \sqrt{\frac{2}{n}\left[\sum_{i=1}^{n} p_i^3 - \left\langle \sum_{i=1}^{n} p_i^2 \right\rangle^2\right]}.$$

Table 1
Allele frequencies and gene diversity of 13 Y-STR loci in 105 Tunisian males

Alleles	DYS19 (n = 104)	DYS385a (n = 105)	DYS385b (n = 105)	DYS389I (n = 104)	DYS389II (n = 105)	DYS390 (n = 105)	DYS391 (n = 105)	DYS392 (n = 105)	DYS393 (n = 104)	DYS436 (n = 105)	DYS437 (n = 104)	DYS438 (n = 105)	DYS439 n = 104)	Genotype	DYS385a-b
8							0.01							10–14	0.0190
9							0.343					0.181		11–13	0.0476
10		0.019					**0.4**			0.038		**0.648**	**0.413**	11–14	0.0381
11		0.105					0.19	**0.857**		**0.962**		0.095	0.356	11–15	0.0190
12		0.048		0.144			0.057	0.009	0.346			0.076	0.154	12–15	0.0190
13	0.365	**0.552**	0.048	**0.500**				0.095	**0.615**				0.077	12–16	0.0190
14	**0.452**	0.124	**0.248**	0.346				0.028	0.038		**0.769**			12–20	0.0095
15	0.135	0.019	0.162	0.010							0.192			13–14	**0.1714**
16	0.038	0.029	0.162								0.038			13–15	0.1143
17	0.010	0.086	0.029					0.009						13–16	0.0571
18			0.152											13–17	0.0190
19		0.019	0.162											13–18	0.0762
20			0.038											13–19	0.0952
21						0.019								13–20	0.0190
22						0.067								14–14	0.0190
23						0.38								14–16	0.0667
24						**0.419**								14–17	0.0095
25						0.114								14–19	0.0286
26														15–15	0.0095
27					0.009									15–19	0.0095
28					0.057									16–16	0.0190
29					0.238									16–18	0.0095
30					**0.543**									17–18	0.0667
31					0.133									17–19	0.0095
32					0.009									17–20	0.0095
33					0.009									19–19	0.0190
GD[a]	0.649	0.657	0.832	0.615	0.633	0.668	0.689	0.258	0.505	0.074	0.373	0.538	0.679	GD	0.931
HD[b]	99.19	98.75	99.30	99.19	99.01	99.06	99.10	99.32	99.28	99.32	99.25	99.32	99.26	HD	98.79

[a] Gene diversity. In bold are the most common allele for each locus.
[b] Haplotype diversity calculated with all Y-STR except this marker.

Table 2
Haplotypes for the 13 Y-STR loci observed in a Tunisian male population ($N = 105$)

H[a]	19	385a	385b	389I	389II	390	391	392	393	436	437	438	439	Observed value	
														n[b]	f[c]
h1	13	12	15	14	33	21	8	11	13	11	14	10	12	1	0.0095
h2	13	13	14	13	29	24	9	11	13	11	14	9	11	1	0.0095
h3	13	13	14	13	29	24	9	11	13	11	14	10	10	2	0.019
h4	13	13	14	14	30	23	9	11	13	11	14	10	10	3	0.0285
h5	13	13	14	14	30	23	9	11	13	11	15	10	10	1	0.0095
h6	13	13	14	14	30	24	9	11	13	11	14	10	10	3	0.0285
h7	13	13	14	14	30	25	10	11	13	11	14	10	11	1	0.0095
h8	13	13	14	14	31	23	9	11	14	11	14	10	10	1	0.0095
h9	13	13	14	15	31	24	9	11	13	11	14	10	10	1	0.0095
h10	13	13	15	12–14	30	24	9	11	13	11	14	10	10	1	0.0095
h11	13	13	15	13	29	24	9	11	13	11	14	10	10	1	0.0095
h12	13	13	15	14	29	24	9	11	13	11	14	10	10	1	0.0095
h13	13	13	15	14	30	24	9	11	13	11	14	10	10	5	0.0476
h14	13	13	15	14	30	25	9	11	13	11	14	10	10	1	0.0095
h15	13	13	15	14	31	24	9	11	13	11	14	10	10	1	0.0095
h16	13	13	16	13	29	24	10	11	12	11	15	9	12	2	0.019
h17	13	13	16	13	30	24	9	11	13	11	14	10	10	1	0.0095
h18	13	13	16	14	30	24	9	11	13	11	14	10	11	1	0.0095
h19	13	13	18	13	30	23	11	11	13	11	14	10	11	1	0.0095
h20	13	14	16	14	30	24	9	11	13	11	14	10	10	1	0.0095
h21	13	16	16	13	30	23	10	11	13	11	15	10	12	1	0.0095
h22	13	16	16	13	30	24	10	11	12	11	14	10	11	1	0.0095
h23	13	17	18	12	29	23	10	11	13	11	14	10	10	2	0.019
h24	13	17	18	12	30	23	10	11	13	11	14	10	10	3	0.0285
h25	13	17	20	14	31	24	10	11	13	11	14	10	12	1	0.0095
h26	14	10	14	12	28	24	11	13	12	11	15	12	12	1	0.0095
h27	14	10	14	14	30	24	11	13	13	11	15	12	11	1	0.0095
h28	14	11	13	12	28	24	10	13	13	10	15	12	13	1	0.0095
h29	14	11	13	13	29	24	10	13	12	10	15	12	12	1	0.0095
h30	14	11	13	13	29	24	10	13	13	10	15	12	12	1	0.0095
h31	14	11	14	13	28	23	10	14	13	11	15	12	12	1	0.0095
h32	14	11	14	13	30	25	11	14	12	11	15	12	12	1	0.0095
h33	14	11	14	14	30	25	11	13	13	11	15	12	12	1	0.0095
h34	14	12	16	13	30	23	9	11	13	11	15–16	10	11–12	1	0.0095
h35	14	12	20	13	30	23	10	11	12	11	14	10	11	1	0.0095
h36	14	13	14	13	30	24	9	11	12	11	14	10	10	1	0.0095
h37	14	13	14	14	30	24	9	11	12	11	14	10	10	1	0.0095
h38	14	13	14	14	31	24	9	11	13	11	14	10	10	3	0.0285
h39	14	13	15	13	30	22	10	11	13	11	16	10	11	1	0.0095
h40	14	13	15	13	30	24	10	11	12	11	15	9	11	1	0.0095
h41	14	13	16	13	29	23	10	11	13	11	14	9	12	1	0.0095
h42	14	13	17	13	30	23	10	11	12	11	14	10	11	1	0.0095
h43	14	13	18	13	30	23	10	11	12	11	14	10	11	1	0.0095
h44	14	13	18	13	30	23	11	11	12	11	14	10	11	1	0.0095
h45	14	13	18	13	30	23	11	11	12–13	11	14	10	11	1	0.0095
h46	14	13	18	13	30	23	12	11	12	11	14	10	11	1	0.0095
h47	14	13	18	13	31	23	11	11	12	11	14	11	11	1	0.0095
h48	14	13	19	13	29	22	11	11	12	11	14	10	11	1	0.0095
h49	14	13	19	13	30	22	10	11	12	11	14	10	11	1	0.0095
h50	14	13	19	13	30	23	11	11	12	11	14	10	11	3	0.0285
h51	14	13	19	13	30	23	12	11	12	11	14	10	10	1	0.0095
h52	14	13	19	13	30	23	12	11	12	11	14	10	11	3	0.0285
h53	14	13	20	13	30	23	11	11	12	11	14	10	11	1	0.0095
h54	14	13	20	14	30	23	10	12	13	11	15	11	11	1	0.0095
h55	14	14	14	14	30	24	9	11	13	11	14	10	10	2	0.019

Table 2 (*Continued*)

H[a]	19	385a	385b	389I	389II	390	391	392	393	436	437	438	439	Observed value	
														n^b	f^c
h56	14	14	16	14	29	23	10	13	13	11	14	9	11	3	0.0285
h57	14	14	16	14	31	23	11	14	13	11	14	9	11	1	0.0095
h58	14	14	17	13	30	23	10	11	12	11	14	11	13	1	0.0095
h59	14	15	19	13	29	23	11	11	12	11	14	10	12	1	0.0095
h60	14	17	18	12	29	23	10	11	13	11	14	10	10	1	0.0095
h61	14	17	19	13	30	25	10	11	13	11	14	10	13	1	0.0095
h62	14	19	19	13	30	25	10	11	13	11	14	10	13	1	0.0095
h63	14	19	19	13	30	25	10	11	13	11	15	10	13	1	0.0095
h64	15	11	13	13	31	25	10	11	13	11	14	11	10	2	0.019
h65	15	11	15	13	30	24	10	11	13	11	14	11	10	1	0.0095
h66	15	11	15	13	31	25	11	11	13	11	14	11	10	1	0.0095
h67	15	13	16	12	28	24	9	11	12	11	15	9	11	1	0.0095
h68	15	13	17	12	30	24	10	11	12	11	16	9	11	1	0.0095
h69	15	13	18	12	29	23	10	11	12	11	14	10	12	1	0.0095
h70	15	13	18	14	30	22	9	11	12	11	15	9	11	1	0.0095
h71	15	13	19	13	29	25	10	11	12	11	14	9	12	1	0.0095
h72	15	14	16	14	32	24	10	13	13	11	14	9	11	1	0.0095
h73	15	14	19	13	29	24	11	11	12	11	15	9	13	1	0.0095
h74	15	15	15	13	28	22	10	17	13	10	14	11	11	1	0.0095
h75	15	16	18	12	27	24	11	11	12	11	14	9	12	1	0.0095
h76	15	17	18	12	29	23	10	11	13	11	14	10	10	1	0.0095
h77	15–16	12	15	12	29	22	9	11	14	11	16	9	11	1	0.0095
h78	16	11	14	13	31	25	12	11	13	11	14	11	10	1	0.0095
h79	16	14	16	12	28	22	10	11	14	11	16	10	11	1	0.0095
h80	16	14	19	13	29	24	11	11	12	11	15	9	13	2	0.019
h81	17	12	16	13	31	21	10	11	14	11	14	11	11	1	0.0095

[a] Haplotype.
[b] The number of males observed for each haplotype.
[c] Frequency of each haplotype in the sample of 105 males.
Haplotype diversity = 0.9932 ± 0.0014, discrimination capacity = 0.7714.

Discrimination capacity was determined by dividing the number of observed haplotypes to the number of sampled individuals [6].

Other remarks: We identified 81 different haplotypes in our study sample (105 unrelated males), 67 of which (82.7%) were unique, 6 were found twice (7.4%) and 7 were found in three individuals (8.6%). The most frequent haplotype was haplotype number 13 (Table 2), shared by 4.7% (five individuals) of the sample. This haplotype matches 26 individuals in Y-chromosome Haplotype Reference Database YHRD (http://www.yhrd.org). It was found in 24 individuals among 246 from different samples of the Tunisian population (6.9%) and two individuals among 689 males (0.29%) from two European samples (France and Portugal). As the hypothesis of these two individuals being of Tunisian origin is likely, haplotype 13 seems to be specific to Tunisia. This is to be corroborated by future investigations.

Haplotype diversity was 0.9932 ± 0.0014 and discrimination capacity was 0.7714 indicating that the STR loci will be useful for human identification in forensic studies and paternity testing in the Tunisian population.

The DYS385a/b had the highest diversity ($D = 0.931$), while locus DYS436 had the lowest ($D = 0.074$). With DYS385a/b, DYS391, DYS439 and DYS390 had the highest gene diversities 0.689, 0.679 and 0.668, respectively. In order to evaluate the informativeness of each marker in a haplotype context, we calculated the HD when this marker is removed from the whole set of the 13 Y-STRs. Markers yielding the highest decrease in HD when removed are the most informative. Table 1 shows that DYS385a/b, DYS389II, DYS390 and DYS391 markers have the highest contribution to haplotype diversity.

Locus multiplication has been reported at several Y-STR loci, including DYS19, DYS390, DYS385 (triplication), DYS393, DYS391, DYS389II, DYS437 and DYS439 [7–12]. In the present study, five duplications were observed in locus DYS19, DYS389I, DYS393, DYS437 and DYS439. Data comparison between our samples and a previously published sample from the Tunisian population [13] was performed for markers which are common to both studies using the exact test for population differentiation implemented in GENEPOP [14]. All comparisons were found non significant (p-values ranging from 0.06 for DYS391 and

DYS385a to 0.90 for DYS389I). We, however, found a new allele for DYS392 (allele 17) which was not described in the previous study [13]. Thirteen haplotypes were found in common between the two populations and exact test for differentiation applied to haplotype frequencies yields the same conclusion ($p = 0.08$).

This paper follows the guidelines for publication of population data requested by the journal [15].

Access to the data: Available upon request by email to: ahmed.rebai@cbs.rnrt.tn.

Acknowledgements

We would like to thank Nathalie Koch (Applied Biosystems) for her technical assistance and recommendations in STR genotyping. We also think an anonymous reviewer whose comments have improved the quality of the paper. This work was supported by the Ministry of Scientific Research, Technology and Competency Development, Tunisia.

References

[1] Q. Ayub, A. Mohyuddin, R. Qamar, K. Mazhar, T. Zerjal, S.Q. Mehdi, C. Tyler-Smith, Identification and characterisation of novel human y-chromosomal microsatellites from sequence database information, Nucl. Acids Res. 20 (2) (2000) e8.

[2] P. Gill, C. Brenner, B. Brinkmann, B. Budowle, A. Carracedo, M.A. Jobling, P. deKnijff, M. Kayser, M. Krawczak, W.R. Mayr, N. Morling, B. Olaisen, V. Pascali, M. Prinz, L. Roewer, P.M. Schneider, A. Sajantila, C. Tyler-Smith, DNA Commission of the International Society of Forensic Genetics: recommendations on forensic analysis using Y-chromosome STRs, Forensic Sci. Int. 124 (2001) 5–10.

[3] M. Nei, Molecular Evolutionary Genetics, Columbia University Press, New York, 1987.

[4] G.F. Sensabaugh, Biochemical markers of individuality, in: R. Saferstein (Ed.), Forensic Science Handbook, Prentice-Hall, Englewood Cliffs, 1982, pp. 340–415.

[5] A. Chakravarti, C.C. Li, The effect of linkage on paternity calculations, in: R.H. Walker (Ed.), Inclusion Probabilities in Parentage Testing, American Association of Blood Banks, Arlington, VA, 1983, pp. 411–420.

[6] C. Robino, S. Varacalli, S. Gino, A. Chatzikyriakidou, A. Kouvatsi, C. Triantaphyllidis, C. Di Gaetano, F. Crobu, G. Matullo, A. Piazza, C. Torre, Y-chromosomal STR haplotypes in a population sample from continental Greece, and the islands of Crete and Chios, Forensic Sci. Int. 145 (2004) 61–64.

[7] A.H. Cakir, A. Celebioğlu, E. Yardimci, Y-STR haplotypes in Central Anatolia region of Turkey, Forensic Sci. Int. 144 (2004) 59–64.

[8] M. Kayser, A. Coaglià, D. Corach, N. Fretwell, C. Gehrig, G. Graziosi, F. Heidorn, S. Herrmann, B. Herzog, M. Hidding, K. Honda, M. Jobling, M. Krawczak, K. Leim, S. Meuser, E. Meyer, W. Oesterreich, A. Pandya, W. Parson, G. Penacino, A. Perez-Lezaun, A. Piccinini, M. Prinz, C. Schmitt, P.M. Schneider, R. Szibor, J. Teifel-Greding, G. Weichhold, P. deKnijff, L. Roewer, Evaluation of Y-chromosomal STRs: a multicenter study, Int. J. Legal Med. 110 (1997) 125–133.

[9] M. Kayser, L. Roewer, M. Hedman, L. Henke, J. Henke, S. Brauer, C. Krûger, M. Krawczak, M. Nagy, T. Doboz, R. Szibor, P. deKnijff, M. Stoneking, A. Sajantila, Characteristics and frequency of Germline mutations at microsatellite loci from the human Y chromosome, as revealed by direct observation in father/son pairs, Am. J. Hum. Genet. 66 (2000) 1580–1588.

[10] R. Kurihara, T. Yamamoto, R. Uchihi, S.L. Li, T. Yoshimoto, H. Ohtaki, K. Kamiyama, Y. Katsumata, Mutations in 14 Y-STR loci among Japanese father–son haplotypes, Int. J. Legal Med. 118 (2004) 125–131.

[11] M. Diederiche, P. Martin, A. Amorim, F. Corte-Real, L. Gusmao, A case of double alleles at three Y-STR loci: forensic implications, Int J. Legal Med. 119 (2005) 223–225.

[12] YHRD database (http://www.yhrd.org).

[13] C. Brandt-Casadevall, M. Ben Dhiab, F. Taroni, V. Castella, N. Dimo-Simonin, M. Zemni, P. Mangin, Tunisian population data on 10 Y-chromosomal loci, Forensic Sci. Int. 135 (2003) 247–250.

[14] M. Raymond, F. Rousset, GENEPOP (version 1.2). Population genetics software for exact tests and ecumenicism, J. Heredity 86 (1995) 248–249.

[15] P. Lincoln, A. Carracedo, Publication of population data of human polymorphism, Forensic Sci. Int. 110 (2000) 3–5.

ELSEVIER

Forensic Science International 164 (2006) 254–256

Forensic Science International

www.elsevier.com/locate/forsciint

Announcement of Population Data

Data for 10 autosomal STR markers in south Tunisian population

N. Mahfoudh-Lahiani [a], A. Rebaï [b], H. Makni [a,*]

[a] *Service de Laboratoire, CHU Hedi Chaker, 3028 Sfax, Tunisia*
[b] *Service de Bioinformatique, Centre de Biotechnologie de Sfax, 3038 Sfax, Tunisia*

Received 18 May 2005; received in revised form 24 October 2005; accepted 24 October 2005
Available online 5 December 2005

Abstract

Allele frequencies, together with some parameters of forensic interest for 10 STRs (D3S1358, vWA, D16S539, D2S1338, D8S1179, D21S11, D18S51, D19S433, TH01 and FGA) were estimated from 201 unrelated individuals originating from southern Tunisia.

Significant deviation from Hardy–Weinberg equilibrium was observed for only one marker. Comparative analyses between our population data and other populations showed that only markers D3S158, vWA and FGA were homogenous among populations. The combination of these 10 STR loci provide a powerful tool for forensic identification in Tunisian population.

Keywords: Tunisian population; STR; Population data; Arab

Population: The population sample is constituted by 201 unrelated volunteer blood donors originating from southern Tunisia (see Fig. 1).

Extraction: The DNA was extracted using phenol chloroform method.

PCR: PCR amplification was performed in Gene Amp PCR system 9600, using the Ampfl STR SGM plus PCR Amplification Kit.

Typing: Electrophoresis of the PCR products was carried out in an ABI Prism 310 DNA analyzer (Applied Biosystems) using gel polyacrylamide (pop 4). Sample genotypes were determined with Genotyper (v3.7) by comparison with supplied allelic ladders and an internal size standard (GS.500 Rx).

Results: See Table 1.

Analysis of data: Exact tests of Hardy–Weinberg equilibrium were performed for the 10 loci. Statistical

Fig. 1. Region from which the population sample was drawn. Names of the major cities of this region are indicated.

* Corresponding author. Tel.: +216 98 445 245.
E-mail address: lahiani.tn@tunet.tn (H. Makni).

0379-0738/$ – see front matter
doi:10.1016/j.forsciint.2005.10.018

Table 1
Allele frequency distribution data for Amp FLSTR SGM Plus loci in a south Tunisian population ($n = 201$)

Allele	D3S1358	vWa	D16S539	D2S1338	D8S1179	D21S11	D18S51	D19S433	THO1	FGA
6									0.24378	
7									0.24129	
8			0.03483		0.00746				0.15423	
9			0.09950		0.00746				0.22139	
9.3									0.09453	
10			0.05224		0.05224		0.00746		0.04478	
10.2							0.00498			
11			0.35572		0.09453		0.00995	0.02488		
11.2							0.00995	0.00498		
12			0.24129		0.14428		0.10448	0.12189		
12.2								0.00498		
13	0.00249	0.00249	0.18159		0.21642		0.14179	0.25871		
13.2								0.02985		
14	0.05970	0.10697	0.03483	0.00249	0.22637		0.09453	0.24378		
14.2							0.00249	0.04478		
15	0.30597	0.10945		0.00498	0.15423		0.16418	0.16169		
15.2								0.04478		
16	0.29353	0.27861		0.08458	0.07463		0.17662	0.04726		
16.2								0.00249		
17	0.21393	0.24627		0.27114	0.01741		0.07960	0.00498		0.00249
17.2								0.00498		
18	0.10448	0.15423		0.09453	0.00498		0.08955			0.00249
19	0.01990	0.06219		0.11692			0.06716			0.06218
20		0.03234		0.12189			0.01990			0.09204
21		0.00498		0.06468			0.01990			0.16915
21.2										0.00249
22		0.00249		0.04726			0.00746			0.14925
23				0.06716						0.18159
24				0.06965		0.00249				0.16169
25				0.03483		0.00249				0.09453
26				0.01493						0.04975
27				0.00498		0.03483				0.00498
28						0.12687				0.01990
29						0.24129				
30						0.23383				0.00498
30.2						0.00995				0.00249
31						0.09240				
31.2						0.07711				
32						0.03230				
32.2						0.08209				
33						0.00498				
33.2						0.04478				
34						0.00498				
34.2						0.00746				
35						0.00498				
P	0.0131	0.550	0.5362	0.3027	0.0003	0.1627	0.4987	0.1919	0.0114	0.1178
H	0.7562	0.7512	0.7761	0.8507	0.7263	0.8009	0.8507	0.8109	0.7313	0.7860
P.D	0.8964	0.9344	0.9039	0.9658	0.9515	0.9488	0.9725	0.9442	0.9272	0.9592
P.E	0.5204	0.5118	0.5554	0.6963	0.4702	0.6008	0.6963	0.6195	0.4783	0.5734
P-comp	0.849	0.481	0.0045	0.0001	0.0001	0.030	0.0001	0.0004	0.0001	0.555

P: uncorrected p-values for exact test of Hardy–Weinberg equilibrium; H: observed heterozygosity; PD: power of discrimination; PE: probability of exclusion; P-comp: exact p-value for test of population stratification between four populations (see text).

forensic parameters were calculated including heterozygosity, power of discrimination and probability of exclusion from genotype and allele frequencies [5]. Data comparison between Arabian populations (Morocco [1], Syria [1] and Tunisia [2,3]) including ours was performed for each marker using an exact test for population differentiation. All computations and tests were performed using GENEPOP (Raymond and Rousset [4]).

Remarks: Only locus D8S1179 showed a significant deviation (after Bonferroni correction) from Hardy–Weinberg equilibrium (Table 1, corrected $p = 0.003$) due to a lack of heterozygosity (observed $H = 73\%$, expected $H = 84.6\%$). The most informative locus was D18S51, as already reported in other populations [1] while the least informative is D3S1358 (PD < 0.90). The average PD and PE values were 0.94 and 0.57, respectively while the combined PD and PE for all 10 STR were 0.999999999999976 and 0.99982, respectively. Comparison between the four populations revealed significant differences in all markers except for D3S1358, vWA and FGA (Table 1). However, when comparing the two Tunisian samples (our data and those of Brandt-Casadevall et al. [3]) we found significant differences for only D8S1179 ($p = 0.00005$) where discrepancies in frequency were observed mainly for alleles 10 (0.052 versus 0.105) and 12 (0.144 versus 0.085).

We can conclude from this analysis that the 10 STR loci reported here are a powerful tool for forensic identification and paternity testing in Arabian populations.

This paper follows the guidelines for publication of population data requested by the journal [6].

Access to the data: Available upon request by email to: lahiani.tn@tunet.tn or ahmed.rebai@cbs.rnrt.tn.

Acknowledgments

This work is supported by the Tunisian Ministry of Health. AR acknowledges support from the Ministry of Scientific Research, Technology and Development of Competences, Tunisia. We are grateful to Imen Ayadi for her help in illustrating the paper.

References

[1] L. Abdin, I. Shimada, B. Brinkmann, C. Hohoff, Analysis of 15 short tandem repeats reveals significant differences between the Arabian populations from Morocco and Syria, Legal Med. 5 (2003) S150–S155.

[2] L. Cherni, B. Loueslati Yaâcoubi, L. Pereira, C. Alves, H. Khodjet El-Kill, A. Ben Ammar El Gaaied, A. Amorim, Data for 15 autosomal STR markers (Powerplex 16 System) from two Tunisian populations: Kesra (Berber) and Zriba (Arab), Forensic Sci. Int. 147 (2005) 101–106.

[3] C. Brandt-Casadevall, M. Ben Dhiab, F. Taroni, C. Gehrig, N. Dimo-Simonin, M. Zemni, P. Mangin, Tunisian population data on 15 PCR-based loci, Forensic Sci. Int. 126 (2002) 272–274.

[4] M. Raymond, F. Rousset, GENEPOP (version 1.2). Population genetics software for exact tests and ecumenicism, J. Hered. 86 (1995) 248–249.

[5] I.W. Evett, B.S. Weir, Interpreting DNA Evidence: Statistical Genetics for Forensic Scientists, Sinauer Associates, Sunderland, MA, 1998, p. 278.

[6] P. Lincoln, A. Carracedo, Publication of population data of human polymorphism, Forensic Sci. Int. 110 (2000) 3–5.

ELSEVIER

Forensic Science International 164 (2006) 257–265

Forensic Science International

www.elsevier.com/locate/forsciint

Announcement of Population Data

Population genetic study in two Transylvanian populations using forensically informative autosomal and Y-chromosomal STR markers

Balazs Egyed *, Sandor Füredi, Zsolt Padar

Department of Haemogenetics, Institute for Forensic Sciences, P.O. Box 314/4, H-1903 Budapest, Hungary

Received 17 August 2005; received in revised form 24 October 2005; accepted 24 October 2005
Available online 28 November 2005

Abstract

Our study provides population genetic data on two population samples collected in a Hungarian speaking region of Transylvania, Romania. Allele frequency and profile databases were generated on 17 autosomal STR loci (D2S1338, D3S1358, D5S818, D7S820, D8S1179, D13S317, D16S539, D18S51, D19S433, D21S11, VWA, FGA, TH01, TPOX, CSF1PO, Penta E and Penta D) as well as at the 12 European Y-STR extended haplotype loci (DYS19, DYS389-I/II, DYS390, DYS391, DYS392, DYS393, DYS385 loci, DYS437, DYS438 and DYS439).

Data were compared to a Central Hungarian (Budapest region) population sample [B. Egyed, S. Füredi, M. Angyal, L. Boutrand, A. Vandenberghe, J. Woller, Z. Padar, Analysis of eight STR loci in two Hungarian populations, Forensic Sci. Int. 113 (2000) 25–27] that was used as a reference group of the Hungarian population. Calculating the F_{ST} indices and with the pairwise comparisons of interpopulation molecular variance (AMOVA) the two populations from Transylvania could be fit into the Hungarian population data showing less substructuring effects as compared to the previous findings in Hungary [B. Egyed, S. Füredi, M. Angyal, L. Boutrand, A. Vandenberghe, J. Woller, Z. Padar, Analysis of eight STR loci in two Hungarian populations, Forensic Sci. Int. 113 (2000) 25–27; B. Egyed, S. Füredi, M. Angyal, I. Balogh, L. Kalmar, Z. Padar, Analysis of the population heterogeneity in Hungary using fifteen forensically informative STR markers, Forensic Sci. Int. 158 (2005) 244–249].

Keywords: Short tandem repeat; Y-STR; Transylvanian population; Romanian population; Population substructure

Populations: The Szekler population sample (see Fig. 1) was collected from 257 unrelated Hungarian speaking individuals (89 males, 168 females) living in Csíkszereda, Transylvania (Miercurea Ciuc, Romania). The Csango samples from Gyimes area were collected from 220 unrelated Hungarian speaking individuals (86 males, 134 females) in a relatively closed population residing in the mountain area of Gyimesfelsőlok, Transylvania (Lunca de Sus, Romania).

Extraction: Genomic DNA was isolated from blood samples applying Proteinase K digestion, organic extraction and Microcon-100 (Millipore) ultrafiltration.

PCR: One to two nanograms template DNA in 25 μl reaction volume following in-house methods and manufacturer's instructions (AmpFlSTR Identifiler PCR System, Applied Biosystems; *GenePrint* PowerPlex® 16 and PowerPlex® Y Systems, Promega).

Typing: ABI 3100 Genetic Analyzer (Applied Biosystems) using reference sequenced ladders and internal standards.

Quality control: GEDNAP blind trial (Stain Commission of the German Society for Legal Medicine); Crime

* Corresponding author. Tel.: +36 1441 1475; fax: +36 1441 1473.
E-mail address: balazs.egyed@mail.orfk.b-m.hu (B. Egyed).

0379-0738/$ – see front matter
doi:10.1016/j.forsciint.2005.10.020

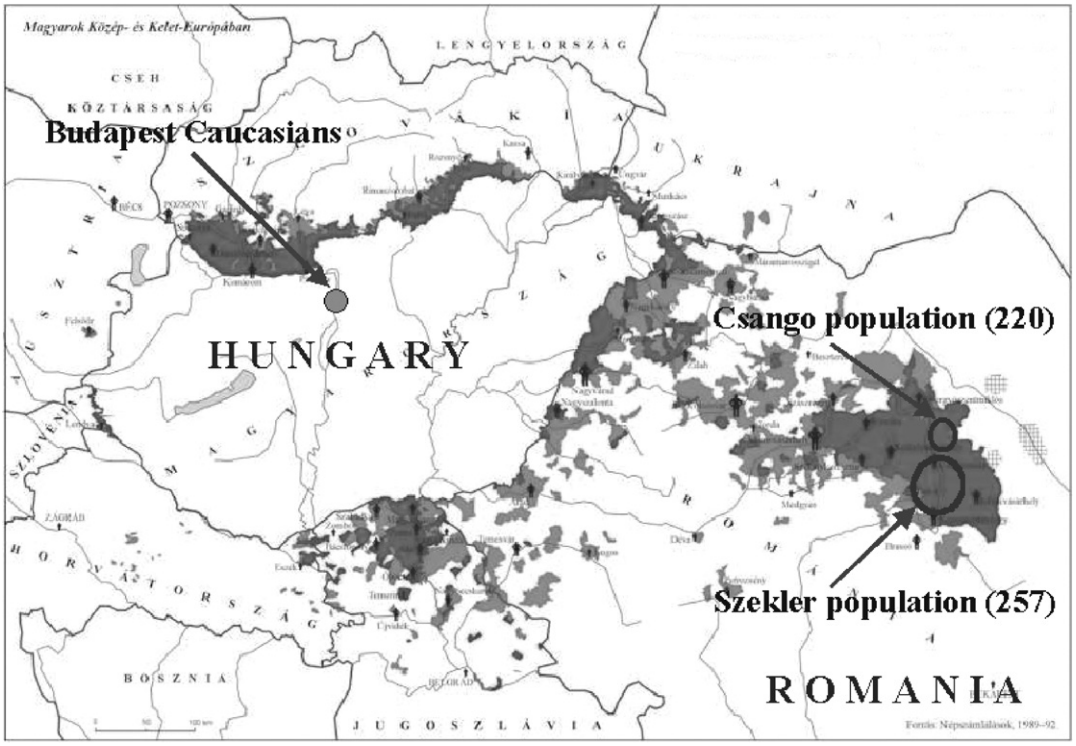

Fig. 1. Map showing the location and the size of the analysed population samples (dark fields surrounding Hungary represent the Hungarian speaking populations in the countries bordering Hungary).

Laboratory Proficiency Testing Program (Collaborative Testing Services, Inc.).

Analysis of data: Possible divergences from Hardy–Weinberg expectations (HWE) were determined using the exact test [3], population substructure was measured by calculating the unbiased single-locus "co-ancestry coefficient" F_{ST} [4] and its Φ-statistic analogue Φ_{ST} in the analysis of molecular variance (AMOVA) [5] using the software ARLEQUIN version 2.000 (http://lgb.unige.ch/arlequin) [6]. The allele frequency profile comparisons were performed by *G*-statistic test using a software dealing with $R \times C$ contingency tables.

Results: The allele frequency data and the forensically informative statistical values of the 17 autosomal STRs are presented in Table 1 following the recommendations of the journal [7]. The combined forensic efficiency values for the examined 17 autosomal markers observed in the Csango population sample [PM = 4.8×10^{-19}; PE = 0.999999894, (PM = matching probability, PE = power of exclusion)] were slightly different to those found in the Szekler database [PM = 1.2×10^{-20}; PE = 0.999999945].

In the analysed 175 male samples, altogether 134 different Y-STR haplotypes were detected which are presented in Table 2. Interestingly, only 6 haplotypes out of 134 were shared by both populations and 80 haplotypes from Szeklers, 48 from Csangos could not be detected in the other population sample. 86 (81 unique) and 54 (39 unique) different haplotypes were found in the Szekler and the Csango population, respectively.

Calculating Wright's F_{ST} indices and with the pairwise comparisons of interpopulation molecular variance (AMOVA) similar values (see Table 3) were found at most autosomal loci as compared to the previous observations in other European populations [8–10]. Our recent data show less substructuring effects than the experienced values in Hungary [1,2,11]. The observed genetic discrepancies between the population pairs are in good accordance with the *G*-statistic findings where the same autosomal loci showed significant differences in the allele frequency distribution. This is especially apparent at locus TPOX in population pairs with Csangos. In the Csango population at locus TPOX an obvious shift of the frequency of allele 8 to 11 can be observed. The F_{ST}-values calculated for the examined Y-STR loci (see Table 3) showed significant genetic differences between population pairs with Csangos. This difference was reinforced at the molecular level in the Szekler/Csango pair by applying AMOVA. The genetic substructuring phenomenon can be explained by a genetic drift or by inbreeding effects in such a closed subpopulation as Csangos.

Access to the data: Available on request: balazs.egyed@orfk.b-m.hu.

Table 1
Allele frequency and forensically informative statistical values on the analysed 17 autosomal STR loci in the Transylvanian Szekler ($N = 257$) and Csango ($N = 220$) population samples

Allele	D8S1179		D21S11		D18S51		FGA		D2S1338	
	Szekler	Csango	Szekler	Csango	Szekler	Csango	Szekler	Csango	Szekler	Csango
8	0.021	0.007								
9	0.008	0.014			0.002					
10	0.070	0.043			0.008	0.005				
11	0.066	0.039			0.008	0.007				
12	0.146	0.166			0.128	0.145				
13	0.338	0.350			0.121	0.093				
14	0.200	0.241			0.204	0.220				
15	0.097	0.102			0.161	0.143				
16	0.048	0.039			0.121	0.141	0.002		0.031	0.055
17	0.004				0.095	0.109	0.002	0.002	0.230	0.211
18					0.045	0.059	0.010	0.014	0.095	0.102
19					0.062	0.055	0.064	0.059	0.099	0.091
20					0.014	0.014	0.119	0.139	0.119	0.086
21					0.010	0.007	0.152	0.159	0.045	0.034
22					0.014	0.002	0.191	0.209	0.029	0.025
22.2							0.014	0.009		
23					0.004		0.136	0.202	0.105	0.143
23.2								0.005		
24					0.004		0.173	0.125	0.105	0.120
24.2							0.002			
25							0.099	0.064	0.126	0.125
25.2							0.002			
26			0.002	0.002			0.029	0.011	0.012	0.005
27			0.025	0.014			0.004	0.002	0.004	0.002
28			0.144	0.132			0.002			
29			0.228	0.245						
29.2			0.002	0.002						
30			0.261	0.289						
30.2			0.033	0.039						
31			0.062	0.070						
31.2			0.088	0.075						
32			0.012	0.007						
32.2			0.093	0.064						
33			0.004							
33.2			0.041	0.048						
34.2			0.006	0.014						
P_{exact}	0.162	0.087	0.566	0.031	0.208	0.163	0.220	0.322	0.859	0.658
H_{obs}	0.817	0.782	0.844	0.773	0.903	0.877	0.871	0.845	0.844	0.863
PD	0.932	0.914	0.952	0.943	0.964	0.958	0.962	0.955	0.970	0.968
PE	0.625	0.577	0.679	0.654	0.741	0.724	0.723	0.693	0.745	0.746

	D19S433		Penta E		Penta D		D3S1358		VWA	
	Szekler	Csango	Szekler	Csango	Szekler	Csango	Szekler	Csango	Szekler	Csango
2.2					0.002					
5			0.078	0.123						
6					0.004					
7			0.158	0.143						
8			0.006	0.007	0.010	0.002				
9				0.007	0.245	0.318				
10		0.002	0.103	0.052	0.126	0.120				
11		0.007	0.097	0.080	0.161	0.191		0.002		
12	0.070	0.055	0.152	0.189	0.195	0.102				
12.2	0.002									
13	0.259	0.245	0.101	0.139	0.160	0.139		0.002		0.005
13.2	0.021	0.020								

Table 1 (*Continued*)

	D19S433		Penta E		Penta D		D3S1358		VWA	
	Szekler	Csango	Szekler	Csango	Szekler	Csango	Szekler	Csango	Szekler	Csango
14	0.340	0.377	0.068	0.043	0.060	0.093	0.113	0.123	0.099	0.075
14.2	0.018	0.016								
15	0.202	0.193	0.072	0.075	0.027	0.032	0.241	0.218	0.086	0.157
15.2	0.039	0.020								
16	0.035	0.034	0.058	0.027	0.010	0.002	0.290	0.225	0.169	0.175
16.2	0.010	0.018								
17	0.004		0.031	0.016			0.220	0.166	0.309	0.259
17.2		0.005								
18			0.041	0.080			0.130	0.216	0.249	0.250
18.2		0.007								
19			0.023	0.016			0.006	0.048	0.076	0.070
20				0.002					0.010	0.009
21			0.004						0.002	
22			0.004	0.002						
24			0.004							
P_{exact}	0.393	0.092	0.190	0.357	0.481	0.610	0.223	0.518	0.484	0.435
H_{obs}	0.755	0.782	0.903	0.814	0.840	0.773	0.790	0.804	0.794	0.759
PD	0.910	0.890	0.977	0.974	0.946	0.938	0.910	0.933	0.924	0.935
PE	0.559	0.544	0.796	0.769	0.660	0.629	0.566	0.619	0.594	0.613

	TH01		TPOX		D5S818		D13S317		D7S820	
	Szekler	Csango	Szekler	Csango	Szekler	Csango	Szekler	Csango	Szekler	Csango
5	0.002									
6	0.216	0.245								
7	0.138	0.120	0.004	0.009	0.002	0.002	0.002		0.021	0.002
8	0.107	0.086	0.560	0.459		0.002	0.152	0.132	0.163	0.195
9	0.228	0.198	0.105	0.132	0.037	0.052	0.101	0.098	0.169	0.145
9.3	0.292	0.336								
10	0.018	0.014	0.054	0.055	0.064	0.075	0.072	0.041	0.288	0.275
11			0.232	0.325	0.323	0.291	0.319	0.361	0.175	0.175
12			0.045	0.020	0.393	0.391	0.243	0.289	0.154	0.184
13					0.173	0.173	0.080	0.064	0.029	0.023
14					0.006	0.014	0.031	0.016		
15					0.002					
P_{exact}	0.731	0.122	0.105	0.465	0.074	0.033	0.279	0.632	0.234	0.342
H_{obs}	0.790	0.809	0.634	0.618	0.685	0.723	0.762	0.741	0.821	0.836
PD	0.919	0.900	0.800	0.837	0.859	0.867	0.927	0.905	0.931	0.925
PE	0.578	0.548	0.382	0.406	0.458	0.489	0.602	0.539	0.616	0.601

	D16S539		CSF1PO	
	Szekler	Csango	Szekler	Csango
8	0.018	0.009	0.008	0.023
9	0.109	0.068	0.043	0.034
10	0.064	0.109	0.280	0.270
11	0.276	0.261	0.272	0.336
12	0.319	0.284	0.298	0.291
13	0.195	0.252	0.084	0.041
14	0.018	0.014	0.016	0.005
15	0.002	0.002		
P_{exact}	0.349	0.944	0.491	0.323
H_{obs}	0.766	0.764	0.786	0.782
PD	0.908	0.908	0.887	0.862
PE	0.553	0.553	0.517	0.479

Szekler: Hungarian speaking population sample from Csíkszereda, Transylvania (Miercurea Ciuc, Romania); Csango: Hungarian speaking population sample from Gyimesfelsőlok, Transylvania (Lunca de Sus, Romania); P_{exact}: Hardy–Weinberg equilibrium (probability of exact test based on 1.000.000 total permutations); H_{obs}: observed heterozygosity; PD: power of discrimination; PE: power of exclusion.

Table 2
Y-STR haplotypes observed in the two examined Transylvanian population samples (134 different haplotypes altogether)

Haplotypes	DYS19	DYS389-I	DYS389-II	DYS390	DYS391	DYS392	DYS393	DYS385	DYS437	DYS438	DYS439	Szekler[a]	Csango[a]
1	13	12	29	24	10	11	13	15–15	14	10	12	1	–
2	13	12	29	24	10	11	13	16–18	14	10	12	1	–
3	13	13	28	24	10	14	13	13–16	14	11	12	–	1
4	13	13	28	24	10	16	13	13–16	14	11	12	–	1
5	13	13	28	24	10	17	13	13–16	14	11	11	1	–
6	13	13	28	24	10	17	13	13–16	14	11	12	–	1
7	13	13	30	24	10	11	13	16–16	14	10	13	1	–
8	13	13	30	24	10	11	13	16–17	14	10	12	1	–
9	13	13	30	24	10	11	13	16–18	14	10	12	–	3
10	13	13	30	24	10	11	14	16–18	14	10	12	1	–
11	13	13	32	25	10	11	13	17–18	14	10	11	1	–
12	13	14	31	22	8	11	13	12–15	14	10	13	2	–
13	14	12	28	22	10	11	12	13–14	16	10	11	1	–
14	14	12	28	22	10	11	13	13–15	15	10	12	1	–
15	14	12	28	22	10	11	13	14–14	16	10	11	1	–
16	14	12	28	22	10	11	13	14–15	16	10	11	–	1
17	14	12	28	22	10	11	14	13–15	16	10	11	1	1
18	14	12	28	23	10	11	11	14–18	15	9	12	1	–
19	14	12	28	23	10	11	12	13–16	15	9	11	–	3
20	14	12	28	23	10	11	13	14–14	16	10	11	1	–
21	14	12	28	24	10	11	12	14–17	16	9	12	1	1
22	14	12	28	24	10	13	12	11–14	15	12	12	1	–
23	14	13	28	24	11	13	13	11–14	15	12	12	1	–
24	14	13	29	22	10	11	12	12–12	14	9	11	–	1
25	14	13	29	22	10	11	13	13–14	16	10	12	1	–
26	14	13	29	23	10	11	12	11–17	15	9	12	1	–
27	14	13	29	23	10	11	12	13–18	14	9	11	–	2
28	14	13	29	23	10	13	13	11–14	15	12	11	1	–
29	14	13	29	23	10	13	13	11–14	15	12	12	1	–
30	14	13	29	23	10	13	13	11–14	15	12	13	1	–
31	14	13	29	24	10	13	13	11–14	15	11	13	1	–
32	14	13	29	24	10	13	13	11–14	15	12	12	1	–
33	14	13	29	24	10	14	12	11–14	15	12	12	1	–
34	14	13	29	24	11	11	13	11–14	15	12	12	–	1
35	14	13	29	24	11	12	13	11–14	15	12	12	–	4
36	14	13	29	24	11	13	13	10–14	15	12	13	1	–
37	14	13	29	25	11	11	12	13–15	15	9	11	2	–
38	14	13	29	25	11	13	13	11–13	15	12	12	1	–
39	14	13	29	25	11	13	13	11–15	15	12	12	1	–
40	14	13	30	24	10	13	13	11–14	14	12	11	1	–
41	14	13	30	24	11	13	12	11–14	15	12	12	1	–
42	14	13	30	24	11	13	13	11–15	15	12	12	–	1
43	14	13	30	24	11	13	13	11–16	15	12	12	–	1
44	14	13	30	24	11	14	12	11–13	15	12	11	–	1
45	14	13	30	24	11	14	12	11–15	15	12	12	1	–
46	14	13	31	24	10	11	12	16–18	14	10	13	1	–
47	14	14	29	23	11	13	13	11–14	15	12	11	1	–
48	14	14	29	23	11	16	15	11–13	14	11	10	1	–
49	14	14	30	23	10	14	14	11–14	14	10	10	1	–
50	14	14	30	23	11	13	13	12–12	15	12	13	–	1
51	14	14	30	23	11	13	13	12–14	15	12	13	2	–
52	14	14	30	23	11	14	14	10–13	14	10	10	1	–
53	14	14	30	23	11	14	14	11–13	14	10	10	2	–
54	14	14	30	24	11	13	12	11–14	15	12	12	1	–
55	14	14	30	25	10	13	12	11–15	14	12	12	1	–
56	14	14	31	23	10	11	12	13–16	14	9	11	1	–
57	14	14	31	23	10	11	12	14–16	14	9	11	–	1

Table 2 (*Continued*)

Haplotypes	DYS19	DYS389-I	DYS389-II	DYS390	DYS391	DYS392	DYS393	DYS385	DYS437	DYS438	DYS439	Szekler[a]	Csango[a]
58	15	11	28	22	10	10	14	15–17	16	10	13	1	–
59	15	11	28	22	10	11	14	14–15	16	10	12	–	3
60	15	12	28	23	9	11	12	15–16	14	9	11	1	–
61	15	12	28	23	10	12	12	15–19	14	9	12	1	–
62	15	12	28	24	10	11	12	14–17	16	9	12	1	1
63	15	12	28	24	10	11	12	14–17	16	9	13	–	1
64	15	12	28	24	10	11	12	14–18	16	10	12	–	1
65	15	12	28	24	10	11	12	14–19	16	10	11	1	–
66	15	12	28	25	10	11	12	15–17	16	9	11	1	–
67	15	12	29	21	11	11	14	13–16	16	10	13	–	1
68	15	12	29	22	10	11	14	14–14	16	10	11	1	1
69	15	12	29	22	10	11	14	14–14	16	10	13	1	–
70	15	12	29	22	10	11	14	14–15	16	10	11	1	–
71	15	12	29	23	10	11	14	14–14	16	10	11	–	1
72	15	12	29	24	10	11	12	14–17	16	10	11	–	3
73	15	13	29	23	9	11	12	13–16	14	9	13	1	–
74	15	13	29	23	10	12	14	15–15	15	8	12	–	1
75	15	13	29	23	10	12	15	16–17	14	10	12	1	–
76	15	13	29	23	10	13	13	11–14	15	13	13	–	1
77	15	13	29	23	10	13	13	16–16	14	9	13	1	–
78	15	13	29	25	10	11	13	11–14	14	11	10	2	6
79	15	13	29	25	10	11	13	11–14	14	11	11	–	1
80	15	13	29	25	10	11	13	11–15	14	11	11	1	–
81	15	13	29	25	11	14	13	11–13	15	12	11	1	–
82	15	13	30	23	10	12	15	16–17	14	10	11	1	–
83	15	13	30	24	10	11	13	11–14	14	11	11	–	1
84	15	13	30	24	11	11	13	11–14	14	11	10	–	1
85	15	13	30	25	11	11	13	11–15	14	11	10	1	–
86	15	13	31	24	11	11	13	14–15	15	10	12	–	3
87	15	13	31	24	11	11	13	14–15	15	10	13	–	2
88	15	13	31	25	11	12	13	14–15	15	10	12	–	2
89	15	13	31	25	11	12	13	14–15	15	10	13	–	2
90	15	14	30	22	10	11	12	15–17	14	9	11	–	1
91	15	14	30	23	9	11	12	15–16	14	10	11	1	–
92	15	14	31	25	11	12	13	11–14	14	11	10	1	–
93	16	12	29	24	11	11	13	14–15	15	10	14	1	–
94	16	12	30	22	10	11	13	14.2–15	16	10	12	1	–
95	16	13	29	23	9	11	12	12–16	14	9	13	1	–
96	16	13	29	23	10	11	13	11–14	14	11	11	1	–
97	16	13	29	23	10	16	13	12–16	15	9	11	1	–
98	16	13	29	24	9	11	12	13–17	14	10	13	1	–
99	16	13	29	24	10	11	13	11–14	14	11	11	1	–
100	16	13	29	24	10	12	15	16–16	14	10	12	1	–
101	16	13	29	25	11	11	13	11–14	14	11	11	1	–
102	16	13	30	22	11	11	12	11–16	15	9	11	1	3
103	16	13	30	22	12	11	12	11–16	15	9	11	–	2
104	16	13	30	24	10	11	13	11–14	14	11	12	1	–
105	16	13	30	25	10	11	13	11–14	14	11	10	1	–
106	16	13	30	25	11	11	13	11–14	14	11	11	1	–
107	16	13	30	25	11	11	14	11–15	14	11	11	–	1
108	16	13	31	23	11	11	13	14–15	15	10	13	–	1
109	16	13	31	24	10	11	13	14–14	14	10	11	–	1
110	16	13	31	24	10	11	13	14–15	15	10	12	–	1
111	16	13	31	24	10	11	13	14–15	15	10	13	–	1
112	16	13	31	24	11	11	13	14–15	15	10	13	1	–
113	16	13	31	24	11	11	13	14–15	16	10	13	1	–
114	16	13	31	24	11	11	13	15–16	15	10	12	1	–
115	16	13	31	25	10	11	13	10–14	14	11	10	–	1
116	16	13	31	25	11	11	13	11–15	14	11	10	–	1

Table 2 (*Continued*)

Haplotypes	DYS19	DYS389-I	DYS389-II	DYS390	DYS391	DYS392	DYS393	DYS385	DYS437	DYS438	DYS439	Szekler[a]	Csango[a]
117	16	13	31	25	11	11	13	14–15	15	10	13	–	1
118	16	13	31	25	11	12	13	14–15	15	10	12	–	1
119	16	13	31	26	10	11	13	14–16	15	10	13	1	–
120	16	13	32	22	10	11	12	13–15	14	9	12	1	–
121	16	13	32	24	11	11	13	14–15	14	10	13	1	–
122	16	14	31	25	10	11	13	11–14	14	11	11	1	–
123	16	14	31	25	11	11	13	11–15	14	11	10	1	–
124	16	14	32	25	11	11	13	11–14	14	11	10	–	1
125	17	13	26	24	11	11	13	14–15	15	10	12	1	–
126	17	13	29	25	11	11	13	11–14	14	11	11	1	–
127	17	13	30	24	10	11	13	10–14	14	11	10	–	1
128	17	13	30	25	10	11	13	10–14	14	11	10	1	–
129	17	13	30	25	11	11	13	14–15	15	10	13	–	1
130	17	13	31	24	11	11	13	14–15	15	10	13	–	1
131	17	13	32	24	10	11	13	14–15	15	10	13	–	2
132	17	14	31	23	11	11	14	11–14	14	11	10	1	–
133	17	14	32	25	10	11	13	10–14	14	11	10	–	5
134	18	13	32	24	10	11	13	14–15	15	10	13	–	1

Szekler: Hungarian speaking population sample from Csíkszereda, Transylvania (Miercurea Ciuc, Romania); Csango: Hungarian speaking population sample from Gyimesfelsőlok, Transylvania (Lunca de Sus, Romania).

[a] Individuals observed for each haplotype in the population sample.

Other remarks: The little evidence for association of alleles at the locus D21S11 and D5S818 in the Csango population sample could not be confirmed using the Bonferroni correction at the individual significance level of 0.003.

By calculating *G*-statistic, allele frequencies were compared to available Romanian population data [12,13], to population data from Serbia, Vojvodina Province [14,15], and to a population from Turkey [16]. In the pairwise comparisons, significant differences were found at least

Table 3
Conventional *F*-statistic (F_{ST}) and AMOVA (Φ_{ST}) values for the analysed STR loci between the two Transylvanian (Szekler, Csango) and Budapest region (BuCa) population pairs

Locus	Szekler/Csango		Szekler/BuCa		Csango/BuCa		Overall populations	
	FST	Φ_{ST}	F_{ST}	Φ_{ST}	F_{ST}	Φ_{ST}	F_{ST}	Φ_{ST}
D8S1179	–	–	–	–	–	+	0.002	0.007
D21S11	–	–	–	–	+	–	0.002	0.001
D18S51	–	–	+	–	+	+	0.002	0.004
FGA	+	+	+	+	+	–	0.003	0.010^{+}
D2S1338	–	–	–	–	–	–	0.000	−0.002
D19S433	–	–	–	–	–	–	0.001	−0.002
Penta E	+	–	–	–	+	–	0.004	−0.001
Penta D	+	–	–	–	+	+	0.007	0.002
D3S1358	+	+	–	–	+	–	0.004	0.005
VWA	+	–	–	+	+	–	0.003	0.002
TH01	–	–	–	–	–	–	0.000	−0.001
TPOX	+	+	–	–	+	+	0.013	0.011^{+}
D5S818	–	–	–	–	–	–	−0.001	−0.001
D13S317	–	–	–	–	–	–	0.000	0.000
D7S820	–	–	–	–	–	–	0.001	0.002
D16S539	+	–	–	–	+	–	0.002	0.000
CSF1PO	–	+	–	–	+	–	0.002	0.002
Overall autosomal STR loci	NT	–	NT	–	NT	–	0.003	0.002
Overall Y-STR loci	0.007^{+}	0.040^{+}	0.000[a]	0.002[a]	0.009[a+]	0.005[a]	0.010	0.014^{+}

+: The *F*-statistic value represents statistically significant difference at the $P = 0.05$ level; −: the *F*-statistic value does not represent statistically significant difference at the $P = 0.05$ level; NT: not tested.

[a] Tested at the European minimal Y-STR haplotype loci.

Table 4
Twelve-locus Y-STR haplotype diversity values in the analysed Transylvanian populations (Szekler, Csango) as well as conventional *F*-statistic (F_{ST}) and AMOVA (Φ_{ST}) values for the European minimal Y-STR haplotypes calculated for the Transylvanian and neighbouring population pairs

	Szekler (0.9987 ± 0.005)[a]		Csango (0.9883 ± 0.016)[a]	
	F_{ST}[b]	Φ_{ST}[b]	F_{ST}[b]	Φ_{ST}[b]
Szekler, Corund [17]	0.002[c]	0.051[c]	0.011[c]	0.083[c]
Romanian, Bukarest [18]	0.000	0.032[c]	0.009[c]	0.011
Bulgarian [19]	0.003[c]	0.022[c]	0.010[c]	0.020[c]
Bulgarian Turks [19]	0.002	0.012	0.009[c]	0.031[c]
Serbian [20]	0.003[c]	0.040[c]	0.012[c]	0.000

[ ]: numbers in brackets are the same in references.
[a] Haplotype diversity (±S.E.).
[b] Genetic structure.
[c] The *F*-statistic value represents statistically significant difference at the $P = 0.05$ level.

two loci (D7S820 and D19S433, Szekler–Serbian pair). Significant differences at the most loci (D21S11, D3S1358, VWA, FGA, D8S1179, D13S317, D7S820, TH01, TPOX, D19S433 and D16S539) were observed between the Csango and the Turkish populations (data not shown).

Comparing the Y-STR haplotypes presented here to previously published Szekler [17], Bukarest Romanian [18], Bulgarian and Bulgarian Turks [19], as well as Serbian [20] population data, significant differences were observed by calculating F_{ST}-values and applying AMOVA (see Table 4). The analysis of the STR loci and the allelic designation was done according to the previously published international guidelines and recommendations [21–23].

References

[1] B. Egyed, S. Füredi, M. Angyal, L. Boutrand, A. Vandenberghe, J. Woller, Z. Padar, Analysis of eight STR loci in two Hungarian populations, Forensic Sci. Int. 113 (2000) 25–27.
[2] B. Egyed, S. Füredi, M. Angyal, I. Balogh, L. Kalmar, Z. Padar, Analysis of the population heterogeneity in Hungary using fifteen forensically informative STR markers, Forensic Sci. Int. 158 (2006) 244–249.
[3] S.W. Guo, E.A. Thompson, Performing the exact test of Hardy–Weinberg proportion for multiple alleles, Biometrics 48 (1992) 361–372.
[4] B.S. Weir, Genetic Data Analysis II, Sinauer Associates, Sunderland, MA, 1996.
[5] Y. Michalakis, L. Excoffier, A generic estimation of population subdivision using distances between alleles with special reference for microsatellite loci, Genetics 142 (1996) 1061–1064.
[6] S. Schneider, D. Roessli, L. Excoffier, Arlequin: a software for population genetics data analysis version 2.000, Genetics and Biometry Lab, Dept. of Anthropology, University of Geneva.
[7] P. Lincoln, A. Carracedo, Publication of population data of human polymorphisms – Editorial, Forensic Sci. Int. 110 (2000) 3–5.
[8] I.W. Evett, P.D. Gill, J.A. Lambert, N. Oldroyd, R. Frazier, S. Watson, S. Panchal, A. Connolly, C. Kimpton, Statistical analysis of data for three British ethnic groups from a new STR multiplex, Int. J. Legal Med. 110 (1997) 5–9.
[9] I.W. Evett, J.A. Lambert, J.S. Buckleton, B.S. Weir, Statistical analysis of a large file of data from STR profiles of British Caucasians to support forensic casework, Int. J. Legal Med. 109 (1996) 173–177.
[10] B. Budowle, R. Chakraborty, Population variation at the CODIS core short tandem repeat loci in Europeans, J. Legal Med. 3 (2001) 29–33.
[11] S. Füredi, J. Woller, Z. Pádár, M. Angyal, Y-STR haplotyping in two Hungarian populations, Int. J. Legal Med. 113 (1999) 38–42.
[12] A. Anghel, C. Marian, M. Pitulescu, A. Daba, I.O. Sirbu, V. Rusu, B. Budowle, Population genetic study of eight short tandem repeat loci CSF1PO, TPOX, TH01, F13A01, FESFPS, vWA, F13B and LPL in the Western Romanian population, Forensic Sci. Int. 131 (2003) 218–219.
[13] L.E. Barbarii, B. Rolf, C. Constantinescu, C. Hohoff, P. Calistru, D. Dermengiu, Allele frequencies of 13 short tandem repeat (STR) loci in the Romanian population, Forensic Sci. Int. 141 (2004) 171–174.
[14] I. Veselinović, M. Kubat, I. Furač, J. Škavić, I. Martinović Klarić, M. Tasić, Allele frequencies of the 15 AmpFlSTR Identifiler loci in the population of Vojvodina Province, Serbia and Montenegro, Int. J. Legal Med. 118 (2004) 184–186.
[15] D. Keckarević, D. Savić, M. Keckarević, M. Stevanović, A. Tarasjev, B. Čuljković, A. Đarmati, S. Vukosavić, S. Romac, Population data on 14 STR loci from population of Serbia and Montenegro (new and renewed data), Forensic Sci. Int. 151 (2005) 315–316.
[16] B.S. Akbasak, B. Budowle, D.J. Reeder, J. Redman, M.C. Kline, Turkish population data with the CODIS multiplex short tandem repeat loci, Forensic Sci. Int. 123 (2001) 227–229.
[17] Z. Beer, K. Csete, T. Varga, Y-chromosome STR haplotype in Szekely population, Forensic Sci. Int. 139 (2004) 155–158.
[18] L.E. Barbarii, B. Rolf, D. Dermengiu, Y-chromosomal STR haplotypes in a Romanian population sample, Int. J. Legal Med. 117 (2003) 312–315.
[19] B. Zaharova, S. Andonova, A. Gilissen, J.J. Cassiman, R. Decorte, I. Kremensky, Y-chromosomal STR haplotypes in three major population groups in Bulgaria, Forensic Sci. Int. 124 (2001) 182–186.
[20] L.B. Lauc, M. Pericic, I.M. Klaric, A. Sijacki, D. Popovic, B. Janicijevic, P. Rudan, Y chromosome STR polymorphisms in a Serbian population sample, Forensic Sci. Int. 150 (2005) 97–101.

[21] B. Olaisen, W. Bär, B. Brinkmann, B. Budowle, A. Carracedo, P. Gill, P. Lincoln, W.R. Mayr, S. Rand, DNA recommendations 1997 of the International Society for Forensic Genetics, Vox Sang. 74 (1998) 61–63.

[22] P. Gill, C. Brenner, B. Brinkmann, B. Budowle, A. Carracedo, M.A. Jobling, P. de Knijff, M. Kayser, M. Krawczak, W.R. Mayr, N. Morling, B. Olaisen, V. Pascali, M. Prinz, L. Roewer, P.M. Schneider, A. Sajantila, C. Tyler-Smith, DNA Commission of the International Society of Forensic Genetics: recommendations on forensic analysis using Y-chromosome STRs, Forensic Sci. Int. 124 (2001) 5–10.

[23] L. Gusmao, J.M. Butler, A. Carracedo, P. Gill, M. Kayser, W.R. Mayr, N. Morling, M. Prinz, L. Roewer, C. Tyler-Smith, P.M. Schneider, DNA Commission of the International Society of Forensic Genetics (ISFG): an update of the recommendations on the use of Y-STRs in forensic analysis, Forensic Sci. Int. 157 (2006) 187–197.

ELSEVIER

Forensic Science International 164 (2006) 266–270

Forensic Science International

www.elsevier.com/locate/forsciint

Announcement of population data

Allele frequencies for 15 autosomal STR loci and admixture estimates in Puerto Rican Americans

J. Zúñiga [a,b,**], M. Ilzarbe [c], V. Acunha-Alonzo [d], F. Rosetti [d], Z. Herbert [c], V. Romero [a], I. Almeciga [a], O. Clavijo [a], J.N.H. Stern [a], J. Granados [f], M. Fridkis-Hareli [a], P. Morrison [c], J. Azocar [e,**], E.J. Yunis [a,*]

[a] *Department of Cancer Immunology and AIDS, Dana-Farber Cancer Institute and Department of Pathology, Harvard Medical School, 44 Binney Street, Boston, MA 02115, United States*
[b] *Instituto Nacional de Enfermedades Respiratorias, Mexico City, Mexico*
[c] *Molecular Biology Core Facilities, Dana Farber Cancer Institute, Harvard Medical School, Boston, MA, United States*
[d] *Escuela Nacional de Antropologia e Historia, Instituto Nacional de Antropologia e Historia, Mexico City, Mexico*
[e] *Northgate Medical Center, Springfield, MA, USA*
[f] *Department of Immunology and Rheumatology, Instituto Nacional de Ciencias Médicas y de la Nutrición Salvador Zubirán, Mexico City, Mexico*

Received 22 November 2005; received in revised form 23 November 2005; accepted 23 November 2005
Available online 19 January 2006

Abstract

Allelic frequencies of 15 short tandem repeats (STR) markers (CSF1PO, FGA, THO1, TPOX, VWA, D3S11358, D5S818, D7S820, D8S1179, D13S317, D16S539, D18S51, D21S11, D19S433 and D2S1338) were determined using the AmpFℓ STR® Identifiler™ PCR Amplification Kit in Puerto Rican American individuals ($N = 205$) from Massachusetts. The FGA, D18S51 and D2S1338 loci had a high power of discrimination (PD) with values of 0.967, 0.965 and 0.961, respectively. Significant deviations from the Hardy–Weinberg (HW) equilibrium were not detected. An important genetic contribution of Caucasian European (76.4%) was detected in Puerto Rican Americans. However, comparative analysis between Puerto Rican American and other neighboring populations from United States mainly with African and Caucasian Americans, revealed significant differences in the distribution of STR markers.

Our results are important for future comparative genetic studies of different American ethnic groups, in particular a cultural group called Hispanic-Americans and should be helpful for forensic and paternity testing.

Keywords: Short tandem repeat; STR; Allelic frequencies; Puerto Rican; AmpFℓ STR® Identifiler™

Population: Two hundred and five non-related Puerto Rican American individuals from Springfield, Massachusetts were studied. All subjects were recruited from the same community and with Puerto Rican ancestry (all four grandparents were born in Puerto Rico and none from Europe or other continents) as self-reported by questionnaire.

DNA extraction: Genomic DNA was extracted from 200 μL of EDTA-blood by using Qiagen columns (Qiagen, Chatsworth, CA).

PCR: CSF1PO, FGA, THO1, TPOX, VWA, D3S11358, D5S818, D7S820, D8S1179, D13S317, D16S539, D18S51,

* Corresponding author. Tel.: +1 617 632 3347; fax: +1 617 632 4466.
** Corresponding authors.
E-mail addresses: Joaquin_zuniga@dfci.harvard.edu (J. Zúñiga), jazocar@comcast.net (J. Azocar), edmond_yunis@dfci.harvard.edu (E.J. Yunis).

0379-0738/$ – see front matter © 2005 Elsevier Ireland Ltd. All rights reserved.
doi:10.1016/j.forsciint.2005.11.022

D21S11, D19S433 and D2S1338 loci along with amelogenin were co-amplified using the AmpFℓ STR® Identifiler™ Kit (Applied Biosystems, Foster City, CA) according to manufacturer's instructions [1].

Typing: The amplified products and reference ladders provided in the kit were analyzed in a ABIPrism 3100 Genetic Analyzer (Applied Biosystems). Electrophoresis results were analyzed using GeneMapper® software Version 3.5.

Results: See Tables 1 and 2.

Quality control: Laboratory internal control standards and kit controls.

Analysis of data: Gene frequencies, observed and expected heterozygosity and Hardy–Weinberg (HW) equilibrium and exact test of population differentiation were calculated using the Arlequin population genetics software v2.1. The significance level 0.05 was corrected by the Bonferroni method, p-values < 0.003 were considered statistically significant ($0.05/15 = 0.003$).

Matching probability, power of discrimination, polymorphism information content, power of exclusion and typical paternity indexes were calculated using the Power Stats v1.2 software.

Admixture estimations were calculated using the maximum likelihood method with the program Leadmix [2] and a Bayesian approach using the program Structure 2.0 [3] (http://pritch.bsd.uchicago.edu). We used Caucasian European (Spaniards), West Africans and Amerindian populations as Puerto Rican ancestral contributors. Previous reported STR data on parental populations Europeans from Spain [4], West Africans [5] and from Mexican Amerindian population [6] were used for the analyses of admixture estimates.

Access to data: The complete data can be accessed: joaquin_zuniga@dfci.harvard.edu.

Other remarks: In this study, we analyzed the frequencies of 15 STR markers in 205 Puerto Rican Subjects from Springfield, Massachusetts, Table 1. Significant deviations from HW equilibrium were not observed. The loci D19S433 and D18S51 had the highest number of alleles (15) compared with the locus TH01 with only six alleles. The locus FGA showed the higher power of discrimination (PD = 0.967) followed by the loci D18S51 and D2S1338 with PD = 0.965 and 0.961, respectively. The combined power of discrimination of all 15 STR was >0.99999999 and the combined power of exclusion was >0.9999992.

These STR frequencies compared with those published before in other populations [4–6] were used for the admixture estimation analysis with the maximum likelihood method [2]. They demonstrated an important contribution of Caucasian European (76.4%), African (17.0%) and Amerindian genes (6.6%) in Puerto Rican American population. Individual ancestry proportions calculated with Structure 2.0 [3] are shown in a triangle plot that shows the distribution of the individual admixture estimates in relation to the parental populations. The results obtained by the above-mentioned Bayesian approach confirm that Puerto Rican Subjects from Massachusetts has a greater Caucasian ancestry contribution, Fig. 1.

Using the population differentiation test, we compared our results in Puerto Rican American individuals with previously published data available online on three populations in the United States [7]: Hispanic American (in the United States, Hispanic Americans refers to individuals originating from Latin America, it is not ethnic but a cultural denomination), African American and Caucasian American http://www.cstl.nist.gov/biotech/strbase. Comparative analyses between pairs of populations are shown as non-differentiation exact probability values in Table 2. We found significant differences between Puerto Rican American and African American populations (6/15 loci with $p < 0.003$) and between Puerto Rican American and Caucasian American populations (4/15 loci with $p < 0.003$). The comparison between Puerto Rican Americans and Random Hispanic Americans showed a significant value in the locus D19S433 ($p = 0.00293$). In addition, important differences between Caucasian American versus African American and Hispanic American versus African American comparisons were observed, Table 2.

Several STR markers have been investigated for application to human identity testing [8,9]. In this study, we used a commercially available multiplex STR typing kit to analyze the allelic frequencies of 15 STR markers in a Puerto Rican American population from Massachusetts. The most informative loci for power of exclusion were FGA, D18S51 and D19S433 and the least informative were D5S818, TPOX, TH01 and CSF1PO. In our study, we also detected an

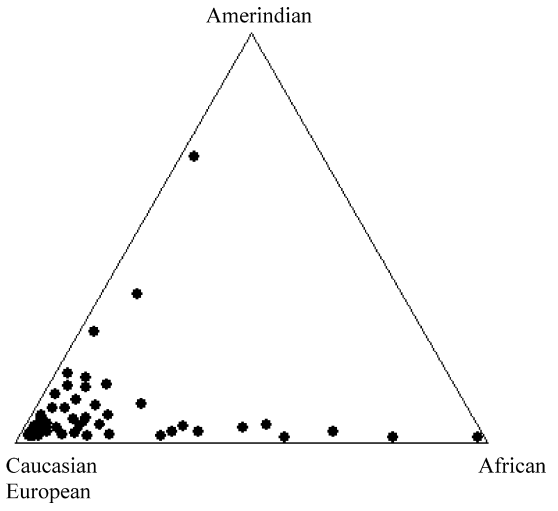

Fig. 1. Estimation of individual ancestry proportions in Puerto Rican Americans. In this analysis, with a three parental population model, the contributions of Caucasian European, African and Amerindian populations in $N = 205$ Puerto Rican American individuals from Massachusetts were calculated. Triangle plot obtained with the Structure 2.0 software shows the ancestry proportions of each individual (●) in the context of the parental populations, which are represented in different angles of the figure.

Table 1
Allele frequencies of 15 STR in Puerto Rican American ($N = 205$)

Allele	D8S1179	D21S11	D7S820	CSF1PO	D3S1358	TH01	D13S317	D16S539	D2S1338	D19S433	vWA	TPOX	D18S51	D5S818	FGA
5	–	–	–	–	–	–	–	–	–	–	–	–	–	–	–
6	–	–	–	–	–	0.200	–	–	–	–	–	0.007	–	–	–
7	–	–	0.022	0.017	–	0.217	–	–	–	–	–	0.002	–	0.049	–
8	0.010	–	0.161	0.022	–	0.127	0.093	0.020	–	–	–	0.398	–	0.002	–
9	0.010	–	0.137	0.015	–	0.210	0.085	0.146	–	0.002	–	0.117	–	0.039	–
9.3	–	–	–	–	–	0.237	–	–	–	–	–	–	–	–	–
10	0.100	–	0.310	0.234	–	0.010	0.059	0.098	–	0.083	–	0.066	0.005	0.049	–
10.2	–	–	–	–	–	–	–	–	–	–	–	–	0.002	–	–
11	0.051	–	0.173	0.261	–	–	0.220	0.329	–	0.027	0.007	0.315	0.005	0.315	–
12	0.122	–	0.141	0.415	0.005	–	0.310	0.237	–	0.098	–	0.090	0.083	0.363	–
12.2	–	–	–	–	–	–	–	–	–	0.010	–	–	–	–	–
13	0.222	–	0.054	0.032	0.016	–	0.166	0.144	–	0.234	–	0.005	0.127	0.173	–
13.2	–	–	–	–	–	–	–	–	–	0.022	–	–	–	–	–
14	0.234	–	0.002	0.002	0.066	–	0.066	0.027	–	0.256	0.088	–	0.163	0.007	–
14.2	–	–	–	–	–	–	–	–	–	0.046	–	–	–	–	–
15	0.212	–	–	–	0.273	–	0.002	–	–	0.112	0.154	–	0.173	0.002	–
15.2	–	–	–	–	–	–	–	–	–	0.056	–	–	–	–	–
16	0.034	–	–	–	0.327	–	–	–	0.056	0.027	0.207	–	0.149	–	–
16.2	–	–	–	–	–	–	–	–	–	0.017		–	–	–	–
17	0.005	–	–	0.002	0.195	–	–	–	0.220	0.007	0.261	–	0.129	–	–
17.2	–	–	–	–	–	–	–	–	–	0.002	–	–	–	–	–
18	–	–	–	–	0.115	–	–	–	0.051	–	0.173	–	0.095	–	0.012
19	–	–	–	–	0.005	–	–	–	0.200	–	0.083	–	0.032	–	0.080
19.2	–	–	–	–	–	–	–	–	–	–	–	–	–	–	–
20	–	–	–	–	0.005	–	–	–	0.090	–	0.024	–	0.017	–	0.098
21	–	–	–	–	–	–	–	–	0.034	–	0.002	–	0.005	–	0.151
21.2	–	–	–	–	–	–	–	–	–	–	–	–	–	–	–
22	–	–	–	–	–	–	–	–	0.051	–	–	–	0.012	–	0.168
22.2	–	–	–	–	–	–	–	–	–	–	–	–	–	–	–
23	–	–	–	–	–	–	–	–	0.095	–	–	–	0.002	–	0.134
23.2	–	–	–	–	–	–	–	–	–	–	–	–	–	–	–
24	–	–	–	–	–	–	–	–	0.095	–	–	–	–	–	0.163
24.2	–	–	–	–	–	–	–	–	–	–	–	–	–	–	–
25	–	–	–	–	–	–	–	–	0.088	–	–	–	–	–	0.080
25.2	–	–	–	–	–	–	–	–	–	–	–	–	–	–	–
26	–	–	–	–	–	–	–	–	0.020	–	–	–	–	–	0.076
26.2	–	0.002	–	–	–	–	–	–	–	–	–	–	–	–	–
27	–	0.024	–	–	–	–	–	–	–	–	–	–	–	–	0.029
28	–	0.107	–	–	–	–	–	–	–	–	–	–	–	–	–
28.2	–	–	–	–	–	–	–	–	–	–	–	–	–	–	–
29	–	0.244	–	–	–	–	–	–	–	–	–	–	–	–	0.004

29.2	–	–	–	–	–	–	–	–	–	–	–	–	–	–	–
30	–	0.261	–	–	–	–	–	–	–	–	–	–	–	–	–
30.2	–	0.029	–	–	–	–	–	–	–	–	–	–	–	–	–
30.3	–	–	–	–	–	–	–	–	–	–	–	–	–	–	–
31	–	0.063	–	–	–	–	–	–	–	–	–	–	–	–	–
31.2	–	0.114	–	–	–	–	–	–	–	–	–	–	–	–	–
32	–	0.007	–	–	–	–	–	–	–	–	–	–	–	–	–
32.2	–	0.083	–	–	–	–	–	–	–	–	–	–	–	–	–
33	–	0.002	–	–	–	–	–	–	–	–	–	–	–	–	–
33.2	–	0.051	–	–	–	–	–	–	–	–	–	–	–	–	–
34	–	–	–	–	–	–	–	–	–	–	–	–	–	–	–
34.2	–	0.007	–	–	–	–	–	–	–	–	–	–	–	–	–
35	–	0.002	–	–	–	–	–	–	–	–	–	–	–	–	–
36	–	–	–	–	–	–	–	–	–	–	–	–	–	–	–
Ho	0.800	0.809	0.834	0.673	0.756	0.741	0.824	0.770	0.853	0.863	0.790	0.658	0.873	0.726	0.897
He	0.824	0.835	0.808	0.704	0.764	0.799	0.806	0.784	0.870	0.846	0.822	0.721	0873	0.736	0.878
HW (p)	0.135	0.111	0.146	0.214	0.335	0.006	0.047	0.157	0.187	0.004	0.867	0.579	0.418	0.824	0.086
MP	0.058	0.049	0.071	0.134	0.096	0.076	0.072	0.078	0.039	0.047	0.056	0.119	0.035	0.113	0.033
PD	0.942	0.951	0.929	0.866	0.904	0.924	0.928	0.922	0.961	0.953	0.944	0.881	0.965	0.887	0.967
PIC	0.80	0.81	0.78	0.65	0.72	0.76	0.78	0.75	0.86	0.83	0.80	0.67	0.86	0.69	0.86
PE	0.599	0.617	0.664	0.388	0.520	0.487	0.645	0.545	0.692	0.731	0.590	0.360	0.741	0.479	0.790
TPI	2.50	2.63	3.10	1.53	2.05	1.90	2.85	2.17	3.31	3.80	2.44	1.44	3.94	1.86	4.88

Ho: Observed heterozygosity; He: expected heterozygosity; HW: Hardy–Weinberg equilibrium, Bonferroni correction significant p-value <0.003. MP: Matching probability; PD: power of discrimination; PIC: polymorphism information content; PE: power of exclusion; TPI: typical paternity index.

Table 2
Comparative analysis between Puerto Rican American (PRA) and other neighboring populations: Hispanic–Americans (HA)[a] [7], Caucasian–Americans (CA) [7] and African–Americans (AA) [7]

Locus	PRA vs. HA	PRA vs. CA	PRA vs. AA	CA vs. AA	CA vs. HA	HA vs. AA
D8S1179	0.21603	0.00098*	0.07722	0.00000*	0.11632	0.02737
D21S11	0.23167	0.24047	0.00000*	0.00000*	0.49462	0.00000*
D7S820	0.04594	0.00587	0.06256	0.00000*	0.00280*	0.00782
CSF1PO	0.11046	0.52297	0.02444	0.02053	0.22385	0.02151
D3S1358	0.98143	0.04399	0.68231	0.01173	0.13881	0.81232
TH01	0.42131	0.00000*	0.00000*	0.00000*	0.00196*	0.00000*
D13S317	0.04203	0.08993	0.00000*	0.00196*	0.08993	0.00000*
D16S539	0.19257	0.46921	0.04301	0.00196*	0.11046	0.05083
D2S1338	0.28543	0.00391*	0.00000*	0.00000*	0.23265	0.00000*
D19S433	0.00293*	0.00000*	0.04888	0.00000*	0.19648	0.00782
vWA	0.24145	0.95210	0.39003	0.31965	0.52493	0.39394
TPOX	0.19062	0.00196*	0.00000*	0.00000*	0.10362	0.00000*
D18S51	0.88465	0.42913	0.00000*	0.00000*	0.82209	0.00587
D5S818	0.49365	0.31672	0.05083	0.02737	0.61193	0.01760
FGA	0.36168	0.35679	0.06940	0.01955	0.12805	0.08309

The significance level 0.05 was corrected by the Bonferroni method for the number of comparisons (0.05/15 = 0.003).
[a] In the United States, Hispanic Americans refers to individuals originating from Latin America, it is not ethnic but a cultural denomination.
* Significant p-values <0.003.

important Caucasian European genetic contribution in Puerto Rican Americans with and adequate number of STR polymorphic markers. Our results support previous studies of admixture estimates using blood groups [10] and other ancestry informative markers [11] that have reported an important contribution of Caucasian genes in Puerto Ricans.

Taken together, our results are important to determine the genetic background of Puerto Ricans living in the United States. STR analysis in this ethnic group showed significant differences between Puerto Rican Americans compared with African American and Caucasian American populations suggesting that the 15 STR system tested would be a useful tool for forensic, paternity testing and population differentiation analysis between neighboring populations living in the United States.

This study is reported following the guidelines for publication of population data requested by the journal [12].

Acknowledgements

This work was supported by NIH grants HL29583 and HL59838. J.Z. was supported in part by grants from the Instituto Nacional de Enfermedades Respiratorias, Mexico and by Fundacion Mexico en Harvard A.C.

References

[1] Applied Biosystems, AmpFℓ STR® Identifiler™ PCR Amplification Kit User's Manual, Foster City, CA, P/N 4323291, 2001.
[2] L. Wang, Maximum likelihood estimation of admixture proportions from genetic data, Genetics 164 (2003) 747–765.
[3] J.K. Pritchard, M. Stephens, P. Donnelly, Inference of population structure using multilocus genotype data, Genetics 155 (2000) 945–959.
[4] P. Sanz, V. Prieto, I. Flores, Y. Torres, M. Lopez-Soto, M.J. Farfan, Population data of 13 STRS in Southern Spain (Andalusia), Forensic Sci. Int. 119 (2003) 113–115.
[5] R. Gonçalves, J. Jesus, A.T. Fernández, A. Brehm, Genetic profile of a multi-ethnic population from Guiné-Bissau (West African Coast) using the new PowerPlex® 16 system kit, Forensic Sci. Int. 129 (2002) 78–80.
[6] C. Barrot, C. Sanchez, M. Ortega, A. Gonzalez-Martin, C. Brand-Casadevall, A. Gorostiza, E. Huguet, J. Corbella, M. Gene, Characterization of three Amerindian populations from Hidalgo State (Mexico) by 15 STR-PCR polymorphisms, Int. J. Legal Med. 119 (2005) 111–115.
[7] J.M. Butler, R. Schoske, P.M. Vallone, J.W. Redman, M.C. Kline, Allele frequencies for 15 autosomal STR loci on U.S. Caucasian, African American and Hispanic populations, J. Forensic Sci. 48 (2003) 1–4.
[8] A. Edwards, A. Civitello, H.A. Hammond, C.T. Caskey, DNA typing and genetic mapping with trimeric and tetrameric tandem repeats, Am. J. Hum. Genet. 49 (2001) 746–756.
[9] P. Gill, DNA as evidence—the technology of identification, N. Engl. J. Med. 352 (2005) 2669–2671.
[10] F.M. Salzano, M.C. Bortolini, The evolution and genetics of Latin American populations, Cambridge Studies in Biological and Evolutionary Anthropology, vol. 28, Cambridge University Press, Cambridge, NY, 2002, xvi (512 pp.).
[11] C. Bonilla, M.D. Shriver, E.J. Parra, A. Jones, J.R. Fernández, Ancestral proportions and their association with skin pigmentation and bone mineral density in Puerto Rican women from New York city, Hum. Genet. 115 (2004) 57–68.
[12] P. Lincoln, A. Carracedo, Publication of population data of human polymorphisms, Forensic Sci. Int. 110 (2000) 3–5.

ELSEVIER

Forensic Science International 164 (2006) 271–275

Forensic Science International

www.elsevier.com/locate/forsciint

Announcement of Population Data

Allelic and haplotypic frequencies at 11 Y-STR loci in Buryats from South-East Siberia

Marcin Woźniak [a,*], Miroslava Derenko [b], Boris Malyarchuk [b], Irina Dambueva [c], Tomasz Grzybowski [a], Danuta Miścicka-Śliwka [a]

[a] *Institute of Molecular and Forensic Genetics, Nicolaus Copernicus University, Collegium Medicum in Bydgoszcz, M. Sklodowskiej-Curie 9, 85-094 Bydgoszcz, Poland*

[b] *Genetics Laboratory, Institute of Biological Problems of the North, Russian Academy of Sciences, Portovaya Str. 18, 685000 Magadan, Russia*

[c] *Institute of General and Experimental Biology, Russian Academy of Sciences, 670047 Ulan-Ude, Russia*

Received 12 August 2005; received in revised form 23 November 2005; accepted 23 November 2005
Available online 13 February 2006

Abstract

We have obtained Y-STR haplotypes in 12 loci (DYS19, DYS385, DYS389I, DYS389II, DYS390, DYS391, DYS392, DYS393, DYS437, DYS438 and DYS439) from 215 Buryat males. We have found that one haplotype (15-11,18-13-28-23-10-11-14-14-10-12) comprises more than 30% of Y chromosomes in this population while another haplotype (14-11,13-14-30-23-10-14-14-14-10-10) comprises additional 14% of chromosomes. The population under study seems to be very homogenous as far as Y chromosome is regarded and the most frequent haplotype seems to be the modal haplotype for Buryats.

Keywords: Buryats; Y-STR; Y chromosome

Population: Buryat samples ($n = 215$) were collected in the villages of the Buryat Republic (Dzhida, Bichursk, Ivolga, Kyakhta, Tunka, Kizhinga, Khorinsk, Zakamensk, Eravna, Selenga, Barguzin and Kabansk districts), Chita (Aginsk district) and Irkutsk (Alarsk, Bayandaevsk, Bokhan, Nukutsk, Olkhon, Ust-Orda, Osa and Ekhirit-Balagansk districts) regions, thus encompassing all territories inhabited by modern Buryats (Fig. 1). Only a few samples were chosen from each locality, limiting the probability of sampling relatives. All of these individuals were paternally and maternally unrelated and originated from the area considered for this study. All samples were collected with approval of an appropriate ethical committee as well as with informed consent.

DNA extraction: The whole blood was obtained by venipuncture and collected into EDTA vacutainer tubes. DNA was extracted by following the standard phenol–chloroform extraction method [1]. The quantity of recovered DNA for most samples was determined using the Quantiblot™ system (Applied Biosystems, Foster City, CA, USA).

PCR amplification: PowerPlex Y® amplification system (Promega) was used to amplify 12 Y-STR loci: DYS19, DYS385, DYS389I/II, DYS390, DYS391, DYS392, DYS393, DYS437, DYS438 and DYS439. Aliquots of DNA samples were diluted at the 1:30 ratio and 1 μL of each dilution was added to the amplification reaction prepared according to the manufacturer's protocol with one exception, i.e. Taq polymerase manufactured by Promega was used instead of AmpliTaq Gold. Cycling conditions

* Corresponding author. Tel.: +48 52 585 3556; fax: +48 52 585 3553.
E-mail address: marcinw@cm.umk.pl (M. Woźniak).

0379-0738/$ – see front matter © 2006 Published by Elsevier Ireland Ltd.
doi:10.1016/j.forsciint.2005.11.023

Table 1
Allele frequencies at 11 Y-STR loci investigated in Buryats ($n = 215$)

Allele	Abs. freq.	Rel. freq.
DYS19		
13	1	0.005
14	48	0.223
15	128	0.595
16	28	0.130
17	8	0.037
18	2	0.009
	LD = 0.5800 ± 0.0293	
DYS389I		
12	9	0.042
13	158	0.735
14	48	0.223
	LD = 0.4103 ± 0.0329	
DYS389II		
27	1	0.005
28	121	0.563
29	45	0.209
30	40	0.186
31	8	0.037
	LD = 0.6063 ± 0.0263	
DYS390		
22	4	0.019
23	161	0.749
24	34	0.158
25	16	0.074
	LD = 0.4103 ± 0.0372	
DYS391		
9	17	0.079
10	185	0.860
11	11	0.051
12	2	0.009
	LD = 0.2518 ± 0.0377	
DYS392		
10	4	0.019
11	162	0.753
12	1	0.005
13	6	0.028
14	42	0.195
	LD = 0.3948 ± 0.0353	
DYS393		
11	1	0.005
12	6	0.028
13	42	0.195
14	165	0.767
15	1	0.005
	LD = 0.3738 ± 0.0349	
DYS437		
13	1	0.005
14	199	0.926
15	8	0.037
16	7	0.033
	LD = 0.1415 ± 0.0320	
DYS438		
9	3	0.014
10	190	0.884
11	19	0.088
13	3	0.014
	LD = 0.2118 ± 0.0356	
DYS439		
10	66	0.307
11	21	0.098
12	96	0.447
13	30	0.140
14	2	0.009
	LD = 0.6805 ± 0.0182	

Haplotype	Abs. freq.	Rel. freq.
DYS385		
10,14	1	0.005
10,19	2	0.009
11,11	1	0.005
11,13	39	0.181
11,14	8	0.037
11,15	3	0.014
11,17	5	0.023
11,18	106	0.493
11,19	6	0.028
12,12	19	0.088
12,13	9	0.042
12,14	1	0.005
12,15	2	0.009
12,19	5	0.023
13,13	1	0.005
13,15	1	0.005
13,16	2	0.009
13,17	2	0.009
13,18	1	0.005
14,14	1	0.005
	LD = 0.7138 ± 0.0283	

Explanations: abs. freq., absolute frequency; rel. freq., relative frequency; LD, locus diversity.

Table 2
Sixty-five distinct Y-STR haplotypes revealed by the analysis of 215 Buryat Y chromosomes

Abs. freq.	Rel. freq.	DYS 19	DYS 385	DYS 389I	DYS 389II	DYS 390	DYS 391	DYS 392	DYS 393	DYS 437	DYS 438	DYS 439
69	0.321	15	11,18	13	28	23	10	11	14	14	10	12
30	0.140	14	11,13	14	30	23	10	14	14	14	10	10
19	0.088	15	11,18	13	28	23	10	11	14	14	10	13
7	0.033	16	12,12	13	29	24	9	11	13	14	10	11
4	0.019	17	12,12	13	29	24	10	11	14	14	10	10
4	0.019	15	11,17	13	28	23	10	11	14	14	10	12
3	0.014	16	12,13	13	29	24	9	11	13	14	10	11
3	0.014	15	11,19	13	28	23	10	11	14	14	10	12
3	0.014	15	11,18	13	28	24	10	11	14	14	10	12
2	0.009	15	11,18	13	28	23	10	11	14	14	9	12
2	0.009	14	11,13	14	30	23	10	14	13	14	10	10
2	0.009	15	11,18	13	28	23	10	11	13	14	10	12
2	0.009	14	13,16	13	29	24	10	11	12	15	10	11
2	0.009	18	12,12	13	29	25	10	11	13	14	10	10
2	0.009	14	11,13	14	29	23	10	14	14	14	10	10
2	0.009	15	11,19	13	28	23	10	11	14	14	10	13
2	0.009	15	12,13	13	29	25	10	11	13	14	10	10
2	0.009	16	10,19	14	29	23	9	13	14	14	13	12
2	0.009	14	12,19	12	29	23	10	10	14	16	11	10
2	0.009	15	12,15	13	28	24	9	11	13	15	11	12
2	0.009	15	11,18	14	29	23	10	11	14	14	10	12
2	0.009	14	12,19	12	28	23	10	10	14	16	11	10
2	0.009	15	11,18	13	28	23	11	11	14	14	10	13
2	0.009	14	11,13	14	31	23	10	14	14	14	10	10
2	0.009	16	11,14	13	29	25	11	11	13	14	11	10
2	0.009	15	12,12	14	31	24	9	11	13	14	10	11
1	0.005	15	11,18	13	28	22	10	11	14	14	10	13
1	0.005	13	13,17	14	29	23	10	12	13	16	10	13
1	0.005	17	12,13	13	29	25	10	11	13	14	10	10
1	0.005	15	11,17	13	29	23	10	11	14	14	10	13
1	0.005	15	12,14	13	29	24	10	11	13	14	11	11
1	0.005	16	11,14	14	31	24	11	11	13	14	11	10
1	0.005	15	11,18	13	28	23	10	11	13	14	10	14
1	0.005	15	11,18	13	28	23	10	11	14	14	10	14
1	0.005	14	11,13	14	30	23	10	13	14	14	10	10
1	0.005	16	13,13	12	28	24	10	13	12	13	10	12
1	0.005	16	12,13	13	29	25	10	11	13	14	10	10
1	0.005	15	11,18	13	29	23	10	11	14	14	10	12
1	0.005	17	12,12	13	29	24	10	11	13	14	10	10
1	0.005	14	11,18	13	28	23	10	11	14	14	10	13
1	0.005	15	11,11	13	28	22	10	14	12	15	10	11
1	0.005	14	12,13	13	29	22	10	14	13	14	10	10
1	0.005	14	11,14	13	29	24	10	13	13	15	13	13
1	0.005	17	11,15	13	31	25	11	11	14	14	11	11
1	0.005	15	11,15	13	30	25	11	11	13	14	11	10
1	0.005	15	11,14	14	31	23	11	11	13	14	10	10
1	0.005	16	11,15	13	30	25	11	11	13	14	11	10
1	0.005	15	11,18	13	28	24	10	11	14	14	10	13
1	0.005	16	13,18	13	30	24	10	13	12	15	9	10
1	0.005	14	11,13	14	30	23	10	14	15	14	10	10
1	0.005	16	10,14	13	29	25	10	11	13	14	11	11
1	0.005	16	11,14	13	29	25	10	11	13	14	11	11
1	0.005	16	12,12	13	29	24	10	11	14	14	10	11
1	0.005	16	12,12	12	28	25	9	11	13	14	10	11
1	0.005	16	12,12	13	29	24	10	11	14	14	10	10
1	0.005	15	12,19	13	28	23	10	11	14	14	10	12

Table 2 (*Continued*)

Abs. freq.	Rel. freq.	DYS 19	DYS 385	DYS 389I	DYS 389II	DYS 390	DYS 391	DYS 392	DYS 393	DYS 437	DYS 438	DYS 439
1	0.005	16	11,14	13	30	25	12	11	13	14	11	10
1	0.005	15	13,17	12	27	23	10	14	12	16	11	12
1	0.005	15	11,19	13	28	23	11	11	14	14	10	12
1	0.005	14	13,15	12	28	24	10	14	11	15	11	13
1	0.005	16	11,18	13	29	23	11	11	14	14	10	12
1	0.005	17	11,14	13	29	24	12	11	13	14	11	10
1	0.005	16	12,13	13	30	25	10	11	13	14	10	10
1	0.005	15	11,13	14	30	23	10	14	14	14	10	10
1	0.005	16	14,14	12	31	22	10	11	14	16	10	12

Explanations: abs. freq., absolute haplotype frequency; rel. freq., relative haplotype frequency.

were set according to the PowerPlex Y kit manufacturer's suggestions.

Electrophoresis and typing: Products of amplification were electrophoresed using ABI3100 Genetic Analyzer with an appropriate filter set prepared on the basis of the relevant PowerPlex® Matrix Standards provided by Promega [2]. Fifty-centimeter capillaries and POP-6 polymer were used for optimal resolution. One microliter of each sample was mixed with 9 μL of deionized formamide (Applied Biosystems) and 0.5 μL of Internal Lane Standard 60–600 (Promega). Electrophoresis results were analyzed using Genscan Version 3.7 and Genotyper Version 3.7 software (Applied Biosystems). Y Power Typer macro (Promega) was used to assign allelic names. Alleles were designated according to the recommendations of the DNA commission of the International Society of Forensic Genetics [3].

Quality: Allelic ladders and control DNA samples provided with the PowerPlex Y kit were used. YHRD quality control exercises passed successfully by the laboratory.

Results: See Tables 1 and 2.

Statistical analysis: Population statistics and FST values were calculated using Arlequin software (Version 2.000) [4]. MDS analysis was performed using STATISTICA Version 7.1 (StatSoft) [5].

Additional data access: Additional data available from corresponding author.

Comments: The Buryats, numbering approximately 436,000, are the largest ethnic minority group in Siberia and are mainly concentrated in the Buryat Republic in central southern part of Siberia border to Mongolia and China. The Buryat language belongs to the Mongolic branch of the Altaic family, and the ancestors of modern Buryats could have been both Mongolic tribes and Tungusic and Turkic nomads who expanded into Baikal region from Central Asia in Neolithic times [6].

Haplotype diversity of the Buryat sample investigated ($n = 215$) was 0.8691 ± 0.0186. The most frequent haplotypes were: 15-11,18-13-28-23-10-11-14-14-10-12 (32.1%), 14-11,13-14-30-23-10-14-14-14-10-10 (14%) and 15-11,18-13-28-23-10-11-14-14-10-13 (8.8%) (order of loci: DYS19, DYS385, DYS389I, DYS389II, DYS390, DYS391, DYS392, DYS393, DYS437, DYS438 and DYS439). The first the third most frequent haplotypes are one-step neighbors and the only difference between them is at DYS439 locus. We have used the minimal haplotype portions of the three most frequent haplotypes (i.e. DYS19, DYS385, DYS389I,

Fig. 1. A map of East Asia. The region where samples were collected is bordered by a thick black line and shaded in gray.

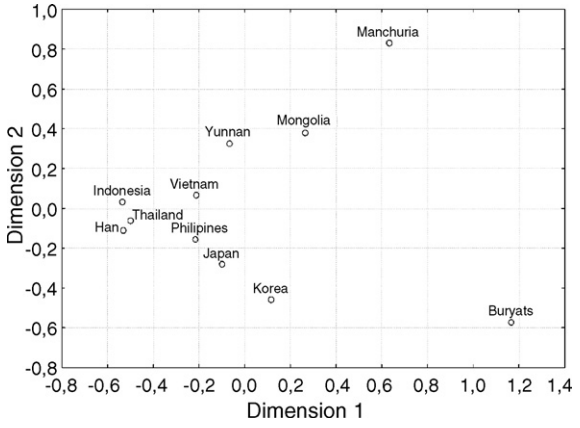

Fig. 2. MDS plot of FST pairwise differences for "minimal Y-STR haplotype" in 11 Asian populations, including Siberian Buryats (denoted in the plot as "Buryats") and 10 Asian populations from Kwak et al. [8].

DYS389II, DYS390, DYS391, DYS392 and DYS393) to scan the YHRD database (Version 16 [7]) for similar haplotypes. It turned out that the most frequent Buryat minimal haplotype (identical for the first and the third most frequent haplotypes in our sample) is not present in the database even though the database contains 42 samples from Mongolia described as Buryats. Thus, the haplotype may represent a modal haplotype for Buryats living in Siberia. Among the most frequent minimal haplotype's one-step neighbors one was found in Vietnamese population (15-11,18-13-29-23-10-11-14, frequency 2/209) but this haplotype turned out to be 10-10 in DYS438 and DYS439 loci so it was not a one-step neighbor if the extended set of loci was regarded. The second one-step neighbor of the Buryats' most frequent minimal haplotype present in the YHRD was 15-11,19-13-28-23-10-11-14, detected in the population of Mongolian Khalks (1/39). The minimal haplotype part of the second most frequent haplotype in Buryats turned out to be present in 10 population samples from Eurasia, including Tatars from Poland (2/124), Turks from Central Anatolia (2/110), Finns (5/399), Buryats (1/42) and Khalks (1/39) from Mongolia, populations of Moscow (1/85), Novogorod (1/50), Vladivostok (1/148) in Russia, Taraz in Kazakhstan (2/175) and population of Sweden (1/405).

Our Buryat sample was compared for ''minimal haplotype'' with other populations of East and South-East Asia, including Buryats from Mongolia, by means of AMOVA analysis based on pairwise FST comparisons. We have used Asian Y-STR data available from literature [8]. The degree if interpopulation variability was 11.16% when Siberian Buryats were included into the dataset while it was equal to 4.78% when the calculations were performed without Siberian Buryats Y-STR data. MDS analysis of the populations under investigation shows significant distance between Siberian Buryats and other Asian populations (Fig. 2).

Homogeneity seems to be the main characteristic of the Buryat population regarding Y-STRs under study. Locus and haplotype diversity indices are lower than usually reported for the loci under study [9–11]. Such a homogeneity was not observed when studying mtDNA diversity from the same subjects [12,13]. This paper follows the guidelines of publication of population data in Forensic Science International [14].

Acknowledgements

We thank all of the donors for making this work possible, Aneta Jakubowska and Maria Perkova for technical assistance. This research has been supported by the grants from the Polish State Committee for Scientific Research (3P04C 04823), Russian Foundation for Basic Research (04-04-48746) and by the Program of Basic Research of Russian Academy of Sciences ''Dynamics of plant, animal and human gene pools''. M.D. was supported in part by the Józef Mianowski Fund.

References

[1] J. Sambrook, E.E. Fritsch, T.R. Maniatis, Molecular Cloning, second ed., Cold Spring Harbour, New York, 1989.
[2] PowerPlex® Matrix Standards, 3100, Technical Bulletin No. 019, Promega, Madison WI, USA (http://www.promega.com/tbs/tbd019/tbd019.pdf).
[3] P. Gill, C. Brenner, B. Brinkmann, et al., DNA Commission of the International Society of Forensic Genetics: recommendations on forensic analysis using Y-chromosome STRs, Forensic Sci. Int. 124 (2001) 5–10.
[4] S. Schneider, D. Roessli, L. Excoffier, Arlequin Ver. 2000: A Software for Population Genetics Data Analysis, Genetics and Biometry Laboratory, University of Geneva, Switzerland, 2000.
[5] StatSoft, Inc., STATISTICA (data analysis software system), Version 7.1, 2005 (www.statsoft.com).
[6] M.G. Levin, L.P. Potapov, The Peoples of Siberia, University of Chicago Press, Chicago, 1964.
[7] Y Chromosome Haplotype Reference Database (http://yhrd.org/index.html).
[8] K.D. Kwak, H.J. Jin, D.J. Shin, J.M. Kim, L. Roewer, M. Krawczak, C. Tyler-Smith, W. Kim, Y-chromosomal STR haplotypes and their applications to forensic and population studies in east Asia, Int. J. Legal Med. 119 (2005) 195–201.
[9] B. Budowle, M. Adamowicz, Z.G. Aranda, C. Barna, R. Chakraborty, D. Cheswick, B. Dafoe, A. Eisenberg, R. Frappier, A.M. Gross, C. Ladd, H.-S. Lee, S.C. Milne, C. Meyers, M. Prinz, M.L. Richard, G. Saladanha, A.A. Tierney, L. Viculis, B.E. Krenke, Twelve short tandem repeat loci Y chromosome haplotypes: genetic analysis on populations residing in North America, Forensic Sci. Int. 150 (2005) 1–15.
[10] H. Khodjet el Khil, R.T. Marrakchi, B.Y. Loueslati, A. Langaney, M. Fellous, A.B. Elgaaied, Distribution of Y chromosome lineages in Jerba island population, Forensic Sci. Int. 148 (2005) 211–218.
[11] A. Hadi Cakir, A. Celebioglu, E. Yardimici, Y-STR haplotypes in Central Anatolia region of Turkey, Forensic Sci. Int. 144 (2004) 59–64.
[12] M.V. Derenko, B.A. Malyarchuk, I.K. Dambueva, G.O. Shaikhaev, C.M. Dorzhu, D.D. Nimaev, I.A. Zakharov, Mitochondrial DNA variation in two South Siberian aboriginal populations: implications for the genetic history of North Asia, Hum. Biol. 72 (2000) 945–973.
[13] M.V. Derenko, T. Grzybowski, B.A. Malyarchuk, I.K. Dambueva, G.A. Denisova, J. Czarny, C.M. Dorzhu, V.T. Kakpakov, D. Miscicka-Sliwka, M. Wozniak, I.A. Zakharov, Diversity of mitochondrial DNA lineages in South Siberia, Ann. Hum. Genet. 67 (2003) 391–411.
[14] P. Lincoln, A. Carracedo, Publication of population data of human polymorphisms, Forensic Sci. Int. 110 (2000) 3–5.

Forensic Science International 164 (2006) 276–277

www.elsevier.com/locate/forsciint

Announcement of Population Data

Nucleotide variability of HV-I in admixed population of the Brazilian Amazon Region

Ana Cecília Feio-dos-Santos, Bruno Maia Carvalho, Sidney Emanuel Batista dos Santos, Ândrea Kely Campos Ribeiro-dos-Santos *

Laboratório de Genética Humana e Médica, Departamento de Patologia, Universidade Federal do Pará, Belém, Pará, Brasil

Received 18 October 2005; received in revised form 24 November 2005; accepted 29 December 2005
Available online 31 January 2006

Abstract

The analysis of genetic variation in the nucleotide sequences of mitochondrial DNA has been used as a tool in the study of history of different human populations, as Amerindians, Afro-descendents populations and furthermore admixed populations. In this study, the mitochondrial DNA was analyzed in 158 unrelated individuals in an admixed population of the Amazonian Region: Santarém-PA-Brazil. The polymorphisms were detected using both levels, analysis of restriction enzyme and direct sequencing. We observed a total of 49 different haplotypes were found determined by 46 variable nucleotides. The more frequent haplotypes (Hap03) was shared by five samples and 43 sequences were unique. The genetic diversity was estimated to 0.989 ± 0.0067 and the probability of two random individuals showed identical mitochondrial DNA (mtDNA) haplotypes were 2.8%.

Keywords: DNA mitochondrial; HV-I; Admixed population; Amazon Region; Santarém

Population: Blood samples were collected from 158 healthy unrelated volunteers from Santarém Population of the Amazon Region. The samples were collected of individuals with the grandparents and parents were born in the city. Thus, we can return to three generations before and prevents migration effect at these samples [1].

Extraction: Fenol–chloroform extraction and ethanol precipitation [2].

Amplification and sequencing of mtDNA: PCR amplification was performed using primers previously described [3–6]. The RFLP analysis was performed employing specific endonucleasis to determine the Amerindians, African, Asian and European haplogroups. The HV-I region was amplified in 60 individuals (23 were identified in null RFLP haplotypes and 37 individuals in random), utilizing specific primer and the products were purified by PureLink (PureLinkTM, Invitrogen) and sequenced employing Big Dye™ Terminator v 3.1 Cycle Sequencing Ready Reaction kit (Applied Biosystems, Foster City, USA). The sequenced products were ethanol precipitated, followed by electrophoresis in ABI 377 Genetic Analyzer (Applied Biosystems, Foster City, USA). We have used the sequencing primers in both forward and reverse directions, thus enhancing the accuracy of the sequences. In all the stages were used negative controls.

Analysis of data: The sequences were edited between positions 16,010 and 16,400. The edited data was aligned with the Cambridge reference sequence [7,8], using BioEdit software [9]. Genetic diversity [10] and nucleotide diversity [11] were calculated using the Arlequin Package software V2.0 [12].

Results: The polymorphic sites observed from the RFLP and sequencing of HV-I region were presented as haplotype data in Table 1.

Access of data: Via electronic mail under request to the communicating author.

Other remarks: The 49 different haplotypes as determined by 46 polymorphic sites were identified by RFLP analysis and the sequencing of HV-I of an admixed population from the Amazon Region, Brazil. Amongst the haplotypes most frequent, one (Hap.03) was shared by only five individuals, one

* Corresponding author at: Universidade Federal do Pará, Centro de Ciências Biológicas, Laboratório de Genética Humana e Médica, Rua Augusto Corrêa, 01 Guamá, Caixa Postal 8615, CEP 66075-970, Belém, Pará, Brasil.
Tel.: +55 91 3249 0373; fax: +55 91 3249 0373.
E-mail address: akely@ufpa.br (Â.K.C. Ribeiro-dos-Santos).

0379-0738/$ – see front matter © 2006 Elsevier Ireland Ltd. All rights reserved.
doi:10.1016/j.forsciint.2005.12.032

Table 1
Description of the variable nucleotides of mitochondrial lineages in Santarém admixed population from the Amazon Region, Brazil

Haplotypes	HG	HV-I[a]	Others polymorphisms
Hap.01	H	CRS	(−) 10,394, (−) 7,025
Hap.02	J	69 126 145 167 231 261	(−) 13,704
Hap.03	A	111 223 290 319 362	(+) 663
Hap.04	A	111 223 290 304 319 362	(+) 663
Hap.05	A	111 192 223 290 319 362	(+) 663
Hap.06	A	111 172 223 290 319 362	(+) 663
Hap.07	A	111 223 290 311 319 362	(+) 663
Hap.08	A	111 223 266 290 319 360 362	(+) 663
Hap.09	A	111 192 223 290 319 360	(+) 663
Hap.10	A	223 290 319 362	(+) 663
Hap.11	A	223 290 319 362 390	(+) 663
Hap.12	B	189 218	Del 9bp
Hap.13	B	189	Del 9bp
Hap.14	B	51 189 217 309 325 360	Del 9bp
Hap.15	B	189 217 390	Del 9bp
Hap.16	B	189 217 223 390	Del 9bp
Hap.17	B	93 111 126 189 223	Del 9bp
Hap.18	B	93 189 362	Del 9bp
Hap.19	C	51 223 298 325 327	(−)13,259
Hap.20	C	51 223 294 298 325 327	CRS
Hap.21	C	223 298 325 327	(−)13,259
Hap.22	C	223 298 325 327 362	Del 9bp
Hap.23	C	126 172 223 298 325 327	(−)13,259
Hap.24	C	129 223 298 325 327	CRS
Hap.25	C	129 223 298 325 327	(−)13,259
Hap.26	C	223 325 327	(−)13,259
Hap.27	C	223 325 327 363	CRS
Hap.28	D	189 223 325 362 390	(−)5,176
Hap.29	D	223 325 362	(−)13,259
Hap.30	D	223 325 362	(−)5,176
Hap.31	D	223 325 362	CRS
Hap.32	D	223 362	(−)5,176
Hap.33	L0a	172 223 311 362	(+) 3,592, (−) 5,176
Hap.34	L2	223 278 362 390	(+)3,592
Hap.35	L2	223 278 294 309 390	(+)3,592
Hap.36	L2	189 192 223 278 294 309 390	(+)3,592
Hap.37	L3a	51 223	(−) 10,394
Hap.38	L3	51 223 327	(+) 663, (+) 3,952
Hap.39	L3e	223 327	(+)2,349, (−) 3,592
Hap.40	L3d	35 129 223 327	(−) 8,616
Hap.41	L3e	129 223 327	(+)2,349, (−) 3,592
Hap.42	L3e	185 223 311 327	(+)2,349, (−) 3,592
Hap.43	L3e	35 185 223 311 327	(+)2,349, (−) 3,592
Hap.44	L3	209 223 311	CRS
Hap.45	L3	209 218 223 256 292 311	CRS
Hap.46	L3d	124 189 223 278 304 311	(−) 8,616
Hap.47	L3b	124 223 278 362	(+)10,084
Hap.48	L3b	223	(+)10,084
Hap.49	?	93 223	CRS

HG: haplogroups names; CRS: Cambridge reference sequence; (+)/(−): presence/absence of the restriction site.
[a] The nucleotides indicated in column HV-I must be increased of 16,000 bp.

(Hap.21) was shared by four individuals, and four haplotypes (Hap.01, Hap.02, Hap.13, Hap.45) were shared by two individuals each one of them. Forty-three unique haplotypes were observed. The genetic diversity was estimated to 0.989 ± 0.0067, the nucleotide diversity was estimated to 0.01258 ± 0.00663 and the probability of two random individuals showed identical mitochondrial DNA (mtDNA) haplotypes were 2.8%.

Acknowledgments

Special thanks to the donors of samples (Santarém Population of the Amazon Region), who enable this study to be carried out. This study was supported by FINEP (*Financiadora de Estudos e Projetos*), CNPq (*Conselho Nacional de Desenvolvimento Científico e Tecnológico*) and UFPA (*Universidade Federal do Pará*).

References

[1] E.J.M. Santos, A.K.C. Ribeiro-dos-Santos, J.F. Guerreiro, G.F.S. Aguiar, S.E.B. Santos, Migration and ethnic change in an admixed population from the Amazon Region (Santarém Pará), Braz. J. Genet. 19 (1996) 511–515.
[2] J. Sambrook, E.F. Frotsch, T. Maniatis, Isolations of DNA from mammalian cells, in: N. Ford, C. Nolan, M. Ferguson (Eds.), Molecular Cloning, Cold Spring Harbor Laboratory Press, New York, 1989, pp. 916–919.
[3] J. Alves-Silva, M.S. Santos, P.E.M. Guimarães, A.C.S. Ferreira, H.-J. Bandelt, S.D.J. Pena, V.F. Prado, The ancestry of Brazilian mtDNA lineages, Am. J. Hum. Genet. 67 (2000) 444–461.
[4] A.C. Stone, M. Stoneking, Ancient DNA from a pre-Columbian Amerindian population, Am. J. Phys. Anthropol. 92 (1993) 463–471.
[5] A. Torroni, T.G. Schurr, C.C. Yang, E.J. Szathmary, R.C. Williams, M.S. Schanfield, G.A. Troup, W.C. Knowler, D.N. Lawrence, K.M. Weiss, D.C. Wallace, Native American mitochondrial DNA analysis indicates that the Amerindian and the Na-Dene populations were founded by two independent migrations, Genetics 130 (1992) 153–162.
[6] S. Horai, R. Kondo, Y. Nakagawa-Hattori, S. Hayashi, S. Sonoda, K. Tajima, Peopling of the Americas, founded by four major lineages of mitochondrial DNA, Mol. Biol. Evol. 10 (1993) 23–47.
[7] S. Anderson, A.T. Bankier, B.G. Barrell, M.H.L. De Bruijn, A.R. Coulson, J. Drouin, I.C. Eperon, D.P. Nierlich, B.A. Rose, F. Sanger, P.H. Schreier, A.J.H. Smith, R. Staden, I.G. Young, Sequence and organization of the human mitochondrial genome, Nature 290 (1981) 457–467.
[8] R.M. Andrews, I. Kubacka, P.F. Chinnery, R.N. Lightowlers, D.M. Turnbull, N. Howell, Reanalysis and revision of the Cambridge reference sequence for human mitochondrial DNA, Nat. Genet. 23 (1999) 457–467.
[9] T.A. Hall, BioEdit: a user-friendly biological sequence alignment editor and analysis program for Windows 95/98/NT, Nucl. Acids. Symp. Ser. 41 (1999) 95–98.
[10] M. Nei, Molecular Evolutionary Genetics, Columbia University Press, New York, 1987.
[11] F. Tajima, Measurement of DNA polymorphism, in: N. Takahata, A.G. Clark (Eds.), Mechanisms of Molecular Evolution, Sinauer Associates Inc., Sunderland, MA, 1993, pp. 37–59.
[12] S. Schneider, D. Roessli, L. Excoffier, Arlequin: A Software for Population Genetic Data, Genetics and Biometry Laboratory, University of Geneva, Switzerland, 2000.

ELSEVIER

Forensic Science International 164 (2006) 278–279

Forensic Science International

www.elsevier.com/locate/forsciint

Letter to the Editor

Shaken baby syndrome: A flawed biomechanical analysis

Keywords: Injury; Infant; Shaken; Baby; Rotational; Acceleration/deceleration; Syndrome; Neck

To the Editor,

We are gravely concerned that the conclusions reached by Bandak [1] may be invalid due to apparent numerical errors in his estimation of forces experienced in an infant neck during vigorous shaking. More specifically, we have repeated the author's calculations and we find values of neck forces that are actually more than 10 times *lower* than those presented in Bandak's Table 3.

Using the free body diagram of the infant head and neck (Fig. 3), Bandak identified the two components of neck force during rotation of the head—the tangential force F_t and the normal force F_n. Bandak described the basic equations for neck forces during a simplified shaking event, but did not present detailed methods for calculating the upper neck loads. We define them here for completeness:

$$F_t = m_{head} a_t = m_{head} r \frac{d^2\theta}{dt^2} \quad (1)$$

$$F_n = m_{head} \frac{v^2}{r} = m_{head} r \left(\frac{d\theta}{dt}\right)^2 \quad (2)$$

where r is the length of the neck in meters, m_{head} the mass of the head in kilograms, a_t the tangential linear head acceleration in meters per second squared, $d^2\theta/dt^2$ the angular acceleration of the head in radians per second squared, v the linear velocity of the head in meters per second, and $d\theta/dt$ the angular velocity of the head in radians per second.[1] As Bandak pointed out, when F_n reaches its maximum value, F_t is at a minimum, so it would be incorrect to sum or otherwise combine peak F_n and F_t to estimate peak neck forces. Yet, using the same angular acceleration and velocity values Bandak reported from the literature, we calculate forces 10 times lower than those presented in Bandak's Table 3.

For example, to calculate neck forces for the most severe shaking event reported in Bandak's Table 3, we used the largest angular acceleration and angular velocity values, the longest neck length and the heaviest head mass provided in Table 3 (15,000 rad/s^2, 150 rad/s, 6.35 cm, and 1.59 kg, respectively). Substituting these values into Eqs. (1) and (2) above, we find that normal force F_n exceeds the tangential force F_t, and is calculated as follows:

$$F_{n,high} = m_{head}(r)\left(\frac{d\theta}{dt}\right)^2 = (1.59\,\text{kg})\left(6.35\,\text{cm} \times \frac{1\,\text{m}}{100\,\text{cm}}\right)\left(150\frac{\text{rad}}{\text{s}}\right)^2 = 2272\,\text{N}$$

However, Bandak reported $F_{n,high}$ at 35,931 N in Table 3, a value 15.8 times higher than the correct value. Similarly, to calculate forces for the least severe shaking event discussed by Bandak, we used the minimum values of each parameter range provided by Bandak's Table 3 and calculated the lower range of the normal force as:

$$F_{n,low} = m_{head}(r)\left(\frac{d\theta}{dt}\right)^2 = (0.68\,\text{kg})\left(3.81\,\text{cm} \times \frac{1\,\text{m}}{100\,\text{cm}}\right)\left(50\frac{\text{rad}}{\text{s}}\right)^2 = 65\,\text{N}$$

The corresponding value reported by Bandak in Table 3 is 1027 N.

We repeated the force calculations for all values in Bandak's Table 3 and our attempts to reproduce these neck force calculations consistently yield values that are at least 10 times *lower* than those reported for shaking in Table 3 and Fig. 4 of Bandak's paper. While in some cases the error appears to be a failure to include the neck length, there is no single, simple explanation responsible for the errors that appear in *every* value in Table 3. Also, Prange and Myers [2] analysis of the same data yielded neck forces similar to what we have calculated here.

DOIs of original articles: 10.1016/j.forsciint.2005.12.017, 10.1016/j.forsciint.2006.01.001.

[1] It is important to note that the equations for tangential and normal acceleration in Bandak's methods and repeated in this letter do not account for chest acceleration, and it is not known if the actual neck forces would be higher or lower if chest acceleration were considered.

0379-0738/$ – see front matter
doi:10.1016/j.forsciint.2005.12.018

Based upon his flawed calculations, Bandak erroneously concluded that the neck forces in even the least severe shaking event far exceed the published injury tolerance of the infant neck. However, when accurately calculated, the range of neck forces is considerably lower, and includes values that are far *below* the threshold for injury. In light of the numerical errors in Bandak's neck force estimations, we question the resolute tenor of Bandak's conclusions that neck injuries would occur in all shaking events. Rather, we propose that a more appropriate conclusion is that the possibility exists for neck injury to occur during a severe shaking event without impact.

References

[1] F.A. Bandak, Shaken baby syndrome: a biomechanics analysis of injury mechanisms, Forensic Sci. Int. 151 (2005) 71–79.
[2] M.T. Prange, B.S. Myers, Evidenced-based biomechanical analysis of craniocervical inflicted neurotrauma, in: Inflicted Childhood Neurotrauma, American Academy of Pediatrics, 2003, pp. 237–243.

Susan Margulies*
University of Pennsylvania, Department of Bioengineering, PA 19104-6392, USA

Michael Prange
Exponent, Inc., 3401 Market Street, Suite 300, Philadelphia, PA 19104, USA

Barry S. Myers
Duke University, Department of Biomedical Engineering, Durham, NC 27708-0281, USA

Matthew R. Maltese
The Children's Hospital of Philadelphia, Philadelphia, PA 19104, USA

Songbai Ji
University of Pennsylvania, Department of Bioengineering, Philadelphia, PA 19104-6392, USA

Xinguo Ning
University of Pennsylvania, Department of Bioengineering, Philadelphia, PA 19104–6392, USA

Jacob Fisher
Exponent, Inc., 3401 Market Street, Suite 300, Philadelphia, PA 19104, USA

Kristy Arbogast
Cindy Christian
University of Pennsylvania, Department of Pediatrics, Philadelphia, PA 19104, USA

*Corresponding author. Tel.: +1 215 898 0882; fax: +1 215 573 2071
E-mail address: margulies@seas.upenn.edu (S. Margulies)

20 July 2005
Available online 24 January 2006

Available online at www.sciencedirect.com
ScienceDirect
Forensic Science International 164 (2006) 280–281
Forensic Science International
www.elsevier.com/locate/forsciint

Letter to the Editor

Keywords: Shaken baby syndrome; Biomechanics; Brain injury

In the paper entitled ''Shaken baby syndrome: A biomechanical analysis of injury mechanism, published in Forensic Science International 15 (2005) 71–79'', a mechanical analogue has been used to model infant head and neck. Neck distraction forces have been calculated for various combinations of head mass, neck length, and head angular velocities. Calculated neck distraction forces have been compared to experimentally observed forces in goats, baboons, and infants. Based on these comparisons, the paper hypothesises, among other things, that neck injury is most likely to occur when a baby is shaken in addition to or before there is brain injury (Table 1).

It is unclear how the head velocities listed in Table 2 were calculated. The free head velocity during shaking is indicated to be 4.31 m/s which perhaps corresponds to the 15 kph figure assigned to Shaking in column 1 of Table 2. Could the author please explain how this 15 kph value was calculated. It will also be interesting to know how this velocity relates to the angular accelerations [5000–15,000 rad/s^2] and angular velocities [50–150 rad/s] which presumably were used to calculate the values of neck distraction forces in Table 3.

The paper indicates on page 76, column 2, para 2, that rotational velocities of 50 rad/s and 150 rad/s were used to compute neck distraction forces presented in Table 3. We were unsuccessful in reproducing the neck distraction forces presented in Table 3 using these values. Presented below is a table with the recomputed values of the neck distraction forces using the neck lengths, head masses used by the author and using a low end rotational velocity of 50 rad/s and an upper end rotational velocity of 150 rad/s. Corresponding values presented in Table 3 of the paper are provided within parenthesis.

The values for neck distraction forces were calculated using the following formula:

$$\text{Neck distraction force}, F_n = \text{mass} \times \frac{\text{velocity}^2}{\text{radius}}$$
$$= \text{mass} \times \text{angular velocity}^2 \times \text{radius} \quad (1)$$

As an example, for a head mass of 0.68 kg, neck length of 0.0381 m, and a rotational velocity of 50 rad/s, neck distraction force is computed as:

$$\text{Neck distraction force} = 0.68 \times 0.0381 \times 50 \times 50$$
$$= 64.77\ \text{N as tabulated below.}$$

Perhaps the author could comment on how the neck distraction forces in Table 3 in the paper were computed. If he finds that the force values are closer to the recomputed values, he might perhaps comment on the validity of the paper's conclusions bearing in mind newly computed much lower values of neck distraction force.

We also reviewed the normal acceleration between the neck and head during shaking experiments conducted by Dr. C. Jenny, MD, et al. (reference [11] in the paper) using a biofidelic dummy. This dummy had a tri-axial accelerometer cluster at the top of the neck, the bottom of the neck and the centre of gravity (C.G.) of the head. The accelerations recorded at the three locations were not completely in phase with respect to each other (i.e. the peaks did not always coincide in time). But they were also not totally out of phase (i.e. the maximum at one location coinciding with the minimum at a second location). The typical peak acceleration at the CG in the normal direction (i.e. trying to pull the neck apart) was about 15 g. The peak accelerations at the top and bottom of the neck were about 5 g at both locations. The maximum difference between the accelerations at the head CG and top of the neck was about 10 g. With a head mass of 1 kg, and $g = 9.81$ m/s^2, this leads to a peak distraction force acting at the top of the neck of about 100 N. In these experiments, head rotational velocity was of the order of 50 rad/s, and accelerations of the order of 3000 rad/s^2.

Eq. (1) can be used to calculate the neck distraction force for this case where the neck length was about 5 cm and head mass about 1 kg. Thus,

$$\text{Neck distraction force}$$
$$= 1\,\text{kg} \times 50\,\text{rad/s}^2 \times 50\,\text{rad/s}^2 \times 0.05\,\text{m} = 125\,\text{N}$$

Even if we assume that the acceleration at the C.G. was totally in opposite phase to the acceleration at the top of the neck, this would lead to a maximum acceleration of

DOIs of original articles: 10.1016/j.forsciint.2005.12.018, 10.1016/j.forsciint.2006.01.001.

0379-0738/$ – see front matter
doi:10.1016/j.forsciint.2005.12.017

Table 1
Recomputed values of neck distraction forces

Calculation basis	Head weight (kg)	Neck length (m)	Neck distraction force (N)
Low end SBS rotational velocity (50 rad/s)	0.68	0.0381	65 (1027)
Low end SBS rotational velocity (50 rad/s)	0.68	0.0635	107 (1711)
Low end SBS rotational velocity (50 rad/s)	1.34	0.0381	128 (1711)
Low end SBS rotational velocity (50 rad/s)	1.34	0.0635	213 (2852)
Low end SBS rotational velocity (50 rad/s)	1.59	0.0381	151 (2395)
Low end SBS rotational velocity (50 rad/s)	1.59	0.0635	252 (3992)
High end SBS rotational velocity (150 rad/s)	0.68	0.0381	582 (9240)
High end SBS rotational velocity (150 rad/s)	0.68	0.0635	971 (15399)
High end SBS rotational velocity (150 rad/s)	1.34	0.0381	1149 (15399)
High end SBS rotational velocity (150 rad/s)	1.34	0.0635	1915 (25665)
High end SBS rotational velocity (150 rad/s)	1.59	0.0381	1363 (21559)
High end SBS rotational velocity (150 rad/s)	1.59	0.0635	2271 (35931)

$15\ g + 5\ g = 20\ g$, which would lead to a distraction force of 200 N, again far below the numbers quoted in the paper, at this level of angular velocity and neck length.

A more interesting calculation is the difference in the accelerations at the top and bottom of the neck column. This would provide an estimate of the actual tension force (or distraction force) acting within the neck. In this case, the time histories of the accelerations follow each other fairly closely, with peak differences rising to about 5 g. This would lead one to conclude that the tension force within the neck column may be quite low.

This might suggest that the mechanical analogue proposed in the paper may not be entirely appropriate when used to model the motion of the head and neck of infants when a baby is shaken. It would be interesting to hear the author s views on the wide variation between experimentally obtained values and those calculated using the formula given in the paper and what this variation indicates about the validity of the proposed analogue.

Duncan (reference [9]) conducted static pull experiments to obtain values of neck distraction forces leading to failure of the neck. Perhaps the author might like to comment on the validity of comparing this failure criterion to predict failures in dynamic situations such as cases where a baby is shaken.

A final point. The paper uses three presentations made at the NHTSA sponsored International Workshop on Human Subject Biomechanics as references [11,20,22]. At the beginning of each of these workshops, the Chairperson of the Workshop announces that material presented in these workshops should not used as references. This is because much work that is presented at these workshops is preliminary in nature and presentations are also used to gather input from experts in the audience. It is discouraging to see the paper use material from the workshop as references thus contravening the spirit of the workshop.

N. Rangarajan*
T. Shams
GESAC, Inc., 125 Orchard Drive Boonsboro, MD 21713, USA

*Corresponding author. Tel.: +1 301 432 5887; fax: +1 301 432 6199
E-mail address: nrangarajan@gesacinc.com (N. Rangarajan)

9 August 2005
Available online 23 February 2006

Forensic Science International 164 (2006) 282–283

www.elsevier.com/locate/forsciint

Response to the Letter to the Editor

I thank the writers for their comments to the editor regarding my article. At the outset, it is evident to me from the letters that the two writers seem to convey a similar construal of my paper. Therefore, I shall provide a combined response to both letters.

As their core message, the writers of the two letters suggest that my calculated SBS neck forces are too high because they are not in accord with what they calculated using the reported velocity values. Rather than concede that the velocities reported for SBS in the literature might be contradictorily low, the writer of one of the letters, instead, chose to believe that numerical errors are the reason for the dissimilarity between my numbers and theirs. In other words, it appears that these writers believe that head accelerations can, over the time duration of shaking, reach the SBS-defined levels[1] high enough to activate the customary rotational acceleration mechanism and cause subdural hematoma (SDH) but, at the same time, not necessarily cause infant neck injury.

These writers claim lower neck forces referring to dummy shaking experiments that produced far lower rotational head accelerations and they cite from an article[2] by Prange and Meyers [1] and one by Jenny et al. [2]. In effect, both writers cite acceleration values that limit the force an adult can impart on an infant and thus bound the head acceleration to far less levels than described for SBS in the literature. In fact, the writers quote a wide range of values for acceleration, which indicates that they are quite aware that human manual shaking alone may be insufficient to activate the above-mentioned rotational injury mechanism that they believe is the cause of SDH in the infant.

Clearly, various articles by M. Prange, S. Margulies, B. Meyers, C. Jenny, and others subscribe to the view that activation of the rotational acceleration mechanism of SDH demands far higher accelerations than those given by the writers in these critiques. In one of the letters, the writer refers to Prange and Meyers [1] who reported shaking accelerations of 4220 rad/s^2 and referred to Duhaime et al. [3] reporting accelerations of 1138 rad/s^2. Prange et al. [4], on the other hand, published a paper the same year that reported shaking accelerations of 2640 rad/s^2. The other writer reports on his analysis of Jenny et al. [2] data to obtain a peak acceleration of 3000 rad/s^2. Jenny et al. [2], however, reported 13252 rad/s^2 for what appears to be the same data.

Essentially, all of the rotational head acceleration values both writers quote are far below the levels described for the SBS. Their letters in effect point out that the levels of the shaking head accelerations defined for the SBS may be unrealistic and possibly unphysical. Disregarding the notion that SBS acceleration levels are unphysical, if one proceeds anyway and analyzes their application for the duration of shaking to the infant head, then a high force outcome on the neck is inevitable. Thus, the dilemma: *SBS calls for very high shaking head accelerations acting over the course of seconds to minutes to cause SDH but does not indicate what is expected to happen to the infant neck as a result of the consequent forces*.

Let me identify the difference between what I have done and what these two writers discuss. Since SBS is referred to in the literature as causing ''acceleration/deceleration'' brain injury, my approach was to directly analyze these accelerations applied for the time course of shaking. I chose a range that includes the highest values of accelerations reported because had I chosen lower values, the analysis would simply exclude the cornerstone mechanism of SBS and therefore, would be rendered moot. In other words, lower values would not be sufficient to activate the customary mechanism of rupturing bridging veins that SBS solely depends on for producing SDH. This of course, is the mechanism garnered for SBS from experiments where the head of a primate was potted in a metal cylinder constrained for acceleration/deceleration along a prescribed arc in a prescribed time frame. Duhaime et al. [3] evaluated this mechanism for infant shaking and impact and provided a time duration for each shaking cycle, which is much longer than that for impact. The SBS literature suggests that a shaking event consists of repeated cycles of shaking, which take place over a reported range from several seconds to more than a minute. I basically integrated the SBS accelerations over the time duration of shaking and obtained values for resulting neck forces. I agree with the writers that the neck forces I obtained are high but not because of numerical error. The forces are high because that is what results when the described SBS accelerations are applied to the infant head for the time duration of shaking.

Finally, more research is needed to advance understanding of the injury mechanisms associated with traumatic infant shaking to help detect and prevent it. It is my hope that discourse such as

DOIs of original articles: 10.1016/j.forsciint.2005.12.018, 10.1016/j.forsciint.2005.12.017.

[1] SBS is cited in the literature as having forces that are as great as those of falls from great heights, by some accounts more than 9 m (30 ft), onto hard surfaces or from high-speed motor vehicle crashes

[2] This article, cited by the writer of one of the letters as ''M.T. Prange and B.S. Myers, *Evidenced-based biomechanical analysis of craniocervical inflicted neurotrauma, Inflicted Childhood Neurotrauma,* American Academy of Pediatrics, 2003, pp. 237–243'', was not found. We found essentially the same citation but apparently the writer of the letter used a different title [1].

0379-0738/$ – see front matter
doi:10.1016/j.forsciint.2006.01.001

this can help energize more interest in the provision for and conduct of innovative research in this very important area.

References

[1] M. Prange, B.S. Meyers, Pathobiology and Biomechanics of Inflicted Childhood Trauma-Response, in Inflicted Childhood Neurotrauma, American Academy of Pediatrics, 2003, pp. 237–243.
[2] C. Jenny, T. Shams, N. Rangarajan, T. Fukuda, Development of a biofidelic 2.5 kg infant dummy and its application to assessing infant head trauma during violent shaking. In: Proceedings of the 30th International Workshop on Injury Biomechanics Research, Ponte Vedra Beach, Florida, 2002, pp. 129–143.
[3] A.-C. Duhaime, S. Margulies, et al., The shaken baby syndrome: a clinical, pathological, and biomechanical study, J. Neurosurg. 66 (1987) 409–415.
[4] M. Prange, S. Margulies, et al., Anthropomorphic simulations of falls, shakes, and inflicted impacts in infants, J. Neurosurg. 99 (2003) 143–215.

Faris A. Bandak*
Department of Neurology, A1036,
F. Edward Hébert School of Medicine,
Uniformed Services University of the Health Sciences,
4301 Jones Bridge Road, Bethesda, MD 20814, USA

*Tel.: +1 301 299 7357
E-mail address: fbandak@usuhs.mil

Available online 10 February 2006